# A Physical Introduction to Fluid Mechanics

## Spring 2014

# A Physical Introduction to Fluid Mechanics

by

## Alexander J. Smits

Professor of Mechanical and Aerospace Engineering
Princeton University
and
Professorial Fellow
Department of Mechanical and Aerospace Engineering
Monash University

Second Edition

December 19, 2013

# Contents

# Preface

## First Edition

The purpose of this book is to summarize and illustrate basic concepts in the study of fluid mechanics. Although fluid mechanics is a challenging and complex field of study, it is based on a small number of principles which in themselves are relatively straightforward. The challenge taken up here is to show how these principles can be used to arrive at satisfactory engineering answers to practical problems. The study of fluid mechanics is undoubtedly difficult, but it can also become a profound and satisfying pursuit for anyone with a technical inclination, and I hope the book conveys that message clearly.

The scope of this introductory material is rather broad, and many new ideas are introduced. It will require a reasonable mathematical background, and those students who are taking a differential equations course concurrently sometimes find the early going a little challenging. The underlying physical concepts are highlighted at every opportunity to try to illuminate the mathematics. For example, the equations of fluid motion are introduced through a reasonably complete treatment of one-dimensional, steady flows, including Bernoulli's equation, and then developed through progressively more complex examples. This approach gives the students a set of tools that can be used to solve a wide variety of problems, as early as possible in the course. In turn, by learning to solve problems, students can gain a physical understanding of the basic concepts before moving on to examine more complex flows. Dimensional reasoning is emphasized, as well as the interpretation of results (especially through limiting arguments). Throughout the text, worked examples are given to demonstrate problem-solving techniques. They are grouped at the end of major sections to avoid interrupting the text as much as possible.

The book is intended to provide students with a broad introduction to the mechanics of fluids. The material is sufficient for two quarters of instruction. For a one-semester course only a selection of material should be used. A typical one-semester course might consist of the material in Chapters 1 to 10, not including Chapter 6. If time permits, one of Chapters 10 to 13 may be included. For a course lasting two quarters, it is possible to cover Chapters 1 to 6, and 8 to 10, and select three or four of the other chapters, depending on the interests of the class. The sections marked with asterisks may be omitted without loss of continuity. Although some familiarity with thermodynamic concepts is assumed, it is not a strong prerequisite. Omitting the sections marked by a single asterisk, and the whole of Chapter 12, will leave a curriculum that does not require a prior background in thermodynamics.

A limited number of Web sites are suggested to help enrich the written material. In particular, a number of Java-based programs are available on the Web to solve specific fluid mechanics problems. They are especially useful in areas where traditional methods limit the number of cases that can be explored. For example, the programs designed to solve potential flow problems by superposition and the programs that handle compressible flow problems, greatly expand the scope of the examples that can be solved in a limited amount of time, while at the same time dramatically reducing the effort involved. A listing of

current links to sites of interest to students and researchers in fluid dynamics may be found at *http://www.princeton.edu/˜gasdyn/fluids.html*. In an effort to keep the text as current as possible, additional problems, illustrations and web resources, as well as a Corrigendum and Errata may be found at *http://www.princeton.edu/˜gasdyn/fluids.html*.

In preparing this book, I have had the benefit of a great deal of advice from my colleagues. One persistent influence that I am very glad to acknowledge is that of Professor Sau-Hai Lam of Princeton University. His influence on the contents and tone of the writing is profound. Also, my enthusiasm for fluid mechanics was fostered as a student by Professor Tony Perry of the University of Melbourne, and I hope this book will pass on some of my fascination with the subject.

Many other people have helped to shape the final product. Professor David Wood of Newcastle University in Australia provided the first impetus to start this project. Professor George Handelman of Rensselaer Polytechnic Institute, Professor Peter Bradshaw of Stanford University, and Professor Robert Moser of the University of Illinois Urbana-Champaign were very helpful in their careful reading of the manuscript and through the many suggestions they made for improvement. Professor Victor Yakhot of Boston University test-drove an early version of the book, and provided a great deal of feedback, especially for the chapter on dimensional analysis. My wife, Louise Handelman, gave me wonderfully generous support and encouragement, as well as advice on improving the quality and clarity of the writing. I would like to dedicate this work to the memory of my brother, Robert Smits (1946–1988), and to my children, Peter and James.

<div align="right">

Alexander J. Smits
Princeton, New Jersey, USA

</div>

## Second Edition

The second edition was initially undertaken to correct the many small errors contained in the first edition, but the project rapidly grew into a major rethinking of the material and its presentation. While the general structure of the book has survived, the material originally contained in chapters 3 and 5 has been re-organized, and many other sections have been given a makeover. More than 120 homework problems have been added, based on exam questions developed at Princeton. It is now presented in two parts: the first part contains the main text, and the second part contains study guides, sample problems, and homework problems (with answers). It continues to be a work in progress, and your comments are invited. My thanks go to Candy Reed for proofreading this and earlier drafts. Any remaining errors or omissions are entirely my fault.

<div align="right">

AJS

</div>

# Chapter 1

# Introduction

Fluid mechanics is the study of the behavior of fluids under the action of applied forces. Typically, we are interested in finding the power necessary to move a fluid through a device, or the force required to move a solid body through a fluid. The speed of the resulting motion, and the pressure, density and temperature variations in the fluid, are also of great interest. To find these quantities, we apply the principles of dynamics and thermodynamics to the motion of fluids, and develop equations to describe the conservation of mass, momentum, and energy.

As we look around, we can see that fluid flow is a pervasive phenomenon in all parts of our daily life. To the ancient Greeks, the four fundamental elements were Earth, Air, Fire, and Water; and three of them, Air, Fire and Water, involve fluids. The air around us, the wind that blows, the water we drink, the rivers that flow, and the oceans that surround us, affect us daily in the most basic sense. In engineering applications, understanding fluid flow is necessary for the design of aircraft, ships, cars, propulsion devices, pipe lines, air conditioning systems, heat exchangers, clean rooms, pumps, artificial hearts and valves, spillways, dams, and irrigation systems. It is essential to the prediction of weather, ocean currents, pollution levels, and greenhouse effects. Not least, all life-sustaining bodily functions involve fluid flow since the transport of oxygen and nutrients throughout the body is governed by the flow of air and blood. Fluid flow is, therefore, crucially important in shaping the world around us, and its full understanding remains one of the great challenges in physics and engineering.

What makes fluid mechanics challenging is that it is often very difficult to predict the motion of fluids. In fact, even to observe fluid motion can be difficult. Most fluids are highly transparent, like air and water, or they are of a uniform color, like oil, and their motion only becomes visible when they contain some type of particle. Snowflakes swirling in the wind, dust kicked up by a car along a dirt road, smoke from a fire, or clouds scudding in a stiff breeze, help to mark the underlying fluid motion (Figure 1.1). It is clear that this motion can be very complicated. By following a single snowflake in a snowstorm, for example, we see that it traces out a complex path, and each flake follows a different path. Eventually, all the flakes end up on the ground, but it is difficult to predict where and when a particular snowflake lands. The fluid that carries the snowflake on its path experiences similar contortions, and generally the velocity and acceleration of a particular mass of fluid vary with time and location. This is true for all fluids in motion: the position, velocity and acceleration of a fluid is, in general, a function of time and space.

To describe the dynamics of fluid motion, we need to relate the fluid acceleration to the resultant force acting on it. For a rigid body in motion, such as a satellite in orbit, we can follow a fixed mass, and only one equation (Newton's second law of motion, $F = ma$) is required, along with the appropriate boundary conditions. Fluids can also move in rigid body motion, but more commonly one part of the fluid is moving with respect to another
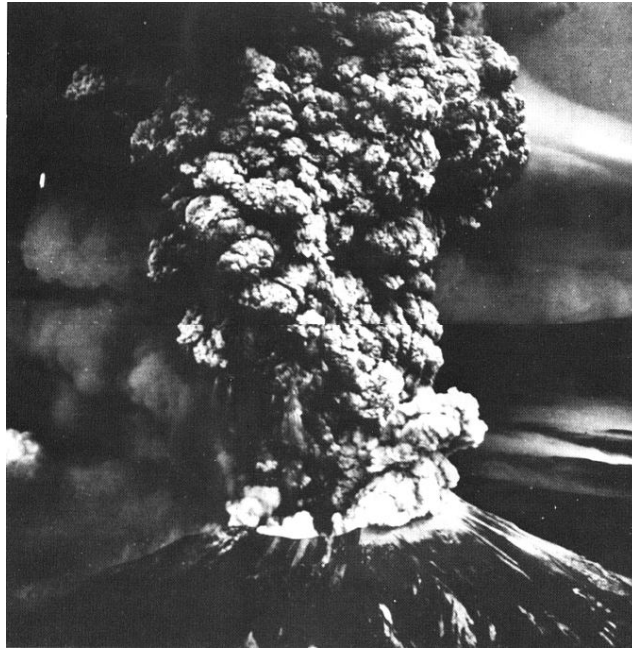
Figure 1.1: The eruption of Mt. St. Helens, May 18, 1980. Austin Post/U.S. Department of the Interior, U.S. Geological Survey, David A. Johnston, Cascades Volcano Observatory, Vancouver, WA.

part (there is *relative* motion), and then the fluid behaves more like a huge collection of particles. We often describe fluid motion in terms of these "fluid particles," where a fluid particle is a small, fixed mass of fluid containing the same molecules of fluid no matter where it ends up in the flow and how it got there. Each snowflake, for example, marks one fluid particle and to describe the dynamics of the entire flow requires a separate equation for each fluid particle. The solution of any one equation will depend on every other equation because the motion of one fluid particle depends on its neighbors, and solving this set of simultaneous equations is obviously a daunting task. It is such a difficult task, in fact, that for most practical problems the exact solution cannot be found even with the aid of the most advanced computers. It seems likely that this situation will continue for many years to come, despite the likely advances in computer hardware and software capabilities.

To make any progress in the understanding of fluid mechanics and the solution of engineering problems, we usually need to make approximations and use simplified flow models. But how do we make these approximations? Physical insight is often necessary. We must determine the crucial factors that govern a given flow, and to identify the factors that can safely be neglected. This is what sometimes makes fluid mechanics difficult to learn and understand: physical insight takes time and familiarity to develop, and the reasons for adopting certain assumptions or approximations are not always immediately obvious.

To help develop this kind of intuition, this book starts with the simplest types of problems and progressively introduces higher levels of complexity, while at the same time stressing the underlying principles. We begin by considering fluids that are in static equilibrium, then fluids where relative motions exist under the action of simple forces, and finally more complex flows where viscosity and compressibility are important. At each stage, the simplifying assumptions will be discussed, although the full justification is sometimes postponed until the later material is understood. By the end of the book, the reader should be able to solve basic problems in fluid mechanics, while understanding the limitations of the tools used in their solution.

Before starting along that path, we need to consider some fundamental aspects of fluids and fluid flow.  In this chapter, we discuss the differences between solids and fluids, and introduce some of the distinctive properties of fluids such as density, viscosity and surface tension.  We will also consider the type of forces that can act on a fluid, and its deformation by stretching, shearing and rotation.  We begin by describing how fluids differ from solids.

## 1.1  The Nature of Fluids

Almost all the materials we see around us can be described as solids, liquids or gases.  Many substances, depending on the pressure and temperature, can exist in all three states.  For example, $H_2O$ can exist as ice, water, or vapor.  Two of these states, liquids and gases are both called fluid states, or simply fluids.

The principal difference between liquids and gases is in their compressibility.  Gases can be compressed much more easily than liquids, but when the change in density of a gas is small, it can often be treated as being incompressible, which is a great simplification.  This approximation will not hold when large pressure changes occur, or when the gas is moving at high speeds (see Section 1.5), but in this text we will ordinarily assume that the fluid is incompressible unless stated otherwise (as in Chapter 11).

The most obvious property of fluids that is not shared by solids is the ability of fluids to flow and change shape; fluids do not hold their shape independent of their surroundings, and they will flow spontaneously within their containers under the action of gravity.  Fluids do not have a preferred shape, and different parts of a fluid may move with respect to each other under the action of an external force.  In this respect, liquids and gases respond differently in that gases fill a container fully, whereas liquids occupy a definite volume.  When a gas and a liquid are both present, an interface forms between the liquid and the surrounding gas called a *free surface* (Figure 1.2).  At a free surface, surface tension may be important, and waves can form.  Gases can also be dissolved in the liquid, and when the pressure changes bubbles can form, as when a soda bottle is suddenly opened.

To be more precise, the most distinctive property of fluids is its response to an applied force or an applied stress (stress is force per unit area).  For example, when a shear stress is applied to a fluid, it experiences a continuing and permanent distortion.  Drag your hand through a basin of water and you will see the distortion of the fluid (that is, the flow that occurs in response to the applied force) by the swirls and eddies that are formed on the free surface.  This distortion is permanent in that the fluid does not return to its original state after your hand is removed from the fluid.  Also, when a fluid is squeezed in one direction (that is, a normal stress is applied), it will flow in the other two directions.  Squeeze a hose in the middle and the water will issue from its ends.  If such stresses persist, the fluid continues to flow.  Fluids cannot offer permanent resistance to these kinds of loads.  This is not true
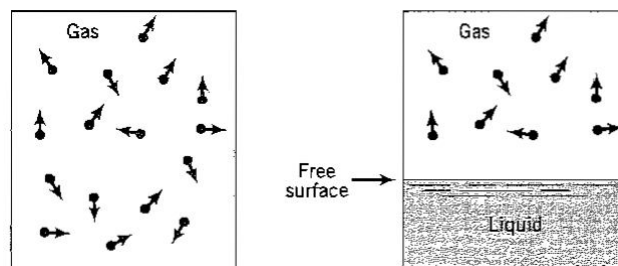


Figure 1.2: Gases fill a container fully (left), whereas liquids occupy a definite volume, and a free surface can form (right).
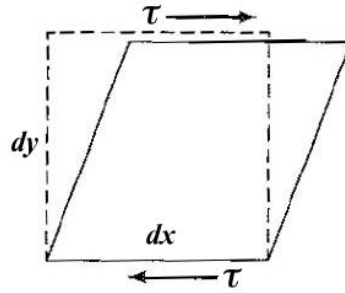
Figure 1.3: When a shear stress $\tau$ is applied to a fluid element the element distorts. It will continue to distort as long as the stress acts.

for a solid; when a force is applied to a solid it will generally deform only as much as it takes to accommodate the load, and then the deformation stops. Therefore,

> A fluid is defined as a material that deforms continuously and permanently under the application of a shearing stress, no matter how small.

So we see that the most obvious property of fluids, their ability to flow and change their shape, is precisely a result of their inability to support shearing stresses (Figure 1.3). Flow is possible without a shear stress, since differences in pressure will cause a fluid to experience a resultant force and an acceleration, but when the shape of the fluid mass is changing, shearing stresses must be present.

With this definition of a fluid, we can recognize that certain materials that look like solids are actually fluids. Tar, for example, is sold in barrel-sized chunks which appear at first sight to be the solid phase of the liquid that forms when the tar is heated. However, cold tar is also a fluid. If a brick is placed on top of an open barrel of tar, we will see it settle very slowly into the tar. It will continue to settle as time goes by — the tar continues to deform under the applied load — and eventually the brick will be completely engulfed. Even then it will continue to move downwards until it reaches the bottom of the barrel. Glass is another substance that appears to be solid, but is actually a fluid. Glass flows under the action of its own weight. If you measure the thickness of a very old glass pane you would find it to be larger at the bottom of the pane than at the top. This deformation happens very slowly because the glass has a very high viscosity, which means it does not flow very freely, and the results can take centuries to become obvious. However, when glass experiences a large stress over a short time, it behaves like a solid and it can crack. Silly putty is another example of a material that behaves like an elastic body when subject to rapid stress (it bounces like a ball) but it has fluid behavior under a slowly acting stress (it flows under its own weight).

## 1.2   Units and Dimensions

Before we examine the properties of fluids, we need to consider units and dimensions. Whenever we solve a problem in engineering or physics, it is important to pay strict attention to the units used in expressing the forces, accelerations, material properties, and so on. The two systems of units used in this book are the SI system (Système Internationale), and the British Gravitational (BG) system. To avoid errors, it is essential to correctly convert from one system of units to another, and to maintain strict consistency within a given system of

units. There are no easy solutions to these difficulties, but by using the SI system whenever possible, many unnecessary mistakes can often be avoided. A list of commonly used conversion factors is given in Appendix B.

It is especially important to make the correct distinction between mass and force. In the SI system, mass is measured in kilograms, and force is measured in newtons. The force required to move a mass of one kilogram with an acceleration of $1\,m/s^2$ is $1\,N$. A mass $m$ in kilograms has a weight in newtons equal to $mg$, where $g$ is the acceleration due to gravity ($= 9.8\,m/s^2$). There is no such quantity as "kilogram-force," although it is sometimes (incorrectly) used. What is meant by kilogram-force is the force required to move a one kilogram mass with an acceleration of $9.8\,m/s^2$, and it is equal to $9.8\,N$.

In the BG system, mass is measured in slugs, and force is measured in pound-force ($lb_f$). The force required to move a mass of one slug with an acceleration of $1\,ft/s^2$ is $1\,lb_f$. A mass $m$ in slugs has a weight in $lb_f$ equal to $mg$, where $g$ is the acceleration due to gravity ($= 32.2\,ft/s^2$). The quantity "pound-mass" ($lb_m$) is sometimes used, but it should always be converted to slugs first by dividing $lb_m$ by the factor 32.2. The force required to move $1\,lb_m$ with an acceleration of $1\,ft/s^2$ is

$$1\,lb_m\,ft/s^2 \;=\; \frac{1}{32.2}\,slug\,ft/s^2 \;=\; \frac{1}{32.2}\,lb_f$$

Remember that $1\,lb_f = 1\,slug\,ft/s^2 = 32.2\,lb_m\,ft/s^2$.

It is also necessary to make a distinction between units and dimensions. The *units* we use depend on whatever system we have chosen, and they include quantities like feet, seconds, newtons and pascals. In contrast, a *dimension* is a more abstract notion, and it is the term used to describe concepts such as mass, length and time. For example, an object has a quality of "length" independent of the system of units we choose to use. Similarly, "mass" and "time" are concepts that have a meaning independent of any system of units. All physically meaningful quantities, such as acceleration, force, stress, and so forth, share this quality.

Interestingly, we can describe the dimensions of any quantity in terms of a very small set of what are called *fundamental* dimensions. For example, acceleration has the dimensions of length/(time)$^2$ (in shorthand, $LT^{-2}$), force has the dimensions of mass times acceleration ($MLT^{-2}$), density has the dimensions of mass per unit volume ($ML^{-3}$), and stress has the dimensions of force/area ($ML^{-1}T^{-2}$) (see Table 1.1).

A number of quantities are inherently nondimensional, such as the numbers of counting. Also, ratios of two quantities with the same dimension are dimensionless. For example, bulk strain $dV/V$ is the ratio of two quantities each with the dimension of volume, and therefore it is nondimensional. Angles are also nondimensional. Angles are usually measured in radians, and since a radian is the ratio of an arc-length to a radius, an angle is the ratio of two lengths, and so it is nondimensional. Nondimensional quantities are independent of the system of units as long as the units are consistent, that is, if the same system of units is used throughout. Nondimensional quantities are widely used in fluid mechanics, as we shall see.

## 1.3   Stresses in Fluids

In this section, we consider the stress distributions that occur within the fluid. To do so, it is useful to think of a fluid particle, which is a small amount of fluid of fixed mass.

The stresses that act on a fluid particle can be split into normal stresses (stresses that give rise to a force acting normal to the surface of the fluid particle) and tangential or shearing stresses (stresses that produce forces acting tangential to its surface). Normal stresses tend to compress or expand the fluid particle without changing its shape. For

| Quantity | Dimension | Units | |
|---|---|---|---|
| | | S.I. | B.G. |
| Mass | $M$ | $kilogram$ | $slug$ |
| Length | $L$ | $meter$ | $foot$ |
| Time | $T$ | $second$ | $second$ |
| Velocity | $LT^{-1}$ | $m/s$ | $ft/s$ |
| Acceleration | $LT^{-2}$ | $m/s^2$ | $ft/s^2$ |
| Velocity gradient (strain rate) | $T^{-1}$ | $s^{-1}$ | $s^{-1}$ |
| Density | $ML^{-3}$ | $kg/m^3$ | $slugs/ft^3$ |
| Force | $MLT^{-2}$ | $newton$ | $lb_f$ |
| Energy | $ML^2T^{-2}$ | $joule$ | $ft \cdot lb_f$ |
| Power | $ML^2T^{-3}$ | $watt$ | $ft \cdot lb_f/s$ |
| Stress | $ML^{-1}T^{-2}$ | $pascal$ | $psi$ |
| Viscosity | $ML^{-1}T^{-1}$ | $Pa \cdot s$ $\left(= N \cdot s/m^2\right)$ | $slugs/ft \cdot s$ $\left(= lb_f \cdot s/ft^2\right)$ |
| Kinematic viscosity | $L^2T^{-1}$ | $m^2/s$ | $ft^2/s$ |
| Surface tension | $MT^{-2}$ | $N/m$ | $lb_f/ft$ |

Table 1.1: Units and dimensions.

example, a rectangular particle will remain rectangular, although its dimensions may change. Tangential stresses shear the particle and deform its shape: a particle with an initially rectangular cross-section will become lozenge-shaped.

What role do the properties of the fluid play in determining the level of stress required to obtain a given deformation? In solids, we know that the level of stress required to compress a rod depends on the Young's modulus of the material, and that the level of tangential stress required to shear a block of material depends on its shear modulus. Young's modulus and the shear modulus are properties of solids, and fluids have analogous properties called the bulk modulus and the viscosity. The bulk modulus of a fluid relates the normal stress on a fluid particle to its change of volume. Liquids have much larger values for the bulk modulus than gases since gases are much more easily compressed (see Section 1.4.3). The viscosity of a fluid measures its ability to resist a shear stress. Liquids typically have larger viscosities than gases since gases flow more easily (see Section 1.6). Viscosity, as well as other properties of fluids such as density and surface tension, are discussed in more detail later in this chapter. We start by considering the nature of pressure and its effects.

## 1.4   Pressure

Consider the pressure in a fluid at rest. We will only consider a gas, but the general conclusions will also apply to a liquid. When a gas is held in a container, the molecules of the gas move around and bounce off its walls. When a molecule hits the wall, it experiences an elastic impact, which means that its energy and the magnitude of its momentum are
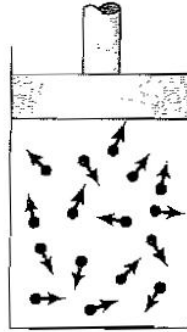
Figure 1.4: The piston is supported by the pressure of the gas inside the cylinder.

conserved. However, its direction of motion changes, so that the wall must have exerted a force on the gas molecule. Therefore, an equal and opposite force is exerted by the gas molecule on the wall during impact. If the piston in Figure 1.4 was not constrained in any way, the continual impact of the gas molecules on the piston surface would tend to move the piston out of the container. To hold the piston in place, a force must be applied to it, and it is this force (per unit area) that we call the gas pressure.

If we consider a very small area of the surface of the piston, so that over a short time interval, $\Delta t$, very few molecules hit this area, the force exerted by the molecules will vary sharply with time as each individual collision is recorded. When the area is large, so that the number of collisions on the surface during the interval $\Delta t$ is also large, the force on the piston due to the bombardment by the molecules becomes effectively constant. In practice, the area need only be larger than about $10\ell_m^2$, where the mean free path $\ell_m$ is the average distance traveled by a molecule before colliding with another molecule. Pressure is therefore a *continuum* property, by which we mean that for areas of engineering interest, which are almost always much larger than areas measured in terms of the mean free path, the pressure does not have any measurable statistical fluctuations due to molecular motions.[1]

We make a distinction between the *microscopic* and *macroscopic* properties of a fluid, where the microscopic properties relate to the behavior on a molecular scale (scales comparable to the mean free path), and the macroscopic properties relate to the behavior on an engineering scale (scales much larger than the mean free path). In fluid mechanics, we are concerned only with the continuum or macroscopic properties of a fluid, although we will occasionally refer to the underlying molecular processes when it seems likely to lead to a better understanding.

## 1.4.1 Pressure: direction of action

Consider the direction of the force acting on a flat solid surface due to the pressure exerted by a gas at rest. On a molecular scale, of course, a flat surface is never really flat. On average, however, for each molecule that rebounds with some amount of momentum in the direction along the surface, another rebounds with the same amount of momentum in the opposite direction, no matter what kind of surface roughness is present (Figure 1.5). The average force exerted by the molecules on the solid in the direction along its surface will be zero. We expect, therefore, that the force due to pressure acts in a direction which is purely normal to the surface.

Furthermore, the momentum of the molecules is randomly directed, and the magnitude of the force due to pressure should be independent of the orientation of the surface on which

---

[1]The mean free path of molecules in the atmosphere at sea level is about $10^{-7}\,m$, which is about 1000 times smaller than the thickness of a human hair.
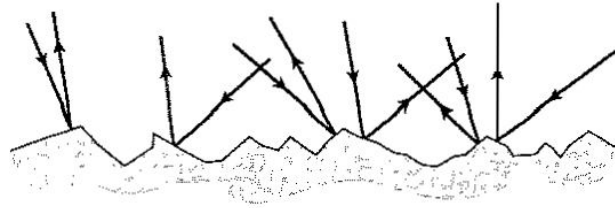
Figure 1.5: Molecules rebounding of a macroscopically rough surface

it acts. For instance, a thin flat plate in air will experience no resultant force due to air pressure since the forces due to pressure on its two sides have the same magnitude and they point in opposite directions. We say that pressure is *isotropic* (based on Greek words, meaning "equal in all directions", or more precisely, "independent of direction").

> The pressure at a point in a fluid is independent of the orientation of the surface passing through the point; the pressure is isotropic.

Pressure is a "normal" stress since it produces a force that acts in a direction normal to the surface on which it acts. That is, the direction of the force is given by the orientation of the surface, as indicated by a unit normal vector $\mathbf{n}$ (Figure 1.6). The force has a magnitude equal to the average pressure times the area of contact. By convention, a force acting to compress the volume is positive, but for a closed surface the vector $\mathbf{n}$ always points outward (by definition). So

> The force due to a pressure $p$ acting on one side of a small element of surface $dA$ defined by a unit normal vector $\mathbf{n}$ is given by $-p\mathbf{n}dA$.

In some textbooks, the surface element is described by a vector $\mathbf{dA}$, which has a magnitude $dA$ and a direction defined by $\mathbf{n}$, so that $\mathbf{dA} = \mathbf{n}dA$. We will not adopt that convention, and the magnitude and direction of a surface element will always be indicated separately.

For a fluid at rest, the pressure is the normal component of the force per unit area. What happens when the fluid is moving? The answer to this question is somewhat complicated.[2] However, for the flows considered in this text, the difference between the pressure in a stationary and in a moving fluid can be ignored to a very good approximation, even for fluids moving at high speeds.

## 1.4.2   Forces due to pressure

Pressure is given by the normal force per unit area, so that even if the force itself is moderate the pressure can become very large if the area is small enough. This effect makes skating possible: the thin blade of the skate combined with the weight of the skater produces intense pressures on the ice, melting it and producing a thin film of water that acts as a lubricant and reduces the friction to very low values.

It is also true that very large forces can be developed by small fluid pressure differences acting over large areas. Rapid changes in air pressure, such as those produced by violent storms, can result in small pressure differences between the inside and the outside of a house. Since most houses are reasonably airtight to save air conditioning and heating costs, pressure differences can be maintained for some time. When the outside air pressure is lower

---

[2]See, for example, I.G. Currie, "Fundamental Fluid Mechanics," McGraw-Hill, 1974.
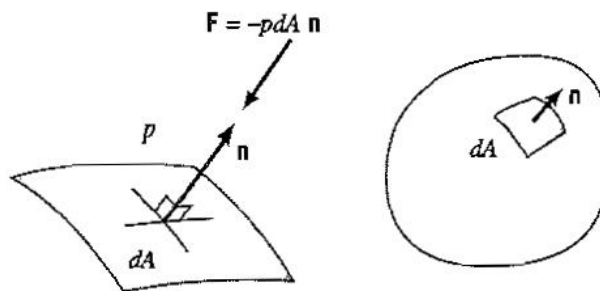
Figure 1.6: The vector force **F** due to pressure $p$ acting on an element of surface area $dA$ with a unit normal vector **n**.

than that inside the house, as is usually the case when the wind blows, the forces produced by the pressure differences can be large enough to cause the house to explode. Example 1.4 illustrates this phenomenon.

This effect can be demonstrated with a simple experiment. Take an empty metal container and put a small amount of water in the bottom. Heat the water so that boils. The water vapor that forms displaces some of the air out of the container. If the container is then sealed, and allowed to cool, the water vapor inside the container condenses back to liquid, and now the mass of air in the container is less than at the start of the experiment. The pressure inside the container is therefore less than atmospheric (since fewer molecules of air hit the walls of the container). As a result, strong crushing forces develop which can cause the container to collapse, providing a dramatic illustration of the large forces produced by small differential pressures. More common examples include the slamming of a door in a draft, and the force produced by pressure differences on a wing to lift an airplane off the ground.

Similarly, to drink from a straw requires creating a pressure in the mouth that is below atmospheric, and a suction cup relies on air pressure to make it stick. In one type of suction cup, a flexible membrane forms the inside of the cup. To make it stick, the cup is pressed against a smooth surface, and an external lever is used to pull the center of the membrane away from the surface, leaving the rim in place as a seal. This action reduces the pressure in the cavity to a value below atmospheric, and the external pressure produces a resultant force that holds the cup onto the surface.

When the walls of the container are curved, pressure differences will also produce stresses within the walls. In Example 1.5, we calculate the stresses produced in a pipe wall by a uniform internal pressure. The force due to pressure acts radially outward on the pipe wall, and this force must be balanced by a circumferential force acting within the pipe wall material, so that the fluid pressure acting normal to the surface produces a tensile stress in the solid.

### 1.4.3 Bulk stress and fluid pressure

Consider a fluid held in a container. In the interior of the fluid, away from the walls of the container, each fluid particle feels the pressure due to its contact with the surrounding fluid. The fluid particle experiences a *bulk* strain and a *bulk* stress since the surrounding fluid exerts a pressure on all the surfaces that define the fluid particle.

We often make a distinction between *body forces* and *surface forces*. Body forces are forces acting on a fluid particle that have a magnitude proportional to its volume. An important example of a body force is the force due to gravity, that is, weight. Surface forces are forces acting on a fluid particle that have a magnitude proportional to its surface area.

An important example of a surface force is the force due to pressure.

When body forces are negligible, the pressure is uniform throughout the fluid. In this case, the forces due to pressure acting over each surface of a fluid particle all have the same magnitude. The force acting on any one face of the particle acts normal to that face with a magnitude equal to the pressure times the area. The force acting on the top face of a cubic fluid particle, for example, is cancelled by an opposite but equal force acting on its bottom face. This will be true for all pairs of opposing faces. Therefore, the resultant force acting on that particle is zero. This result will also hold for a spherical fluid particle (an element of surface area on one side will always find a matching element on the opposite side), and, in fact, it will hold for a body of any arbitrary shape. Therefore there is no resultant force due to pressure acting on a body if the pressure is uniform in space, regardless of the shape of the body. Resultant forces due to pressure will appear only if there is a pressure variation within the fluid, that is, when pressure gradients exist.

The force due to pressure acts to compress the fluid particle. This type of strain is called a bulk strain, and it is measured by the fractional change in volume, $dv/v$, where $v$ is the volume of the fluid particle. The change in pressure $dp$ required to produce this change in volume is linearly related to the bulk strain by the bulk modulus, $K$. That is,

$$dp = -K\,\frac{dv}{v} \qquad (1.1)$$

The minus sign indicates that an increase in pressure causes a decrease in volume (a compressive pressure is taken to be positive). We can write this in terms of the fractional change in density, where the density of the fluid $\rho$ is given by its mass divided by its volume (see Section 2.2). Since the mass $m$ of the particle is fixed,

$$\rho = \frac{m}{v}$$

so that

$$v = \frac{m}{\rho}$$

and

$$\frac{dv}{v} = \frac{d(m/\rho)}{(m/\rho)} = \rho\, d\left(\frac{1}{\rho}\right) = -\frac{d\rho}{\rho}$$

equation 1.1 becomes

$$dp = K\,\frac{d\rho}{\rho} \qquad (1.2)$$

This compressive effect is illustrated in Examples 1.6 and 1.7. Note that the value of the bulk modulus depends on how the compression is achieved; the bulk modulus for isothermal compression (where the temperature is held constant) is different from its adiabatic value (where there is no heat transfer allowed) or its isentropic value (where there is no heat transfer and no friction).

### 1.4.4   Pressure: transmission through a fluid

An important property of pressure is that it is transmitted through the fluid. For example, when an inflated bicycle tube is squeezed at one point, the pressure will increase at every other point in the tube. Measurements show that the increase is (almost) the same at every point and equal to the applied pressure; if an extra pressure of $5\,psi$ were suddenly applied at the tube valve, the pressure would increase at every point in the tube by almost exactly this amount (small differences will occur due to the weight of the air inside the tube – see Chapter 2, but in this particular example the contribution is very small). This property of transmitting pressure undiminished is a property possessed by all fluids, not just gases.

However, the transmission does not occur instantaneously. It depends on the speed of sound in the medium and the shape of the container. The speed of sound is important because it measures the rate at which pressure disturbances propagate (sound is just a small pressure disturbance traveling through a medium). The shape of the container is important because pressure waves refract and reflect off the walls, and this process increases the distance and time the pressure waves need to travel. The phenomenon may be familiar to anyone who has experienced the imperfect acoustics of a poorly designed concert hall.

### 1.4.5 Ideal gas law

Take another look at the piston and cylinder example shown in Figure 1.4. If we double the number of molecules in the cylinder, the density of the gas will double. If the extra molecules have the same speed (that is, the same temperature) as the others, the number of collisions will double, to a very good approximation. Since the pressure depends on the number of collisions, we expect the pressure to double also, so that at a constant temperature the pressure is proportional to the density.

On the other hand, if we increase the temperature without changing the density, so that the speed of the molecules increases, the impact of the molecules on the piston and walls of the cylinder will increase. The pressure therefore increases with temperature, and by observation we know that the pressure is very closely proportional to the absolute temperature.

These two observations are probably familiar from basic physics, and they are summarized in the ideal gas law, which states that

$$p = \rho R T \tag{1.3}$$

where $R$ is the gas constant. Gas constants for a number of different gases are given in Table Appendix-C.10. For air, $R = 287.03\, m^2/s^2 K = 1716.4 ft^2/s^2 R$.

Equation 1.3 is an example of an equation of state, in that it relates several thermodynamic properties such as pressure, temperature and density. Most gases obey equation 1.3 to a good approximation, except under conditions of extreme pressure or temperature where more complicated relationships must be used.

## 1.5 Compressibility in Fluids

All fluids are compressible, which means that the density can vary. However, under some range of conditions, it is often possible to make the approximation that a fluid is incompressible. This is particularly true for liquids. Water, for example, only changes its density and volume very slightly under extreme pressure (see, for instance, Example 1.6). Other liquids behave similarly, and under commonly encountered conditions of pressure and temperature we generally assume that liquids are incompressible.

Gases are much more compressible. The compressibility of air, for example, is part of our common experience. By blocking off a bicycle pump and pushing down on the handle, we can easily decrease the volume of the air by 50% (Figure 1.7), so that its density increases by a factor of two (the mass of air is constant). See also Example 1.7.

Even though gases are much more compressible than liquids (by perhaps a factor of $10^4$), small pressure differences will cause only small changes in gas density. For example, a 1% change in pressure at constant temperature will change the density by 1%. In the atmosphere, a 1% change in pressure corresponds to a change in altitude of about 85 meters, so that for changes in height of the order of tall buildings we can usually assume air has a constant pressure and density.

Velocity changes will also affect the fluid pressure and density. When a fluid accelerates from velocity $V_1$ to velocity $V_2$ at a constant height, the change in pressure $\Delta p$ that occurs
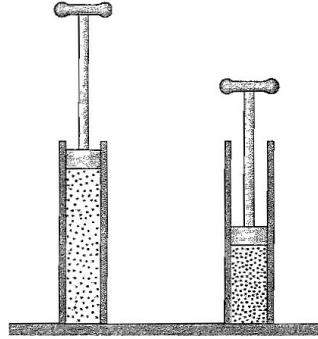
Figure 1.7: Air compressed in a bicycle pump.

is given by

$$\Delta p \; = \; -\tfrac{1}{2}\rho \left( V_2^2 - V_1^2 \right) \tag{1.4}$$

according to Bernoulli's equation (see Section 4.2). The pressure decreases as the velocity increases, and vice versa. What are the consequences for the density? If air at sea level accelerates from rest to, say, $30\,m/s$, its pressure will decrease by $450 Pa$, which represents only a -0.5% change in ambient pressure. The corresponding density change for an isentropic process would be -0.7%, which is obviously very small.

When do velocity variations lead to significant density changes? A common yardstick is to compare the flow velocity $V$ to the speed of sound $a$. This ratio is called the Mach number $M$, so that

$$M = \frac{V}{a} \tag{1.5}$$

The Mach number is a nondimensional parameter since it is defined as the ratio of two velocities. That is, it is just a number, independent of the system of units used to measure $V$ and $a$ (see Section 1.2 and Chapter 7). It is named after Ernst Mach, who was an early pioneer in studies of sound and compressibility.

When the Mach number is less than about 0.3, the flow is usually assumed to be incompressible. To see why this is so, consider air held at $20°C$ as it changes its speed from zero to $230\,mph$ ($114\,m/s$). The speed of sound in an ideal gas is given by

$$a = \sqrt{\gamma R T} \tag{1.6}$$

where $T$ is the absolute temperature, $R$ is the gas constant ($= 287.03\,m^2/s^2K$ for air), and $\gamma$ is the ratio of specific heats ($\gamma = 1.4$ for air). At $20°C$, the speed of sound in air is $343\,m/s = 1126\,ft/s = 768\,mph$. Therefore, at this temperature, $230\,mph$ corresponds to a Mach number of 0.3. At sea level, according to equation 1.4, the pressure will decrease by about $7,800\,Pa$ at the same time, which is less than 8% of the ambient pressure. If the process were isentropic, the density would decrease by 11%. We see that relatively high speeds are required for the density to change significantly. However, when the Mach number approaches one, compressibility effects become very important. Passenger transports, such as the Boeing 747 shown in Figure 1.8, fly at a Mach number of about 0.8, and the compressibility of air is a crucial factor affecting its aerodynamic design.

## 1.6   Viscous Stresses

As indicated earlier, when there is no flow the stress distribution is completely described by its pressure distribution, and the bulk modulus relates the pressure to the fractional change

Figure 1.8: A Boeing 747 cruising at $35,000\,ft$ at a Mach number of about 0.82. Courtesy of United Airlines.

in volume (the compression strain). When there is flow, however, shearing stresses may become important, and additional normal stresses can also come into play. The magnitude of these stresses depends on the fluid viscosity. Viscosity is a property of fluids, and it is related to the ability of a fluid to flow freely. Intuitively, we know that the viscosity of motor oil is higher than that of water, and the viscosity of water is higher than that of air (see Section 1.6.3 for more details). To be more precise about the nature of viscosity, we need to consider how the viscosity of a fluid gives rise to viscous stresses.

## 1.6.1 Viscous shear stresses

When a shear stress is applied to a solid, the solid deforms by an amount that can be measured by an angle called the shear angle $\Delta\gamma$ (Figure 1.9). We can also apply a shear stress to a fluid particle by confining the fluid between two parallel plates, and moving one plate with respect to the other. We find that the shear angle in the fluid will grow indefinitely if the shear stress is maintained. The shear stress $\tau$ is not related to the magnitude of the shear angle, as in solids, but to the rate at which the shear angle is changing. For many fluids, the relationship is linear, so that

$$\tau \propto \frac{d\gamma}{dt}$$
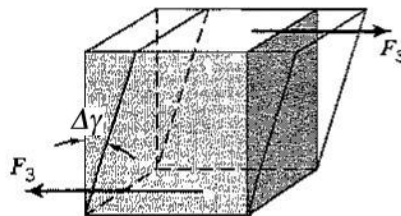


Figure 1.9: Solid under shear.
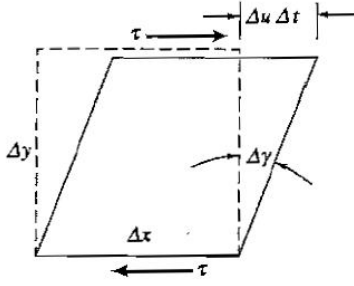
Figure 1.10: A fluid in shear.
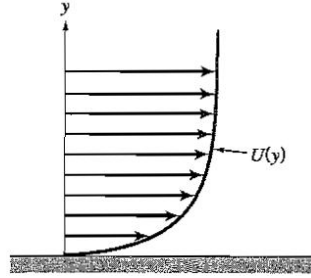


Figure 1.11: Velocity profile in the region near a solid surface.

That is

$$\tau = \mu \frac{d\gamma}{dt}$$

where the coefficient of proportionality $\mu$ is called the *dynamic viscosity* of the fluid, or simply the fluid *viscosity*.

Imagine an initially rectangular fluid particle of height $\Delta y$, where the tangential force is applied to the top face, and its base is fixed (Figure 1.10). In time $\Delta t$, the top face of the particle moves a distance $\Delta u \Delta t$ relative to the bottom face, where $\Delta u$ is the velocity of the top face relative to the bottom face. If $\Delta \gamma$ is a small angle, $\sin \Delta \gamma \approx \Delta \gamma$, and so

$$\Delta y \sin \Delta \gamma \approx \Delta y \Delta \gamma \approx \Delta u \Delta t, \quad \text{so that} \quad \frac{\Delta \gamma}{\Delta t} \approx \frac{\Delta u}{\Delta y}$$

In the limit of a very small cube we obtain

$$\frac{d\gamma}{dt} = \frac{du}{dy}$$

so that

$$\tau_{yx} = \mu \frac{du}{dy} \tag{1.7}$$

The subscript $yx$ indicates that the shear stress in the $x$-direction is associated with a strain rate in the $y$-direction. Note that $du/dy$ has dimensions of a strain rate (1/time, or $T^{-1}$).

Fluids which obey a linear relationship between stress and strain rate such as that given in equation 1.7 are called *Newtonian* fluids. Most common fluids are Newtonian, including air and water over very wide ranges of pressures and temperatures. The density and viscosity of some common fluids are shown in Table 1.2. A more complete listing appears in Appendix A.

Not all fluids obey a Newtonian stress-strain relationship. An enormous variety of non-Newtonian or *visco-elastic* fluids exists that obey more complicated relationships between stress and strain rate. The relationships can be nonlinear, similar to the plastic deformation of solids, or demonstrate history effects, where the stress history needs to be known before the deformation can be predicted. Such fluids are commonly encountered in the plastics and chemical industries.

## 1.6.2   Viscous normal stresses

Viscosity is also important when normal stress differences occur. Consider a length of taffy. Taffy behaves a little like a fluid in that it will continue to stretch under a constant load, and it has very little elasticity, so that it does not spring back when the load is removed. Imagine that we pull lengthwise on the taffy (call it the $x$-direction). Its length will increase

in the direction of the applied load, while its cross-sectional area will decrease. Normal stress differences are present. For example, as the taffy stretches, the point in the center will remain in its original location, but all other points move outward at speeds that increase with the distance from the center point. If the velocity at any point is $u$, we see that $u$ varies with $x$, and that a velocity gradient or strain rate $du/dx$ exists. The resistance to the strain rate depends on the properties of the taffy.

A fluid behaves somewhat similarly to taffy, in that fluids offer a resistance to stretching or compression. The magnitude of the stress depends on a fluid property called the *extensional* viscosity. For Newtonian fluids, the viscosity is isotropic, so that the shear viscosity and the extensional viscosity are the same. So, for a fluid in simple extension or compression, the normal stress is given by

$$\tau_{xx} = \mu \frac{du}{dx} \tag{1.8}$$

The subscript $xx$ indicates that the stress in the $x$-direction is associated with a strain rate in the $x$-direction.

### 1.6.3   Viscosity

We have seen that when fluids are in relative motion, shear stresses develop which depend on the viscosity of the fluid. Viscosity is measured in units of $Pa \cdot s$, $kg/(m\,s)$, $lb_m/(ft \cdot s)$, $N \cdot s/m^2$, or $Poise$ (a unit named after the French scientist Jean Poiseuille). It has dimensions of mass per unit length per unit time ($M/LT$)

Because a viscous stress is developed (that is, a viscous force per unit area), we know from Newton's second law that the fluid must experience a rate of change of momentum. Sometimes we say that momentum "diffuses" through the fluid by the action of viscosity. To understand this statement, we need to examine the basic molecular processes that give rise to the viscosity of fluids. That is, we will take a microscopic point of view.

A flowing gas has two characteristic velocities: the average molecular speed $\bar{v}$, and the speed at which the fluid mass moves from one place to another, called the *bulk velocity*, $V$. For a gas, $\bar{v}$ is equal to the speed of sound. Consider a flow where the fluid is maintained at a constant temperature, so that $\bar{v}$ is the same everywhere, but where $V$ varies with distance as in Figure 1.12. As molecules move from locations with a bulk velocity that is smaller to locations where the bulk velocity is larger (from B to A in Figure 1.12), the molecules will interact and exchange momentum with their faster neighbors. The net result is to reduce the local average bulk velocity. At the same time, molecules from regions of higher velocity will migrate to regions of lower velocity (from A to B in Figure 1.12), interact with the surrounding molecules and increase the local average velocity.

We see that the exchange of momentum on a microscopic level tends to smooth out, or diffuse, the velocity differences in a fluid. On a macroscopic scale, we see a change in

|  | $\rho$ $(kg/m^3)$ | $\mu$ $(N\,sec/m^2)$ |
|---|---|---|
| Air | 1.204 | $18.2 \times 10^{-6}$ |
| Water | 998.2 | $1.002 \times 10^{-3}$ |
| Sea water | 1,025 | $1.07 \times 10^{-3}$ |
| SAE 30 motor oil | 919 | 0.04 |
| Honey | $\approx 1430$ | $\approx 1.4$ |
| Mercury | 13,600 | $1.57 \times 10^{-3}$ |

Table 1.2: Density and viscosity of some common fluids (at $20°C$ and $1\,atm$).
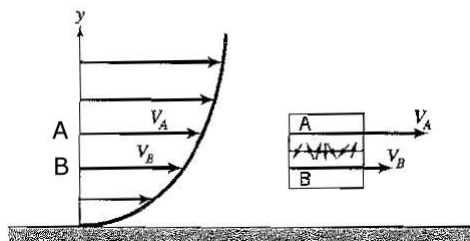
Figure 1.12: Momentum exchange by molecular mixing. Velocity profile in the vicinity of a solid surface.

momentum in the bulk fluid and infer the action of a stress — we call it the viscous shear stress, with a diffusion coefficient called the viscosity.

Because the interactions among molecules occur within a distance comparable to the mean free path, the viscosity must depend on the average molecular speed $\bar{v}$, the density $\rho$ and the mean free path $\ell_m$. Viscosity is therefore a property of the fluid, and for a gas it can be estimated from molecular gas dynamics. Typically, the dynamic viscosity is very small. Air at $20°C$, for example, has a viscosity of about $\mu = 18.2 \times 10^{-6}\,N \cdot s/m^2$ (see Table Appendix-C.1). Nevertheless, the stress is given by the product of the viscosity and the velocity gradient, and viscous stresses can become very important when the magnitude of the velocity gradient is large even when the viscosity itself is very small. This happens in regions close to a solid surface, such as that shown in Figure 1.12.

The molecular interpretation of viscosity also helps us to know what to expect when the temperature of the gas increases. Since the number of collisions will increase, enhancing the momentum exchange among molecules, the viscosity should increase. Figure Appendix-C.1 confirms this expectation.

The opposite behavior is found for liquids, where the viscosity decreases as the temperature increases. This is because liquids have a much higher density than gases, and intermolecular forces are more important. As the temperature increases, the relative importance of these bonds decreases, and therefore the molecules are more free to move. As a consequence, the viscosity of liquids decreases as their temperature increases (see Figure A-C.1).

Finally, we note that it is sometimes convenient to use a parameter called the *kinematic viscosity*, $\nu$, defined as the dynamic viscosity divided by the density,

$$\nu = \frac{\mu}{\rho}$$

The dimensions of kinematic viscosity are length$^2$/time ($L^2/T$), and common units are $m^2/s$ or $ft^2/s$.

## 1.6.4   Measures of viscosity

We have seen that viscosity is associated with the ability of a fluid to flow freely. For example, honey has about 1000 times the viscosity of water, and it is obvious that it takes a much greater force to stir honey than water (at the same rate). The fact that viscosity and flow rate are directly connected is sometimes used to measure the fluid viscosity. Motor oils, for example, are rated by the Society of Automobile Engineers in terms of the time it takes for $60\,mL$ of the oil to flow through a calibrated hole in the bottom of a cup under the action of gravity. An oil rated as SAE 30 will take about 60 seconds, and a SAE 120 oil will take 240 seconds, and so forth. The instrument is called a Saybolt viscometer (Figure 1.13).
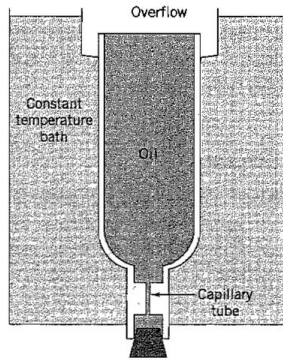
Figure 1.13: Society of Automobile Engineers of America (SAE) standard viscosity test. With permission, "Fluid Mechanics," Streeter & Wylie, 8th ed., published by McGraw-Hill, 1985.
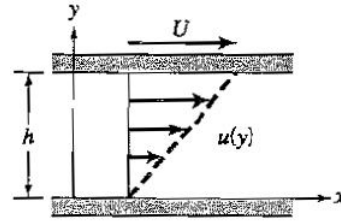


Figure 1.14: Linear Couette flow.

Alternatively, it is possible to use the relationship given in equation 1.7 to measure the viscosity. If we consider two plates, separated by a gap $h$, and fill the gap with a fluid of viscosity $\mu$, the force required to move one plate with respect to the other is a measure of the fluid viscosity. If the top plate moves with a velocity $U$ relative to the bottom plate, and if the gap is small enough, the velocity profile becomes linear, as shown in Figure 1.14. This flow is called plane Couette flow. The stress at the wall, $\tau_w$ is related to the velocity gradient at the wall, where

$$\tau_w = \mu \left. \frac{\partial u}{\partial y} \right|_w$$

By finding $\tau_w$, the force per unit area required to move the top plate at a constant speed, the viscosity can be found as shown in Example 1.10 in the Study Guide.

It is also possible to use a circular geometry, where the fluid fills the annular gap between two concentric cylinders, and the two cylinders move at different speeds. This flow is called circular Couette flow. Another common "viscometer" uses a cone rotating in a cup (see Figure 7.2 in the Study Guide.

### 1.6.5 Energy and work considerations

For the velocity profile shown in Figure 1.11, the local shear stress at any distance from the surface is given by equation 1.7. To overcome this viscous stress, work must be done by the fluid. If no further energy were supplied to the fluid, all motion would eventually cease because of the action of viscous stresses. For example, after we have finished stirring our coffee we see that all the fluid motions begin to slow down and finally come to a halt. Viscous stresses *dissipate* the energy associated with the fluid motion. In fact, we often say that viscosity gives rise to a kind of friction within the fluid.

Viscosity also causes a drag force on a solid surface in contact with the fluid: the viscous stress at the wall, $\tau_w = \mu(\partial u/\partial y)_w$, transmits the fluid drag to the surface, as illustrated in Figure 1.15.

Example 1.10 shows how the drag force on a solid surface can be found from the velocity profile by evaluating the velocity gradient at the wall and integrating the surface stress over the area of the body. If the stress is constant over the area, the viscous force $F_v$ is simply given by the shear stress at the wall times the area over which it acts. If the body moves at a constant velocity $U_b$, it must do work to maintain its speed. If it moves a distance $\Delta x$ in
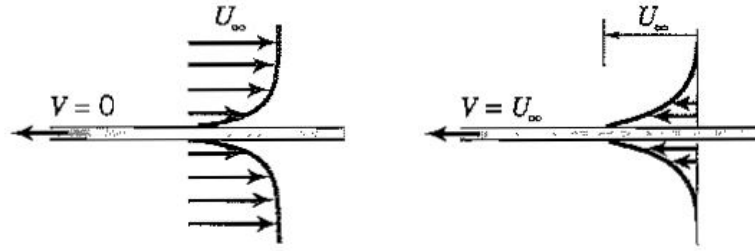
Figure 1.15: A long flat plate moving at constant speed in a viscous fluid. On the right is shown the velocity distributions as they appear to a stationary observer, and on the left they are shown as they appear to an observer moving with the plate.

a time $\Delta t$, it does work equal to $F_v \Delta x$, and it expends power equal to $F_v \Delta x / \Delta t$, that is, $F_v U_b$.

## 1.7  Boundary Layers

Viscous effects are particularly important near solid surfaces, where the strong interaction of the molecules of the fluid with the molecules of the solid causes the relative velocity between the fluid and the solid to become almost exactly zero. For a stationary surface, therefore, the fluid velocity in the region near the wall must reduce to zero (Figure 1.16). This is called the *no-slip condition*.

We see this effect in nature when a dust cloud driven by the wind moves along the ground. Not all the the dust particles are moving at the same speed; close to the ground they move more slowly than further away. If we were to look in the region very close to the ground we would see that the dust particles there are almost stationary, no matter how strong the wind. Right at the ground, the dust particles do not move at all, indicating that the air has zero velocity at this point. This is evidence for the no-slip condition, in that there is no relative motion between the air and the ground at their point of contact. It follows that the flow velocity varies with distance from the wall; from zero at the wall to its full value some distance away, so that significant velocity gradients are established close to the wall. In most cases, this region is thin (compared to a typical body dimension), and it is called a *boundary layer*. Within the boundary layer, strong velocity gradients can occur, and therefore viscous stresses can become important (as indicated by equation 1.7).

The no-slip condition is illustrated in Figure 1.17. Here, water is flowing above and below a thin flat plate. The flow is made visible by forming a line of hydrogen bubbles in the water (the technique is described in Section 4.1). The line was originally straight,
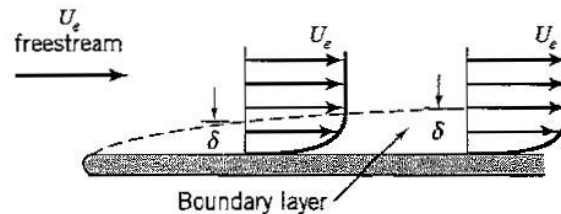


Figure 1.16: Growth of a boundary layer along a stationary flat plate. Here, $\delta$ is the boundary layer thickness, and $U_e$ is the freestream velocity, that is, the velocity outside the boundary layer region.
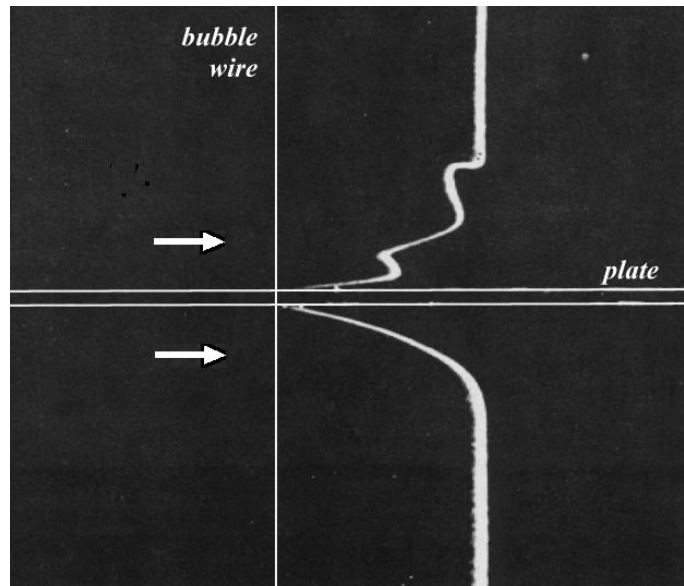
Figure 1.17: The no-slip condition in water flow past a thin plate. Flow is from left to right. The upper flow is turbulent, and the lower flow is laminar. With permission, *Illustrated Experiments in Fluid Mechanics*, (*The NCMF Book of Film Notes*, National Committee for Fluid Mechanics Films, Education Development Center, Inc., © 1972).

but as the flow sweeps the bubbles downstream (from left to right in Figure 1.17), the line changes its shape because bubbles in regions of faster flow will travel further in a given time than bubbles in regions of slower flow. The hydrogen bubbles therefore make the velocity distribution visible. Bubbles near the surface of the plate will move slowest of all, and *at* the surface they are stationary with respect to the surface because of the no-slip condition. The upper and lower flows in Figure 1.17 are different (the upper one is turbulent, and the lower one is laminar — see Section 1.8), but the no-slip condition applies to both.

## 1.8   Laminar and Turbulent Flow

We have described boundary layer flow as the flow in a region close to a solid surface where viscous stresses are important. When the layers of fluid inside the boundary layer slide over each other in a very disciplined way, the flow is called *laminar* (the lower flow in Figure 1.17). Whenever the size of the object is small, or the speed of the flow is low, or the viscosity of the fluid is large, we observe laminar flow. However, when the body is large, or it is moving at a high speed, or the viscosity of the fluid is small, the entire nature of the flow changes. Instead of smooth, well-ordered, laminar flow, irregular eddying motions appear, signaling the presence of *turbulent* flow (the upper flow in Figure 1.17).

   Turbulent flows are all around us. We see it in the swirling of snow in the wind, the sudden and violent motion of an aircraft encountering "turbulence" in the atmosphere, the mixing of cream in coffee, and the irregular appearance of water issuing from a fully-opened faucet. Turbulent boundary layers are seen whenever we observe the dust kicked up by the wind, or look alongside the hull of a ship moving in smooth water, where swirls and eddies are often seen in a thin region close to the hull. Inside the eddies and between them, fluid layers are in relative motion, and local viscous stresses are causing energy dissipation. Because of the high degree of activity associated with the eddies and their fluctuating velocities, the viscous energy dissipation inside a turbulent flow can be very much greater than in a

laminar flow.

We suggested that laminar flow is the state of fluid flow found at low velocities, for bodies of small scale, for fluids with a high kinematic viscosity. In other words, it is the flow state found at *low* Reynolds number, where the Reynolds number is a nondimensional ratio defined by

$$Re = \frac{\rho V D}{\mu} = \frac{V D}{\nu}$$

where $V$ is the velocity and $D$ is a characteristic dimension (the body length, the tube diameter, etc.). Turbulent flow is found when the velocity is high, on large bodies, for fluids with a low kinematic viscosity. That is, turbulent flow is the state of fluid flow found at *high* Reynolds number. Because the losses in turbulent flow are much greater then in laminar flow, the distinction between these two flow states is of great practical importance.

## 1.9   Surface Tension

At the free surface that forms between a gas and a liquid, a fluid property called *surface tension* becomes important.

By observation, we know that the surface of a liquid tends to contract to the smallest possible area, behaving as though its surface were a stretched elastic membrane. For example, small drops of liquid in a spray become spherical, because a sphere has the smallest surface area for a given volume. Spherical lead shot (as found in shotgun pellets) used to be made by dropping molten lead from a high tower (they are often called "shot" towers). The drops of liquid lead would take a spherical form because of surface tension, and maintain this form as they cooled and solidified during their fall. Also, when a brush is wet, the hairs cling together, because the films between them tend to contract. Some insects can walk on water, and a steel needle placed carefully on a water surface will float.

These surface tension phenomena are due to the attractive forces that exist between molecules. The forces fall off quickly with distance, and they are appreciable only over a very short distance (of the order of $5 \times 10^{-6}\,m$, that is, $5\,\mu m$). This distance forms the radius of a sphere around a given molecule, and only molecules contained in this sphere will attract the one at the center (Figure 1.18). For a molecule well inside the body of the liquid, its "sphere of molecular attraction" lies completely in the liquid, and the molecule is attracted equally in all directions by the surrounding molecules, so that the resultant force acting on it is zero. For a molecule near the surface, where its sphere of attraction lies partially outside the liquid, the resultant force is no longer zero; the surrounding molecules of the liquid tend to pull the center molecule into the liquid, and this force is not balanced by the attractive force exerted by the surrounding gas molecules because they are fewer in number (because the gas has a much lower density than the liquid). The resultant force on molecules near the surface is inward, tending to make the surface area as small as possible.
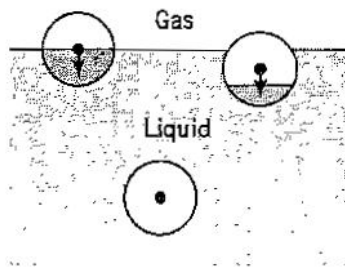


Figure 1.18: Surface tension and "spheres of molecular attraction."

The coefficient of surface tension $\sigma$ of a liquid is the tensile force per unit length of a line on the surface. Common units are $lb_f/ft$ or $N/m$, and its dimensions are $M/T^2$. A typical value at $20°C$ for air-water is $\sigma = 0.0050\,lb_f/ft = 0.073\,N/m$, and for air-mercury $\sigma = 0.033\,lb_f/ft = 0.48\,N/m$. Additional values are given in Tables Appendix-C.3, C.4 and C.11. Generally, dissolving an organic substance in water, such as grease or soap, will lower the surface tension, whereas inorganic substances raise the surface tension of water slightly. The surface tension of most liquids decreases with temperature, and this effect is especially noticeable for water.

We will now describe some particular phenomena due to surface tension, including the excess pressure in a drop or bubble, the formation of a meniscus on a liquid in a small-diameter tube, and *capillarity*.

## 1.9.1 Drops and bubbles

The surfaces of drops or bubbles tend to contract due to surface tension, which increases their internal pressure. When the drop or bubble stops growing, it is in equilibrium under the action of the forces due to surface tension and the excess pressure $\Delta p$ (the difference between the internal and external pressures).

Figure 1.19a shows one half of a spherical drop of radius $r$. The resultant upward force due to the excess pressure is $\pi r^2 \Delta p$, where $\pi r^2$ is the cross-sectional arae of the drop. Because the drop is in static equilibrium (that is, it is not accelerating and it is not growing), this force must be balanced by the surface tension force $2\pi r\sigma$, acting around the edge of the hemisphere (we neglect its weight). Therefore, for a drop

$$\pi r^2 \Delta p = 2\pi r\sigma$$

That is,

$$\Delta p = \frac{2\sigma}{r}$$

In the case of a bubble [Figure 1.19(b)] there are two surfaces to be considered, inside and out, so that for a bubble:

$$\Delta p = \frac{4\sigma}{r}$$

## 1.9.2 Forming a meniscus

The free surface of a liquid will form a curved surface when it comes in contact with a solid. Figure 1.20(a) shows two glass tubes, one containing mercury and the other water. The free surfaces are curved, convex for mercury, and concave for water. The angle between the solid surface $AB$ and the tangent $BC$ to the liquid surface at the point of contact [Figure 1.20(b)] is called the *angle of contact*, $\theta$. For liquids where the angle is less than $90°$ (for example,



(a)          (b)
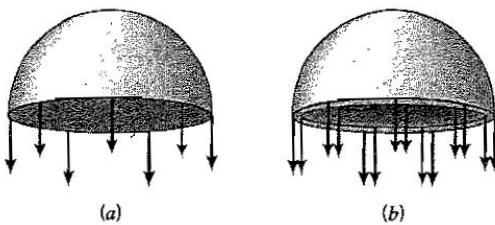
Figure 1.19: Equilibrium of (a) drop and (b) bubble, where the excess pressure is balanced by surface tension.
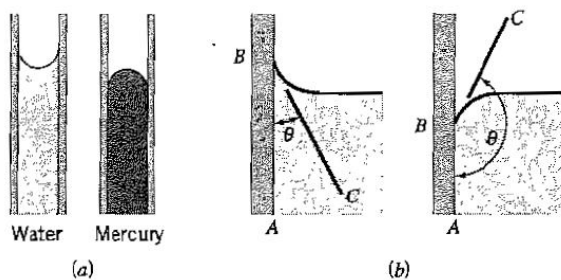
Figure 1.20: Angle of contact: (a) Free surface shape of water and mercury in glass tubes. (b) A wetting, and a non-wetting liquid.

water on glass), the liquid is said to *wet* the surface. For liquids where the angle is greater than 90° (for example, mercury on glass), the liquid is said not to wet the surface. For pure water on clean glass, the angle of contact is approximately zero, and for various metal surfaces it lies between 3° and 11°. For mercury on glass, its value is 130° to 145°.

Water wets glass because the attractive forces between the water molecules and the glass molecules exceed the forces between water molecules. The reverse holds true for mercury. That the contact angle depends on the nature of the surface is clearly illustrated by the behavior of water droplets. On a clean glass plate, $\theta \approx 0$, and a drop of water will spread out to wet the surface. However, on a freshly waxed surface such as a car hood, drops will "bead up," showing that $\theta > 0°$. Figure 1.21 ilustrates how the nature of the surface will change the contact angle for water drops on different glass surfaces.

Consider also a drop of water pressed between two plates a small distance $t$ apart (Figure 1.22). The radius of the circular spot made by the drop is $R$. The pressure inside the drop is less than the surrounding atmosphere by an amount depending on the tension in the free surface. To pull the plates apart, a force $F$ is required. If $\theta$ is the angle of contact, the upward component of surface tension is $\sigma \cos \theta$ [see Figure 1.20(b)], and it produces an upward force of $2\pi r \sigma \cos \theta$ around the perimeter of the drop. There is an identical force acting in the downward direction, and so the total force due to surface tension is given by $4\pi R \sigma \cos \theta$. This force is balanced by the reduced pressure acting on the circumferential area of the squeezed drop (only the radial component needs to be taken into account), given
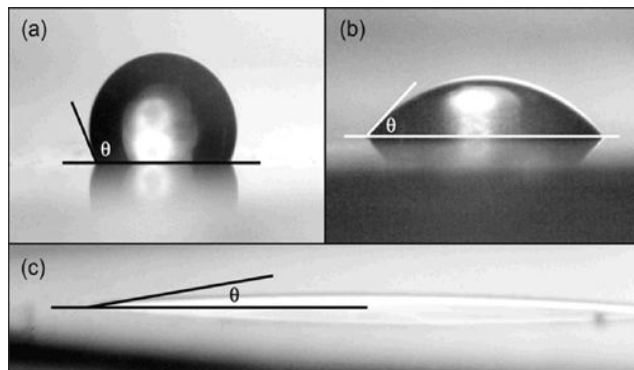


Figure 1.21: Water droplet contact angle measurements on 3 different borosilicate glass surfaces. From Sumner *et al. The Nature of Water on Surfaces of Laboratory Systems and Implications for Heterogeneous Chemistry in the Troposphere*, Phys. Chem. Chem. Phys. (2004) **6** 604-613. With permission of The Royal Society of Chemistry.
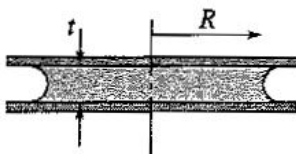
Figure 1.22: A drop of liquid squeezed between two glass plates.

by $2\pi Rt$. That is,

$$2\pi Rt\Delta p = 4\pi R\sigma \cos\theta$$

In turn, the force required to pull the plates apart is given by the reduced pressure times the area of the spot, which is approximately equal to $\pi R^2$. Hence

$$F = \pi R^2 \Delta p = \frac{2\sigma\pi R^2 \cos\theta}{t} \tag{1.9}$$

This force can be quite large if the film thickness $t$ is small or $R$ is large. For example, when a pot sits on a wet kitchen bench, the gap between the pot and the bench fills with water, and the pot can be remarkably difficult to pull off the bench. This force is due to surface tension.

### 1.9.3 Capillarity

Another phenomenon due to surface tension is capillarity. When a clean glass tube of radius $r$ is inserted into a dish of water, the water will rise inside the tube a distance $h$ above the surface (Figure 1.23). This happens because the attraction between glass and water molecules is greater than that between water molecules themselves, producing an upward force. The liquid rises until the weight of the liquid column balances the upward force due to surface tension. If $\theta$ is the angle of contact, the upward component of surface tension is $\sigma \cos\theta$ [see Figure 1.20(b)], and it produces an upward force of $2\pi r\sigma \cos\theta$ around the inside perimeter of the tube. If we neglect the contribution of the curved surface to the height of the column, then the weight of the column of liquid is equal to its volume times the fluid density $\rho$ times the acceleration due to gravity $g$, that is, $\rho g\pi r^2 h$. Hence,

$$\rho g\pi r^2 h = 2\pi r\sigma \cos\theta$$

and

$$h = \frac{2\sigma \cos\theta}{\rho gr}$$
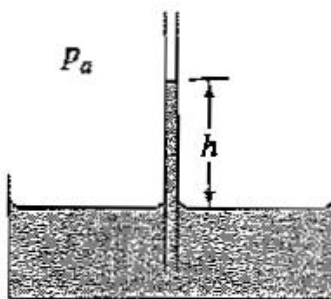


Figure 1.23: Water in a glass tube: a demonstration of capillarity.

The capillary rise $h$ is therefore inversely proportional to the tube radius. For water on clean glass, $\theta \approx 0$, and $h = 2\sigma/(\rho gr)$. For mercury in a glass tube, $\theta > 90°$ and $h$ is negative, so that there is a capillary depression.

# Chapter 2

# Fluid Statics

In this chapter, we consider fluids in static equilibrium. To be in static equilibrium, the fluid must be at rest, or it must be moving in such a way that there are no relative motions between adjacent fluid particles. There can be no velocity gradients, and consequently there will be no viscous stresses. A fluid in static equilibrium, therefore, is acted on only by forces due to pressure and its own weight, and perhaps by additional body forces due to externally imposed accelerations. In general, for a fluid in static equilibrium

$$\Sigma \mathbf{F} = 0 \quad \text{and} \quad \Sigma \mathbf{M} = 0$$

where $\mathbf{F}$ are all the forces acting on it, and $\mathbf{M}$ are all the moments.

The simplest case of a fluid in static equilibrium occurs when the fluid is at rest. For example, if a liquid is poured into a bucket and left to stand until all relative motions have died out, the fluid is then in static equilibrium. At this point, there are no resultant forces or moments acting on the fluid.

It is also possible to have a moving fluid in static equilibrium, as long as no part of the fluid is moving with respect to any other part. This is called *rigid body motion*. When the fluid and its container are moving at constant speed, for instance, it is in equilibrium under the forces due to pressure and its own weight (think of the coffee in a cup that is in a car moving at constant velocity). However, when this system is accelerating, the inertia force due to acceleration needs to be taken into account, as we shall see in Section 2.12.

## 2.1   The Hydrostatic Equation

We begin by considering a fluid at rest. We choose a small fluid element, that is, a small fixed volume of fluid located at some arbitrary point with dimensions of $dx$, $dy$ and $dz$ in the $x$-, $y$- and $z$-directions, respectively. When the fluid is in static equilibrium, there are no relative motions, and so the fluid element (a fixed volume) occupies the same space as a fluid particle (a fixed mass of fluid). The $z$-axis points in the direction opposite to the gravitational vector (see Figure 2.1) so that the positive direction is vertically up.

The only forces acting on the fluid particle are those due to gravity and pressure differences. Because there is no resultant acceleration of the fluid particle, these forces must balance. The force due to gravity acts only in the vertical direction, and we see immediately that the pressure cannot vary in the horizontal plane. In the $x$-direction, for example, the force due to pressure acting on the left face of the particle ($abef$) must cancel the force due to pressure acting on the right face of the particle ($cdgh$), since there is no other force acting in the horizontal direction. The pressures on these two faces must be equal, and so the pressure cannot vary in the $x$-direction. Similarly, it cannot vary in the $y$-direction.
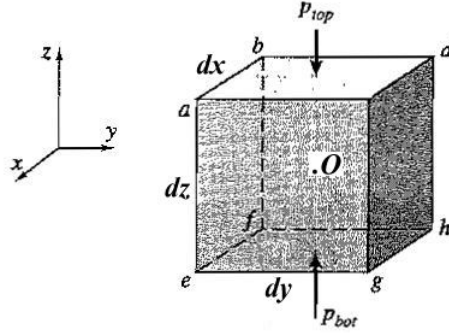
Figure 2.1: Static equilibrium of a small particle of fluid under the action of gravity and fluid pressure.

For the vertical direction, we use a Taylor-series expansion to express the pressure on the top and bottom faces of the particle in terms of pressure at the center of the particle, $p_0$, and its derivatives at that point (see Section Appendix-A.10). That is,

$$p_{top} = p_0 + \frac{dz}{2} \left.\frac{dp}{dz}\right|_0 + \frac{1}{2!} \left(\frac{dz}{2}\right)^2 \left.\frac{d^2p}{dz^2}\right|_0 - \ldots \tag{2.1}$$

The positive sign on the first derivative reflects the fact that when we move from the center of the cube to the top face, we move in the positive $z$-direction. The dots indicate higher order terms (terms involving higher order derivatives). Similarly, on the bottom face of the cube

$$p_{bot} = p_0 - \frac{dz}{2} \left.\frac{dp}{dz}\right|_0 + \frac{1}{2!} \left(\frac{dz}{2}\right)^2 \left.\frac{d^2p}{dz^2}\right|_0 + \ldots \tag{2.2}$$

where the negative sign on the first derivative reflects the fact that when we move from the center of the cube to the top face, we move in the negative $z$-direction. As the volume becomes infinitesimally small, the resultant force due to pressure is given by

$$F_{press} = (p_{bot} - p_{top}) \, dxdy = - \left.\frac{dp}{dz}\right|_0 dxdydz \tag{2.3}$$

which acts in the positive $z$-direction (opposite to the direction of $\mathbf{g}$). The second-order terms cancel exactly, and the third- and higher-order terms become negligible as the volume of the element becomes very small.

For the particle to remain at rest, the force due to the pressure differences, $F_{press}$, must be balanced by the weight of the fluid particle. To find the weight of the particle, we will assume that the density (like the pressure) is only a function of $z$, since we expect a direct relationship between pressure and density. The densities at the top and bottom of the cube, $\rho_{top}$ and $\rho_{bot}$, are given by equations similar to equations 2.1 and 2.2, respectively, with the pressure $p$ replaced by the density $\rho$. The average density, $\rho$, is given by

$$\rho = \tfrac{1}{2} \left(\rho_{top} + \rho_{bot}\right) = \tfrac{1}{2} \left(2\rho_0 + \ldots\right)$$

and so the weight of the fluid particle is given by

$$F_{weight} = (\rho_0 + \ldots) \, g \, dxdydz \tag{2.4}$$

where the higher order terms go to zero as the particle becomes infinitesimally small. The weight acts in the negative $z$-direction (in the direction of $\mathbf{g}$). For static equilibrium, $F_{press} -$
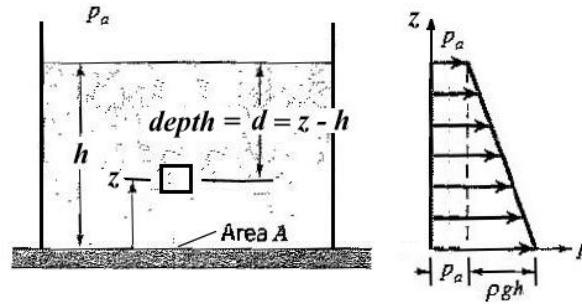
Figure 2.2: Container open to atmosphere, showing a particle of fluid located at a depth $d = z - h$ below the free surface. The graph on the right is a plot of the pressure as a function of depth.

$F_{weight} = 0$, and so from Equations 2.3 and 2.4 we obtain the *hydrostatic equation* describing the variation of pressure in a fluid under the action of gravity

$$\frac{dp}{dz} = -\rho g \qquad (2.5)$$

Remember that $z$ points in the direction *opposite* to that of **g** (that is, it points vertically up). The subscript 0 identifying the center of the particle has been dropped because the final result applies to any point in the fluid.

Consider a vessel filled to a depth $h$ with a liquid of constant density $\rho$. The top of the container is open to the atmosphere, so that the pressure at the surface of the liquid is equal to atmospheric pressure, $p_a$ (Figure 2.2). The $z$-direction is positive going up, as in equation 2.5. The hydrostatic equation (equation 2.5) is a first-order, linear, ordinary differential equation, so we need only one boundary condition to solve it. We have at $z = h$, $p = p_a$, and so

$$p - p_a = -\rho g(z - h) = \rho g(h - z) \qquad (2.6)$$

indicating that the pressure increases with depth $d = h - z$, with a constant slope equal to $\rho g$. That is,

> For a constant density fluid, the pressure increases linearly with depth.

The pressure variation with depth is shown on the right in Figure 2.2. At the free surface where $d = 0$ ($z = h$), the pressure is equal to atmospheric pressure, and then it increases linearly with depth so that at the bottom of the container where $d = h$ ($z = 0$) the pressure is equal to $p_a + \rho g h$. The arrows indicate the direction of the force produced by the pressure acting on the side wall of the container.

It is often useful to check relationships by examining their behavior "in the limit." When using the hydrostatic equation, for example, it is important to check that the depth is expressed correctly since it is easy to get the sign wrong. Remember that the pressure should have its maximum value at the maximum depth. We see that equation 2.6 has the right behavior: when $z = 0$, the depth is $h$ and the pressure takes its maximum value.

## 2.2  Density and Specific Gravity

Density is defined as the mass per unit volume, and it is measured in $kg/m^3$, or *slugs* ($1\,slug = 32.2\,lb_m$). The usual symbol is $\rho$. At $4°C$, water has a density of $1000\,kg/m^3$,

so that at this temperature one cubic meter contains $1000\,kg$ of water. At $20°C$, water has a density of $998.2\,kg/m^3$. In contrast, air has a density of $1.204\,kg/m^3$ at atmospheric pressure and $20°C$, so that its density is about 830 times smaller than water (see Tables 1.2 and Appendix-C.7).

It is common practice to express the density of other liquids relative to that of water. This is called the *specific gravity*. Formally, the specific gravity (SG) of a solid or liquid is the ratio of its density to that of water, that is,

$$SG = \frac{\text{density of substance}}{\text{density of water}}$$

Note that the specific gravity is a ratio of like quantities, and so it has no dimensions. It is an example of what is called a nondimensional parameter. Since the density is mass per unit volume, an equivalent definition is

$$SG = \frac{\text{mass of a given volume of substance}}{\text{mass of an equal volume of water}}$$

as long as the temperatures of the substance and the water are equal. Therefore air has a specific gravity of $1.204/998.2 = 0.001206$ at $20°C$. One type of alcohol widely used in manometers (and alcoholic beverages) is ethanol, which has a density of $789\,kg/m^3$ at $20°C$, so that its specific gravity is $789/998.2 = 0.790$. These concepts are further illustrated in Example 2.1.

Substances with a specific gravity less than one, such as ethanol, will float on water. Steel, on the other hand, has a density of $7850\,kg/m^3$, so that its specific gravity is 7.86, and it will not float on water, except possibly through the action of surface tension (see Section 1.9). Ice will float on water since it has a specific gravity of 0.917. For an iceberg, floating in sea water (which has a specific gravity of 1.025), this means that only about 10% of its bulk will be visible above the sea surface (Figure 2.3). This result is demonstrated in Example 2.10.

## 2.3   Absolute and Gauge Pressure

In equation 2.6, $p$ is the *absolute* pressure, since it is measured relative to an absolute vacuum. Absolute pressure is the pressure that appears in the ideal gas law (equation 1.3). When the pressure is measured relative to atmospheric pressure, such as $p - p_a$, it is called *gauge* pressure.

Gauge pressure is often useful when pressures above (or below) atmospheric are of interest. Most pressure instruments measure gauge pressures. A tire gauge, for instance, measures the pressure in a tire over and above the local atmospheric pressure. A vacuum gauge, in contrast, will measure the pressure below atmospheric (in common engineering usage a *vacuum* is any pressure lower than the ambient atmospheric pressure).

Air pressure can often assumed to be constant. Consider a simple container like that shown in Figure 2.2. The pressure difference measured from the top to the bottom of the liquid is given by $\rho g h$, where $\rho$ is the density of the liquid. Outside the container, atmospheric pressure acts, and the air pressure changes by $\rho_a g h$ over the same distance $h$, where $\rho_a$ is the density of air. The pressure change for air relative to water over the same distance is therefore given by the ratio

$$\frac{\rho_a g h}{\rho g h} = \frac{\rho_a}{\rho}$$

If the liquid was water, this ratio is equal to about $1.2/1000 = 0.0012$, and for alcohol it would be about $1.2/800 = 0.0015$. So the relative change of pressure in air compared to
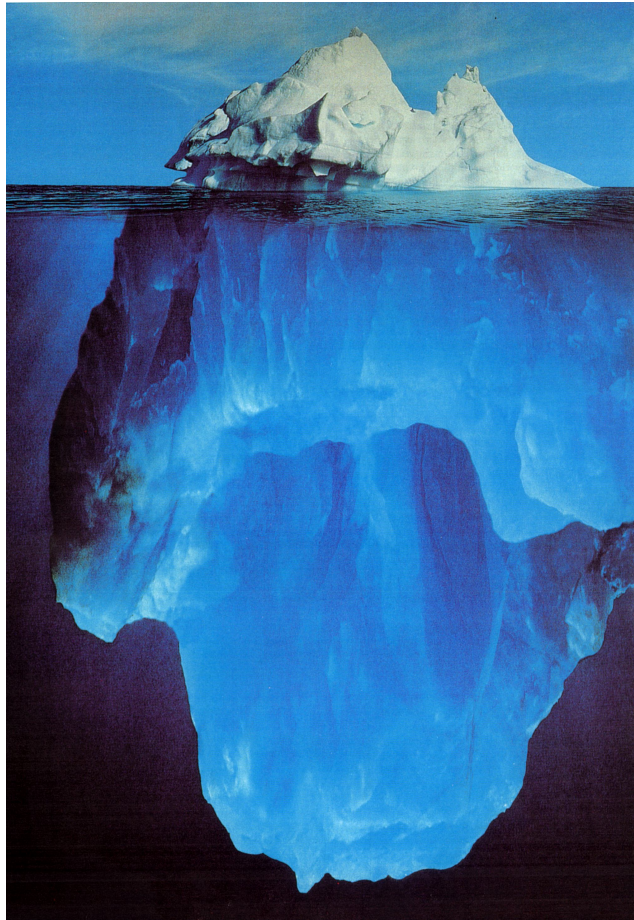
Figure 2.3: Iceberg, above and below the sea surface. Corbis/Ralph A. Clevenger.

a liquid over the same depth is always very small, simply because the density of a gas at moderate pressures is always much smaller than the density of a liquid. In many problems involving the pressure change due to a change in depth of a liquid, therefore, the change in air pressure over the same distance can be neglected and the air pressure can be assumed to be constant.

When this is the case, problems can often be solved using gauge pressures rather than absolute pressures. We will see additional examples later, but for now we consider the resultant force exerted on the bottom of the container shown in Figure 2.2. We will assume that the air pressure can be taken to be constant everywhere.

First, we use absolute pressures. The absolute pressure acting on the bottom of the container from the outside, where air pressure acts, is simply $p_a$, and the absolute pressure exerted on the bottom of the container from the inside by the liquid is $p_b$, where

$$p_b = p_a + \rho g h$$

If the area of the bottom is $A$, then the resultant force $F$ acting on the bottom surface is

$$F = (p_a + \rho g h) A - p_a A = \rho g h A$$

Second, we use gauge pressures. The gauge pressure acting on the outside of the tank is zero, by definition. Inside the tank, the gauge pressure at the bottom of the container is

$p_b - p_a = \rho g h$, and so

$$F = \rho g h A$$

as before. In this case, the air simply adds a constant pressure to the pressure developed hydrostatically in the liquid. Since the same pressure acts on the bottom of the container from the outside in the opposite direction, the forces due to air pressure cancel out and they do not contribute to the resultant force.

## 2.4   Applications of the Hydrostatic Equation

### 2.4.1   Pressure variation in the atmosphere

We can think of atmospheric pressure as being equal to the weight (per unit area) of all the air above our point of measurement. As we increase our height above sea level, this weight decreases, and therefore pressure decreases with altitude. However, the pressure will not be given by a simple relationship such as $\rho g d$ (where $d$ is the depth) because the density varies with altitude. We need to return to equation 2.5 and find the solution from first principles.

That is,

$$\frac{dp}{dz} = -\rho g \tag{2.7}$$

The variation of temperature, density and pressure with altitude is usually described in terms of a Standard Atmosphere (see Tables Appendix-C.5, C.6, and Figure 13.1). For the first $10,000\,m$, the temperature variation is almost linear, and it is closely approximated by

$$T = T_0 + m\,(z - z_0)$$

From Table Appendix-C.5, we see that with $T_0 = 288.2°K$ $(= 15.0°C)$ and $z_0 = 0$, $m = -0.0065°K/m$. From the hydrostatic equation (equation 2.7) and the ideal gas law (equation 1.3),

$$\frac{dp}{dz} = -\frac{p}{RT}\,g$$

That is, with $z_0 = 0$,

$$\frac{dp}{p} = -g\,\frac{dz}{RT} = -\frac{g}{mR}\left(\frac{m\,dz}{T_0 + mz}\right)$$

By integration

$$\ln\left(\frac{p}{p_0}\right) = -\frac{g}{mR}\ln\left(\frac{T_0 + mz}{T_0}\right)$$

That is, the pressure in the first $10,000\,m$ of the Standard Atmosphere varies with altitude according to

$$\frac{p}{p_0} = \left(\frac{T_0 + mz}{T_0}\right)^{-g/mR}$$

At an altitude of $1000\,m$, for example, the the pressure decreases by about $11\%$.

In Chapter 13, we will see that the actual variation of temperature with altitude in the atmosphere at a given location is a strong function of the local weather conditions (see, for example, Figure 13.6, and the Standard Atmosphere represents a longterm average taken over many seasons.

### 2.4.2 Density variation in the ocean

What about the variation of density with depth in the ocean? We saw earlier that water is slightly compressible, and that this leads to a small increase in density with increasing depth. The density varies almost linearly with pressure, and the coefficient is given by the bulk modulus $K$. With $z$ measured from the surface downward, and substituting for $dp$ using equation 1.2, we obtain the pressure gradient in the ocean in terms of the density gradient. That is,

$$\frac{dp}{dz} = \frac{K}{\rho}\frac{d\rho}{dz} = \rho g$$

That is,

$$\frac{d\rho}{dz} = \frac{g}{K}\rho^2$$

so that

$$\frac{d\rho}{\rho^2} = \frac{g}{K}dz$$

If we assume that $K$ remains constant,

$$\rho = \frac{\rho_0}{1 - \frac{\rho_0 g z}{K}}$$

where $\rho_0$ is the density at the point where $z = 0$. Seawater has a bulk modulus of $K = 2.34 \times 10^9\,Pa$ at $20°C$ (see Table Appendix-C.11). If we neglect the variation of $K$ with temperature, then at a depth of $1000\,m$ the density of seawater is different from its value at the surface by about 0.5%.

### 2.4.3 Manometers

Manometers are used to measure pressure differences. A simple manometer can be made using a U-shaped tube, filled to some depth with a liquid (Figure 2.4). Water is easy, but many manometers use alcohol to prevent the growth of algea or bacteria. Alcohol can also be easily dyed to make it clearly visible. The two sides of the manometer are connected by tubes to the points of interest, which may, for example, be located on the upper and lower surfaces of the wing on an airplane. In that case, since the lift generated by the wing supports the weight of the airplane, we expect the pressure on the bottom surface of the wing, $p_1$, to be greater than the pressure on the top surface, $p_2$. Using the hydrostatic equation for a constant density fluid (equation 2.6), we obtain

$$p_1 - p_2 = \rho_m g(z_2 - z_1)$$

where $\rho_m$ is the density of the manometer fluid. That is,

$$p_1 - p_2 = \rho_m g \Delta h$$

Therefore we can find the pressure difference $p_1 - p_2$ by measuring the deflection of the manometer fluid, $\Delta h$.

In deriving this result, we assumed that the pressures at points A and B are equal. This assumption is perfectly correct, since the pressure in a fluid under the action of gravity alone does not vary in the horizontal plane. In other words, any horizontal line is an *isobar*, which is a line connecting points of equal pressure. This is a general principle, as long as the path from A to B can be drawn within the same liquid. Points A and B are then called *simply connected*. If, for example, there was a slug of different fluid (an air pocket, perhaps) along the path between A and B, they are no longer simply connected, and the pressures at A and B would be different. For the manometer shown in Figure 2.5, $p_1 = p_6 = p_a$ and
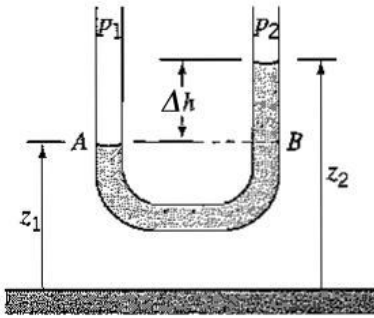
Figure 2.4: A simple U-tube manometer.
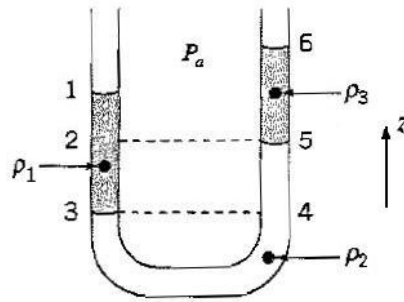


Figure 2.5: A U-tube manometer with multiple manometer fluids, open to atmospheric pressure.

$p_3 = p_4$, but $p_2 \neq p_5$. A manometer problem similar to this one is worked out in detail in Example 2.2.

When a pressure is transmitted to a manometer through a tube, it is important to wait long enough for the pressure to be felt fully by the manometer, and this will take longer for smaller diameter tubes. Again, this occurs because pressure disturbances travel slowly along tubes of small diameter since they reflect and refract off the walls of the tube. If we wait long enough, however, the full pressure will always be felt at the manometer, because of the transmissibility of pressure in a fluid (see Section 1.4.4).

### 2.4.4   Barometers

Barometers are devices that measure the atmospheric pressure relative to a complete vacuum. In a complete vacuum, the absolute pressure is zero, so that barometers measure the absolute atmospheric pressure, $p_a$.

A mercury barometer consists of a vertical tube that contains mercury. One end is in contact with a vacuum where the absolute pressure is zero, and the other end is exposed to atmospheric pressure. A simple way to make a mercury barometer is to take a glass tube about $1\,m$ long, close it at one end and fill it with mercury. Invert the tube and put the open end below the surface of a pool of mercury in a bowl. This will create a near vacuum in a small space at the closed end of the tube. The level of the mercury in the tube will settle at a height of about $760\,mm$ ($30\,in.$) above the level of the mercury in the bowl (see Figure 2.6). This is exactly what the Italian scientist Evangalista Torricelli did in 1643. He explained this observation by saying that the atmosphere must be exerting a pressure on the free surface of the mercury and that this pressure must be equal to that exerted by the mercury column. For the barometer shown in Figure 2.6, with the very good approximation that $p_2 = 0$,

$$p_a = \rho g \Delta h = \text{absolute pressure}$$

One of the units of pressure, the *torr*, is named in honor of Torricelli for his observations on the nature of pressure, and his contributions to the development of barometers to measure atmospheric pressure.

When the barometer fluid is mercury, $\Delta h \approx 760\,mm$ ($30\,in.$), and when it is water, $\Delta h \approx 10\,m$ ($34\,ft$). It is possible, therefore, to express atmospheric pressure in terms of an equivalent height of a column of fluid. This is common practice for all kinds of pressures, so we can talk about a pump developing a *head* of 60 feet of water, which is just a way of saying that it develops a pressure equal to that found at the bottom of 60 feet of water,
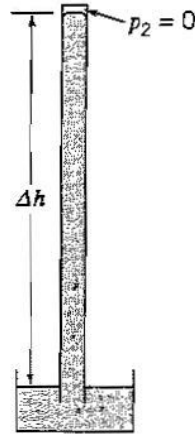
Figure 2.6: Mercury barometer as devised by Torricelli.
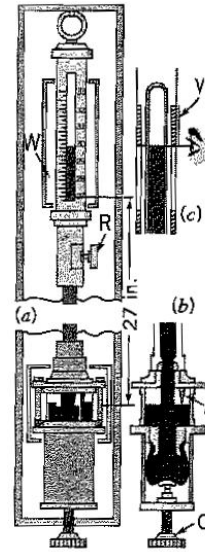


Figure 2.7: Fortin barometer. From Martin and Conner, *Basic Physics*, 8th ed., published by Whitcombe & Tombs Pty. Ltd., Melbourne, Australia, 1962, with permission.

that is, a pressure of about 1.8 atmospheres, or $26 \, psi$. More exact equivalences are given in Table 2.1.

The type of mercury barometer most widely used in fluid mechanics laboratories is called a Fortin barometer (see Figure 2.7). The scale is fixed and the level of the mercury in the bowl is adjustable. Before making the reading, the free mercury surface is brought to the scale zero by turning the knob $C$ until the free surface just touches the tip of the pointer $A$. The vernier scale $V$ is then moved up and down by means of a rack and pinion $R$, until the top of the mercury column and the lower front and back edges are seen in the same straight line [Figure 2.7(c)]. A white surface $W$ behind the tube helps to make this adjustment. The reading needs to be adjusted for ambient temperature since the length of the mercury

$$
\begin{array}{rcl}
1 \, \text{atmosphere} & = & 101,325 \, N/m^2 \quad (= Pa) \\
& = & 1.01325 \, bar \\
& = & 14.70 \, psi \quad (= lb_f/in^2) \\
& = & 2,116 \, psf \quad (= lb_f/ft^2) \\
& = & 29.92 \, in. \, Hg \\
& = & 760.0 \, mm \, Hg \\
& = & 760.0 \, torr \\
& = & 10.33 \, m \, H_2O \\
& = & 33.90 \, ft \, H_2O
\end{array}
$$

Table 2.1: Common equivalent units for atmospheric pressure.
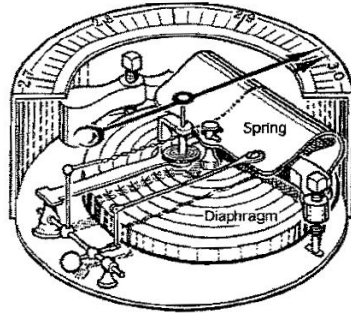
Figure 2.8: Aneroid barometer.

column and the length of the scale both increase with temperature. Also, moist air is less dense than dry air at the same temperature and pressure, since the molecular weight of water is less than that of air (18 compared to 28.96), and so the barometer reading decreases as the moisture of the atmosphere increases.

Another type of barometer is the aneroid barometer, which consists of an evacuated metal box (Figure 2.8). The air pressure acting on the outside of the box causes the box to deform, and this deformation is amplified by a series of levers and springs to move a pointer over a graduated scale.

The height of the mercury column, or the reading of the aneroid barometer, will vary with altitude, since the atmospheric pressure decreases with height. If it is known how the pressure varies with altitude, this property can be used to find the height above sea level. A modified aneroid barometer is commonly used as an airplane altimeter.

## 2.5   Vertical Walls of Constant Width

So far, we have used the hydrostatic equation to find the variation with pressure due to height. We will now consider the forces exerted by pressure differences on the walls of a container.

Pressure is an isotropic stress. That is, at a given point in the fluid, the pressure that acts on a vertical surface passing through the point has the same value as it has on a horizontal surface passing through the same point. In a container filled with water, the hydrostatic pressure acting on the bottom of the vessel is equal to the hydrostatic pressure acting on the side wall at the same depth. The pressure on the side wall increases with increasing depth according to the hydrostatic equation, and so the side wall feels a linearly varying pressure distribution.

Consider the vertical wall of a reservoir, with water of depth $h$ on one side (see Figure 2.9). A plot of the pressure as a function of depth is shown on the left. At the free surface, the pressure is atmospheric and below the surface, the pressure increases linearly with depth to a maximum value of $p_a + \rho g h$. What is the resultant force due to the water pressure acting over the area of the reservoir wall, and where does it act? That is, if we were to replace the distributed force due to pressure by a single resultant force, what is its magnitude and direction, and where must it be placed?

We begin by noting that air pressure acts everywhere, on the free surface as well as on the outside of the wall. The wall is of constant width, $W$ (into the page), and the $z$-direction is chosen to be positive in the direction of increasing altitude (that is, it is in the direction opposite to the gravitational force). The force acting on a local element of area on the vertical wall, $dA$, depends only on the depth, that is, the distance below the free surface, given here by $(h - z)$. In the case shown here, $dA = W\,dz$, so that the elemental area we
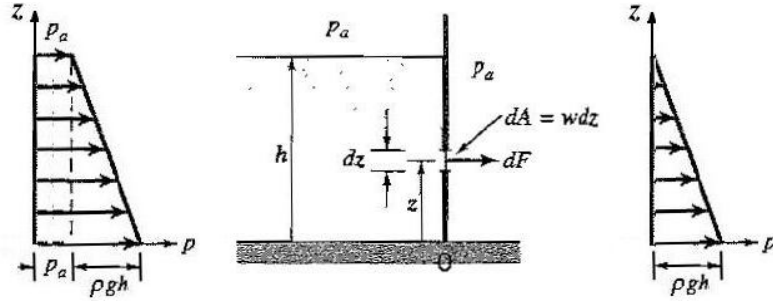
Figure 2.9: Vertical wall with water pressure acting on one side, atmospheric pressure on the other. The graph on the left shows the absolute pressure as a function of depth, and the graph on the right shows the gauge pressure as a function of depth.

consider is a strip of width $W$ and height $dz$.

## 2.5.1 Solution using absolute pressures

First, we use absolute pressures. From the hydrostatic equation (equation 2.5), the pressure at any depth is given by

$$p - p_a = \rho g(h - z)$$

(remember, the $z$-direction is positive going up). On the side of the wall where the water acts, the pressure $p$ acts on element $dA$ to produce a force $dF_x$ that acts to the right. So

$$dF_x = p\, dA = p\, dA = (p_a + \rho g(h - z))\ dA$$

On the other side of the wall, air pressure acts, and we will assume that this pressure is constant (see Section 2.3) so that the force due to air pressure acting on $dA$ is $p_g dA$. The resultant force, $dF$, acting on the area $dA$ is therefore given by

$$dF = dF_x - p_a\, dA$$

and it acts to the right. That is,

$$dF = (p_a + \rho g(h - z))\ dA - p_a\, dA = \rho g(h - z)W\, dz \tag{2.8}$$

where we have used $dA = W\, dz$. Integrating equation 2.8 from $z = 0$ to $z = h$ gives the resultant force

$$F = \int_0^h \rho g\,(h - z)W\, dz$$

so that

$$F = \tfrac{1}{2}\rho g W h^2 \tag{2.9}$$

## 2.5.2 Solution using gauge pressures

If instead we use gauge pressure $p_g$, where $p_g = p - p_a$, we can ignore the contributions made by the air pressure since it acts equally on both sides of the wall. Hence,

$$dF = p_g\, dA = \rho g(h - z)W\, dz \tag{2.10}$$

just as in equation 2.8. The force $F$ is then found by integration, yielding the same result as that given in equation 2.9.

### 2.5.3   Moment balance

Where should the resultant force $F$ be placed so that it exerts the same moment as the distributed force due to pressure? In order to take moments, we must specify the axis about which the moments are taken, and determine the lever arm or moment arm, which is the *perpendicular* distance to the line of action of the force. It is the minimum distance between the moment axis and the line of action of the force. A convenient place to take moments for the problem shown in Figure 2.9 is the axis passing through the point where $z = 0$. Any other axis will do fine, but this one happens to make the problem simpler. Let $M_0$ be the resultant moment about the axis through the origin due to the total force $F$ exerted on the wall by the water pressure, so that

$$M_0 = \bar{z} \times F$$

where $\bar{z}$ is the moment arm of $F$ about the axis, and where a clockwise moment is taken to be positive. We can find $M_0$ by considering the elemental moment $dM_0$ due to $dF$ about the moment axis. That is,

$$dM_0 \;=\; z \times dF \;=\; \rho g(h - z)zW\,dz$$

where we have substituted for $dF$ from either equation 2.8 or 2.10. Here, $z$ is the moment arm of the force $dF$ about the axis through $z = 0$. Integrating from $z = 0$ to $z = h$ gives the resultant moment

$$M_0 = \int_0^h \rho g(h - z)zW\,dz = \tfrac{1}{6}\rho gWh^3$$

By definition, the resultant force times its moment arm must be equal to the moment exerted by the force acting on the wall, so that

$$M_0 = \bar{z} \times F = \tfrac{1}{6}\rho gWh^3 = \tfrac{1}{3}h\left(\tfrac{1}{2}\rho gWh^2\right) = \tfrac{1}{3}h \times F$$

Hence,

$$\bar{z} = \tfrac{1}{3}h$$

When atmospheric pressure acts everywhere, therefore, the resultant force exerted by a fluid of depth $h$ acting on a vertical wall of constant width is given by

$$F = \tfrac{1}{2}\rho gWh^2 \tag{2.11}$$

and it acts a distance $\tfrac{1}{3}h$ from the bottom of the reservoir.

In finding the resultant force and moment in statics problems, there are many similarities with methods that are usually taught in mechanics of solids. The problem just considered is very similar to finding the resultant force acting on a cantilever beam under a distributed load, where the load per unit area of beam is $p$, varying from its minimum value of zero at $z = h$ to its maximum value of $\rho gh$ at $z = 0$ (compare Figures 2.9 and 2.10). The resultant force is given by the integral of the distributed force over the length of the beam. That is, it is given by the area of the triangle describing the load distribution. The point at which the force acts will be at the centroid of the triangle, which is one-third the distance from the point where the load is a maximum. In fluid statics, the point through which the resultant force acts is called the *center of pressure* (see also Section 2.9).

### 2.5.4   Gauge pressure or absolute pressure?

For the problem we just solved, air pressure acted on top of the water surface so that it added a constant pressure $p_a$ to the pressure at any point inside the water. Since we assumed that the atmospheric pressure was constant everywhere outside the reservoir, it also acts
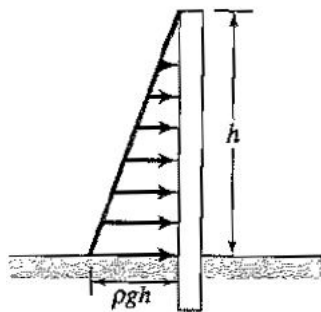
Figure 2.10: Cantilever under the action of a distributed load similar to that produced by hydrostatic pressure.
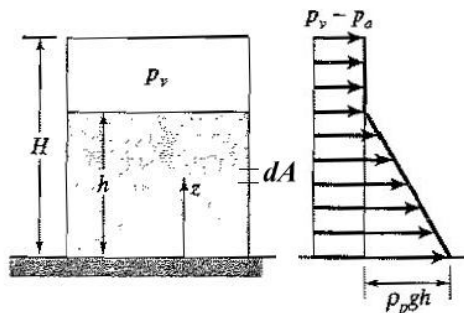
Figure 2.11: Closed propane container where the gaseous phase exerts a pressure on the liquid phase.

with the same value of $p_a$ at any position on the outside of the wall. Since air pressure acts on the inside and the outside of the wall with the same value, it cancels out. The only pressure that contributes to the resultant force is the "excess" pressure, that is, the gauge pressure. It is always a good idea to look at a problem before starting its solution to see if the ambient pressure by itself is going to add to the resultant force. If not, the problem can usually be made considerably simpler by using gauge pressure.

To give an example where this is not the best approach, consider the closed gas container shown in Figure 2.11, which is similar to the kind of propane container used in a gas grill. Here, the container happens to have a square cross-section with dimensions $W \times W$, and a height $H$. The liquid propane fills the container to a depth $h$. The rest of the container is filled with propane vapor at a pressure $p_v$, equal to its vapor pressure at the ambient temperature. Since the density of the gaseous phase of propane is much less than the density of the liquid phase (this is true for any fluid not near its critical point), the vapor pressure can be taken to be constant throughout the container. Similarly, air pressure acts with a constant value $p_a$ everywhere outside the gas container. What is the resultant force due to all the pressures acting on a side wall of the container and where does it act?

In problems like this, it is best to use absolute pressures. Consider the pressure acting on a small element of area $dA$ on the right side wall. On the inside of the container we have a pressure $p_v + p_\ell$ acting on $dA$, where $p_\ell$ is the pressure in the liquid, and on the outside of the container we have a pressure $p_a$. Hence

$$dF = (p_v + p_\ell - p_a)\, dA$$

The pressures $p_a$ and $p_v$ are constant, but $p_\ell$ varies with depth according to the hydrostatic equation. This allows us to split up the problem into two parts, starting with the pressures that are constant; $p_v$ and $p_a$. The resultant force due to these pressures is simply $(p_v - p_a)\, WH$, acting to the right. Within the liquid, the pressure $p_\ell$ varies according to its depth $p_\ell = \rho_p g(h - z)$ (where $\rho_p$ is the density of the liquid propane). From our earlier work, we know this gives rise to a resultant force $\frac{1}{2}\rho_p g W h^2$, acting to the right. So for the right side wall, the total resultant force $F$ acting to the right due to all the fluid pressures is

$$F = (p_v - p_a)\, WH + \tfrac{1}{2}\rho_p g W h^2$$

To find out where this resultant force acts, we can again split up the problem into two parts. The resultant force due to the constant pressures $p_v$ and $p_a$ will act at $z = H/2$, for the same reason the resultant force on a beam due to a constant distributed load acts at

the center of the beam. We found earlier that the resultant force due to the liquid acts at a distance $\frac{1}{3}h$ from the bottom. When we take moments about the axis through the point $z = 0$, we have

$$\bar{z} \times F = \tfrac{1}{2}H \times (p_v - p_a)\,WH + \tfrac{1}{3}h \times \tfrac{1}{2}\rho_p gWh^2$$

which can then be solved for $\bar{z}$ because we have already found $F$.

## 2.6    Sloping Walls of Constant Width

What happens when the wall is sloping? Consider a straight wall of constant width $W$ leaning over at an angle of $\theta$ to the horizontal (Figure 2.12). The pressure acts in a direction normal to the surface, so that the resultant force due to water pressure will now have a horizontal and a vertical component ($F_x$ and $F_z$, respectively). What is the magnitude of the resultant force $F$, and where does it act? Atmospheric pressure is taken to act everywhere.

We will solve this problem in two different ways. We begin by finding $F_x$ and $F_z$ separately, and obtain the resultant force using $F = \sqrt{F_x^2 + F_z^2}$. We will then find $F$ directly, without first finding $F_x$ and $F_z$.

### 2.6.1    Horizontal force

Since atmospheric pressure acts everywhere, we can use gauge pressure, $p_g$. Then, at any depth below the surface,

$$p_g = \rho g(h - z)$$

This pressure acts normal to the wall, so that the force $dF$ on the element $dA$ is given by

$$dF = p_g\,dA$$

Here, $dA = W\,ds$, where $s$ is the coordinate along the direction of the wall, measured from the origin, where $s = 0$ and $z = 0$. From the geometry, we have

$$z = s\sin\theta$$

and

$$dz = ds\sin\theta$$
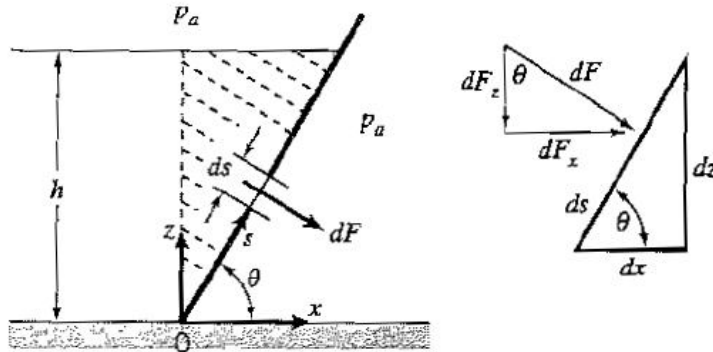


Figure 2.12:  Pressure acting on a sloping wall of constant width.

The horizontal component of the force acting on $dA$ is then given by

$$
\begin{aligned}
dF_x &= dF \sin\theta = p_g \, dA \sin\theta \\
&= p_g W \, ds \, \sin\theta \\
&= p_g W \frac{dz}{\sin\theta} \sin\theta
\end{aligned}
$$

That is,

$$
dF_x = p_g W \, dz = \rho g \, (h-z) \, W \, dz
$$

and by integration,

$$
F_x = \rho g \int_0^h (h-z) \, W \, dz = \tfrac{1}{2}\rho g W h^2 \tag{2.12}
$$

This is the same result found for a vertical wall (equation 2.8), and we note that the horizontal component of the force due to hydrostatic pressure on an inclined wall of constant width is equal to that on a vertical wall at the same depth. As we shall see in Section 2.7, this is a result that also applies to any wall of constant width, including curved walls.

### 2.6.2 Vertical force

Consider now the vertical component of the force acting on $dA$. This is given by

$$
\begin{aligned}
dF_z &= dF \cos\theta = p_g \, dA \cos\theta \\
&= p_g W \, ds \, \cos\theta \\
&= p_g W \frac{dz}{\sin\theta} \cos\theta = \rho g \, (h-z) \, W \frac{dz}{\tan\theta}
\end{aligned}
$$

By integration

$$
F_z = \rho g \int_0^h (h-z) \, W \, \frac{dz}{\tan\theta} = \frac{\rho g W h^2}{2\tan\theta} \tag{2.13}
$$

which acts downwards if $\theta$ is positive.

If instead we consider the weight of the fluid "supported" by the wall (the hatched area in Figure 2.12), we obtain

$$
\text{weight of fluid} = \frac{1}{2}\left(\rho g W h\right) \times \frac{h}{\tan\theta} = F_z
$$

as we might expect.

### 2.6.3 Resultant force

The resultant force is given by

$$
F = \sqrt{F_z^2 + F_x^2}
$$

Using the results given in Equations 2.12 and 2.13, we obtain

$$
F = \frac{\rho g W h^2}{2\sin\theta} \tag{2.14}
$$

We can arrive at the same result by considering the force $dF$ directly, rather than first finding the horizontal and vertical components. Here we use the $s$-coordinate system rather than the $[x,y]$ system. Then,

$$
dF = p_g \, dA = \rho g \, (h-z) \, W \, ds = \rho g \, (h-z) \, W \frac{dz}{\sin\theta} \tag{2.15}
$$

By integration

$$F = \int_0^h -\rho g\,(z-h)\,W\,\frac{dz}{\sin\theta} \;\; = \;\; \frac{\rho gWh^2}{2\sin\theta} \tag{2.16}$$

as in equation 2.14.

### 2.6.4   Moment balance

To find where this resultant force acts we need to take moments. Let $M_0$ be the resultant moment about the axis through the origin (see Figure 2.12) due to the force exerted by the water pressure, so that

$$M_0 = \bar{s} \times F$$

where $\bar{s}$ is the moment arm of $F$ about the axis, and where a clockwise moment is taken to be positive. We can find $M_0$ by considering the elemental moment $dM_0$ due to $dF$ about the moment axis. That is,

$$dM_0 \;\; = \;\; s \times dF \;\; = \;\; \rho g(h-z)sW\,ds$$

where we have used the result for $dF$ from equation 2.15. Integration gives

$$M_0 \;\; = \;\; \int \rho gW(h-z)s\,ds$$

With $z = s\sin\theta$, and $dz = ds\sin\theta$

$$\bar{s} \times F \;\; = \;\; M_0 \;\; = \;\; \int_0^h \rho gW(h-z)\frac{z}{\sin\theta}\frac{dz}{\sin\theta}$$

$$= \;\; \frac{\rho gW}{\sin^2\theta}\left[\frac{z^2 h}{2} - \frac{z^3}{3}\right]_0^h \;\; = \;\; \frac{\rho gWh^3}{6\sin^2\theta}$$

By using the result for $F$ given in equation 2.16, we obtain

$$\bar{s} = \frac{h}{3\sin\theta}$$

We can check the solution by examining its behavior "in the limit." For example, if $\theta \to \pi/2$, the wall becomes vertical and we find $\bar{s} = \frac{1}{3}h$, as we expect.

## 2.7   Hydrostatic Forces on Curved Surfaces

So far we have considered only plane surfaces. In many cases, the surfaces are curved. For example when building a dam, the bottom of the dam needs to be stronger than the top because the pressure increases with depth. To achieve this with minimum material, the thickness of the dam must increase with depth, so that the strength of the dam matches the increasing force and moments due to pressure.

To see how the hydrostatic forces and moments acting on curved surfaces can be found, consider the parabolic wall shown in Figure 2.13. Atmospheric pressure acts everywhere. We will find the resultant force acting on the wall, and its point of action.
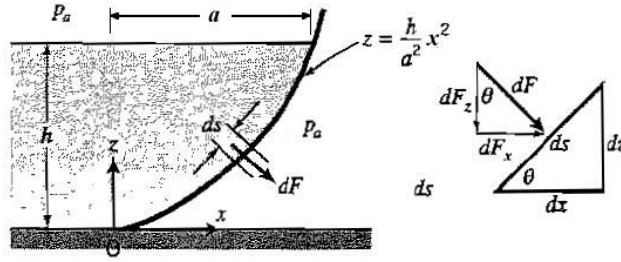
Figure 2.13: Pressure acting on a parabolic wall of constant width.

## 2.7.1 Resultant force

We begin by defining a coordinate system so that the shape of the wall can be expressed as simply as possible. For the system shown, the equation describing the shape of the wall is $z = \frac{h}{a^2}x^2$, where $a$ is the extent of the wall in the $x$-direction. Let $dF$ be the net force due to the water pressure acting on the element $dA$, and $dA = W\,ds$, where the coordinate $s$ is measured along the surface of the wall and $W$ is the width of the wall. Then, using gauge pressure,

$$dF = p_g\,dA = \rho g(h - z)W\,ds$$

For curved walls it is probably simpler to find the horizontal and vertical components of the resultant force separately, starting with the horizontal component $F_x$. Now

$$dF_x = dF \sin\theta = \rho g(h - z)W\,ds\,\sin\theta$$

Since

$$z = s \sin\theta \quad \text{and} \quad dz = ds \sin\theta$$

we have

$$dF_x = \rho g(h - z)W\,dz$$

By integration

$$F_x = \rho g \int_0^h (h - z)W\,dz = \tfrac{1}{2}\rho g W h^2$$

This is the same result found for the horizontal force acting on an inclined wall (see Section 2.6). It is, in fact a general result.

> The horizontal component of the force due to hydrostatic pressure on a wall of constant width is independent of its slope and it is equal to that on a vertical wall at the same depth.

Now we find the vertical component of the resultant force, $F_z$. Following the same approach as we did in finding $dF_x$, we have

$$dF_z = dF \cos\theta = p_g\,dA \cos\theta = \rho g(h - z)W\,ds\,\cos\theta$$

Since

$$x = s \cos\theta \quad \text{and} \quad dx = ds \cos\theta$$

we have

$$dF_z = \rho g(h - z)W\,dx$$

By integration:

$$F_z = \rho g W \int_0^a \left( h - \frac{h}{a^2} x^2 \right) dx = \rho g W \left[ hx - \frac{hx^3}{3a^2} \right]_0^a = \tfrac{2}{3} \rho g W h a$$

We can also show that this vertical force is equal to the weight of fluid supported by the wall (see Section 2.10).

The total force may be found by vector addition. That is,

$$F = \sqrt{F_x^2 + F_z^2} = \tfrac{1}{2} \rho g W h^2 \sqrt{\left( 1 + \frac{16a^2}{9h^2} \right)} \tag{2.17}$$

We could also try to find this resultant force directly by using

$$dF = \rho g (h - z) W \, ds$$
$$\text{and} \qquad F = \int_0^h \rho g (h - z) W \, \frac{dz}{\sin \theta}$$

For a curved wall, $\theta$ varies with depth. Therefore, we need to substitute for $\sin \theta$ in the expression for $dF$. Using trigonometry, we obtain

$$\frac{dz}{\sin \theta} = \sqrt{(dx)^2 + (dz)^2} = dx \sqrt{1 + \left( \frac{dz}{dx} \right)^2} = dx \sqrt{1 + \frac{4h^2}{a^4} x^2}$$

Therefore

$$F = \rho g W \int_0^a \left( h - \frac{h}{a^2} x^2 \right) \sqrt{1 + \frac{4h^2}{a^4} x^2} \, dx$$

Clearly, this integration is not straightforward, and although we can show that it gives the same result as given by equation 2.17, we will not proceed further. If it is possible to get the resultant force directly, it can save some effort, but in most curved-wall cases it is easier to deal with the two components of the resultant force separately.

## 2.7.2   Line of action

To find where the resultant force acts, we take moments for each force component in turn. First, we take moments of horizontal force components about the $y$-axis, which is the line passing through the origin of the coordinate system pointing into the page. The moment arm for $F_x$ is $\bar{z}$, so that

$$\bar{z} \times F_x = \rho g W \int_0^h z(h - z) \, dz$$

and we can show that

$$\bar{z} = \tfrac{1}{3} h$$

We could have anticipated this result from our earlier analysis; the horizontal component of the resultant force on a plane wall of constant width acts at a point one-third from the bottom of the wall, regardless of the inclination of the wall.

Next, we take moments of the vertical force component about the $y$-axis. The moment arm for $F_z$ is $\bar{x}$, so that

$$\bar{x} \times F_z = \rho g W \int_0^a (h - z) x \, dx = \rho g W \int_0^a \left( h - h \frac{x^2}{a^2} \right) x \, dx$$

and we find that

$$\bar{x} = \tfrac{3}{8} a$$

This also happens to be the line passing through the centroid of the volume of water supported by the parabolic wall. We obtained a similar conclusion for a plane, inclined wall. In fact, this is a general result.

> The vertical component of the resultant force on any surface acts at the centroid of the volume of fluid it supports (usually called the *displaced* volume), regardless of the shape of the wall.

This observation will be considered further in Section 2.10.

## 2.8 Two-Dimensional Surfaces

The next level of complexity in hydrostatic problems is the case where the surface is flat, but it has a width that varies. The surface is two-dimensional, and the force acting on a two-dimensional surface depends on its depth and its width. An example using a triangular plate is given in Figure 2.14 where a side view and a plan view are shown. The plate is symmetrical, with a height $\ell$ and a base width $2a$. Its apex is located a depth $L \sin \theta$ below the surface of the water. The surface of the water, and the outer face of the plate, are open to the atmosphere, so that we can use gauge pressure. What is the resultant force due to the water pressure, and where does it act?

We begin by defining a coordinate system. A good choice is to put the origin $O$ at the apex, so that the $y$-coordinate lies along the centerline of the plate, pointing towards the base. Next, we mark an element of area $dA$ on the surface of the plate, where $dA = dx\,dy$. The depth of the element $dA$ is $(y + L) \sin \theta$, and therefore the gauge pressure acting on $dA$ is $p_g = \rho g(y + L) \sin \theta$, and the force acting on $dA$ is

$$dF = p_g\, dA = \rho g(y + L) \sin \theta\, dA = \rho g(y + L) \sin \theta\, dx\, dy$$

so that

$$F = \iint \rho g(y + L) \sin \theta \ dx\, dy$$

This is a double integral, with one integration in $x$ and one in $y$. We can choose which one to do first, and since the pressure depends only on depth, that is, it depends only on $y$ and not on $x$, it is probably better to perform the $x$ integration first. We can write this as

$$F = \int \rho g(y + L) \sin \theta \left( \int dx \right) dy$$

The $x$-integration is done at a constant $y$, so that the limits of integration must go from one side of the plate to the other side, at a given $y$. The $x$-value on the positive edge of the plate is $ay/\ell$, and on the negative edge it is $-ay/\ell$. The $x$-integration expands the original square element $dA$ into a strip of width $dy$ and length $2ay/\ell$. The subsequent $y$-integration expands this strip into the whole area of the plate, so that the limits on $y$ are 0 and $\ell$. That is,

$$
\begin{aligned}
F &= \int_0^\ell \rho g(y + L) \sin \theta \left( \int_{\frac{-ay}{\ell}}^{\frac{ay}{\ell}} dx \right) dy \\[2mm]
&= \int_0^\ell \rho g(y + L) \sin \theta \left( \frac{2ay}{\ell} \right) dy \\[2mm]
F &= \rho g a \ell \left( L + \frac{2\ell}{3} \right) \sin \theta
\end{aligned}
\tag{2.18}
$$
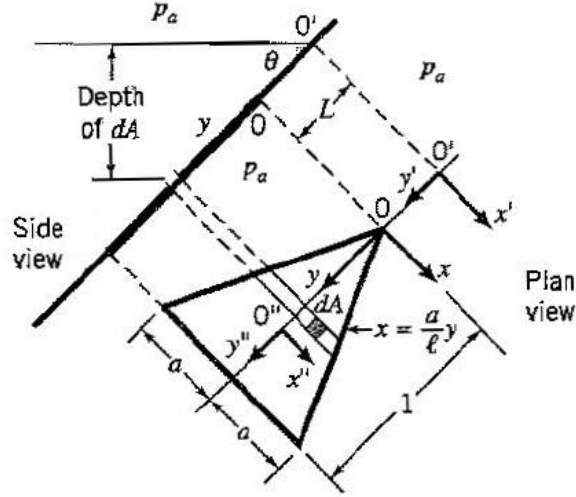
Figure 2.14: Triangular plate, with water pressure on one side, and air pressure on the other. Side and plan views.

Completing the $y$-integration gives

$$F = \rho g a \ell \left( L + \frac{2\ell}{3} \right) \sin \theta \tag{2.19}$$

To find the point of action of $F$ we need to take moments. The area is symmetrical and therefore the point of action lies somewhere along the $y$-axis. To find exactly where, we will take moments about the $x$-axis. The moment arm of the force $dF$ about the $x$-axis is given by $y$, so that $dM_O$, the moment of $dF$ about the $x$-axis, is given by:

$$dM_O = y \times dF = \rho g \left( y + L \right) \sin \theta \, y \, dA$$

The total moment $M_O$ can be found by integration. Since $M_O$ is also given by the resultant force $F$ multiplied by its moment arm $\bar{y}$ about the $x$-axis

$$M_O = F \times \bar{y} = \rho g \sin \theta \iint (y + L) y \, dx \, dy$$

Using equation 2.19, we obtain

$$\bar{y} \;=\; \frac{1}{a\ell \left( L + \frac{2\ell}{3} \right)} \int_0^\ell y(y + L) \left( \int_{\frac{-ay}{\ell}}^{\frac{ay}{\ell}} dx \right) dy$$

and so

$$\bar{y} \;=\; \frac{2\ell}{3} \left( \frac{L + \frac{3\ell}{4}}{L + \frac{2\ell}{3}} \right) \tag{2.20}$$

To demonstrate the consequences of choosing a different moment axis, we choose the moment axis through the point $O'$, where $O'$ is located at the point where the $y$-axis intersects the water surface (see Figure 2.14). We still measure $y$ and $\bar{y}$ from the point $O$. Then:

$$dM_{O'} = (y + L) \times dF = \rho g \sin \theta (y + L)^2 \, dA$$

Hence

$$M_{O'} = (\bar{y} + L) \times F = \rho g \sin\theta \iint (y + L)^2 \, dx \, dy$$

and so

$$\bar{y} + L = \frac{1}{a\ell\left(L + \frac{2\ell}{3}\right)} \int_0^l (y + L)^2 \left(\frac{2ay}{\ell}\right) dy$$

$$= \frac{1}{6\left(L + \frac{2\ell}{3}\right)} \left(3\ell^2 + 8\ell L + 6L^2\right)$$

Hence,

$$\bar{y} = \frac{1}{6\left(L + \frac{2\ell}{3}\right)} \left(3\ell^2 + 8\ell L + 6L^2 - 6L^2 - 4\ell L\right)$$

and

$$\bar{y} = \frac{2\ell}{3} \left(\frac{L + \frac{3\ell}{4}}{L + \frac{2\ell}{3}}\right) \tag{2.21}$$

We obtain the same answer as before (see equation 2.20), but the calculations were more complicated. It is always a good idea to think carefully before choosing the coordinate system for a particular problem. The "right" choice will help to reduce the overall algebraic complexity and the likelihood of making a mistake.

## 2.9   Centers of Pressure, Moments of Area

There are other ways to find these forces and moments. One way that is popular in many textbooks is to note that hydrostatics has a lot in common with the mechanics of solids. In particular, for the problem with the triangular plate (Figure 2.14), we know that the centroid of the triangle is located at a depth $\left(L + \frac{2\ell}{3}\right)\sin\theta$ below the water surface. The gauge pressure at this point is $\rho g \left(L + \frac{2\ell}{3}\right)\sin\theta$, so that from the result given in equation 2.20 we can see that the resultant force acting on the triangular plate is equal to the pressure at the centroid, $p_c$, times the area of the plate ($a\ell = A$). That is,

$$F = p_c A \tag{2.22}$$

This is a general result for flat surfaces of any shape. However, this observation is only useful if we know where the centroid is located.

Another interesting result can be obtained by considering the sum of the moments. If we choose a new coordinate system $[x', y']$ located at the point $O'$ (see Figure 2.14), and we measure the moment arm $\bar{y}'$ from the $x'$-axis, then, taking moments about the $x'$-axis

$$dM_{O'} = y \times dF = y' \left(\rho g \sin\theta \, y'\right) dA$$

That is

$$M_{O'} = \bar{y}' \times F = \rho g \sin\theta \int y'^2 \, dA = \rho g \sin\theta \, I_{x'} \, dA$$

where $I_{x'} = \int y'^2 dA$. This integral can be recognized as the second moment of the area with respect to the $x'$-axis.

We can continue by adding another coordinate system $[x'', y'']$ with its origin located at the centroid of the triangular plate $O''$, located a distance $[x_c, y_c]$ from $O'$. Hence, $y' = y'' + y_c$, and

$$I_{x'} = \int y'^2 \, dA = \int \left(y''^2 + 2y_c y'' + y_c^2\right) dA = \int y''^2 \, dA + 2y_c \int y'' \, dA + y_c^2 \int dA$$

The integral $\int y'' dA$ is the first moment of area about an axis passing through the centroid, which is identically zero by the definition of a centroid. So

$$I_{x'} = \int y''^2 \, dA + y_c^2 \int dA = \int y''^2 \, dA + A y_c^2$$

or

$$I_{x'} = I_{xc} + A y_c^2$$

This is the *theorem of parallel axes*, where $I_{x'}$ is the second moment of area with respect to an arbitrary $x'$-axis, $I_{xc}$ is the second moment of area with respect to the $x''$-axis passing through the centroid, and $y_c$ is the distance between the $x'$-axis and the $x''$-axis. Finally,

$$\bar{y}' \times F = \rho g \, \sin\theta \, I_{x'}$$

so that

$$\bar{y}' = \frac{\rho g \sin\theta \, I_{x'}}{F} = \frac{\rho g \sin\theta \, I_{x'}}{p_c A} = \frac{\rho g \sin\theta \, I_{x'}}{\rho g y_c \sin\theta \, A}$$

That is

$$\bar{y}' = \frac{I_{x'}}{y_c A} = \frac{I_{xc} + A y_c^2}{y_c A} = \frac{I_{xc}}{y_c A} + y_c$$

Therefore, if the position of the centroid is known, and the moment of area about the centroid is known, the line of action can be found using

$$\bar{y}' = \frac{I_{xc}}{y_c A} + y_c \tag{2.23}$$

This result also shows that the line of action of the resultant force is always lower than the position of the centroid. To illustrate this point more physically, consider a simple rectangular plate oriented vertically. The pressure acting over the area increases with depth so that it has a higher value at greater depth, and therefore the resultant force will always act below the middle of the plate, that is, it acts below the centroid of the area.

Methods based on centroids and moments of area are one way to solve problems in hydrostatics. They require you to know the position of the centroid and the moment of inertia for the shape in question, and although many common shapes are tabulated in handbooks, irregular shapes still need to be evaluated from first principles. In addition, unless great care is taken, shifting axes to find moments of area about axes other than the standard ones is a process open to many errors. Finally, these approaches tend to obscure the basic physics underlying the problem. For all these reasons, we prefer to use methods based on the hydrostatic equation, as outlined in Section 2.8.

## 2.10   Archimedes' Principle

We saw in Sections 2.6 and 2.7 that the vertical force acting on a sloping wall or a curved wall was equal to the weight of the fluid supported by the wall, and that it acted through the centroid of the fluid volume. More can be done with this result.

Consider a V-shaped "boat" floating in water, where the weight of the boat is $mg$, and its length is $L$ (Figure 2.15). The lowest point of the boat is a distance $h$ below the surface of the water. The boat is in equilibrium, so that the resultant force acting on it is zero (the resultant moment must be zero also). The horizontal component of the force due to water pressure acting on the left half of the hull is equal and opposite to that acting on the right half, and so they cancel. As for the vertical forces, we know that the weight of the boat is
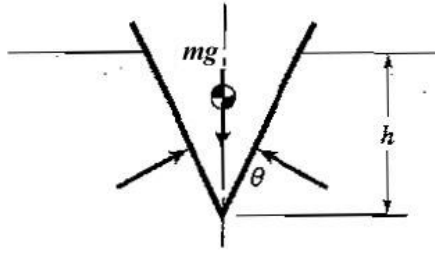
Figure 2.15: A V-shaped boat floating in water.

balanced by the sum of the vertical forces due to water pressure acting on the two halves of the hull. Using the result found in Section 2.6

$$mg = 2 \times \frac{\rho g L h^2}{2 \tan \theta} = \rho g \frac{L h^2}{\tan \theta}$$

Note that the volume of the displaced fluid is $Lh^2/\tan\theta$, and its weight is $\rho g L h^2/\tan\theta$. In other words, the weight of the boat is balanced by a *buoyancy* force equal to the weight of water displaced by the boat. Since there is no resultant moment (all moments cancel), the resultant force must act through the centroid of the displaced fluid, in line with the weight force. These observations can be written in a general way, known as Archimedes principle.

> The buoyancy force on an object is equal to the weight of fluid it has displaced, and it acts through the centroid of the displaced volume.

The centroid of the displaced fluid is also know as the *center of buoyancy*.

For a different example involving buoyancy forces, consider a barge floating in a small pond. The barge contains a number of steel bars, and therefore displaces a certain amount of water (the weight of the fluid displaced must equal the weight of the barge plus the weight of the steel bars). The maximum depth of the water is $h_1$ (Figure 2.16). An accident upsets the barge so that all the steel bars fall in the water, and since they have a greater density than water, they sink to the bottom. The maximum depth of the water is now $h_2$. How does $h_1$ compare to $h_2$? There are three possible answers: $h_1 > h_2$, $h_1 = h_2$ or $h_1 < h_2$. Which one is right?

Initially, the total weight of water displaced equals the weight of the barge plus the weight of the steel bars. Since the specific gravity of steel is 7.86, the volume of water displaced is 7.86 times the volume of steel. After the barge is upset and the steel bars have sunk to
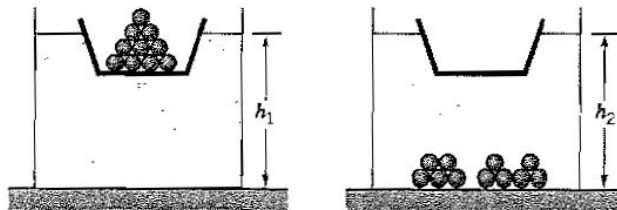


Figure 2.16: Floating barge, containing steel bars (left), and empty (right).
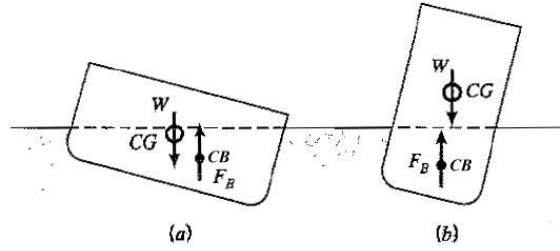
Figure 2.17: Stability of floating bodies. (a) Stable. (b) Unstable.

the bottom, the water displaced by the barge is such that the weight of the displaced water equals the weight of the barge. Water is also displaced by the steel bars, but since they are not floating they only displace a volume of water equal to the volume of the steel bars. This volume is much less than the volume displaced by the steel bars when they were floating, so the correct answer is $h_1 > h_2$.

## 2.11   Stability of Floating Bodies

Floating bodies are in equilibrium under the action of body forces (the weight of the vessel) and buoyancy forces (the weight of the displaced fluid). The lines of action of these forces determine the stability of the body (Figure 2.17).   The weight $W$ acts through the center of gravity of the body, $CG$, and the buoyancy force $F_B$ acts through the centroid of the displaced fluid volume, that is, the center of buoyancy $CB$. The body is *neutrally stable* if the lines of action are co-linear, and *stable* if they produce a moment which tends to right the vessel [Figure 2.17(a)]. It is *unstable* if the moment tends to capsize the vessel [Figure 2.17(b)].

## 2.12   Fluids in Rigid Body Motion

We noted earlier that a fluid in motion can be in static equilibrium as long as all parts of the fluid are moving together as a rigid body. In *rigid body motion*, there can be no relative motion within the liquid; no part of the fluid can be moving with respect to any other part. When the fluid and its container are moving at constant speed, such a system is in simple translation and there are no additional forces acting. However, when this system is accelerating, the inertia force due to the acceleration needs to be taken into account.

### 2.12.1   Vertical acceleration

Consider fluid in a container that is moving in the vertical direction with an acceleration $a_z$. The fluid is in rigid body motion. Newton's second law states that for an accelerating mass of fluid

$$\left\{ \begin{array}{c} \text{mass of fluid} \\ \times \text{ acceleration} \end{array} \right\} = \left\{ \begin{array}{c} \text{forces due to} \\ \text{pressure differences} \end{array} \right\} + \left\{ \begin{array}{c} \text{weight of} \\ \text{fluid} \end{array} \right\}$$

For a small particle of fluid of volume $dx\,dy\,dz$, where the positive $z$-direction is vertically up as in Figure 2.18,

$$(\rho\,dxdydz)\,a_z = \left( p_0 - \left.\frac{dp}{dz}\right|_0 \frac{dz}{2} \right) dxdy - \left( p_0 + \left.\frac{dp}{dz}\right|_0 \frac{dz}{2} \right) dxdy - (\rho\,dxdydz)\,g$$
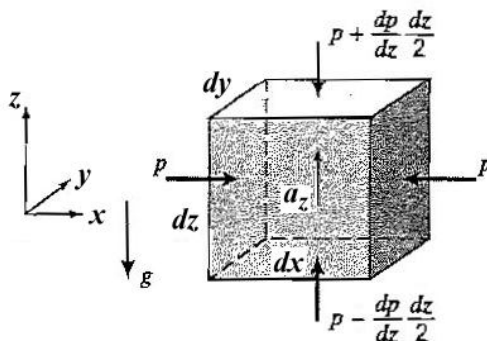
Figure 2.18: Static equilibrium of a fluid particle under the action of gravity and a constant vertical acceleration.

where we have used a first order Taylor series expansion (Section Appendix-A.10) to express the pressures on the top and bottom faces of the particle in terms of $p_0$, the pressure at the center. Collecting terms gives

$$\rho a_z = - \left. \frac{dp}{dz} \right|_0 - \rho g$$

We can drop the subscript 0 because the result should not depend on the particular point that was considered. Hence

$$\frac{dp}{dz} = -\rho \left( g + a_z \right) \tag{2.24}$$

This result is identical to the hydrostatic equation (equation 2.5) with the inclusion of the additional acceleration $a_z$ due to the motion of the container.

What happens when the container is falling freely under gravity? In this case, $a_z = -g$ since $z$ is positive going up, and the hydrostatic pressure variations in the container go to zero. This is true for all fluids in free fall. For example, a jet of water issuing from a tank will be in free fall under gravity, and there will be no hydrostatic pressure variations within the jet. When in space, where there is zero gravity because the spacecraft is essentially in free fall, the pressure in any fluid will be constant and the only thing keeping a fluid together in an open container is surface tension.

In contrast, when the container is accelerating upwards at the same rate, $a_z = +g$, and the pressure variations in the fluid increase above their static values. Astronauts accelerating into space at high "g-levels" need to lie at right angles to the acceleration vector so that the pressure differences across their bodies are minimized, and their hearts can cope with the extra load imposed by the increased pressure differences.

## 2.12.2 Vertical and horizontal accelerations

We now consider a container that experiences accelerations in both the horizontal and vertical directions, $a_x$ and $a_z$, respectively (Figure 2.19). The equation of motion in the $z$-direction is given by equation 2.24), so that

$$\frac{\partial p}{\partial z} = -\rho \left( g + a_z \right) \tag{2.25}$$

Partial derivatives are needed because the pressure is now a function of $x$ and $z$. Using a first order Taylor Series expansion, the equation of motion in the horizontal $x$-direction gives

$$\left( \rho \, dx dy dz \right) a_x = \left( p_0 - \left. \frac{dp}{dx} \right|_0 \frac{dx}{2} \right) dy dz - \left( p_0 + \left. \frac{dp}{dx} \right|_0 \frac{dx}{2} \right) dy dz$$
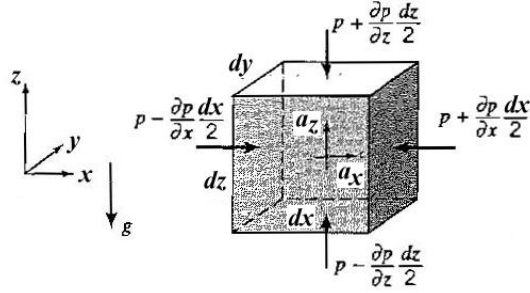
Figure 2.19: Static equilibrium of a fluid element under the action of gravity and constant vertical and horizontal accelerations.

Since the result is independent of the point chosen, we drop the subscript 0 and obtain

$$\frac{\partial p}{\partial x} = -\rho a_x \tag{2.26}$$

Equations 2.25 and 2.26 are a pair of first-order partial differential equations which can be solved as follows. Integrating equation 2.25 with respect to $z$ we obtain

$$p = -\rho\left(g + a_z\right)z + f(x) + C_1 \tag{2.27}$$

where $f(x)$ is an unknown function of $x$, and $C_1$ is a constant of integration. Integrating equation 2.26 with respect to $x$ we obtain

$$p = -\rho a_x x + g(z) + C_2 \tag{2.28}$$

where $g(z)$ is an unknown function of $z$ (only), and $C_2$ is another constant of integration. From equations 2.27 and 2.28 we see that

$$p = -\rho\left(g + a_z\right)z - \rho a_x x + C \tag{2.29}$$

(When solving simultaneous partial differential equations, it is always recommended to check that the original equations, in this case equations 2.25 and 2.26, are recovered by differentiating the solution.)

For a surface of constant pressure (an *isobaric* surface), the left hand side of equation 2.29 is constant. The slope of an isobaric surface can be found by differentiating this equation while holding $p$ constant. That is, the slope of an isobaric surface is given by

$$\frac{dz}{dx} = -\frac{a_x}{g + a_z} \tag{2.30}$$

At the free surface, the pressure is constant and equal to the atmospheric pressure, so that it is an isobaric surface. Hence, equation 2.30 gives the slope of the free surface. Because $a_x$ and $a_z$ are constant throughout the fluid, all isobaric surfaces have the same slope so that they are all parallel to the free surface.

### 2.12.3   Rigid body rotation

A similar analysis will apply to a volume of fluid that is rotating at a constant angular speed, as shown in Figure 2.20. In that case, an element of fluid experiences a radial acceleration $V^2/r$, where $V$ is the circumferential component of velocity, and $r$ is the distance from the axis of rotation. There is also an acceleration in the vertical direction due to gravity, so
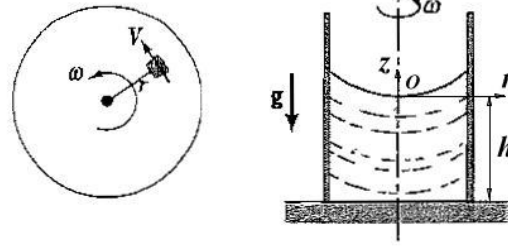
Figure 2.20: Fluid in rigid body motion under rotation.

that the pressure is a function of $r$ and $z$. If the rate of rotation is $\omega\ rad/s$, the equation of motion in the $r$-direction becomes

$$\frac{\partial p}{\partial r} = \rho\frac{V^2}{r} = \rho\omega^2 r \tag{2.31}$$

For the $z$-direction (where the positive $z$-direction is vertically up), we get the usual hydrostatic variation

$$\frac{\partial p}{\partial z} = -\rho g \tag{2.32}$$

Integrating equation 2.31 with respect to $r$ we obtain

$$p = \tfrac{1}{2}\rho\omega^2 r^2 + f'(z) + C_3 \tag{2.33}$$

and integrating equation 2.32 with respect to $z$ we obtain

$$p = -\rho g z + g'(x) + C_4 \tag{2.34}$$

From equations 2.33 and 2.34

$$p = -\rho g z + \tfrac{1}{2}\rho\omega^2 r^2 + C' \tag{2.35}$$

To find $C'$, we need to know the pressure at a given point. At the free surface, the pressure is equal to atmospheric pressure, so that $p = p_a$ at $r = 0$, $z = 0$, and

$$p - p_a = -\rho g z + \tfrac{1}{2}\rho\omega^2 r^2$$

so that

$$z = \frac{\omega^2 r^2}{2g} - \frac{p - p_a}{\rho g} \tag{2.36}$$

On the axis, where $r = 0$, the radial acceleration is zero, and the slope of the free surface is horizontal. Further from the axis of rotation, the surface is inclined to the horizontal, and we see that the free surface actually forms a parabola of revolution, as do all other isobaric surfaces (Figure 2.20). Question: For a cylindrical container, where is the maximum pressure found?

# Chapter 3

# Equations of Motion in Integral Form

Here, we consider the basic principles governing fluid motion: conservation of mass, momentum, and energy, as applied to large control volumes. This leads to the derivation of the general equations of motion expressed in integral form. Before doing so, we introduce the concepts of fluid particles and control volumes.

## 3.1   Fluid Particles and Control Volumes

Imagine what happens when a glass of water spills on the ground. The water spreads out in all directions, and parts of the water that were originally close together can end up in very different places. In other words, there exist relative motions among different parts of the fluid. How are we to describe the displacement, velocity and acceleration of all these parts? We can either use a *fluid particle*, or a *control volume* approach. In the fluid particle, or *Lagrangian* approach, we identify and follow small, fixed masses of fluid, as illustrated in Figure 3.1(a). The fluid making up the particle is always the same, no matter how much the particle deforms. As the particle moves through the duct, forces act on it and it may experience an acceleration so that its velocity changes. In the control volume, or *Eulerian* approach, we do not follow individual fluid particles. Instead, we draw an imaginary box around a fluid system. The box can be large or small, and it can be stationary or moving at a constant velocity. Generally, there will be flow in and out of the control volume through its surfaces, and the fluid inside the control volume is changing all the time, even if the boundary conditions are constant in time. [Figure 3.1(b)].
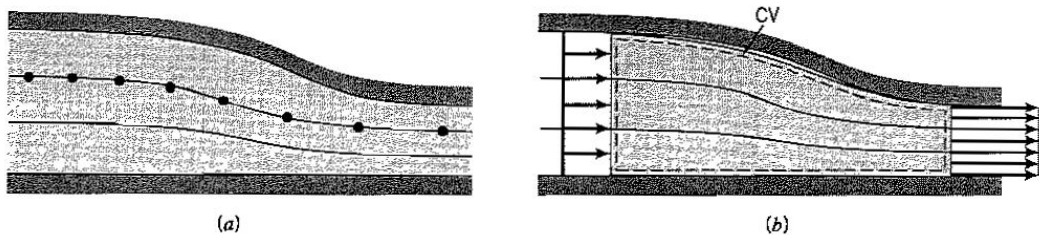


Figure 3.1: (a) Following a fluid particle in time; (b) Using a fixed control volume.

### 3.1.1   Lagrangian system

In the Lagrangian system we use *fluid particles*, which are small parts of the fluid of fixed mass. They are called particles in analogy with the dynamics of solid bodies. We follow an individual fluid particle as it moves through the flow, and the particle is identified by its position at some initial time and the time elapsed since that instant. Consider a velocity field described by

$$\mathbf{V} = u\mathbf{i} + v\mathbf{j} + w\mathbf{k}$$

where $\mathbf{i}$, $\mathbf{j}$ and $\mathbf{k}$ are the unit vectors in a Cartesian $[x, y, z]$ coordinate system, and $u$, $v$, and $w$ are the corresponding velocity components. In Lagrangian terms, then, the velocity of a fluid particle that was located at point $[x_0, y_0, z_0]$ at time $t = t_0$ is given by $\mathbf{V} = \partial \mathbf{x}/\partial t$, and its acceleration is given by $\partial \mathbf{V}/\partial t$.

This particle description is the one normally used in describing the dynamics of rigid bodies because the particles tend to be few in number and easily identified. To describe a fluid flow, however, we need to follow many fluid particles, and to resolve the smallest details of the flow we may need to follow a very large number of them. The motion of each particle can be described by a separate ordinary differential equation (ODE), such as Newton's second law, and each equation is coupled to all the others (that is, the solution of one equation depends on the solution of all others), because the motion of each particle will depend on the motion of all its neighboring particles. The solutions of these coupled ODE's are usually difficult to find because of their large number. The Lagrangian approach, therefore, is not widely used in fluid mechanics, except in some problems such as in tracking the dispersion of pollutants.

### 3.1.2   Eulerian system

In the Eulerian system we try to find a description which gives the details of the entire flow field at any position and time. Instead of describing the fluid motion in terms of the movement of individual particles, we look for a "field" description. In other words, we search for a description that gives the velocity and acceleration of any fluid particle at any point $[x, y, z]$ at any time $t$. For example, if we were given a Cartesian velocity field described by $\mathbf{V} = 2x^2\mathbf{i} - 3t\mathbf{j} + 4xy\mathbf{k}$, we would know its velocity at every point in the flow, at any time.

At first sight, this approach appears to be very straightforward. However, we are no longer explicitly following fluid particles of fixed mass; at a given point in the flow, new particles are arriving all the time. This makes it difficult to apply Newton's second law since it applies only to particles of fixed mass. We therefore need a relationship that gives the acceleration of a fluid particle in terms of the Eulerian system, and this proves to be somewhat complicated, as we shall see. Nevertheless, the Eulerian system is generally preferred for solving problems in fluid mechanics.

### 3.1.3   Small control volumes: fluid elements

In deriving the equations of motion, we often choose fixed, infinitesimally small control volumes. Such "fluid elements" are control volumes that are small enough so that the variations in fluid properties over its volume, such as density, temperature, velocity and stress, are approximately linear. That is, we need to take only the first two terms in a Taylor series expansion (see Section Appendix-A.10). Fluid elements are different from fluid particles, in that

> A fluid element has a fixed volume and it is fixed in space. A fluid particle has a fixed mass and moves with the flow.
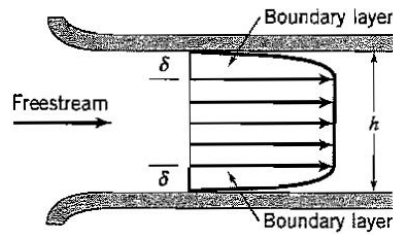
Figure 3.2: Flow in a duct, showing boundary layers near the walls.
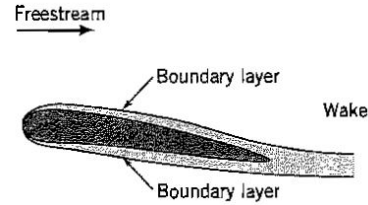
Figure 3.3: Flow over an airfoil, showing boundary layers near the surface, and the formation of a wake downstream of the airfoil.

There are upper and lower limits on the size of the element. The characteristic dimension of the element, $\ell$ (its height, width or length), should always be large compared to the mean free path $\ell_m$ so that the continuum approximation holds ($\ell \gg \ell_m$) (see Section 1.4). At the other end of the scale, $\ell$ should be small enough so that the changes in fluid velocity or pressure across the element can be found by linear interpolation. In other words, the fluid element needs to be small compared to the characteristic scale of the flow field. For example, if we have a duct of height $h$, then we should certainly make sure that $\ell \ll h$. In addition, near solid walls, thin boundary layers can form. To be able to say something about the flow inside the boundary layer, we need $\ell \ll \delta$, where $\delta$ is a measure of the boundary layer thickness (see Figures 3.2 and 3.3).

### 3.1.4 Large control volumes

Instead of using a small fluid element as a control volume, we can choose a large control volume that encloses the entire flow [for instance, the flow inside the duct shown in Figure 3.1(b)]. Whatever their size, control volumes allow us to think in terms of overall balances of mass, momentum and energy. For example, mass must be conserved in any fluid flow. That is, we need to account for all the mass of fluid entering and leaving the control volume, as well as the rate of change of the amount of mass contained inside the volume. A piping system, for instance, will have a number of places where fluid enters, and a number of other places where fluid exits. If the amount of mass entering over a given time exceeds the amount of mass leaving during the same time, we know that mass must be accumulating somewhere inside the system.

In this book we will generally use fixed control volumes, large and small, although it is sometimes useful to follow a fluid particle or use a moving control volume. The large control volume approach is one of the most basic tools for the study of fluid flow, in that it can give many insights into fluid flow problems without solving all the detailed aspects of the fluid behavior inside the control volume.

On the other hand, it is sometimes essential to know the details in the control volume. For instance, the aerodynamic performance of an airplane wing depends critically on its shape, and using a large control volume that encloses the entire wing cannot give any guidance as to its correct shape. To design the wing shape, we need to use sufficiently small control volumes or fluid elements, since this is the only way to obtain detailed information on the pressure distribution and velocity field generated by the wing.

Consider a large control volume such as that shown in Figure 3.1(b). Usually, there is fluid flowing in and out of the control volume through its surfaces. The collection of matter inside the control volume at any given time, therefore, is continually changing. However, all

physical laws are originally stated in terms of a *system*, which is a particular collection of matter. For example, the law of conservation of mass states that the mass of a system does not change. Newton's second law states that the force acting on a system is equal to the time rate of change of momentum of the system. To apply these physical laws to a control volume, we need to consider the system that occupies the control volume at the instant of our analysis. Because the system properties may be changing in time, and the system itself is generally moving relative to the control volume, we need to relate the system properties to the control volume properties. For large control volumes, this relationship is called the *Reynolds transport theorem* (see Section A.15), and for infinitesimally small control volumes, it is called the *total derivative* (see Section 5.1).

### 3.1.5 Steady and unsteady flow

Another very important concept is the idea of a *steady* flow. If we have a large, fixed control volume, it is possible that the inflow and outflow conditions do not change with time. If the fluid properties inside the control volume are also independent of time, we say that the flow is steady. However, if we followed an individual fluid particle passing through the control volume, as shown in Figure 3.1(a), we see that its velocity can change as it moves, and therefore the particle experiences unsteady conditions. Whether the flow is steady or unsteady often depends on how we choose our point of view. In the case of the large control volume with boundary conditions that are independent of time, we may see variations of velocity, momentum, and energy in space, but no variation in time, whereas when we move with a fluid particle we would see only a variation in time.

It is sometimes possible to change an unsteady flow into a steady flow by changing the point of view of the observer. For instance, if you stand by the side of the road as a car is approaching, you will feel no air flow at first, then a sudden rush as the car goes by, and then, later, nothing again. Standing by the side of the road, you experience an unsteady flow. However, if you were traveling with the car, and the car was moving at a constant velocity, the flow relative to your new vantage point would not vary with time: it is steady. Steady flows are much more easily analyzed than unsteady flows, and it is always useful if a coordinate transformation can be found whereby an unsteady flow becomes steady.

### 3.1.6 Dimensionality of a flow field

The dimensionality of a flow field is governed by the number of space dimensions needed to define the flow field completely. For example, in a one-dimensional flow the flow variables can only vary in one direction. The direction might coincide with a coordinate axis such as $x$, or it may be directed along the flow direction, as in Figure 3.4(a). In a two-dimensional flow, the flow variables vary along the flow direction as well as across it, as in Figure 3.4(b), and in a three-dimensional flow they vary in all three directions.

---

The dimensionality of a flow field is equal to the number of space dimensions needed to define the flow field.

---

Perfectly one-dimensional flows are not often found in nature. For example, if the flow diverges so that its cross-sectional area increases with distance, the flow will also diverge [Figure 3.4(a)], and it will no longer be strictly one-dimensional. Even if the streamwise velocity is constant over the area of a duct, the other components need not be. For instance, in a symmetric diverging flow in the $x$-$y$ plane, $v = 0$ on the centerline, but $v$ will be positive above the centerline and negative below (Figure 3.5).
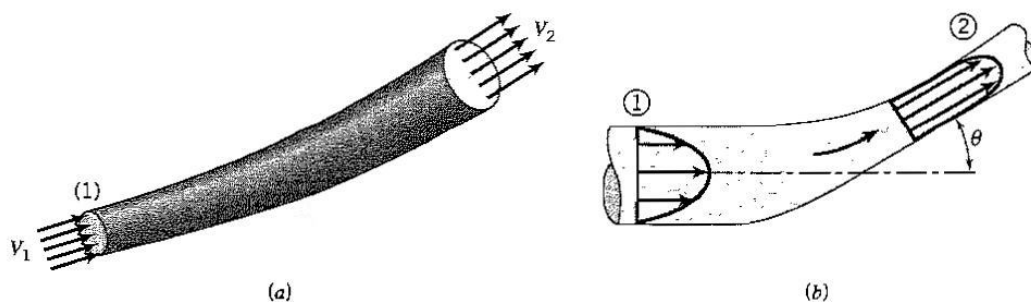
Figure 3.4: (a) One-dimensional flow; (a) Two-dimensional flow.
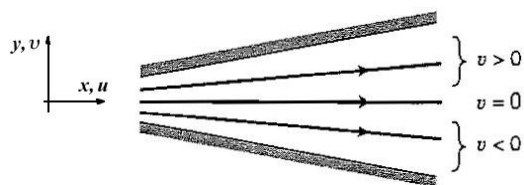


Figure 3.5: Flow in a symmetrically diverging duct.

We therefore define a class of "quasi" one-dimensional flows where the flow variables, including the streamwise velocity, are assumed to be constant across the flow area. This will be a good approximation to one-dimensional flow as long as the other components of velocity ($v$ and $w$) are small compared to the streamwise component, $u$.

In addition, for the flow in a duct or pipe, the no-slip condition guarantees that the flow velocity at the wall must be zero (see Section 1.7 and Example 3.5), so that there will always be a variation in velocity across the duct, even if the bulk of the flow has a relatively constant velocity. Nevertheless, the concept of a one-dimensional flow, or a quasi-one-dimensional flow, is still a very useful approximation in many cases.

## 3.2 Conservation of Mass

We are now ready to consider the first principle of fluid motion: conservation of mass. To see how mass conservation places restrictions on the velocity field, consider the steady flow of fluid through a duct. We will use a large control volume enclosing the duct ($CV$ in Figure 3.6). The inflow and outflow are one-dimensional, so that the velocity $V$ and density $\rho$ are constant over the inlet and outlet areas.

It is useful to consider what happens to the mass of fluid that is coincident with the control volume at time $t = 0$. This mass of fluid is called the *system*. At time $t + \Delta t$, the mass has moved a small distance downstream. Over $A_1$, it has moved a distance $V_1 \Delta t$, and over $A_2$, it has moved a distance $V_2 \Delta t$. In terms of the control volume, there is a certain amount of mass that has entered the control volume, and a certain amount that has left. Mass conservation in a steady flow requires that whatever mass flows into the control volume must leave the control volume at the same rate (if the mass inflow was greater than the outflow, for example, mass would accumulate inside the control volume and the flow could not be steady). Over the time interval $\Delta t$, therefore, for steady flow

$$\text{volume flow in over } A_1 \;\; = \;\; A_1 V_1 \Delta t$$
$$\text{volume flow out over } A_2 \;\; = \;\; A_2 V_2 \Delta t$$
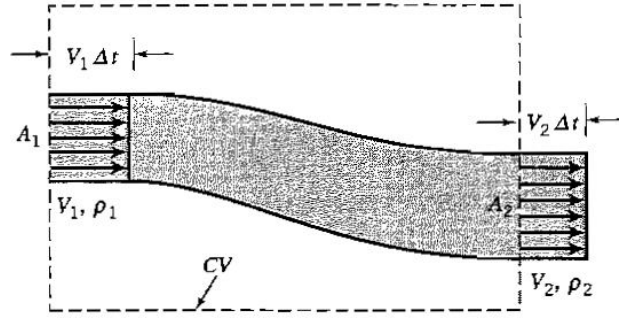
Figure 3.6: Steady, one-dimensional duct flow.

That is,

$$\text{mass flow in over } A_1 = \rho_1 A_1 V_1 \Delta t$$
$$\text{mass flow out over } A_2 = \rho_2 A_2 V_2 \Delta t$$

By the conservation of mass for a steady flow

$$\rho_2 A_2 V_2 = \rho_1 A_1 V_1$$

or

$$\boxed{\rho_2 A_2 V_2 - \rho_1 A_1 V_1 = 0} \tag{3.1}$$

That is, the net rate of change in mass flow rate (expressed as the outflow minus the inflow) is zero. This is a statement of the principle of mass conservation for a steady, one-dimensional flow, with one inlet and one outlet. For a control volume with $N$ inlets and outlets,

$$\sum_{i=1}^{N} \rho_i A_i V_i = 0 \tag{3.2}$$

where outflows are positive and inflows are negative. This equation is called the *continuity equation* for steady one-dimensional flow through a fixed control volume. It is understood that the velocities are normal to the inlet and outlet areas, regardless of the directions of the inflow and outflow. The dimensions of the product $\rho AV$ are given by

$$[\rho AV] = \frac{M}{L^3} L^2 \frac{L}{T} = \frac{M}{T} = \frac{mass}{unit\ time}$$

(see Section 1.2). That is, the product $\rho AV$ is a mass flow rate. It is commonly denoted by the symbol $\dot{m}$, and it is measured in units of $kg/s$, $lb_m/s$ or $slugs/s$.

When the density is constant,

$$\sum_{i=1}^{N} A_i V_i = 0$$

The dimensions of the product $AV$ are given by

$$[AV] = L^2 \frac{L}{T} = \frac{L^3}{T} = \frac{volume}{unit\ time}$$

That is, the product $AV$ is a volume flow rate. Volume flow rate is commonly denoted by the symbol $\dot{Q}$, but this is also the symbol used to denote a heat transfer rate. To avoid

confusion, we will use the symbol $\dot{q}$ to represent volume flow rate. It is measured in units of $m^3/s$, $ft^3/s$, $liters/s$, $gallon/hr$, cubic feet per minute $(cfm)$, or $m^3/s$.

Mass flow rate and volume flow rate are scalars, and they are independent of direction.

## 3.3 Flux

What happens when the flow is neither one-dimensional, nor steady? To extend the concept of mass conservation to these more complex flows, we introduce the important concept of flux.

When a fluid flows across the surface area of a control volume, it carries with it many properties. For example, if the fluid has a certain density, it carries this density with it across the surface into the control volume. If it has a particular temperature, it also carries this temperature with it. The fluid can also carry momentum and energy. This "transport" of fluid properties by the flow across a surface is embodied in the concept of *flux*.

> The flux of (something) is the amount of that (something) being transported across a surface per unit time.

We begin with the concept of *volume flux*, that is, the volume of all fluid particles going through an area $dA$ in time $\Delta t$ [see Figure 3.7(a)]. Consider a three-dimensional, time-dependent flow, where the velocity and density vary in space and time. If we mark a number of fluid particles and visualize their motion over a short time $\Delta t$, we can identify the fluid particles that pass through $dA$ during this time interval [Figure 3.7(b)]. If the area $dA$ is small enough, the distributions of $\rho$ and $\mathbf{V}$ can be approximated by their average values over the area.

We can now find the volume which contains all the particles that will pass through $dA$ in time $\Delta t$. From Figure 3.7b, this volume is given by $(V\Delta t \cos\theta)\,dA$. By introducing vector notation, we can express this volume as $(\mathbf{n} \cdot \mathbf{V}\Delta t)\,dA$, where $\mathbf{n}$ is the unit normal vector which defines the orientation of the surface $dA$ (Figure 3.7c). That is,

$$\left\{ \begin{array}{c} \text{amount of volume per unit time} \\ \text{transported across an area} \\ dA \text{ with a direction } \mathbf{n} \end{array} \right\} = \left\{ \begin{array}{c} \text{total} \\ \text{volume} \\ \text{flux} \end{array} \right\} = (\mathbf{n} \cdot \mathbf{V})dA$$

The volume flux $\mathbf{n} \cdot \mathbf{V}dA$ has dimensions of volume flow rate, $\dot{q}$ $(L^3 T^{-1})$.
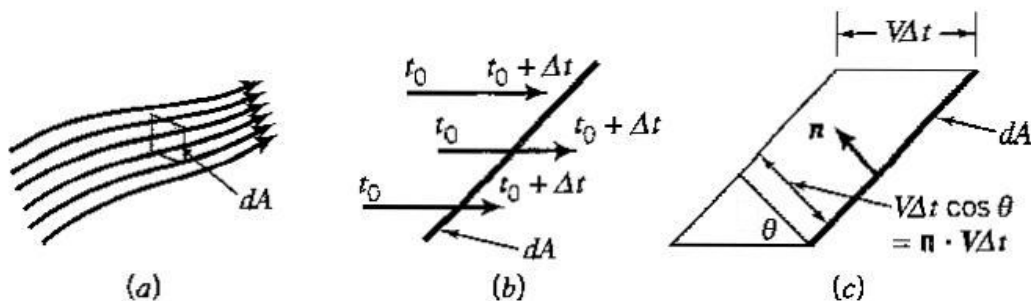


Figure 3.7: (a) Three-dimensional, unsteady flow field with $\mathbf{V}(x, y, z, t)$ and $\rho(x, y, z, t)$. (b) Edge-on view of element of control surface of area $dA$. (c) Volume swept through $dA$ in time $\Delta t$.
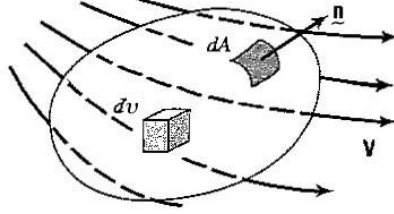
Figure 3.8: General control volume, with a surface area element $dA$, and a volume element $dv$.

Once we have obtained the volume flux we can easily write down other fluxes, such as

$$
\begin{aligned}
\text{mass flux} &= \mathbf{n} \cdot \rho \mathbf{V} \, dA \\
\text{momentum flux} &= (\mathbf{n} \cdot \rho \mathbf{V}) \mathbf{V} \, dA \\
\text{kinetic energy flux} &= (\mathbf{n} \cdot \rho \mathbf{V}) \tfrac{1}{2} V^2 \, dA
\end{aligned}
$$

The dimensions of mass flux are the same as that of the mass flow rate, $\dot{m}$ $(MT^{-1})$. The momentum flux has the dimensions of force $(MLT^{-2})$, and the kinetic energy flux has dimensions of force $\times$ velocity, that is, power $(ML^2T^{-3})$.

These fluxes are given for the flow through a small area $dA$. When this elemental area forms part of a larger area $A$, we can find the total flux by integrating over the area. For a control volume such as that shown in Figure 3.8, we can find the net fluxes leaving the control volume by integrating over its entire surface area. That is,

$$
net \text{ volume flux} = \int \mathbf{n} \cdot \mathbf{V} \, dA \tag{3.3}
$$

$$
net \text{ mass flux} = \int \mathbf{n} \cdot \rho \mathbf{V} \, dA \tag{3.4}
$$

$$
net \text{ momentum flux} = \int (\mathbf{n} \cdot \rho \mathbf{V}) \mathbf{V} \, dA \tag{3.5}
$$

$$
net \text{ kinetic energy flux} = \int (\mathbf{n} \cdot \rho \mathbf{V}) \tfrac{1}{2} V^2 \, dA \tag{3.6}
$$

The volume, mass, and kinetic energy fluxes are scalars. The momentum flux, however, is a vector, with a direction given by the velocity vector $\mathbf{V}$. Outfluxes are positive, since $\mathbf{V}$ will have a non-zero component in the direction of the outward-facing unit normal vector $\mathbf{n}$. Conversely, influxes will be negative.

## 3.4   Continuity Equation

To find the integral form of the continuity equation, we will use the fixed control volume $CV$ shown in Figure 3.9. At any instant of time, a given mass of fluid occupies the space defined by the control volume. If we follow this particular mass of fluid (often called the "system" in mechanics and thermodynamics) as it moves, then its mass will not change. However, to apply the conservation of mass to the fixed control volume, we need to consider the instantaneous mass flux through its surface, and the corresponding rate of change of mass contained inside. That is, for a fixed control volume,

$$
\left\{ \begin{array}{c} \text{rate of increase of mass} \\ \text{inside control volume} \end{array} \right\} + \left\{ \begin{array}{c} \text{net mass flux} \\ \text{out of control volume} \end{array} \right\} = \left\{ \, 0 \, \right\}
$$
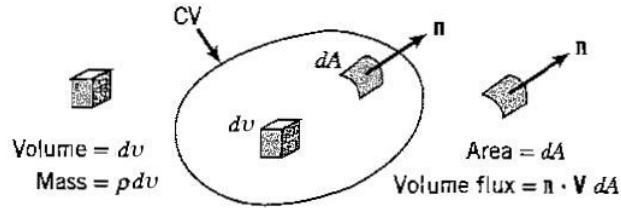
Figure 3.9: Fixed control volume for derivation of the integral form of the continuity equation. The unit vector normal to the surface, **n**, is defined to be positive when pointing outward.

We begin by considering the net mass flux leaving the control volume. For a small element of surface area $dA$, the mass outflux through $dA$ per unit time $= \mathbf{n} \cdot \rho\mathbf{V}\,dA$ (see Section 3.3). Therefore

$$\text{net mass flux out of CV} \; = \; \int \mathbf{n} \cdot \rho\mathbf{V}\,dA \tag{3.7}$$

As noted in the previous section, the integrand will be positive when the direction of the flow is in the same direction as the outward-facing unit normal vector **n** (an outflux), and negative when the direction of the flow is opposite to that of **n** (an influx).

If the flow is unsteady, the influx and outflux of mass are not equal, and we need to consider the rate of change of mass contained in the control volume. A fluid element of volume $dv$ contained within the control volume has a mass $\rho\,dv$. The total mass contained in the control volume is found by integration, and its rate of change with time is found by differentiating with respect to time. Hence,

$$\text{rate of change of mass in CV} \; = \; \frac{\partial}{\partial t} \int \rho\,dv \tag{3.8}$$

This rate of change of mass will be negative if the mass inside the control volume is decreasing with time (that is, when the outflux exceeds the influx). The partial derivative with respect to time is used to emphasize that, since the volume is fixed in shape and location, the integral is only a function of time.

From equations 3.7 and 3.8, the conservation of mass requires that

$$\boxed{\frac{\partial}{\partial t} \int \rho\,dv + \int \mathbf{n} \cdot \rho\mathbf{V}\,dA \; = \; 0} \tag{3.9}$$

This is the integral form of the continuity equation for a fixed control volume, in a three-dimensional, time-dependent flow.

When the mass inside the control volume is fixed,

$$\boxed{\int \mathbf{n} \cdot \rho\mathbf{V}\,dA \; = \; 0} \qquad \text{fixed mass} \tag{3.10}$$

When the flow is steady the flow properties do not depend on time, and since the control volume is fixed,

$$\boxed{\int \mathbf{n} \cdot \rho\mathbf{V}\,dA \; = \; 0} \qquad \text{steady flow} \tag{3.11}$$

Equations 3.10 and 3.11 are identical, although the first applies when the mass inside the control volume is fixed, and the second when the flow is steady. These conditions have somewhat different implications, depending on the flow. When the flow is steady, for example, the inlet and outlet mass flow rates, and the mass inside the control volume, do not change with time. When the only restriction is that the mass inside the control volume is constant in time, however, it is possible for the inlet and outlet mass flow rates to be unsteady, as long as they are equal.

Finally, for steady or unsteady constant density flow,

$$\int \mathbf{n} \cdot \mathbf{V} dA \; = \; 0 \qquad\qquad \text{constant density} \qquad\qquad (3.12)$$

## 3.5 Conservation of Momentum

We now consider the second principle of fluid motion: conservation of momentum. We will first construct the momentum equation for one-dimensional, steady flow by applying Newton's second law of motion to the flow through a large control volume. We will then develop the general integral form of the momentum equation by using the concept of flux. To begin, we need to consider the kinds of forces that can act to change the momentum of a fluid.

### 3.5.1 Forces

What causes a fluid to move? Fluids will begin to move when a nonzero resultant force acts on them. For example, when the pressure in one location is higher than in another location, the fluid will tend to move toward the region of lower pressure. Such pressure differences play a major role in establishing weather patterns, for example. Gravity can also cause a fluid to move: liquids flow downhill, trading their potential energy for kinetic energy of motion. Similarly, temperature differences will cause one part of a fluid to have a lower density compared to another part, and the lighter fluid will tend to rise.

There is also friction. When one layer of fluid moves with respect to an adjacent layer, a viscous shear stress develops which tends to speed up the flow in the slower layer and slow down the speed of the faster layer (see Section 1.6). Sometimes we consider fluids where the viscosity is zero. These *inviscid* fluids do not exist in nature because all real fluids are viscous, but we can often use this approximation when the effects of viscosity are small. However, we must be careful, because neglecting viscosity can sometimes lead to spectacularly wrong answers (see, for instance, Section 6.9).

Forces due to stress differences are called *surface* forces because they are proportional to the total surface area over which they act. For instance, if a constant shear stress $\tau$ acts over an area $A$, the resultant shear force is equal to $\tau A$, so that the force is proportional to the area. In contrast, the acceleration due to gravity $g$ acting on a fluid mass $m$ introduces a force that is proportional to the mass of the fluid, $mg$, and it is called a *body* force.

We must also include forces exerted by solid surfaces. This becomes clear when we think of a jet of water hitting a flat plate — there is a force exerted on the plate by the water, and by Newton's third law the plate exerts an equal but opposite force on the water (which acts to change the direction of motion of the fluid and therefore changes its momentum).

Other forces may also be important. For instance, if the fluid is electrically charged it can be made to move by applying a magnetic field, and Coriolis forces can be important in a rotating flow (they are another crucial factor in forming our weather patterns — see Chapter 13). Mostly, however, we will only consider the forces due to pressure differences, viscous stress differences, solid surfaces, and gravity.
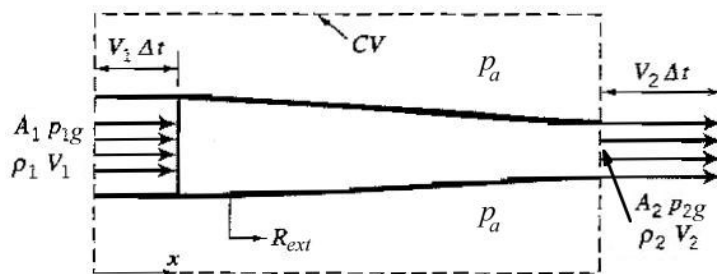
Figure 3.10: Flow in a one-dimensional duct where the inlet and outlet directions are aligned.

## 3.5.2 Flow in one direction

Consider the simple case shown in Figure 3.10, where the inflow and outflow are in the same direction, and the flow is steady and one-dimensional. How can we find, for example, the force $F_D$ required to hold the duct in place as the fluid flows through it? To answer this question, we choose a rectangular control volume, labeled $CV$ in Figure 3.10. The pressure outside the duct is equal to the atmospheric pressure, but over the inflow area $A_1$ the gauge pressure is $p_{1g}$, and over the outflow area $A_2$ it is $p_{2g}$.

We will now apply Newton's second law to the fluid flowing through the control volume. Newton's second law applies to a fixed mass of fluid. As in the case of mass conservation, we consider the mass of fluid that is coincident with the control volume at time $t = 0$ (the *system*). At time $t + \Delta t$, the mass has moved a small distance downstream. Over $A_1$, it has moved a distance $V_1 \Delta t$, and over $A_2$, it has moved a distance $V_2 \Delta t$. In terms of the control volume, a certain amount of momentum has entered, and a certain amount has left. If the momentum of the system has changed, then forces have acted on the system. We therefore examine the surfaces of the control volume to see where the flow momentum enters and leaves, and what forces are acting on the fluid contained in the control volume at the instant of our analysis. In this particular example, we only need to consider the momentum equation in the $x$-direction because the flow is one-dimensional..

As the fluid moves through the control volume, its velocity varies along the flow direction. Specifically, the inflow and outflow velocities, $V_1$ and $V_2$, are different. Relative motions exist, and fluid particles accelerate as they move from entry to exit. Even though the velocity field is independent of time, there is a fluid acceleration because of spatial variations in velocity. We know from Newton's second law that a resultant force must therefore be acting on the fluid. We have seen that these forces will come from pressure differences, viscous stress differences, solid surfaces, and gravity. Hence,

(1) The force due to pressure differences acting on the fluid contained in the control volume acts on the surface of the control volume. The only places where pressures other than atmospheric pressure act are over areas $A_1$ and $A_2$. The atmospheric pressure by itself does not contribute to the resultant force since it acts equally over the complete surface area of the control volume. Therefore the forces due to pressure differences are entirely due to the gauge pressures acting on areas $A_1$ and $A_2$. Since compressive pressures are taken to be positive,

$$\text{force due to pressure acting on area } A_1 \quad = \quad p_{1g}A_1 \text{ to the right}$$
$$\text{force due to pressure acting on area } A_2 \quad = \quad p_{2g}A_2 \text{ to the left}$$

(2) There is a force exerted *by* the duct *on* the fluid (the external forces included in the momentum equation are always the forces acting *on* the fluid). This is intuitive,

in that the duct will experience a force due to the action of the fluid, and therefore the duct exerts an equal but opposite force on the fluid. We call this a force due to external surfaces, and we use the symbol $R_{ext}$. Unless otherwise given, we will always assume that forces like $R_{ext}$ act in the positive $x$-direction. If the solution shows that $R_{ext}$ is negative, it simply means that it acts in the negative $x$-direction.

(3) Forces due to friction and gravity can also be important. For the simple example considered here, they will be neglected.

The resultant force $F$ acting on the fluid, therefore, is given by

$$F = R_{ext} + p_{1g}A_1 - p_{2g}A_2$$

This resultant force changes the momentum of the fluid. To find this momentum change we note that for the system

$$\text{the mass entering during } \Delta t = \rho_1 A_1 V_1 \Delta t$$
$$\text{the } x\text{-momentum entering during } \Delta t = (\rho_1 A_1 V_1 \Delta t) V_1$$
$$\text{the } x\text{-momentum leaving during } \Delta t = (\rho_2 A_2 V_2 \Delta t) V_2$$

Since outflows are taken to be positive

$$\text{the net change of } x\text{-momentum during } \Delta t = \left(\rho_2 A_2 V_2^2 - \rho_1 A_1 V_1^2\right) \Delta t$$
$$\text{the net rate change of } x\text{-momentum} = \rho_2 A_2 V_2^2 - \rho_1 A_1 V_1^2$$

This is the rate of increase in $x$-momentum experienced by the fluid in passing through the duct. Note that the quantity $\rho A V^2$ has the dimensions of force $(MLT^{-2})$ and it is measured in units of $N$ or $lb_f$.

The flow is steady, so that the momentum of the fluid inside the control volume is not changing with time. Therefore the net rate of change of fluid momentum is equal to the resultant force acting on the fluid. That is,

$$F = R_{ext} + p_{1g}A_1 - p_{2g}A_2 = \rho_2 A_2 V_2^2 - \rho_1 A_1 V_1^2$$

This equation is Newton's second law of motion as applied to a simple one-dimensional, steady flow. In this example, the force acts in the $x$-direction, and there is no resultant force in the $y$-direction. Note that the force $R_{ext}$ is the force exerted *by* the duct *on* the fluid. By Newton's third law, the force exerted *on* the duct *by* the fluid is given by $-R_{ext}$. To hold the duct in place, there must be an external restraining force acting on the duct, $F_D$, equal to $-(-R_{ext})$, that is $F_D = R_{ext}$. Hence, the force required to hold the duct in place is

$$F_D = R_{ext} = -(p_{1g}A_1 - p_{2g}A_2) + \rho_2 A_2 V_2^2 - \rho_1 A_1 V_1^2 \qquad (3.13)$$

The solution for $F_D$ is somewhat complicated, and without further information of the flow conditions it is difficult to tell whether it is positive or negative. It is good practice, therefore, not to try to anticipate the direction of $F_D$ or $R_{ext}$ at the start of the problem.

### 3.5.3   Flow in two directions

Consider now the case shown in Figure 3.11, where the inlet and outlet directions are not aligned. All other conditions are the same as in the previous example; the flow is steady, one-dimensional, and we neglect friction and gravity. Also, $p_{1g}$ and $p_{2g}$ are the gauge pressures over the inlet and outlet areas, respectively. In this example, however, as the fluid passes through the duct, its momentum changes in magnitude and direction. The entering
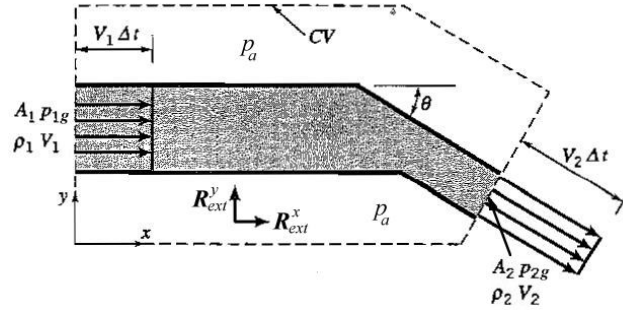
Figure 3.11: Flow in a one-dimensional duct where the inlet and outlet directions are not aligned.

momentum is all in the $x$-direction, whereas the exiting momentum has components in the $x$- and the $y$-directions. Therefore the force due to pressure differences also has two components, and so will the force exerted by the duct on the fluid. This force due to external surfaces is shown as $R_{ext}^x$ and $R_{ext}^y$ in Figure 3.11, and we will assume that the components act in the positive $x$- and $y$-directions, respectively. The solution will reveal if this assumption is correct.

We will now apply Newton's second law to the fluid passing through the control volume in order to find the force $F_R$ required to hold the duct in place.

We begin by considering the forces acting on the fluid in the $x$-direction. First, we have $R_{ext}^x$. Second, we have the net force due to pressure differences. Because atmospheric pressure acts everywhere, only nonzero gauge pressures give rise to a resultant force. The $x$-component of the force due to pressure differences is therefore given by $p_{1g}A_1 - p_{2g}A_2 \cos\theta$. Hence, the resultant force acting on the fluid in the $x$-direction, $F_x$, is given by

$$F_x = R_{ext}^x + p_{1g}A_1 - p_{2g}A_2 \cos\theta$$

This force causes the fluid momentum in the $x$-direction to change. During the short time interval $\Delta t$, the $x$-momentum of the fluid entering the control volume is $(\rho_1 V_1 A_1 \Delta t)V_1$, and the $x$-momentum of the fluid leaving the control volume is $(\rho_2 V_2 A_2 \Delta t)V_2 \cos\theta$. That is,

$$\text{net change of } x\text{-momentum} = (\rho_2 V_2 A_2 \Delta t)V_2 \cos\theta - (\rho_1 V_1 A_1 \Delta t)V_1$$

and

$$\text{net rate of change of } x\text{-momentum} = (\rho_2 V_2 A_2)V_2 \cos\theta - (\rho_1 V_1 A_1)V_1 \qquad (3.14)$$

Hence, by Newton's second law

$$R_{ext}^x + p_{1g}A_1 - p_{2g}A_2 \cos\theta = \rho_2 A_2 V_2^2 \cos\theta - \rho_1 A_1 V_1^2$$

and so

$$R_{ext}^x = -\left(p_{1g}A_1 - p_{2g}A_2 \cos\theta\right) - \left(\rho_1 A_1 V_1^2 - \rho_2 A_2 V_2^2 \cos\theta\right)$$

We now go through the same procedure to find the force $R_{ext}^y$. The force due to pressure differences in the $y$-direction is given by $p_{2g}A_2 \sin\theta$ (this component is positive because it acts in the positive $y$-direction). There is no vertical contribution from the force due to pressure acting on $A_1$ since it acts purely in the $x$-direction. Hence, the resultant force acting on the fluid in the $y$-direction, $F_y$, is given by

$$F_y = R_{ext}^y + p_{2g}A_2 \sin\theta$$

This force causes the fluid momentum in the $y$-direction to change. We see that the momentum entering the control volume has no component in the $y$-direction, but the momentum leaving the control volume does. So

$$\text{net rate of change of } y\text{-momentum} = -(\rho_2 A_2 V_2)V_2 \sin\theta \qquad (3.15)$$

where the minus sign indicates that the $y$-component of the momentum leaves the control volume in the negative $y$-direction. Hence,

$$R^y_{ext} + p_{2g} A_2 \sin\theta = -\rho_2 A_2 V_2^2 \sin\theta$$

That is,

$$R^y_{ext} = -p_{2g} A_2 \sin\theta - \rho_2 A_2 V_2^2 \sin\theta$$

Finally, the resultant force by the duct on the fluid is given by

$$\mathbf{R_{ext}} = R^x_{ext}\mathbf{i} + R^y_{ext}\mathbf{j}$$

Hence the force *by* the fluid *on* the duct is given by $-\mathbf{R_{ext}}$, and therefore $F_D$, the force required to hold the duct in place, is given by $-(-\mathbf{R_{ext}}) = \mathbf{R_{ext}}$.

It is important to make sure that the rate of change of momentum has the correct sign. Note that each term on the right hand side of equation 3.14 is of the form (mass-flow rate) × (velocity component in $x$-direction). Similarly, each term on the right hand side of equation 3.15 is of the form (mass-flow rate) × (velocity component in $y$-direction). Hence, for a one-dimensional flow over any inlet or outlet

> The $i$-component of the fluid momentum is given by the mass-flow rate times the $i$-component of the velocity. Similarly for the $j$- and $k$-components.

In this example, the momentum enters enters the duct in one direction and leaves in another direction, so that there must be both $x$- and $y$-components of the force acting on the duct. This observation can help give a simple explanation for the lift generated by an airfoil. When a flow is deflected from its original direction by an airfoil, the airfoil must be exerting a force on the fluid. Therefore, by Newton's third law, there will be an equal and opposite force acting on the airfoil. The component normal to the incoming flow contributes to the lift, and the component in the direction of the incoming flow contributes to the drag.

## 3.6　Momentum Equation

We can now examine the conservation of momentum for the general case of three-dimensional, time-dependent flows. To derive the integral form of the general momentum equation, we use a fixed control volume similar to that used in the derivation of the continuity equation (see Figure 3.12). The momentum of the particular mass of fluid occupying the control volume at any instant (the "system") will change under the action of a resultant force according to Newton's second law. To express the rate of change of momentum of this mass in terms of a fixed control volume, we need to consider the instantaneous momentum flux through its surface and the rate of change of momentum of the fluid contained inside. That is, for a fixed control volume,

$$\left\{ \begin{array}{c} \text{rate of change of} \\ \text{momentum inside} \\ \text{control volume} \end{array} \right\} + \left\{ \begin{array}{c} \text{net momentum} \\ \text{flux out of} \\ \text{control volume} \end{array} \right\} = \left\{ \begin{array}{c} \text{resultant force} \\ \text{acting on fluid} \\ \text{in control volume} \end{array} \right\}$$
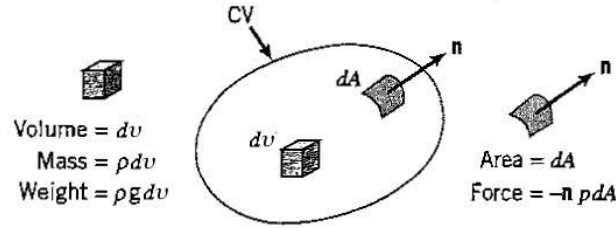
Figure 3.12: Fixed control volume for derivation of the integral form of the momentum equation.

We begin by considering the net momentum flux leaving the control volume. For a small element of surface area $dA$, the mass outflux through $dA$ per unit time $= \mathbf{n} \cdot \rho \mathbf{V}\, dA$, and the momentum flux is given by $(\mathbf{n} \cdot \rho \mathbf{V})\, \mathbf{V} dA$ (see Section 3.3). Therefore

$$\left\{ \text{ net momentum flux out of } CV \right\} = \int (\mathbf{n} \cdot \rho \mathbf{V})\, \mathbf{V}\, dA \qquad (3.16)$$

The integrand will be positive when the direction of the flow is in the same direction as the outward-facing unit normal vector $\mathbf{n}$ (an outflux), and negative when the direction of the flow is opposite to that of $\mathbf{n}$ (an influx).

If the flow is unsteady, we need to consider also the rate of change of mass contained in the control volume. A fluid element of volume $dv$ contained within the control volume has a mass $\rho\, dv$, and its momentum is $\rho \mathbf{V}\, dv$. The total momentum contained in the control volume is found by integration, and its rate of change with time is found by differentiating with respect to time. Hence,

$$\left\{ \begin{array}{c} \text{rate of change of momentum} \\ \text{inside control volume} \end{array} \right\} = \frac{\partial}{\partial t} \int \rho \mathbf{V}\, dv \qquad (3.17)$$

This rate of change of momentum is positive if the momentum inside the control volume is increasing with time. The partial derivative with respect to time is used to emphasize that, since the volume is fixed in shape and location, the integral (but not the integrand) depends only on time.

The resultant force acting on the fluid in the control volume is the sum of the surface forces, body forces and forces due to external surfaces. They act on the fluid mass that is coincident with the control volume at a particular instant of time.

Surface forces include viscous forces and forces due to pressure differences acting over the surface of the control volume. For now we will write the force due to viscous friction simply as $\mathbf{F_v}$. With respect to the force due to pressure differences, consider an element of surface area $dA$. The force due to pressure acts with a magnitude $pdA$. The direction of the force is normal to the surface, and by convention pressure forces are positive if they are compressive, so that the vector force due to pressure acting on $dA$ is $-\mathbf{n}\,pdA$. That is

$$\left\{ \begin{array}{c} \text{resultant force due to pressure} \\ \text{differences acting on the fluid} \\ \text{contained in the control volume} \end{array} \right\} = -\int \mathbf{n}\, p\, dA \qquad (3.18)$$

Body forces include gravitational, magnetic and electrical forces acting over all the fluid contained in the control volume. The only body force considered here is the force due to gravity. An element of volume $dv$ has a mass $\rho dv$, and the vector force due to gravity acting on this mass is $\rho \mathbf{g}\, dv$. That is

$$\left\{ \begin{array}{c} \text{resultant force due to gravity} \\ \text{acting on the fluid contained} \\ \text{in the control volume} \end{array} \right\} = \int \rho \mathbf{g}\, dv \qquad (3.19)$$

where $\int \rho \, dv$ is the total mass of fluid contained in the control volume.

The forces due to external surfaces, $\mathbf{R_{ext}}$, are the forces applied to the fluid by the walls of a duct, the surfaces of a deflector, or the forces acting in the solid cut by the control volume. An example of the latter is when a control volume is drawn to cut through the solid walls of a duct: we must include the forces exerted by the walls in the force balance on the fluid. (Remember: when a fluid exerts a force on a solid surface, an equal but opposite force acts on the fluid.)

By combining the terms given in equations 3.16 to 3.19, and including the viscous forces ($\mathbf{F_v}$) and the forces due to external surfaces ($\mathbf{R_{ext}}$), we obtain

$$\frac{\partial}{\partial t} \int \rho \mathbf{V} \, dv + \int (\mathbf{n} \cdot \rho \mathbf{V}) \, \mathbf{V} \, dA \;=\; -\int \mathbf{n} \, p \, dA + \int \rho \mathbf{g} \, dv + \mathbf{F_v} + \mathbf{R_{ext}} \qquad (3.20)$$

This is the integral form of the momentum equation for a fixed control volume, in a three-dimensional, time-dependent flow. It is a vector equation, so that in Cartesian coordinates it has components in the $x$-, $y$- and $z$-directions. Note that it is written in the form "rate of change of momentum equals resultant force," rather than the other way round. This is the usual practice in fluid mechanics.

## 3.7   Viscous Forces and Energy Losses

Whenever viscous forces are present, there will also be energy dissipation. Fluid flows are irreversible (in a thermodynamic sense) because whenever velocity gradients appear in the flow viscous stresses appear, and work needs to be done to overcome these stresses. Energy is not conserved. [1] However in some cases, viscous effects are small compared to other effects. For instance, in the flow through a large duct where the boundary layers are very thin, viscous effects are confined to a rather small region, and then the viscous forces may sometimes be neglected compared to the other forces that are acting. This is not the case for many practical flows. In most pipe and duct flows, for example, the velocity gradients extend over the entire cross-section and frictional stresses are important everywhere.

Even if the boundary layers are thin to begin with, when the flow decelerates rapidly, or when it tries to change direction rapidly, it can *separate*. When a flow separates, it no longer follows the shape of the solid boundary, and regions of recirculating flow appear where some of the fluid particles are moving in a direction opposite to that of the main flow. For example, in the flow shown in Figure 3.13, as the flow enters the diverging section of the duct (the "diffuser") it hardly turns at all and continues to go almost straight downstream. A region of separated flow marked by large recirculating eddies forms over the diffuser walls. Large losses can occur, as the mechanical energy of the fluid is used to drive large unsteady eddying motions, which eventually dissipate into heat. This type of flow can occur for quite small diffuser angles. To avoid the large losses associated with separation, the angle of divergence needs to be very small: the included angle $\theta$ needs to be less than about $7°$.

In contrast, when the flow is in the direction of decreasing area, as in a "contraction," there is little risk of creating large regions of separated flow, even for large values of $\theta$ (up to $45°$), and consequently losses are generally small (see Figure 3.14).

We see that great care needs to be taken in considering frictional effects; sometimes they are negligible, and sometimes they are not. When separation occurs, however, frictional effects and mechanical energy losses are always important. It is worth noting that sharp corners almost always produce a separated flow. The sudden expansion and contraction

---

[1]Energy is conserved only if there are no velocity gradients anywhere, or if the fluid is inviscid, but inviscid fluids are mathematical constructs and do not exist in nature.
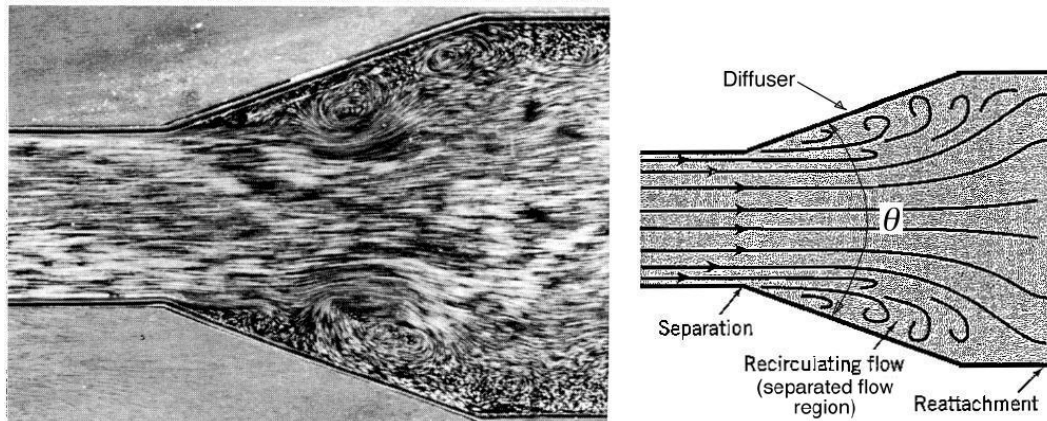
Figure 3.13: Separated diffuser flow. The included angle $\theta = 40°$). Flow is from left to right. From *Visualized Flow*, Japan Society of Mechanical Engineers, Pergamon Press, 1988.
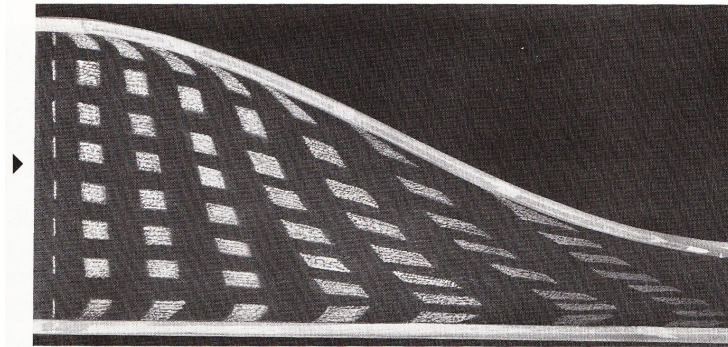


Figure 3.14: Flow in a smooth, asymmetric contraction. Flow is from left to right. From *Visualized Flow*, Japan Society of Mechanical Engineers, Pergamon Press, 1988.

flows shown in Figure 3.15 also demonstrate the problem. The direction of the flow greatly influences the flow pattern and the resulting energy loss. The flow in the sudden expansion is therefore expected to cause greater losses than the flow in the sudden contraction.

## 3.8  Energy Equation

We will now derive the integral form of the energy equation for a fixed control volume. The first law of thermodynamics states that the total change in energy of a system is the result of work and heat transfers to the system. That is,

$$\Delta E_{sys} = Q_{sys} + W_{sys}$$

In fluid mechanics, a "system" is a fixed mass of fluid. The "total change in energy," $\Delta E$, contains contributions from all motions of matter that make up the system. By "work and heat transfers" we mean the work $W$ done on or by the system, and the heat $Q$ transferred to or from the system. Work and heat transferred *from* the surroundings *to* the system are taken to be positive. Cooling the system, so that heat is transferred from the system, is a negative heat transfer. Lifting the system to a higher elevation means that work is done on the system, and it is a positive work transfer.
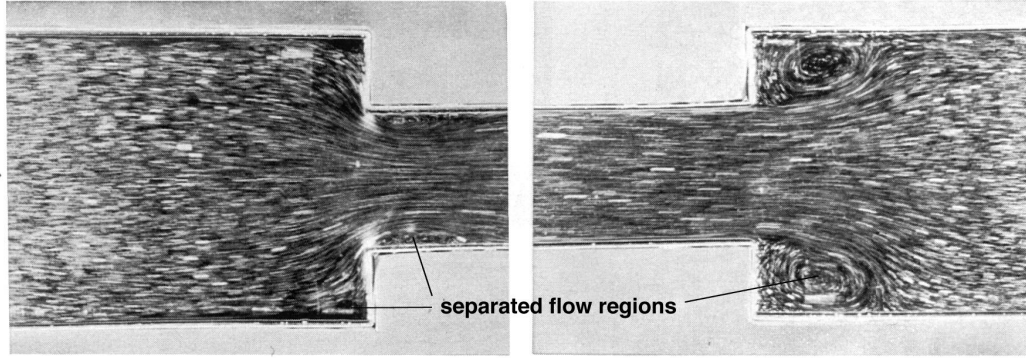
Figure 3.15: Flow through a sudden contraction (left), and a sudden expansion (right). Flow is from left to right. From *Visualized Flow*, Japan Society of Mechanical Engineers, Pergamon Press, 1988.

If the heat and work transfers are slow enough for the system to be in equilibrium (this is not difficult to satisfy even in supersonic flows), the first law will also hold in terms of rates of change. That is, for a fixed mass of fluid, the first law of thermodynamics states that

$$
\left\{ \begin{array}{c} \text{rate of change of} \\ \text{total energy of} \\ \text{a system} \end{array} \right\} = \left\{ \begin{array}{c} \text{net rate of energy} \\ \text{addition by heat} \\ \text{transfer to system} \end{array} \right\} + \left\{ \begin{array}{c} \text{net rate of energy} \\ \text{addition by work} \\ \text{done on system} \end{array} \right\}
$$

That is,

$$\Delta \dot{E}_{sys} = \dot{Q}_{sys} + \dot{W}_{sys} \tag{3.21}$$

The first law applies to a closed system. In fluid mechanics, we are interested in "open" systems, that is, control volumes. For the rate of change of total energy inside a control volume, consider an element of volume $dv$, as in Figure 3.12. The mass of this volume is $\rho dv$, and its total energy is $\rho e dv$, where $e$ is the total energy per unit mass. The total energy contained in the control volume is found by integration, and its rate of change with time is found by differentiating with respect to time, so that

$$
\left\{ \begin{array}{c} \text{rate of change of total energy} \\ \text{inside control volume} \end{array} \right\} = \frac{\partial}{\partial t} \int \rho e \, dv \tag{3.22}
$$

There is also a flux of total energy through the surface of the control volume. For an element of surface area $dA$, we have a mass flux given by $\mathbf{n} \cdot \rho \mathbf{V} dA$, and the total energy flux is given by $(\mathbf{n} \cdot \rho \mathbf{V}) e dA$. The net flux is found by integration, so that

$$
\left\{ \begin{array}{c} \text{net outflux of total energy} \\ \text{from control volume} \end{array} \right\} = \int (\mathbf{n} \cdot \rho \mathbf{V}) \, e \, dA \tag{3.23}
$$

Combining equations 3.21, 3.22, and 3.23 gives

$$\frac{\partial}{\partial t} \int \rho e \, dv + \int (\mathbf{n} \cdot \rho \mathbf{V}) \, e \, dA = \dot{Q} + \dot{W} \tag{3.24}$$

where $\dot{Q}$ and $\dot{W}$ are the heat and work energies transferred to the fluid contained in the control volume at time $t$. It is understood that we refer to a system, so the subscript has been dropped.

For a flowing fluid, the total energy is the sum of its internal energy and its kinetic energy. The internal energy is the energy stored in the fluid due to molecular activity and

molecular bonding forces, and the kinetic energy is due to the bulk motion of the fluid. Expressing this per unit mass, the total energy is $e$, the internal energy is $\hat{u}$, and the kinetic energy is $\frac{1}{2}V^2$. That is, $e = \hat{u} + \frac{1}{2}V^2$.

The work done on the fluid inside the control volume can be split four ways:

$$\dot{W} = \dot{W}_{pressure} + \dot{W}_{grav} + \dot{W}_{viscous} + \dot{W}_{shaft}$$

where $\dot{W}_{pressure}$ is the rate that work is done by forces due to pressure, $\dot{W}_{grav}$ is the rate that work is done against gravity, $\dot{W}_{viscous}$ is the rate that shear work is done by viscous stresses, and $\dot{W}_{shaft}$ is the rate that shaft work is done by machines that may be inside the control volume (a pump, fan, piston, and so forth).

For a surface element $dA$, the rate of doing work by pressure forces is given by the force due to pressure times the velocity component normal to the surface into the control volume. That is

$$d\dot{W}_{pressure} = -p\left(\mathbf{n} \cdot \mathbf{V}\right) dA$$

where $-\mathbf{n}$ is the direction of the force exerted by the pressure.

The mass of a volume element is $\rho d\upsilon$ and so its weight is $\rho \mathbf{g} d\upsilon$. The rate of doing work against gravity in the direction of $\mathbf{V}$ is given by $\rho \mathbf{g} \cdot \mathbf{V} d\upsilon$. We can write $\mathbf{g}$ in terms of a gravitational potential $\phi_g$ (see Section Appendix-A.13, such that $\mathbf{g} = -g\nabla\phi_g$. That is, the rate of doing work against gravity is given by

$$d\dot{W}_{grav} = -\rho g\left(\nabla\phi_g \cdot \mathbf{V}\right) d\upsilon$$

Finally, by a suitable choice of control volume, the shear work can often be made zero. For example, at a solid surface, the no-slip condition makes the velocity at the wall zero, so that the rate of work by viscous forces is also zero. At an inlet or outlet, the flow is usually normal to the surface, and then the shear work is again zero. The shear work is rarely important for large control volumes, and we will neglect it from now on.

The total work term is then found by integrating over the surface area of the control volume. By using the theorems given in Section Appendix-A.9), we obtain

$$\dot{W} = -\int p\left(\mathbf{n} \cdot \mathbf{V}\right) dA - \int g\phi_g\left(\mathbf{n} \cdot \rho\mathbf{V}\right) dA + \dot{W}_{shaft}$$

Hence, with $e = \hat{u} + \frac{1}{2}V^2$, and recognizing that $\phi_g = z$, equation 3.24 becomes

$$\frac{\partial}{\partial t}\int \rho\left(\hat{u} + \frac{1}{2}V^2\right) d\upsilon + \int \left(\mathbf{n} \cdot \rho\mathbf{V}\right)\left(\hat{u} + \frac{p}{\rho} + \frac{1}{2}V^2 + gz\right) dA = \dot{Q} + \dot{W}_{shaft} \qquad (3.25)$$

This is the integral form of the energy equation for a fixed control volume. The pressure work term has been combined with the energy flux term, as is common practice.

# Chapter 4

# Kinematics and Bernoulli's Equation

We are now interested in describing what happens inside the control volume. Instead of integral equations that describe the overall balance os mass and momentum, we will need differential equations that describe the local behavior of the fluid particles. We will derive these differential equations of motion in Chapter 5, but before we do so we introduce the concepts of streamlines and pathlines, and Bernoulli's equation. Streamlines and pathlines help us to describe fluid motion inside the control volume, and so encompass the kinematics of the flow field. Bernoulli's equation is a special form of the momentum equation, which describes the dynamics of the flow field. Its application requires some knowledge about the flow behavior inside the control volume, as we shall make clear.

## 4.1 Streamlines and Flow Visualization

It is important to know how fluid motion can be described, and how it can be visualized. The most common methods of flow visualization introduce smoke or dye particles in the flow, and then we follow their motion to infer the behavior of the velocity field. We are particularly interested in identifying streamlines and particle paths.

### 4.1.1 Streamlines

Velocity is a vector, and therefore it has a magnitude and a direction.

> A streamline is defined as a line that is everywhere tangential to the instantaneous velocity direction.

Since the velocity at any point in the flow has a single value, streamlines cannot cross (the flow cannot go in more than one direction at the same time).[1]

To visualize a streamline in a flow, imagine the motion of a small marked particle of fluid. For instance, we could mark a drop of water with fluorescent dye and illuminate it using a laser so that it fluoresces. If we took a short exposure photograph as the drop moves according to the local velocity field (where the exposure needs to be short compared to the

---

[1]*Singular points* can occur in the flow at points where the velocity magnitude is zero. Consequently, their nature depends strongly on the velocity of the observer. At a critical point, the velocity direction is indeterminate, and streamlines can meet. One example of a singular point is a stagnation point — see Figure 4.8 and Section 4.3.1.
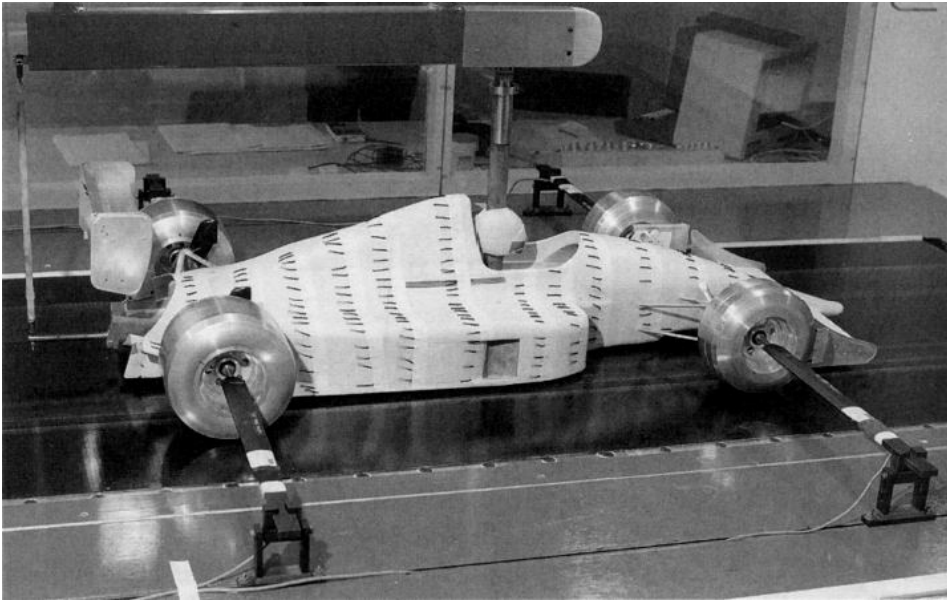
Figure 4.1: Surface tufts for surface-flow visualization. From *Race Car Aerodynamics*, J. Katz, Robert Bentley Publishers, 1995. Originally from MIRA. With permission.

time it takes for the velocity to change appreciably), we would see a short streak, with a length $V\Delta t$ and a direction tangential to the instantaneous velocity direction. If we mark many drops of water in this way, all the streamlines in the flow would become visible.

Particle Image Velocimetry (PIV) is a technique to measure the instantaneous velocity field by visualizing the motion of individual particles. First, small particles are introduced into the flow, small enough so that they faithfully follow the flow. Second, a laser light sheet is used to illuminate the particles in a plane in the flow field. Third, two images are taken of the particle distributions a short time $\Delta t$ apart. The velocity magnitude in the plane of the laser sheet can then be found by measuring the displacements of each particle, $V\Delta t$ and by knowing $\Delta t$, and the instantaneous velocity direction is given by the direction of the displacement.

In the absence of flow visualization, we can find the shape of the streamlines if we the velocity field is known. From the definition of a streamline, it follows that for a flow in the $[x, y]$-plane, the slope of a streamline, $dy/dx$, must be equal to $v/u$, where $u$ and $v$ are the instantaneous velocity components in the $x$- and $y$-directions. respectively. For a streamline in a three-dimensional flow,

$$\frac{dy}{dx} = \frac{v}{u} \qquad \frac{dy}{dz} = \frac{v}{w} \qquad \frac{dx}{dz} = \frac{u}{w}$$

The procedure for finding the shape of the streamlines is illustrated in Examples 4.1 and 4.2.

*Surface streamlines* are the streamlines followed by the flow very close to a solid surface. Small, flexible tufts of yarn are sometimes attached to the body, and because of the drag on the tufts by the flow, the tufts will align themselves in the local flow direction (see, for example, Figure 4.1).

### 4.1.2  Pathlines

There are other ways to make the flow visible. For example, we can trace out the path followed by a fluorescent drop using a long-exposure photograph. When the drop is small

enough, we will record the path taken by a fluid particle. This line is called a *pathline*, and it is similar to what you see when you take a long-exposure photograph of car lights on a freeway at night. Each light marks a specific point on a car, and the photograph will show the path of this material point as the car moves through traffic. It is possible for pathlines to cross, as you can imagine from the freeway analogy: as a car changes lanes, the pathline traced out by its lights might cross another pathline traced out by another vehicle at an earlier time.

> A pathline is the line traced out by a fluid particle as it moves through the flow field.

Since we are following fluid particles along a pathline, it is a Lagrangian concept. For a pathline in a two-dimensional flow, we use the fact that $u = dx/dt$, and $v = dy/dt$. If we know how $u$ and $v$ depend on time, and a sufficient number of boundary conditions are given, we can integrate $u$ and $v$ with respect to time to find the particle path coordinates $x$ and $y$ as functions of time. By eliminating time from the expressions for $x$ and $y$, the particle path in $[x, y]$-space can be found (see Examples 4.1 and 4.2).

### 4.1.3 Streaklines

Another way to visualize flow patterns is by *streaklines*.

> A streakline is the line traced out by particles that pass through a particular point.

For instance, if we emit fluorescent dye continuously from a fixed point, the dye makes up a streakline as it passes downstream. To use the freeway analogy again, a streakline is the line made by the movement of the lights on all the vehicles that passed through the same toll booth. If they all follow the same path (a steady flow), a single line results, but if succeeding cars follow different paths (unsteady flow), it is possible for lines to cross over each other as well as themselves. As an example, Figure 4.3(b) shows how streaklines can be used to visualize the flow over a circular cylinder.

*Surface streaklines* are the streaklines followed by the flow very close to a solid surface. For example, raindrops falling on a windscreen will tend to trace out a path representing a surface streakline.

In unsteady flow, streamlines, pathlines and streaklines are all different, but it may be shown that

> In steady flow, streamlines, pathlines and streaklines are identical.

### 4.1.4 Streamtubes

Imagine a set of streamlines starting at points on a closed loop (Figure 4.2). These streamlines form a tube that is impermeable since the walls of the tube are made up of streamlines, and there can be no flow normal to a streamline (by definition). This tube is called a *streamtube*. For a steady, one-dimensional flow, the mass-flow rate passing through a streamtube is constant (see Section 3.2). If the density is constant, and the area decreases, the velocity increases. The cross-sectional area of the streamtube therefore gives information on the local velocity magnitude. In a two-dimensional flow, the distance between adjacent streamlines gives similar insight; as the distance decreases, the velocity increases.
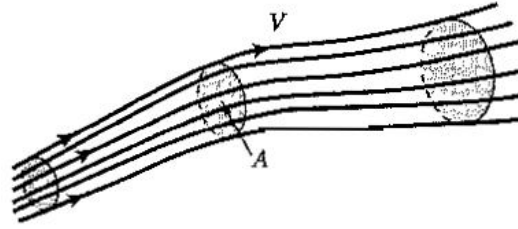
Figure 4.2: Streamlines forming a streamtube.

### 4.1.5 Hydrogen bubble visualization

The hydrogen bubble technique is a very useful method for visualizing water flows. An example of the technique is given in Figure 4.3, showing the flow over a circular cylinder. To form the bubbles, a thin wire is mounted transverse to the stream and connected to the cathode of a voltage source. An anode is placed in the water at some other location. By passing a current between the anode and cathode, hydrogen is generated by electrolysis at the wire (the cathode) in the form of bubbles. If the hydrogen bubbles are small enough, the buoyancy force on them can be neglected (it is proportional to the volume of the bubbles), and the bubbles follow the flow. By covering up parts of the thin wire cathode, and applying a continuous current to the wire, streaklines are formed, as shown in Figure 4.3(b). Upstream of the cylinder, the flow is steady so that streaklines are also streamlines, and we see that they diverge as the flow approaches the cylinder, indicating that the flow is slowing down. The central streamline stops at the cylinder surface at a point called the *stagnation point*, and this particular streamline is called the *stagnation streamline* (see also Figure 4.8). Downstream of the cylinder we see a region of reduced velocity called the *wake*. In the wake, large eddies are formed, first from one side, and then from the other. The flow is highly unsteady, and streamlines, pathlines, and streaklines are all different.

If in the hydrogen bubble technique the wire is not selectively covered up, and a short pulse of current is used, a line of bubbles is formed at the wire and is swept downstream by the flow. The line formed by the bubbles is an example of a *timeline*.

A timeline is a line made up of fluid particles that were all marked at the same time.

Timelines, streaklines, and timelines in combination with streaklines, are shown for the flow over a cylinder in Figure 4.3.

## 4.2 Bernoulli's Equation

For steady flows, we have seen that streamlines and pathlines are identical. Therefore, if we can identify a streamline, we know that fluid particles follow the same path. We can now examine the forces acting on the particle that follows this path, which leads us directly to Bernoull's equation.

Bernoulli's equation is obtained by applying Newton's second law between two points on a streamline (the complete derivation is given in Sections 4.2.1 and 4.2.2). It states that

$$p_1 + \tfrac{1}{2}\rho V_1^2 + \rho g z_1 = p_2 + \tfrac{1}{2}\rho V_2^2 + \rho g z_2 = \text{constant} \qquad (4.1)$$
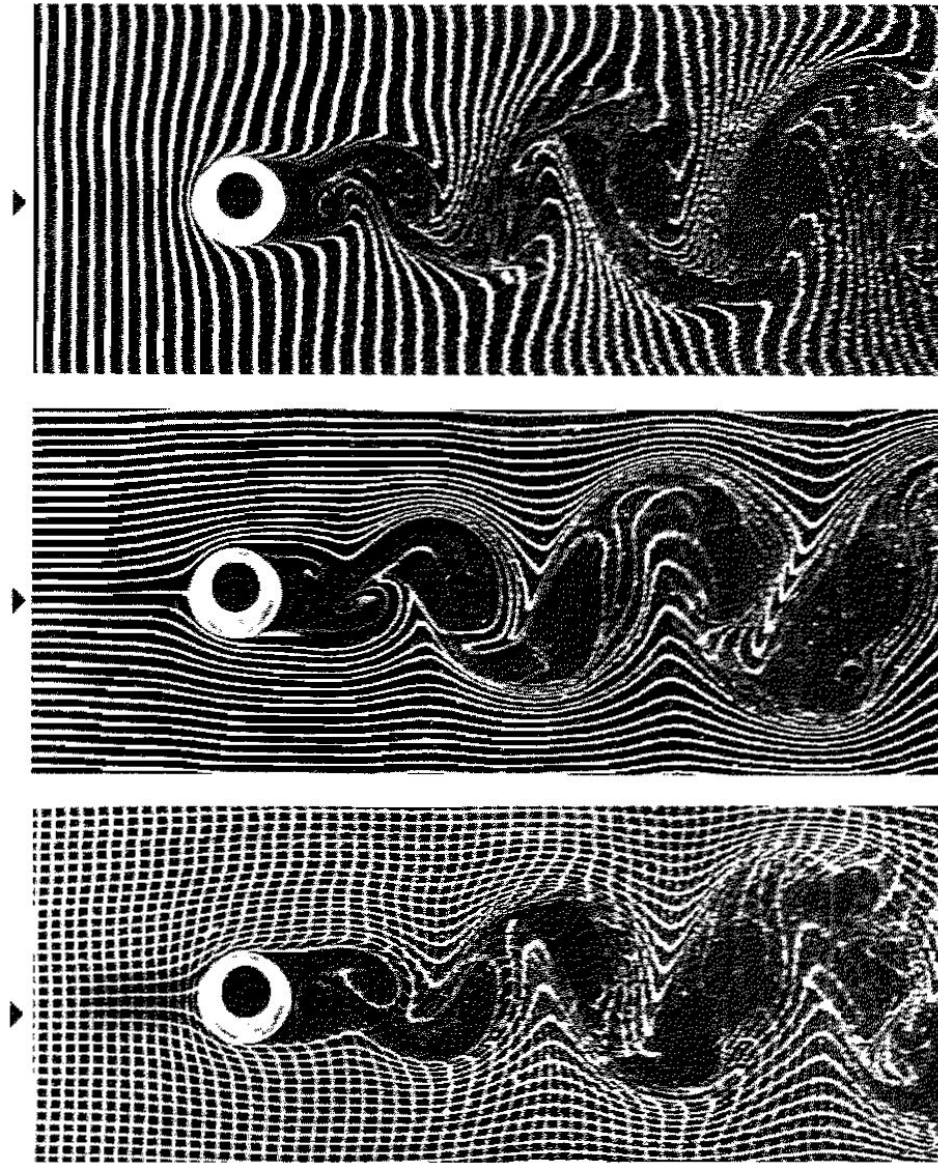
Figure 4.3: Flow over a cylinder at a Reynolds number of 170 made visible using the hydrogen bubble technique. (a) Timelines. (b) Streaklines. (c) Timeline and streakline combination. From *Visualized Flow*, Japan Society of Mechanical Engineers, Pergamon Press, 1988.

where $g$ is the gravitational constant, $z_1$ and $z_2$ are the heights or elevations of points 1 and 2 above some horizontal reference plane, and $p_1$ and $p_2$, and $V_1$ and $V_2$, are the pressures and velocities at these same points, respectively. Most important, it is required that

1. Points 1 and 2 lie on the same streamline;

2. The fluid has constant density;

3. The flow is steady; and

4. The flow is inviscid (there are no losses).

The requirement that points 1 and 2 lie along a streamline can be relaxed in an "irrotational" flow field, which is defined as a region where $\vec{\Omega} = \nabla \times \mathbf{V} = 0$ (see Chapter 6). In that case, Bernoulli's equation can be used across streamlines. Also, in practice, the "fluid has a constant density" statement means that density changes in the flow field need to be small compared to the mean density. The "flow is steady" statement not only excludes unsteady flows, but also all turbulent flows. The "flow is inviscid" statement means that the losses due to viscous effects need to be negligible, so that our interests lie outside regions where viscous stresses are important, as it is in boundary layers and wakes.

Although these restrictions sound severe, Bernoulli's equation is very useful, partly because it is so simple, but mostly because it can give great insight into the balance among the pressure, velocity and height in the motion of a fluid particle.

Bernoulli's equation can be derived directly from the Euler or Navier-Stokes equations, as shown in Section A.14. In the following section, it is obtained by applying Newton's second law along a streamline. We assume steady flow, so that fluid particles follow streamlines.

## 4.2.1   Force balance along streamlines

Consider a particle of fluid moving in a steady two-dimensional flow in the $z$-$y$ plane of a constant density fluid (Figure 4.4). Because the flow is steady, the particle moves along a streamline (see Section 4.1). Its velocity at a point along the streamline is $V$. The $z$-direction is measured vertically up from a horizontal reference plane, so that it increases in a direction opposite to the direction of gravity, and the $x$-direction is into the page. The $s$-direction is along the streamline, and the $n$-direction is normal to it.

If we neglect friction, the only forces acting on the particle are those due to its weight, and those due to pressure differences. The weight of the fluid particle is $dW = \rho g \, dn ds dx$, and its component in the $s$-direction is $dW_s = -\rho g \sin \beta \, dn ds dx$. Since $\sin \beta = \partial z / \partial s$ (see Figure 4.4),

$$dW_s = -\rho g \frac{\partial z}{\partial s} \, dn ds dx$$

The force due to pressure differences acting in the $s$-direction is $dF_{ps}$. By using a first order Taylor Series expansion (Section Appendix-A.10), we obtain

$$dF_{ps} = \left( p_0 - \left. \frac{\partial p}{\partial s} \right|_0 \frac{ds}{2} \right) dn dx - \left( p_0 + \left. \frac{\partial p}{\partial s} \right|_0 \frac{ds}{2} \right) dn dx \;\; = \;\; - \left. \frac{\partial p}{\partial s} \right|_0 dn ds dx$$

Hence, $F_s$, the resultant force per unit volume in the $s$-direction, is given by

$$F_s = \frac{dW_s}{dn ds dx} + \frac{dF_{ps}}{dn ds dx} \;\; = \;\; -\frac{\partial p}{\partial s} - \rho g \frac{\partial z}{\partial s} \tag{4.2}$$

where we have dropped the subscript 0 because the result should not depend on the particular point that was considered. This force will accelerate the fluid particle as it moves along the streamline. In a short distance $ds$, the velocity changes from $V$ to $V + \frac{\partial V}{\partial s} ds$, so that the rate of change of momentum of the fluid particle, per unit volume, is given by

$$\rho \frac{\left( V + \frac{\partial V}{\partial s} ds \right) - V}{dt} = \rho \frac{ds}{dt} \frac{\partial V}{\partial s} = \rho V \frac{\partial V}{\partial s}$$

since $V = ds/dt$. Using equation 4.2, we obtain (by Newton's second law)

$$\boxed{\rho V \frac{\partial V}{\partial s} \;\; = \;\; -\frac{\partial p}{\partial s} - \rho g \frac{\partial z}{\partial s}} \tag{4.3}$$
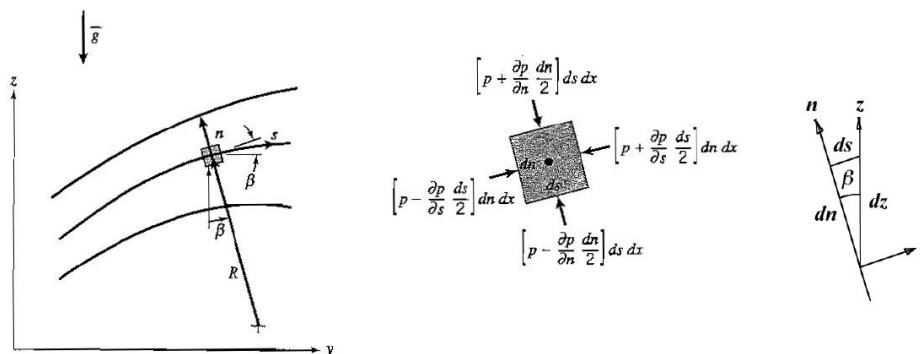
Figure 4.4: Fluid particle moving along a streamline.

This equation is called the one-dimensional Euler equation for steady flow, or the Euler equation *along* a streamline. By multiplying through by $ds$, we get

$$\frac{\partial p}{\partial s}ds + \rho V\frac{\partial V}{\partial s}ds + \rho g\frac{\partial z}{\partial s}ds = 0 \tag{4.4}$$

Now, since $s$ is the coordinate along the streamline,

$$\frac{\partial p}{\partial s}ds \;=\; dp \;=\; \text{change in pressure along streamline}$$

$$\frac{\partial V}{\partial s}ds \;=\; dV \;=\; \text{change in velocity along streamline}$$

$$\frac{\partial z}{\partial s}ds \;=\; dz \;=\; \text{change in elevation along streamline}$$

so that equation 4.4 becomes

$$\frac{dp}{\rho} + V\,dV + g\,dz \;=\; 0 \tag{4.5}$$

No restrictions have yet been placed on the density of the fluid particle, and so this relationship holds for flows with variable density. When the density is constant, however, we can integrate this relationship along the streamline to obtain

$$\frac{p}{\rho} + \frac{1}{2}V^2 + gz \;=\; \text{constant}$$

which is Bernoulli's equation for steady, constant density flow, without friction, along a streamline.

Since Bernoulli's equation was derived by applying Newton's second law along a streamline, it is a form of the momentum equation. Interestingly, however, each term in Bernoulli's equation has the dimensions of energy, or work, per unit mass. The quantity $\frac{1}{2}V^2$ is the kinetic energy per unit mass, $gz$ is the potential energy per unit mass, and $p/\rho$, being the integral of $dp/\rho$, is the work done by a unit mass of fluid against the change in pressure. For steady, constant density flow, without friction, Bernoulli's equation indicates that the sum of pressure work, kinetic energy, and potential energy remains constant along a streamline. This connection with the energy equation is explored further in Section 8.11.

## 4.2.2 Force balance across streamlines

Another useful result can be obtained by considering the force balance across streamlines for a steady inviscid, constant density flow. The weight of the fluid particle is $dW = \rho g\,dndsdx$,

and its component in the $n$-direction is $dW_n = -\rho g \cos \beta \, dndsdx$. Since $\cos \beta = \partial z / \partial n$ (see Figure 4.4),

$$dW_n = -\rho g \frac{\partial z}{\partial n} \, dndsdx$$

The force acting on the fluid particle due to pressure differences acting in the $n$-direction is $dF_{pn}$. By using a first order Taylor Series expansion (Section Appendix-A.10), we obtain

$$dF_{pn} = \left( p - \frac{\partial p}{\partial n} \frac{dn}{2} \right) dsdx - \left( p + \frac{\partial p}{\partial n} \frac{dn}{2} \right) dsdx \;\; = \;\; -\frac{\partial p}{\partial n} \, dndsdx$$

Hence, $F_n$, the resultant force per unit volume in the $s$-direction, is equal to

$$F_n = \frac{dF_{pn}}{dndsdx} + \frac{dW_n}{dndsdx} \;\; = \;\; -\frac{\partial p}{\partial n} - \rho g \frac{\partial z}{\partial n} \tag{4.6}$$

This force will accelerate the fluid particle in the direction normal to the streamline. The centripetal acceleration is given by $-V^2/R$, where $R$ is the local radius of curvature (see Figure 4.4), so that the rate of change of momentum of the fluid particle in the $n$-direction, per unit volume, is given by $-\rho \frac{V^2}{R}$. Using equation 4.6, we obtain (by Newton's second law)

$$\boxed{\rho \frac{V^2}{R} \;\; = \;\; \frac{\partial p}{\partial n} + \rho g \frac{\partial z}{\partial n}} \tag{4.7}$$

This is the momentum equation for steady, constant density flow without friction, *across* streamlines.

We see that, as the streamlines become straight and the radius of curvature becomes very large, the pressure across streamlines can only vary through hydrostatic pressure differences. If the effects of gravity are not important, and $R \to \infty$, then equation 4.7 gives that $\partial p / \partial n = 0$, that is, the pressure is constant across streamlines. Therefore, for a steady, inviscid flow,

---

The pressure across straight streamlines is constant when the effects of gravity can be neglected.

---

This is a very important result, and we shall make good use of it.

## 4.2.3   Pressure–velocity variation

Consider the flow shown in Figure 4.5, which was first considered in Section 3.5.2 using a large control volume. The flow is steady, and we will assume that there are no losses, and the density is constant. Because the streamlines are parallel at the entry and exit to the duct, the pressure is constant across the duct, except for hydrostatic pressure differences. If we ignore gravity, then the pressures over the inlet and outlet areas are constant. Along a streamline on the centerline, the Bernoulli equation and the one-dimensional continuity equation give, respectively,

$$p_1 - p_2 \;\; = \;\; \tfrac{1}{2} \rho \left( V_2^2 - V_1^2 \right)$$

$$\text{and} \qquad A_1 V_1 \;\; = \;\; A_2 V_2$$

Note that

$$\text{With } \; A_2 < A_1, \quad V_2 > V_1 \quad \begin{bmatrix} \text{decreasing area} \\ \text{increasing velocity} \end{bmatrix}$$
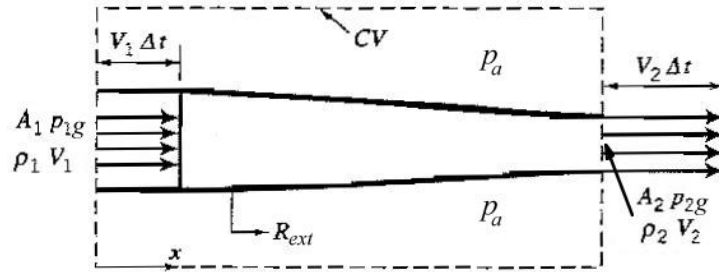
Figure 4.5: Flow in a one-dimensional duct where the inlet and outlet directions are aligned. This flow case was first analyzed using a large control volume in Section 3.5.2.

$$\text{With} \quad V_2 > V_1, \quad p_2 < p_1 \quad \left[ \begin{array}{c} \text{increasing velocity} \\ \text{decreasing pressure} \end{array} \right]$$

These two observations are illustrated in Figure 4.6. They provide an intuitive guide for analyzing fluid flows, even when the flow is not one-dimensional. For example, when fluid passes over a solid body the flow velocity increases, the streamlines get closer together, and the pressure decreases (see, for example, the steady flow over a cylinder shown in Figure 4.3).

### 4.2.4 Experiments on Bernoulli's equation

We see that when height differences along a streamline are not important, Bernoulli's equation expresses the relationship between velocity and pressure variations. Pressure differences can lead to large forces, as illustrated in the following simple experiments.

1. An easy experiment to demonstrate the force produced by an airstream requires a piece of notebook paper and two books of about equal thickness. Place the books four to five inches apart, and cover the gap with the paper. When you blow through the passage made by the books and the paper, what do you see? Why?

2. As a variation on this experiment, hold a piece of regular note paper by your fingertips at the corners on the short side. Then blow over the top in the direction of the long side. What do you see, and why?

3. In another experiment, use a hair dryer to make a jet of air that blows vertically up. Insert a table tennis ball in the center of the jet, and let it go. It will remain suspended by the jet of air. Push the ball down, and it will spring back up to its equilibrium position; push it sideways, and it will rapidly return to its original position in the center of the jet.



Figure 4.6: Pressure–velocity variation according to Bernoulli's equation.

Figure 4.7: Attracted disk experiment.

Why does this happen? In the vertical direction, the weight of the ball is balanced by a force due to pressure differences: the pressure over the rear half of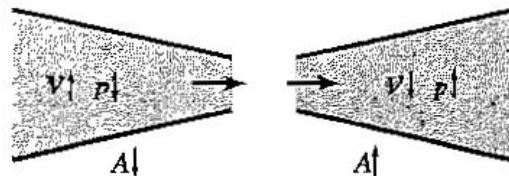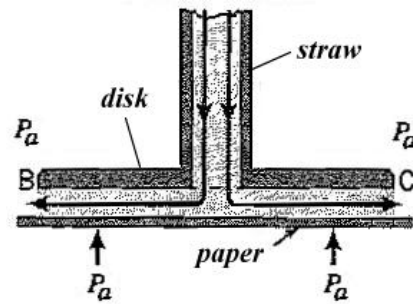 the sphere is lower than over the front half because of losses that occur in the wake. To understand the balance of forces in the horizontal direction, remember that if the streamlines in the jet flow are approximately parallel, the pressure inside the jet in the absence of the sphere is the same as the pressure outside the jet, so that the pressure is equal to atmospheric pressure everywhere. Now imagine the ball placed on the edge of the jet, so that one half is exposed to the flow, and the other half is not. On the side exposed to the jet, the flow velocity increases as it passes around the sphere, and the pressure falls below atmospheric. On the side outside the jet, the pressure remains atmospheric. The differences in pressure tend to move the ball back towards the center, and therefore it is stable.

4. Finally, cut a $50\,mm$ disk out of cardboard, punch a small hole in the center, and attach a straw to the hole. Place the assembly over a horizontal sheet of paper, as shown in Figure 4.7. When air is blown through the straw, the sheet of paper is forced against the disk instead of being blown off as might be expected. The explanation is based on the relationship between pressure and velocity. The velocity in the gap between the paper and disk is initially high, but it begins to decrease as the fluid flows outward since the area through which the flow passes increases with radius. At the same time, the pressure rises. However, at the exit ($B$ and $C$), the pressure must be equal to atmospheric pressure since the streamlines at the exit are parallel. The pressure in the gap must, therefore, be everywhere less than atmospheric. Since the pressure on the outside of the gap is atmospheric, and inside the gap it is less than atmospheric, there is a resultant force holding the paper against the disk due to pressure differences.

## 4.3   Applications of Bernoulli's Equation

One common use of Bernouli's equation is as a third equation, in addition to the continuity and momentum equations, for solving flow problems. Consider again the flow shown in Figure 4.5. The flow is steady, and we will assume that there are no losses, and the density is constant ($\rho_1 = \rho_2 = \rho$), so that we can apply the Bernoulli equation along a streamline. Hence,

$$p_1 + \frac{1}{2}\rho V_1^2 \;=\; p_2 + \frac{1}{2}\rho V_2^2$$

since $z_1 = z_2$. That is,

$$p_{2g} = p_{1g} + \frac{1}{2}\rho\left(V_1^2 - V_2^2\right)$$

and by using the continuity equation, we obtain

$$p_{2g} \; = \; p_{1g} + \frac{1}{2}\rho V_1^2 \left(1 - \frac{A_1^2}{A_2^2}\right)$$

Then, from the analysis given in Section 3.5.2 (specifically equation 3.13),

$$F_D = \rho A_1 V_1^2 \left(\frac{A_1}{A_2} - 1\right) + p_{1g}(A_2 - A_1) + \frac{1}{2}\rho V_1^2 A_2 \left(1 - \frac{A_1^2}{A_2^2}\right)$$

where $F_D$ is the force required to hold the duct in place. Bernoulli's equation was used to find the pressure $p_{2g}$, so that the force $F_D$ can now be found if $p_{1g}$, $V_1$, $A_1$ and $A_2$ are known.

We can go one step further and divide both sides by $\frac{1}{2}\rho V_1^2 A_1$, so that

$$\frac{F_D}{\frac{1}{2}\rho V_1^2 A_1} = 2\left(\frac{A_1}{A_2} - 1\right) + \frac{p_1}{\frac{1}{2}\rho V_1^2 A_1}(A_2 - A_1) + \frac{A_2}{A_1}\left(1 - \frac{A_1^2}{A_2^2}\right)$$

This step makes both sides of the equation nondimensional. The parameter on the left hand side is an example of a nondimensional force coefficient. This process of *nondimensionalization* is standard practice in fluid mechanics since it makes the answer more useful and elegant, as we shall see in Chapter 7.

## 4.3.1 Stagnation pressure and dynamic pressure

Bernoulli's equation leads to some interesting conclusions regarding the variation of pressure over solid bodies. Consider a steady flow of a constant density fluid impinging on a perpendicular plate, such as that shown in Figure 4.8. There is one streamline that divides the flow in half. Above this streamline, all the flow goes up the plate and below this streamline, all the flow goes down the plate. Along this dividing streamline, the fluid moves towards the plate. Since the flow cannot pass through the plate, the fluid must come to rest at the point where it meets the plate. In other words, it "stagnates." The fluid along the dividing, or *stagnation streamline* slows down and eventually comes to rest without deflection at the *stagnation point*.[2]

---

[2]At a stagnation point, the magnitude of the velocity is zero and its direction is indeterminate. This is an example of a singular or critical point, which is a point where streamlines can meet.
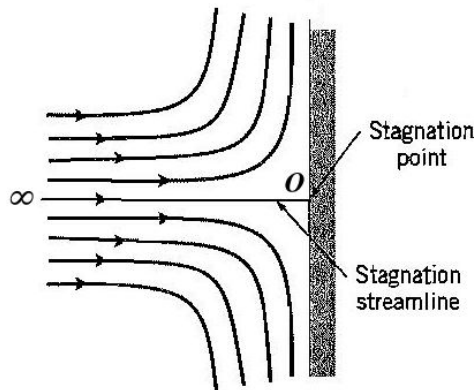


Figure 4.8: Stagnation point flow.

Neglecting viscous effects, Bernoulli's equation along the stagnation streamline gives

$$p_\infty + \tfrac{1}{2}\rho V_\infty^2 + \rho g z_\infty = p_0 + \tfrac{1}{2}\rho V_0^2 + \rho g z_0$$

where the point $\infty$ is far upstream and point 0 is at the stagnation point (Figure 4.8). Since $z_\infty = z_0$, and $V_0 = 0$,

$$\boxed{p_0 \;=\; p_\infty + \tfrac{1}{2}\rho V_\infty^2 \;=\; \text{stagnation pressure}} \tag{4.8}$$

The *stagnation* or *total* pressure, $p_0$, is the pressure measured at the point where the fluid comes to rest. It is the highest pressure found anywhere in the flow field, and it is the sum of the *static* pressure ($p_\infty$) and the *dynamic* pressure ($\tfrac{1}{2}\rho V_\infty^2$) measured far upstream. The quantity $\tfrac{1}{2}\rho V_\infty^2$ is called the dynamic pressure because it arises from the motion of the fluid. The dynamic pressure is not really a pressure at all: it is simply a convenient name for the quantity $\tfrac{1}{2}\rho V_\infty^2$, which represents the decrease in pressure due to the increase in fluid velocity.

We can also express the pressure anywhere in the flow in the form of a nondimensional pressure coefficient $C_p$, where

$$C_p \equiv \frac{p - p_\infty}{\tfrac{1}{2}\rho V_\infty^2}$$

At the stagnation point $C_p = 1$, which is its maximum value. In the freestream, far from the plate, $C_p = 0$.

### 4.3.2   Pitot tube

One of the most immediate applications of Bernoulli's equation is in the measurement of velocity with a Pitot tube. The Pitot tube (named after the French scientist and engineer Henry Pitot, 1695–1771) is perhaps the simplest and most useful fluid flow instrument ever devised (Figure 4.9). By pointing the tube directly into the flow and measuring the difference between the pressure sensed by the tube and the pressure in the surrounding air flow, the Pitot probe can provide a very accurate measure of the velocity. In fact, it is probably the most accurate method available for measuring flow velocity on a routine basis, and accuracies better than 1% are easily possible. Pitot tubes are widely used in flow measurement applications. For instance, they are standard equipment on airplanes, where a Pitot tube is combined with a static port located somewhere on the fuselage to measure the relative airspeed.

To see how the Pitot tube works, consider the example of a Pitot tube mounted in a wind tunnel. Bernoulli's equation along the streamline that begins far upstream of the tube and comes to rest in its mouth (station 0) gives

$$p_\infty + \tfrac{1}{2}\rho_a V_\infty^2 + \rho_a g z_\infty = p_0 + \tfrac{1}{2}\rho_a V_0^2 + \rho_a g z_0$$

where $\rho_a$ is the density of air. Since $z_\infty = z_0$, and $V_0 = 0$,

$$p_0 = p_\infty + \tfrac{1}{2}\rho_a V_\infty^2 \tag{4.9}$$

We see that the Pitot tube measures the stagnation pressure in the flow. We can also write

$$p_0 - p_\infty = \tfrac{1}{2}\rho_a V_\infty^2 \tag{4.10}$$

Therefore, to find the velocity $V_\infty$, we need to know the density of air and the pressure difference $p_0 - p_\infty$. The density can be found from standard tables if the temperature and the atmospheric pressure are known.    The pressure difference $p_0 - p_\infty$ is usually found
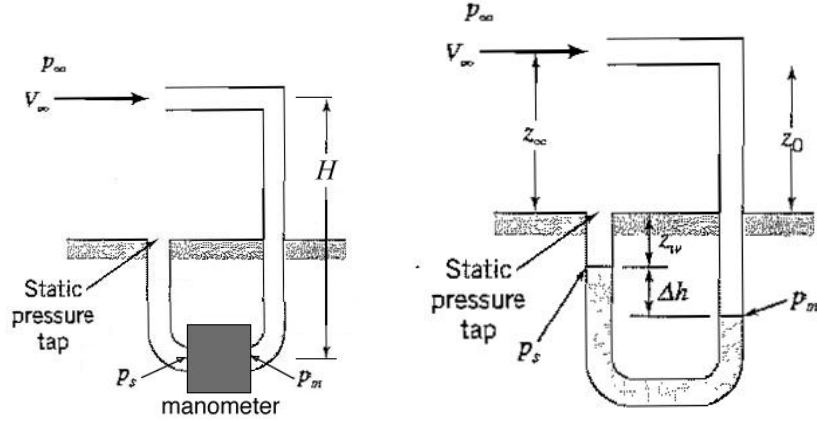
Figure 4.9: Pitot tube in a wind tunnel. (a) Electronic manometer. (b) Liquid manometer.

indirectly by using a *static pressure tap* located on the wall of the wind tunnel (as shown in Figure 4.9). A differential electronic manometer [Figure 4.9(a)] will measure the difference $p_m - p_s$, and by using the hydrostatic equation twice we obtain

$$
\begin{aligned}
p_s &= p_\infty + \rho_a g H \\
p_m &= p_0 + \rho_a g H
\end{aligned}
$$

so that

$$
p_m - p_s = p_0 - p_\infty = \tfrac{1}{2}\rho_a V_\infty^2
$$

Therefore,

$$
V_\infty = \sqrt{\frac{2}{\rho_a}\left(p_m - p_s\right)}
$$

If a liquid manometer is used, as in Figure 4.9(b), we apply the hydrostatic equation three times to find

$$
\begin{aligned}
p_s &= p_\infty + \rho_a g \left(z_w + z_0\right) & (4.11) \\
p_m &= p_0 + \rho_a g \left(z_w + z_0 + \Delta h\right)
\end{aligned}
$$

$$
\text{and} \qquad p_m - p_s = \rho_m g \Delta h
$$

where $\rho_m$ is the density of the manometer fluid. Hence,

$$
p_0 - p_\infty = \rho_m g \Delta h - \rho_a g \Delta h.
$$

Using equation 4.10, we obtain

$$
V_\infty^2 = 2g\frac{\rho_m}{\rho_a}\left(1 - \frac{\rho_a}{\rho_m}\right)\Delta h \qquad (4.12)
$$

Since $\rho_m$ is always much greater than $\rho_a$, we have, to a very good approximation,

$$
V_\infty = \sqrt{2g\frac{\rho_m}{\rho_a}\Delta h} \qquad (4.13)
$$

Therefore, the velocity can be found by measuring the manometer deflection, and by knowing the density of air and the density of the manometer fluid.

Figure 4.10: Pitot-static tube of the Prandtl type. From Rae & Pope *Low-Speed Wind Tunnel Testing*, 2nd. ed., Wiley-Interscience, 1984.

The Pitot tube is sometimes combined with a static tube to make a single unit called a Pitot-static tube (Figure 4.10). A static tube is a closed tube aligned with the flow direction. At some distance from the nose, small pressure tappings are drilled in the tube wall to measure the local static pressure. In a Pitot-static tube, the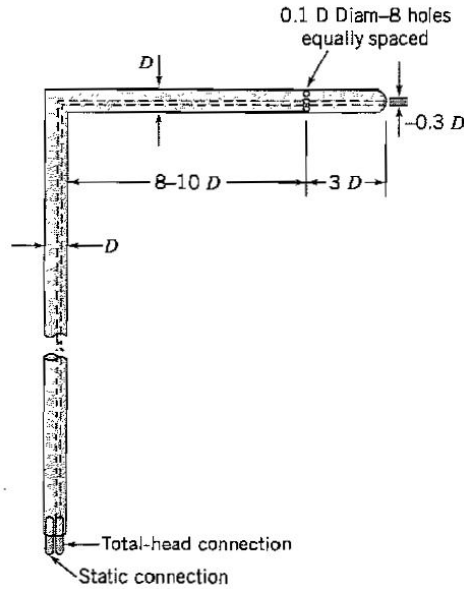 two tubes are installed one inside the other. The inner tube is open at the end and measures the total pressure, while the outer tube serves as a static tube to measure the static pressure. The two tubes can be connected to a manometer to read the dynamic pressure. The accuracy of the Pitot-static tube depends on its construction and installation. It is more sensitive to misalignment with the flow direction than a Pitot tube, and to achieve high accuracy it should be calibrated against a known standard. Such calibrated Pitot-static tubes are readily available commercially.

### 4.3.3   Venturi tube and atomizer

The relationship between pressure and velocity expressed by Bernoulli's equation is used in the design of the Venturi tube (Figure 4.11). This device is made up of a contracting section followed by a diverging section, and its shape is chosen to minimize losses due to friction or flow separation. One application of the Venturi tube is as a flow measurement device for the steady flow of a constant-density fluid. As the fluid passes through the tube, it reaches its maximum velocity and minimum pressure at the smallest cross-sectional area. Using the one-dimensional continuity equation and Bernoulli's equation, we have

$$V_A A_A = V_B A_B$$

$$\frac{p_A}{\rho} + \tfrac{1}{2}V_A^2 = \frac{p_B}{\rho} + \tfrac{1}{2}V_B^2$$

so that

$$p_A - p_B = \tfrac{1}{2}\rho V_A^2 \left( \left( \frac{A_A}{A_B} \right)^2 - 1 \right)$$

By measuring the pressure difference $p_A - p_B$ and knowing the dimensions of the Venturi tube and the density of the fluid, we can find the flow velocity. The Venturi tube is used
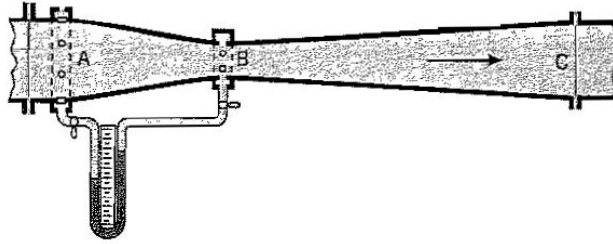
Figure 4.11: Venturi tube. From Martin and Conner, *Basic Physics*, 8th ed., published by Whitcombe & Tombs Pty. Ltd., Melbourne, Australia, 1962, with permission.

when an accurate velocity measurement is required in a piping system without introducing substantial losses.

Carburetors also make use of the Venturi principle. Here, the low pressure at the throat of the Venturi tube is used to draw fuel into the main flow stream. If the pressure is low enough at the throat, the fuel will break up into drops and vaporize before entering the engine combustion chamber.

A further use of this concept is in an atomizer (Figure 4.12). A stream of air blown through the pipe $A$ passes directly above the open end of the tube $B$, the other end of which dips into a liquid in the container $C$ which is open to the atmosphere. The tube is designed so that the airstream diverges after passing $B$. Far from the tube exit, at $F$, the pressure must be atmospheric, so that the pressure at $B$ must be below atmospheric (since the flow must slow down as it goes from $B$ to $F$). Therefore the pressure of the atmosphere acting on the surface of the liquid in $C$ forces it up to $B$ where it is entrained in the airstream and carried forward as a spray. Paint sprayers, perfume sprayers and snowmakers at ski resorts all operate in this way.

### 4.3.4   Siphon

A siphon can be used to drain liquid from an open tank. It consists of a tube, with one end immersed in the liquid and the other end kept outside the liquid and below the level of the free surface (see Figure 4.13). If there are no losses, and the flow is steady, we can use Bernoulli's equation to find the speed of the jet issuing from the open end of the tube, and the minimum pressure in the tube.

When the tank is large, the level of the water falls very slowly and we can assume that the velocity of the free surface is almost zero. This is called the *quasi-steady* assumption, where the flow is not really steady but it is steady enough to apply Bernoulli's equation, for example. To draw a streamline, we should remember that a streamline is a line which is tangential to the instantaneous velocity vector. If we took a short-exposure photograph of some marked fluid particles, we would see that the velocity vectors throughout most of the tank are directed towards the entrance of the tube. So we can start the streamline at the bottom of the tank, or halfway up, or at the surface of the water. However, to make a particular streamline useful, it must connect a point where we have information with a point where we need information. At the free surface in the tank we know that $V_1 = 0$, and that the pressure is atmospheric. Since two parameters are known at the surface, this is a good starting place for the streamline. To find the conditions at the exit of the tube, we draw the streamline to connect to a point in the exit plane. Then, if there are no losses, and the flow is steady (or at least quasi-steady),

$$\frac{p_a}{\rho} + 0 + gz_3 \;=\; \frac{p_3}{\rho} + \tfrac{1}{2}V_3^2 + 0$$
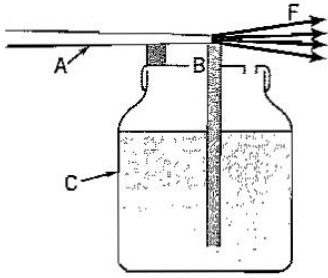
Figure 4.12: Atomizer. From Martin and Conner, *Basic Physics*, 8th ed., published by Whitcombe & Tombs Pty. Ltd., Melbourne, Australia, 1962, with permission..
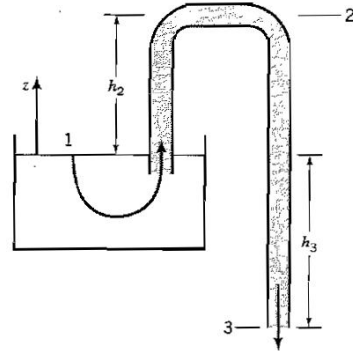
Figure 4.13: Siphon, used to transfer liquids from a higher to a lower level.

What about the pressure at the exit of the tube, $p_3$? Close to the exit the flow streamlines are nearly parallel and the pressure surrounding the jet is atmospheric. In a steady flow, the pressure can only vary across straight streamlines due to hydrodynamic pressure gradients (see Section 4.2.2). There can be no hydrostatic pressure differences across the jet, since it is in free fall, so that with $V_1 = 0$ and $p_3 = p_1 = p_a$,

$$V_3 = \sqrt{2gz_3} \tag{4.14}$$

To obtain this result, we assumed that the flow was along a streamline, the fluid had a constant density, the flow was steady, and there were no losses. We also implicitly assumed that the flow was one-dimensional. These are all approximations, and perhaps the most questionable assumptions were that the flow was one-dimensional and that it experienced no losses. We know that the flow in a tube is subject to the no-slip condition, and therefore there will be viscous forces acting and energy losses taking place. One way to think about this is to recognize that equation 4.14 can be interpreted as indicating that the potential energy of the fluid available at point 1 has all been converted to kinetic energy at point 1. If there were losses along the way, we would expect that the kinetic energy at the exit would be less than the available potential energy, so that $V_3 < \sqrt{2gz_3}$. Therefore equation 4.14 gives the maximum possible value of $V_3$, and in practice we would expect to see a lower value.

We can also use Bernoulli's equation to track the pressure variation along the tube. The cross-sectional area of the tube does not vary, and therefore by continuity the velocity in all parts of the tube is equal to $V_3$. Since the velocity in the tube is constant, the minimum pressure will occur at the maximum height of the tube, that is, at point 2. Here,

$$\frac{p_1}{\rho} + \tfrac{1}{2}V_1^2 + 0 \; = \; \frac{p_2}{\rho} + \tfrac{1}{2}V_2^2 + gz_2$$

With $V_1 = 0$, $p_1 = p_a$, and $V_2 = V_3 = \sqrt{2gz_3}$

$$\frac{p_a}{\rho} \; = \; \frac{p_2}{\rho} + gz_3 + gz_2$$

That is,

$$\frac{p_2}{\rho} \; = \; \frac{p_a}{\rho} - g\left(z_3 + z_2\right)$$

We see that the pressure at point 2 is below atmospheric.

### 4.3.5 Vapor pressure

If the elevation of point 2 in Figure 4.13 is high enough, the pressure can become equal to the vapor pressure of the liquid. The vapor pressure $p_v$ of a liquid is the equilibrium pressure of a vapor above its liquid, that is, the pressure of the vapor that comes from the evaporation of a liquid in a closed container. If the liquid pressure is greater than the vapor pressure, the only exchange between the liquid and vapor phases is evaporation at a free surface. If the liquid pressure falls below the vapor pressure, vapor bubbles begin to appear in the body of the liquid. That is, the liquid will begin to boil. For water at $100°C$, the vapor pressure is $101,325\,Pa$, which is equal to atmospheric pressure. Therefore water boils at $100°C$ under standard atmospheric conditions. For water at $20°C$ the vapor pressure is $2338\,Pa$ (see Table Appendix-C.3), which is equal to $0.0232\,atm$. Since $1\,atm = 10.33\,m$, we find that for the siphon shown in Figure 4.13, if

$$z_2 + z_3 > (1 - 0.0232) \times 10.33\,m = 10.1\,m$$

the water will boil and a vapor lock could form that would prevent proper functioning of the siphon.

Because the air pressure decreases with increasing altitude, it will approach the vapor pressure of water with increasing altitude, and water will start to boil at a lower temperature. At an altitude of $13000\,m$, for example, where the atmospheric pressure is $70,120\,Pa$ (Table Appendix-C.5), water boils at $90°C$, not $100°C$.

A liquid can also boil if its velocity is high enough so that the static pressure in the liquid drops below the vapor pressure. The formation of vapor bubbles, when followed by their collapse, is then called *cavitation*, and it can cause severe erosion on marine propellers, where low pressure regions are found near the tips of the blades (Figure 7.1). Just below the water surface, the static pressure equals the vapor pressure at a speed of about $15\,m/s$ ($50\,ft/s$, or $= 34\,mph$). Cavitation can therefore be a problem at relatively modest speeds, although in practice it may not occur until the pressure is well below the vapor pressure. At greater depths, the pressure in the surrounding fluid increases according to the hydrostatic equation, and the onset of cavitation is delayed to higher velocities.

### 4.3.6 Draining tanks

Consider water draining out of a large tank (Figure 4.14). The tank is large enough so that we can use the quasi-steady assumption. Along a streamline connecting a point at the free surface with a point in the exit plane of the jet, we have

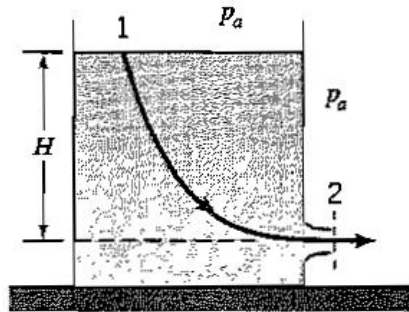$$\frac{p_1}{\rho} + 0 + gH \;=\; \frac{p_2}{\rho} + \tfrac{1}{2}V_2^2 + 0$$



Figure 4.14: Water draining out of a large tank.
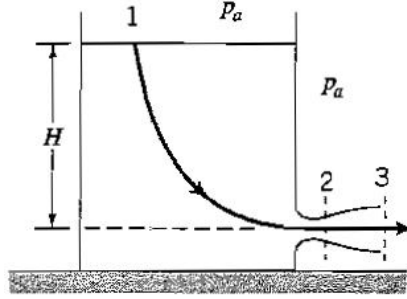
Figure 4.15: Tank exit with an expanding drain.

If the streamlines at the exit of the jet are parallel, $p_2 = p_a$. Also, the jet is in free fall, so that hydrostatic pressure differences across the jet are zero. With $V_1 = 0$, and $p_2 = p_1 = p_a$,

$$V_2 = \sqrt{2gH}$$

This is known as Torricelli's formula.

What is the discharge rate? The volume discharge $\dot{q}$ is the volume outflow per unit time, that is, the volume flow rate out of the tank, given by $A_2 V_2$, where $A_2$ is the cross-sectional area of the jet. So the volume outflow per unit time is simply $A_2 V_2$. Similarly, the mass flow discharge, or the mass flow rate leaving the tank, is given by $\rho A_2 V_2$. Hence, for the flow leaving the tank,

$$\dot{q} \;=\; \text{volume discharge rate} \;=\; A_2 V_2 \;=\; A_2 \sqrt{2gH}$$
$$\dot{m} \;=\; \text{mass discharge rate} \;=\; \rho A_2 V_2 \;=\; \rho A_2 \sqrt{2gH}$$

What if the orifice was modified to have a diverging section, so that the area increases from $A_2$ to $A_3$ (Figure 4.15)? If the streamlines are parallel at the exit, the pressure at the exit, $p_3$, is atmospheric. If there are no losses, we see that the exit velocity is still $\sqrt{2gH}$. The volume discharge, however, has increased to $A_3\sqrt{2gH}$ so that it is greater than before by the ratio $A_3/A_2$. Provided there are no losses, the exit velocity is independent of the exit area but the discharge increases as the exit area increases.

What has happened at the point $A_2$? Because of mass conservation, the velocity at $A_2$ is larger than the velocity at $A_3$ by the ratio $A_3/A_2$. Since the pressure at $A_3$ is atmospheric, the pressure at $A_2$ is below atmospheric, and the exit nozzle acts similar to a Venturi tube (see Section 4.3.3). If the pressure at station 2 drops below the vapor pressure, cavitation can occur (see Section 4.3.5).

# Chapter 5

# Differential Equations of Motion

In Chapter 3, we used large control volumes to find the overall balances of mass, momentum and energy, without describing the specific flow behavior inside the control volume. These balances were expressed by a set of equations in integral form (equations 3.9, 3.20, and 3.25). For some purposes this approach can provide very useful information, as in finding the forces exerted by the fluid on an object held inside the control volume. For many other purposes we need to have a more detailed knowledge of the flow behavior. For instance, as we pointed out in Section 3.1, the performance of an airplane depends critically on its shape. For an airplane in cruise, the lift is primarily generated by the pressure differences between the bottom and top surfaces of the wing. A large part of the drag, on the other hand, is due to the viscous friction between the fluid and the surface of the airplane. Both lift and drag depend strongly on the shapes of the wing and the fuselage. A large control volume cannot give very specific insight into how these shapes can be designed.

In Chapter 4, we saw that in some cases we can use Bernoulli's equation to gain insight in the distribution of velocity and pressure within the flow field. Bernoulli's equation was derived by applying Newton's second law to the motion of fluid particles along streamlines, and itapplies only for steady, incompressible flow with no viscous effects. To derive the general form of the equations of motion as they apply to all points within a flow field, so that we can understand the complete flow behavior, we will use very small control volumes or fluid elements, which means we will adopt an Eulerian description of the flow field. This approach leads to a set of differential equations describing the detailed motion of the fluid. We will derive the continuity and momentum equations, but we will not consider the differential form of the energy equation.

We could obtain these equations directly from their integral forms. This is done in Section A.12. Here, we choose to derive them from first principles. To begin this analysis, we need to express the rate of change of velocity, density and pressure of a fluid particle in the Eulerian system.

## 5.1   Rate of Change Following a Fluid Particle

How are we to describe the displacement, velocity and acceleration of a fluid? As indicated in Section 3.1, there are two possibilities: the Lagrangian system and the Eulerian system. In the Lagrangian system, we follow fluid particles which are of fixed mass, whereas in the Eulerian system we look for a "field" description which gives all the details of the entire flow field at any position and time, and we do not follow individual fluid particles.

To apply Newton's laws of mechanics, as well as other principles such as the conservation of mass and energy, it is necessary to refer to fixed quantities of matter, that is, fluid particles. A Lagrangian system would therefore seem ideal for deriving the equations of motion of a

fluid. However, a full description of the flow field in a Lagrangian system requires that a very large number of fluid particles be followed, and it is usually easier to adopt an Eulerian description instead.

To make the Eulerian representation useful, we need to find a way to express the rate of change of properties of a fluid particle of fixed mass at a fixed point in the flow field. The *total derivative* provides us with the required link between the Lagrangian and Eulerian descriptions for small, fixed control volumes, in the same way as the Reynolds transport theorem (Section A.15) provides a link between the two descriptions for large, fixed control volumes.

In the Eulerian system, density, pressure and velocity are functions of four independent variables. In Cartesian coordinates, for example, $\rho = \rho(x, y, z, t)$. Similarly, $\mathbf{V} = u\mathbf{i} + v\mathbf{j} + w\mathbf{k}$, where $u$, $v$ and $w$ are the velocity components in the $x$-, $y$- and $z$-directions, and each component is a function of $x$, $y$, $z$ and $t$.

Consider a fluid particle as it moves a distance $\Delta x$, $\Delta y$ and $\Delta z$ in space during a time $\Delta t$. The velocity changes by an amount $\Delta \mathbf{V}$, and by the chain rule of differentiation

$$\Delta \mathbf{V} \;=\; \frac{\partial \mathbf{V}}{\partial t}\Delta t + \frac{\partial \mathbf{V}}{\partial x}\Delta x + \frac{\partial \mathbf{V}}{\partial y}\Delta y + \frac{\partial \mathbf{V}}{\partial z}\Delta z$$

Dividing through by $\Delta t$

$$\frac{\Delta \mathbf{V}}{\Delta t} \;=\; \frac{\partial \mathbf{V}}{\partial t} + \frac{\partial \mathbf{V}}{\partial x}\frac{\Delta x}{\Delta t} + \frac{\partial \mathbf{V}}{\partial y}\frac{\Delta y}{\Delta t} + \frac{\partial \mathbf{V}}{\partial z}\frac{\Delta z}{\Delta t}$$

and as $\Delta t$ approaches small values,

$$\frac{d\mathbf{V}}{dt}\bigg|_{sys} = \frac{\partial \mathbf{V}}{\partial t} + \frac{\partial \mathbf{V}}{\partial x}\frac{dx}{dt}\bigg|_{sys} + \frac{\partial \mathbf{V}}{\partial y}\frac{dy}{dt}\bigg|_{sys} + \frac{\partial \mathbf{V}}{\partial z}\frac{dz}{dt}\bigg|_{sys}$$

where we have identified the derivatives pertaining to the properties of the fluid particle (the "system"). We use the following shorthand notation:

$$\frac{D}{Dt} \equiv \frac{d}{dt}\bigg|_{sys}$$

so that

$$\frac{D\mathbf{V}}{Dt} \;=\; \frac{\partial \mathbf{V}}{\partial t} + u\frac{\partial \mathbf{V}}{\partial x} + v\frac{\partial \mathbf{V}}{\partial y} + w\frac{\partial \mathbf{V}}{\partial z} \tag{5.1}$$

because $u = dx/dt$, $v = dy/dt$, and $w = dz/dt$. The special symbol $D/Dt$ denotes the *total derivative*, that is, the derivative of a system quantity that depends on three space variables as well as time. In Cartesian coordinates,

$$\frac{D}{Dt} \;=\; \frac{\partial}{\partial t} + u\frac{\partial}{\partial x} + v\frac{\partial}{\partial y} + w\frac{\partial}{\partial z} \tag{5.2}$$

The first term in the definition of the total derivative represents the variation with time at a given point. It is called the *local* part of the total derivative, and it is the only source of variation in a field that is uniform in space. When the flow is unsteady, the local part is non-zero. In other words, if the partial derivative of the velocity, pressure or density with respect to time is not zero, the flow field is unsteady.

The last three terms in the definition of the total derivative represent the variation that occurs in space, and it is called the *convective* part of the total derivative. In a non-uniform flow field, the velocity can vary in all three directions. As a fluid particle passes through a given point, its velocity changes in response to the spatial variations of velocity. The rate
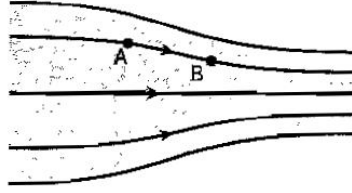
Figure 5.1: Steady flow through a converging duct.

at which its velocity is changing will depend on the spatial gradients of the velocity, and the speed at which it is moving from one point to another. To be more explicit, consider the steady, constant density flow through a converging duct shown Figure 5.1. The velocity at point A does not vary with time, but we know the velocity at point B is greater than at point A because the cross-sectional area is smaller. Therefore a fluid particle experiences an acceleration as it moves from A to B: this part of the acceleration is described by the convective acceleration. If the mass flow rate through the duct was also unsteady, the local acceleration would then make a contribution because the velocity at each point would change with time as well as with position.

The total derivative, therefore, gives the rate at which the properties of a fluid particle change when the flow field is expressed in an Eulerian system.

> The total derivative $D/Dt$ is the rate of change of a fluid property following a fluid particle.

It is also called the *particle derivative*, the *substantial derivative* or the *material derivative*.

The symbol $D/Dt$ denotes an "operator" which, when acting on the velocity, gives the acceleration in an Eulerian system (see equation 5.1). It is sometimes written as the sum of the local and convective accelerations, so that

$$\frac{D}{Dt} = \frac{\partial}{\partial t} + \mathbf{V} \cdot \nabla$$

It is incorrect to think of $\mathbf{V} \cdot \nabla$ as the scalar product of two vectors. It is best thought of as another operator such that, in Cartesian coordinates,

$$\mathbf{V} \cdot \nabla = u\frac{\partial}{\partial x} + v\frac{\partial}{\partial y} + w\frac{\partial}{\partial z}$$

Scalar products are commutative, which means that the order of multiplication does not change the result. In contrast, $\mathbf{V} \cdot \nabla$ and $\nabla \cdot \mathbf{V}$ are not the same at all: one is an operator and the other is an operation (see Section A.11).

## 5.1.1 Acceleration in Cartesian coordinates

Equation 5.1 expresses the *total acceleration* following a fluid particle in Cartesian coordinates. It is the sum of the local acceleration and the convective acceleration, and it contains time and space derivatives of the vector velocity $\mathbf{V}$. With $\mathbf{V} = u\mathbf{i} + v\mathbf{j} + w\mathbf{k}$, we have

$$\frac{\partial \mathbf{V}}{\partial t} = u\frac{\partial \mathbf{i}}{\partial t} + \mathbf{i}\frac{\partial u}{\partial t} + v\frac{\partial \mathbf{j}}{\partial t} + \mathbf{j}\frac{\partial v}{\partial t} + w\frac{\partial \mathbf{k}}{\partial t} + \mathbf{k}\frac{\partial w}{\partial t} = \mathbf{i}\frac{\partial u}{\partial t} + \mathbf{j}\frac{\partial v}{\partial t} + \mathbf{k}\frac{\partial w}{\partial t}$$

since the unit vectors $\mathbf{i}$, $\mathbf{j}$ and $\mathbf{k}$ have a constant magnitude and direction, and therefore their derivatives are zero. Similarly,

$$\frac{\partial \mathbf{V}}{\partial x} = \mathbf{i}\frac{\partial u}{\partial x} + \mathbf{j}\frac{\partial v}{\partial x} + \mathbf{k}\frac{\partial w}{\partial x}$$

$$\frac{\partial \mathbf{V}}{\partial y} = \mathbf{i}\frac{\partial u}{\partial y} + \mathbf{j}\frac{\partial v}{\partial y} + \mathbf{k}\frac{\partial w}{\partial y}$$

$$\frac{\partial \mathbf{V}}{\partial z} = \mathbf{i}\frac{\partial u}{\partial z} + \mathbf{j}\frac{\partial v}{\partial z} + \mathbf{k}\frac{\partial w}{\partial z}$$

so that

$$
\frac{D\mathbf{V}}{Dt} = \left(\frac{\partial u}{\partial t} + u\frac{\partial u}{\partial x} + v\frac{\partial u}{\partial y} + w\frac{\partial u}{\partial z}\right)\mathbf{i}
$$
$$
+ \left(\frac{\partial v}{\partial t} + u\frac{\partial v}{\partial x} + v\frac{\partial v}{\partial y} + w\frac{\partial v}{\partial z}\right)\mathbf{j}
$$
$$
+ \left(\frac{\partial w}{\partial t} + u\frac{\partial w}{\partial x} + v\frac{\partial w}{\partial y} + w\frac{\partial w}{\partial z}\right)\mathbf{k} \tag{5.3}
$$

which reveals the full complexity of the acceleration in an Eulerian description. In particular, consider a term like $u\partial u/\partial x$, which can be written as $\frac{1}{2}\partial u^2/\partial x$. We recognize that this term is nonlinear, and the complexity that nonlinearity introduces in describing the motion of fluids is discussed in Section 5.3.2.

### 5.1.2  Acceleration in cylindrical coordinates

The form of the operator $D/Dt$ depends on the coordinate system. In a cylindrical coordinate system, $\mathbf{V}(r,\theta,z,t) = u_r\mathbf{e_r} + u_\theta\mathbf{e_\theta} + u_z\mathbf{e_z}$, where $u_r$, $u_\theta$ and $u_z$ are the velocity components, and $\mathbf{e_r}$, $\mathbf{e_\theta}$ and $\mathbf{e_z}$ are the unit vectors in the $r$, $\theta$, and $z$-directions, respectively (see Figure 5.2). Given that

$$u_r = \frac{dr}{dt}, \quad u_\theta = r\frac{d\theta}{dt} \quad \text{and} \quad u_z = \frac{dz}{dt}$$

we find that

$$\frac{D\mathbf{V}}{Dt} = \frac{\partial \mathbf{V}}{\partial t} + u_r\frac{\partial \mathbf{V}}{\partial r} + \frac{u_\theta}{r}\frac{\partial \mathbf{V}}{\partial \theta} + u_z\frac{\partial \mathbf{V}}{\partial z} \tag{5.4}$$

To find the derivatives of the velocity, we need to remember that $\mathbf{e_r}$ and $\mathbf{e_\theta}$ are not constant vectors: they depend on $\theta$, and their derivatives with respect to $\theta$ do not vanish. When the coordinate $\theta$ changes by a small amount $d\theta$, the unit vectors $\mathbf{e_r}$ and $\mathbf{e_\theta}$ change by an amount $d\mathbf{e_r}$ and $d\mathbf{e_\theta}$. From Figure 5.3, we see that the direction of $d\mathbf{e_\theta}$ is opposite to the direction of $\mathbf{e_r}$. Since the triangles $abc$ and $lmn$ are similar, the magnitude of $d\mathbf{e_\theta}$ is $d\theta$, and therefore

$$d\mathbf{e_\theta} = -\mathbf{e_r}\,d\theta$$

Similarly,

$$d\mathbf{e_r} = \mathbf{e_\theta}\,d\theta$$

and so we have

$$\frac{\partial \mathbf{e_r}}{\partial \theta} = \mathbf{e_\theta} \qquad \text{and} \qquad \frac{\partial \mathbf{e_\theta}}{\partial \theta} = -\mathbf{e_r}$$

That is:

$$
\frac{\partial \mathbf{V}}{\partial \theta} = \mathbf{e_r}\frac{\partial u_r}{\partial \theta} + u_r\frac{\partial \mathbf{e_r}}{\partial \theta} + \mathbf{e_\theta}\frac{\partial u_\theta}{\partial \theta} + u_\theta\frac{\partial \mathbf{e_\theta}}{\partial \theta} + \mathbf{e_z}\frac{\partial u_z}{\partial \theta}
$$
$$
= \mathbf{e_r}\frac{\partial u_r}{\partial \theta} + u_r\mathbf{e_\theta} + \mathbf{e_\theta}\frac{\partial u_\theta}{\partial \theta} - u_\theta\mathbf{e_r} + \mathbf{e_z}\frac{\partial u_z}{\partial \theta}
$$
$$
= \left(\frac{\partial u_r}{\partial \theta} - u_\theta\right)\mathbf{e_r} + \left(u_r + \frac{\partial u_\theta}{\partial \theta}\right)\mathbf{e_\theta} + \frac{\partial u_z}{\partial \theta}\mathbf{e_z}
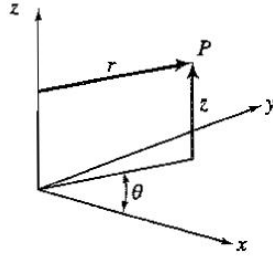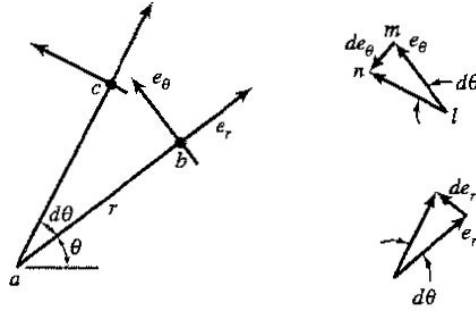$$

Figure 5.2: Cylindrical coordinate system.

Figure 5.3: Rate of change of unit vectors in a cylindrical coordinate system.

It follows that the acceleration in cylindrical coordinates is given by

$$
\begin{aligned}
\frac{D\mathbf{V}}{Dt} &= \left( \frac{\partial u_r}{\partial t} + u_r \frac{\partial u_r}{\partial r} + \frac{u_\theta}{r} \frac{\partial u_r}{\partial \theta} + u_z \frac{\partial u_r}{\partial z} - \frac{u_\theta^2}{r} \right) \mathbf{e_r} \\
&+ \left( \frac{\partial u_\theta}{\partial t} + u_r \frac{\partial u_\theta}{\partial r} + \frac{u_\theta}{r} \frac{\partial u_\theta}{\partial \theta} + u_z \frac{\partial u_\theta}{\partial z} + \frac{u_r u_\theta}{r} \right) \mathbf{e_\theta} \\
&+ \left( \frac{\partial u_z}{\partial t} + u_r \frac{\partial u_z}{\partial r} + \frac{u_\theta}{r} \frac{\partial u_z}{\partial \theta} + u_z \frac{\partial u_z}{\partial z} \right) \mathbf{e_z}
\end{aligned}
\tag{5.5}
$$

## 5.2  Continuity Equation

We are now ready to derive the continuity equation in differential form for an Eulerian system, in Cartesian coordinates. Consider the elemental volume $dx\,dy\,dz$ shown Figure 5.4). The rate of change of mass contained in the volume plus the net rate of mass flow out of the volume must be zero. We begin by finding the net mass flow rate out of the volume. We do this by finding the mass passing through through each of the six faces and summing the result. We start with faces $abcd$ and $efgh$ which have an area $dA = dydz$. During a short time interval $\Delta t$,

$$
\begin{aligned}
\text{mass flow in} \\
\text{through } abcd &= (\rho u\,dA)_{abcd}\,\Delta t \\
&= \left( \rho_0 - \left.\frac{\partial \rho}{\partial x}\right|_0 \frac{dx}{2} \right) \left( u_0 - \left.\frac{\partial u}{\partial x}\right|_0 \frac{dx}{2} \right) dy\,dz\,\Delta t \\
&= \left( \rho_0 u_0 - u_0 \left.\frac{\partial \rho}{\partial x}\right|_0 \frac{dx}{2} - \rho_0 \left.\frac{\partial u}{\partial x}\right|_0 \frac{dx}{2} \right) dy\,dz\,\Delta t
\end{aligned}
$$

where we have used a first order Taylor series expansion around the center of the volume, indicated by the subscript 0. Similarly, during the interval $\Delta t$,

$$
\begin{aligned}
\text{mass flow out} \\
\text{through } efgh &= (\rho u\,dA)_{efgh}\,\Delta t \\
&= \left( \rho_0 + \left.\frac{\partial \rho}{\partial x}\right|_0 \frac{dx}{2} \right) \left( u_0 + \left.\frac{\partial u}{\partial x}\right|_0 \frac{dx}{2} \right) dy\,dz\,\Delta t
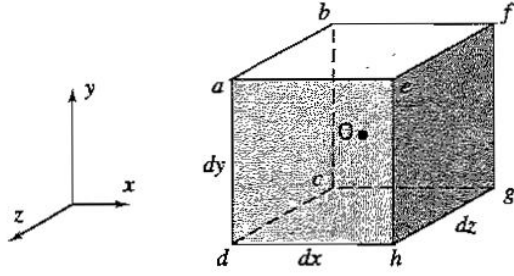\end{aligned}
$$

Figure 5.4: Elemental control volume for derivation of the differential form of the continuity equation.

$$= \left( \rho_0 u_0 + u_0 \left. \frac{\partial \rho}{\partial x} \right|_0 \frac{dx}{2} + \rho_0 \left. \frac{\partial u}{\partial x} \right|_0 \frac{dx}{2} \right) dy\, dz\, \Delta t$$

Dropping higher order terms and dividing through by $\Delta t$, we find

$$\begin{aligned} \text{net mass flow rate out} \\ \text{through } abcd \text{ and } efgh \end{aligned} = \left( u_0 \left. \frac{\partial \rho}{\partial x} \right|_0 + \rho_0 \left. \frac{\partial u}{\partial x} \right|_0 \right) dx\, dy\, dz$$

$$= \left. \frac{\partial(\rho u)}{\partial x} \right|_0 dx\, dy\, dz$$

Similar expressions can be derived for the other faces. We find

$$\text{net mass flow rate out through } cdhg \text{ and } abfe = \left. \frac{\partial(\rho v)}{\partial y} \right|_0 dx\, dy\, dz$$

$$\text{net mass flow rate out through } cbfg \text{ and } aehd = \left. \frac{\partial(\rho w)}{\partial z} \right|_0 dx\, dy\, dz$$

By adding up the contributions over all six faces, we obtain

$$\text{total net mass outflow rate} = \left( \frac{\partial(\rho u)}{\partial x} + \frac{\partial(\rho v)}{\partial y} + \frac{\partial(\rho w)}{\partial z} \right) dx\, dy\, dz$$

where we have dropped the subscript 0 because the result should not depend on the particular point that was considered.

This net mass flux must be equal to the decrease in mass contained in this volume during the same time interval since mass must be conserved. Since the volume of the fluid element remains fixed,

$$\text{Decrease in mass during } \Delta t = -dx\, dy\, dz\, \frac{\partial \rho}{\partial t} \Delta t$$

Hence,

$$\left[ \frac{\partial(\rho u)}{\partial x} + \frac{\partial(\rho v)}{\partial y} + \frac{\partial(\rho w)}{\partial z} \right] dx\, dy\, dz\, \Delta t = -dx\, dy\, dz\, \frac{\partial \rho}{\partial t} \Delta t$$

so that we obtain the continuity equation in Cartesian coordinates

$$\frac{\partial(\rho u)}{\partial x} + \frac{\partial(\rho v)}{\partial y} + \frac{\partial(\rho w)}{\partial z} = -\frac{\partial \rho}{\partial t} \tag{5.6}$$

The continuity equation in cylindrical coordinates is given by

$$\frac{1}{r} \frac{\partial(r\rho u_r)}{\partial r} + \frac{1}{r} \frac{\partial(\rho u_\theta)}{\partial \theta} + \frac{\partial(\rho u_z)}{\partial z} = -\frac{\partial \rho}{\partial t} \tag{5.7}$$

We can now write the continuity equation using vector notation by introducing the divergence operator (see Section A.5). That is,

$$\boxed{\nabla \cdot \rho \mathbf{V} \ = \ -\frac{\partial \rho}{\partial t}} \tag{5.8}$$

We can find an alternative form by expanding equation 5.6 to give

$$u\frac{\partial \rho}{\partial x} + \rho\frac{\partial u}{\partial x} + v\frac{\partial \rho}{\partial y} + \rho\frac{\partial v}{\partial y} + w\frac{\partial \rho}{\partial z} + \rho\frac{\partial w}{\partial z} \ = \ -\frac{\partial \rho}{\partial t}$$

By collecting terms, we can introduce the total derivative and obtain

$$\frac{\partial u}{\partial x} + \frac{\partial v}{\partial y} + \frac{\partial w}{\partial z} \ = \ -\frac{1}{\rho}\frac{D\rho}{Dt}$$

or, by using vector notation,

$$\boxed{\nabla \cdot \mathbf{V} \ = \ -\frac{1}{\rho}\frac{D\rho}{Dt}} \tag{5.9}$$

Equations 5.8 and 5.9 are two forms of the continuity equation in differential form. They are written in vector form, so that they are independent of the coordinate system.

We now introduce the concept of *incompressible* flow. By definition,

An incompressible flow is one where either $D\rho/Dt = 0$, or equivalently where $\nabla \cdot \mathbf{V} = 0$.

An incompressible flow field is sometimes called *solenoidal*. In vector calculus a solenoidal vector field is one where the divergence of the vector field is zero everywhere.

When the fluid has a constant density, the flow field is obviously incompressible, but it is possible to have an incompressible flow field with a fluid of variable density, as long as $D\rho/Dt = 0$. One example would be a stratified liquid, as found in the ocean where salinity gradients cause the density of sea water to change with depth.

## 5.3   Momentum Equation

Here we derive the momentum equation in differential form. When the fluid is inviscid, the equation that results is called the Euler equation, or the momentum equation for inviscid flow. When the fluid is viscous, the equation is known as the Navier-Stokes equation. We begin with inviscid flows.

### 5.3.1   Euler equation

Consider a fixed, control volume of infinitesimal size (Figure 5.5). There is flow through the six faces of the volume element, and surface forces and body forces act on the fluid particle that occupies the volume at a particular instant in time. The only surface force taken into account is that due to pressure differences, and the only body force considered is that due to gravity. The volume element $dxdydz$ is similar to the one used to derive the continuity equation, except that only one face is shown, and this face has an arbitrary orientation with respect to the gravitational vector $\mathbf{g}$ (that is, $\mathbf{g}$ may have components in or out of the page, as well as being at an angle to the $x$- and $y$-axes). That is,

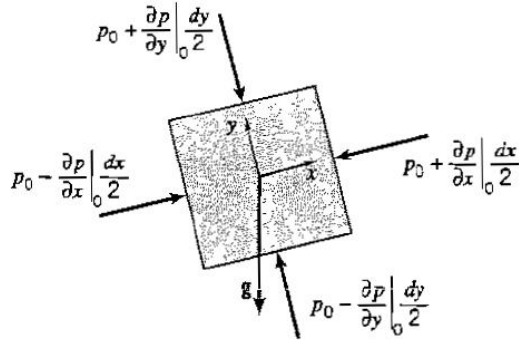$$\mathbf{g} = g_x\mathbf{i} + g_y\mathbf{j} + g_z\mathbf{k}$$

Figure 5.5: Elemental control volume for derivation of the differential form of the momentum equation.

where $g_x$, $g_y$, and $g_z$ are the components of $\mathbf{g}$ in the $x$, $y$ and $z$-directions, respectively.

The resultant force in the $x$-direction, $F_x$, then has two contributions: the force due to pressure differences acting on the two faces of area $dy\,dz$, and the $x$-component of the force due to the weight of the fluid contained in the volume $dx\,dy\,dz$. Using a first order Taylor series expansion about the center of the volume, we have

$$F_x = \left( p_0 - \frac{\partial p}{\partial x}\bigg|_0 \frac{dx}{2} \right) dydz - \left( p_0 + \frac{\partial p}{\partial x}\bigg|_0 \frac{dx}{2} \right) dydz + \rho_0 g_x\, dxdydz$$

That is,

$$F_x = -\frac{\partial p}{\partial x}\bigg|_0 dxdydz + \rho_0 g_x\, dxdydz$$

Similarly for the $y$- and $z$-directions:

$$F_y = -\frac{\partial p}{\partial y}\bigg|_0 dxdydz + \rho_0 g_y\, dxdydz$$

$$F_z = -\frac{\partial p}{\partial z}\bigg|_0 dxdydz + \rho_0 g_z\, dxdydz$$

so that

$$\begin{aligned}
\mathbf{F} &= F_x \mathbf{i} + F_y \mathbf{j} + F_z \mathbf{k} \\
&= -\left( \mathbf{i}\frac{\partial p}{\partial x} + \mathbf{j}\frac{\partial p}{\partial y} + \mathbf{k}\frac{\partial p}{\partial z} \right) dxdydz + \rho\left( g_x \mathbf{i} + g_y \mathbf{j} + g_z \mathbf{k} \right) dxdydz
\end{aligned}$$

where we have dropped the subscript 0 because the result should not depend on the particular point that was considered. Introducing the gradient operator (see Section A.4), we obtain

$$\mathbf{F} = (-\nabla p + \rho \mathbf{g})\, dxdydz$$

By Newton's second law of motion, $\mathbf{F}$ is equal to the rate of change of momentum following a fluid particle. For a velocity field in an Eulerian system, the acceleration following a fluid particle is given by $D\mathbf{V}/Dt$, and

$$\left\{ \begin{array}{c} \text{the rate of change of momentum} \\ \text{following a fluid particle} \end{array} \right\} = \rho\, dxdydz\, \frac{D\mathbf{V}}{Dt}$$

Therefore:

$$\boxed{\rho \frac{D\mathbf{V}}{Dt} = -\nabla p + \rho \mathbf{g}} \tag{5.10}$$

This is the differential form of the linear momentum equation for an inviscid fluid, in vector form. It states that, at any point in the flow of an inviscid fluid, the inertia force (mass × acceleration) acting on a fluid particle is equal to the sum of the forces due to pressure differences and gravity. It is also called the Euler equation, and it holds for compressible and incompressible flows.

In Cartesian coordinates:

$$\frac{\partial u}{\partial t} + u\frac{\partial u}{\partial x} + v\frac{\partial u}{\partial y} + w\frac{\partial u}{\partial z} = -\frac{1}{\rho}\frac{\partial p}{\partial x} - g_x \tag{5.11}$$

$$\frac{\partial v}{\partial t} + u\frac{\partial v}{\partial x} + v\frac{\partial v}{\partial y} + w\frac{\partial v}{\partial z} = -\frac{1}{\rho}\frac{\partial p}{\partial y} - g_y \tag{5.12}$$

$$\frac{\partial w}{\partial t} + u\frac{\partial w}{\partial x} + v\frac{\partial w}{\partial y} + w\frac{\partial w}{\partial z} = -\frac{1}{\rho}\frac{\partial p}{\partial z} - g_z \tag{5.13}$$

In cylindrical coordinates:

$$\frac{\partial u_r}{\partial t} + u_r\frac{\partial u_r}{\partial r} + \frac{u_\theta}{r}\frac{\partial u_r}{\partial \theta} + u_z\frac{\partial u_r}{\partial z} - \frac{u_\theta^2}{r} = -\frac{1}{\rho}\frac{\partial p}{\partial r} - g_r \tag{5.14}$$

$$\frac{\partial u_\theta}{\partial t} + u_r\frac{\partial u_\theta}{\partial r} + \frac{u_\theta}{r}\frac{\partial u_\theta}{\partial \theta} + u_z\frac{\partial u_\theta}{\partial z} + \frac{u_r u_\theta}{r} = -\frac{1}{\rho r}\frac{\partial p}{\partial \theta} - g_\theta \tag{5.15}$$

$$\frac{\partial u_z}{\partial t} + u_r\frac{\partial u_z}{\partial r} + \frac{u_\theta}{r}\frac{\partial u_z}{\partial \theta} + u_z\frac{\partial u_z}{\partial z} = -\frac{1}{\rho}\frac{\partial p}{\partial z} - g_z \tag{5.16}$$

In streamline coordinates for steady flow (see equations 4.3 and 4.7)

$$V\frac{\partial V}{\partial s} = -\frac{\partial p}{\partial s} - \rho g\frac{\partial z}{\partial s} \tag{5.17}$$

$$\rho\frac{V^2}{R} = \frac{\partial p}{\partial n} + \rho g\frac{\partial z}{\partial n} \tag{5.18}$$

## 5.3.2 Navier-Stokes equations

We now consider the momentum equation for a Newtonian viscous fluid. In Section 1.6, we indicated that the viscous stress for a Newtonian fluid is given by the coefficient of viscosity times the velocity gradient. We need to add that this is strictly true only for incompressible flow, and the following derivation will similarly be restricted to incompressible flow.

Consider the case where the only velocity gradient present is $\partial u/\partial y$, the gradient of the $x$-component of velocity in the $y$-direction (as in Figure 5.6). The only shear stress that acts on the fluid particle that occupies the volume at a particular instant in time is then $\tau_{yx} = \mu\left(\partial u/\partial y\right)$, where the subscript $yx$ denotes a stress that acts in the $x$-direction and is associated with a velocity gradient in the $y$-direction. The resultant force acting on the fluid particle due to this viscous stress is $F_{vx}$. Using a first order Taylor Series expansion, we obtain

$$\begin{aligned}
F_{vx} &= \left(\tau_{yx} + \frac{\partial \tau_{yx}}{\partial y}\bigg|_0 \frac{dy}{2}\right)dxdz - \left(\tau_{yx} - \frac{\partial \tau_{yx}}{\partial y}\bigg|_0 \frac{dy}{2}\right)dxdz \\
&= \frac{\partial \tau_{yx}}{\partial y}\,dxdydz \\
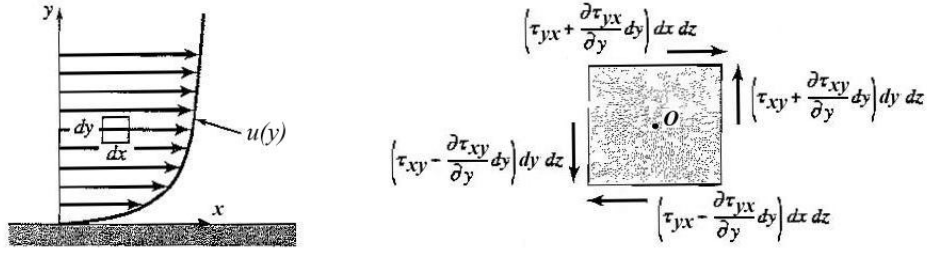&= \frac{\partial}{\partial y}\left(\mu\frac{\partial u}{\partial y}\right)dxdydz
\end{aligned}$$

Figure 5.6: Viscous flow showing an element in shear. Left: the velocity $U = U(y)$, so that $\tau = \tau_{yx}$. Right: Notation for a fluid element.

That is, for the case where $\partial u / \partial y$ is the only velocity gradient and $\mu$ is constant, the resultant force due to viscous friction in the $x$-direction, per unit volume, is given by

$$\frac{F_{vx}}{dxdydz} = \frac{\partial \tau_{yx}}{\partial y} = \mu \frac{\partial^2 u}{\partial y^2}$$

We see that this force is proportional to the gradient of the stress $\tau_{yx}$. If the shear stress is uniform throughout the flow, fluid particles will distort but there will be no resultant force due to viscous stresses. In other words, there must exist viscous stress *gradients* for the viscous stress to contribute to the acceleration of fluid particles.

Normal stresses due to extensional strain rates also lead to viscous stresses (see Section 1.6). A similar analysis to that given previously shows that for a flow where $\partial u / \partial x$ is the only velocity gradient and $\mu$ is constant, the resultant force due to viscous friction in the $x$-direction, per unit volume, is given by

$$\frac{F_{vx}}{dxdydz} = \frac{\partial \tau_{xx}}{\partial x} = \mu \frac{\partial^2 u}{\partial x^2}$$

where the subscript $xx$ denotes a stress that acts in the $x$-direction and is associated with a velocity gradient also in the $x$-direction.

In the general case, where velocity gradients act in all directions, the $x$-component of the viscous force per unit volume in Cartesian coordinates becomes

$$\frac{F_{vx}}{dxdydz} = \mu \left( \frac{\partial \tau_{xx}}{\partial x} + \frac{\partial \tau_{yx}}{\partial y} + \frac{\partial \tau_{zx}}{\partial z} \right)$$

By expressing the stresses in terms of the velocity gradients, and using the continuity equation (equation 5.6) to simplify the result, we obtain:

$$\frac{F_{vx}}{dxdydz} = \mu \left( \frac{\partial^2 u}{\partial x^2} + \frac{\partial^2 u}{\partial y^2} + \frac{\partial^2 u}{\partial z^2} \right) = \mu \nabla^2 u$$

where $\nabla^2$ is the Laplacian operator (see Section A.6). In vector notation, therefore, the viscous force per unit volume is given by $\mu \nabla^2 \mathbf{V}$. This force can simply be added to the Euler equation, and we obtain the momentum equation for the flow of a viscous fluid:

$$\rho \frac{D\mathbf{V}}{Dt} = -\nabla p + \rho \mathbf{g} + \mu \nabla^2 \mathbf{V} \tag{5.19}$$

This equation is known as the Navier-Stokes equation. In the form written here it only applies to incompressible, constant viscosity (Newtonian) flows.

The Euler and Navier-Stokes equations are nonlinear, partial differential equations, and no general solutions exist. The main source of difficulty in both equations is the nonlinear part of the acceleration term, as noted in Section 5.1.1. Analytical solutions exist only under particular conditions, such as incompressible, irrotational flow (Chapter 6), fully developed flows where the acceleration term is zero (Chapter 8), or Stokes flow where the acceleration term is small compared to the viscous term (Section 13.6). Numerical techniques must be used for other cases, and it is now routinely possible, for instance, to solve the Euler equation for an entire airplane at transonic Mach numbers, as long as it is not maneuvering too quickly. When viscous effects are included, however, numerical solutions require a great deal more computer speed and memory, and full Navier-Stokes solutions are currently possible only at low Reynolds numbers, that is, at Reynolds numbers not much greater than the value where transition from laminar to turbulent flow occurs.

### 5.3.3 Boundary conditions

The differential equations of motion are complete once the boundary conditions are specified. We will only consider the specific boundary conditions introduced by the presence of a wall since they are of most interest here. The Navier-Stokes equation includes the viscous stress, so that the no-slip condition must be satisfied (see Section 1.7). The no-slip condition means that the fluid in contact with a solid surface has no relative velocity with respect to the surface. That is, at the wall

$$\mathbf{V} = \mathbf{V}_w \tag{5.20}$$

The Euler equation does not include the viscous stress so that it cannot satisfy the same boundary conditions as the Navier-Stokes equation. In particular, it cannot satisfy the no-slip condition, and slip is allowed. However, relative to the solid surface the velocity of the fluid normal to a solid surface must still go to zero so that there is no flow through the surface. That is, the boundary condition for the Euler equation at the wall is

$$\mathbf{n} \cdot \mathbf{V} = \mathbf{n} \cdot \mathbf{V}_w \tag{5.21}$$

## 5.4 Rigid Body Motion Revisited

When a fluid is in static equilibrium, there are no relative motions in the fluid. If the entire body of fluid is moving with an acceleration $\mathbf{a}$ ($= a_x\mathbf{i} + a_y\mathbf{j} + a_z\mathbf{k}$) so that there are no relative motions, we say that it is in rigid body motion (Section 2.12). All the fluid particles are then moving with the same acceleration, and therefore $D\mathbf{V}/Dt = \mathbf{a}$, everywhere. The momentum equation (equation 5.10) becomes

$$\rho\,\mathbf{a} = -\nabla p + \rho\mathbf{g}$$

Consider the case where $a_y = 0$, so that the motion is in the $x$-$z$ plane, and that the $x$-direction is horizontal and the $z$-direction is vertically up, so that $\mathbf{g} = -g\mathbf{k}$. Then

$$\rho a_x\mathbf{i} + \rho a_z\mathbf{k} = -\frac{\partial p}{\partial x}\mathbf{i} - \frac{\partial p}{\partial z}\mathbf{k} - \rho g\mathbf{k}$$

For the $z$-direction we obtain

$$\frac{\partial p}{\partial z} = -\rho\left(g + a_z\right) \tag{5.22}$$

and for the $x$-direction

$$\frac{\partial p}{\partial x} = -\rho a_x \tag{5.23}$$

which are the same results obtained in Section 2.12.2 for rigid body motion with vertical and horizontal accelerations.

When the acceleration $\mathbf{a} = \mathbf{0}$, equations 5.22 and 5.23 reduce to

$$\frac{\partial p}{\partial z} = \frac{dp}{dz} = -\rho g$$

and we recover the hydrostatic equation first derived in Section 2.1. We see that the hydrostatic equation is just a special case of the momentum equation for a fluid in static equilibrium and with zero acceleration.

# Chapter 6

# Irrotational, Incompressible Flows

We saw in Chapter 5 that the flow field is described completely by the continuity equation and the Navier-Stokes equation (as long as energy considerations are not important). These equations are complex and difficult to solve, but it is possible to find solutions under some conditions. Specifically, it is possible to solve these equations when the flow is irrotational.

What does *irrotational* mean? If a flow is irrotational, it does not mean that the flow is not rotating: an irrotational flow can be in rectilinear or rotating motion relative to some reference frame. What is important is the rotation of fluid particles, and s flow is said to be irrotational if the average angular velocity of every fluid particle is zero. We will show that this occurs when the curl of the velocity field is zero, that is, when $\nabla \times \mathbf{V} = 0$. Therefore,

---

A flow is irrotational if the average angular velocity of every fluid particle is zero. so that $\nabla \times \mathbf{V} = 0$.

---

We call the quantity $\nabla \times \mathbf{V}$ the *vorticity*, $\vec{\Omega}$, so that, equivalently, the flow is irrotational when $\vec{\Omega} = 0$.

When the flow is irrotational, the equations of motion are greatly simplified because we can express the vector velocity field in terms of a scalar function $\phi$, called the *velocity potential*. Lines of constant velocity potential are somewhat like contour lines on a map, and the magnitude of the local velocity is larger where the equipotential lines are closer together. If the flow is also incompressible, the equations of motion become even simpler, because then the velocity potential (and hence the velocity) obeys a linear partial differential equation (Laplace's equation $\nabla^2 \phi = 0$), which makes it possible to find analytical solutions for many useful flow cases.

Alternatively, if the flow is incompressible and two-dimensional, the equations can also be greatly simplified. In this case, the velocity can be expressed in terms of another scalar function $\psi$, called the *stream function*. Lines of constant $\psi$ correspond to streamlines. If the flow is also irrotational, the stream function (and hence the velocity) can be found by solving Laplace's equation for $\psi$, that is, $\nabla^2 \psi = 0$.

To know whether a flow is irrotational or not, it is necessary to understand the role of the viscous stresses. In particular, whenever viscous stresses are important the flow will be *rotational* (that is, not irrotational). Boundary layer flows, fully developed pipe and duct flows, and wakes are all rotational. Outside these viscous regions, however, the flow is often irrotational. For example, the flow over a streamlined shape such as an airfoil is rotational inside the boundary layer and wake, and irrotational in the rest of the flow field.

If we now consider flows that are inviscid everywhere, so that we neglect the presence of boundary layers and wakes, the flow will be irrotational everywhere. We can then use velocity potentials and stream functions to find the velocity field, and by using Bernoulli's equation we can determine the pressure distributions. In the case of the flow over an airfoil, this approach can give very good estimates of the lift force. The lift is due primarily to the pressure difference between the upper and lower surfaces of the airfoil, and these pressure differences are not affected significantly by the presence of the boundary layers and wake (as long as the flow is not separated). However, this approach cannot be used to find the drag force. The drag acting on the airfoil is primarily due to the viscous stresses acting in the boundary layer and wake, so that when the flow is assumed to be inviscid, there is no longer any drag.

## 6.1  Vorticity and Rotation

Here, we consider the connection between the rotation of a fluid particle, and the vorticity $\vec{\Omega} = \nabla \times \mathbf{V}$. The rotation of a fluid particle is defined by the rotation vector $\vec{\omega}$, which is the average angular velocity of two originally perpendicular lines "attached" to the fluid particle. Consider a fluid particle in a flow with velocity gradients acting only in the $x$-$y$ plane. In a short time interval $dt$, the particle will move and distort as shown in Figure 6.1. The velocity gradient $\partial u/\partial y$ will cause a rotation $-d\beta$, and the velocity gradient $\partial v/\partial x$ will cause a rotation $d\alpha$ (counterclocwise rotations are taken to be positive). The average angular rotation about the $z$-axis is then given by $\frac{1}{2}(d\alpha - d\beta)$, and so the $z$-component of the rotation vector is given by

$$\omega_z = \frac{1}{2dt}(d\alpha - d\beta)$$

For small angles,

$$d\alpha \; \approx \; \tan d\alpha \; = \; \frac{\left(v_0 + \frac{\partial v}{\partial x}\big|_0 dx\right)dt - v_0 dt}{dx - u_0 dt + \left(u_0 + \frac{\partial u}{\partial x}\big|_0 dx\right)dt} \; = \; \frac{\partial v}{\partial x}\bigg|_0 dt$$

where the origin 0 is taken to be at the lower left corner of the particle, and higher order terms have been neglected. Similarly, we have

$$d\beta \; \approx \; \tan d\beta \; = \; \frac{\left(u_0 + \frac{\partial u}{\partial y}\big|_0 dy\right)dt - u_0 dt}{dy - v_0 dt + \left(v_0 + \frac{\partial v}{\partial y}\big|_0 dy\right)dt} \; = \; \frac{\partial u}{\partial y}\bigg|_0 dt$$
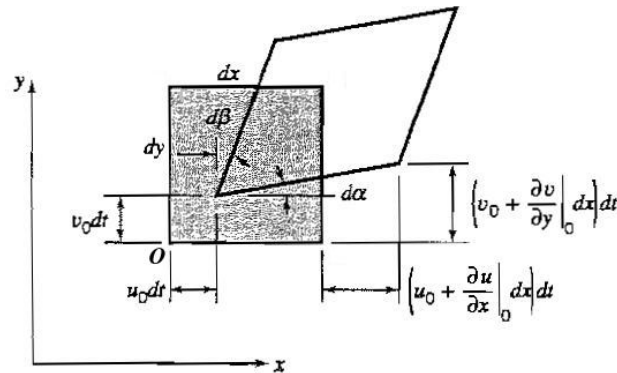


Figure 6.1: Rotation and translation of a fluid particle. The origin 0 is taken to be at the lower left corner of the particle.

Dropping the subscript because the location of the origin is arbitrary gives

$$\omega_z = \frac{1}{2dt}(d\alpha - d\beta) = \frac{1}{2}\left(\frac{\partial v}{\partial x} - \frac{\partial u}{\partial y}\right)$$

Similarly, for a three-dimensional flow field with velocity gradients in all directions, we can show that the rotations about the $y$- and $x$-directions are given by

$$\omega_y = \frac{1}{2dt}\left(\frac{\partial u}{\partial z} - \frac{\partial w}{\partial x}\right) \quad \text{and} \quad \omega_x = \frac{1}{2}\left(\frac{\partial w}{\partial y} - \frac{\partial v}{\partial z}\right)$$

Therefore

$$\vec{\omega} = \frac{1}{2}\left[\left(\frac{\partial w}{\partial y} - \frac{\partial v}{\partial z}\right)\mathbf{i} - \left(\frac{\partial w}{\partial x} - \frac{\partial u}{\partial z}\right)\mathbf{j} + \left(\frac{\partial v}{\partial x} - \frac{\partial u}{\partial y}\right)\mathbf{k}\right]$$

In Cartesian coordinates,

$$\nabla \times \mathbf{V} = \left(\frac{\partial w}{\partial y} - \frac{\partial v}{\partial z}\right)\mathbf{i} - \left(\frac{\partial w}{\partial x} - \frac{\partial u}{\partial z}\right)\mathbf{j} + \left(\frac{\partial v}{\partial x} - \frac{\partial u}{\partial y}\right)\mathbf{k} \qquad (6.1)$$

(see Section A.7), so that

$$\vec{\omega} = \tfrac{1}{2}\nabla \times \mathbf{V} = \text{rotation vector}$$

When $\vec{\omega} = 0$, the average angular velocity of the fluid particle is zero, and the flow is irrotational. The factor of a half is suppressed by defining the vorticity vector such that

$$\boxed{\vec{\Omega} \equiv 2\vec{\omega} = \nabla \times \mathbf{V}} \qquad (6.2)$$

The magnitude of the vorticity at any point is just twice the local rate of rotation of a fluid particle located at that point, and it is given by the curl of the velocity field. When $\vec{\omega} = 0$, then $\vec{\Omega} = 0$, and the flow is irrotational. There is no net rotation of fluid particles, although their shape can distort as they move.

We noted earlier that in regions where viscous stresses are important, as in boundary layers, pipe flows, duct flows, and wakes, the flow is not irrotational. To illustrate this point, consider a two-dimensional boundary layer such as that shown in Figure 1.11. Since the flow is two-dimensional, the vorticity vector has only one component, given by

$$\nabla \times \mathbf{V} = \left(\frac{\partial v}{\partial x} - \frac{\partial u}{\partial y}\right)\mathbf{k}$$

Since the boundary layer thickness grows with distance along the surface, the streamlines inside the boundary layer gradually get displaced further from the surface, so that, in addition to the principal velocity gradient $\partial u/\partial y$, the wall-normal velocity $v$ varies with $x$ so that $\partial v/\partial x \neq 0$ (see Section 9.2.2). However, the boundary layer only grows slowly with distance, so that $\partial v/\partial x$ is always small compared to $\partial u/\partial y$, and therefore $\nabla \times \mathbf{V} \neq 0$. The flow in the boundary layer is rotational, and methods developed for irrotational flows, such as those discussed in this chapter, cannot be used.

## 6.2 The Velocity Potential $\phi$

The condition of irrotational flow ($\nabla \times \mathbf{V} = 0$) means that, in Cartesian coordinates

$$\frac{\partial u}{\partial y} = \frac{\partial v}{\partial x}, \qquad \frac{\partial v}{\partial z} = \frac{\partial w}{\partial y}, \quad \text{and} \quad \frac{\partial w}{\partial x} = \frac{\partial u}{\partial z} \qquad (6.3)$$

(see equation 6.1). It is possible to satisfy these equations by defining a function $\phi$, called the *velocity potential*, such that

$$u = \frac{\partial \phi}{\partial x}, \qquad v = \frac{\partial \phi}{\partial y}, \quad \text{and} \quad w = \frac{\partial \phi}{\partial z} \tag{6.4}$$

Hence

$$\frac{\partial u}{\partial y} = \frac{\partial^2 \phi}{\partial x \partial y}, \qquad \frac{\partial v}{\partial x} = \frac{\partial^2 \phi}{\partial y \partial x}$$

and so on. The function $\phi$ will always satisfy the condition of irrotational flow (equation 6.3) since the order of differentiation is immaterial as long as $\phi$ is well-behaved. We see that the velocity is related to $\phi$ according to

$$\mathbf{V} = u\mathbf{i} + v\mathbf{j} + w\mathbf{k} = \frac{\partial \phi}{\partial x}\mathbf{i} + \frac{\partial \phi}{\partial y}\mathbf{j} + \frac{\partial \phi}{\partial z}\mathbf{k}$$

so that

$$\mathbf{V} = \nabla \phi \tag{6.5}$$

For irrotational flow, therefore, it is always possible to write the velocity as the gradient of a scalar function called the velocity potential $\phi$. Irrotational flows are often called *potential flows* because of this connection.

We now take one more step. Using the result from vector calculus that the curl of a gradient is always zero, we see that the velocity potential $\phi$ obeys Laplace's equation

$$\boxed{\nabla^2 \phi = 0} \tag{6.6}$$

For irrotational flows, therefore, the vector velocity field can be described by the gradient of a velocity potential $\phi$, and the Navier-Stokes equation is replaced by Laplace's equation as the governing equation of motion.

### Cylindrical coordinates

In cylindrical coordinates,

$$\vec{\Omega} = \nabla \times \mathbf{V} = \left( \frac{1}{r}\frac{\partial u_z}{\partial \theta} - \frac{\partial u_\theta}{\partial z} \right)\mathbf{e_r} + \left( \frac{\partial u_r}{\partial z} - \frac{\partial u_z}{\partial r} \right)\mathbf{e_\theta} + \frac{1}{r}\left( \frac{\partial r u_\theta}{\partial r} - \frac{\partial u_r}{\partial \theta} \right)\mathbf{e_z} \tag{6.7}$$

(see Section A.7), and the condition for irrotational flow requires that

$$\frac{1}{r}\frac{\partial u_z}{\partial \theta} = \frac{\partial u_\theta}{\partial z}, \qquad \frac{\partial u_r}{\partial z} = \frac{\partial u_z}{\partial r}, \quad \text{and} \quad \frac{\partial r u_\theta}{\partial r} = \frac{\partial u_r}{\partial \theta}$$

These equations are satisfied when

$$u_r = \frac{\partial \phi}{\partial r}, \qquad u_\theta = \frac{1}{r}\frac{\partial \phi}{\partial \theta}, \quad \text{and} \quad u_z = \frac{\partial \phi}{\partial z} \tag{6.8}$$

and again we have

$$\mathbf{V} = \nabla \phi$$

## 6.3 The Stream Function $\psi$

For a two-dimensional, incompressible flow (which can be unsteady, and/or rotational), the continuity equation in Cartesian coordinates is given by

$$\nabla \cdot \mathbf{V} = \frac{\partial u}{\partial x} + \frac{\partial v}{\partial y} = 0 \tag{6.9}$$

We can define a function $\psi$ such that

$$u = \frac{\partial \psi}{\partial y} \qquad \text{and} \qquad v = -\frac{\partial \psi}{\partial x} \tag{6.10}$$

and from equation 6.9

$$\nabla \cdot \mathbf{V} = \frac{\partial}{\partial x}\left(\frac{\partial \psi}{\partial y}\right) + \frac{\partial}{\partial y}\left(-\frac{\partial \psi}{\partial x}\right) = 0$$

We see that the function $\psi$ was defined so that the continuity equation is always satisfied. In terms of $\psi$ the velocity may be written as

$$\mathbf{V} = u\mathbf{i} + v\mathbf{j} = \frac{\partial \psi}{\partial y}\mathbf{i} - \frac{\partial \psi}{\partial x}\mathbf{j}$$

Hence, for two-dimensional incompressible flows, the vector velocity field can be described by a single scalar function $\psi$, called the *stream function*.

If the flow is also irrotational, then $\psi$ will satisfy Laplace's equation. To see why, consider an irrotational flow field in two dimensions. That is,

$$\nabla \times \mathbf{V} = \left(\frac{\partial v}{\partial x} - \frac{\partial u}{\partial y}\right)\mathbf{k} = \left(-\frac{\partial^2 \psi}{\partial x^2} - \frac{\partial^2 \psi}{\partial y^2}\right)\mathbf{k} = 0$$

Hence

$$\boxed{\nabla^2 \psi = 0} \tag{6.11}$$

Most importantly, we can show that lines of constant stream function are streamlines of the flow. Consider a fluid particle as it moves a distance $dx$ and $dy$ in a two-dimensional flow field. The stream function changes by an amount $d\psi$, and by the chain rule of differentiation

$$d\psi = \frac{\partial \psi}{\partial x}dx + \frac{\partial \psi}{\partial y}dy = -v\,dx + u\,dy$$

When $\psi$ is constant, $d\psi = 0$. Then

$$\frac{dy}{dx} = \frac{v}{u} \tag{6.12}$$

which shows that lines of constant $\psi$ have a direction that is tangential to the instantaneous flow direction. Hence, lines of constant stream function are streamlines.

### Cylindrical coordinates

A stream function can also be defined for a cylindrical coordinate system. The continuity equation for a two-dimensional, incompressible flow is given by

$$\nabla \cdot \mathbf{V} = \frac{\partial r u_r}{\partial r} + \frac{\partial u_\theta}{\partial \theta} = 0$$

Substituting the stream function defined by

$$u_r = \frac{1}{r}\frac{\partial \psi}{\partial \theta} \qquad \text{and} \qquad u_\theta = -\frac{\partial \psi}{\partial r} \tag{6.13}$$

we obtain

$$\nabla \cdot \mathbf{V} = \frac{\partial}{\partial r}\left(\frac{\partial \psi}{\partial \theta}\right) + \frac{\partial}{\partial \theta}\left(-\frac{\partial \psi}{\partial r}\right) = 0$$

and we see that this form of the stream function always satisfies the continuity equation, as required.

## 6.4    Flows Where Both $\psi$ and $\phi$ Exist

The velocity potential can be defined for any irrotational flow field, and the stream function can be defined for any two-dimensional, incompressible flowfield.[1]  Therefore when the flow is two-dimensional, irrotational and incompressible, $\phi$ and $\psi$ both exist.  The flow can be steady or unsteady.

Under these conditions, it can be shown that lines of constant $\phi$ intersect lines of constant $\psi$ at right angles. We can write

$$d\phi = \frac{\partial \phi}{\partial x}dx + \frac{\partial \phi}{\partial y}dy = u\,dx + v\,dy$$

When $\phi$ is constant, $d\phi = 0$. Then

$$\frac{dy}{dx} = -\frac{u}{v} \tag{6.14}$$

Hence, from equations 6.12 and 6.14,

$$\left.\frac{dy}{dx}\right|_\phi \times \left.\frac{dy}{dx}\right|_\varphi = -1$$

which shows that $\phi$ and $\psi$ form an orthogonal flownet. Two observations can be made. First, streamlines are tangential to the flow direction, given by the direction of the vector velocity $\mathbf{V}$. Second, the gradient operator points in the direction of the maximum rate of change, which locally will always be in a direction normal to a line of constant potential (see Section A.4). Since $\mathbf{V} = \nabla\phi$, the lines of constant stream function must be orthogonal to lines of constant velocity potential.

## 6.5    Summary of Definitions and Restrictions

We have defined a potential function $\phi$ such that

$$\mathbf{V} = \nabla\phi \tag{6.15}$$

where $\phi$ satisfies the condition of irrotationality. In two-dimensional flow

$$u = \frac{\partial \phi}{\partial x}, \qquad \text{and} \qquad v = \frac{\partial \phi}{\partial y} \tag{6.16}$$

$$\text{or} \qquad u_r = \frac{\partial \phi}{\partial r}, \qquad \text{and} \qquad u_\theta = \frac{1}{r}\frac{\partial \phi}{\partial \theta} \tag{6.17}$$

---

[1]It is, in fact, also possible to define a stream function $\psi$ for a two-dimensional, steady, compressible flow, as shown by, for example, Milne-Thomson *Theoretical Aerodynamics*, 4th edition, published by Macmillan, 1966.

Similarly, a stream function $\psi$ was defined such that the two-dimensional, incompressible continuity equation is always satisfied. In two-dimensional flow

$$u = \frac{\partial \psi}{\partial y}, \qquad \text{and} \qquad v = -\frac{\partial \psi}{\partial x} \qquad (6.18)$$

$$\text{or} \qquad u_r = \frac{1}{r}\frac{\partial \psi}{\partial \theta}, \qquad \text{and} \qquad u_\theta = -\frac{\partial \psi}{\partial r} \qquad (6.19)$$

If either $\phi$ or $\psi$ can be found, the velocity $\mathbf{V}$ is known, and for steady flows the pressure can be obtained from Bernoulli's equation.

It is clear that flows exist where a velocity potential can be defined, but not a stream function. In what follows, we will always assume that the flow is incompressible, irrotational and two-dimensional, so that both a potential function and a stream function exist.

## 6.6  Laplace's Equation

Using the continuity equation for incompressible flow ($\nabla \cdot \mathbf{V} = 0$), and the definition of the velocity potential ($\mathbf{V} = \nabla\phi$), we can write

$$\nabla \cdot \mathbf{V} \;=\; \nabla \cdot (\nabla\phi) \;=\; \nabla^2 \phi \;=\; 0$$

where $\nabla^2$ is the Laplacian operator (see Section A.6). That is,

$$\boxed{\nabla^2 \phi \;=\; 0} \qquad (6.20)$$

Therefore the velocity potential satisfies Laplace's equation for irrotational, incompressible flow. In Cartesian coordinates,

$$\frac{\partial^2 \phi}{\partial x^2} + \frac{\partial^2 \phi}{\partial y^2} + \frac{\partial^2 \phi}{\partial z^2} \;=\; 0 \qquad (6.21)$$

and in cylindrical coordinates,

$$\frac{\partial^2 \phi}{\partial r^2} + \frac{1}{r}\frac{\partial \phi}{\partial r} + \frac{1}{r^2}\frac{\partial^2 \phi}{\partial \theta^2} + \frac{\partial^2 \phi}{\partial z^2} \;=\; 0 \qquad (6.22)$$

Consider now the stream function in two-dimensional, irrotational flow. Here,

$$\nabla \times \mathbf{V} \;=\; \left(\frac{\partial v}{\partial x} - \frac{\partial u}{\partial y}\right)\mathbf{k} \;=\; -\left(\frac{\partial^2 \psi}{\partial x^2} + \frac{\partial^2 \psi}{\partial y^2}\right)\mathbf{k} \;=\; 0$$

so that, in Cartesian coordinates,

$$\frac{\partial^2 \psi}{\partial x^2} + \frac{\partial^2 \psi}{\partial y^2} \;=\; 0$$

That is,

$$\boxed{\nabla^2 \psi \;=\; 0} \qquad (6.23)$$

Therefore the stream function satisfies Laplace's equation for irrotational, two-dimensional, incompressible flow.

Laplace's equation can be used to find the velocity potential or the stream function (with the appropriate boundary conditions). Once $\phi$ or $\psi$ is known, $\mathbf{V}$ can be found, and the pressure is found from Bernoulli's equation, if the flow is also steady.

Laplace's equation is useful in many fields and a great deal has been written on its solutions (see, for instance, Lamb's *Hydrodynamics*, reprinted by Dover, 1945). Here, we are concerned with only one aspect of this equation — its linearity. An equation is linear if, when two separate solutions are known, the sum of these two solutions is also a solution of the equation.

If we have, for example, two known solutions to Laplace's equation, $\psi_1$ and $\psi_2$, consider $\psi = \psi_1 + \psi_2$. In Cartesian coordinates,

$$
\begin{aligned}
\frac{\partial^2 \psi}{\partial x^2} + \frac{\partial^2 \psi}{\partial y^2} &= \left( \frac{\partial^2 \psi_1}{\partial x^2} + \frac{\partial^2 \psi_1}{\partial y^2} \right) + \left( \frac{\partial^2 \psi_2}{\partial x^2} + \frac{\partial^2 \psi_2}{\partial y^2} \right) \\
&= 0 + 0 = 0
\end{aligned}
$$

Therefore $\nabla^2 \psi = 0$, demonstrating that the equation is linear.

The linearity of Laplace's equation means that we can construct new solutions by combining known solutions. In the next few sections, we will find simple solutions to Laplace's equation and show how they can be combined to construct more complex flows.

## 6.7   Examples of Potential Flow

Here we consider a number of simple flows in terms of their corresponding velocity potentials and stream functions. The results are summarized in Table 6.1. These simple flows are very useful because, as we saw in Section 6.6, they can be used as the basic building blocks to construct more complex flows by linear addition.

### 6.7.1   Uniform flow

For uniform flow to the right (Figure 6.2), $u = U$, and $v = 0$. From equation 6.17

$$ u = \frac{\partial \phi}{\partial x} = U $$

| | Cartesian coordinates | | Cylindrical coordinates | |
|---|---|---|---|---|
| | $\phi$ | $\psi$ | $\phi$ | $\psi$ |
| Uniform flow | $Ux$ | $Uy$ | $Ur\cos\theta$ | $Ur\sin\theta$ |
| Point source | $\frac{\dot{q}}{2\pi} \ln \sqrt{x^2+y^2}$ | $\frac{\dot{q}}{2\pi} \tan^{-1}\left(\frac{y}{x}\right)$ | $\frac{\dot{q}}{2\pi} \ln r$ | $\frac{\dot{q}}{2\pi}\theta$ |
| Point sink | $-\frac{\dot{q}}{2\pi} \ln \sqrt{x^2+y^2}$ | $-\frac{\dot{q}}{2\pi} \tan^{-1}\left(\frac{y}{x}\right)$ | $-\frac{\dot{q}}{2\pi} \ln r$ | $-\frac{\dot{q}}{2\pi}\theta$ |
| Potential vortex (counterclockwise) | $\frac{\Gamma}{2\pi} \tan^{-1}\left(\frac{y}{x}\right)$ | $-\frac{\Gamma}{2\pi} \ln \sqrt{x^2+y^2}$ | $\frac{\Gamma}{2\pi}\theta$ | $-\frac{\Gamma}{2\pi} \ln r$ |
| Doublet | $\frac{Kx}{x^2+y^2}$ | $-\frac{Ky}{x^2+y^2}$ | $\frac{K\cos\theta}{r}$ | $-\frac{K\sin\theta}{r}$ |
| $u = \frac{\partial\phi}{\partial x} = \frac{\partial\psi}{\partial y}, \quad v = \frac{\partial\phi}{\partial y} = -\frac{\partial\psi}{\partial x}; \qquad u_r = \frac{\partial\phi}{\partial r} = \frac{1}{r}\frac{\partial\psi}{\partial\theta}, \quad u_\theta = \frac{1}{r}\frac{\partial\phi}{\partial\theta} = -\frac{\partial\psi}{\partial y}$ | | | | |

Table 6.1: Potential functions and stream functions for simple flows.

$$\text{so that} \quad \phi = Ux + g(y) + \text{constant}$$

$$\text{and} \quad v = \frac{\partial \phi}{\partial y} = 0$$

$$\text{Hence} \quad \phi = Ux + \text{constant}$$

Since we are ultimately interested in the velocity, and since the velocity is the gradient of $\phi$ (remember $\mathbf{V} = \nabla\phi$), the constant of integration is arbitrary and we can give it any value we like. For convenience, we set it equal to zero. Therefore a uniform flow field can be expressed in terms of the velocity potential $\phi$ according to

$$\phi = Ux$$

Also, from equation 6.19,

$$u = \frac{\partial \psi}{\partial y} = U$$

$$\text{so that} \quad \psi = Uy + f'(x) + \text{constant}$$

$$\text{and} \quad v = -\frac{\partial \psi}{\partial x} = 0$$

$$\text{Hence} \quad \psi = Uy + \text{constant}$$

We will set the constant of integration to zero, and therefore a uniform flow field can be expressed in terms of the stream function $\psi$ according to

$$\psi = Uy$$

To summarize, for a uniform flow in Cartesian coordinates:

$$\phi = Ux \quad \text{and} \quad \psi = Uy \tag{6.24}$$

In cylindrical coordinates,

$$\phi = Ur\cos\theta \quad \text{and} \quad \psi = Ur\sin\theta \tag{6.25}$$

As seen in Figure 6.2, lines of constant velocity potential and stream function are orthogonal. Furthermore, lines of constant stream function are streamlines, and they are parallel, as required for a uniform flow.

## 6.7.2  Point source and sink

A point *source* in a two-dimensional flow is a point where fluid enters the flow field and flows out equally in all directions, as shown in Figure 6.3. It is an example of a critical or singular point, where streamlines can meet. The mass flow supplied by the source is constant, and because we have restricted ourselves to incompressible flows the volume flow rate $\dot{q}$ is also constant. Since the flow is two-dimensional, $\dot{q}$ is the volume flux per unit length, and its dimensions are volume/length/unit time ($L^2 T^{-1}$).

Cylindrical coordinates are the natural coordinates for this flow, so that by continuity $\dot{q} = 2\pi r u_r$, where $u_r$ is the velocity in the radial direction, and $r$ is the radial coordinate. For a point source, $\dot{q}$ is positive and

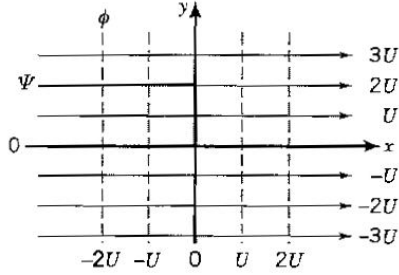$$u_r = \frac{\dot{q}}{2\pi r} \quad \text{and} \quad v_\theta = 0$$
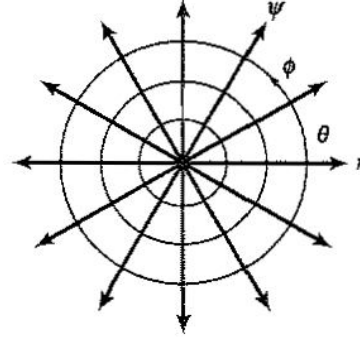
Figure 6.2: Uniform flow.



Figure 6.3: Source flow. Sink flow has the directions of all the arrows reversed.

Hence

$$u_r \;=\; \frac{\dot{q}}{2\pi r} \;=\; \frac{\partial \phi}{\partial r} \;=\; \frac{1}{r}\frac{\partial \psi}{\partial \theta}$$

In cylindrical coordinates, therefore,

$$\phi = \frac{\dot{q}}{2\pi}\ln r \qquad \text{and} \qquad \psi = \frac{\dot{q}}{2\pi}\theta \tag{6.26}$$

In Cartesian coordinates,

$$\phi = \frac{\dot{q}}{2\pi}\ln\sqrt{x^2+y^2} \qquad \text{and} \qquad \psi = \frac{\dot{q}}{2\pi}\tan^{-1}\left(\frac{y}{x}\right) \tag{6.27}$$

A point *sink* is a point where fluid exits the flow field and fluid flows in equally from all directions. It is a source with a negative volume flux, so that

$$\phi = -\frac{\dot{q}}{2\pi}\ln r \qquad \text{and} \qquad \psi = -\frac{\dot{q}}{2\pi}\theta \tag{6.28}$$

In appearance a sink looks exactly as in Figure 6.3, but with all the flow directions reversed.

### 6.7.3    Potential vortex

A *free* or *potential* vortex is a flow with circular streamlines around a common axis, as shown in Figure 6.4, where the velocity distribution is such that the flow is irrotational. Since $\nabla \times \mathbf{V} = 0$, all components of the vorticity vector must be zero. The flow is two-dimensional and confined to the $r$-$\theta$ plane, and the vorticity has only one component, in the $z$-direction. According to equation 6.7

$$\frac{\partial r u_\theta}{\partial r} - \frac{\partial u_r}{\partial \theta} \;=\; 0$$

A potential vortex also has circular symmetry, so that all derivatives with respect to $\theta$ are zero. Hence

$$\frac{\partial r u_\theta}{\partial r} \;=\; \frac{d r u_\theta}{dr} \;=\; 0$$

The quantity $r u_\theta$ is therefore a constant, and the velocity distribution for a potential vortex is given by
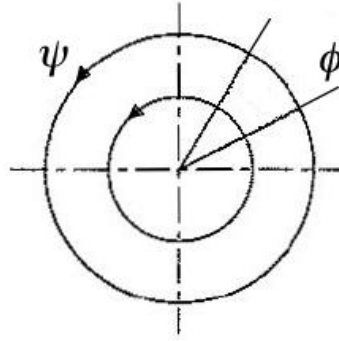
$$u_\theta = \frac{\text{constant}}{r}$$

Figure 6.4: A potential vortex (counterclockwise rotation is positive).

By convention, we set the constant equal to $\Gamma/2\pi$, where the new constant, $\Gamma$, is called the *circulation*, and it is positive for counterclockwise rotation. Therefore a potential vortex is described by

$$u_\theta = \frac{\Gamma}{2\pi r} \tag{6.29}$$

where the circulation $\Gamma$ is often called the strength of the vortex.

Now that we know the tangential velocity distribution in the irrotational parts of the flow (equation 6.29), we can find the velocity potential $\phi$ and the stream function $\psi$. Using the definition of the velocity potential (equation 6.8), we obtain

$$u_\theta = \frac{\Gamma}{2\pi r} = \frac{1}{r}\frac{\partial \phi}{\partial \theta}$$

Hence

$$\phi = \frac{\Gamma}{2\pi}\theta$$

We see that a free vortex has a potential proportional to $\theta$, so that equipotential lines are radial lines with $\theta = $ constant, and the flow describes concentric circles.

In terms of the stream function, we have

$$u_\theta = \frac{\Gamma}{2\pi r} = -\frac{\partial \psi}{\partial r}$$

Hence

$$\psi = -\frac{\Gamma}{2\pi}\ln r$$

To summarize, for a potential vortex in cylindrical coordinates

$$\phi = \frac{\Gamma}{2\pi}\theta \qquad \text{and} \qquad \psi = -\frac{\Gamma}{2\pi}\ln r \tag{6.30}$$

where $\Gamma$ is positive for counterclockwise rotation and negative for clockwise rotation. In Cartesian coordinates,

$$\phi = \frac{\Gamma}{2\pi}\tan^{-1}\left(\frac{y}{x}\right) \qquad \text{and} \qquad \psi = -\frac{\Gamma}{2\pi}\ln\sqrt{x^2+y^2} \tag{6.31}$$

From equation 6.29 we see that, as $r$ goes to zero, the tangential velocity of a potential vortex $u_\theta$ approaches infinity. This cannot happen in a real fluid. At some point viscosity will become important in a real fluid, and it will prevent the velocity from becoming infinite.
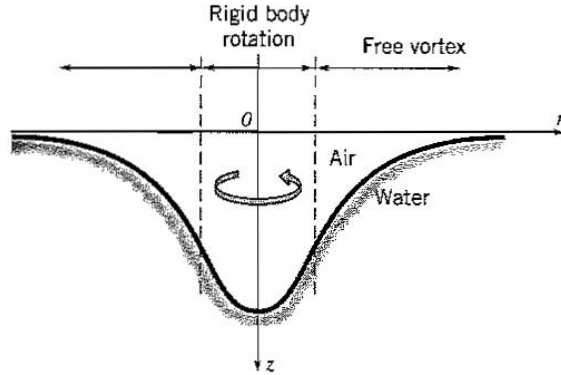
Figure 6.5: Surface shape of a whirlpool, showing the transition from free vortex motion at large $r$ to rigid body rotation at small $r$.

In fact, viscous friction will cause the core of the vortex to start rotating as a solid body, and the flow in this region will no longer be irrotational.

Outside this viscous region, in the irrotational part of the flow, Bernoulli's equation applies between any two points as long as the flow is steady. If the pressure far from the center of the vortex $(r \to \infty)$ is $p_\infty$, and we can ignore gravity, Bernoulli's equation gives

$$p + \tfrac{1}{2}\rho V^2 \;=\; p_\infty$$

At any position $r$, $V = u_\theta$, so that

$$p \;=\; p_\infty - \frac{\rho \Gamma^2}{8\pi^2 r^2}$$

As the radius decreases, the velocity increases and the pressure decreases. Near the core of a free vortex, very low pressures can be found. It is this low pressure that makes trailing vortices in the wake of airplanes visible by allowing the water vapor in the air to condense and show up as *vapor trails*.[2]

A good approximation of a potential vortex can be generated by rotating a cylinder in an otherwise stationary, viscous fluid. On the surface of the cylinder the no-slip condition must be satisfied, and therefore a boundary layer is formed close to the surface. Within the boundary layer, viscous stresses are important and the flow is rotational, but outside the boundary layer the flow is irrotational, and the flow field resembles that of a potential vortex, with a strength equal to twice the angular velocity of the cylinder rotation. In this respect, the cylinder acts like the core of a free vortex in a viscous fluid where the viscous stresses cause to fluid to rotate like a solid body.

A whirlpool in water behaves very similarly. Here, the free surface is a constant-pressure surface, and according to Bernouli's equation

$$\tfrac{1}{2}V^2 + gh \;=\; gh_\infty$$

As the velocity increases toward the axis of the whirlpool, the height of the free surface decreases, and a dimple is formed, as illustrated in Figure 6.5. Since at any position $r$, $V = u_\theta$, the shape of the free surface is given by

$$h \;=\; h_\infty - \frac{\Gamma^2}{8g\pi^2 r^2} \tag{6.32}$$

----

[2]Vapor trails are often visible on take-off or landing under humid conditions, originating at the wing tip or the junction between the wing and a control surface. However, the structures seen in the wake of airplanes cruising at high altitude are not vapor trails but *contrails*, which are formed from water vapor produced as a byproduct of combustion as it freezes and forms ice particles.

We see why the center of a whirlpool is marked by a sharp depression in the water surface. However, near its center, viscous friction will become important and the water will begin to rotate as a rigid body. From Section 2.12, we know that rigid body rotation of a liquid produces a parabolic free surface, so that as $r$ decreases the surface profile changes from that given by equation 6.32 to a parabolic shape.

## 6.8   Source and Sink in a Uniform Flow

To find the flow pattern that results when a source is placed in a uniform flow, we use the linearity of the governing equation (Laplace's equation). That is, we add the stream functions for a source and a uniform flow to obtain the combined stream function $\psi$.

$$
\begin{aligned}
\psi \;=\; \psi_1 + \psi_2 \;&=\; Uy + \frac{q}{2\pi}\theta \\
&=\; Uy + \frac{q}{2\pi}\tan^{-1}\frac{y}{x}
\end{aligned}
$$

The stream function pattern for the combination is shown in Figure 6.6.  The lines of constant stream function represent streamlines.

We can also find the lines of constant velocity potential for the same flow by adding the potentials for a source and a uniform flow to obtain the combined velocity potential $\phi$.

$$
\begin{aligned}
\phi \;=\; \phi_1 + \phi_2 \;&=\; Ux + \frac{\dot{q}}{2\pi}\ln r \\
&=\; Ux + \frac{\dot{q}}{2\pi}\ln\sqrt{x^2 + y^2}
\end{aligned}
$$

The lines of constant potential are everywhere normal to the lines of constant stream function (see Section 6.4).

When a sink is placed in a uniform flow, we obtain the streamlines shown in Figure 6.7. Note that this flow is the mirror image of the flow produced by a source in a uniform flow (shown in Figure 6.6).

The lines of constant $\psi$ represent streamlines. By definition, there can be no flow across streamlines, and therefore a line of constant $\psi$ can be used to represent a solid wall in an inviscid flow. In an inviscid flow, the no-slip boundary condition does not apply, and the boundary condition at a solid surface reduces to the impermeability condition given by equation 5.21, that is, at the surface

$$
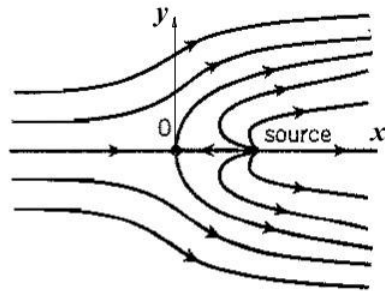\mathbf{n} \cdot \mathbf{V} = \mathbf{n} \cdot \mathbf{V}_w
$$



Figure 6.6:  Stream function pattern for a source in a uniform flow.
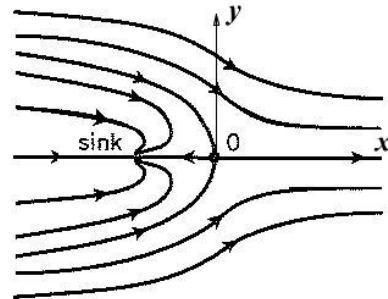


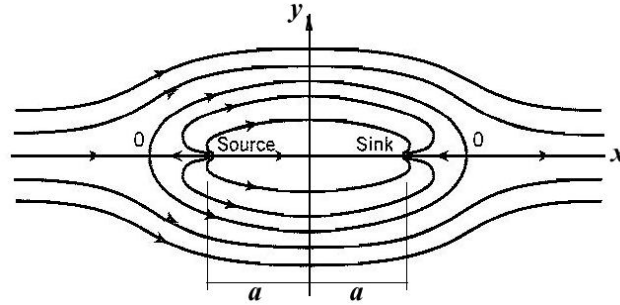Figure 6.7: Stream function pattern for a sink in uniform flow.

Figure 6.8: Stream function pattern generated by a source and sink of equal strength in a uniform flow.

Since there can be no flow across a streamline, each streamline is equivalent to a solid surface. Figures 6.6 and 6.7, therefore, represent the flow over an infinite number of different half-bodies, one for each streamline. The streamline passing through the stagnation point (point O) describes the shape of a particularly interesting body. Furthermore, the straight streamline that acts as a line of symmetry could represent another solid surface, so that the top half of the flow field can be used to represent the flow over a hill of a particular shape. By changing the relative strengths of the freestream flow and the source or sink, many different shapes can be generated. In this way, we can find the velocity and pressure field around a variety of solid bodies in inviscid flow. We cannot take account of the boundary layers, but it is still a very useful technique.

We can take this idea of superposition one step further by considering the flow generated when a source *and* a sink of equal strengths are placed in a uniform flow. With a distance $2a$ separating the source from the source along the $x$-axis, the combined stream function $\psi$ is given by

$$\psi \; = \; Uy + \frac{q}{2\pi} \tan^{-1} \left( \frac{y}{x+a} \right) - \frac{q}{2\pi} \tan^{-1} \left( \frac{y}{x-a} \right) \tag{6.33}$$

The streamline pattern is as shown in Figure 6.8. We see that a closed streamline appears (0-0 in Figure 6.8). Inside the closed streamline, all the flow originating from the source is absorbed by the sink. The closed streamline acts like a solid body, and by changing the strength of the uniform flow relative to that of the source-sink pair, bodies of many different aspect ratios may be generated.

## 6.9   Potential Flow Over a Cylinder

One very useful application of potential flow methods is to find the flow over a cylinder. This flow can be generated by placing a sink and a source close together in a uniform flow. The general streamline pattern appears as in Figure 6.8, and it might be inferred that as the sink and the source come closer together, the shape of the closed streamline will look more and more like a circle. We could guess that the closed streamline becomes a circle when the source and the sink occupy the same location. This may sound difficult to accomplish, since we would expect the source and the sink to cancel each other, leaving us with undisturbed, uniform flow. This is not necessarily the case, as we shall see from the following analysis.

When we add the stream functions for a source and a sink, separated by a distance $2a$, the combined stream function is as given in equation 6.33. In cylindrical coordinates, the stream function for the source-sink pair can be written as

$$\psi \; = \; -\frac{\dot{q}}{2\pi} \left( \theta_1 - \theta_2 \right) \tag{6.34}$$
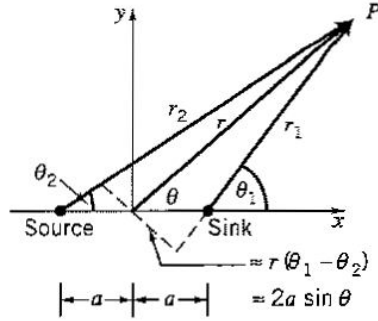
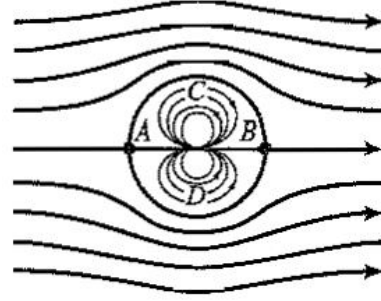Figure 6.9: Notation for a doublet.        Figure 6.10: Doublet in a uniform flow.

where the angle $\theta$ is measured from a common origin, and the source is labeled with subscript 2, and the sink is labeled with subscript 1 (Figure 6.9). When the distance $a$ is small, the angle $\theta_1 - \theta_2$ is also small, so that $r(\theta_1 - \theta_2) \approx 2a \sin \theta$, and

$$\theta_1 - \theta_2 \approx \frac{2a \sin \theta}{r}$$

so that

$$\psi = -\frac{\dot{q}a \sin \theta}{r} \tag{6.35}$$

As $a$ becomes very small compared to $r$, we let $\dot{q}$ increase so that the product $\dot{q}a$ remains finite and constant. That is,

$$\psi = -\frac{K \sin \theta}{r} \tag{6.36}$$

Under these conditions, the source-sink pair is called a *doublet*, and $K = \dot{q}a/\pi$ is called the *strength* of the doublet. The velocity potential of a doublet is given by

$$\phi = \frac{K \cos \theta}{r} \tag{6.37}$$

When a uniform flow is added to the doublet, we obtain the the combined stream function

$$\psi = Uy - \frac{K \sin \theta}{r} = Ur \left( 1 - \frac{K}{Ur^2} \right) \sin \theta = Ur \left( 1 - \frac{R^2}{r^2} \right) \sin \theta \tag{6.38}$$

(since $y = r \sin \theta$). The lines of constant stream function are shown in Figure 6.10. For the closed streamline $\psi = 0$, and so $r = \sqrt{K/U}$, which is a constant. We see that the closed streamline is a circle of radius $R \ (= \sqrt{K/U})$, and therefore the combination of a doublet and a uniform flow models the inviscid flow over a cylinder.

The stagnation streamlines and the closed streamline describing the cylinder meet at front and rear stagnation points, A and B respectively. The true flow pattern around a cylinder at reasonable Reynolds numbers does not look like that shown in Figure 6.10, especially in the wake region (see, for example, Figure 4.3). The inviscid flow is symmetrical front to back, whereas the viscous flow is not. We will consider these differences further after we have found the velocity and pressure distributions for the inviscid flow.

From equation 6.38, we find

$$u_r = \frac{1}{r} \frac{\partial \psi}{\partial \theta} = U \left( 1 - \frac{R^2}{r^2} \right) \cos \theta$$

and

$$u_\theta = -\frac{\partial \psi}{\partial r} = -U \left( 1 + \frac{R^2}{r^2} \right) \sin \theta$$

On the surface of the cylinder, $r = R$, and therefore $u_r = 0$ (as expected, since the surface is a streamline). Along the surface, $u_\theta = u_{\theta s}$, where

$$u_{\theta s} = -2U \sin \theta \qquad (6.39)$$

We see that the inviscid flow does not satisfy the no-slip condition, and therefore boundary layers do not form on the surface of the cylinder. This is one of the most important differences between the inviscid flow solution, and a "real" viscous flow.

### 6.9.1   Pressure distribution

Since the flow is steady, inviscid, irrotational and incompressible, we can find the pressure distribution using Bernoulli's equation. If the pressure far from the cylinder is $p_\infty$, then, along the stagnation streamline and around the cylinder,

$$p_\infty + \tfrac{1}{2}\rho U^2 = p_s + \tfrac{1}{2}\rho u_{\theta s}^2$$

where $p_s$ is the surface pressure, and $u_{\theta s}$ is the flow velocity along the surface of the cylinder, given by equation 6.39. The inviscid pressure distribution over the cylinder surface is therefore given by

$$p_s = p_\infty + \tfrac{1}{2}\rho U^2 \left(1 - 4 \sin^2 \theta\right)$$

In terms of the coefficient of pressure, $C_p$, we obtain

$$C_p = \frac{p_s - p_\infty}{\tfrac{1}{2}\rho U^2} = 1 - 4 \sin^2 \theta$$

Figure 6.11 shows a comparison of the inviscid and the experimental pressure distributions. The comparison is good for $\theta > 135°$, but the inviscid solution predicts a much lower pressure at the shoulder ($\theta = 90°$) than what is found by experiment. In the wake ($\theta < 90°$), the analysis predicts a full pressure recovery to its stagnation point value at the rear stagnation point ($\theta = 0°$), whereas the experiment indicates that the pressure at the rear stagnation point recovers to only a fraction of its original value.

   We noted earlier that potential flow methods cannot be used to find the drag on a body. For the flow over a cylinder, we see that the inviscid, potential flow solution gives a symmetric pressure distribution, and in the streamwise direction the force due to pressure acting on the front face is exactly balanced by the force due to pressure acting on the back face. The drag on the cylinder is zero. This is obviously not true for the flow of a real fluid where the boundary layers and wake play a major role.

### 6.9.2   Viscous effects

Over the front face of the cylinder ($\beta < 90°$), the pressure is decreasing, so the flow is accelerating. The boundary layer in this region remains very thin, and the pressure changes very little across its thickness because the streamlines are almost parallel. Hence, the pressure on the surface in a viscous flow is very close to its value in an inviscid, irrotational flow (see Figure 6.11). Near the shoulder where $\beta = 90°$, the pressure gradient changes from being negative (decreasing pressure, called a *favorable pressure gradient*) to positive (increasing pressure, called an *adverse pressure gradient*). The force in the flow direction due to pressure differences changes sign from being an accelerating force to being a retarding force. In response, the flow slows down. However, the fluid in the boundary layer already has a reduced momentum because of viscous stresses, and it does not have enough momentum to overcome the retarding force. As the pressure rises, some fluid particles near the wall actually reverse direction, and the flow separates. Large eddying motions are formed in the

$$C_p = \frac{p - p_0}{\frac{1}{2}\rho U^2}$$

Inviscid theory
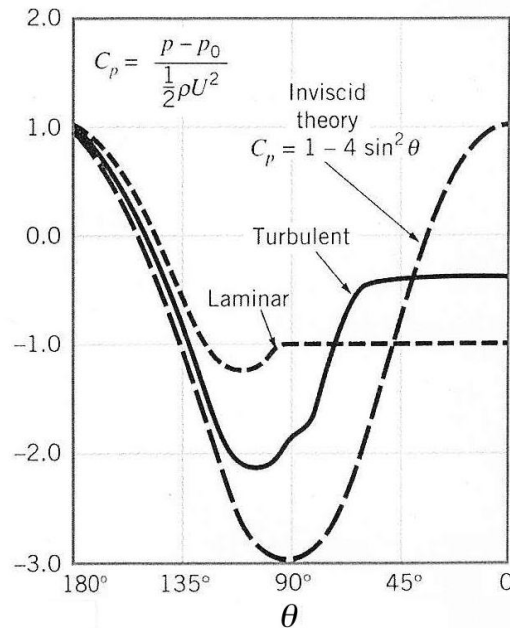
$$C_p = 1 - 4\sin^2\theta$$

Turbulent

Laminar

Figure 6.11: A comparison of the inviscid pressure distribution on a circular cylinder with a typical experimental distribution. Adapted from Munson, Young & Okiishi *Fundamentals of Fluid Mechanics*, John Wiley & Sons, 1998.

wake, and large pressure losses occur. The pressure distribution then departs dramatically from the inviscid solution. The wake also exerts an upstream influence on the boundary layer, and for the case shown in Figure 6.11, separation actually takes place upstream of the shoulder, somewhere near $\beta = 80°$.

The drag on the cylinder is made up of two components: a minor part due to the viscous friction acting on the surface, and a major part due to pressure differences between the front and the rear of the cylinder. Bodies where the pressure losses dominate the total drag force are called *bluff* bodies, and the cylinder is a good example of a bluff body. Bodies where the pressure losses are small and the viscous stresses dominate the total drag force are called *streamlined* bodies, and a good example of a streamlined body flow is the flow over an airfoil at small angles of attack.

So, despite the fact that the viscosities of common fluids are very low, a substantial drag force is found on most bodies. This was puzzling to scientists in the nineteenth century who believed that, since the viscosity was so small, the inviscid assumption should hold to a high degree of accuracy. The discrepancy was called "d'Alembert's Paradox," after the famous French scientist who studied this problem. The paradox was resolved by Prandtl in 1904, when he described for the first time the nature of the boundary layers that are formed near the surface due to the action of viscosity. Prandtl noted that in a thin layer near the wall, strong velocity gradients were present, and that despite the small magnitude of the viscosity, the viscous stress, being the product of the viscosity and the velocity gradient, could become very significant — viscosity could not be ignored. Mathematically, we could say that inviscid flow cannot satisfy the boundary conditions of a real flow: specifically, inviscid flows allow slip at the surface, whereas viscous flows do not.
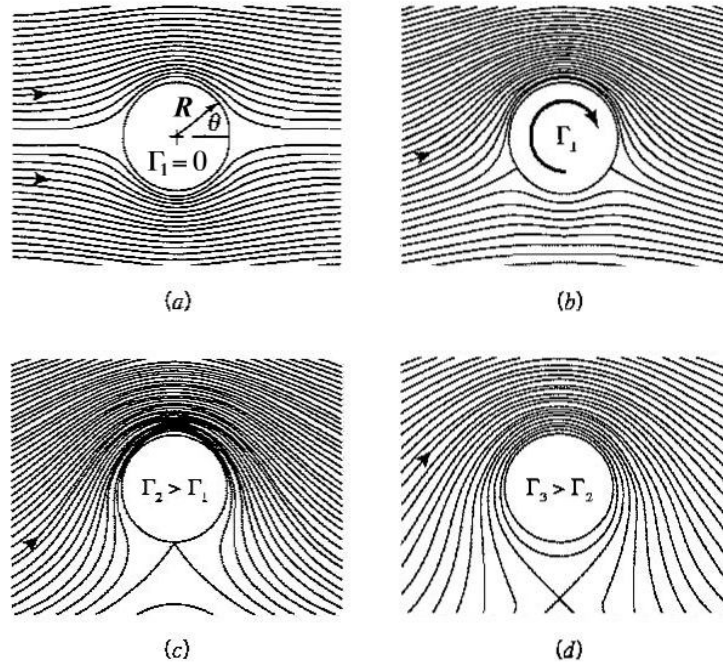
Figure 6.12: The addition of a vortex of increasing strength to a uniform flow over a circular cylinder. Adapted from F. M. White, *Fluid Mechanics*, 2nd ed., McGraw-Hill, 1986.

## 6.10   Lift

A very interesting flow is generated when we add a vortex of strength $\Gamma$ to the uniform flow over a circular cylinder. The combined stream function is given by

$$\psi \ = \ Ur\left(1 - \frac{R^2}{r^2}\right)\sin\theta + \frac{\Gamma}{2\pi}\ln r \qquad (6.40)$$

where the vortex was chosen to have a clockwise rotation. The streamline pattern is shown in Figure 6.12 for increasing vortex strength, starting with $\Gamma = 0$. We can show that the streamline where $\psi = 0$ always remains a closed circle of radius $R$.

As seen in Figure 6.12, the vortex moves the stagnation points away from the line of horizontal symmetry. The streamlines over the upper part of the cylinder come closer together, whereas those near the lower part move further apart. At the same time, the pressure decreases on the upper part, and increases on the lower part. A lift is generated. As the strength of the vortex increases, the stagnation points come closer together, and eventually they move off the surface of the cylinder. The lift keeps increasing at the same time.

By following a similar procedure to that given in Section 6.9, we can find the velocity and pressure on the surface of the cylinder, and by integrating the pressure distribution we can show that the resultant lift force $F_L$ (per unit span) is given by

$$F_L = \rho U \Gamma \qquad (6.41)$$

so that the lift is proportional to the strength of the vortex.

This flow field, made up of a vortex and a uniform flow over a circular cylinder, helps us to understand and quantify two very significant phenomena: the lift generated by a spinning cylinder, and the lift generated by an airfoil.
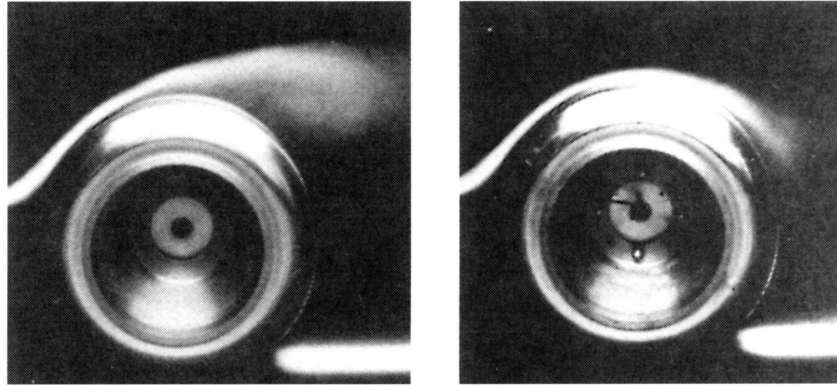
Figure 6.13: Visualization of the flow on a counter-rotating (left) and a non-rotating (right) wheel. The Reynolds number is $0.53 \times 10^6$. From *Race Car Aerodynamics*, J. Katz, Robert Bentley Publishers, 1995. Copyright AIAA, 1977, with permission.

### 6.10.1 Magnus effect

The flow field shown in Figure 6.12 is for inviscid flow. However, in a viscous fluid, a cylinder spinning in an otherwise uniform flow can generate a flow field that looks remarkably similar. A thin layer of air (the boundary layer) is forced to spin with the cylinder because of viscous friction, and its effect on the surrounding flow is similar to that produced by the vortex on the flow over a non-spinning cylinder. In region where the direction of motion of the moving surface is the same as that of the external air stream [the top of the cylinder in Figure 6.12(b)], the velocities sum, the streamlines come closer together, and the pressure in this region is relatively low. In the region of the flow where the motion due to spin is opposite to that of the air stream [the bottom of the cylinder in Figure 6.12(b)], there is a region of low velocity where the streamlines diverge and the pressure is relatively high. The cylinder experiences a lift force acting in a direction normal to the freestream [vertically up in Figure 6.12(b)]. In effect, the spin produces a circulation around the cylinder, and the strength of this "virtual" vortex depends on the spin rate of the cylinder.

The appearance of a side force on a spinning cylinder or sphere is called the *Magnus effect*, after the Swedish physicist Gustav Magnus who first described it clearly in 1853. Its effect is well known to all participants in ball sports, especially golf, baseball, cricket and tennis, where backspin creates a vertical lift force. For additional observations on the fluid mechanics of sports balls, see Section 9.7.

The Magnus effect is also seen in spinning cylinders and disks. The effect of rotation on the flow field around an automobile wheel is shown in Figure 6.13. The rotation is in the sense of a car traveling right to left, and so the motion of the upper surface of the tire is in a direction opposite to the incoming flow direction. As a result, the velocity outside the boundary layer in that region is lower than in the case of a non-spinning wheel, and the pressure is higher. As a result, there is a down force on the wheel. In addition, the fact that the viscous flow in the boundary layer experiences a stronger deceleration moves the upper separation point forward, increasing the size of the wake. As a result, the rate of rotation can strongly affect both the lift and drag forces developed by the wheel.

### 6.10.2 Airfoils and wings

In Section 3.5.3, we noted that when a flow is deflected by a solid surface, the surface must be exerting a force on the fluid. By Newton's third law, there will be an equal and opposite force exerted by the fluid on the surface. By adding a vortex to the flow over a circular
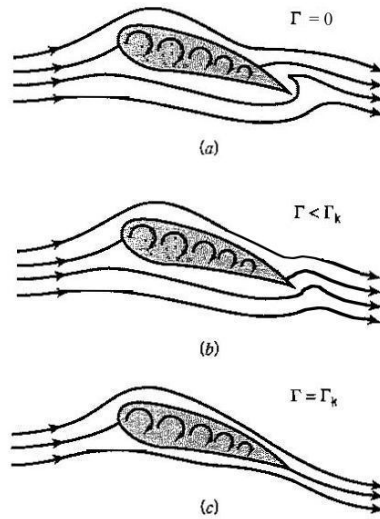
Figure 6.14: The addition of a vortex of increasing strength to a uniform flow over an airfoil shape. Adapted from F. M. White, *Fluid Mechanics*, 2nd ed., McGraw-Hill, 1986.

cylinder, a similar flow deflection occurs, and we can infer that a lift force is generated. Furthermore, the stronger the deflection, the stronger the lift force, and from equation 6.41 we see that the lift force is proportional to the strength of the vortex. We will now consider the potential flow over an airfoil, and the effect of adding a vortex of strength $\Gamma$.

All practical airfoils have rounded leading edges, and sharp trailing edges. If we were to solve the potential flow over a typical airfoil shape, we would see a streamline pattern similar to that shown in Figure 6.14(a). One of the stagnation points is always located near the leading edge, and in a potential flow the other is typically located somewhere on the upper surface. By analyzing the pressure distribution over the surface, we would find that an airfoil in potential flow generates no lift and no drag, which is completely contrary to our experience of "real" airfoils.

In fact, the flow shown in Figure 6.14(a) cannot occur in any real fluid. Viscosity always plays a very important role. For example, the potential flow over the sharp trailing edge indicates that the flow in this region needs to changes its direction by almost 180° *instantaneously* to follow the contour of the body. The slope of the surface changes discontinuously at the trailing edge, which implies that the fluid has to change its velocity infinitely fast, which gives rise to an infinite strain rate. For a viscous fluid, this would be associated with an infinite shear stress.

Clearly, this is unrealistic, and when we look at the real flow over an airfoil (Figure 6.15), we see that the flow near the trailing edge does not behave at all like that shown in Figure 6.14(a). The flow leaves the trailing edge smoothly, which means that the trailing edge is also a stagnation point. Under these conditions, all shear stresses are finite. The question is, how can we modify the potential flow solution to make it resemble the real flow?

If we add a clockwise vortex to the flow in Figure 6.14(a) we can move the stagnation points, as we did for the cylinder flow in Figure 6.12. By increasing the strength of the vortex, the flow pattern changes from that shown in Figure 6.14(a), to that shown in Figure 6.14(b). At the same time, the airfoil begins to generate lift. In effect, the addition of a clockwise vortex increases the average velocity over the top surface of the airfoil, and reduces the average velocity over the bottom, and by Bernoulli's equation we can see that this results in a lift force due to the pressure difference between the top and bottom surfaces. For
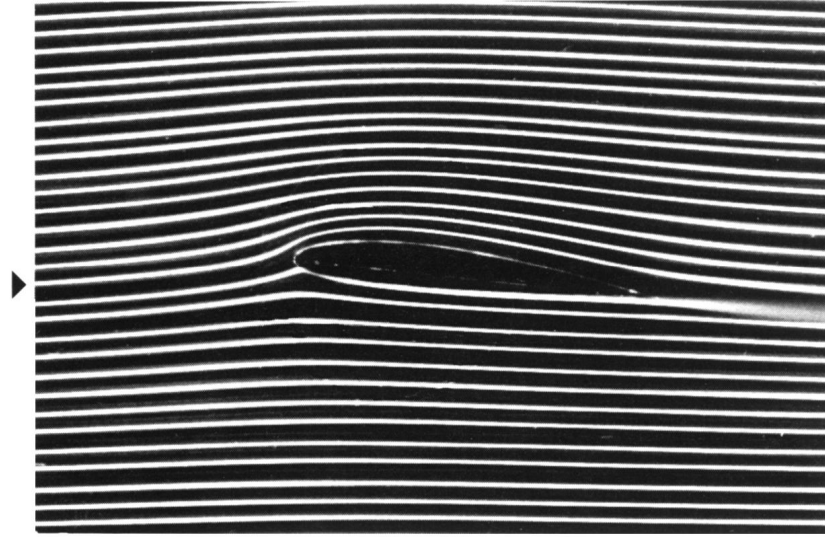
Figure 6.15: Streamlines over an airfoil shape made visible using smoke in air. Reynolds number based on chord length $R_c = 2.1 \times 10^5$, angle of attack $\alpha = 5°$. From *Visualized Flow*, Japan Society of Mechanical Engineers, Pergamon Press, 1988.

a particular vortex strength, $\Gamma_K$, the rear stagnation point will be located at the trailing edge [Figure 6.14(c)]. The lift force produced by the airfoil under this condition (per unit span) is remarkably similar to that acting on a cylinder with an imposed circulation (see equation 6.41, and it is given by

$$F_L = \rho U_\infty \Gamma_K \tag{6.42}$$

This is called the *Kutta-Joukowski theorem*, named after a German and a Russian aerodynamicist active in the early part of the 20th century. The boundary condition imposed on the flow, that is, the requirement that the rear stagnation point coincides with the trailing edge, is called the *Kutta condition*.

The Kutta-Joukowski theorem applies to the flow of an inviscid fluid over a two-dimensional body in steady motion. It holds for bodies of arbitrary shape, and so it also predicts the lift generated by a cylinder with any level of imposed circulation, although the corresponding Kutta condition only applies to bodies with a sharp trailing edge. The Kutta-Joukowski theorem is the basis for the theory of lift on wings, and the thrust of fan and propeller blades. Experiments show that it is in very good agreement with measurements of lift on two-dimensional airfoils.

An important parameter is the *angle of attack*, which is the angle the chord line makes with the incoming flow direction.[3] As the angle of attack increases, the circulation required to satisfy the Kutta condition also increases, and therefore the lift increases as well. It can be shown that for small angles of attack $\alpha$, the lift coefficient $C_L$ is given by

$$C_L = \frac{F_L}{\frac{1}{2}\rho U_\infty^2 c} = 2\pi\alpha \tag{6.43}$$

where $c$ is the chord length.[4] This result is compared with data in Figure 9.13. It holds for most airfoil shapes for $\alpha$ less than about 12 to 15°, at which point the boundary layer on

---

[3]The airfoil *chord* is the straight line drawn from the leading edge to the trailing edge.

[4]See, for example, *Foundations of Aerodynamics*, 4th edition, by A. M. Kuethe and C.-Y. Chow, published by John Wiley & Sons, 1986.
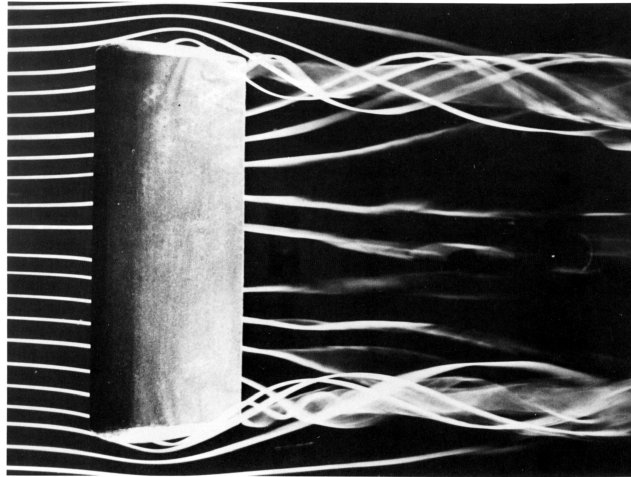
Figure 6.16: The formation of trailing vortices from a wing of finite span. In this view, the flow is from left to right, and the top surface has a lower pressure. From M. R. Head, in *Flow Visual II*, ed. W. Merzkirch, pp. 339-403, published by Hemisphere.

the rear part of the upper surface can begin to separate, a condition known in aerodynamics as *stall*. Once the airfoil stalls, the drag increases significantly, and there may be a sudden loss of lift.

### 6.10.3   Trailing vortices

The vortex that was added to the potential flow to satisfy the Kutta condition is a theoretical construct. In the case of an airfoil moving through a viscous fluid, however, we often think of a virtual "bound" vortex contained in the airfoil. It is real in the sense that, on average, the flow over the top surface of the airfoil is faster than that over the bottom surface, and so the sense of the circulation is clockwise if the flow over the airfoil is moving from left to right.

So far, we have only dealt with two-dimensional airfoils that have, in effect, an infinite wingspan. For an airfoil with finite wingspan, however, a very consistent observation is made. Near the tips of the wing, trailing vortices form which can be made visible using smoke, as in Figure 6.16. Where do they come from? In one interpretation, trailing vortices are formed near the wingtips because the flow tends to spill over the wingtip in response to the pressure difference between the top and bottom surface of the wing. The pressure on the top is lower than on the bottom, so near each wing tip there is a tendency for the flow to move from the bottom to the top of the wing. If we are looking from some point downstream of the wing back toward the wing, we see the formation of a clockwise vortex near the left wing tip, and a counterclockwise vortex near the right wing tip (see Figure 6.16).

In another interpretation, the trailing vortices are seen as the physical continuation of the virtual vortex "bound" in the wing (see Figure 6.14). Since it is known from theory and experiment that a vortex is shed from the airfoil when it starts its motion, we have a simple picture of the vortex system of a finite wing, comprising a bound vortex, a starting vortex, and two trailing vortices (Figure 6.17). We have a closed vortex loop of circulation $\Gamma_K$ at all points along the loop. This view was developed by Lanchester in England and Prandtl in Germany, and it is often called the Prandtl lifting line theory. In reality, the distribution of vorticity is more complex than that implied by Figure 6.17, but it still represents a powerful concept in learning to understand three-dimensional airfoil behavior.

One result is that the wingtip vortices have the same strength as the bound vortex.
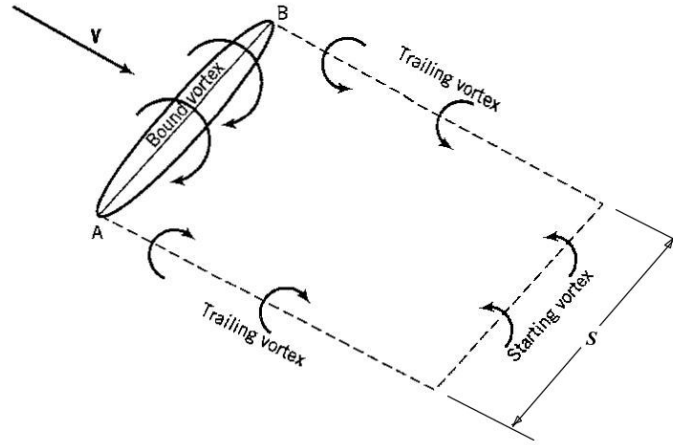
Figure 6.17: Vortex system of a finite wing.

When the lift increases, the strength of the bound vortex increases, and so do the strengths of the trailing vortices. When the lift is maximum, as in takeoff and landing, the trailing vortices have their maximum strength. If a following airplane encounters one of the trailing vortices, it will experience a strong overturning moment which can flip the airplane. All airports, therefore, have minimum time intervals between successive takeoffs and landings to avoid this danger.

A second result is that the trailing vortices generate circulating flow fields. This is true for all vortices, but in the case of trailing vortices the flow field due to one vortex interacts with the flow field of the other vortex. This vortex-vortex interaction is the subject of the next section.

## 6.11   Vortex Interactions

The superposition of two vortex flow fields leads to some interesting phenomena. A good example is the wake of an airplane where two trailing vortices are present (see Figure 6.17). Once the airplane has taken off, the starting vortex has been left far behind. The trailing vortex flow may then be idealized as two infinitely long, line vortices, separated by a distance $S$, where one vortex has a clockwise circulation $-\Gamma$, and the other has a counterclockwise circulation $\Gamma$. The combined velocity field will be the linear superposition of the two potential vortex flow fields. We say that each vortex "induces" its own velocity field with a distribution given by equation 6.29, which is

$$u_\theta = \frac{\Gamma}{2\pi r}$$

There will be a velocity induced by the right hand, counterclockwise vortex on the left hand, clockwise vortex, which tends to push the left hand vortex down. The left hand vortex, in turn, is associated with an induced velocity field that tends to push the right hand vortex down. We see that the interaction of a pair of line vortices of opposite sign causes the pair to move down together with a propagation velocity $u_p$ given by

$$u_p = \frac{\Gamma}{2\pi S} \tag{6.44}$$

where $S$ is the distance between the vortices. As a result of this induced motion, the trailing vortex system in the wake of a wing moves downward as it is left behind.

This self-induced propagation can also be seen by moving a flat plate through water in a bath or in a large bucket. Move the plate while holding it vertical and at right angles to the direction of motion for a short distance and then remove it from the liquid. Vortices of opposite sign are produced at the vertical edges, and they will continue to move under their own induced velocity field after the plate is withdrawn.

A similar phenomenon is seen in the motion of a vortex ring. A vortex ring can be generated and visualized using a cardboard cylinder (a handtowel roll works well) sealed off at both ends with paper diaphragms. A $5\,mm$ circular hole needs to be made in one diaphragm, and the cylinder should be filled with smoke from a cigarette or a stick of incense. If the end without the hole is lightly tapped, a smoke ring will emanate from the hole in the other end. Each part of the smoke ring induces a velocity that acts on all other parts of the ring, and through this interaction the ring propagates at a constant velocity through the air. The resulting motion of the smoke-filled vortex ring is quite beautiful to watch.

# Chapter 7

# Dimensional Analysis

Dimensional analysis is the process by which the dimensions of equations and physical phenomena are examined to give new insight into their solutions. This analysis can be extremely powerful. Besides being rather elegant, it can greatly simplify problem solving, and for problems where the equations of motion cannot be solved it sets the rules for designing model tests, which can help to reduce the level of experimental effort significantly.

The principal aim of dimensional analysis in fluid mechanics is to identify the important nondimensional parameters that describe any given flow problem. Thus far, we have already encountered a number of nondimensional parameters, each of which has a particular physical interpretation. For example, in Section 1.8 we described the Reynolds number, $Re = UD/\nu$, as the parameter that indicates the onset of turbulent flow. Another nondimensional parameter, the pressure coefficient $C_p = (p - p_\infty)/\frac{1}{2}\rho V^2$ was discussed in Section 4.3.1, and we see that it is the ratio of static pressure differences to the dynamic pressure. The lift and drag coefficients, $C_L$ and $C_D$, were defined in Example 3.9 in the Study Guide,and in Section 1.5 we introduced the Mach number $M$, which we interpreted as the ratio of a wave speed to the flow velocity.

Nondimensional parameters are widely used in fluid mechanics, and there are good reasons for this.

1. Dimensional analysis leads to a reduced variable set. A problem where the "output" variable, such as the lift force, is governed by a set of $(N-1)$ "input" variables (for example, a length, a velocity, the density, the viscosity, the speed of sound, a roughness height, etc.), can generally be expressed in terms of a total of $(N-3)$ nondimensional groups (for example, the lift coefficient, the Reynolds number, the Mach number, etc.).

2. When testing a scale model of an object, such as a car or an airplane, dimensional analysis provides the guidelines for scaling the results from a model test to the full-scale. In other words, dimensional analysis sets the rules under which full similarity in model tests can be achieved.

3. Nondimensional parameters are more convenient than dimensional parameters since they are independent of the system of units. In engineering, dimensional equations are sometimes used, and they contribute to confusion, errors and wasted effort. Dimensional equations depend on using the required units for each of the variables, or the answer will be incorrect. They are common in some areas of engineering, such as in the calculation of heat transfer rates and in describing the performance of turbomachines.

4. Nondimensional equations and data presentations are more elegant than their dimensional counterparts. Engineering solutions need to be practical, but they are always more attractive when they display a sense of style or elegance.
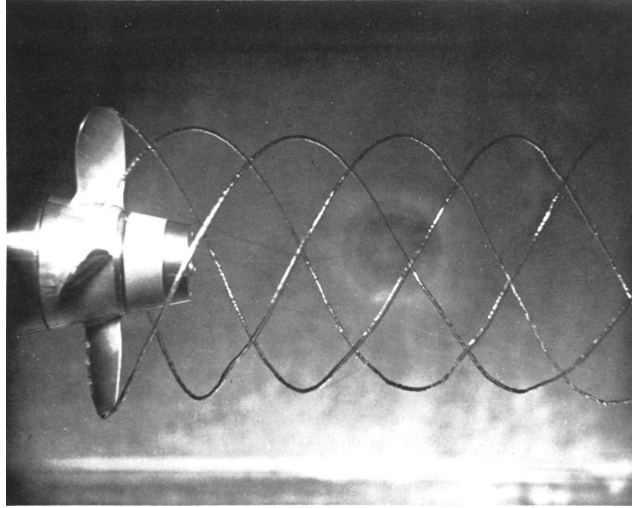
Figure 7.1: Cavitation on a model propeller. The bubbles are generated near the tip of each blade, and from a helical pattern in the wake. Photograph courtesy of the Garfield Thomas Water Tunnel, Pennsylvania State University.

The most powerful application of dimensional analysis occurs in situations where the governing equations cannot be solved. This is often the case in fluid mechanics. Very few exact solutions of the equations of motion can be found, and for the vast majority of engineering problems involving fluid flows we need to use an approximate analysis where the full equations are simplified to some extent, or we need to perform experiments to determine empirically the behavior of the system empirically over some range of interest (we may, for example, need to understand cavitation on marine propellers, as illustrated in Figure 7.1). In both cases, dimensional analysis plays a critical role in reducing the amount of effort involved and by providing physically meaningful interpretations for the answers obtained. Instead of solving the equations directly, we try to identify the important variables (such as force, velocity, density, viscosity, the size of the object, etc.), arrange these variables in nondimensional groups, and write down the functional form of the flow behavior. This procedure establishes the conditions under which similarity occurs, and it always reduces the number of variables that need to be considered.

It is rare for dimensional analysis to actually yield the analytical relationship governing the behavior. Usually, it is just the functional form that can be found, and the actual relationship must be determined by experiment. The experiments will also verify if any parameters neglected in the analysis were indeed negligible. To see how dimensional analysis works, we first need to define what system of dimensions we will use, and what is meant by a "complete physical equation."

## 7.1  Dimensional Homogeneity

When we write an algebraic equation in engineering, we are rarely dealing with just numbers. We are usually concerned with quantities such as length, force or acceleration. These quantities have a dimension (e.g., length or distance) and a unit (e.g., inch or meter). In fluid mechanics, the four fundamental dimensions are usually taken to be mass $M$, length $L$, time $T$ and temperature $\theta$. An alternative system uses force, length, time and temperature, but it will not be used in this book.

Some common variables and their dimensions are as follows (the square brackets are

used as shorthand for "the dimensions of .... are").

$$[\text{angular velocity}] \; = \; \frac{\text{angular measure}}{\text{time}} \; = \; T^{-1}$$

$$[\text{density}] \; = \; \frac{\text{mass}}{\text{volume}} \; = \; ML^{-3}$$

$$[\text{velocity}] \; = \; \frac{\text{length}}{\text{time}} \; = \; LT^{-1}$$

$$[\text{acceleration}] \; = \; \frac{\text{length}}{(\text{time})^2} \; = \; LT^{-2}$$

$$[\text{force}] \; = \; \text{mass} \times \text{acceleration} \; = \; MLT^{-2}$$

$$[\text{pressure}] \; = \; \frac{\text{force}}{\text{area}} \; = \; ML^{-1}T^{-2}$$

$$[\text{work}] \; = \; \text{force} \times \text{distance} \; = \; ML^2 T^{-2}$$

$$[\text{torque}] \; = \; \text{force} \times \text{distance} \; = \; ML^2 T^{-2}$$

$$[\text{power}] \; = \; \text{force} \times \text{velocity} \; = \; ML^2 T^{-3}$$

$$[\text{dynamic viscosity}] \; = \; \frac{\text{stress}}{\text{velocity-gradient}}$$

$$= \; \frac{(\text{force/area})}{(\text{velocity/length})} \; = \; ML^{-1}T^{-1}$$

$$[\text{kinematic viscosity}] \; = \; \frac{\text{viscosity}}{\text{density}} \; = \; \frac{\text{viscosity}}{(\text{mass/volume})} \; = \; L^2 T^{-1}$$

$$[\text{surface tension}] \; = \; \frac{\text{force}}{\text{length}} \; = \; MT^{-2}$$

Some quantities are already dimensionless. These include pure numbers, angular degrees or radians, and strain.

The concept of a dimension is important because we can only add or compare quantities which have similar dimensions: lengths to lengths, and forces to forces. In other words, all parts of an equation must have the same dimension — this is called the *principle of dimensional homogeneity*, and if the equation satisfies this principle it is called a *complete physical equation*. Take, for example, Bernoulli's equation

$$\frac{p}{\rho} + \tfrac{1}{2}V^2 + gh \; = \; B \tag{7.1}$$

where $B$ is a constant. We can examine the dimensions of each term in the equation by writing the dimensional form of the equation:

$$\frac{M}{L^2}\frac{L}{T^2} \times \frac{L^3}{M} \; + \; \frac{L^2}{T^2} \; + \; \frac{L}{T^2} \times L \; = \; [B]$$

(the number $\tfrac{1}{2}$ is just a counting number with no dimensions). That is,

$$\frac{L^2}{T^2} + \frac{L^2}{T^2} + \frac{L^2}{T^2} \; = \; [B]$$

All the parts on the left hand side have the same dimensions of (velocity)$^2$, and the equation is dimensionally homogeneous. The constant on the right hand side must have the same dimensions as the parts on the left, so that in this case the constant $B$ also has the dimensions of (velocity)$^2$.

If we rewrote equation 7.1 as

$$\frac{p}{\rho g} + \tfrac{1}{2}\frac{V^2}{g} + h \;\; = \;\; B_1$$

$$\text{or} \quad p + \tfrac{1}{2}\rho V^2 + \rho g h \;\; = \;\; B_2$$

then in the first case each term has dimensions of length (including $B_1$), and in the second case each term has dimensions of pressure (including $B_2$).  Thus we have the principle of dimensional homogeneity

> All physically meaningful equations are dimensionally homogeneous.

To put this another way, in order to measure any physical quantity we must first choose a unit of measurement, the size of which depends solely on our own particular preference. This arbitrariness in selecting a unit size leads to the following postulate: any equation that describes a real physical phenomenon can be formulated sothat its validity is independent of the size of the units of the primary quantities. Such equations are therefore called complete physical equations.  All equations given in this book are complete in this sense.  When writing down an equation from memory, it is always a good idea to check the dimensions of all parts of the equation — just to make sure it was remembered correctly.  It also helps in verifying an algebraic manipulation or proof where it can be used as a quick check on the answer.

## 7.2   Applying Dimensional Homogeneity

In this section we will show how the principle of dimensional homogeneity can be used to reduce the number of parameters describing a given problem.  To appreciate how this is achieved, we first need to understand how relationships that are expressed in functional form can be manipulated, and what is meant by independent variables. These concepts are illustrated using the following examples.

### 7.2.1   Example: Hydraulic jump

Consider a hydraulic jump. This is the name given to stationary, breaking waves in a water flow. A simple example can be seen by letting a stream of water fall on a flat surface such as a plate. The water spreads out on the plate in a thin layer, and then at some distance from the point of impact, a sudden rise in water level occurs. This is a circular hydraulic jump. A planar jump can be seen as the sudden increase in water height at the bottom of a dam spillway, as shown in Figure 7.2. In that case, the change in water height can be described by a simple relationship known as the hydraulic jump relationship

$$\frac{H_2}{H_1} \;\; = \;\; \frac{1}{2}\left(\sqrt{1 + 8F_1^2} - 1\right) \tag{7.2}$$

where $F_1 = V_1/\sqrt{gH_1}$ is a nondimensional quantity called the Froude number, $H$ is the water depth, and the suffixes 1 and 2 refer to conditions upstream and downstream of the jump. This relationship is derived and discussed in Chapter 11, but here we will only use it as an example to illustrate the concept of a functional dependence, and the principle of dimensional homogeneity.

The hydraulic jump relationship of equation 7.2 can also be written as

$$\frac{H_2}{H_1} = \phi\left(F_1\right) \tag{7.3}$$
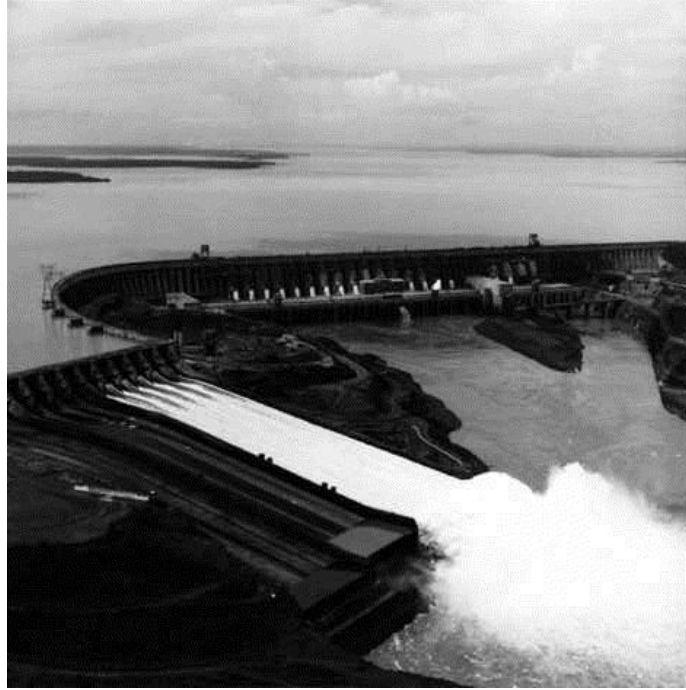
Figure 7.2: A hydraulic jump formed near the bottom of a spillway. From Siemens, with permission.

where the notation $\phi\left(F_1\right)$ denotes a functional dependence on $F_1$. Equation 7.3 states that the ratio of water depths across a hydraulic jump depends only on the upstream Froude number $F_1$. Alternatively, we can write equation 7.2 as a functional dependence in dimensional form, so that

$$H_2 = \phi'\left(H_1, V_1, g\right) \tag{7.4}$$

Four observations can now be made. First, the nondimensional form (equation 7.3) contains only two *nondimensional* parameters, whereas the dimensional form (equation 7.4) contains four *dimensional* parameters.

Second, we have included the dimensional constant $g$. It is absolutely essential to include all dimensional "constants" (such as $g$, the speed of sound, the density of water, etc.) in any dimensional analysis because the dimensions of constants are just as important as the dimensions of any variables. The only universal constants are dimensionless constants.

Third, the relationship given in equation 7.3 could be written in a number of alternative forms. For example, we can write it as

$$\frac{H_2}{H_1} = \phi_1\left(\frac{1}{F_1}\right)$$

Using the inverse of the Froude number instead of the Froude number itself, changes the form of the function, but it does not change the fact that the height of the jump depends only on the Froude number.

Fourth, consider the alternative functional relationship

$$\frac{H_2}{H_1} = \phi\left(F_1, \rho\right) \tag{7.5}$$

Since the left hand side is dimensionless, the right hand side must also be dimensionless. Any term on the right hand side that involves the Froude number by itself would be fine, but

terms that involve some function of density cannot be dimensionless. equation 7.5 cannot be correct; since the right hand side must be dimensionless, it cannot depend on the density by itself. This observation leads to two conclusions, based purely on dimensional grounds: either the density should be eliminated from the problem as stated in equation 7.5, or there are other variables in the problem that we have left out. If we were convinced that the density was important, another parameter is needed that has the same dimensions so that the density could be made nondimensional. One parameter that suggests itself is the viscosity $\mu$. This by itself does not have the dimensions of density, but combining the viscosity with some of the existing quantities can make it so. For example, the combination $\mu/V_1 H_1$ has the dimensions of mass per unit volume, so that one possibility for a dimensionally correct hydraulic jump relationship that includes density as one of the variables is

$$\frac{H_2}{H_1} = \phi\left(F_1, \frac{\rho V_1 H_1}{\mu}\right)$$

We recognize the new nondimensional group as the Reynolds number based on upstream flow conditions.

## 7.2.2   Example: Drag on a sphere

Suppose we need to find the drag force $F_D$ acting on a sphere of diameter $D$ in a viscous fluid flow of velocity $V$. The equations of motion for this flow can only be solved under very restricted conditions, and the full equations are too complex to allow a general solution. We must resort to dimensional analysis, and experiment.

We will assume that the drag force $F_D$ depends only on the fluid density $\rho$, the stream velocity $V$, the diameter $D$ and the fluid viscosity $\mu$. That is,

$$F_D = f\left(\rho, V, D, \mu\right) \tag{7.6}$$

where $f$ is the unknown functional dependence. Other variables may enter the problem, such as the roughness of the surface or the speed of sound, but for now we will keep it simple.

Given this functional form, what would it take to find the drag force experimentally over a wide range of variation in velocity, diameter, density and viscosity? For the sake of illustration, suppose that it takes about 10 points to define an experimental curve [Figure 7.3(a)]. To find the effect of velocity, we need to run the experiment for 10 different values of $V$, while holding all the other variables constant. To find the effect of diameter at each velocity, we need to find $F_D$ for 10 different values of $D$ for each velocity, while holding the other variables constant, so that the total number of experiments has grown to 100. For each $V$ and each $D$ we will need 10 values of of $\mu$ [Figure 7.3(b)] and 10 values of $\rho$ [Figure 7.3(c)], making a grand total of 10,000 experiments!

Instead, let us rearrange these variables into nondimensional groups, step by step. We can do this in a number of ways, but the object of each step is to make all the variables in the functional relationship, except one, dimensionless with respect to one of the fundamental dimensions. The dimensional variable that remains can then be deleted, as will be shown. We will use the three fundamental dimensions length $L$, mass $M$ and time $T$.[1]

All the variables except the density are first made dimensionless in mass. There is no need to start with density and mass, but it turns out to be convenient. Divide both sides of equation 7.6 by $\rho$, in order to change the dependent variable to $F_D/\rho$, which has dimensions

---

[1]The following treatment was adapted from *Dimensional Analysis for Engineers* by E.S. Taylor, published by Clarendon Press, Oxford (1974), and *Engineering Applications of Fluid Mechanics* by Hunsaker & Rightmire, published by McGraw-Hill (1947).
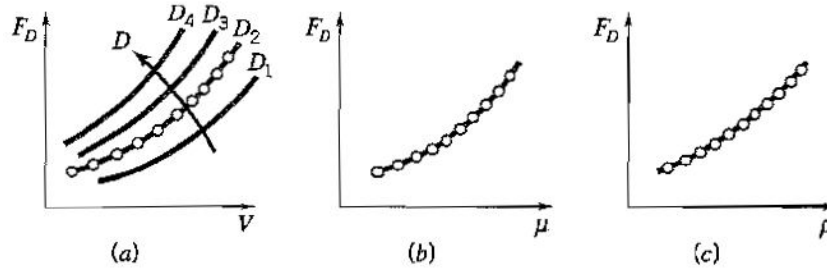
Figure 7.3: Experiments to find the drag force on a sphere. (a) Varying $V$ for different $D$, holding $\rho$ and $\mu$ constant; (b) For each point in (a), vary the viscosity, holding $\rho$ constant; (c) For each point in (b), vary the density.

$\left[MLT^{-2}/ML^{-3}\right] = \left[L^4T^{-2}\right]$. So

$$\frac{F_D}{\rho} = \frac{f\left(\rho, V, D, \mu\right)}{\rho} \tag{7.7}$$

or

$$\frac{F_D}{\rho} = f_1\left(\rho, V, D, \mu\right) \tag{7.8}$$

The step taken in going from equation 7.7 to 7.8 is perfectly legitimate: equation 7.7 states that $F_D/\rho$ depends on density, velocity, diameter and viscosity, and equation 7.8 states the same thing, although function $f_1$ is clearly different from function $f$.

In equation 7.8, the viscosity $\mu$ is the only independent variable (besides $\rho$) that has nonzero dimensions in mass. Let us define a new independent variable $\mu/\rho$, having dimensions $\left[ML^{-1}T^{-1}/ML^{-3}\right] = \left[L^2T^{-1}\right]$. So

$$\frac{F_D}{\rho} = f_2\left(\rho, V, D, \frac{\mu}{\rho}\right) \tag{7.9}$$

This change from $\mu$ to $\mu/\rho$ is permissible, since equations 7.8 and 7.9 still express the same functional dependence because $\rho$ and $\mu$ are *independent*. Independence means that in determining the drag we can vary $\rho$ and $\mu$ separately (as for equation 7.8), or vary $\rho$ and $\mu/\rho$ separately (as for equation 7.9).

The change of variables made in going from equation 7.8 to equation 7.9 cannot have any effect on the dimensional homogeneity of the equation. The validity of equation 7.9 must therefore be unaffected by a change in the particular mass unit that is used, as in going from slugs to kilograms, for example. The ratio of $F_D/\rho$ is unaffected by this change because it is independent of the mass unit. The value of $f_2\left(\rho, V, D, \frac{\mu}{\rho}\right)$ must likewise be unaltered. The values of $V$, $D$ and $\mu/\rho$ remain the same, but the value of $\rho$ would be different. Consequently, $f_2$ cannot depend on $\rho$, but only on $V$, $D$ and $\mu/\rho$. This was the same reasoning that led us to conclude that equation 7.5 could not be correct. In that case the density was eliminated on dimensional grounds, and the same argument applies here. The density is therefore deleted, and

$$\frac{F_D}{\rho} = f_2\left(V, D, \frac{\mu}{\rho}\right) \tag{7.10}$$

This procedure is more clearly illustrated using the *matrix of dimensions*. In this matrix, the columns are the governing variables, and the rows are the dimensions. The entries are

the exponents of the dimensions of each variable. The matrix of dimensions corresponding to equation 7.6 is

|     | $F_D$ | $\rho$ | $V$ | $D$ | $\mu$ |
|-----|-------|--------|-----|-----|-------|
| $M$ | 1     | 1      | 0   | 0   | 1     |
| $L$ | 1     | $-3$   | 1   | 1   | $-1$  |
| $T$ | $-2$  | 0      | $-1$| 0   | $-1$  |

Starting with the mass row, all the variables containing mass are made nondimensional in mass, except the density, by dividing all the variables in that row by the density.

|     | $F_D/\rho$ | $\rho$ | $V$ | $D$ | $\mu/\rho$ |
|-----|-----------|--------|-----|-----|-----------|
| $M$ | 0         | 1      | 0   | 0   | 0         |
| $L$ | 4         | $-3$   | 1   | 1   | 2         |
| $T$ | $-2$      | 0      | $-1$| 0   | $-1$      |

This is the matrix of dimensions corresponding to equation 7.9. The density is the only variable that still has a mass dimension and therefore it must be removed for equation 7.9 to be dimensionally homogeneous. Therefore

|     | $F_D/\rho$ | $V$ | $D$ | $\mu/\rho$ |
|-----|-----------|-----|-----|-----------|
| $M$ | 0         | 0   | 0   | 0         |
| $L$ | 4         | 1   | 1   | 2         |
| $T$ | $-2$      | $-1$| 0   | $-1$      |

The mass row is now empty, and we can delete it. So

|     | $F_D/\rho$ | $V$ | $D$ | $\mu/\rho$ |
|-----|-----------|-----|-----|-----------|
| $L$ | 4         | 1   | 1   | 2         |
| $T$ | $-2$      | $-1$| 0   | $-1$      |

which is the matrix of dimensions corresponding to equation 7.10.

A similar procedure can be used to give all the remaining variables, except the velocity, zero dimensions in time. Change $F_D/\rho$ to $F_D/\rho V^2$, which has dimensions $\left[L^4 T^{-2}/L^2 T^{-2}\right] = \left[L^2\right]$, and change $\mu/\rho$ to $\mu/\rho V$, which has dimensions $\left[L^2 T^{-1}/LT^{-1}\right] = [L]$. Then

$$\frac{F_D}{\rho V^2} = f_3\left(V, D, \frac{\mu}{\rho V}\right)$$

Can this result be correct? It appears that the left hand side was divided by $V^2$, whereas on the right hand side only one term was changed, and it was divided by $V$. What is really happening, though, is that we are making the quantities on the left and right hand sides independent of time by using $V$ (which contains time as a fundamental dimension) in whatever way necessary. As long as the variables remain independent, that is, they can be changed in ways that are different from the way the other variables change, this is a legitimate process and does not alter the basic functional dependence, although it will change the function itself (see also Section 7.4, step 5(c)).

According to our previous arguments, we can delete $V$ by virtue of the principle of dimensional homogeneity (since a change in the unit of time measurement will affect $V$ but no other variable), and we get

$$\frac{F_D}{\rho V^2} = f_3\left(D, \frac{\mu}{\rho V}\right)$$

The matrix of dimensions reduces to

$$
\begin{array}{c|ccc}
 & F_D/\left(\rho V^2\right) & D & \mu/\left(\rho V\right) \\
\hline
L & 2 & 1 & 1
\end{array}
$$

A last application of the same reasoning leads to

$$
\frac{F_D}{\rho V^2 D^2} \;=\; f_4\left(D, \frac{\mu}{\rho V D}\right) \;=\; f_4\left(\frac{\mu}{\rho V D}\right)
$$

That is

$$
\frac{F_D}{\rho V^2 D^2} \;=\; f_5\left(\frac{\rho V D}{\mu}\right)
$$

Finally

$$
\frac{F_D}{\frac{1}{2}\rho V^2 \left(\frac{\pi}{4}D^2\right)} \;=\; g\left(\frac{\rho V D}{\mu}\right) \tag{7.11}
$$

In the last step we included the nondimensional numbers $\frac{1}{2}$ and $\frac{\pi}{4}$ in the denominator of the left hand side, so that the denominator is of the form "dynamic pressure $\times$ cross-sectional area." For a sphere, the nondimensional drag coefficient $C_D$ is defined by

$$
C_D \;\equiv\; \frac{F_D}{\frac{1}{2}\rho V^2 \left(\frac{\pi}{4}D^2\right)} \tag{7.12}
$$

This allows us to write the functional dependence as

$$
C_D = g\left(Re\right) \tag{7.13}
$$

that is, the drag coefficient is only a function of Reynolds number.

This process has achieved a major result: equation 7.6, which involves five dimensional variables, has been simplified by purely dimensional reasoning to equation 7.13, which involves only two nondimensional variables.

One of the many consequences is that experimental data can be correlated more easily by means of equation 7.11 than equation 7.6. Using our earlier methodology, we would need only 10 experiments rather than 10,000 to determine the drag behavior. The actual data are shown in Figure 7.4. The data were obtained using spheres of different sizes, over a very wide velocity range, and for a number of different fluids. It applies to dust particles settling in the atmosphere, bubbles rising in a glass of beer, droplets formed by a fuel injector, soccer balls, and slow cannon balls (slow because compressibility effects become important at high speed and these were not taken into account). By using a nondimensional representation, all these results can be collapsed onto a single curve described by equation 7.13.

We should note that, although our analysis reduced the number of variables from five dimensional ones to two nondimensional ones, the answer is not unique: equation 7.11 is not the only form that can be obtained by starting from equation 7.6. By operating with $\mu$ instead of $\rho$, or by multiplying the left hand side of equation 7.11 by the Reynolds number, we can also get

$$
\frac{F}{\mu V D} \;=\; g_1\left(\frac{\rho V D}{\mu}\right) \tag{7.14}
$$

It is found that, except at very low Reynolds numbers, equation 7.11 is more useful than equation 7.14, because $F/\frac{1}{2}\rho V^2(\frac{\pi}{4}D^2)$ varies less than $F/\mu V D$ in the practical range of the independent variable $\rho V D/\mu$.

We see that more than one result is possible, and the choice of which nondimensional groups to use is somewhat arbitrary. We usually try to choose groups which have some
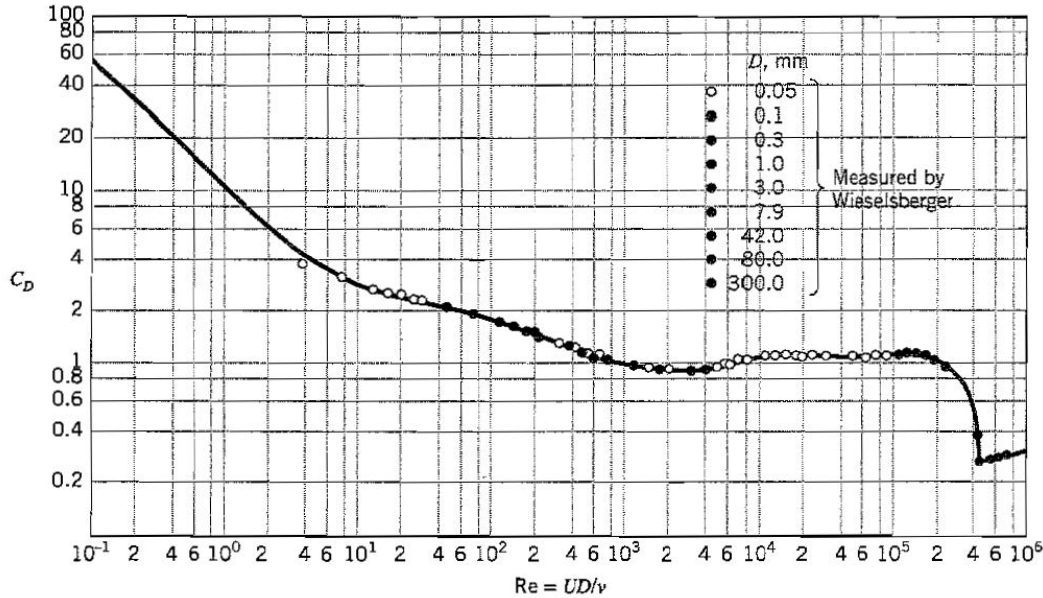
Figure 7.4: Drag of a sphere. Adapted from Schlichting *Boundary Layer Theory*, 7th edition, McGraw-Hill, 1979.

meaning, that is, groups that have a physical interpretation such as the Reynolds number, Froude number, and so forth. We will discuss this issue further in Section 7.6.

The first formal treatment of this successive application of dimensional homogeneity was given by E. Buckingham in 1892, in what became known as the "Buckingham Π theorem." Nondimensional parameters are sometimes called Π-products because of this connection with the Buckingham Π theorem.

To summarize, the number of variables can always be reduced by non-dimensionalization. Each time we make the functional relationship dimensionless with respect to one of the fundamental dimensions, the number of variables is reduced by one. So we can expect that, for a total of $N$ variables (including "input" and "output" variables) the number of nondimensional groups or Π-products $= N-$ (number of fundamental dimensions). The validity of this statement is discussed in the next section.

## 7.3   The Number of Dimensionless Groups

What is the validity of the rule "the number of Π-products $= N-$ (the number of fundamental dimensions)"? It is relatively easy to show that it fails in some cases. For instance, say that we needed to find the functional dependence of the speed of sound $a$. It could be a function of pressure $p$ and density $\rho$. We have a total of 3 parameters, and if we choose $M$, $L$ and $T$ as fundamental dimensions, our rule would suggest that no dimensionless groups can be found. However, the combination $\rho a^2/p$ is dimensionless, so at least one Π-product exists.

A universal rule can be found by examining the matrix of dimensions. For the sphere

drag example used in the previous section, we have

|   | $F_D$ | $\rho$ | $V$ | $D$ | $\mu$ |
|---|---|---|---|---|---|
| $M$ | 1 | 1 | 0 | 0 | 1 |
| $L$ | 1 | $-3$ | 1 | 1 | $-1$ |
| $T$ | $-2$ | 0 | $-1$ | 0 | $-1$ |

The rule that works every time is the one that says

> The number of dimensionless groups is equal to the total number of parameters minus the rank of the matrix of dimensions.

The rank of a matrix is the order of the largest determinant in the matrix with a nonzero value (see Section A.1). By trying different determinants of order 3 in the matrix for the sphere problem, we can find at least one determinant that is nonzero (for example, try the columns headed by $F_D$, $\rho$ and $V$) and so the rank of that matrix is 3. The number of $\Pi$-products is therefore $5 - 3 = 2$, as found earlier.

What about the speed of sound example? The matrix of dimensions for that case is

|   | $a$ | $p$ | $\rho$ |
|---|---|---|---|
| $M$ | 0 | 1 | 1 |
| $L$ | 1 | $-1$ | $-3$ |
| $T$ | $-1$ | $-2$ | 0 |

There is only one determinant of order 3 that can fit, and it is equal to zero. Therefore the rank of the matrix cannot be equal to 3. Is it 2? Yes, because it is easy to find one determinant of order 2 which is nonzero. The number of dimensionless groups is therefore $3 - 2 = 1$, and it is given by

$$\Pi_1 = \frac{\rho a^2}{p}$$

When only one nondimensional group exists, as in this case, it cannot be a function of anything else, since that would naturally require another nondimensional parameter. Therefore

> When only one nondimensional group exists, that group must be a constant.

In the case of the sound speed problem, the value of the constant depends on the particular fluid under consideration. For a perfect gas, it is the ratio of specific heats, $\gamma$ (see Section 11.4.4).

A similar problem regarding viscosity was first considered in Section 1.6.3. There, we noted that the viscosity of a gas depends on the average molecular speed $\bar{v}$, the density $\rho$, and the mean free path $\ell_m$. That is,

$$\mu = \psi\left(\bar{v}, \rho, \ell_m\right)$$

Then

|   | $\mu$ | $\bar{v}$ | $\rho$ | $\ell_m$ |
|---|---|---|---|---|
| $M$ | 1 | 0 | 1 | 0 |
| $L$ | $-1$ | 1 | $-3$ | 1 |
| $T$ | $-1$ | $-1$ | 0 | 0 |

The rank of the matrix is 3, so that the number of dimensionless parameters is $N - 3 = 1$. Hence

$$\Pi_1 \ = \ \frac{\rho \ell_m \bar{v}}{\mu}$$

Therefore $\Pi_1$ is a constant, and a simple kinetic model gives $\Pi_1 = \frac{5\pi}{32}$.

Consider one more example, based on the hydraulic jump (see Section 7.2.1). We start with equation 7.4

$$H_2 = \phi' \left( H_1, V_1, g \right)$$

Then

|   | $H_2$ | $H_1$ | $V_1$ | $g$ |
|---|---|---|---|---|
| $M$ | 0 | 0 | 0 | 0 |
| $L$ | 1 | 1 | 1 | 1 |
| $T$ | 0 | 0 | $-1$ | $-2$ |

The rank of this matrix cannot be 3 because of the zeros in the top row; no variable contains the mass dimension. We find that the rank is 2 so that the number of dimensionless parameters is $N - 2 = 2$. We already know that this yields the result first given by equation 7.3

$$\frac{H_2}{H_1} = \phi \left( \frac{V_1}{\sqrt{gH_1}} \right) = \phi \left( F_1 \right)$$

What if we include the density in the list of parameters? Then

|   | $H_2$ | $H_1$ | $V_1$ | $g$ | $\rho$ |
|---|---|---|---|---|---|
| $M$ | 0 | 0 | 0 | 0 | 1 |
| $L$ | 1 | 1 | 1 | 1 | $-3$ |
| $T$ | 0 | 0 | $-1$ | $-2$ | 0 |

The rank of this new matrix is 3, so that the number of dimensionless parameters is $5 - 3 = 2$. But we already have 2: the ratio of depths and the Froude number. The density does not belong since there is no other parameter with a mass dimension that could be used together with the density to make a new nondimensional parameter (we argued this from first principles in Section 7.2).

Dimensional analysis therefore helps us to find the right number of dimensionless groups or $\Pi$-products. It can tell us that a certain dimensional variable does not belong, and it can also tell us if another variable is missing. For example, if we really believed that the hydraulic jump depends on the density of the fluid, then we need another variable with a non-zero dimension in mass, such as the pressure, to make the density dimensionless in mass. We then end up with 3 nondimensional groups: the ratio of depths, the Froude number and a pressure coefficient. Alternatively, if we included the viscosity, which also has mass in its dimensions, the Reynolds number would make an appearance.

Dimensional analysis cannot tell us which $\Pi$-products are important in any particular flow problem. The results of the analysis should always be tested by experiment, and it is the experiment that will finally show which $\Pi$-products are important to describe the flow.

## 7.4   Non-Dimensionalizing Problems

In problems where dimensional analysis is likely to be useful, we use the following procedure.

**Step 1**: Determine $N$, the total number of variables, including input and output variables (in the sphere example, we had five: $F$, $V$, $D$, $\mu$, and $\rho$). This is the most crucial step in the process, since it defines the problem. It is also the most difficult step.

**Step 2**: Select a set of fundamental dimensions, usually mass, length and time ($M$, $L$ and $T$).

**Step 3**: Write down the matrix of dimensions. In this matrix, the columns are the governing parameters and the rows are the dimensions. The entries are the exponents of the dimensions of each parameter.

**Step 4**: Find the rank $r$ of the matrix of dimensions (the rank of a matrix is the order of the largest determinant in the matrix with a nonzero value). There will always be $N - r$ dimensionless parameters. In most cases, but not always, the rank of the matrix will be 3 since there are usually 3 fundamental dimensions (see Section 7.3).

**Step 5**: Establish these $N - r$ dimensionless parameters by

**(a)** Using your intuition. For example, in problems where viscosity is important, the Reynolds number usually makes an appearance. Similarly, if high-speed flow is present, the Mach number should be considered, and if waves or a free surface are present, the Froude number is certain to be useful. In other problems it is usually possible to take the dependent variable (the output), and choose a number of input variables that when combined with the dependent variable make a nondimensional group. This process can then be repeated to make dimensionless groups using only input variables. The matrix of dimensions can be very useful in this regard. Remember, the answer is not unique. This does not mean any answer will do, just that more than one answer is possible. Nevertheless, some answers are "better" than others (those that use standard $\Pi$-products, for example).[2]

**(b)** Check the result. That is, check that each $\Pi$-product really is nondimensional.

**(c)** Check that all the $\Pi$-products are independent. That is, if one of the dimensionless parameters is simply a combination of others, or just another raised to some power, it is not independent. A good check for independence is to see that each of the $\Pi$-products contains one variable that none of the other groups does.

**Step 6**: See if any of the dimensionless parameters are not important, and then neglect them. This requires considerable judgment.

**Step 7**: Test your results experimentally. This step is very important, since it will verify or refute all your assumptions, especially Steps 1, 5, and 6.

## 7.5 Pipe Flow Example

Consider flow through a circular, horizontal pipe of length $L$ and diameter $D$. The average velocity, integrated across the cross-section, is $\overline{V}$, so that

$$\overline{V} = \frac{1}{A} \int u \, dA \tag{7.15}$$

Note that $\overline{V}$ is equal to the volume flow rate divided by the cross-sectional area $A$. Develop a functional dependence for the pressure drop $\Delta p$, and express the result nondimensionally.

Step 1: Determine $N$, the total number of variables. We expect that $\Delta p$ will depend on $L$, $D$, $\overline{V}$, $\rho$, $\mu$, but what else? It might depend on the roughness of the surface $k$, where

---

[2] Some texts recommend the *method of indices* to find the $\Pi$-products. I have found this approach to be totally nonintuitive and full of opportunities for error, and therefore I strongly advise against its use.

$k$ is some measure of the average roughness height. It should not depend on gravity since the pipe is horizontal. It might depend on the speed of sound, but if the Mach number is small we can probably neglect it. Let's start with the minimum number of variables so that $N = 7$, and

$$\Delta p \;=\; \phi_1\left(L, D, \overline{V}, \rho, \mu, k\right)$$

Step 2: Select a set of fundamental units. Here, we choose $M$, $L$ and $T$.

Step 3: Write down the matrix of dimensions.

|   | $F$ | $\rho$ | $\overline{V}$ | $D$ | $k$ | $L$ | $\mu$ |
|---|-----|--------|----------------|-----|-----|-----|-------|
| $M$ | 1 | 1 | 0 | 0 | 0 | 0 | 1 |
| $L$ | 1 | $-3$ | 1 | 1 | 1 | 1 | $-1$ |
| $T$ | $-2$ | 0 | $-1$ | 0 | 0 | 0 | $-1$ |

Step 4: Find the number of nondimensional parameters. Since the rank of the matrix is 3, we will have $N - 3 = 4$ dimensionless parameters or $\Pi$-products.

Step 5a: Pick dimensionless parameters. According to Step 4, we need to find four. Let us start with the pressure drop. To make it nondimensional , we need a combination of the other variables that has the dimension of pressure. One likely candidate is the dynamic pressure $\frac{1}{2}\rho\overline{V}^2$. The first nondimensional group becomes

$$\Pi_1 \;=\; \frac{\Delta p}{\frac{1}{2}\rho\overline{V}^2}$$

The second possible nondimensional group is the length-to-diameter ratio

$$\Pi_2 \;=\; \frac{L}{D}$$

This ratio tells us if the pipe is short or long, compared to its diameter. The third nondimensional group is the relative roughness

$$\Pi_3 \;=\; \frac{k}{D}$$

which is more meaningful than $k/L$ since a large value of $k/D$ can be interpreted immediately as indicating a severe blockage effect due to roughness. What is left? The viscosity has not been used so far, so we can use the Reynolds number as the fourth nondimensional group

$$\Pi_4 \;=\; \frac{\rho\overline{V}L}{\mu}$$

Finally

$$\frac{\Delta p}{\frac{1}{2}\rho\overline{V}^2} \;=\; \phi_1\left(\frac{\rho\overline{V}D}{\mu}, \frac{L}{D}, \frac{k}{D}\right) \tag{7.16}$$

Step 5b: Check that the $\Pi$-groups are really nondimensional . Here, this step is straightforward: we recognize the left hand side of equation 7.16 as a pressure coefficient, and the right hand side contains ratios of lengths and a Reynolds number.

Step 5c: Check the independence of the nondimensional groups. None of the dimensionless parameters we found can be formed by a combination of the others, and of them is just

another raised to some power. Also, each $\Pi$-product has something which none of the others have: $\Delta p$ in the first, $\mu$ in the second, $L$ in the third and $k$ in the fourth. So these $\Pi$-products are independent.

Step 6: Decide if all the $\Pi$-products are all important. One suggestion might be that, since pipes are typically long compared to their diameter, an asymptotic state will exist where the flow properties do not change with further increase in length. From observation, we know that after 40–100 diameters the flow properties are free of entrance effects and the mean velocity profile is *fully developed*, which means that it is independent of position along the pipe. In that case, the parameter $\frac{L}{D}$ should no longer be important, and it can be dropped. This would also imply that we should not use the pressure drop along the whole length of the pipe (since a fully developed flow is independent of the distance along the pipe), but instead we should use the pressure drop per unit length, expressed in terms of the number of diameters. This thinking would suggest that equation 7.16 could be written as

$$\frac{\left(\frac{\Delta p}{L}\right) D}{\frac{1}{2}\rho \overline{V}^2} = \phi\left(\frac{\rho \overline{V} D}{\mu}, \frac{k}{D}\right) \tag{7.17}$$

The nondimensional group on the left hand side is called the friction factor $f$, defined by

$$f \equiv \frac{\left(\frac{\Delta p}{L}\right) D}{\frac{1}{2}\rho \overline{V}^2} \tag{7.18}$$

The most widely used correlation for the pressure drop in fully developed pipe flow uses the functional dependence expressed in equation 7.17. The experimental data are generally given in the form of a chart called the Moody diagram (Figure 8.7), where the friction factor $f$ is plotted as a function of Reynolds number based on diameter and average velocity, for different values of the relative roughness $k/D$. The curves shown in Figure 8.7 hold for all Newtonian fluids: water, air, milk, alcohol, natural gas, and so on. A fuller discussion of the pressure drop in pipe flow is given in Section 8.6.

## 7.6 Common Nondimensional Groups

We have noted that it is possible to have more than one correct answer in dimensional analysis. For example, in the sphere example given in Section 7.2, we started by eliminating the mass dimension by using the density, and we found that

$$\frac{F}{\frac{1}{2}\rho V^2 D^2} = g\left(\frac{\rho V D}{\mu}\right) \tag{7.19}$$

As was pointed out then, we could have started with the viscosity instead of the density. In that case, we would have found that

$$\frac{F}{\mu V D} = g_1\left(\frac{\rho V D}{\mu}\right) \tag{7.20}$$

Both answers are correct, but one may be preferable to or "better" than the other for a particular problem. To understand what constitutes a better answer generally requires physical insight into the problem, which may take a considerable amount of experience to develop. In some cases, however, it is reasonably obvious. For example, we could write the sphere drag relationship as

$$\frac{F}{\frac{1}{2}\rho V^2 D^2} = g_3\left(\sqrt{\frac{\mu}{\rho V D}}\right) \tag{7.21}$$

This does not change its "correctness" (both sides are still nondimensional), but we recognize the second $\Pi$-product as being a mutation of the Reynolds number, and we would probably choose to write equation 7.21 in the form given in equation 7.19. We might also recognize that it is the frontal area that governs the drag. Therefore, equation 7.19 could be "improved" by changing the left hand side to include the frontal area $\frac{\pi}{4}D^2$ instead of $D^2$, so that

$$\frac{F}{\frac{1}{2}\rho V^2 \frac{\pi}{4}D^2} = g_4\left(\frac{\rho V D}{\mu}\right)$$

The left hand side of this equation is now the drag coefficient for a sphere, as defined by equation 7.12. By using the frontal area in the definition of drag coefficients, we can more easily compare the drag coefficients obtained for a sphere to those obtained for other shapes.

## 7.7  Non-Dimensionalizing Equations

There are a large number of possible $\Pi$-products, but only a rather limited set is in common use. The most compelling reason for the popularity of this subset is that these parameters, such as the Reynolds number and the nondimensional force coefficients, often come naturally out of the equations of motion themselves.

For example, consider Bernoulli's equation. If at some point we know the reference static pressure $p_\infty$ and velocity $V_\infty$, then we could use them to non-dimensionalize Bernoulli's equation. If we start with equation 7.1

$$\frac{p}{\rho} + \tfrac{1}{2}V^2 + gh = B$$

each term has the dimensions of $V^2$. If we divide through by $\frac{1}{2}V_\infty^2$, we obtain the dimensionless form

$$\frac{p}{\frac{1}{2}\rho V_\infty^2} + \frac{V^2}{V_\infty^2} + \frac{gh}{\frac{1}{2}V_\infty^2} = B_3$$

The first term is a pressure coefficient of some sort, the second is a velocity ratio, and the third term contains a Froude number (squared). We can go one step further and subtract the constant quantity $p_\infty/\frac{1}{2}\rho V_\infty^2$ from both sides, giving

$$\frac{(p - p_\infty)}{\frac{1}{2}\rho V_\infty^2} + \left(\frac{V}{V_\infty}\right)^2 + \frac{gh}{\frac{1}{2}V_\infty^2} = B_4$$

so that the first term now takes the form of the pressure coefficient $C_p$ as defined in Section 4.3.1.

To take another example, consider the Navier-Stokes equation for constant density flow

$$\rho\frac{D\mathbf{V}}{Dt} = -\nabla p + \rho\mathbf{g} + \mu\nabla^2\mathbf{V}$$

This is the momentum equation for a viscous fluid in differential form (see Section 5.3, equation 5.19). Here, $\nabla^2$ is the Laplacian operator which represents a second order differentiation with respect to the space variables (see Section A.6).

If at some reference position in the flow we know the pressure $p_\infty$ and the velocity $V_\infty$, and if we can identify a reference length $L$, we can form the nondimensional variables

$$\begin{aligned} x' &= x/L \\ y' &= y/L \\ z' &= z/L \end{aligned}$$

$$t' = V_\infty t/L$$
$$\mathbf{V}' = \mathbf{V}/V_\infty$$
$$p' = (p - p_\infty)/\tfrac{1}{2}\rho V_\infty^2$$

We also have $\nabla' = L\nabla$, the nondimensional form of the gradient operator, and $\nabla'^2 = L^2\nabla^2$, the nondimensional form of the Laplacian operator.

Rewriting the Navier-Stokes equation in terms of these nondimensional variables gives

$$\frac{\rho V_\infty^2}{L}\frac{D\mathbf{V}'}{Dt'} = -\frac{1}{L}\tfrac{1}{2}\rho V_\infty^2 \nabla'p' + \rho\mathbf{g} + \frac{\mu V_\infty}{L^2}\nabla'^2\mathbf{V}'$$

so that

$$\frac{D\mathbf{V}'}{Dt'} = -\tfrac{1}{2}\nabla'p' + \frac{\mathbf{g}L}{V_\infty^2} + \frac{\nu}{V_\infty L}\nabla'^2\mathbf{V}' \qquad (7.22)$$

Three widely used nondimensional parameters have appeared: a nondimensional time, $t' = V_\infty t/L$ which is the inverse of the Strouhal number (see Section 9.5), the square of the Froude number $F_\infty = V_\infty/\sqrt{gL}$, and the Reynolds number $Re_\infty = V_\infty L/\nu$. I By inserting these nondimensional groups into equation 7.22, we obtain the nondimensional form of the Navier-Stokes equation

$$\frac{D\mathbf{V}'}{Dt'} = -\tfrac{1}{2}\nabla'p' + \frac{1}{F_\infty^2}\frac{\mathbf{g}}{g} + \frac{1}{Re_\infty}\nabla'^2\mathbf{V}' \qquad (7.23)$$

The significance of the Reynolds number in the Navier-Stokes equation is especially interesting. If the length and velocity scales that were used in the non-dimensionalization are the appropriate ones, then all the derivative terms should be of $O(1)$, and then the coefficients in the non-dimensional equation indicate the relative importance of each term. We see that as the Reynolds number becomes very large, the magnitude of the viscous term becomes very small compared to the other terms. In particular, the viscous term becomes small compared to the inertia term on the left hand side. The magnitude of the Reynolds number is therefore often interpreted as a measure of the importance of the inertia force compared to the viscous force.

We can also use the Couette flow shown in Figure 1.14 to illustrate this interpretation of the Reynolds number. The viscous force acting on the fluid at any point in the flow, $F_v$, is given by the viscous stress times the area, so that

$$F_v = \frac{\mu U}{h}A$$

We can estimate the magnitude of the corresponding inertial force, $F_i$, by finding the change in the momentum of the fluid between the top and bottom plates. Since the momentum of the flow in contact with the bottom plate is zero, the change in momentum is $\rho U^2 A$, and so

$$F_i = \rho U^2 A$$

Hence

$$\frac{F_i}{F_v} = \frac{\rho U^2 A}{\frac{\mu U}{h}A} = \frac{\rho U h}{\mu} = Re$$

From this example, we see again that the Reynolds number represents the ratio of a typical inertia force to a typical viscous force.

When the Reynolds number is very large, it would seem possible to neglect the viscous stress term in the Navier-Stokes equation. Very close to a solid surface, however, where boundary layers form, the relevant Reynolds number must be based on some measure of the viscous layer thickness, since that is the proper scale for the velocity gradient, and the resulting viscous stresses. Therefore, near a solid surface, within the boundary layer, the viscous term always remains important. Outside the boundary layer, it can often be ignored.
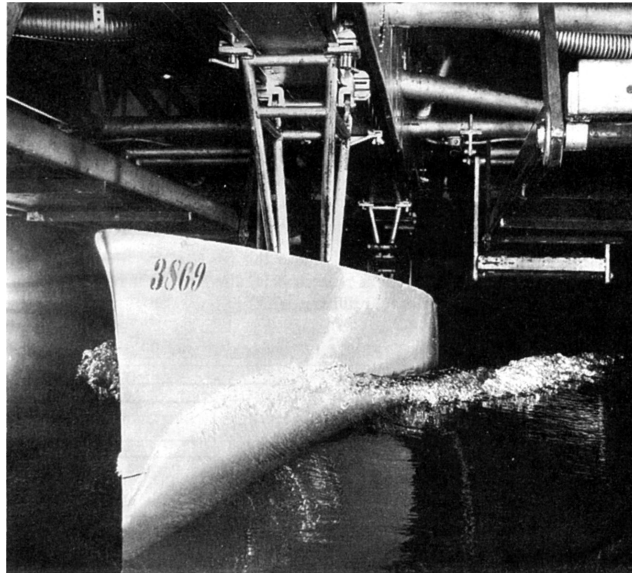
Figure 7.5: Testing a model ship in a towing tank at the Naval Ship Research and Development Center, Carderock, Maryland.

## 7.8   Scale Modeling

Dimensional analysis is particularly useful for problems where we cannot find solutions to the equations of motion, and where we need to conduct experiments to determine the flow behavior. When investigating the flow over vehicles, it is often useful to test scale models of full-scale vehicles. To design a new airplane, for example, many hours of wind tunnel tests are performed to test scale models of different wings and fuselage shapes. To help design boats and ships, scale models are often tested in towing tanks (Figure 7.5).

Scale models are used to save money since it is much cheaper to build a series of models than a series of full-scale vehicles, and model tests can be used to develop scaling laws. Scaling laws are needed to predict full-scale results from model tests. However, it is not always possible to test a scale model so that the flow conditions are exactly similar to those experienced by the full-scale vehicle. In that case, different size models are often used to give information on how the results might be extrapolated to the full scale.

We have seen how dimensional analysis can be used to find and interpret the nondimensional parameters that govern problems in fluid mechanics. It can also be used to determine the conditions for similarity in scale modeling. A scale model will only give correct results if the flow is similar to the full scale prototype. What do the words "similar" or "similarity" mean in this context? We have three levels of similarity that must be satisfied before a model can be said to be completely similar: geometric, kinematic, and dynamic similarity.

### 7.8.1   Geometric similarity

The model must have the same shape as the prototype, that is, it must be geometrically similar. This requires that corresponding lengths are related by a constant ratio. A model car, for instance, will be geometrically similar to the full-scale vehicle if

$$\frac{(\text{length})_m}{(\text{length})_p} \;=\; \frac{(\text{width})_m}{(\text{width})_p} \;=\; \frac{(\text{height})_m}{(\text{height})_p} \;=\; r_g \qquad (7.24)$$
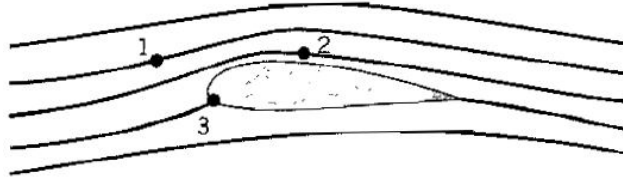
Figure 7.6: Flow over an airfoil.

and so on, where the subscripts $m$ and $p$ denote model and full-scale prototype, respectively, and $r_g$ is the scaling constant. When buying a model airplane kit, for example, the model might be advertised as a 1/72-scale model, which means that $r_g = 1/72$, and all corresponding dimensions are in the ratio 1:72.

## 7.8.2 Kinematic similarity

A flow field is kinematically similar if, at corresponding points in the flow, the velocities (at corresponding times) are in a constant ratio, $r_k$. For example, the flow over a model airfoil (Figure 7.6) will be kinematically similar to the full-scale airfoil if

$$\frac{V_{1m}}{V_{1p}} = \frac{V_{2m}}{V_{2p}} = \frac{V_{3m}}{V_{3p}} = r_k \qquad (7.25)$$

and so on, where $V_m$ and $V_p$ are the velocities in the model and prototype. respectively. If this condition is satisfied, the two flow fields will have exactly the same appearance.

## 7.8.3 Dynamic similarity

For dynamic similarity, corresponding forces need to be in a constant ratio. For instance, the forces acting on a fluid element are those due to pressure, viscous stresses, gravity and inertia. So

$$\frac{(\text{force due to viscous stresse})_m}{(\text{force due to viscous stresses})_p} = \frac{(\text{inertia force})_m}{(\text{inertia force})_p} = r_d \qquad (7.26)$$

and so on for the other forces. In this case, all forces are in model are in the proper ratio when compared to the full scale prototype.

We see that to make the flow over a model completely similar to the flow over the prototype, we need to satisfy geometric, kinematic, and dynamic similarity. For geometric similarity we require the condition given in equation 7.24. This condition can be written with model quantities on one side and full scale quantities on the other, so that, for geometric similarity

$$\left(\frac{L}{W}\right)_m = \left(\frac{L}{W}\right)_p \qquad (7.27)$$

where $L$ is the length, and $W$ is the width, for example. For kinematic similarity we require the condition given in equation 7.25, which can be written as

$$\left(\frac{V_1}{V_2}\right)_m = \left(\frac{V_1}{V_2}\right)_p \qquad (7.28)$$

For dynamic similarity we require the condition given in equation 7.26, which can be written as

$$\left(\frac{F_i}{F_v}\right)_m = \left(\frac{F_i}{F_v}\right)_p \qquad (7.29)$$

where $F_i$ is the force due to inertia, and $F_v$ is the force due to viscous stresses.

We recognize the ratios in equations 7.27, 7.28, and 7.29 as nondimensional groups, and we see that

> For two flows to be dynamically similar, all of the nondimensional groups must have the same value.

We know many of these nondimensional parameters by name. For example

$$\frac{F_i}{F_v} = \frac{\text{inertia force}}{\text{viscous force}} = \text{Reynolds number} = Re$$

$$\frac{\text{inertia force}}{\text{gravitational force}} = \text{Froude number} = F$$

$$\frac{\text{pressure force}}{\text{inertia force}} = \text{pressure coefficient} = C_p$$

$$\frac{\text{lift force}}{\text{inertia force}} = \text{lift coefficient} = C_L$$

$$\frac{\text{drag force}}{\text{inertia force}} = \text{drag coefficient} = C_D$$

$$\frac{\text{flow speed}}{\text{sound speed}} = \text{Mach number} = M$$

$$\frac{\text{unsteady time scale}}{\text{flow time scale}} = \text{Strouhal number} = St$$

$$\frac{\text{inertia force}}{\text{surface tension force}} = \text{Weber number} = We$$

The physical significance of these nondimensional groups is largely derived from the equations of motion, as noted in Section 7.7. It is the concept of similarity, and the basic equations of motion that underlie this concept, which helps us to understand the physical significance of the nondimensional parameters in common use.

For any given problem, many different forces could be acting. For example, the flow of a viscous fluid in a narrow open channel, for instance, could be affected by viscous forces, inertia forces, gravitational forces, surface tension, and other such forces. To model this flow accurately, the Reynolds number, Froude number and Weber number must all be the same as in the full scale flow. This is not usually possible, but in most cases some approximations can be made. Some forces may be more important than others, and therefore some effects may be neglected. A limited type of similarity can then be achieved which may be accurate enough. If the channel flow considered in this example is not too narrow and the fluid viscosity is not all that important, then a sufficient level of dynamic similarity may be achieved if the ratio of the inertia force to the gravitational force (the Froude number) is the same for model and prototype.

# Chapter 8

# Viscous Internal Flows

## 8.1  Introduction

In this chapter and in Chapter 9, we examine viscous flows. Viscous flows are flows where viscous stresses exert significant forces on the fluid, and viscous energy dissipation is important. Here, we concentrate on *internal* flows, that is, flows through pipes and ducts, and in Chapter 9 we examine *external* flows, which include the flow over the surfaces of airplanes, ships and automobiles.

The flow of fluids through pipes and ducts of different shapes is extremely important in all kinds of engineering applications, including the transport of water, oil, natural gas and sewage, and the design of heating and air conditioning systems in buildings and vehicles, as well as heat exchanger systems of all kinds. In biological systems, the flow of blood and air through the respiratory and circulatory systems are also dominated by viscous effects.

Three basic phenomena are important to the understanding of viscous flows.

1. The appearance of viscous stresses due to the relative motion of fluid particles.

2. The development of velocity gradients by the no-slip condition whenever the fluid is in contact with a solid surface.

3. The transition of laminar to turbulent flow as the Reynolds number increases.

For flow through long ducts, there is an additional phenomenon where the velocity profile far from the entry to the duct becomes fully developed, which means it becomes independent of the distance from the entry. Some of these concepts were introduced as early as Chapter 1, but we will now study each phenomenon in detail as a necessary prelude to analyzing laminar and turbulent flow in pipes, ducts, and piping systems.

## 8.2  Viscous Stresses and Reynolds Number

In Chapter 1, it was noted that the most characteristic property of fluids, their capacity to flow and change shape, is a result of their inability to support shearing stresses. Whenever a fluid is undergoing a deformation, relative motions occur, and shearing stresses become important. The magnitude of the shear stress $\tau$ is related to the rate of deformation, that is, the rate at which one part of the fluid is moving with respect to another part. In other words, $\tau$ depends on the strength of the velocity gradients, so that, for a simple two-dimensional flow in the $x$-$y$ plane

$$\tau_{yx} = \mu \frac{\partial u}{\partial y}$$

(see Section 1.6.1). Many common fluids obey this "Newtonian" relationship where the stress is proportional to the strain rate, including air and water over very wide ranges of pressures and temperatures.

When the viscous stresses are included in the differential form of the momentum equation, we obtain the Navier-Stokes equation. For an incompressible fluid, this equation is

$$\frac{D\mathbf{V}}{Dt} \; = \; -\frac{1}{\rho}\nabla p + \mathbf{g} + \nu\nabla^2\mathbf{V} \tag{8.1}$$

The Navier-Stokes equation is a nonlinear, partial differential equation, and no general solution exists (see Section 5.3.2). Nevertheless, some insight may be gained by non-dimensionalizing this equation, as shown in Section 7.6. With a suitable choice of length and velocity scales, the coefficients in the non-dimensional equation indicate the relative importance of each term. The coefficient on the viscous term was given by the reciprocal of a Reynolds number (see equation 7.23), so that the Reynolds number gives a measure of how important the inertia force is compared to the viscous force.

When the Reynolds number is small (less than one, say), we would expect the viscous terms to be important everywhere in the flow field. Small Reynolds numbers mean very slow flow, or very small characteristic lengths, or very high kinematic viscosity, or all three. For example, a fish of length $1\,mm$, swimming at $1\,mm/s$ in water, where $\nu = 10^{-6}\,m^2/s$, has a Reynolds number of one. Dust particles settling in the atmosphere may have Reynolds numbers of order 0.01. The flow of oil in a bearing where the clearances are typically very small, is also dominated by viscous stresses. We call these flows *creeping flows*.

In this chapter, we are interested in flows of more general engineering interest, where the Reynolds numbers are considerably larger, of order 100 to 1000 (at least). Under these conditions, viscous effects only become important in relatively thin regions where the velocity gradients are large, such as in boundary layers, fully developed internal flows, jets, and wakes.

## 8.3   Boundary Layers and Fully Developed Flow

When a viscous fluid flows over a solid surface, the no-slip condition requires that right at the surface there is no relative motion between the fluid and the surface (see Section 1.7). As a result, strong velocity gradients appear in the region near the surface. At Reynolds numbers very large compared to one, this region is always very thin and it is called the boundary layer. By definition, the boundary layer is the region where velocity gradients are large enough to produce significant viscous stresses, and significant dissipation of mechanical energy. The region outside the boundary layer is called the *freestream*. It is also sometimes called the inviscid freestream, not because the fluid there is inviscid but because there are no significant velocity gradients in that region and viscous stresses are negligible.

Consider the simple flow of a viscous fluid over a flat surface aligned with the flow direction. At any given point within the boundary layer, viscous diffusion tends to smooth out velocity differences. That is, the viscous stresses tend to decrease the velocity of the flow on the high speed side of the point in question, and increase the velocity on the low speed side. At the edge of the boundary layer, therefore, viscous action will also tend to slow the freestream fluid, and as we proceed downstream, more and more of the freestream flow is affected by friction. Therefore the thickness of the boundary layer will grow with distance downstream (see Figure 1.16).

For an internal flow, such as that in a pipe or a duct, the boundary layers will eventually meet at the center, and at this point they cannot grow any further. The velocity profile reaches an asymptotic state where the flow is said to be fully developed. The effects of viscous friction are then important over the whole cross-section of the flow, and all adjacent
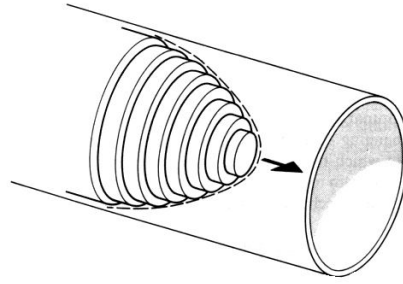
Figure 8.1: Idealized fully developed laminar pipe flow. With permission, *Engineering Fluid Mechanics*, A. Mironer, MacGraw-Hill, 1979.

layers of fluids slide over each other, as shown in Figure 8.1. There is no further change in the velocity profile with distance downstream, and so there is no further flow acceleration.

For an external flow, such as the flow over the hull of a ship, the velocity profile will not reach an asymptotic state and the boundary layer continues to grow. Nevertheless, the boundary layer thickness (that is, the region where appreciable flow deceleration has occurred) will always remain small compared to the length of the surface over which the boundary layer develops. That is, the boundary layer is "thin."

In laminar pipe flow, fully developed flow is attained within about $0.03Re_D$ diameters of the entrance, where $Re_D$ is the Reynolds number based on the diameter and the average velocity. That is, with $Re_D = 1000$, the flow is fully developed for $x > 30D$. For turbulent pipe flow, it takes about 25 to 40 pipe diameters,[1] so that in many pipe flow applications (laminar or turbulent) the flow is fully developed almost along its entire length. When the flow is fully developed, there is no flow acceleration, and the fluid velocity at any distance from the wall is constant with streamwise distance. The left-hand side of equation 8.1 must be zero, and the viscous force on the fluid must be balanced exactly by forces due to gravity, or by pressure gradients. In the absence of these forces, the fluid would decelerate and eventually come to rest, and so work must be done on the system to keep the motion going.

Viscous, frictional stresses also cause energy dissipation in the fluid, which appears as heat. This heat generation is not usually important at subsonic speeds since the resulting temperature changes are typically very small. However, one example of a subsonic flow where this heat generation is important is the flow around a closed circuit wind tunnel, where the air is pumped around and around the same circuit. There is a continual energy input through the work done by the fan on the air, and although some of this energy will be lost by heat transfer to the walls of the tunnel, at high speeds this heat transfer may not be sufficient to keep the air temperature from rising to unacceptable levels. Cooling coils may be necessary to control the temperature.

At supersonic speeds where the Mach number $M > 1$, very strong velocity gradients occur within the boundary layer and sufficient heat may be generated by viscous dissipation to change the density of the fluid significantly. At hypersonic speeds, where $M \gg 1$, frictional heating can be sufficient to cause the molecules to ionize and dissociate, as occurs during re-entry, and thermal protection systems are necessary to avoid damage to the spacecraft.

## 8.4 Transition and Turbulence

We have described the flow near a solid surface in terms of the slipping of adjacent fluid layers, where relative motion between the layers produces shearing stresses. This type of flow

---

[1] Schlichting *Boundary Layer Theory*, 7th edition, published by McGraw-Hill, 1979.
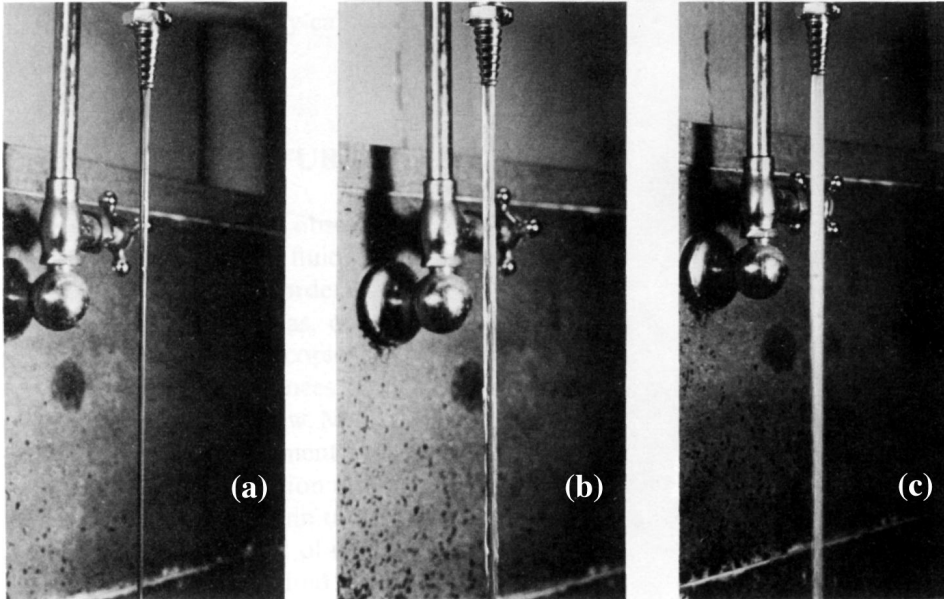
Figure 8.2: Transition in water flow issuing from a faucet: (a) laminar, (b) transitional, and (c) turbulent flow. With permission, *Engineering Fluid Mechanics*, A. Mironer, MacGraw-Hill, 1979.

is called laminar flow, and it is seen whenever the Reynolds number is small (here "small" means less than about 1000 to 10,000 based on the freestream velocity and the characteristic length of the flow). At higher Reynolds numbers, the flow changes its nature, and instead of smooth, well-ordered, laminar flow, irregular eddying motions appear indicating the presence of turbulent flow. Because of the high degree of activity associated with turbulent eddies and their fluctuating velocities, the viscous energy dissipation inside a turbulent flow can be very much greater than in a laminar flow.

We can observe this transition from laminar to turbulent flow by examining the flow from a faucet. If the faucet is turned on very slowly, a smooth, orderly flow is observed. This is laminar flow [Figure 8.2(a)]. When the faucet is opened a little more, perturbations will start to appear in the surface of the jet. Occasionally, the whole of the jet takes on an irregular appearance, and then it may revert to its laminar state [Figure 8.2(b)]. If the faucet is now opened fully, the jet will become fully turbulent [Figure 8.2(c)] and its appearance will change in a seemingly random way. Although its average motion is in one direction (downward), within the flow there are irregularities in the velocity everywhere. Have you ever watched cigarette smoke rise smoothly for a short distance, then burst into a seemingly chaotic flow? This is another example of transition and turbulence. For example, a smoke particle would, on average, move in the principal flow direction (upward) but it would jitter as well, sometimes moving to one side, or up, or down. Turbulent flow, while proceeding on average in a particular direction, like laminar flow, has the added complexity of three-dimensional random velocity fluctuations. These random motions help to mix turbulent flows, so that temperature and velocity differences, for example, are smoothed out much more quickly in turbulent flow than they would be in a laminar flow.

> Turbulence, or the presence of eddies in a moving fluid, gives rise to the twofold effect of a pronounced mixing of the fluid and a subsequent dissipation of energy. Like solid friction, fluid turbulence is sometimes a blessing to mankind, and sometimes a curse. Without the mixing which eddies produce, both the water in boiler tubes and the air surrounding the earth would be very poor distributors

> *of heat; steam engines would prove too costly to run, and the atmosphere would be incapable of supporting life. On the other hand, dust storms would not then occur, nor would rivers transport their tremendous loads of silt from the foothills to the sea. Without means of producing eddies in the process of propulsion, moreover, a swimmer—or an ocean liner—could make little headway, just as a car would remain at rest if friction provided no tractive force. Yet, paradoxically, were turbulence not produced by the motion of a body through a fluid, the process of streamlining would be quite unnecessary.[2]*

## 8.5 Poiseuille Flow

It is possible to find exact solutions to equation 8.1 for fully developed pipe flow, as long as the flow is laminar and not turbulent (this is called Poiseuille flow). It is also possible to find a solution for fully developed, laminar flow in a rectangular duct (this is called plane Poiseuille flow). Here, we will derive the solutions for these two cases from first principles, starting with duct flow. The results are very similar, and they differ only in the constants that appear in the equations.

### 8.5.1 Fully developed duct flow

Consider laminar, two-dimensional, steady, constant density duct flow, far from the entrance, so that the flow is fully developed. The duct is rectangular in cross-section, of width $W$ and height $D$ so that $W >> D$, and it is horizontal, so we do not need to include the forces due to gravity. For a duct, laminar flow requires that the Reynolds number $\overline{V}D/\nu$ is less than about 2000, where $\overline{V}$ is the average velocity. We can find the velocity profile and the friction factor, as follows.

We start with the Navier-Stokes equation (equation 8.1). The notation is as given in Figure 8.3. For negligible body forces and fully developed flow (where the acceleration is zero), this equation reduces to

$$0 = -\frac{1}{\rho}\nabla p + \nu\nabla^2\mathbf{V} \tag{8.2}$$

The streamlines are parallel, and the flow is two-dimensional, so that $v = w = 0$, and $\mathbf{V} = u\mathbf{i}$. In addition, the pressure gradient is constant across any cross-section of the duct, so that it can only vary in the streamwise direction, $p = p(x)$. It follows that

$$\boxed{\frac{1}{\rho}\frac{dp}{dx} = \nu\frac{d^2u}{dy^2}} \tag{8.3}$$

Equation 8.3 holds for all fully developed flows in the absence of body forces. It can be solved by separation of variables, since the pressure term only depends on $x$, and the viscous term only depends on $y$. Therefore the equation can only be satisfied if both terms are equal to a constant, $-K$, say. Hence

$$\frac{dp}{dx} = -K \tag{8.4}$$

$$\text{and} \quad \mu\frac{d^2u}{dy^2} = -K \tag{8.5}$$

We see that the pressure varies linearly with distance. In addition, we expect $K$ to be a positive constant since the pressure must decrease with distance along the duct.

---

[2] *Elementary Mechanics of Fluids*, by H. Rouse, published by Dover Edition, 1978.
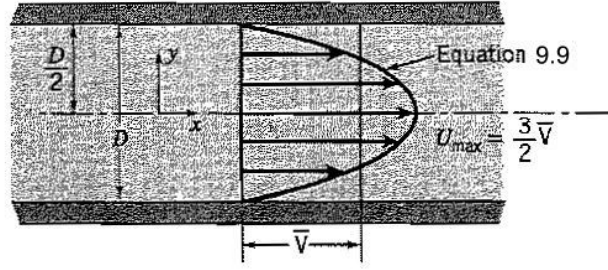
Figure 8.3: Parabolic velocity profile in fully developed laminar duct flow.

We can integrate equation 8.5 twice to obtain the velocity profile. The boundary conditions are

$$u = 0, \quad \text{at} \quad y = \pm D/2 \quad \text{(no-slip)}$$

$$\text{and} \quad \frac{du}{dy} = 0, \quad \text{at} \quad y = 0 \quad \text{(symmetry)}$$

Hence

$$u = \frac{KD^2}{8\mu}\left[1 - \left(\frac{2y}{D}\right)^2\right] \tag{8.6}$$

The average velocity $\overline{V}$ is defined by (equation 7.15). For a duct, the average velocity is given by

$$\overline{V} = \frac{1}{A}\int u\,dA = \frac{1}{WD}\int_{-D/2}^{D/2} u\,W\,dy = \frac{KD^2}{12\mu} \tag{8.7}$$

Therefore

$$K = -\frac{dp}{dx} = \frac{12\mu\overline{V}}{D^2} \tag{8.8}$$

From equations 8.6 and 8.8 we obtain

$$\boxed{\frac{u}{\overline{V}} = \frac{3}{2}\left[1 - \left(\frac{2y}{D}\right)^2\right]} \tag{8.9}$$

We find that the laminar velocity profile is parabolic, as illustrated in Figure 8.3, with a maximum velocity $U_{max} = 3\overline{V}/2$. The friction factor (see equation 7.18) is given by

$$f = \frac{\frac{\Delta p}{L}D}{\frac{1}{2}\rho\overline{V}^2} = \frac{-\frac{dp}{dx}D}{\frac{1}{2}\rho\overline{V}^2} = -\frac{dp}{dx}\frac{2D}{\rho\overline{V}^2} = \frac{24\mu}{\rho\overline{V}D}$$

where the pressure gradient was eliminated using equation 8.8. That is,

$$\boxed{f = \frac{24}{Re}} \tag{8.10}$$

which holds for smooth rectangular ducts where $Re_D = \rho\overline{V}D/\mu$ is less than about 1400 (the exact Reynolds number value depends on the aspect ratio of the duct).
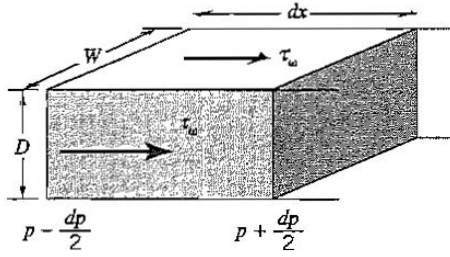
Figure 8.4: Integral control volume for fully developed flow in a rectangular duct.

We can find the stress at the wall ($y = -D/2$) by differentiating equation 8.6. That is,

$$\tau_w = \mu \left. \frac{\partial u}{\partial y} \right|_w = -\frac{D}{2} \frac{dp}{dx} \tag{8.11}$$

The same result can be obtained using a control volume. Consider the control volume of length $dx$ shown in Figure 8.4. If the flow is fully developed, the influx and outflux of momentum have the same magnitude but opposite sign and so they cancel. Since there is no change in the flow momentum, the flow must be in equilibrium under the applied forces: the force acting on the fluid due to the pressure drop is balanced by the force due to the viscous stress acting on the interior surface of the duct. The pressure over the inflow area is $p - (dp/dx)\frac{dx}{2}$, and over the outflow area it is $p + (dp/dx)\frac{dx}{2}$. The force due to pressure differences acts over the cross-sectional area $WD$. The shear stress on the surface $\tau_w$ acts on the area $2(w + D) dx$. Hence

$$0 = \left(p + \tfrac{1}{2}dp\right) wD - \left(p - \tfrac{1}{2}dp\right) wD + 2\tau_w \left(w + D\right) dx$$

and so

$$\frac{dp}{dx} = -2\tau_w \frac{(w + D)}{wD}$$

For a two-dimensional flow $w \gg D$, and we can show that

$$\tau_w = -\frac{D}{2} \frac{dp}{dx}$$

which is the same result obtained in equation 8.11.

## 8.5.2 Fully developed pipe flow

Here we consider fully developed laminar flow in a smooth, circular, horizontal pipe. In Chapter 7, this flow was examined using dimensional analysis (Section 7.5). For a smooth pipe of length $L$ and diameter $D$, we found

$$\frac{\Delta p}{\frac{1}{2}\rho \bar{V}^2} = \phi_1 \left( \frac{\rho \bar{V} D}{\mu}, \frac{L}{D} \right)$$

where the pressure drop over the length $L$ is $\Delta p$, and $\bar{V}$ is the average velocity over the cross-section of the pipe. That is, the non-dimensional pressure drop depends on the Reynolds number based on the average velocity and the pipe diameter, and the length-to-diameter ratio of the pipe. When the pipe is long compared to its diameter, an asymptotic, fully developed state exists where the flow properties do not change with further increase in length. As in fully developed duct flow, the mean velocity profile is then independent of the

distance along the pipe. In that case, the parameter $L/D$ should no longer be important, in which case the resistance relationship for fully developed smooth pipe flow becomes

$$f \equiv \frac{\left(\frac{\Delta p}{L}\right) D}{\frac{1}{2}\rho \bar{V}^2} = \phi\left(\frac{\rho \bar{V} D}{\mu}\right) = \phi\left(Re_D\right)$$

where $f$ is the friction factor. Here, we have chosen to represent the pressure drop in terms of a pressure gradient, $\Delta p/L$. We see that for fully developed pipe flow, the friction factor depends only on the Reynolds number, $Re_D$.

For fully developed flow, we can solve the Navier-Stokes equation to find the functional relationship. We begin with form given by equation 8.2, which, for two-dimensional flow in cylindrical coordinates, reduces to

$$\frac{1}{\rho}\frac{dp}{dx} = \frac{\nu}{r}\frac{d}{dr}\left(r\frac{du}{dr}\right) \tag{8.12}$$

The notation is as given in Figure 8.5. This equation can be satisfied only if the left hand side and the right hand side are equal to a constant, $-K'$, say. Hence

$$\frac{dp}{dx} = -K' \tag{8.13}$$

$$\frac{\nu}{r}\frac{d}{dr}\left(r\frac{du}{dr}\right) = -K' \tag{8.14}$$

The pressure varies linearly with distance, and we expect $K'$ to be a positive constant since the pressure must decrease with distance along the pipe.

We can integrate equation 8.14 to give

$$r\frac{du}{dr} = -K'\frac{r^2}{2\nu} + c_1$$

or

$$\frac{du}{dr} = -K'\frac{r}{2\nu} + \frac{c_1}{r}$$

Integrating one more time gives

$$u = -K'\frac{r^2}{4\nu} + c_1\ln r + c_2$$

Using the boundary conditions

$$u = 0, \quad \text{at} \quad r = \pm D/2 \qquad \text{(no-slip)}$$

$$\frac{du}{dr} = 0, \quad \text{at} \quad r = 0 \qquad \text{(symmetry)}$$

we find $c_1 = 0$, and $c_2 = K'D^2/16\mu$, so that

$$u = \frac{K'D^2}{16\mu}\left[1 - \left(\frac{2r}{D}\right)^2\right] \tag{8.15}$$

The average velocity $\overline{V}$ for a pipe is given by

$$\overline{V} = \frac{1}{A}\int u\,dA = \frac{1}{\frac{\pi}{4}D^2}\int_0^{D/2} u\,2\pi r\,dr = \frac{K'D^2}{32\mu} \tag{8.16}$$
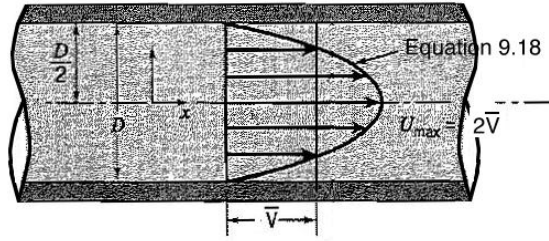
Figure 8.5: Parabolic velocity profile in fully developed laminar pipe flow.

Therefore

$$K' = -\frac{dp}{dx} = \frac{32\mu\overline{V}}{D^2} \tag{8.17}$$

From equations 8.15 and 8.17 we obtain

$$\frac{u}{\overline{V}} = 2\left[1 - \left(\frac{2r}{D}\right)^2\right] \tag{8.18}$$

We find that the velocity profile for laminar pipe flow is parabolic, as in the case of the rectangular duct, but this time with a maximum velocity $U_{max} = 2\overline{V}$. The friction factor is given by

$$f = \frac{\frac{\Delta p}{L}D}{\frac{1}{2}\rho\overline{V}^2} = \frac{-\frac{dp}{dx}D}{\frac{1}{2}\rho\overline{V}^2} = \frac{64\mu}{\rho\overline{V}D}$$

where the pressure gradient was eliminated using equation 8.16. That is,

$$f = \frac{64}{Re} \tag{8.19}$$

which holds for smooth circular pipes and tubes where $Re_D = \rho\overline{V}D/\mu$ is less than 2300.

We can find the stress at the wall $(y = -D/2)$ by differentiating equation 8.15. That is,

$$\tau_w = \mu\left.\frac{\partial u}{\partial r}\right|_w = -\frac{D}{4}\frac{dp}{dx} \tag{8.20}$$

The same result can be obtained using a control volume. Consider the control volume of length $dx$ shown in Figure 8.6. The pressure over the inflow area is $p - (dp/dx)\frac{dx}{2}$, and
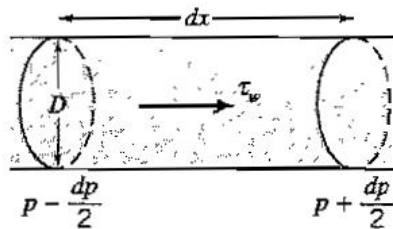


Figure 8.6: Integral control volume for fully developed flow in a circular pipe.

over the outflow area it is $p + (dp/dx)\frac{dx}{2}$. Since the flow is fully developed, the flow is in equilibrium under the applied forces. The pressure drop acts on the cross-sectional area $\pi D^2/4$, and the viscous stress acts on the area $2\pi D dx$. Hence

$$0 \;=\; \left(p + \tfrac{1}{2}dp\right)\frac{\pi D^2}{4} - \left(p - \tfrac{1}{2}dp\right)\frac{\pi D^2}{4} + \tau_w \pi D\, dx$$

so that

$$\tau_w \;=\; -\frac{D}{4}\frac{dp}{dx}$$

which is the same result obtained in equation 8.20.

## 8.6   Transition in Pipe Flow

The experimental friction factors for circular pipes and tubes are shown in Figure 8.7. This is called the Moody diagram, after Lewis Ferry Moody, a former Princeton professor. As expected from the dimensional analysis given in Section 7.5, all the data collapse onto curves that depend on just three nondimensional groups: the friction factor $f$, the Reynolds number $Re_D$, and the relative roughness $k/D$. This is true for laminar and turbulent flows.

The Moody diagram displays only one curve for $Re_D < 2300$: this is the laminar flow regime where the layers of fluid slide over each other, and all the pressure drop is due to viscous stresses set up by the velocity gradient. Surface roughness does not affect the drag in the laminar flow regime. However, for Reynolds numbers greater than 2300, transition to turbulence can occur. The precise value of the Reynolds number where transition occurs depends on many factors, including surface roughness, vibrations, and noise levels.

To understand why these factors are important, and to appreciate the role of the Reynolds number in governing the stability of the flow, it is helpful to think in terms of a spring-damper system such as the suspension system of a car. Driving along a bumpy road, the springs act to smooth the movement experienced by the car body. If there were no shock absorbers, however, there would be no damping of the motion, and the car would continue to oscillate long after the bump has been left behind. So the shock absorbers, through a viscous damping action, dissipate the energy in the oscillations and reduce their amplitude. If the viscous action is strong enough, the oscillations will die out very quickly and the car can proceed smoothly. If the shock absorbers are not in good shape, the oscillations may not die out. The oscillations can actually grow if the excitation frequency is in the right range, and the system can experience resonance. The car becomes unstable, and it is then virtually uncontrollable.

The stability of a fluid flow is similarly dependent on the relative strengths of the flow acceleration and the viscous damping. This is expressed by the Reynolds number, which is the ratio of a typical inertia force to a typical viscous force (see Section 7.7). At low Reynolds numbers, the viscous force is large compared to the inertia force, and the flow behaves in some ways like a car with a good suspension system. Small disturbances in the velocity field, created perhaps by small roughness elements on the surface, or by pressure perturbations from external sources such as vibrations of the pipe, or even the presence of loud noises, will be damped out and not allowed to grow. This is the case for pipe flow at Reynolds numbers smaller than the critical value of 2300. As the Reynolds number increases, however, the viscous damping action becomes comparatively smaller, and at some point it becomes possible for small perturbations to grow, just as in the case of a car with poor shock absorbers. The flow can become unstable, and it can experience transition to a turbulent state where large variations in the velocity field can be maintained.

The point where the disturbances will grow rather than decay will also depend on the magnitude and frequency of the disturbances. If the disturbances are very small, as in the

case where the walls are very smooth, or if the frequency of the disturbance is not close to resonance, transition to turbulence will occur at a Reynolds number higher than the critical value.  The point of transition does not correspond to a single Reynolds number, and it is possible to delay transition to relatively large Reynolds numbers by controlling the disturbance environment.  At very high Reynolds numbers, however, it is impossible to maintain laminar flow since under these conditions even minute disturbances will be amplified into turbulence.

## 8.7   Turbulent Pipe Flow

In turbulent flow, a significant part of the mechanical energy in the flow goes into forming and maintaining randomly eddying motions which eventually dissipate their kinetic energy into heat. At a given Reynolds number, therefore, we expect the drag of a turbulent flow to be higher than the drag of a laminar flow, and the results shown in the Moody diagram (Figure 8.7) confirm this expectation. Also, turbulent flow is affected by surface roughness, in that the friction factor for turbulent flow is larger than for laminar flow, at the same Reynolds number.  The roughness elements can create additional turbulence by shedding vortices, so that increasing roughness increases the drag. If the roughness is large enough, and the Reynolds number is large enough, the drag becomes independent of Reynolds number and the friction factor then becomes a function of the relative roughness only.  For example, when $k/D = 0.006$ and $Re_D > 3 \times 10^5$, Figure 8.7 shows that $f$ is a constant equal to 0.032.

The unsteady eddying motions in turbulent flow are in constant motion with respect to each other, producing fluctuations in the flow velocity and pressure. If we were to measure
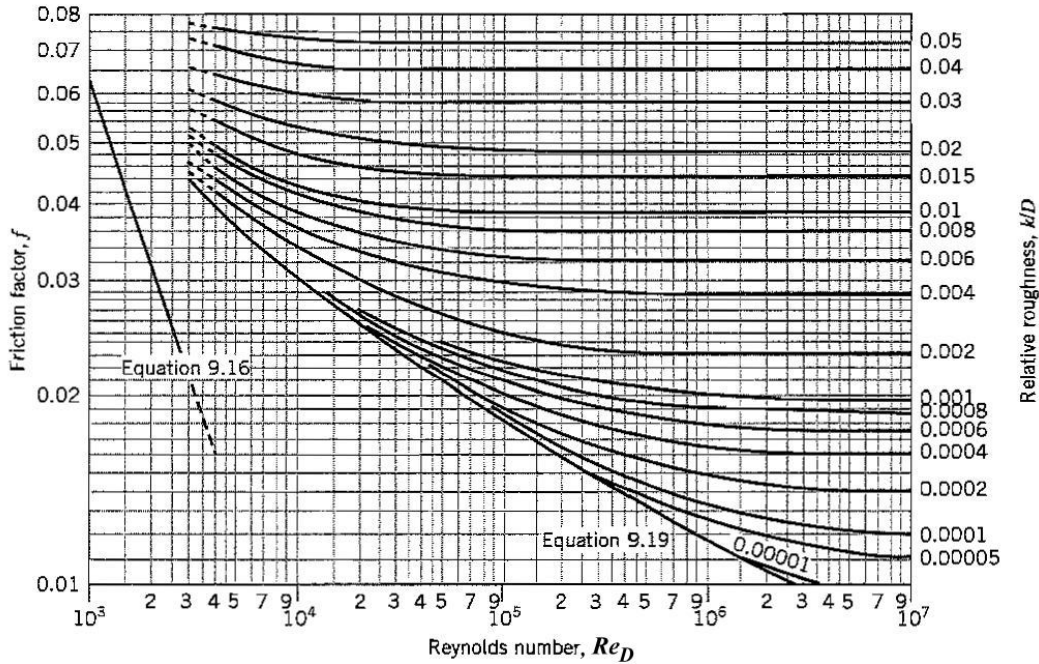


Figure 8.7: Moody diagram for fully developed flow in circular pipes. Laminar flow is described by equation 8.19. Prandtl's universal law of friction for turbulent smooth pipes is given by equation 8.25. Adapted from Moody, L.F. "Friction factors for pipe flow," *Trans. ASME*, **66**, 671–684, with permission.
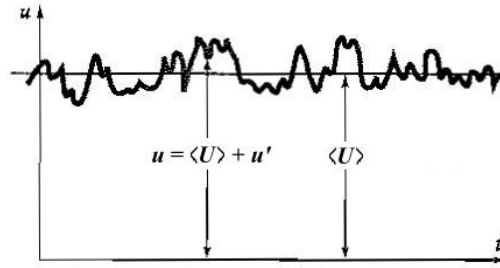
Figure 8.8: Velocity at a point in a turbulent flow as a function of time.

the instantaneous streamwise velocity in turbulent pipe flow, we would see a variation in time as shown in Figure 8.8. We define a time-averaged or "mean" value, $\langle U \rangle$, by

$$\langle U \rangle \;\equiv\; \lim_{T \to \infty} \frac{1}{T} \int\limits_{t}^{t+T} u \, dt \qquad\qquad (8.21)$$

and a fluctuating value $u'$ $(= u - \langle U \rangle)$, so that $\langle U \rangle$ is not a function of time, but $u'$ is. We can also define an rms turbulence intensity, $u_{rms} = \sqrt{\overline{u'^2}}/\langle U \rangle$, where

$$\overline{u'^2} \;\equiv\; \lim_{T \to \infty} \frac{1}{T} \int\limits_{t}^{t+T} (u - \langle U \rangle)^2 \, dt \qquad\qquad (8.22)$$

Turbulence is three-dimensional, so that the velocity fluctuations have three components: $u'$, $v'$, and $w'$.

The turbulent eddies interact with each other as they move around, and they can exchange momentum and energy. For example, an eddy that is near the centerline of the pipe (and therefore has a relatively high average velocity), may move towards the wall and interact with eddies near the wall (which typically have lower average velocities). As they mix, momentum differences are smoothed out. This process is superficially similar to the action of viscosity, which tends to smooth out momentum gradients by molecular interactions, and therefore turbulent flows are sometimes said to have an equivalent *eddy viscosity*. Because turbulent mixing is such an effective transport process, the eddy viscosity is typically several orders of magnitude larger than the molecular viscosity.

The important point is that turbulent flows are very effective at mixing: the eddying motions can very quickly transport mass, momentum and energy from one place to another. As a result, velocity, temperature and concentration differences get smoothed out more effectively than in a laminar flow, and, for example, the time-averaged velocity profile in a turbulent pipe flow is much more uniform than in a laminar flow (see Figure 8.9). We call this profile "fuller", and it has higher velocities near the wall. The velocity profile is no longer parabolic, and it is sometimes approximated by a power law, such as

$$\frac{\langle U \rangle}{U_{CL}} = \left(\frac{2y}{D}\right)^{1/n} \qquad\qquad (8.23)$$

where $U_{CL}$ is the mean velocity on the centerline, and the exponent $n$ varies with Reynolds number (for a Reynolds number $Re_D$ of about 100,000, $n = 7$).

As a result of this mixing, the velocity gradient at the wall is higher than that found in a laminar flow at the same Reynolds number, so that the shear stress at the wall is
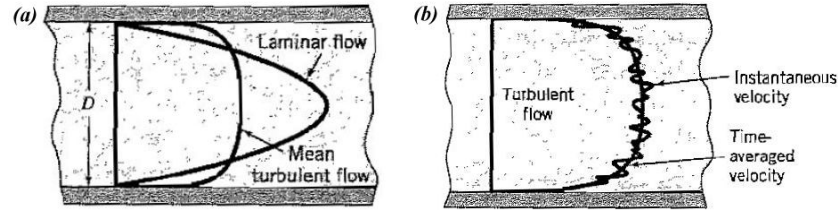
Figure 8.9: Distributions of streamwise velocity in laminar and turbulent pipe flow. (a) Comparison of laminar and time-averaged turbulent velocity profiles. (b) Comparison of turbulent instantaneous and time-averaged velocity profiles.

correspondingly larger [see Figure 8.9(a)]. This observation agrees with the fact that, since the energy losses in a turbulent flow are higher than in a laminar flow, the pressure drop per unit length will be greater. From the momentum balance considered in Section 8.5.2, we know that there must be a larger frictional stress at the wall, which in turn requires a higher velocity gradient at the wall. Note that we cannot evaluate the wall stress from equation 8.23 since this approximation to the velocity profile actually gives an infinite velocity gradient (and therefore an infinite stress) at the wall (where $y = 0$). Near the wall, equation 8.23 cannot be correct. However, for turbulent flow there are no exact solutions available for either the velocity profile or the friction factor variation with Reynolds number. Instead, we must always rely on experimental data, and scaling arguments based on dimensional analysis.

For the friction factor in turbulent pipe flow at Reynolds numbers less than about $10^5$, the Blasius friction relationship is often used, where

$$f = \frac{0.3164}{Re_D^{0.25}} \tag{8.24}$$

For Reynolds numbers greater than $10^5$, we often use the semi-empirical relation

$$\frac{1}{\sqrt{f}} = 2.0 \log \left( Re_D \sqrt{f} \right) - 0.8 \tag{8.25}$$

which is known as Prandtl's universal law of friction for smooth pipes. The line in Figure 8.7 that corresponds to turbulent flow in a smooth pipe is a combination of equations 8.24 and 8.25. A more accurate form is given by

$$\frac{1}{\sqrt{f}} = 1.873 \log \left( Re_D \sqrt{f} \right) - 0.2631 - \frac{233}{\left( Re_D \sqrt{f} \right)^{0.90}} \tag{8.26}$$

which describes the friction factor to within $1.4\%$ for Reynolds numbers from $10 \times 10^3$ to $35 \times 10^6$.[3]

## 8.8 Energy Equation for Pipe Flow

So far, we have considered only simple ducts and pipes, without worrying about how these elements fit into a piping or ducting system. Whenever a duct changes its size, either through a gradual diffuser or by a sudden expansion, or when a valve is installed somewhere along the pipe, or when a pipe flow enters or leaves a tank in a non-ideal way, there will be additional losses in the system, manifesting themselves as a drop in pressure. Roughness

---

[3]B.J. McKeon, M.V. Zagarola & A.J. Smits, *J. Fluid Mech.*, **538**, 429–443, 2005.

can also be very important. When a pipe system ages, corrosion can roughen the surface of the pipes, and scale can build up, so that the losses due to friction can increase dramatically. As we will show in Section 8.9, for a given available pressure head, increased losses in the system will reduce the flow rate. The Moody diagram (Figure 8.7) can be used to find the friction factor for laminar and turbulent pipe and duct flows, but to design piping systems we need to know the effects of pipe fittings, valves, diffusers, etc.

Piping and ducting systems are commonly analyzed using the energy equation. In order to do so, two modifications are necessary. First, viscous internal flows are two-dimensional, and in order to use the one-dimensional energy equation we introduce the *kinetic energy coefficient*, $\alpha$. This coefficient allows us to define an average velocity so that a two-dimensional field can be represented as an "equivalent" one-dimensional field.

Second, friction factors and loss coefficients are introduced into the energy equation to represent the kinetic energy losses in the system. These coefficients are determined from theory (when that is possible), or from empirical relationships established from experience.

### 8.8.1   Kinetic energy coefficient

Consider the steady flow of an incompressible fluid through a pipe of variable cross section. We draw a control volume as shown in Figure 8.10, and apply the steady flow energy equation in integral form (equation 3.25). That is,

$$\int (\mathbf{n} \cdot \rho \mathbf{V}) \left( \hat{u} + \frac{p}{\rho} + \tfrac{1}{2} V^2 + gz \right) dA \;=\; \dot{Q} + \dot{W}_{shaft}$$

where $\dot{Q}$ is the heat transferred to the fluid, $\dot{W}_{shaft}$ is the rate of doing work on the fluid by a machine (for example, by a pump or turbine), and $\hat{u}$ is the internal energy of the fluid per unit mass.. If the pressures and internal energy at stations 1 and 2 are uniform,

$$
\begin{aligned}
\dot{Q} + \dot{W}_{shaft} \;=\;& \dot{m} \left( \hat{u}_2 - \hat{u}_1 \right) + \dot{m} \left( \frac{p_2}{\rho} - \frac{p_1}{\rho} \right) + \dot{m} g \left( z_2 - z_1 \right) \\
&+\; \int \rho V_2 \left( \tfrac{1}{2} V_2^2 \right) dA_2 - \int \rho V_1 \left( \tfrac{1}{2} V_1^2 \right) dA_1
\end{aligned}
\tag{8.27}
$$

When the velocity varies across the pipe, the kinetic energy also varies across the pipe. To treat the flow as one-dimensional, we need to introduce an equivalent kinetic energy, based on the average velocity $\overline{V}$ rather than the spatially varying velocities $V_1$ and $V_2$. The advantage of using an average velocity $\overline{V}$ is that it is relatively easy to measure (for example, if the fluid was a liquid, we could use a bucket and a stopwatch to find the volume flow rate, and then $\overline{V}$ is found by dividing the volume flow rate by the interior cross-sectional area of the pipe).
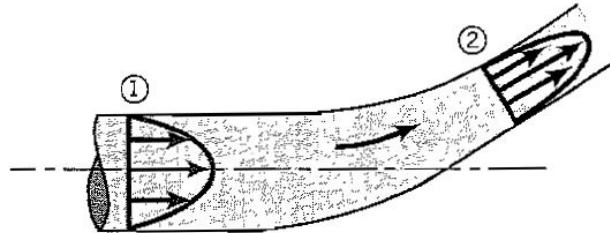


Figure 8.10: Control volume applied to steady, two-dimensional flow through a pipe of varying cross section.

How do we achieve this aim of finding an equivalent kinetic energy? The important requirement is that the kinetic energy flux through the pipe is accurately represented. Specifically, we would like to define an *average* kinetic energy flux based on the mean velocity, which is equal to the *actual* kinetic energy flux. For a pipe flow, the actual kinetic energy flux through area $A$ is given by

$$\text{actual KE flux} = \int \tfrac{1}{2}\rho V^3\, dA$$

where the velocity $V$ varies across the area. The average kinetic energy flux through the pipe is given by the volume flow rate times the average kinetic energy. The average kinetic energy may be written as some multiple of $\tfrac{1}{2}\rho \overline{V}^2$, say $\alpha \tfrac{1}{2}\rho \overline{V}^2$, where the value of the coefficient $\alpha$ depends only on the shape of the velocity profile. Therefore

$$\text{average KE flux} = \tfrac{1}{2}\alpha\rho \overline{V}^3 A$$

By equating the actual and the average kinetic energy fluxes we obtain

$$\alpha = \frac{1}{A\overline{V}^3} \int V^3\, dA \tag{8.28}$$

which defines the *kinetic energy coefficient*, $\alpha$. This coefficient can be found if the velocity profile shape is known. In Section 8.5.2 we showed that velocity profile for laminar pipe flow is parabolic, which gives $\alpha = 2.0$. Turbulent pipe flow has a considerably flatter profile so that the velocity over much of the cross-section is close to the average value, and we find by experiment that $1.08 > \alpha > 1.03$. It is commonly assumed that $\alpha = 1$ for turbulent flow, which is also the value for a flow that is precisely one-dimensional where $V = \overline{V}$.

We can now write the energy equation for a two-dimensional flow in an equivalent one-dimensional form, using

$$\text{KE flux} = \int \tfrac{1}{2}\rho V^3\, dA = \tfrac{1}{2}\alpha\rho \overline{V}^3 A = \rho \overline{V} A \left(\tfrac{1}{2}\alpha \overline{V}^2\right) = \dot{m}\left(\tfrac{1}{2}\alpha \overline{V}^2\right)$$

Equation 8.27 then becomes

$$(\hat{u}_2 - \hat{u}_1) + \left(\frac{p_2}{\rho} - \frac{p_1}{\rho}\right) + g\,(z_2 - z_1) + \left(\tfrac{1}{2}\alpha_2 \overline{V}_2^2 - \tfrac{1}{2}\alpha_1 \overline{V}_1^2\right) = \frac{\dot{Q} + \dot{W}_{shaft}}{\dot{m}}$$

At this stage, we could introduce the enthalpy $h$ here, since $h = \hat{u} + p/\rho$, but for pipe flow problems it is more useful to write

$$\left(\frac{p_1}{\rho} + gz_1 + \tfrac{1}{2}\alpha_1 \overline{V}_1^2\right) - \left(\frac{p_2}{\rho} + gz_2 + \tfrac{1}{2}\alpha_2 \overline{V}_2^2\right) = (\hat{u}_2 - \hat{u}_1) - \frac{\dot{Q} + \dot{W}_{shaft}}{\dot{m}} \tag{8.29}$$

For pipe flow, the change in internal energy $(\hat{u}_2 - \hat{u}_1)$ is written as $gh_\ell$, where $h_\ell$ is called the *total head loss* and it represents the irreversible conversion of mechanical energy to heat (see Section 8.8.1). It has the dimensions of length.

Finally, we have the energy equation in a form that is convenient for pipe flow analysis, in that

$$\left(\frac{p_1}{\rho} + gz_1 + \tfrac{1}{2}\alpha_1 \overline{V}_1^2\right) - \left(\frac{p_2}{\rho} + gz_2 + \tfrac{1}{2}\alpha_2 \overline{V}_2^2\right) = gh_\ell - \frac{\dot{Q} + \dot{W}_{shaft}}{\dot{m}} \tag{8.30}$$

| Type | $k$ $(mm)$ | $k$ $(ft)$ |
|------|------------|------------|
| Glass | Smooth | Smooth |
| Asphalted cast iron | 0.12 | 0.0004 |
| Galvanized iron | 0.15 | 0.0005 |
| Cast iron | 0.26 | 0.00085 |
| Wood stave | 0.18–0.90 | 0.006–0.003 |
| Concrete | 0.30–3.0 | 0.001–0.01 |
| Riveted steel | 1.0–10 | 0.003–0.03 |
| Drawn tubing | 0.0015 | 0.000005 |

Table 8.1: Roughness height $k$ of common pipe materials. Source: *Introduction to Fluid Mechanics*, John & Haberman, Prentice-Hall, 1988.

## 8.8.2   Major and minor losses

We now consider how the total head loss $h_\ell$ may be calculated. In a piping network, the total head loss is the sum of *major* losses and *minor* losses. That is,

$$h_\ell \;=\; h_{\ell,maj} + h_{\ell,min}$$

Major losses are due to friction. For a given length $L$ of pipe with a constant diameter $D$, carrying a fluid with an average velocity $\overline{V}$, these losses can be written as

$$h_{l,maj} \;=\; \text{major losses} \;=\; f\frac{L}{D}\frac{\overline{V}^2}{2g}$$

where $f$ is the *friction factor*. The Moody diagram gives the value of $f$ as a function of Reynolds number and relative roughness height $k/D$ (see Figure 8.7). The minimum roughness is called *smooth*, or *hydraulically smooth*. Equivalent roughness heights for different pipe materials are listed in Table 8.1.

Minor losses are due to entrances, fittings, area changes, and so forth. Whenever a pipe flow goes around a bend, or changes its cross-sectional area, or it is throttled by a valve, flow separation and secondary flows can occur. When a flow separates, the fluid is no longer smoothly flowing in the intended direction. Significant parts of the fluid are eddying and recirculating in a way that absorbs a lot of mechanical energy without doing any useful work. Some examples are given in Figure 8.11. In addition, when the flow passes through a bend, the path followed by the fluid often becomes twisted, so that the flow downstream of the bend has two components of velocity: a component in the downstream direction, and a circumferential or "secondary" component. The secondary flow absorbs flow energy, and therefore contributes to the loss of total energy.

Minor losses for inlets, exits, enlargements and contractions are written as

$$h_{l,min} \;=\; (\text{minor losses})_a \;=\; K\frac{\overline{V}^2}{2g}$$

where $K$ is a *loss coefficient*, which depends on the type of fitting. Typical values of $K$ are 0.6 for a sudden two-fold increase in diameter, and 0.5 for a square-edged entry from a reservoir into a pipe (a sudden very large decrease in diameter). Even a minor rounding of the entry to the pipe reduces the loss coefficient significantly. For example, with a radius of curvature at entry equal to just 15% of the pipe diameter, the loss coefficient reduces to 0.04 (see Table 8.2). Also, the introduction of guide vanes into bends can help to reduce the
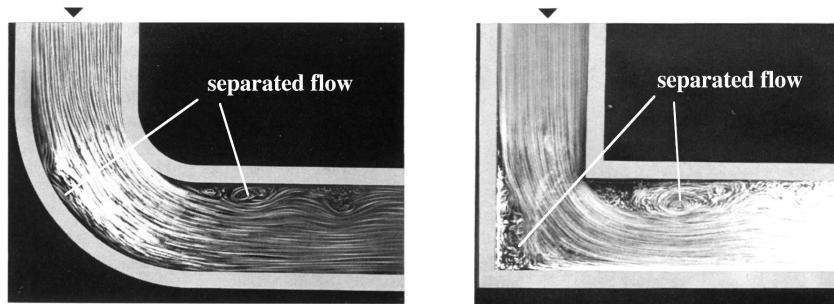
Figure 8.11: Flow through round and square bends showing regions of separation. From *Visualized Flow*, Japan Society of Mechanical Engineers, Pergamon Press, 1988.

| Entrance type | $K$ |
|---|---|
| Re-entrant | 0.78 |
| Square-edged | 0.5 |
| Rounded ($r/D = 0.02$) | 0.28 |
| Rounded ($r/D = 0.06$) | 0.15 |
| Rounded ($r/D \geq 0.15$) | 0.04 |
| Exit type | $K$ |
| Abrupt | 1.0 |

Table 8.2: Typical loss coefficients for pipe entrances and exits ($D$ is the diameter of the pipe, and $r$ is the radius of the rounded entry). Source: Data from Crane Co., NY, Technical Paper No. 410, 1982.

regions of separated flow, thereby reducing the loss coefficient significantly (see Figure 8.12).

For pipe bends, tee fittings and valves, minor losses are sometimes written in terms of an equivalent length of straight pipe, $L_e$. In that case, for fully developed pipe flow with a friction factor $f$ and average velocity $V$, the losses due to pipe bends, tees and valves are
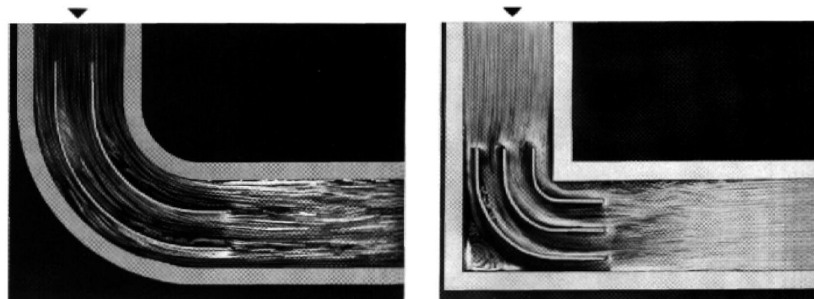


Figure 8.12: Flow through round and square bends with guide vanes. From *Visualized Flow*, Japan Society of Mechanical Engineers, Pergamon Press, 1988.

| Valve or fitting | $\frac{L_e}{D}$ | $K$ |
|---|---|---|
| Gate valve (open) | 8 | 0.20 |
| Globe valve (open) | 340 | 6.4 |
| Angle valve (open) | 150 | |
| Ball valve (open) | 3 | |
| Standard 45° elbow | 16 | 0.35 |
| Standard 90° elbow | 30 | 0.75 |
| Long-radius 90° elbow | | 0.45 |
| Standard tee (flow through run) | 20 | 0.4 |
| Standard tee (branch flow) | 60 | 1.5 |

Table 8.3: Typical loss coefficients for pipe fittings. From *Introduction to Fluid Mechanics*, Whitaker, Prentice-Hall, 1968, and Crane Co., NY, Technical Paper No. 410, 1982.

given by

$$h_{l,min} \;=\; (\text{minor losses})_b \;=\; f\frac{L_e}{D}\frac{\overline{V}^2}{2g}$$

Typical values of $L_e/D$ are 3 for a ball valve, 8 for a gate valve, 340 for a globe valve (all valves wide open), and 30 for a standard 90° elbow, where the radius of curvature is equal to the diameter of the pipe (see Table 8.3).

Additional information on minor loss coefficients, with an extensive discussion of pipe flow losses, may be found in Munson, Young & Okiishi *Fundamentals of Fluid Mechanics*, John Wiley & Sons, 1998.

On a practical note, we can write the friction factor $f$ in terms of the volume flow rate $\dot{q} = \pi D^2 \overline{V}/4$:

$$f = \frac{\Delta p D}{\frac{1}{2}\rho \overline{V}^2 L} = \frac{\Delta p\,\pi^2 D^5}{8\rho\dot{q}^2 L}$$

That is,

$$\Delta p = \frac{8f}{\pi^2}\frac{\rho\dot{q}^2 L}{D^5}$$

This relationship for the pressure drop is very useful for design engineers when the expected Reynolds number is large enough for the friction factor to be moderately insensitive to changes in the Reynolds number. What happens if your client wants to double the volume flow rate? We see that the pressure drop would quadruple. What happens if your client wants to maintain the volume flow rate at a constant value, but halve the recommended pipe diameter to save money? The pressure drop would increase by a factor of 32.

## 8.9   Valves and Faucets

For the discharge from a tank, the exit velocity is independent of the exit area but the discharge increases as the exit area increases, provided there are no losses. This result, obtained in Section 4.3.6, appears to contradict our common experience with valves. Opening a faucet further does not change the exit area and yet it increases the discharge rate. Why? Valves work because they introduce losses into the system.

Imagine a constant pressure supply, such as a large tank of water, connected to a pipe of constant diameter with a valve located somewhere along its length. Assume all the losses

are small except in the valve. The pressure difference from the surface of the tank to the exit of the tube is fixed by the depth of water in the tank, because the pressures at the free surface of the tank and at the exit of the pipe are equal to atmospheric pressure. This means, in effect, that there is a certain amount of potential energy available to push the fluid through the piping system. If there are no losses anywhere, all of this potential energy can be converted to kinetic energy of fluid motion. The relationship describing the exit velocity in the absence of losses, $V_e = \sqrt{2gH}$ came from the relationship $\frac{1}{2}\rho V_e^2 = \rho g H$ (Section 4.3.6), which makes this connection between kinetic and potential energies clear. If losses occur, as in a valve or faucet, there is less potential energy available for conversion to kinetic energy: as a result, the velocity of the outflow is reduced. More losses mean a lower velocity and a reduced discharge, and so valves control the flow rate by changing the losses in the system.

Where do the losses in a valve come from? Valves come in many shapes and sizes, but a common design such as a gate valve uses a simple sliding gate with a sharp edge that moves in and out of the flow. As the flow passes over the gate, the edge of the gate causes the flow to separate and a recirculating region forms downstream where many losses occur. These losses cause the pressure to drop across the valve because some of the available mechanical energy is dissipated in the eddying motions that characterize the separated zone.

Some valves are designed to have very little energy loss when they are fully opened. In a ball valve, for example, the valve mechanism consists of a ball with a hole drilled through it where the hole has the same diameter as the connecting pipes. By turning the handle, the ball rotates, so that when it is fully opened the hole in the ball is aligned with the flow direction and there is very little disturbance to the flow. However, when it is partially opened, losses occur as the flow passes over the edge of the misaligned hole and the flow rate can be controlled.

The throttling effect produced by energy losses can also be observed using a garden hose. Kinking the hose will control the flow rate (at least until the kink is severe enough to stop the flow altogether). A kink produces losses by flow separation downstream of the kink, and so it acts like a valve.

Another example is given by the losses due to pipe friction. The friction inside rough pipes can be much greater than in clean, smooth pipes. For a given driving pressure, additional work needs to be done to overcome the extra friction, and so less potential energy is available in a rough pipe for conversion to kinetic energy than in a smooth pipe. The velocity, and the discharge will be reduced. For this reason, replacing old copper bathroom pipes that have corroded and developed a high degree of internal roughness with new plastic pipes can improve the discharge from your shower head dramatically.

These considerations also help to explain why squeezing a hose near its exit will result in a higher exit velocity. According to our earlier analysis, if there are no losses in the system, reducing the exit area of the hose has no effect on the exit velocity. Therefore the explanation for a higher exit velocity is connected with the losses occurring in the system. By squeezing the end, we form a nozzle. The nozzle increases the fluid velocity and drops its pressure, but since the pressure at the exit of the nozzle is always atmospheric, the pressure just upstream of the nozzle must be higher than atmospheric. Inside the entire hose (except for the nozzle itself), the driving pressure has decreased (assuming the upstream pressure remains constant), and therefore the velocity in that part of the hose actually decreases. Since the losses are now smaller, more pressure is available to drive the nozzle flow, which can then reach very high exit velocities, depending on the contraction ratio. Squeezing the hose to increase the exit velocity works particularly well if the losses due to friction in the hose are large, so that $fL/D \gg 1$.

## 8.10    Hydraulic Diameter

To find the friction factor for ducts with non-circular cross-section, there exists a useful approximation, called the hydraulic diameter $D_H$, which allows the flow in different conduits to be compared. It is defined by

$$D_H \;\equiv\; \frac{4 \times \text{cross-sectional area}}{\text{perimeter}} \tag{8.31}$$

The hydraulic diameter is used to define equivalent Reynolds numbers $\overline{V} D_H / \nu$ and the relative roughness factors $k/D_H$, so that the Moody diagram can be used to estimate the relevant friction factor. It can also be used to define equivalent head loss factors $h_L = f(L/D_H)\overline{V}^2/2g$ to estimate the losses due to pipe fittings.

To show how this works, say we were asked to estimate the friction factor for a laminar flow in a high aspect ratio rectangular duct by using the known result for a circular pipe (equation 8.19). For a duct, the hydraulic diameter is given by

$$D_H \;=\; \frac{4wD}{2(D+w)}$$

Since $w \gg D$, $D_H = 2D$. Substituting $D_H$ for the diameter in equation 8.19, we have an estimate for the friction factor for the duct flow

$$f = \frac{64}{Re} = \frac{64\nu}{\overline{V} D_H} = \frac{32\nu}{\overline{V} D}$$

This result is 33% larger than the actual result for a two-dimensional duct given in equation 8.10. So the concept of a hydraulic diameter does not work very well for laminar flow in a two-dimensional duct. It tends to work better for flow in ducts with aspect ratios closer to one, such as square ducts, or triangular ones, where the errors for laminar flow are probably less than 10 or 15%. The approach works best for turbulent flows, where the errors in the friction factor are probably less than 10 or 15% for all duct shapes.

## 8.11    Relationship of the Energy Equation to Bernoulli's Equation

When there are no heat interactions (adiabatic flow), and no shaft work interactions, the pipe flow energy equation (equation 8.30) becomes

$$\frac{p_1}{\rho_1} + \tfrac{1}{2}\alpha_1 \overline{V}_1^2 + gz_1 = \frac{p_2}{\rho_2} + \tfrac{1}{2}\alpha_2 \overline{V}_2^2 + gz_2 + gh_\ell \tag{8.32}$$

For one-dimensional flow, this reduces to

$$\frac{p_1}{\rho_1} + \tfrac{1}{2}V_1^2 + gz_1 = \frac{p_2}{\rho_2} + \tfrac{1}{2}V_2^2 + gz_2 + gh_\ell \tag{8.33}$$

This form of the energy equation is very similar to the Bernoulli equation (equation 4.1), except that the energy equation takes account of the changes in density and internal energy, and it allows for losses. For constant density, frictionless flow, the one-dimensional energy equation reduces precisely to Bernoulli's equation, even though one was derived from the first law of thermodynamics, and the other from Newton's second law.

As we pointed out earlier, the terms in Bernoulli's equation all have the dimensions of energy per unit mass, and the equation can be interpreted as expressing the conservation of mechanical energy. The energy equation, however, is more general. In particular, if there is

friction, mechanical energy will not be conserved along streamlines and Bernoulli's equation cannot be used. Similarly, if there is work done on the fluid by a pump, for instance, we must use the energy equation.

This thinking is sometimes expressed in terms a quantity called the Bernoulli constant, $B$. The Bernoulli equation can be written as

$$\frac{p}{\rho} + \tfrac{1}{2}V^2 + gz \;=\; B \tag{8.34}$$

Here, $B$ is constant when the Bernoulli equation is applied to the steady, frictionless flow of a constant density fluid along a streamline. By comparing this equation with the one-dimensional energy equation (equation 8.33), we see that when losses occur ($h_\ell > 0$) the Bernoulli constant will decrease, and the amount it decreases may be identified with the amount of mechanical energy dissipated (see, for example, Section 10.8. Alternatively, adding heat to the fluid or passing it through a pump will increase the Bernoulli constant (both processes add energy to the flow). See also Section 10.8.

# Chapter 9

# Viscous External Flows

## 9.1 Introduction

In the previous chapter we examined viscous, *internal* flows, where the flow was fully developed. For fully developed flow, the fluid does not accelerate, and the nonlinear acceleration term in the Navier-Stokes equation ($D\mathbf{V}/Dt$) is identically zero. When a body moves through a viscous fluid, a boundary layers develop over its surface, but for such external flows, the flow never becomes fully developed. The boundary layers continue to grow in the streamwise direction, and the acceleration of the fluid cannot be neglected. The boundary layers produce a viscous resistance to the motion of the body. Near the rear of the body, the boundary layers can separate, and a wake forms which can increase the overall resistance. In this chapter, we consider external flows where boundary layers and wakes are important.

## 9.2 Laminar Boundary Layer

When a fluid flows over a solid surface at reasonable Reynolds numbers, we know that the no-slip condition causes steep velocity gradients to occur in a thin region near the surface (see Section 1.7). As the flow proceeds downstream, the thickness of this boundary layer grows because slower layers of fluid exert friction on the faster layers, and more and more fluid is decelerated by viscous stresses. In an internal flow, the layers eventually meet, and further growth stops.

However, in an external flow, such as the flow over the hull of a ship, the fuselage of an airplane, or a flat plate placed in the center of a wind tunnel, the boundary layer continues to grow and there is no fully developed state. The analysis is consequently more difficult because the nonlinear acceleration term in the Navier-Stokes equation is no longer zero. Nevertheless, for a simple flow such as that over a flat plate at zero angle of attack, it is possible to determine approximately the growth rate of the layer and the drag exerted by the flow on the plate by using the integral forms of the continuity and momentum equations.

### 9.2.1 Control volume analysis

We will begin by analyzing a laminar boundary layer. We are interested in finding the drag force exerted on the plate by the fluid, and the rate of growth of the boundary layer. A laminar boundary layer is the flow that occurs over a flat plate when the Reynolds number $Re_x = \rho U_e x/\mu$ is less than about 100,000, where $x$ is the distance from the leading edge, and $U_e$ is the velocity of the flow outside the boundary layer. The flow is as shown in Figure 9.1. The velocity $U_e$ is taken to be constant so that $\partial p/\partial x = 0$. We will assume that the boundary layer is thin, so that the streamlines within the boundary layer are nearly
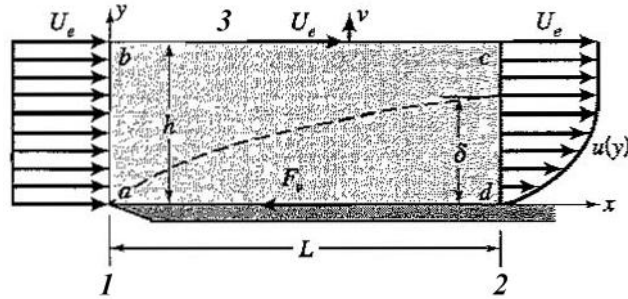
Figure 9.1: Control volume for the analysis of a laminar boundary layer.

parallel and therefore $\partial p/\partial y \approx 0$. Hence, the pressure is taken to be constant everywhere. The flow is steady and the fluid has a constant density.

Consider a rectangular control volume extending a distance $L$ from the leading edge, with a height $h$ (Figure 9.1). The incoming velocity is uniform, and the outgoing profile is decelerated near the wall because of friction, so that for a distance $y \leq \delta$ the streamwise velocity $u(y) < U_e$. Actually, $u$ approaches the freestream value asymptotically, so that the *boundary layer thickness* $\delta$ is defined as the distance where the $u$ is virtually indistinguishable from $U_e$. The most common definition of the boundary layer thickness is that

$$\text{at} \quad y = \delta, \quad u = 0.99 U_e$$

Since the boundary layer thickness grows with downstream distance, $\delta = \delta(x)$.

We begin with the conservation of mass. Since $u(y) < U_e$ there is a greater mass flux into the control volume over face 1 (marked $ab$ in Figure 9.1) than out of the control volume over face 2 ($cd$), and there must be a mass flux out of the control volume through face 3 ($bc$). On face 3, the velocity in the $x$-direction is constant and equal to $U_e$, but the $y$-component of the velocity $v$ is unknown. The vector velocities are on face 1: $\mathbf{V} = U_e\mathbf{i}$, face 2: $\mathbf{V} = u\mathbf{i}$, and face 3: $\mathbf{V} = U_e\mathbf{i} + v\mathbf{j}$. Using the continuity equation, we obtain

$$\int_0^h (\mathbf{n_1} \cdot U_e\mathbf{i})\, W\, dy + \int_0^h (\mathbf{n_2} \cdot u\mathbf{i})\, W\, dy + \int_0^L [\mathbf{n_3} \cdot (U_e\mathbf{i} + v\mathbf{j})]\, W\, dx \; = \; 0$$

where $W$ is the width of the plate, and $\mathbf{n_1}$, $\mathbf{n_2}$ and $\mathbf{n_3}$ are the unit normal vectors on faces 1, 2 and 3, respectively. Since $\mathbf{n_1} = -\mathbf{i}$. $\mathbf{n_2} = \mathbf{i}$, $\mathbf{n_3} = \mathbf{j}$,

$$-U_e h + \int_0^h u\, dy + \int_0^L v\, dx \; = \; 0 \tag{9.1}$$

where $u = u(y)$ and $v = v(x)$.

Next, we use the $x$-component of the momentum equation. Here, $F_v$ is the force exerted by the plate on the fluid. It is assumed to be acting to the left, so that

$$-F_v \;=\; \mathbf{i} \cdot \int_0^h (\mathbf{n_1} \cdot \rho U_e\mathbf{i})\, U_e\mathbf{i}\, W\, dy + \mathbf{i} \cdot \int_0^h (\mathbf{n_2} \cdot \rho u\mathbf{i})\, u\mathbf{i}\, W\, dy$$

$$+\, \mathbf{i} \cdot \int_0^L [\mathbf{n_3} \cdot \rho\, (U_e\mathbf{i} + v\mathbf{j})]\, (U_e\mathbf{i} + v\mathbf{j})\, W\, dx$$

That is,

$$-F_v = -\int_0^h \rho U_e^2 \, W \, dy + \int_0^h \rho u^2 \, W \, dy + \int_0^L \rho v U_e \, W \, dx$$

and so

$$-\frac{F_v}{\rho W} = -U_e^2 h + \int_0^h u^2 \, dy + \int_0^L v U_e \, dx$$

The continuity equation can now be used to eliminate the unknown velocity $v(x)$. Multiplying equation 9.1 by $U_e$ and subtracting the result from the momentum equation gives

$$-\frac{F_v}{\rho W} = -U_e^2 h + \int_0^h u^2 \, dy + U_e^2 h - \int_0^h u U_e \, dy = \int_0^h \left( u^2 - u U_e \right) \, dy$$

Hence

$$\frac{F_v}{\rho W U_e^2} = \frac{1}{U_e^2} \int_0^h \left( u U_e - u^2 \right) \, dy = \int_0^h \left( \frac{u}{U_e} - \frac{u^2}{U_e^2} \right) \, dy$$

Finally

$$\frac{F_v}{\rho W U_e^2} = \int_0^h \frac{u}{U_e} \left( 1 - \frac{u}{U_e} \right) \, dy = \int_0^\delta \frac{u}{U_e} \left( 1 - \frac{u}{U_e} \right) \, dy \qquad (9.2)$$

since $u = U_e$ for $y \geq \delta$. To proceed further with the analysis, we need to know (or guess) the shape of the velocity profile. That is, we need to know how $u$ varies with $y$. This requires some additional input.

## 9.2.2  Blasius velocity profile

It was shown by Ludwig Prandtl in 1904 that for the flow in a boundary layer, it is possible to make some approximations to the full Navier-Stokes equation. The approximations are based on the observation that a boundary layer grows slowly, and therefore the streamlines within the layer are nearly parallel. In particular, the pressure across the layer is then nearly constant (as assumed in the control volume analysis given in Section 9.2.1). These approximations yield an equation called the *boundary layer equation*, and for a zero pressure gradient laminar flow it is given by

$$u \frac{\partial u}{\partial x} + v \frac{\partial u}{\partial y} = \nu \frac{\partial^2 u}{\partial y^2} \qquad (9.3)$$

with the boundary conditions given by $u = v = 0$ at $y = 0$, and $u = U_e$ at $y = \infty$.

Paul Blasius, one of Prandtl's students, showed that this equation has a "similarity" solution. He first proposed that the velocity distribution was a function only of the freestream velocity $U_e$, the density $\rho$, the viscosity $\mu$, the distance from the wall $y$, and the distance along the plate $x$. Dimensional analysis then gives

$$\frac{u}{U_e} = f \left( \frac{U_e x}{\nu}, \frac{y}{x} \right).$$

Blasius then showed that, instead of depending on two dimensionless variables, the velocity distribution was a function of only one composite dimensionless variable $\eta$, so that

$$\frac{u}{U_e} = f'(\eta) \qquad (9.4)$$

| $y(U_e/\nu x)^{1/2}$ | $u/U_e$ | $y(U_e/\nu x)^{1/2}$ | $u/U_e$ |
|:---:|:---:|:---:|:---:|
| 0.0 | 0.0 | 2.8 | 0.81152 |
| 0.2 | 0.06641 | 3.0 | 0.84605 |
| 0.4 | 0.13277 | 3.2 | 0.87609 |
| 0.6 | 0.19894 | 3.4 | 0.90177 |
| 0.8 | 0.26471 | 3.6 | 0.92333 |
| 1.0 | 0.32979 | 3.8 | 0.94112 |
| 1.2 | 0.39378 | 4.0 | 0.95552 |
| 1.4 | 0.45627 | 4.2 | 0.96696 |
| 1.6 | 0.51676 | 4.4 | 0.97587 |
| 1.8 | 0.57477 | 4.6 | 0.98269 |
| 2.0 | 0.62977 | 4.8 | 0.98779 |
| 2.2 | 0.68132 | 5.0 | 0.99155 |
| 2.4 | 0.72899 | $\infty$ | 1.00000 |
| 2.6 | 0.77246 | | |

Table 9.1: Dimensionless velocity profile for a laminar boundary layer: tabulated values prepared by by L.N. Howarth, *Proc. Roy. Soc. London A*, 1938. Adapted from F.M. White, *Fluid Mechanics*, 2nd ed., McGraw-Hill, 1986.

where $\eta = y\sqrt{U_e/(\nu x)}$. The variables $u/U_e$ and $\eta$ are called similarity variables, which means that if the velocity distribution is plotted using these non-dimensional variables (instead of dimensional variables such as $u$ and $y$), it is defined by a universal curve, for any Reynolds number and any position along the plate. This solution is shown in Figure 9.2.

These particular similarity variables transform the boundary layer equation (a *PDE*) into an *ODE* which can be solved numerically. The solution is called the Blasius velocity profile, and the results are usually given in the form of a table (see Table 9.1). The Blasius velocity profile matches the experimental data, such as those shown in Figure 9.2, very well, thereby justifying the assumptions that were made.[1] Note that in these experiments the boundary layer remained laminar up to $Re_x = 1.24 \times 10^6$.

### 9.2.3   Parabolic velocity profile

The Blasius solution is not an analytical solution, and tabulated values do not reveal the physics very well. It is convenient to have an analytical form for the velocity profile, and it turns out that a parabola is a reasonable curve-fit (as can be seen from Figure 9.6). That is, we can use the approximation that

$$\frac{u}{U_e} = 2\left(\frac{y}{\delta}\right) - \left(\frac{y}{\delta}\right)^2 \qquad \text{for} \quad y \le \delta \tag{9.5}$$

and $u/U_e = 1$ for $y > \delta$. This approximation satisfies the boundary conditions $u = 0$ at $y = 0$, and $u = U_e$ at $y = \delta$. Most importantly, it retains the correct similarity scaling, as we will see.

We now have an analytical expression for the velocity distribution, and so we can evaluate

---

[1] Excellent discussions of this topic, and a guide to more general boundary layer problems, may be found in Schlichting *Boundary Layer Theory*, 7th ed., McGraw-Hill, 1979, and White *Viscous Fluid Flow*, 2nd ed., McGraw-Hill, 1991.
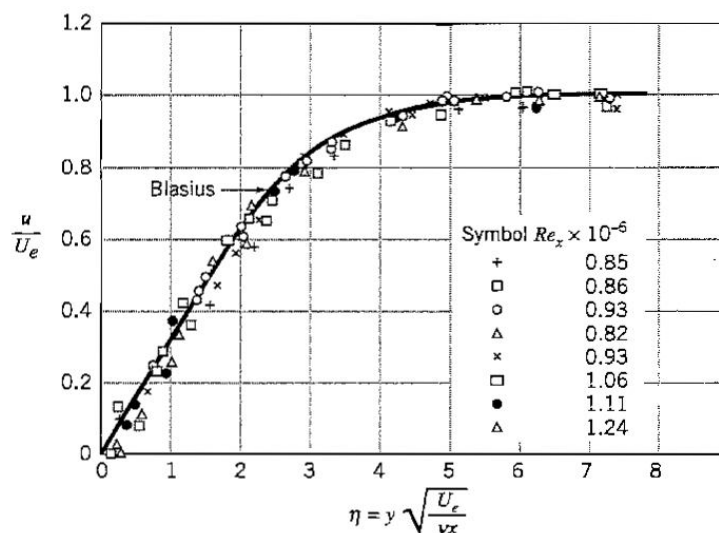
Figure 9.2: Dimensionless velocity profile for a laminar boundary layer: comparison with experiments by H.W. Liepmann, *NACA Rept. 890*, 1943. Adapted from F.M. White, *Viscous Flow*, McGraw-Hill, 1991.

the integral in equation 9.2 and find $F_v$. That is,

$$\frac{F_v}{\rho W U_e^2} \;=\; \int\limits_0^\delta \frac{u}{U_e}\left(1 - \frac{u}{U_e}\right)\,dy \;=\; \frac{2}{15}\delta \tag{9.6}$$

To eliminate the unknown boundary layer thickness $\delta$, we use the fact that the total force due to friction $F_v$ is the integral of the shear stress at the wall $\tau_w$ over the area of the plate. That is,

$$F_v = \int\limits_0^L \tau_w\, W\, dx$$

By differentiating, we obtain

$$\tau_w = \frac{1}{W}\frac{dF_v}{dx} \tag{9.7}$$

The stress at the wall is related to the velocity gradient at the wall (see Example 1.10 in the Study Guide), so that

$$\tau_w = \mu \left.\frac{\partial u}{\partial y}\right|_w$$

For the parabolic profile approximation used here,

$$\tau_w = \frac{2\mu U_e}{\delta} \tag{9.8}$$

Combining this result with equation 9.6 to eliminate $\delta$, we obtain

$$F_v \frac{dF_v}{dx} \;=\; \frac{4}{15}\mu\rho U_e^3 W^2$$

By integration,

$$\int F_v\, dF_v = \frac{4}{15}\mu\rho U_e^3 W^2 \int_0^L dx$$

so that

$$F_v = \sqrt{\tfrac{8}{15}\mu\rho U_e^3 W^2 L}$$

This result can be written as

$$\frac{F_v}{\frac{1}{2}\rho U_e^2 LW} = \frac{\sqrt{32/15}\sqrt{\mu}}{\sqrt{\rho U_e L}} \tag{9.9}$$

so that

$$C_F = \frac{1.46}{\sqrt{Re_L}}$$

for a parabolic velocity profile. The skin friction coefficient $C_F$ and the Reynolds number $Re_L$ are defined by

$$C_F = \frac{F_v}{\frac{1}{2}\rho U_e^2 LW} \qquad \text{and} \qquad Re_L = \frac{\rho U_e L}{\mu} \tag{9.10}$$

$C_F$ is called the *total* skin friction coefficient since it measures the total viscous drag on the plate.

This result holds for a parabolic velocity profile. If we had assumed a different approximation to the Blasius velocity distribution, such as a linear variation where $u/U_e = y/\delta$, we would obtain the same result given in equation 9.10, except the constant would be equal to 1.155 instead of 1.46.

We can now find the variation of boundary layer thickness with streamwise distance by using the result given in equation 9.6 to eliminate $F_v$ in equation 9.9. For the parabolic profile approximation used here:

$$\frac{\delta}{L} = \frac{5.48}{\sqrt{Re_L}}$$

For any position along the plate, therefore,

$$\frac{\delta}{x} = \frac{5.48}{\sqrt{Re_x}} \tag{9.11}$$

This can be written as

$$\delta = \frac{5.48\sqrt{x}}{\sqrt{U_e/\nu}}$$

and we see that the boundary layer thickness grows as $\sqrt{x}$.

The total skin friction coefficient $C_F$ expresses the magnitude of the viscous *force* acting on a plate of width $W$ and length $L$. We can find the local wall shear ıstress acting at any position $x$ along the plate from equations 9.8 and 9.11. For the parabolic velocity profile we otain

$$C_f = \frac{0.73}{\sqrt{Re_x}} \tag{9.12}$$

where the local skin friction coefficient $C_f$ is defined as

$$C_f \equiv \frac{\tau_w}{\frac{1}{2}\rho U_e^2} \tag{9.13}$$

$C_f$ is called the *local* skin friction coefficient since it measures the local viscous stress on the plate. The stress at the wall decreases with distance downstream because the velocity gradient at the wall decreases as a result of the boundary layer growth.

In summary, for a parabolic velocity profile

$$C_F = \frac{1.46}{\sqrt{Re_L}}, \qquad \frac{\delta}{x} = \frac{5.48}{\sqrt{Re_x}} \quad \text{and} \quad C_f = \frac{0.73}{\sqrt{Re_x}}$$

We can compare these approximate results with the exact results obtained by Blasius, who found that

$$C_F = \frac{1.328}{\sqrt{Re_L}}, \qquad \frac{\delta}{x} = \frac{5.0}{\sqrt{Re_x}} \quad \text{and} \quad C_f = \frac{0.664}{\sqrt{Re_x}} \qquad (9.14)$$

We see that the parabolic velocity profile approximation gives the correct dependence on Reynolds number (that is, it gives the correct scaling), but the skin friction coefficients and the boundary layer thickness are about 10% high.

## 9.3  Displacement and Momentum Thickness

As we noted earlier, the velocity $u$ near the edge of the boundary layer approaches the freestream value $U_e$ asymptotically, so that the boundary layer thickness $\delta$ is defined to be the distance where the $u$ is "close enough" to $U_e$. The most common definition of the boundary layer thickness is that

$$\text{at} \quad y = \delta, \quad u = 0.99 U_e$$

Two other thicknesses can be defined, the displacement thickness $\delta^*$, and the momentum thickness $\theta$.

### 9.3.1  Displacement thickness

By definition, the displacement thickness is given by

$$\delta^* \equiv \int_0^\infty \left( 1 - \frac{u}{U_e} \right) dy \qquad (9.15)$$

What is the purpose of defining the displacement thickness? To answer this question, we rewrite equation 9.15 as

$$\rho U_e \delta^* = \int_0^\infty \rho \left( U_e - u \right) dy$$

We see that the mass flux passing through the distance $\delta^*$ in the *absence* of a boundary layer is the same as the deficit in mass flux due to the *presence* of the boundary layer.

To make this point further, consider a velocity profile where $u = 0$ for $y \leq \Delta$, and $u = U_e$ for $y > \Delta$ (see Figure 9.3). For this profile,

$$\delta^* = \int_0^\infty \left( 1 - \frac{u}{U_e} \right) dy = \int_0^\Delta dy = \Delta$$

Therefore, from the point of view of the flow outside the boundary layer, $\delta^*$ can be interpreted as the distance that the presence of the boundary layer appears to "displace" the flow outward from the plate (hence the name). To the external flow, this streamline displacement also looks like a slight thickening of the body shape.

To illustrate an application of this concept, consider the entrance region of a two-dimensional duct of width $W$ and height $2h$. The flow is steady and incompressible. Boundary layers will grow on the top and bottom surfaces, as shown in Figure 9.4. By continuity, if the flow near the wall is slowed down, the fluid outside the boundary layers (in the "core"
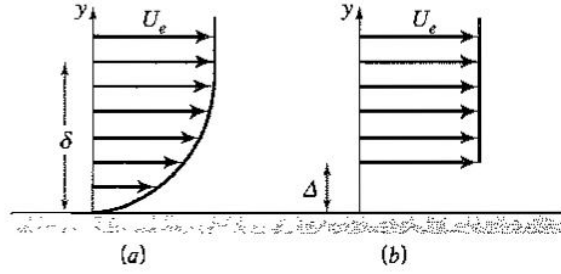
Figure 9.3: Displacement thickness. (a) Velocity profile. (b) Interpretation.

region) must speed up. If the incoming velocity has a value $U_\infty$, what is the core velocity $U_e$ at a point where the boundary layer thickness is $\delta$?

For the control volume shown in Figure 9.4, the continuity equation gives

$$-U_\infty 2hW + \int_{-h}^{h} u\,W\,dy = 0$$

This may be rewritten as

$$U_\infty 2h = \int_{-h}^{h} U_e\,dy - \int_{-h}^{h} (U_e - u)\,dy = U_e D - 2U_e \int_{0}^{h} \left(1 - \frac{u}{U_e}\right) dy$$

where we have used symmetry to simplify the integration. Hence

$$\frac{U_\infty}{U_e} = 1 - \frac{2}{2h} \int_{0}^{h} \left(1 - \frac{u}{U_e}\right) dy \approx 1 - \frac{1}{h} \int_{0}^{\delta} \left(1 - \frac{u}{U_e}\right) dy = 1 - \frac{\delta^*}{h}$$

where we have made the approximation, that, as far as the contribution to the displacement thickness is concerned, $\delta \approx h \approx \infty$. This assumption is commonly made because at $y = \delta$ the velocity is very close to its asymptotic freestream value, and the contribution to the integral for $y > \delta$ is negligible. Hence we obtain

$$U_e = U_\infty \left(\frac{h}{h - \delta^*}\right)$$

We see that the increase in the freestream velocity is given by the effective decrease in the cross-sectional area due to the growth of the boundary layers, and this decrease in area is measured by the displacement thickness.
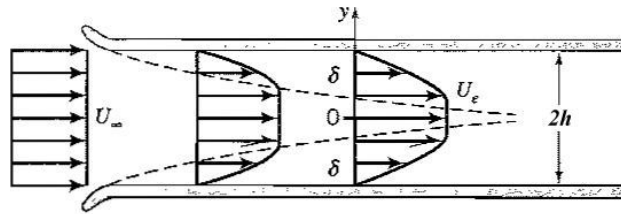


Figure 9.4: Flow in the entrance region of a two-dimensional duct.

### 9.3.2 Momentum thickness

By definition, the momentum thickness is given by

$$\theta \equiv \int_0^\infty \frac{u}{U_e}\left(1 - \frac{u}{U_e}\right)dy \tag{9.16}$$

To interpret the momentum thickness physically, we rewrite equation 9.16 as

$$\rho U_e^2 \theta = \int_0^\infty \rho u \left(U_e - u\right) dy$$

We see that the momentum flux passing through the distance $\theta$ in the absence of a boundary layer is the same as the deficit in momentum flux due to the presence of the boundary layer.

To illustrate this concept, we return to the analysis of the laminar, two-dimensional boundary layer. We start by writing equation 9.2 as

$$\frac{F_v}{\rho W U_e^2} = \int_0^\delta \frac{u}{U_e}\left(1 - \frac{u}{U_e}\right)dy$$

If we make the approximation, that, as far as the contribution to the momentum thickness is concerned, $\delta \approx \infty$, then

$$\frac{F_v}{\rho W U_e^2} = \theta$$

so that

$$F_v = \rho U_e^2 W \theta$$

Therefore the momentum flux passing through the cross-sectional area $W\theta$ at $x = L$, say, in the *absence* of a boundary layer is a measure of the drag on a plate of width $W$ and length $L$ due to the ɪpresence of the boundary layer.

We can also differentiate this relationship and use equation 9.7 to obtain

$$\frac{d\theta}{dx} = \frac{\tau_w}{\rho U_e^2}$$

That is,

$$\frac{d\theta}{dx} = \frac{C_f}{2} \tag{9.17}$$

where the local skin friction coefficient $C_f$ was defined in equation 9.13. The nondimensional rate of change of the momentum thickness with distance is therefore equal to local frictional stress at the wall. Equation 9.17 is called the *momentum integral equation* for a boundary layer in a zero pressure gradient. Although we did not show it, this equation applies equally to laminar and turbulent boundary layers.

### 9.3.3 Shape factor

Another term that is often encountered in discussions of boundary layer behavior is the *form* or *shape* factor $H$, where $H$ is defined as the ratio of the displacement thickness to the momentum thickness:

$$H \equiv \frac{\delta^*}{\theta}$$

By comparing equations 9.15 and 9.16, we see that $\delta^* > \theta$, and so $H > 1$. For a laminar boundary layer the Blasius solution gives $H = 2.59$, and for a turbulent boundary layer experiment shows that $1.4 < H < 1.15$, where $H$ decreases with the Reynolds number. Smaller values of $H$ indicate a "fuller" velocity profile (that is, one with higher velocities near the wall).

## 9.4   Turbulent Boundary Layers

As in pipe flows (Section 8.7), boundary layers become turbulent at high Reynolds number. Transition to turbulence in boundary layers can occur for $Re_x$ greater than about 100,000, where $Re_x$ is the Reynolds number based on the freestream velocity, $U_e$, and the distance from the leading edge, $x$. The actual value depends on many factors, including surface roughness, vibrations, and noise (see also Section 8.6).

In a pipe, the flow is turbulent everywhere, but in a boundary layer the turbulence is bounded on one side by the wall, and the other side by an external freestream. There exists a reasonably well-defined edge between the turbulent fluid in the layer and the non-turbulent fluid in the freestream. An instantaneous picture of the flow in a turbulent boundary layer reveals that this edge is highly convoluted (Figure 9.5), and the instantaneous boundary layer thickness is continually varying in time. We generally prefer to use a time-averaged boundary layer thickness $\delta$ defined so that

$$\text{at} \qquad y = \delta, \quad \langle U \rangle = 0.99 U_e$$

where $\langle U \rangle$ is the time-averaged velocity defined by equation 8.21, so that $\delta$ has a similar meaning in laminar and turbulent flows.

Within the boundary layer, the turbulent fluctuations mixes momentum very efficiently, and as a result the velocity profile is fuller than in a laminar flow (a comparison is shown in Figure 9.6). No analytical or numerical solution exists for the velocity distribution in a turbulent boundary layer, and so we must rely on experiment. The actual mean flow profile is sometimes approximated by a power law similar to that used to describe turbulent pipe flow. That is,

$$\frac{\langle U \rangle}{U_e} \approx \left(\frac{y}{\delta}\right)^{1/n} \tag{9.18}$$

where the exponent $n$ varies with Reynolds number. For a Reynolds number $Re_x$ of about 500,000, $n = 7$, but for higher Reynolds numbers it may increase to about 9.
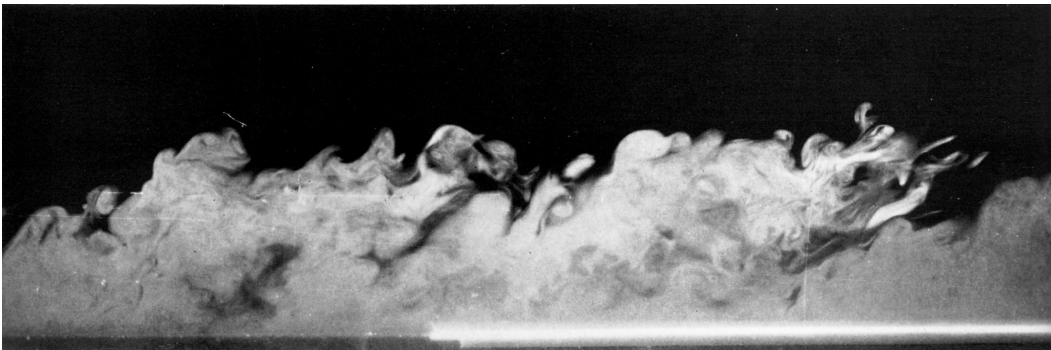


Figure 9.5: Streamwise section of a turbulent boundary layer made visible using small oil droplets. Flow is from left to right. The Reynolds number based on momentum thickness is about 4000. R.E. Falco, *Physics of Fluids* **20**, 1977.
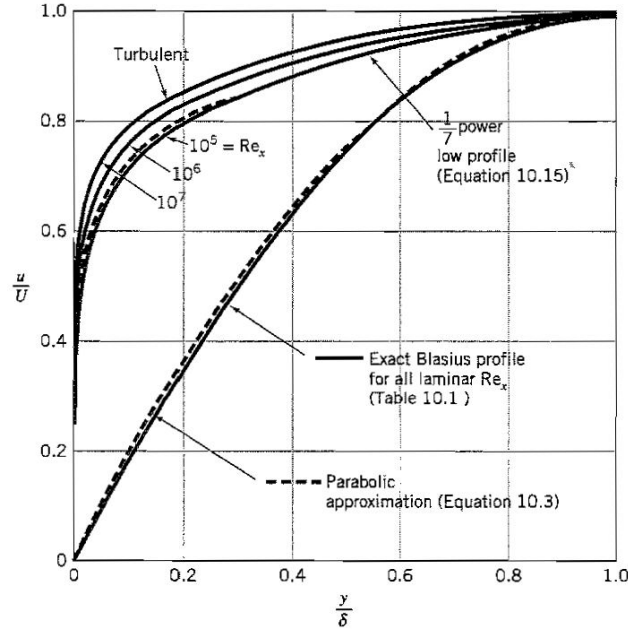
Figure 9.6: Comparison of dimensionless laminar and turbulent flat-plate velocity profiles. Adapted from F.M. White, *Fluid Mechanics*, 2nd ed., McGraw-Hill, 1986.

This power law approximation is reasonably accurate for the outer part of the velocity distribution, as seen in Figure 9.6, but it is a very poor approximation near the wall. Specifically, the velocity gradient at the wall is infinite, implying an infinite wall stress $\tau_w$. Therefore a power law profile cannot be used to find the skin friction in a turbulent flow. Instead, we use the empirical result that the wall stress is given approximately by

$$C_f = \frac{\tau_w}{\frac{1}{2}\rho U_e^2} = \frac{0.0576}{Re_x^{0.2}} \tag{9.19}$$

where $C_f$ is the local skin friction coefficient defined originally by equation 9.13. The skin friction distributions for laminar and turbulent flow on a flat plate are shown in Figure 9.7. At a given Reynolds number, the turbulent skin friction is always higher than the laminar value, reflecting the fact that the turbulent velocity profile is fuller, and therefore the velocity gradient at the wall will be steeper.

To find the total skin friction coefficient, we need the total viscous drag on the plate $F_v$, where

$$F_v = \int_0^L \tau_w\,W\,dx$$

where $W$ is the width of the plate, and $L$ its length. Hence,

$$C_F = \frac{F_v}{\frac{1}{2}\rho U_e^2 LW} = \frac{0.072}{Re_L^{0.2}}$$

If the constant is changed to 0.074, this result is in good agreement over a reasonable Reynolds number range with experimental data for plates that are turbulent along their entire length.[2] Therefore, by experiment

$$C_F = \frac{0.074}{Re_L^{0.2}} \qquad \text{for} \quad 5 \times 10^5 < Re_L < 10^7 \tag{9.20}$$

---

[2]H. Schlichting *Boundary Layer Theory*, 7th edition, published by McGraw-Hill, 1979.
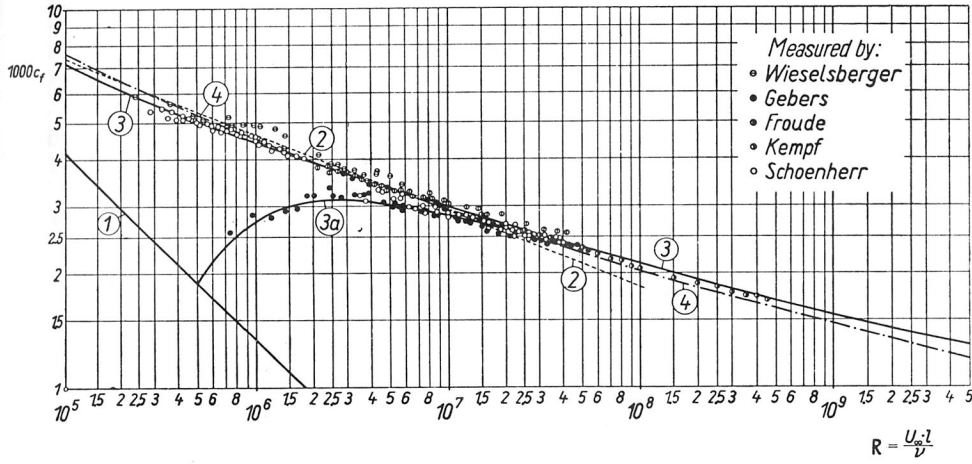
Figure 9.7: Local skin friction coefficient in a flat plate boundary layer as a function of Reynolds number based on freestream velocity and streamwise distance. Laminar flow, labeled (1), is described by equation 9.14, and turbulent flow, labeled (2) is described by equation 9.19 with the constant equal to 0.074. From H. Schlichting, *Boundary Layer Theory*, 7th ed., McGraw-Hill, 1979.

Despite the fact that the shear stress at the wall cannot be found from a power law approximation to the velocity profile, this representation can still be useful. For example, it can give a good estimate of how the boundary layer thickness varies with Reynolds number. To find this estimate, we repeat the analysis given in Section 9.2.3 using the power law profile given by equation 9.18, and the empirical skin friction variation with Reynolds number given by equation 9.19. We obtain

$$\frac{\delta}{x} = \frac{0.37}{Re_x^{0.2}} \tag{9.21}$$

This result agrees reasonably well with experiment. Equation 9.21 can be rewritten as

$$\delta = \frac{0.37x}{Re_x^{0.2}} = \frac{0.37x^{0.8}}{(\nu/U_e)^{0.2}}$$

We see that a turbulent boundary layer grows approximately as $x^{0.8}$, which is faster than a laminar boundary layer, which grows as $x^{0.5}$ (equation 9.14). This increased growth rate is a consequence of the fact that turbulence mixes momentum more efficiently than viscosity.

Also, for a power law profile, we find that

$$\frac{\delta^*}{\delta} = \frac{1}{n+1} \tag{9.22}$$

and

$$\frac{\theta}{\delta} = \frac{n}{(n+1)(n+2)} \tag{9.23}$$

and the shape factor

$$H = \frac{\delta^*}{\theta} = \frac{n+2}{n}$$

For $n = 7$,

$$\frac{\delta^*}{\delta} = \frac{1}{8}, \qquad \frac{\theta}{\delta} = \frac{7}{72}, \quad \text{and} \quad H = \frac{9}{7} \tag{9.24}$$

These estimates for $\delta^*$, $\theta$, and $H$ apply reasonably well for moderate Reynolds numbers where the 1/7th power law is a reasonable approximation. With increasing Reynolds number, $n$ changes from about 7 to about 9, but it is clear that for turbulent flow $\delta^*$, $\theta$, and $H$ are all smaller than in a laminar boundary layer, again because the turbulent velocity profile is fuller than the laminar boundary layer velocity profile.

## 9.5 Separation, Reattachment and Wakes

Now we consider external flows that separate and form wakes. In studying internal flows, we noted that sharp corners almost always produce a separated flow. The sudden expansion and contraction flows shown in Figure 3.15 also demonstrate the formation of large separated regions whenever the duct suddenly changes its area. Sharp corners are not the only cause of separation. For example, whenever a flow changes direction suddenly, we can expect to see regions of separated flow.

This phenomenon is very common, and it is illustrated in Figure 9.8 for the case of external flow over the front of a car. Note that the flow is shown relative to an observer traveling with the car, so that it appears to be approaching the car from left to right. The flow is initially uniform and steady, but as it comes into contact with the surface of the car a boundary layer forms, which then separates as the flow makes the turn over the front part of the hood. The flow *reattaches* at some point downstream, so that the boundary layer re-forms, grows some more and then separates again as the flow meets the windscreen and is forced to turn again. The separation behavior of boundary layers strongly depends on the local pressure gradient: when the pressure rises in the flow direction, a resultant force due to the pressure differences acts to slow the incoming flow. If the force due to pressure differences is strong enough, the flow can reverse direction, which is what we call separation. This behavior is discussed further in Section 9.6.

Note that turbulent flow and separated flow are two different phenomena. In separated flow there is backflow, so that some fluid particles are moving in a direction opposite to the principal flow direction, and there may be significant unsteadiness and fluctuation observed in the flow field. In turbulent flow, all the fluid is moving in the principal flow direction, although the velocity fluctuates about an average value, and the fluctuations have components in all three directions.
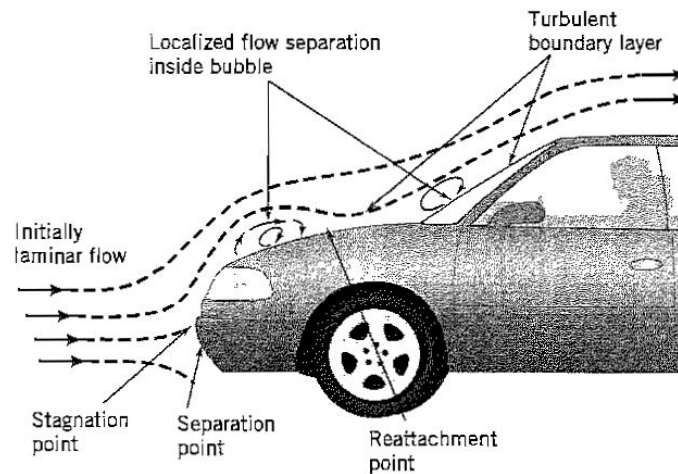


Figure 9.8: Sketch of the flow over the front of a car, showing points of separation and reattachment. From *Race Car Aerodynamics*, J. Katz, Robert Bentley Publishers, 1995. With permission.
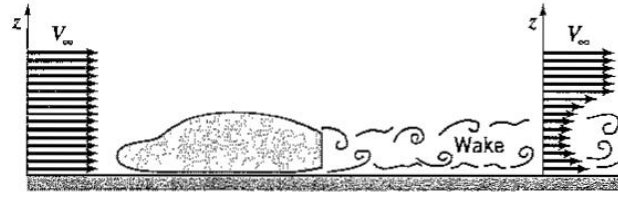
Figure 9.9: Wake flow behind a road vehicle (with flow separation and vortex shedding in the base area). From *Race Car Aerodynamics*, J. Katz, Robert Bentley Publishers, 1995, with permission.
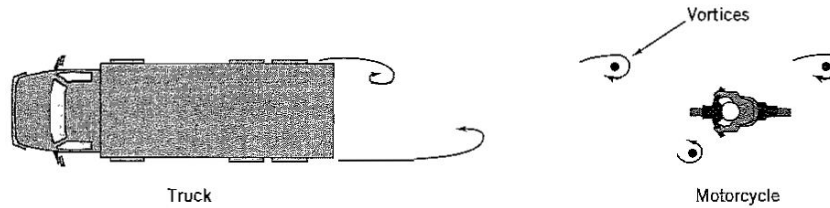


Figure 9.10: Periodic vortex formation in the wake of a large truck. From *Race Car Aerodynamics*, J. Katz, Robert Bentley Publishers, 1995, with permission.

Separated flows are often found in the wake of a moving body. Wakes almost always contain large eddying motions which are shed downstream. For some wakes, such as those produced by cylinders, bluff plates, cars and trucks and other bluff bodies, they often appear at very regular frequencies (see Figures 9.9 and 9.10). In other cases, they are shed more irregularly. For instance, the wake of a boat often contains large eddying motions, in more or less random patterns. Similar flow patterns are observed downstream of pylons supporting a bridge, and in the wake of airfoils.

The wake of a cylinder is particularly interesting. A large region of separated flow occurs, and coherent vortices are shed downstream, as seen in Figure 9.11 (see also Figure 4.3). The flow pattern shown in Figure 9.11 is made visible by illuminating small bubbles suspended in the fluid. A short exposure photograph is used to create short streaklines that approximate the instantaneous velocity vector (that is, we see instantaneous streamlines). The flows over the front and rear of the cylinder are quite different. In the front, the flow passes smoothly over the cylinder, but in the rear the wake is highly unsteady and large eddies or vortices are shed downstream. The large eddies are formed at a regular frequency and they produce pressure disturbances in the flow, which we can sometimes hear as sound . When we talk of the wind whistling in the trees, it is the sound of eddies being shed from the smallest branches. An ancient Greek instrument, the Aolian harp, made use of this regular vortex shedding to produce music. In 1911, Theodore von Kármán made an analysis of this flow pattern of alternating vortices, which is now generally known as the Kármán *vortex street*. The shedding frequency is determined by the nondimensional Strouhal number, which for a cylinder of diameter $D$ is defined as

$$St = \frac{fD}{V} \tag{9.25}$$

where $f$ is the frequency of vortex shedding from one side of the cylinder (in $Hz$), and $V$ is the freestream velocity. In general, the Strouhal number is a function of Reynolds number (see Figure 9.12), but for Reynolds numbers from about 100 to $10^5$, the Strouhal number has an almost constant value of about 0.21.

The wake of a body is always characterized by a region of low velocity, which marks a region of momentum loss associated with the formation of eddying motions in the wake
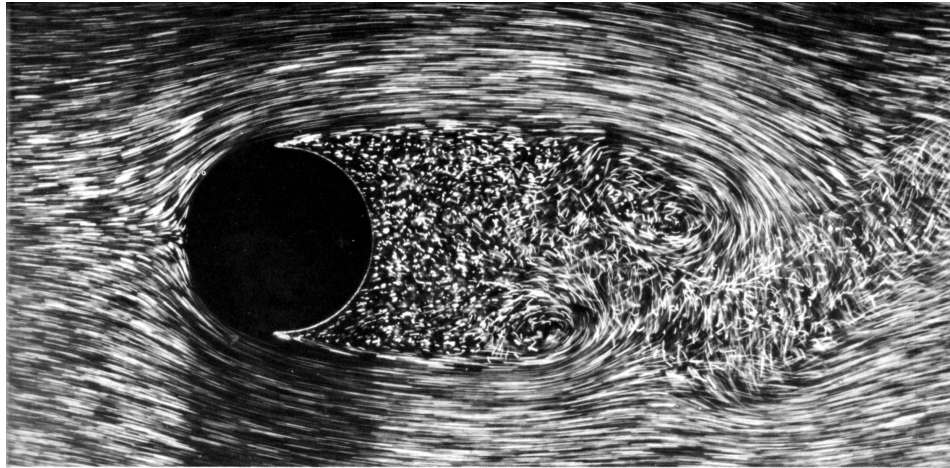
Figure 9.11: Flow over a single cylinder at a Reynolds number of 2000, visualized using small air bubbles in water. ONERA photograph, Werlé & Gallo, 1972.
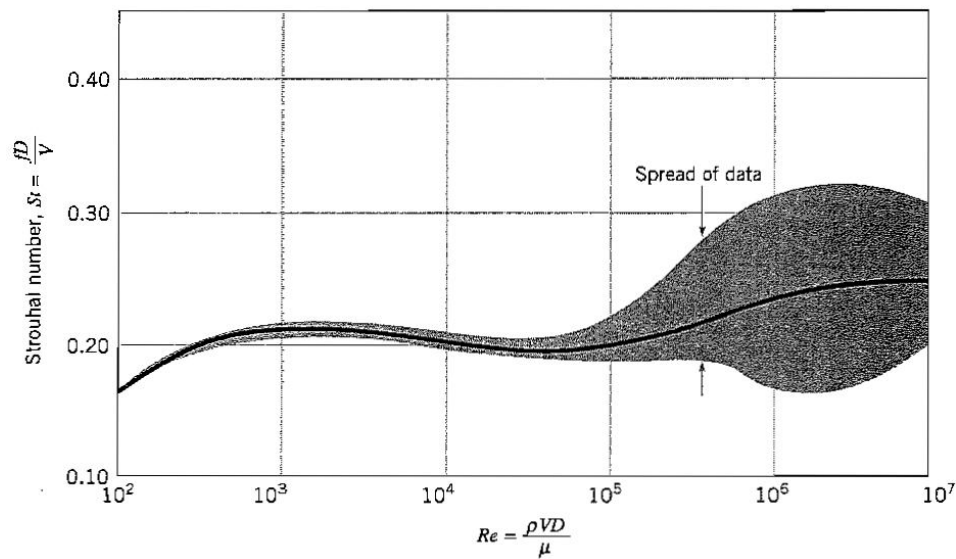


Figure 9.12: Dimensionless shedding frequency from a circular cylinder (Strouhal number) as a function of Reynolds number. Adapted from A. Roshko, *Turbulent Wakes from Vortex Streets*, NACA Rept. 1191, 1954.

(see, for example, Figure 9.9. The pressure in this region does not recover to its stagnation value because of these losses, as we see from the pressure distribution shown in Figure 6.11. In addition, the alternate shedding of vortices produces fluctuating lift and drag forces on the cylinder. If the frequency of the shedding couples to a natural frequency of the cylinder or its supports, large cross-stream oscillations can occur in the cylinder position. This kind of aerodynamic instability was responsible for the destruction of the Tacoma Narrows suspension bridge in the state of Washington in 1940,[3] and it has led to spectacular cooling tower failures in England.

---

[3]A short video is available at *http://media.efluids.com/galleries/all?medium=8*.

## 9.6   Drag of Bluff and Streamlined Bodies

We have seen that boundary layers exert a drag force on a body moving through a fluid. In addition, the formation of a wake is associated with eddying motions that lead to a loss of momentum. The total drag force experienced by a body as it moves through a fluid is therefore usually divided into two components called *viscous drag*, and *pressure drag*. Viscous drag is associated with the viscous stresses developed within the boundary layers, and it scales with Reynolds number as we have seen. Pressure drag comes from the eddying motions that are set up in the wake downstream of the body, and it is usually less sensitive to Reynolds number than viscous drag. Formally, both types of drag are due to viscosity (if the body was moving through an an inviscid fluid there would be no drag at all), but the distinction is useful because the two types of drag are due to different flow phenomena. Viscous drag is important for attached flows (that is, when there is no separation), and it is related to the surface area exposed to the flow. Pressure drag is important for separated flows, and it is related to the cross-sectional area and shape of the body.

We can see the role played by viscous drag (sometimes called frictional drag) and pressure drag (sometimes called form drag) by considering an airfoil at different angles of attack. At small angles of attack, the boundary layers on the top and bottom surfaces experience only mild pressure gradients, and they remain attached along almost the entire chord length [see Figure 9.13(a) and (b)]. The wake is very small, and the drag is dominated by the viscous stresses inside the boundary layers. At a given Reynolds number, the drag will be higher for turbulent flow than for laminar flow. As the angle of attack increases, however, pressure drag will become more important. With an increased angle of attack, the pressure gradients on the airfoil increase in magnitude. In particular, the pressure increases toward the rear portion of the top surface, so that the pressure gradient in that region is positive. This "adverse" pressure gradient may become sufficiently strong to produce a separated flow [see Figure 9.13(c) and (d), and also Section 6.9]. Separation will increase the size of the wake, and increase the magnitude of the pressure losses in the wake due to eddy formation. Therefore the pressure drag increases. At a higher angle of attack, a large fraction of the flow over the top surface of the airfoil may be separated, and the airfoil is said to be *stalled* [see Figure 9.13(e)]. At this stage, the pressure drag is much greater than the viscous drag.

When the pressure losses are small and the overall drag is mainly due to viscous drag, we say the body is *streamlined*. When the viscous drag is small and the total drag is dominated by pressure losses, we describe the body as *bluff*. Whether the flow is viscous-drag dominated or pressure-drag dominated depends entirely on the shape of the body. A fish, or an airfoil at small angles of attack, behaves like a streamlined body, whereas a brick, a cylinder, or an airfoil at large angles of attack behaves like a bluff body. For a given frontal area and velocity, a streamlined body will always have a lower resistance than a bluff body. For example, the drag of a cylinder of diameter $D$ is about ten times larger than a streamlined shape of the same thickness.

Cylinders and spheres are considered bluff bodies because at Reynolds numbers much greater than one, the drag is dominated by the pressure losses in the wake. The variation of the drag coefficients with Reynolds number is shown in Figure 9.14 and the corresponding flow patterns are shown in Figure 9.15. We see that as the Reynolds number increases the variation in the drag coefficient (based on cross-sectional area) decreases, and over a large range in Reynolds number it is nearly constant.

At a Reynolds number between $10^5$ and $10^6$, the drag coefficient takes a sudden dip. The dip indicates that the pressure losses in the wake have suddenly become smaller, and experiments show that the size of the wake decreases, and that the boundary layer separation on the cylinder or sphere occurs further along the surface than before. What has happened?

The sudden decrease in drag is related to the differences between laminar and turbulent
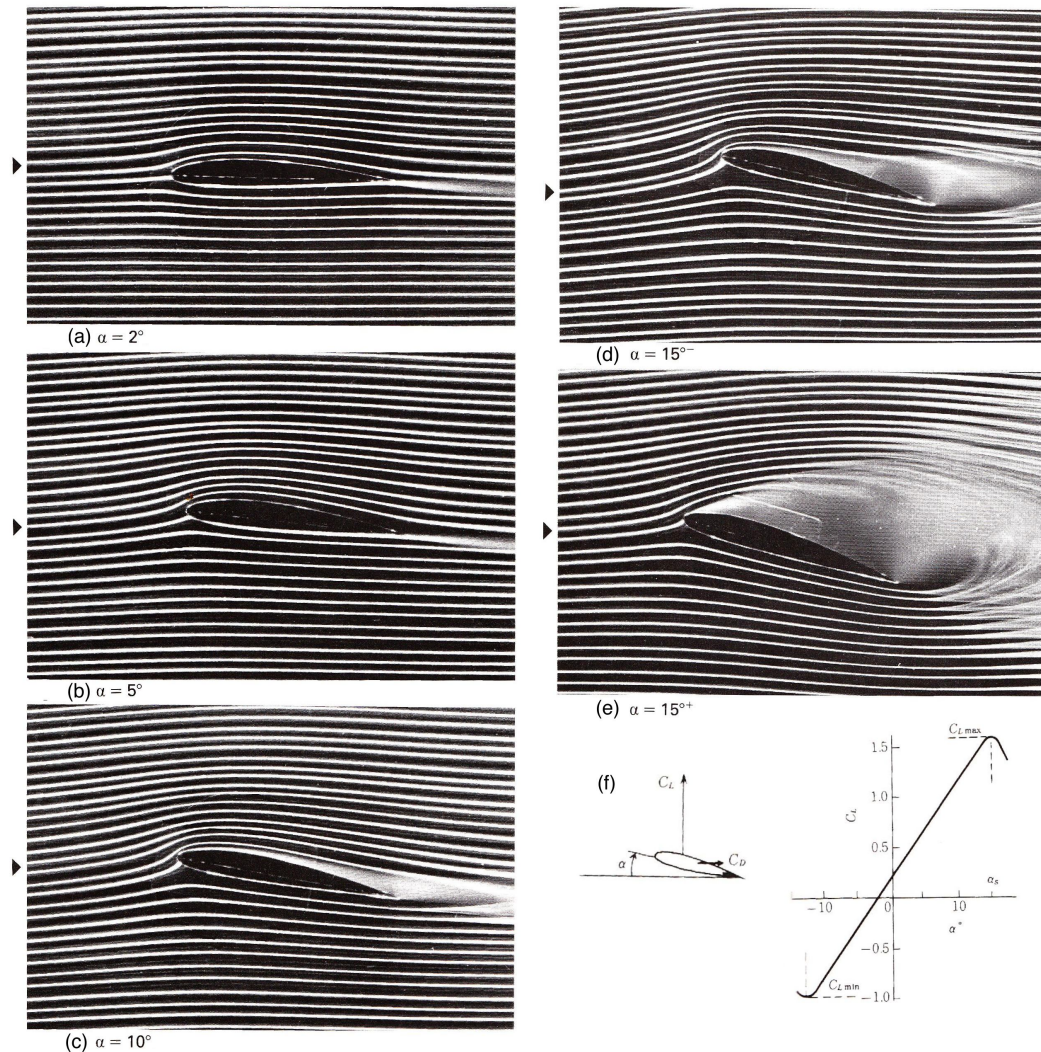
Figure 9.13: Flow over a NACA 4412 airfoil section at Reynolds number based on chord length of $2.1 \times 10^6$. (a) $\alpha = 2°$, (b) $\alpha = 5°$, (c) $\alpha = 10°$, (d) $\alpha < 15°$, (e) $\alpha > 15°$, (f) Lift coefficient versus angle of attack. From *Visualized Flow*, Japan Society of Mechanical Engineers, Pergamon Press, 1988.

boundary layers. We saw in Section 6.9 that the boundary layer and its interaction with the local pressure gradient plays a major role in affecting the flow over a cylinder. In particular, near the shoulder, the pressure gradient changes from being negative (decreasing pressure, a *favorable* pressure gradient) to positive (increasing pressure, an *adverse* pressure gradient). The force due to pressure differences changes sign from being an accelerating force to being a retarding force. In response, the flow slows down. However, the fluid in the boundary layer has already given up some momentum to overcome the viscous stresses, and it does not have enough momentum to overcome the retarding force. Some fluid near the wall, where the momentum was low to begin with, actually reverses direction, and the flow separates.

A turbulent boundary layer has more momentum near the wall than a laminar boundary layer (see Figure 9.6) because turbulence is a very effective mixing process. More importantly, turbulent transport of momentum is very effective at replenishing the near-wall momentum. When a turbulent boundary layer enters a region of adverse pressure gradient,
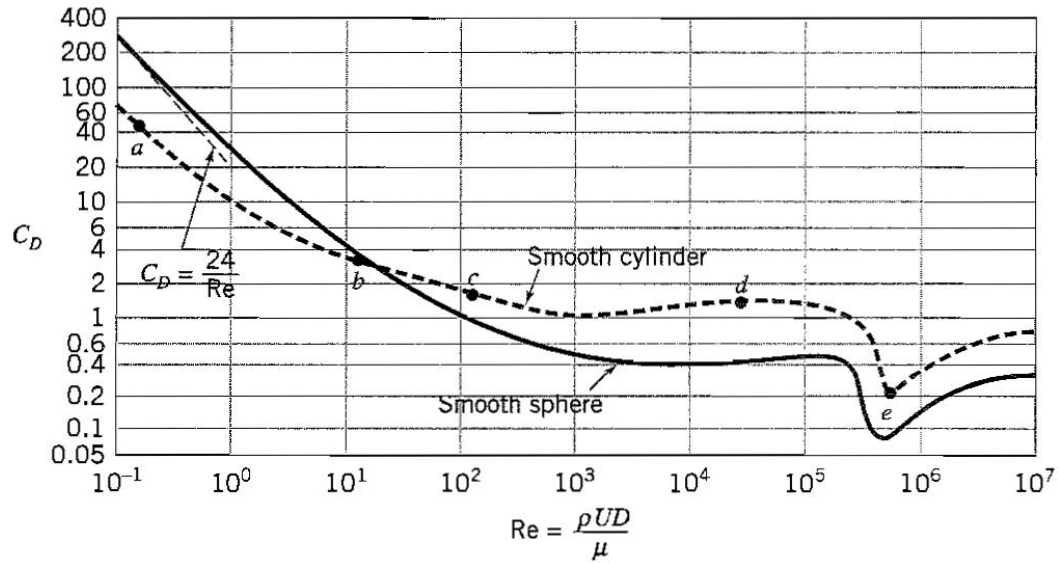
Figure 9.14: Drag coefficient as a function of Reynolds number for smooth circular cylinders and smooth spheres. From Munson, Young & Okiishi *Fundamentals of Fluid Mechanics*, John Wiley & Sons, 1998.
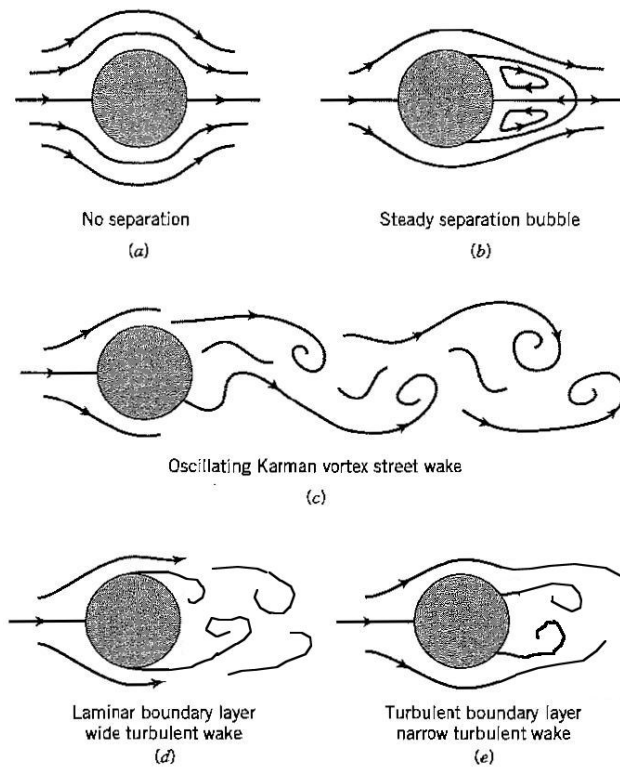


Figure 9.15: Flow patterns for flow over a cylinder. (a) Reynolds number = 0.2; (b) 12; (c) 120; (d) 30,000; (e) 500,000. Patterns correspond to the points marked on Figure 9.14. Adapted from Munson, Young & Okiishi *Fundamentals of Fluid Mechanics*, John Wiley & Sons, 1998.

it can therefore persist for a longer distance without separating (compared to a laminar flow) because its momentum near the wall is higher to begin with, and it is continually (and quickly) being replenished by turbulent mixing.

We can now reconsider the dip in the drag coefficient that occurs at a Reynolds number of about 250,000 (Figure 9.14). The boundary layer over the front face of a sphere or cylinder is laminar at lower Reynolds numbers, and turbulent at higher Reynolds numbers. The dip in the drag coefficient occurs at the point where the boundary layer changes from laminar to turbulent. When it is laminar ($Re < 10^5$), separation starts almost as soon as the pressure gradient becomes adverse [very near the shoulder, Figure 9.15(d)], and a large wake forms. When it is turbulent ($Re > 10^6$), separation is delayed [to a point about $20°$ past the shoulder, Figure 9.15(e)] and the wake is correspondingly smaller. The Reynolds number where the flow switches and the drag suddenly decreases is called the *critical* Reynolds number.

It follows that, if the boundary layer of a sphere could be made turbulent at a Reynolds number lower than the critical value, the drag should also decrease at the same time. This can be demonstrated by using a *trip wire*. A trip wire is simply a wire placed axisymmetrically on the front face of the sphere. As the flow passes over the wire, it introduces a large disturbance into the boundary layer which causes an early transition to turbulence. Its effect on the size of the wake is quite dramatic, as shown in Figure 9.16. A similar result can be achieved using surface roughness to "trip" the boundary layer, and Figure 9.17 shows the effect of increasing surface roughness on the drag coefficient of a sphere.

Elliptical and airfoil shapes display a similar dip in the drag curve at a critical Reynolds number (see Figure 9.18). Bodies with sharp edges typically do not, at least for Reynolds numbers greater than about 3000, as in the case of a flat plate set at right angles to the flow direction. Here the points of separation are fixed at the edges, and they do not change with position with Reynolds number. The drag coefficients for a number of sharp-edged bodies are given in Table 9.2. Drag coefficients for a wide variety of other interesting shapes are shown in Table 9.3.

## 9.7  Golf Balls, Cricket Balls and Baseballs

Tripping the boundary layer to reduce the drag of spheres is widely used in sports. For example, golf balls are dimpled. The dimples act as a very effective trip wire, and the consequent delay in separation reduces the drag on the ball and allows the ball to travel further for the same amount of effort. A good golfer can easily make a golf ball carry 250 yards, but the same golfer using a smooth ball will only drive it about 100 yards. Figure 9.17 shows how different degrees of roughness reduce the drag on a sphere at high Reynolds number, and how effective dimples are.

The same principle is used in cricket. A cricket ball has a single, circumferential seam which looks remarkably like a trip wire. If a cricket ball is bowled without spin so that its seam is tilted forward on the top of the ball, then the boundary layer over the top surface becomes turbulent, whereas the boundary layer on the bottom surface remains laminar. The wake becomes asymmetric, and a downward force is produced so that the ball dips sharply. A similar effect can be obtained with a baseball or a tennis ball if the seam is held correctly. The seam on a baseball is more convoluted than on a cricket ball, but its tripping effect is similar.

The addition of spin complicates this picture enormously. We saw in Section 4.3 and Figure 6.12 that spin can produce a side force on a ball due to the Magnus effect. The effect depends strongly on the orientation of the seam. Knuckleball pitchers typically pitch a baseball with very little spin, and they do not use the Magnus effect. Instead, they rely largely on the uneven tripping of the boundary layer. Even a little spin will make
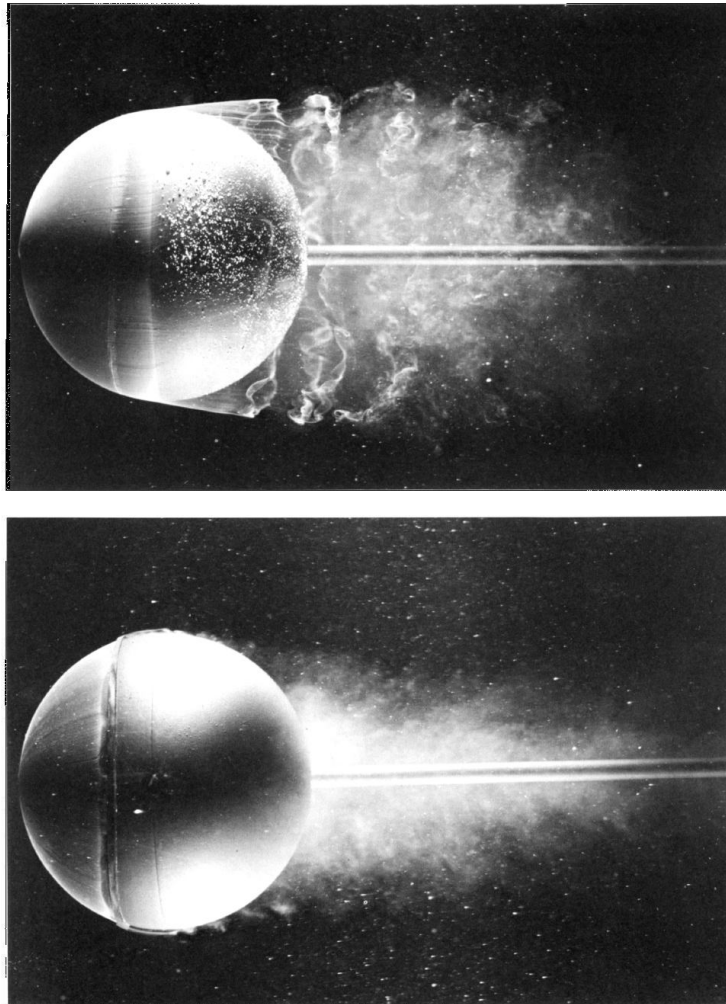
Figure 9.16: Flow over a sphere. (a) Reynolds number = 15,000 (laminar separation). (b) Reynolds number = 30,000, with trip wire (turbulent separation). From van Dyke, *Album of Fluid Motion*, Parabolic Press, 1982. Original photographs by Werlé, ONERA, 1980.

the direction of the side force change dramatically, however, and it is no wonder that the behavior of a knuckleball is highly unpredictable.[4]

## 9.8   Automobile Flow Fields

As a final topic in this chapter, we examine some aspects of the flow over automobiles. As we have already seen in Figures 4.1, 6.13, 9.8, 9.9 and 9.10, boundary layers form, which can separate at points where the flow makes a sudden turn, and where adverse pressure gradients occur. A typical pressure distribution over a car model is shown in Figure 9.19. The region of favorable pressure gradient on the roof is indicated by the negative slope in the upper pressure distribution (where $\partial p/\partial x < 0$). The region of adverse pressure gradient near the rear of the car is indicated by the positive slope in the upper pressure distribution (where

---

[4]To learn more about these matters, see the article by R. Mehta, "Aerodynamics of sports balls," *Annual Review of Fluid Mechanics*, **17**:151–189, 1985.
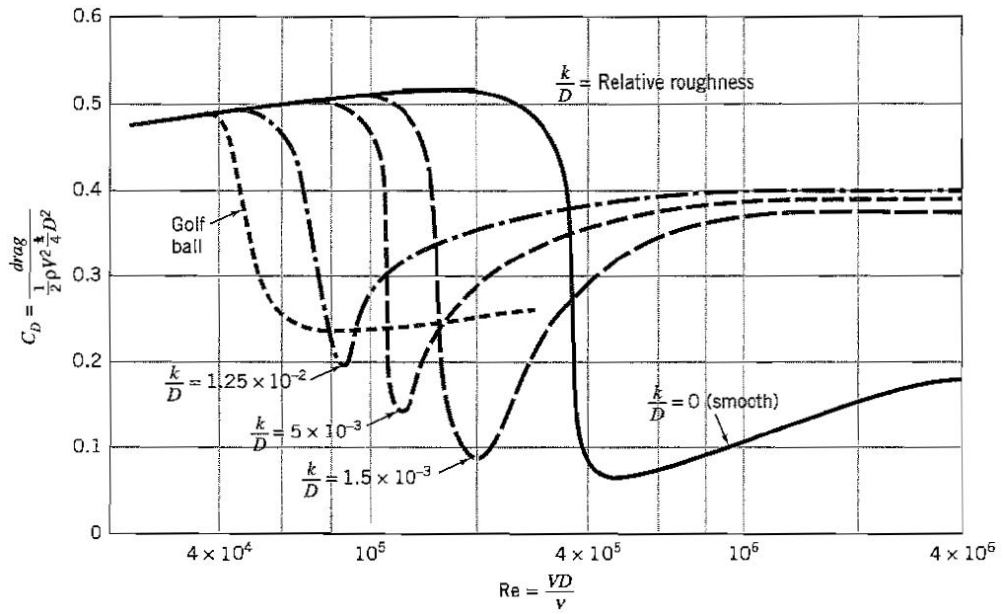
Figure 9.17: Drag coefficient as a function of Reynolds number for spheres with different degrees of roughness. From Munson, Young & Okiishi *Fundamentals of Fluid Mechanics*, John Wiley & Sons, 1998.
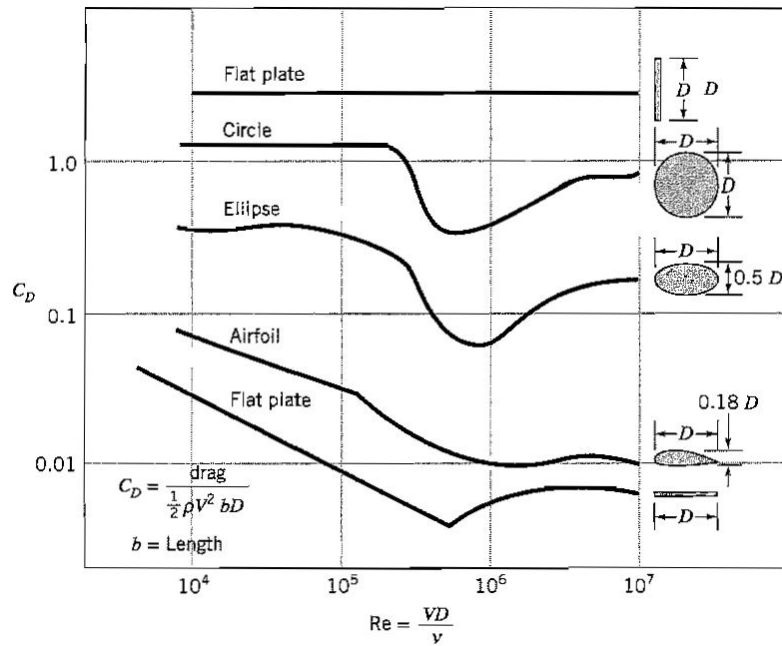


Figure 9.18: Drag coefficients of bluff and streamlined bodies. From Munson, Young & Okiishi *Fundamentals of Fluid Mechanics*, John Wiley & Sons, 1998.

$\partial p/\partial x > 0$), and this is where the boundary layer is susceptible to separation. Similar regions of adverse pressure gradient are found on the hood, and on the rear underside of the car.
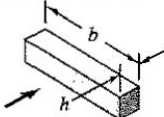
| Object | Diagrams | $C_D$ $(Re \gtrsim 10^{-1})$ | |
|---|---|---|---|
| Square cylinder | | $b/h = \infty$ | 2.05 |
| | | $b/h = 1$ | 1.05 |
| Disk | | | 1.17 |
| Ring | | | $1.20^b$ |
| Hemisphere (open end facing flow) | | | 1.42 |
| Hemisphere (open end facing downstream) | | | 0.38 |
| C-section (open side facing flow) | | | 2.30 |
| C-section (open side facing downstream) | | | 1.20 |

Table 9.2: Drag coefficient data for sharp-edged bodies. From Fox & McDonald, *Introduction to Fluid Mechanics*, 4th ed., John Wiley & Sons, 1992. [a]Original data from Hoerner, Fluid-Dynamic Drag, 2nd ed., Midland Park, NJ. Published by the author. [b]Based on area of ring.

The regions of separated flow on the car body, and the presence of a wake, dominate the aerodynamic drag on the vehicle (on most cars, the viscous, boundary layer drag makes only a small contribution to the total drag, and therefore cars are frequently considered to be bluff bodies).

At low speeds, the major source of resistance on a car is the rolling resistance due to friction between the moving parts in the drivetrain and the flexing of the tires. As the speed increases, however, the aerodynamic drag increases rapidly, approximately as the square of the speed if the drag coefficient is constant with Reynolds number (see Figure 9.20). For the particular car shown in Figure 9.20, the aerodynamic resistance becomes the major source of drag at about $80\,km/h$, that is, $50\,mph$. At $120\,km/h$ ($75\,mph$), the aerodynamic resistance accounts for two-thirds of the total drag.

Typical values of lift and drag coefficients for car-shaped bodies are given in Table 9.4. The most streamlined shape listed in the table has a drag coefficient as low as 0.04, but when this shape is modified to look like a ground vehicle, it increases to about 0.15, which might be taken as a realistic lower limit. Most modern cars have values closer to 0.4. Somewhat surprisingly, race cars have generally higher drag coefficients, primarily because there are other constraints on their shape, such as a requirement for strong negative lift to help cornering performance, and the presence of air inlets for the engine and the water and oil coolers. Also, the downforce generated by wings and other lifting surfaces has a strong effect on the drag coefficient of a race car, with a corresponding effect on its maximum speed. The results shown in Figure 9.21 were obtained by using the maximum engine rpm for each downforce adjustment under full throttle conditions to estimate the drag force.
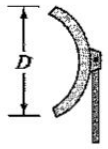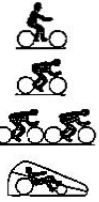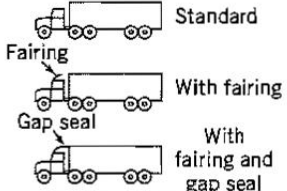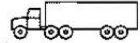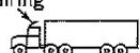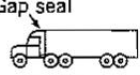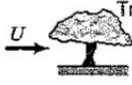
| Shape | Reference area | Drag coefficient $C_D$ |
|---|---|---|
| Parachute | Frontal area $A = \frac{\pi}{4}D^2$ | 1.4 |
| Porous parabolic dish | Frontal area $A = \frac{\pi}{4}D^2$ | Porosity: 0 \| 0.2 \| 0.5<br>→ 1.42 \| 1.20 \| 0.82<br>← 0.95 \| 0.90 \| 0.80<br>Porosity = open area/total area |
| Average person | Standing<br>Sitting<br>Crouching | $C_D A = 9$ ft$^2$<br>$C_D A = 6$ ft$^2$<br>$C_D A = 2.5$ ft$^2$ |
| Fluttering flag | $A = lD$ | $l/D$ \| $C_D$<br>1 \| 0.07<br>2 \| 0.12<br>3 \| 0.15 |
| Empire State Building | Frontal area | 1.4 |
| Six-car passenger train | Frontal area | 1.8 |
| Bikes — Upright commuter | $A = 5.5$ ft$^2$ | 1.1 |
| Racing | $A = 3.9$ ft$^2$ | 0.88 |
| Drafting | $A = 3.9$ ft$^2$ | 0.50 |
| Streamlined | $A = 5.0$ ft$^2$ | 0.12 |
| Tractor-trailor trucks — Standard | Frontal area | 0.96 |
| With fairing | Frontal area | 0.76 |
| With fairing and gap seal | Frontal area | 0.70 |
| Tree: $U = 10$ m/s<br>$U = 20$ m/s<br>$U = 30$ m/s | Frontal area | 0.43<br>0.26<br>0.20 |
| Dolphin | Wetted area | 0.0036 at Re = $6 \times 10^6$<br>(flat plate has $C_{Df} = 0.0031$) |
| Large birds | Frontal area | 0.40 |

Table 9.3: Drag coefficient data for selected objects. From Munson, Young & Okiishi *Fundamentals of Fluid Mechanics*, John Wiley & Sons, 1998.
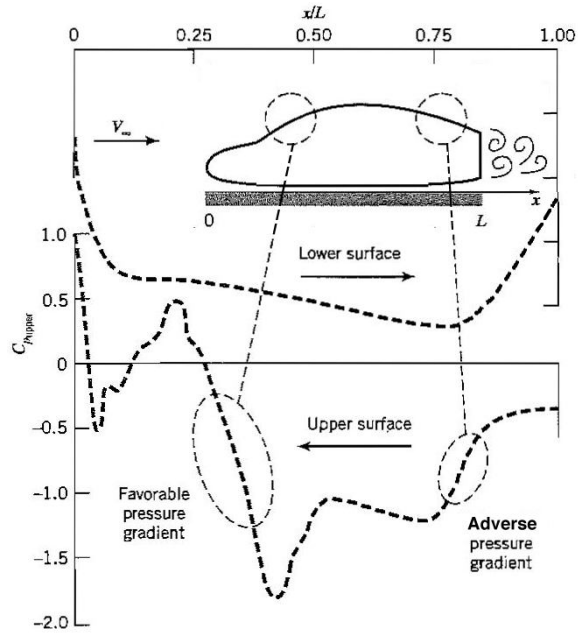
Figure 9.19: Distribution of measured pressure coefficients over a two-dimensional automobile shape. Adapted from *Race Car Aerodynamics*, J. Katz, Robert Bentley Publishers, 1995, with permission.
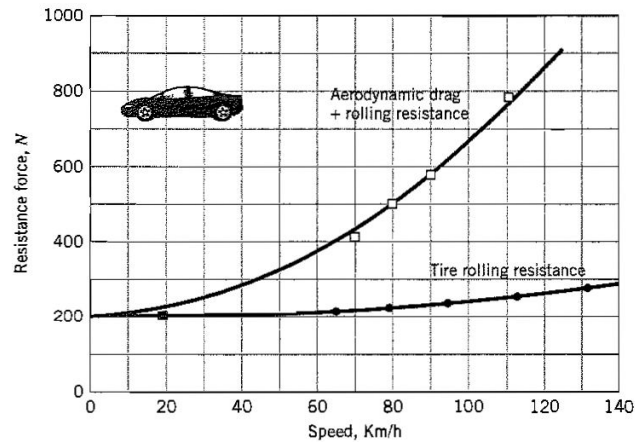


Figure 9.20: Aerodynamic and rolling resistances for an average sedan car. From *Race Car Aerodynamics*, J. Katz, Robert Bentley Publishers, 1995, with permission.

Another interesting aspect of the flow over cars is the phenomenon of drafting or "tail-gating." It is well-known that the air resistance of a car is reduced when it follows another in close proximity, and the leading car acts as a shield for the trailing car. The resulting flow field is sketched in Figure 9.22. The data shown in Figure 9.23 indicate a significant decrease in drag coefficient for the trailing car when the separation is less than about one car length. Interestingly, the drag coefficient of the leading car is decreased by an even greater margin, suggesting that under race conditions both cars will travel faster in tandem than they could by themselves.
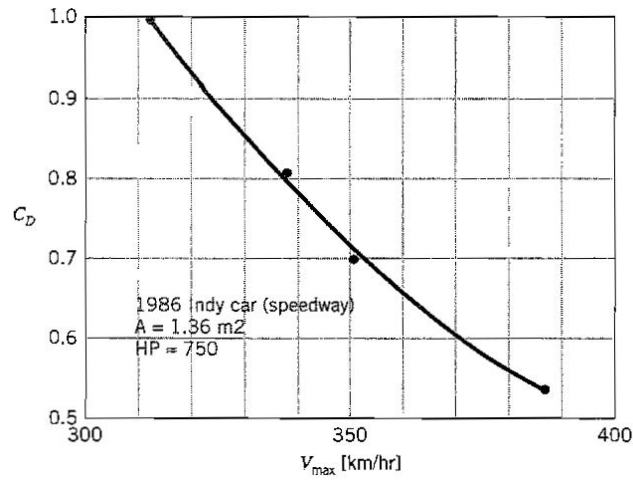
Figure 9.21: effect of the drag coefficient on the maximum speed of an Indy-class speedway car. From *Race Car Aerodynamics*, J. Katz, Robert Bentley Publishers, 1995, with permission.
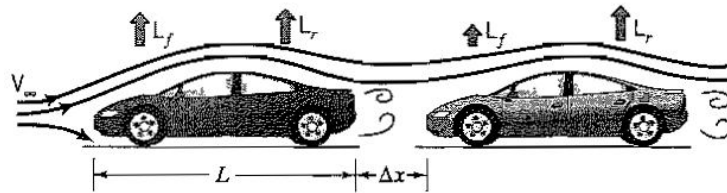


Figure 9.22: Sketch of the flow over two cars, separated by a distance $\Delta x$. From *Race Car Aerodynamics*, J. Katz, Robert Bentley Publishers, 1995, with permission.
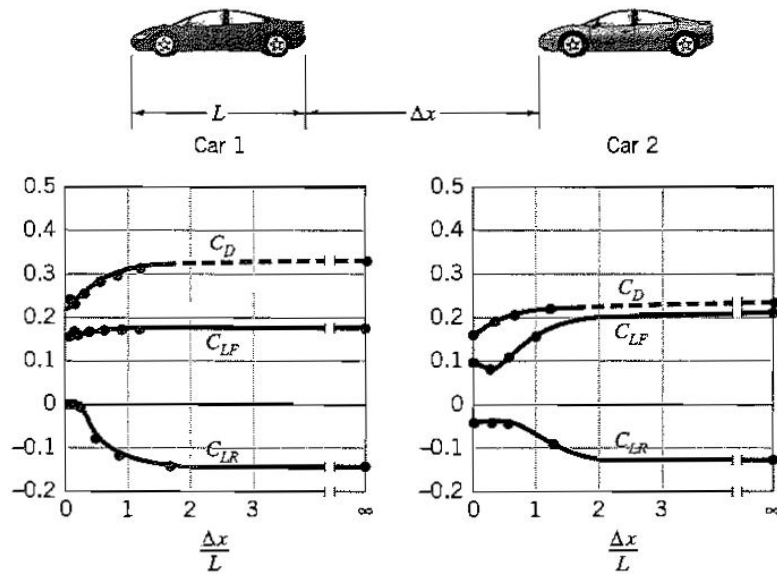


Figure 9.23: Lift and drag coefficients for two cars, separated by a distance $\Delta x$. Notation as in Figure 9.22. From *Race Car Aerodynamics*, J. Katz, Robert Bentley Publishers, 1995, with permission.
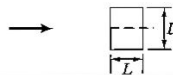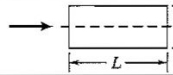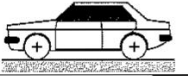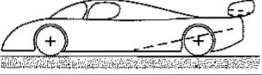
| | | | $C_L$ | $C_D$ |
|---|---|---|---|---|
| 1 | Circular plate | | 0 | 1.17 |
| 2 | Circular cylinder $L/D < 1$ | | 0 | 1.15 |
| 3 | Circular cylinder $L/D > 2$ | | 0 | 0.82 |
| 4 | Low drag body of revolution | | 0 | 0.04 |
| 5 | Low drag vehicle near the ground | | 0.18 | 0.15 |
| 6 | Generic automobile | | 0.32 | 0.43 |
| 7 | Prototype race car | | −3.00 | 0.75 |

Table 9.4:  Typical lift and drag coefficients.  From *Race Car Aerodynamics*, J. Katz, Robert Bentley Publishers, 1995, with permission.

# Chapter 10

# Open Channel Flow

## 10.1  Introduction

In this chapter we examine flows where there is a *free surface*. A free surface is the interface between a liquid and a gas, a place where the pressure at the interface is effectively constant. For the case of water flowing in a channel that is open to the atmosphere, the pressure at the free surface is assumed to be constant and equal to atmospheric pressure. If there are no strong disturbances present, such as breaking waves, and the flow is steady, Bernoulli's equation can be used along the surface. Below the free surface, the pressure will vary with depth: even if the flow has parallel streamlines, hydrostatic pressure still acts and the forces due to hydrostatic pressure differences must be taken into account in the momentum equation.

One of the most interesting aspects of flows with a free surface is the formation of surface waves. We shall see that the propagation of waves is determined by the Froude number, $F$, which is the ratio of the speed of the flow to the speed of propagation of small amplitude waves. As the Froude number changes from subcritical values (where $F < 1$) to supercritical values (where $F > 1$), the nature of the wave propagation changes radically. This phenomenon has a profound influence on the nature of the flow, and it is very similar to the behavior of sound waves in a gas, where subsonic flows ($M < 1$) behave entirely differently from supersonic flows ($M > 1$). In the next chapter, we examine compressible flows, where the similarity between wave propagation in open channel flows and sound waves in gases will be explored further. Here, we examine open channel flows.

## 10.2  Small Amplitude Gravity Waves

To begin the study of open channel flows, we will consider the behavior of *small amplitude gravity waves* moving in a *shallow, open channel flow*. A small amplitude gravity wave is a wave that is driven by, with a height that is small compared to its wavelength. Energy losses are very small and the equations of motion can be linearized (see following discussion). Shallow means that the depth of the water is small compared to the length of the waves, so that the one-dimensional form of the equations of motion can be used. Open channel flow means that the flow is open to the atmosphere (it has a free surface where the pressure is atmospheric).

Consider a long, shallow, open channel containing a stationary liquid. A small disturbance is initiated at one end of the channel, perhaps by using a paddle to raise the water level a small amount and then releasing it. The disturbance will move along the channel with velocity $c$, as shown in Figure 10.1. We call this small-amplitude disturbance a wave,
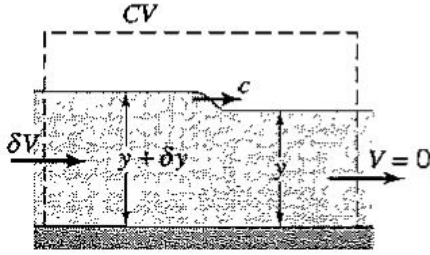
Figure 10.1: Control volume for a small amplitude wave in an open channel: unsteady flow.
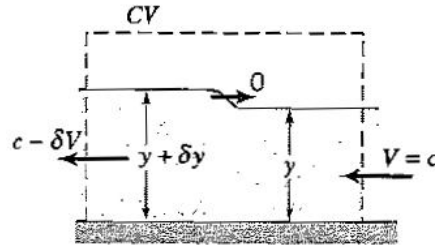


Figure 10.2: Control volume for a small amplitude wave in an open channel: steady flow.

although it is not periodic. It is strictly a *bore*, which is a type of single-sided wave found in shallow channel flows (see Section 10.7 for more details). For the case considered here, the wave is a plane wave, in that it is straight and does not vary across the channel.

We can analyze this flow using a control volume approach, together with Bernoulli's equation. When the control volume is stationary, as shown in Figure 10.1, we see that before the arrival of the wave, the control volume contains a motionless body of water of depth $y$. The wave then arrives from the left, and as it enters the control volume the depth of the water behind the wave increases to $y + \delta y$. With respect to this stationary control volume, the flow is unsteady. Also, we see that the fluid behind the wave is moving to the right with velocity $\delta V$. Why is this fluid moving? As the wave passes through the control volume, the mass of water contained in the control volume increases. The extra mass was brought in by a mass flux through the left hand face of the control volume, so that the fluid behind the wave must be moving with a small velocity in the direction of motion of the wave. This velocity $\delta V$ is called the *drift* velocity, and it is typically a small fraction of the wave speed.

The analysis becomes simpler if you imagine yourself moving with the wave. The wave is now stationary relative to yourself, but the water in front of the wave is coming towards you at a speed $c$. Therefore, if we use a control volume that moves at speed $c$ to the right, the wave is always at the same location in the control volume and the flow is steady (Figure 10.2). The shallow channel approximation implies that $\delta V$ is constant over the depth $y + \delta y$, and that the flow can be treated as one-dimensional. The continuity equation then gives

$$(c - \delta V)(y + \delta y) = c\,y$$

Expanding, and keeping only first order terms ($\delta y \ll y$, and $\delta V \ll c$), we obtain:

$$c\,\delta y = y\,\delta V \tag{10.1}$$

If we also assume there are no losses, we can apply Bernoulli's equation along the surface (the surface is a streamline where the pressure is constant), so that

$$\tfrac{1}{2}(c - \delta V)^2 + g(y + \delta y) = \tfrac{1}{2}c^2 + gy$$

Expanding, and keeping only first order terms gives

$$g\,\delta y = c\,\delta V \tag{10.2}$$

Equations 10.1 and 10.2 yield

$$\boxed{c = \sqrt{gy}}$$

We find that the speed of a small amplitude gravity wave moving over the surface of shallow water is $\sqrt{gy}$.

## 10.3 Waves in a Moving Fluid

What happens if, instead of being motionless with respect to a fixed observer, the water ahead of the wave was moving with velocity $V$ to the right? To make this flow steady, we would have to move with a velocity $V + c$. In this new framework, a similar analysis to that given above would lead to the result that the speed of the wave is $V + \sqrt{gy}$, relative to a stationary observer. Similarly, if the water ahead of the wave was flowing with a velocity $V$ to the left, we would find that the wave moves at the speed $V - \sqrt{gy}$. That is, the wave moves at a speed $\sqrt{gy}$ *relative to the moving fluid*.

So far, we have examined plane waves. Consider instead a circular wave that is generated by point disturbance on the surface of the water. For example, fill a sink or bath to a depth of about $10\,mm$. Take a sponge that is soaked with water and, while holding it stationary, squeeze it gently to make it drip onto the water surface. We expect the ripples made by the drops of water to propagate outward in concentric circular patterns at a speed $\sqrt{gy}$ ($\approx 0.3\,m/s$).[1] You can check this with a stopwatch. Now move the sponge slowly as you squeeze it. As each drop hits the water, a circular disturbance travels outward, as before, but the parts of the circles that lie in the same direction as the motion of the sponge are closer together than the parts in the opposite direction. This produces the same effect as holding the dripping sponge stationary over a flowing body of water. If we were stationary, and the water was moving, it would appear that the waves move slower upstream then they do downstream [see Figure 10.3(a)]. The wave speed is constant, so that the wave shape remains circular, but the wave is also convected downstream by the moving fluid. Relative to a stationary observer, the parts of the wave that are moving upstream move more slowly than the parts of the wave moving downstream where the wave velocity and the fluid velocity are in the same direction. The pattern shown in Figure 10.3(a) is observed whenever the fluid velocity is less than the speed of the wave.

The ratio of fluid speed $V$ to wave speed $V/\sqrt{gy}$ is called the Froude number.

$$\text{Froude number} \;=\; F \;\equiv\; \frac{V}{\sqrt{gy}} \tag{10.3}$$

The Froude number is named after William Froude, who performed many experiments to study the waves produced by ships. The pattern shown in Figure 10.3(a) is observed when $F < 1$. This is called *sub-critical* flow. This phenomenon is similar to the Doppler effect for sound waves. The Doppler effect explains why the sound of a whistle on a train that is moving towards you has a higher pitch (higher frequency, smaller wavelength) than when it is moving away from you, where it has a lower pitch (lower frequency, longer wavelength).

Let us return to our experiment. As we move the sponge faster, there is a point where it will be moving with the same velocity as the wave velocity. That is, $F = 1$. If the sponge was stationary and the water was moving, the parts of the wave moving upstream at speed $\sqrt{gy}$ will be swept downstream at the same speed, and so all the wavefronts collect along a line [Figure 10.3(b)]. This is called *critical* flow.

When the water moves still faster, so that $F > 1$, we obtain the pattern shown in Figure 10.3(c). Here, the wave fronts are being swept downstream by the current faster than they can move upstream, and a wedge-shaped pattern forms with a characteristic angle $\alpha$ (see Section 10.4). This is called *supercritical* flow.

---

[1]It can be shown that a circular wave spreads at the same speed as a planar wave, that is, at a speed $\sqrt{gy}$ far from the center of the disturbance.
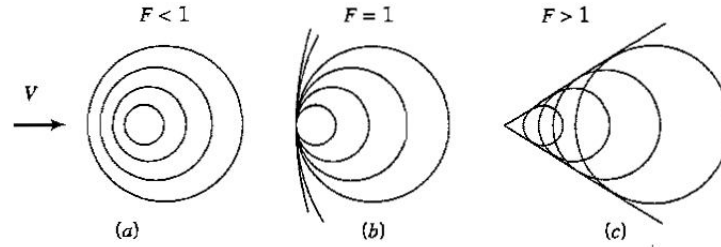
Figure 10.3: Wave patterns made by a point disturbance on the free surface of a moving liquid. (a) $V < \sqrt{gy}$ (subcritical). (b) $V = \sqrt{gy}$ (critical). (c) $V > \sqrt{gy}$ (supercritical).

Some interesting observations can be made. For example, consider a fisherman in his boat, moored in a river some distance upstream of the point where a disturbance is creating waves. In subcritical flow, where $F < 1$, the waves, relative to the stationary fisherman, spread out at different speeds depending on the direction, but they will all reach him eventually. Even if he was not looking at the waves, he would learn of their presence by the rocking of the boat. All this changes when $F = 1$ (the *critical Froude number*). At this point, the waves collect along a line downstream of the fisherman, and they never reach the boat. He never receives the information that waves are being generated. The line of waves divides the flow into two zones: a downstream zone that is influenced by the presence of waves and an upstream zone that is not. When $F > 1$, the zone that is influenced by the waves shrinks to the wedge-shaped region shown in Figure 10.3(c).

## 10.4    Froude Number

The Froude number always makes an appearance when gravity is important. It comes directly from the equations of motion, as we saw from the nondimensional form of the Navier-Stokes equation (equation 7.23). For flow in an open channel, $F = V/\sqrt{gy}$, and it gives the ratio of the flow velocity to the speed of a small amplitude disturbance. The Froude number will be small compared to 1 when the velocity is low and/or when the water depth is large. Large rivers are likely to have low Froude numbers. The Froude number will be large compared to 1 when the velocity is large and/or the depth is small. As we indicated, this is called supercritical flow, but it is also sometimes called *shooting flow* because of its appearance.

Another interpretation for the Froude number can be found by squaring it and multiplying the numerator and denominator by the density. Hence

$$F^2 = 2 \left( \frac{\frac{1}{2}\rho V^2}{\rho g y} \right) \tag{10.4}$$

and so the Froude number is related to the ratio of the fluid kinetic energy to its potential energy. Fast flow in a shallow channel has a large Froude number, and its kinetic energy is large compared to its potential energy. Alternatively, from this from of the Froude number, we could interpret it as the ratio of the dynamic pressure to a typical hydrostatic pressure.

We saw in Section 10.3 that when the Froude number is supercritical ($F > 1$), a wedge-shaped pattern of waves forms, with a characteristic angle $\alpha$ (Figure 10.4). In a given time interval $\Delta t$, the center of the disturbance is convected by the flow a distance $V\Delta t$, while the wave front moves a distance $\sqrt{gy}\Delta t$. Hence

$$\sin \alpha = \frac{\sqrt{gy}\Delta t}{V\Delta t} = \frac{\sqrt{gy}}{V} = \frac{1}{F} \tag{10.5}$$
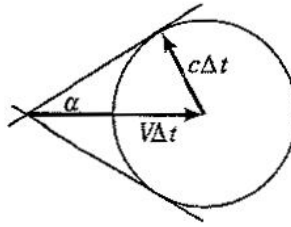
Figure 10.4: Wave patterns made at supercritical Froude numbers.

The Froude number can be estimated, therefore, by measuring the angle the wave fronts make with the flow direction, as long as the waves have small amplitudes. The angle $\alpha$ is sometimes called the *Froude angle*. The line defined by this angle defines the line of propagation of small disturbances in supercritical flow.

## 10.5 Breaking Waves

If we have a long water channel, we can create a large planar disturbance traveling down the channel by using a wave maker (a sort of oscillating airfoil) or a large paddle hinged at the bottom of the channel. As the wave moves down the channel, it will grow larger and steeper, and possibly "break" like a wave at the beach.

Why does it steepen and break? To a stationary observer, the front of the wave initially moves at a speed close to $\sqrt{gh_2}$, that is, the local speed of a small disturbance (Figure 10.5). The back of the wave moves at a speed very nearly equal to $\sqrt{gh_1} + \delta V$, that is, the local speed of a small amplitude disturbance plus the drift speed $\delta V$. Since $\sqrt{gh_1} + \delta V > \sqrt{gh_2}$, the back of the wave catches up with the front and the wave steepens. Eventually, it will break and it is then sometimes called a *positive surge*.

A similar phenomenon occurs at the beach. There the steepening of the wave is aided by the slope of the bottom: the water depth decreases in the direction of wave movement, accentuating the differences between the speeds of the front and back of the wave (see Figures 10.6 and 10.7). In addition, there is significant undertow, which is the result of mass conservation: as the wave brings water up the beach, there must be a current near the bottom to bring it back. This undertow accentuates the effects due to the slope of the beach and hastens the formation of the breaking wave. The most common explanation for the formation of breaking waves on a beach ascribes the phenomenon to "bottom friction." Although there are always effects due to friction, this explanation misses one of the more important mechanisms.
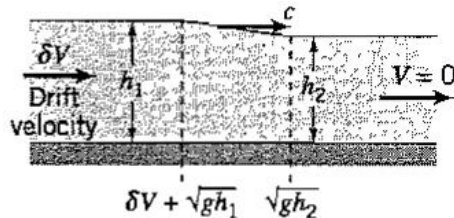


Figure 10.5: Notation for a steepening wave (stationary observer).
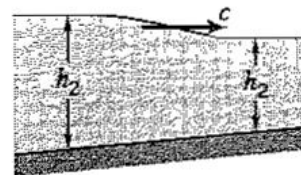


Figure 10.6: Waves forming on a sloping beach.

# 10.6    Tsunamis[2]

ESASHI, Japan, July 14.  They can travel as fast as jet planes.  They can carry off entire houses.  They can inundate coastal communities with violent flooding.  Some English speakers call them tidal waves, but they have nothing to do with tides; much of the world recognizes them by their Japanese name, tsunami.

Huge tsunamis inundated northern Japan Monday night, minutes after a powerful earthquake struck the Sea of Japan west of the northern island of Hokkaido.  A tsunami contributed heavily to damage along the coast and to the virtual demolition of the Aonae district on Okushiri, a small island known for fishing and resorts.

People were swept away by huge waves and drowned.  Cars were flushed into the sea.  Ships were thrown onto land where they crashed into buildings.  And hundreds of houses were destroyed in a torrent of water.  One of the most striking television images of the quake was that of what looked to be an entire house floating out to sea, its roof protruding above the water.

Many things contributed to the damage in the quake, which measured 7.8 on the Richter Scale.  There was the shaking, the landslides that ruined roads and buried a hotel, and fires, probably caused by the explosion of ruptured gas lines.  But perhaps the most spectacular phenomenon was the tsunami.

### Waves outran warning

While Japan, perhaps the world's most earthquake-prone country, has learned how to build structures to withstand earthquakes, it apparently has not yet been able to fully cope with tsunamis.

'Even wooden houses in Japan are built strong enough to withstand the shaking of an earthquake,' said Nobuo Shuto, a professor of tsunami engineering at Tohoku University in Sendai.

Japan has a warning system for tsunamis, but on Monday night the waves reached Okushiri at about the same time as the warning, five minutes after the earthquake.  'Under this kind of situation, maybe there is little you can do,' Professor Shuto said.  'The only way to save human lives is to evacuate immediately, even without a warning.'

### Waves up to 35-feet high

Professor Shuto estimated that the wave that struck Okushiri ranged from 10 to 16 feet high, but noted that he said he had not completed his calculations.  A researcher for the Meteorological Agency estimated, based on a survey of the site, that the waves were as high as 35 feet.

Tsunamis are gigantic versions of the ripples produced by a pebble tossed into a still pond.  But in tsunamis, the water is displaced not by a pebble, but by an earthquake, volcanic eruption or other violent undersea movement (Figure 10.7).  A huge mass of water can be displaced.

The tsunami's speed depends on the depth of the water above the displaced sea bed.  In the case of the tsunami on Monday, where the water was about 6,000 feet deep, the wave travels at 300 miles per hour.

As the wave approaches the land and the ocean becomes shallower, the water in the back of the wave catches up to the water in the front, and the wave height mounts.

### Report seeing 10 waves

Depending on the structure of the coastline, a tsunami might strike one time and recede, or reverberate, hitting the shoreline many times.  Professor Shuto said some witnesses on Okushiri reported seeing as many as 10 waves.

The professor said that while Japan is most known for tsunamis, they occur elsewhere, and can strike with deadly force thousands of miles from their source.  A huge

---

[2]From the article "A Wall of Water Traveling at the Speed of a Jet Plane" by Andrew Pollack, *New York Times*, July 14, 1994.
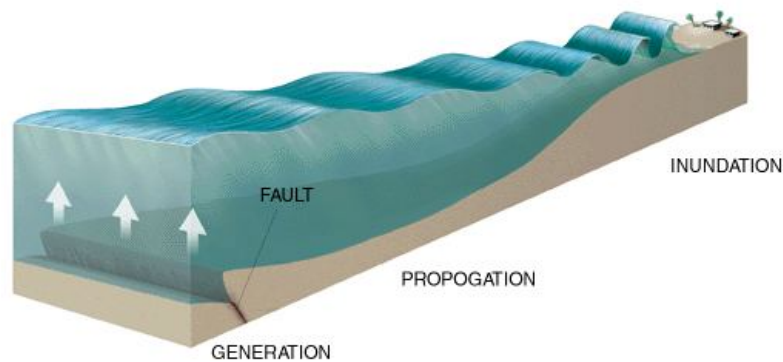
Figure 10.7: Formation of tsunamis. From *Scientific American*, May, 1999.

tsunami occurred off the Aleutian Islands of Alaska on April 1,1946, and traveled to Hawaii. Hawaiians thought warnings of a sea disturbance were an April Fool's joke and ignored them, he said, and 159 people were killed.

Japan began constructing defenses against tsunamis after it was hit by what Professor Shuto said was the strongest tidal wave in its recorded history, with waves up to 40 feet high. The tsunami, which struck in 1960 started off the coast of Chile and took 23 hours to cross the Pacific before slamming into Japan's Pacific Coast.[3]

A graphic animation of the July 17, 1998, Papua New Guinea Tsunami is given at *http://walrus.wr.usgs.gov/docs/tsunami/PNGhome.html* (produced by the U. S. Geological Survey). Note the generation of multiple waves by a single earthquake.

## 10.7 Hydraulic Jumps

To understand breaking waves or tsunamis in more detail, we consider a stationary *hydraulic jump*. Hydraulic jumps may be seen at home by turning on a faucet and letting the stream of water fall on a flat, horizontal surface such as a plate. The water spreads out from its point of impact in a thin layer, and then at some point a sudden rise in water level occurs. This is a circular hydraulic jump. Waves breaking on a beach are planar hydraulic jumps, and hydraulic jumps are also often seen in a shallow river bed where a sudden change in river depth occurs, or in the region just downstream of a large rock (white water enthusiasts know and love hydraulic jumps). In an open channel water tunnel (sometimes called a *flume*), we can form a hydraulic jump by first letting the water flow over a bump (we will see later that this is a mechanism for making the flow supercritical), and then placing an obstacle downstream. The hydraulic jump will form upstream of the obstacle, and it will be stationary with respect to the flume. In the laboratory, we can also produce a planar hydraulic jump by suddenly removing a barrier between two bodies of water of different depth. The motion has two parts: a hydraulic jump moving into the region of lower depth, and a smooth *expansion wave* moving in the opposite direction into the region of higher depth.

---

[3]With an average Pacific Ocean depth of $15,000\,ft$, the wave speed $\sqrt{gy}$ is about $700\,ft/s$, or $470\,mph$. The distance traveled in 23 hours is therefore about 11,000 miles, which is almost exactly the distance between Chile and Japan. Tidal waves travel as small amplitude disturbances for long distances (the wave height may only be several feet, with a very large wavelength), and they only become destructive near the shore where huge breaking waves can form.

Figure 10.8: A moving hydraulic jump (called a *bore*) traveling upstream in the Severn River in England. The bore is caused by the tide moving into the mouth of the river. Photograph by D.H. Peregrine, with permission.


Moving hydraulic jumps are sometimes called *bores* or *surges*. A tidal bore is caused by a high tide entering a shallow bay or river inlet (see Figure 10.8). As the water proceeds against the current, a bore is formed by the same mechanism responsible for breaking waves. Surges, for example, are formed when a river dam breaks. Bores and surges can be very hazardous, but they can also be useful. For example, they can be used to decelerate a stream of fluid to reduce scouring in a river or channel bed, and Figure 7.2 shows a hydraulic jump formed for this purpose near the bottom of a spillway.

To analyze the features of a hydraulic jump, consider a stationary, planar jump formed in a horizontal, two-dimensional channel flow of width $W$ (Figure 10.9). We will use a control volume that starts well upstream of the jump where the depth of the water is $H_1$, and that ends well downstream of the jump where the depth is $H_2$. Large disturbances such as hydraulic jumps dissipate a lot of energy, so that mechanical energy is not conserved and Bernoulli's equation cannot be used. We can, however, use the continuity and momentum equations.

First, consider the continuity equation. We will assume that the velocities across areas $WH_1$ and $WH_2$ are constant, so that

$$\rho U_1 W H_1 = \rho U_2 W H_2$$

That is,

$$U_1 H_1 = U_2 H_2 \tag{10.6}$$

Next, consider the momentum equation. In the undisturbed part of the channel flow, the streamlines are parallel, so that the pressure varies with depth because of the hydrostatic pressure gradient. In problems involving air or other gases, we have generally ignored these hydrostatic pressures since they were small. With liquids, however, the hydrostatic pressures must be taken into account. Since the depth increases across the jump, the force due to hydrostatic pressure acting on the right hand face of the control volume is larger than that due to hydrostatic pressure acting on the left hand face. This appears as a resultant force due to pressure differences in the momentum equation. If we ignore any viscous forces that might act on the channel bed, there will be no external forces acting on the control
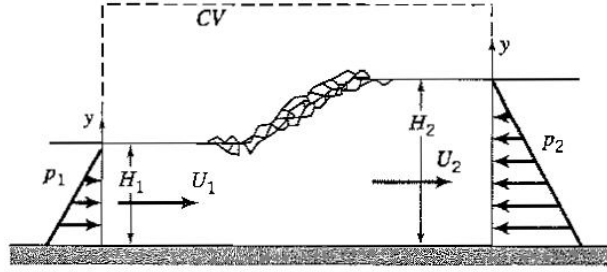
Figure 10.9: Control volume for the analysis of a hydraulic jump.

volume, and the force due to hydrostatic pressure differences is equal to the net outflux of momentum. The $x$-momentum equation becomes:

$$-\mathbf{i} \cdot \int p\mathbf{n}\, dA \;=\; \mathbf{i} \cdot \int (\mathbf{n} \cdot \rho\mathbf{V})\, \mathbf{V}\, dA$$

By using gauge pressure, we obtain:

$$\int_0^{H_1} p_1 W\, dy - \int_0^{H_2} p_2 W\, dy \;=\; (-\rho U_1)\, U_1 W H_1 + (\rho U_2)\, U_2 W H_2$$

The pressures are hydrostatic, so that

$$\int_0^{H_1} \rho g\, (H_1 - y)\, dy - \int_0^{H_2} \rho g\, (H_2 - y)\, dy \;=\; -\rho U_1^2 H_1 + \rho U_2^2 H_2$$

That is,

$$\tfrac{1}{2} g H_1^2 - \tfrac{1}{2} g H_2^2 \;=\; U_2^2 H_2 - U_1^2 H_1 \tag{10.7}$$

Combining equations 10.6 and 10.7 gives

$$\left(\frac{H_2}{H_1}\right)^2 + \left(\frac{H_2}{H_1}\right) - 2F_1^2 = 0 \tag{10.8}$$

where $F_1$ is the upstream Froude number ($= U_1/\sqrt{gH_1}$). This quadratic equation has the solutions

$$\frac{H_2}{H_1} = \frac{-1 \pm \sqrt{1 + 8F_1^2}}{2}$$

We can reject the negative solution because $H_2$ is always positive. Hence

$$\boxed{\frac{H_2}{H_1} \;=\; \frac{1}{2}\left(\sqrt{1 + 8F_1^2} - 1\right)} \tag{10.9}$$

This is called the hydraulic jump relationship, and it applies to stationary, planar hydraulic jumps, in channels with negligible bottom friction.

We see that the height of the jump depends only on the upstream Froude number. When $F_1 > 1$, $H_2 > H_1$, and the jump is "up." When $F_1 = 1$, $H_2 = H_1$, and there is no jump at all. When $F_1 < 1$, $H_2 < H_1$, and the jump is "down." We will show in Section 10.8,

however, that jumps that go down are not possible because of thermodynamic considerations (entropy cannot decrease). Therefore

> A hydraulic jump occurs only if $F_1 > 1$. As a result, $H_2 > H_1$.

How does a hydraulic jump form?  Consider supercritical flow in an open channel. Because $F > 1$, a wave generated by a small change in flow elevation cannot travel upstream. If a large bump or a barrier is placed on the channel bottom, the flow cannot adjust smoothly because the "information" about the presence of the obstacle cannot be signaled upstream, and therefore the flow will change abruptly close to the obstacle. A hydraulic jump will occur just upstream of the obstacle.

What about the Froude number downstream of the hydraulic jump? We first write the continuity equation nondimensionally, as follows. Equation 10.6 gives

$$U_1 H_1 \;=\; U_2 H_2$$

Dividing through by $\sqrt{gH_1}$ gives

$$\frac{U_1}{\sqrt{gH_1}} H_1 \;=\; \frac{U_2}{\sqrt{gH_1}} H_2 \;=\; \frac{U_2}{\sqrt{gH_1}} \frac{\sqrt{gH_2}}{\sqrt{gH_2}} H_2$$

That is

$$F_1 H_1 \;=\; \frac{U_2}{\sqrt{gH_2}} \frac{\sqrt{gH_2}}{\sqrt{gH_1}} H_2$$

and

$$F_2 = \left(\frac{H_1}{H_2}\right)^{3/2} F_1 \tag{10.10}$$

Equation 10.10 is just another way of writing the continuity equation for flow in a channel of constant width, but it is particularly useful because it is written in terms of nondimensional parameters such as the Froude number. Writing the equations in terms of nondimensional parameters can be very effective in solving problems, particularly in problems concerning open channel flows.

The downstream Froude number can now be found by combining the continuity equation in the form given by equation 10.10 with the hydraulic jump relationship given by equation 10.9. That is,

$$F_2^2 \;=\; \left(\frac{H_1}{H_2}\right)^3 F_1^2 \;=\; \left(\frac{H_1}{H_2}\right)^3 \frac{1}{8}\left[\left(\frac{2H_2}{H_1}+1\right)^2 - 1\right]$$

That is,

$$F_2^2 \;=\; \frac{1}{2}\frac{H_1}{H_2}\left(\frac{H_1}{H_2}+1\right)$$

For $F_1 > 1$, $H_1/H_2 < 1$ (jumps go up), and therefore $F_2$ is always less than 1. That is,

> A hydraulic jump occurs only if $F_1 > 1$. As a result, $F_2 < 1$.

## 10.8 Hydraulic Drops?

The hydraulic jump relationship (equation 10.9) implies that it is possible to have hydraulic jumps that go down ($H_2 < H_1$) when $F_1 < 1$. To show that such hydraulic "drops" are not possible, consider what happens to the Bernoulli constant $B$ through this flow. The Bernoulli constant was defined in Section 8.11, and it is constant if energy is conserved. At the surface of the water upstream of the jump $B_1 = \frac{1}{2}U_1^2 + gH_1$, and downstream of the jump $B_2 = \frac{1}{2}U_2^2 + gH_2$. That is,

$$B_1 \;=\; \tfrac{1}{2}U_1^2 + gH_1 \;=\; gH_1\left(\tfrac{1}{2}F_1^2 + 1\right)$$

$$\text{Similarly} \qquad B_2 \;=\; gH_2\left(\tfrac{1}{2}F_2^2 + 1\right)$$

We know there are energy losses in the hydraulic jump because they are turbulent, so that $B_2 < B_1$. When $F_1 > 1$, then $B_2 < B_1$, as required, so that jumps that go *up* are allowed. However, when $F_1 < 1$, then $B_2 > B_1$, which is not allowed, and so jumps that go *down* are not possible.

To demonstrate this result, we first form the ratio of the Bernoulli constants.

$$\frac{B_2}{B_1} \;=\; \frac{H_2}{H_1}\frac{\left(1 + \frac{F_2^2}{2}\right)}{\left(1 + \frac{F_1^2}{2}\right)}$$

By using the continuity equation (equation 10.10), we obtain

$$\frac{B_2}{B_1} \;=\; \frac{H_2}{H_1}\left[\frac{1 + \left(\frac{H_1}{H_2}\right)^3 \frac{F_1^2}{2}}{1 + \frac{F_1^2}{2}}\right] \tag{10.11}$$

We can find an expression for $F_1$ using the hydraulic jump relationship (equation 10.9). That is,

$$F_1^2 = \frac{1}{2}\frac{H_2}{H_1}\left(\frac{H_2}{H_1} + 1\right)$$

and use this result to substitute for $F_1$ in equation 10.11 to obtain

$$\frac{B_2}{B_1} \;=\; \frac{H_2}{H_1}\left[\frac{1 + \frac{1}{4}\left(\frac{H_1}{H_2}\right)^2\left(\frac{H_2}{H_1} + 1\right)}{1 + \frac{1}{4}\left(\frac{H_2}{H_1}\right)\left(\frac{H_2}{H_1} + 1\right)}\right] \tag{10.12}$$

This relationship is plotted in Figure 10.10 for a small range of $H_2/H_1$. For $H_2 > H_1$, we see that $B_2 < B_1$, indicating that energy is dissipated by the hydraulic jump, as observed. When $H_2 < H_1$, $B_2 > B_1$, implying that energy is created by a hydraulic drop, which is not possible. Hydraulic drops cannot occur, and only hydraulic jumps are allowed.

## 10.9 Surges and Bores

A surge or a bore is a moving hydraulic jump. It may be caused by a tidal flow entering a shallow estuary (the mouth of a river), as shown in Figure 10.8, or by a sudden increase in water level, as when a dam on a river is breached. They are similar to tsunamis, but tsunamis are coastal features where the breaking wave is usually formed on a sloping beach.

Consider a surge, moving with a constant velocity $V_S$ into a region where the velocity is zero and the bottom is level (Figure 10.11). This is an unsteady flow, but if we adopt
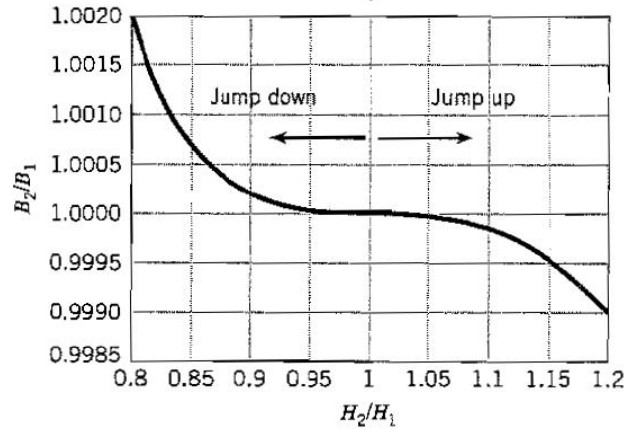
Figure 10.10: The ratio of downstream to upstream Bernoulli constants for a hydraulic jump as a function of the ratio of downstream to upstream water depths. Note the similarity to Figure 11.12.

a frame of reference moving at the same speed as the wave, it becomes a steady problem (Figure 10.12). The analysis is identical to that followed for the stationary hydraulic jump given in Section 10.7, with $V_S$ replacing $U_1$, and $V_S - U_2$ replacing $U_2$. To see this, imagine riding on the wave as a surfer might. What the surfer sees coming towards her is not a stagnant body of water, but water that appears to be moving towards her at a speed $V_S$. When she looks back, she sees water moving away from her at a speed $V_S - U_2$. So the relationship for a surge or bore moving into a stagnant pool of water with a level bottom is simply

$$\frac{H_2}{H_1} = \frac{1}{2}\left(\sqrt{1 + 8F_S^2} - 1\right)$$

where $F_S = V_S/\sqrt{gH_1}$, and $V_S$ is the speed of the bore relative to a stationary observer. Since the appropriate Froude number is based on the bore velocity, this Froude number must be supercritical ($F_S > 1$) if a jump is to take place.

## 10.10    Flow Through a Smooth Constriction

To illustrate further the behavior of subcritical and supercritical flows, consider the steady flow of water through an open channel where the sides of the channel form a symmetric constriction so that the widths of the inlet and outlet are the same, as shown in Figure 10.13.
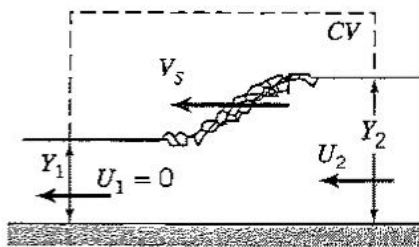


Figure 10.11:  Surge in a frame of reference where the flow is unsteady.
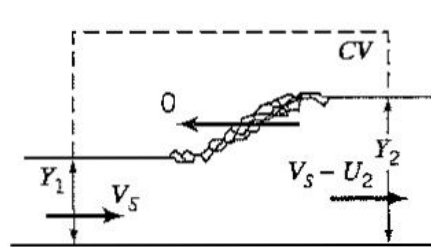
Figure 10.12:  Surge in a frame of reference where the flow is steady.
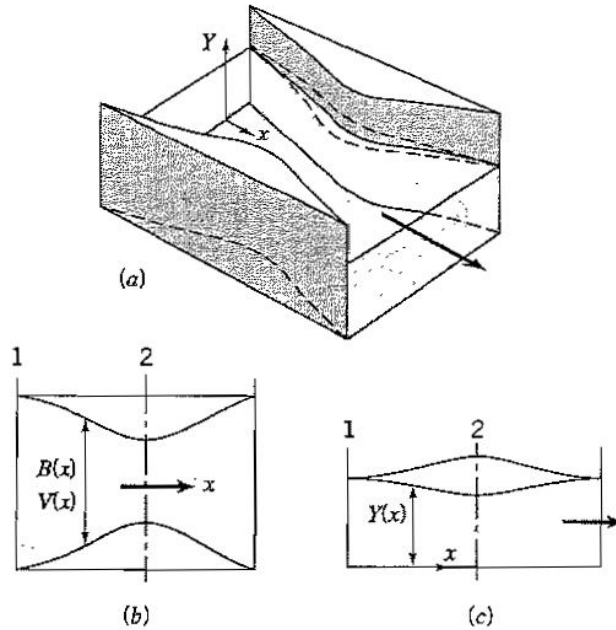
Figure 10.13: Steady flow through a smooth constriction. (a) Perspective view. (b) Plan view. (c) Elevation.

We will assume that the flow is approximately one-dimensional and that there are no losses, so that there are no hydraulic jumps. A flow where there are no losses is sometimes called "smooth," so this is a smooth constriction.

As the flow passes through the constriction, what happens to the water surface? Does the water level go down, or does it go up? To answer this question we will use the one-dimensional continuity equation, and apply Bernoulli's equation along the surface stream-line. The continuity equation gives

$$B_1 Y_1 V_1 = BYV \tag{10.13}$$

where the subscript 1 denotes the inlet conditions upstream of the constriction, and $B$, $Y$, and $V$ are, respectively, the width of the channel, the depth of the stream and the average velocity in a cross-section of the flow at some location $x$ inside the constriction. Non-dimensionalizing equation 10.13 in the same way as we did earlier (see equation 10.10), we obtain

$$F^2 = \left(\frac{B_1}{B}\right)^2 \left(\frac{Y_1}{Y}\right)^3 F_1^2 \tag{10.14}$$

which is just the continuity equation in nondimensional form. Here, $F$ is the local Froude number at the location $x$.

Bernoulli's equation for steady, incompressible, frictionless flow along the surface stream-line, where $p_1 = p_2$, gives

$$\tfrac{1}{2}V_1^2 + gY_1 = \tfrac{1}{2}V^2 + gY$$

Non-dimensionalizing this equation by dividing through by $gY_1$ gives

$$\tfrac{1}{2}F_1^2 + 1 = \tfrac{1}{2}F^2 \frac{Y}{Y_1} + \frac{Y}{Y_1} \tag{10.15}$$

By combining equations 10.14 and 10.15, we obtain (after some algebra) a third-order polynomial for $Y/Y_1$

$$\left(\frac{Y}{Y_1}\right)^3 - \left(\frac{Y}{Y_1}\right)^2 \left(1 + \frac{F_1^2}{2}\right) + \left(\frac{B_1}{B}\right)^2 \frac{F_1^2}{2} \;=\; 0 \tag{10.16}$$

Since this is a cubic, there are in general three solutions. One solution is usually nonphysical (for example, it could be negative), so that there are at most two nontrivial solutions. These solutions show that $Y/Y_1$ can be greater than one, or less than one. To answer the question regarding the behavior of the water surface: the water level can go up, or it can go down, depending on the values of $F_1$ and $B/B_1$.

Instead of solving this equation for a wide range of inputs, we can learn a great deal about the behavior of the water level by examining the slope of the water surface. To find the slope, we differentiate equation 10.16, and we can show that

$$\boxed{\frac{dY}{dx} = \frac{\frac{Y}{B}F^2}{1 - F^2}\frac{dB}{dx}} \tag{10.17}$$

where $F = V/\sqrt{gY}$ is the local Froude number.

Clearly, this is an interesting result. In particular, the slope of the surface changes sign when the Froude number changes from being less than one, to being greater than one. We can also anticipate some problems when $F = 1$. Before we proceed further, we need one more result.

By differentiating the continuity equation for this flow (equation 10.13), we have

$$BY\frac{dV}{dx} + BV\frac{dY}{dx} + YV\frac{dB}{dx} \;=\; 0$$

That is,

$$-\frac{Y}{V}\frac{dV}{dx} \;=\; \frac{Y}{B}\frac{dB}{dx} + \frac{dY}{dx}$$

By using equation 10.17, we obtain

$$-\frac{Y}{V}\frac{dV}{dx} \;=\; \frac{F^2}{1-F^2}\frac{Y}{B}\frac{dB}{dx} + \frac{Y}{B}\frac{dB}{dx} \;=\; \frac{1}{1-F^2}\frac{Y}{B}\frac{dB}{dx}$$

Finally

$$\boxed{\frac{dV}{dx} \;=\; -\frac{\frac{V}{B}}{1-F^2}\frac{dB}{dx}} \tag{10.18}$$

which provides information on how the flow accelerates or decelerates as it passes through the smooth constriction.

We will avoid the case where $F = 1$ for now, and consider the two cases where either $F < 1$ everywhere, or $F > 1$ everywhere.

1. When $F < 1$ everywhere, then with

   (a) $\dfrac{dB}{dx} < 0$,   we find   $\dfrac{dY}{dx} < 0$,   and   $\dfrac{dV}{dx} > 0$

   (b) $\dfrac{dB}{dx} > 0$,   we find   $\dfrac{dY}{dx} > 0$   and   $\dfrac{dV}{dx} < 0$
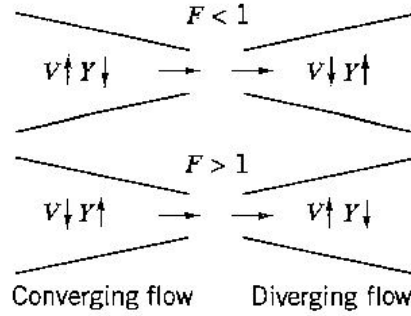
Figure 10.14: Summary of flow variation in subcritical and supercritical channels.

2. When $F > 1$ everywhere, then with

(a) $\dfrac{dB}{dx} < 0$, we find $\dfrac{dY}{dx} > 0$ and $\dfrac{dV}{dx} < 0$

(b) $\dfrac{dB}{dx} > 0$, we find $\dfrac{dY}{dx} < 0$ and $\dfrac{dV}{dx} > 0$

These results are summarized in Figure 10.14.

When the Froude number is subcritical everywhere, the water level falls as the flow speeds up in the converging part of the constriction, and it rises as the flow slows down in the diverging part of the constriction. When the Froude number is supercritical everywhere, the water level rises as the flow slows down in the converging part of the constriction, and it falls as the flow speeds up in the diverging part of the constriction (Figure 10.15). It is possible, therefore, to know whether the flow is subcritical or supercritical by observing its behavior as it passes through a constriction.

What happens when the Froude number becomes critical ($F = 1$) somewhere? The initial conclusion from equation 10.17 is that the slope of the water surface becomes infinite. This is not possible in the real world. It is also not the only conclusion that can be drawn. The slope of the water surface depends on the value of $dB/dx$ as well as the Froude number, and it is possible for the Froude number to be equal to one, as long as $dB/dx = 0$ at the
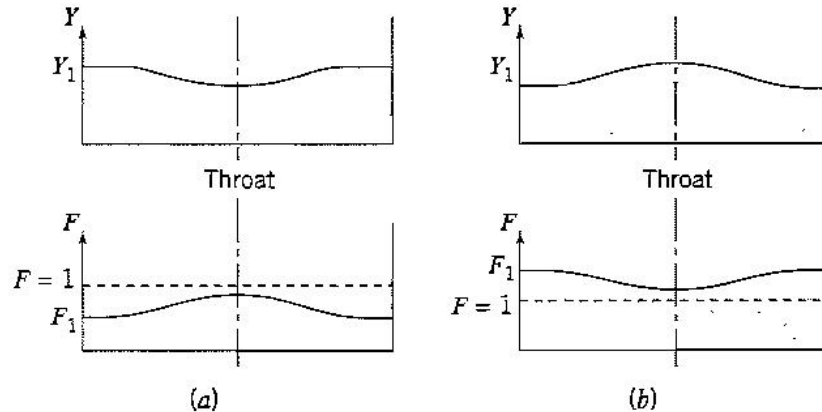


Figure 10.15: Steady flow through a smooth constriction. (a) Subcritical flow everywhere. (b) Supercritical flow everywhere.

same location.  In that case, the numerator and denominator of equation 10.17 are both zero, and although the slope is now indeterminate, it is finite, and physically meaningful solutions can exist.  This means that

**1.**  The only place where $F = 1$ must be where $dB/dx = 0$, that is, at the point of minimum area of the constriction. This is called the *throat*. The Froude number cannot be one anywhere else.

**2.**  When $F = 1$ at the throat, the slope of the water at the throat cannot be found using equation 10.17. Additional information regarding the downstream flow conditions is required before the solution can be determined, as discussed in the following sections.

What happens if we try to increase $F_1$ beyond the condition where the throat Froude number is 1? Our first suggestion might be that $F$ becomes unity at some point upstream where $dB/dx \neq 0$. But equation 10.17 indicates that when $F = 1$ and $dB/dx \neq 0$, $dY/dx$ becomes infinite. This is not possible.  The only place where the flow can become critical is at the throat. If $F = 1$ at the throat, and the upstream flow velocity $V_1$ is somehow increased, then $Y_1$ will increase such that $F_1$ remains as before, and $F$ at the throat remains equal to one.

### 10.10.1    Subcritical flow in contraction

Consider a stream that is initially subcritical everywhere ($F < 1$). This corresponds to the flow conditions given in the upper part of Figure 10.14. As the water passes through the constriction, its level falls and its velocity increases. Consequently, the local Froude number $F$ increases, and its maximum value will occur at the throat where the area is a minimum. Downstream of the throat, the flow recovers so that the water level rises and the Froude number decreases. If the upstream and downstream widths of the constriction are equal, the flow returns to its upstream state (neglecting losses).

When the incoming Froude number $F_1$ is increased, there comes a point when the Froude number becomes critical somewhere. As we saw previously, this will occur at the throat: it is the first place where $F$ can become critical, and it is the *only* place it can occur. From equation 10.17, we see that when $F = 1$ the slope of the water surface is indeterminate, and so we cannot say what happens to the water level downstream of the throat. Will it go up, or continue to go down? The answer depends on the conditions downstream of the throat.

If we now return to the original equation for the flow through the constriction (equation 10.16), we find that there exist two possible solutions that have $F = 1$ at the throat. That is, two possibilities exist for a continuous surface profile in a steady flow without losses, and they must satisfy one of two particular boundary conditions at the exit from the constriction. In other words, under the conditions where there are no losses, only two flows are possible with $F = 1$ at the throat, and they can only exist if the downstream water level $Y_3$ is one of two values, $Y_3'$ or $Y_3''$ in Figure 10.16.

**1.**  When $Y_3 = Y_3'$, the flow returns to subcritical Froude number values, and the water level rises in the diverging part of the constriction.

**2.**  When $Y_3 = Y_3''$, the flow becomes supercritical in the diverging part of the constriction, and the water level falls.

If $F = 1$ at the throat, and the downstream water level $Y_3$ takes a value not equal to $Y_3'$ or $Y_3''$, a continuous surface profile without losses cannot be found. For example, if $Y_3$ was such that $Y_3'' < Y_3 < Y_3'$ (in Figure 10.16, this value of $Y_3$ is shown as $Y_3'''$), the flow will be supercritical for some distance downstream of the throat. However, when the Froude number is such that a jump is possible (according to equation 10.9), a hydraulic
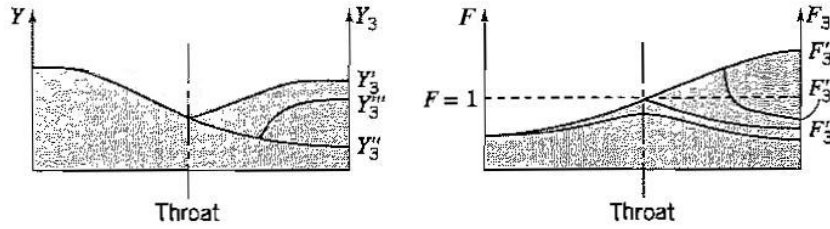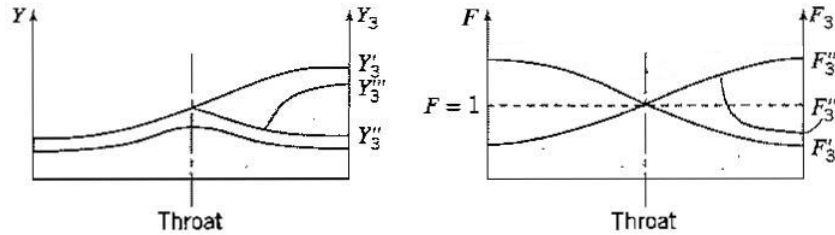
Figure 10.16: Steady flow through a smooth constriction, with subcritical flow upstream, and critical flow ($F = 1$) at the throat.

jump occurs and the flow becomes subcritical. Downstream of the hydraulic jump, the flow will be subcritical, and the water surface begins to rise as it passes through the rest of the constriction until $Y_3 = Y_3'''$ at the exit. The actual location of the hydraulic jump is given by the point where the jump height corresponding to the local Froude number is such as to match the downstream water level.

The lowest value that $Y_3'''$ can take will occur when the hydraulic jump is located at the end the diverging section. This jump is the strongest jump that can be found in the constriction, because at this point the Froude number has its highest value and the change in water level is the largest possible.

What happens if no hydraulic jump is possible? That is, what happens when the hydraulic jump relationship cannot be satisfied at any location in the diverging part of the constriction? In this case, no solution exists, neither without losses, nor in the presence of a hydraulic jump. However, our analysis has been restricted to one-dimensional flow. In practice, oblique hydraulic jumps will appear downstream of the constriction, but the analysis of oblique jumps is beyond the scope of this text.

What happens if $Y_3 > Y_3'$? There is no steady solution: the channel will *drown*. That is, the water will flow back upstream and subcritical flow will be established everywhere.

What happens if $Y_3 < Y_3''$? In this case, there is no one-dimensional solution, and oblique expansion waves will appear downstream of the constriction.

## 10.10.2 Supercritical flow in contraction

When the conditions are such that the Froude number of the flow is supercritical everywhere in the converging part of the constriction, the water level will rise, and the local Froude number will decrease. This corresponds to the flow conditions given in the lower part of Figure 10.14.. If the Froude number decreases such that the Froude number becomes critical ($F = 1$) at the throat, the flow downstream of the throat has the same two solutions considered in the previous section.

If there are no losses and equation 10.16 applies, the downstream part of the flow has the same two possible solutions as before, where $Y_3 = Y_3'$ or $Y_3 = Y_3''$ (see Figure 10.17), no matter what the Froude number is upstream of the throat. If $Y_3'' < Y_3 < Y_3'$, then the flow will be supercritical for some distance downstream of the throat and when the Froude number is such that, for the given $Y_3$, a jump is possible (according to the hydraulic jump relationship, equation 10.9), a hydraulic jump occurs, and the flow becomes subcritical.

An important point is that, once the Froude number at the throat is equal to one, the upstream and downstream parts of the flow become independent. There is no communication between them, even if they were both subcritical. The location where $F = 1$ acts as a barrier to communication: disturbances in water level such as waves and ripples cannot pass upstream of this location. Therefore any changes downstream of the throat cannot be transmitted to the flow upstream of the throat.

Figure 10.17: Steady flow through a smooth constriction, with supercritical flow upstream, and critical flow ($F = 1$) at the throat.

### 10.10.3    Flow over bumps

We have seen that when a subcritical open channel flow passes through a smooth constriction, the Froude number can become critical at the throat and supercritical in the diverging part of the constriction. A bump on the floor of a channel of constant width can also make the flow become supercritical. For example, if the depth of the water decreases approaching the bump, and then continues to decrease downstream of the bump, we can show that the flow has become supercritical as it passed over the bump. A throat must have formed near the crest of the bump. This type of flow is often seen in river rapids, where the depth of the water decreases as the water passes over a submerged rock. Usually, a hydraulic jump forms a short distance downstream of the rock, indicating that the flow became supercritical as it passed over the rock. For the flow approaching a bump, if we see that the depth of the water begins to increase, we know that it is initially supercritical. If the depth continues to increase downstream of the bump, we know that the flow became subcritical as it passed over the bump.

# Chapter 11

# Compressible Flow

## 11.1 Introduction

To demonstrate why the compressibility of fluids is important, consider the example of a piston in a long, straight tube filled with gas (Figure 11.1). The piston is initially at rest, and so is the gas. If the piston suddenly starts moving at a constant speed, what happens to the fluid? The fluid in contact with the piston must start to move when the piston does, but what about the fluid further down the tube? If the fluid were incompressible, the gas would behave like a solid body and the entire mass of fluid would move with the piston. As soon as the piston begins to move, all the fluid in the tube must start to move at the same speed, even the fluid far from the piston. In other words, the effect of the piston motion would travel through the gas at an infinite speed.

Real fluids do not behave like this. Real fluids are compressible. As the piston starts to move, the gas near the piston gets compressed first (the gas far away has not started to move yet, so the gas near the piston gets squeezed into a smaller volume), and then the gas a little further away, and so on. The motion of the piston propagates through the tube as a pressure wave at a finite speed.

We can identify the "front" between the compressed gas and the undisturbed gas and measure the speed at which it travels. If the pressure disturbance caused by the piston motion is small compared to the ambient pressure, this compression front travels at the local speed of sound (sound waves are just very weak pressure waves). In fact, the most common evidence of the compressibility of fluids is the propagation of sound waves — if a fluid were truly incompressible, sound waves could not travel through it. In contrast, if the pressure disturbances caused by the piston motion are not small, shock waves will appear. A shock wave is a very thin region where the velocity, pressure, temperature and density all change significantly. For the case of a shock forming in a tube, the shock is planar, and it travels into the gas at a speed somewhere between the speed of sound in the undisturbed gas ahead of it, and the speed of sound in the compressed gas behind it.

We have all heard shock waves: the thunder that accompanies lightning, the boom that comes with an explosion, and the crack of a whip, are all examples of shock waves. We know from experience that shock waves produce rapid changes in pressure. In fact, they often produce such rapid changes that the changes are said to occur "discontinuously." For example, an explosion generates a very intense pressure and temperature rise, and the pressure disturbance travels out as a shock wave. In this case, the shock wave is spherical and it weakens as it travels outward so that the pressure jump across the shock decreases with distance. When a bullet issues from a barrel, the hot, high pressure gas that is expelled from the muzzle also generates a spherical shock. The bullet itself typically travels at a supersonic speed (that is, at a speed greater than the speed of sound in the undisturbed
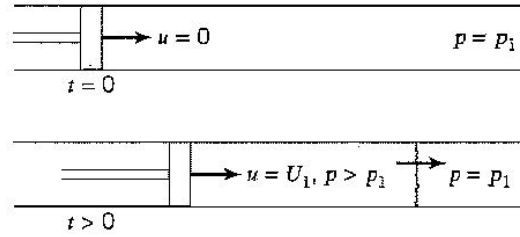
Figure 11.1: The motion of a piston in a tube filled with a gas produces a pressure disturbance, which travels down the tube at a finite speed.

gas), and its motion will generate shock waves. In fact, whenever a body of finite size travels through a gas at a supersonic speed, shocks will appear. For example, the crack of a whip is the audible evidence of shock formed by the supersonic motion of its tip, as shown in Figure 11.2.

In this chapter, we focus on high speed gas flows where compressibility effects are important, and analyze the behavior of shocks and other wave phenomena that occur when bodies travel at supersonic speed.

## 11.2   Pressure Propagation in a Moving Fluid

The propagation of sound waves in high-speed flow displays many similarities to the propagation characteristics of small amplitude gravity waves examined in Chapter 11. For example,
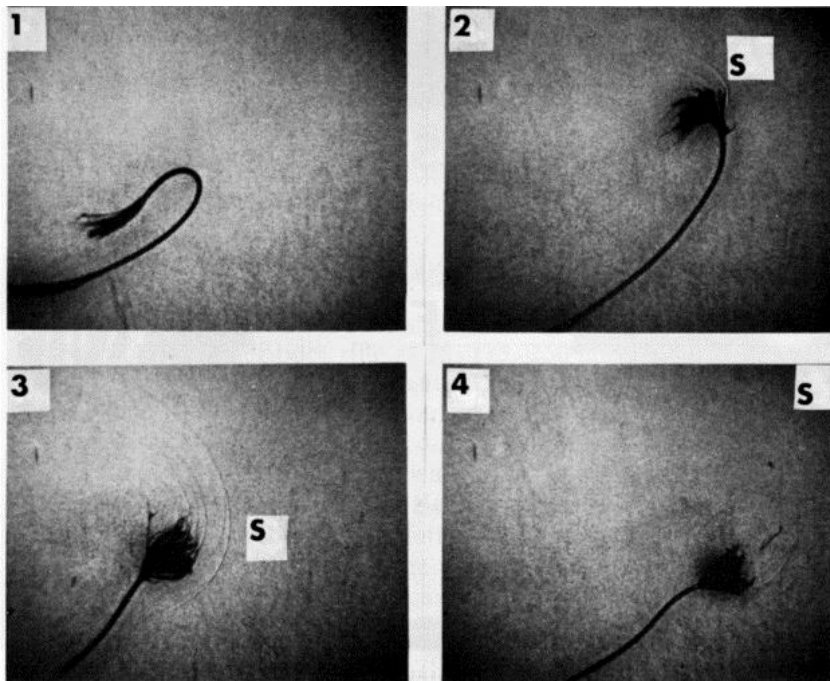


Figure 11.2: The motion of the tip of a bull whip is shown to produce shock waves in these four sequential pictures. The shocks are visible as thin lines near the letter $S$ in each picture. The tip speed is $1400\,ft/s$, compared to the sound speed of $1100\,ft/s$. Courtesy, Naval Research Laboratory.

imagine a body suddenly placed in a subsonic air flow [see Figure 11.3(a)]. The presence of the body creates pressure disturbances, which travel outward from the body at the speed of sound (as long as the pressure waves are small). It is by the transmission of pressure waves that the rest of the flow finds out about the presence of the body, in the same way the fisherman in Section 10.2 found out about the presence of a wave source through the ripples that traveled outward on the free surface of the water.

An important parameter is the Mach number $M$, defined as the ratio of the bulk velocity of the fluid $V$ to the speed of sound $a$. That is,

$$M = \frac{V}{a}$$

In a *subsonic* flow ($M < 1$), the whole of the flow field will be affected by the pressure waves, and this explains why the flow at some distance upstream of the body adjusts to the presence of the body: it "knows" that the body is there because pressure waves transmit the information regarding its presence. For a cylinder, this distance is of the order of 10 diameters. In mathematical terms, the flow field is "elliptic," which means that all parts of the flow are affected by all other parts since information is freely transmitted throughout the flow field.

If the body was placed in a *sonic* flow field ($M = 1$), the pressure waves would travel outward at the speed of sound, but they would also be swept downstream by the flow at the same speed [see Figure 11.3(b)]. The waves all collect along a line normal to the flow direction, and the flow upstream of the body never feels the presence of the body. The adjustment of the flow to the presence of the body is no longer gradual, but sudden.

When the flow is *supersonic* ($M > 1$), the pressure waves still travel outward at the speed of sound, but they are swept downstream at an even greater speed so that the waves are confined to a wedge-shaped region [see Figure 11.3(c)]. Only the flow inside this region feels the presence of the body. The angle made by the envelop of waves is $\alpha_M$, where

$$\sin \alpha_M \; = \; \frac{1}{M} \tag{11.1}$$

(see Figure 11.4). The angle $\alpha_M$ is called the *Mach angle*, and it is the angle a weak pressure wave makes with the flow direction in a supersonic flow. The weak pressure wave is often called a *Mach wave*.

If the body has a finite size, the pressure disturbances it generates will no longer be small. At supersonic speeds, the flow cannot adjust gradually to its presence, and a sudden, steep adjustment of pressure (a *shock wave*) is necessary to let the flow pass over the body. Shock wave patterns made by a sphere moving at Mach 4.01 are shown in Figure 11.5. A similar phenomenon occurs in open channel flows at the critical Froude number ($F = 1$), where an obstruction of finite size forms a sudden change in water level called a hydraulic jump.
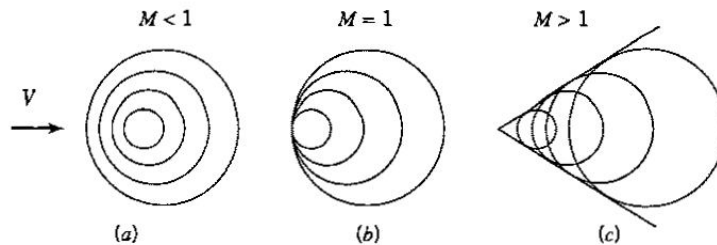


Figure 11.3: Wave patterns made by a point disturbance. (a) $U < a$ (subsonic). (b) $U = a$ (sonic). (c) $U > a$ (supersonic).

$$\sin \alpha = \frac{a \Delta t}{V \Delta t} = \frac{1}{M}$$
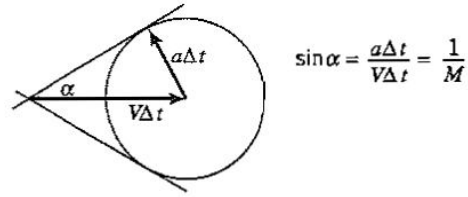
Figure 11.4: Wave patterns made at supersonic Mach numbers.

For a body in a sonic flow, the shock wave that forms in front of the body is at right angles to the flow direction, and it is called a normal shock. For a supersonic flow, the shock is inclined to the flow direction, and it is called an oblique shock wave.[1] You may have heard shock waves when an airplane flies over you at sonic or supersonic speeds. If you had your eyes closed, the first indication that an airplane was present would have been the passage of the shock wave created by the plane. Until the airplane passed over you, the sound waves generated by the plane could not have reached you because the source of the sound was moving faster than the speed of sound. If you have had this experience, you would also know that the shock wave is a large pressure disturbance, and even at considerable distances from the plane, the *sonic boom* can be very unpleasant. In fact, the pressure jump can be so large that the increased pressure, acting over the area of a window pane, can

[1]For very weak shocks, the angle made by an oblique shock $\beta$ is equal to the Mach angle $\alpha_M$. This is not true for shocks of finite strength.
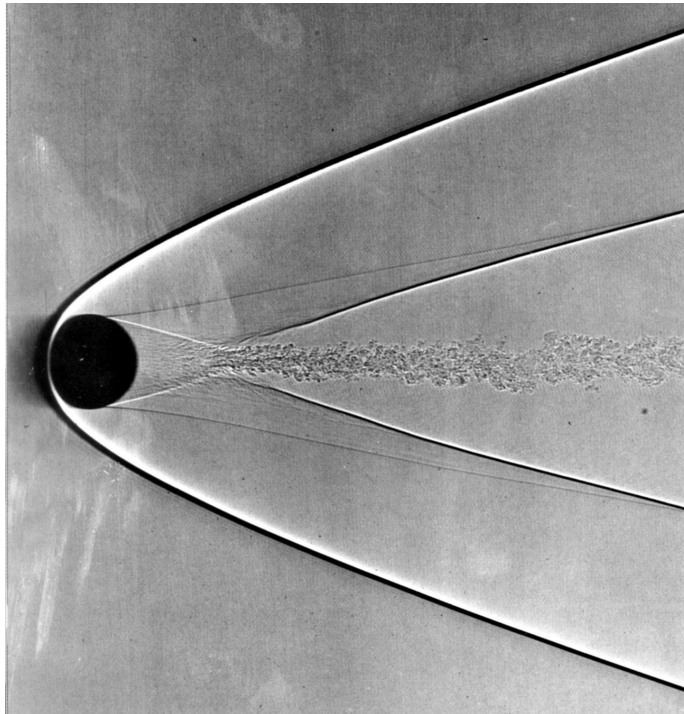


Figure 11.5: Shock wave patterns made by a $0.5\,in.$ sphere in free flight in atmospheric air at Mach 4.01. A strong shock wave is formed upstream of the sphere. The boundary layer separation just behind the equator is accompanied by a weak shock wave, and a second shock is formed near the point where the separated shear layers meet. Photograph courtesy of A.C. Charters.

cause it to break. The wave field generated by a supersonic vehicle is considered further in Section 11.11.

## 11.3 Regimes of Flow

A flow at very low Mach number can generally be assumed to be incompressible, as long as we are not concerned with the mechanics of sound propagation. As the Mach number increases, there comes a point where compressibility effects become important. At what Mach number does this occur? In Section 1.5, it was suggested that density changes due to variations in flow velocity can be neglected, as long as the dynamic pressure is small compared to the static pressure. We see that

$$M^2 \;=\; \frac{V^2}{a^2} \;=\; 2\left( \frac{\frac{1}{2}\rho V^2}{\gamma\, p} \right)$$

so that the Mach number is related to the ratio of the dynamic pressure to the absolute pressure. If we accept a 1% level as a tolerable change in density, then if the temperature remains constant the corresponding change in pressure is 1%.[2] This requires $\frac{1}{2}\rho V^2 < 0.01$, so that at sea level where the density of air is about $1.2\, kg/m^3$, we are limited to velocities less than $40\, m/s$ ($132\, ft/s$ or $90\, mph$), which correspond to Mach numbers less than about 0.12.

The limit for the assumption of incompressible flow is often given as $M < 0.3$. This corresponds to a maximum change in density of about 5% for an isentropic process. This may seem somewhat generous, but there are good reasons why changes in density are often considered to be less important than changes in pressure. When we consider the forces acting on a wing, for example, the pressure differences acting over the top and bottom surfaces of the wing give rise to a lift force. The pressure differences also generate density differences, which lead to a buoyancy force. This buoyancy force is almost always negligible compared to the lift force and density differences can be ignored.

At higher Mach numbers, changes in density become more and more important, especially at transonic and supersonic Mach numbers where shocks are formed. Under certain conditions, compressibility effects can even be important at relatively low Mach numbers. Just after take-off, for example, the wings on an airplane are developing very high lift. The flow velocities near the leading edge of the wing can be very high, so that even though the aircraft may be moving at a Mach number of 0.3, the local Mach number can be supersonic and shocks can form.

Based on these considerations, we can identify three regimes of fluid flow:

**1.** Acoustics, where fluid velocities are very small compared with the speed of sound, but the fractional changes in pressure, temperature and density are important;

**2.** Incompressible flow, where fluid velocities are small compared with the speed of sound, and the fractional changes in density are not significant; however, fractional changes in pressure and temperature may be very important;

**3.** Compressible flow ("gasdynamics"), where fluid velocities are comparable to the speed of sound, and the fractional changes in pressure, temperature and density are all important.

In this chapter, we will consider flows in the gasdynamics regime. Before we begin this analysis, we need to review some basic thermodynamic principles and relationships.

---

[2]The process is more likely to be isentropic, but that does not change the argument very much.

## 11.4    Thermodynamics of Compressible Flow

In thermodynamics, we often speak of "systems." In fluid mechanics, we talk about "control volumes." They are identical concepts, in that systems and control volumes both describe a specific three-dimensional region bounded by a surface. Mass, momentum and energy may flow through the control volume surface, and the concept of flux can be used to describe this transport (Section 3.3).

Basic thermodynamic concepts and "state variables" such as total and internal energy were introduced in Section 3.8.[3] In our earlier considerations of the energy equation, it was always assumed that the system was in "equilibrium." That is, the heat and work interactions were assumed to be slow enough for the thermodynamic state of the system to be described completely by the first law of thermodynamics. What about non-equilibrium states? In compressible flows where high speeds are common and strong velocity and pressure gradients exist, systems may not be in equilibrium. It has been found by experiment, however, that the flow still attains an instantaneous local equilibrium, as long as the temperatures and pressures are not too extreme. This continues to hold even inside shock waves. For many flows, therefore, no new non-equilibrium phenomena need to be considered. For the flows examined here, all systems will be assumed to be in equilibrium at all times.

### 11.4.1    Ideal gas relationships

The behavior of compressible flow depends critically on the properties of the gas we are considering. Many gases, including air at reasonable temperatures and pressures, behave like an "ideal" gas. That is, they obey the ideal gas law (equation 1.3)

$$p = \rho R T \qquad \text{or} \qquad pv = RT \tag{11.2}$$

where $v = 1/\rho$ is the specific volume. All fluids considered here are assumed to follow the ideal gas law.

It is important to remember that in all thermodynamic and compressible gas relationships, absolute values are used, so that for temperature we use the Kelvin or Rankine scales, and for pressure we always use the absolute value, never the gauge value. Also, in equation 11.2,

$$R = \frac{A}{MW} \tag{11.3}$$

where $A = 8,314\,m^2/s^2K$ (or $8,314\,J/kg\,K$) is the universal gas constant, and $MW$ is the molecular weight of the gas. For air, $MW = 28.98$ and $R = 287.03\,m^2/s^2K = 1716.4\,ft^2/s^2R$.

### 11.4.2    Specific heats

The heat input to a system is related to temperature changes. The change in temperature for a given heat interaction depends on material properties such as its specific heats. For the SI system of units

> Specific heat is defined as the amount of heat required to raise the temperature of $1\,kg$ of substance by $1\,K$.

A different amount of heat is usually required if the process occurs at a constant volume, or at a constant pressure. The specific heats at constant volume, $C_v$, and at constant pressure,

---

[3]An excellent introduction to more general thermodynamic principles is given in *An Introduction to Thermal-Fluid Engineering* by Z. Warhaft, published by CUP, 1997.

$C_p$ are defined as

$$C_v = \left(\frac{\partial \hat{u}}{\partial T}\right)_v \quad \text{and} \quad C_p = \left(\frac{\partial h}{\partial T}\right)_p \tag{11.4}$$

where $\hat{u}$ is the internal energy per unit mass $(= \hat{U}/\rho)$, and $h$ is the enthalpy per unit mass, defined by

$$h = \hat{u} + \frac{p}{\rho} \quad \text{or} \quad h = \hat{u} + pv \tag{11.5}$$

The units of $C_v$ and $C_p$ are $J/(kg\,K)$, that is, $N \cdot m/(kg\,K)$, or $ft \cdot lb_f/(slug\,R)$.

For an ideal gas, the internal energy per unit mass $\hat{u}$ is a function of temperature only, and

$$C_v \equiv \left(\frac{\partial \hat{u}}{\partial T}\right)_v = \frac{d\hat{u}}{dT}$$

For a constant specific heat (a reasonable approximation for moderate changes in temperature), in an ideal gas

$$\boxed{\hat{u}_2 - \hat{u}_1 = C_v \left(T_2 - T_1\right)} \tag{11.6}$$

For an ideal gas, $\hat{u}$ and $p/\rho$ depend only on temperature. It follows that the enthalpy $(h = \hat{u} + pv)$ is a function of temperature only, and

$$C_p \equiv \left(\frac{\partial h}{\partial T}\right)_p = \frac{dh}{dT}$$

For a constant specific heat, in an ideal gas

$$\boxed{h_2 - h_1 = C_p \left(T_2 - T_1\right)} \tag{11.7}$$

For air at 20°C, $C_v = 718\,J/kgK$, and $C_p = 1005\,J/kgK$. Note that if the mass of fluid is thermally insulated from its surroundings, so that all heat interactions are zero, the change of state of the fluid is called "adiabatic."

We can also derive some useful relationships between $C_v$ and $C_p$. From the definition of enthalpy and the ideal gas law

$$h = \hat{u} + RT$$

Differentiating, we obtain

$$dh = d\hat{u} + R\,dT$$

or

$$\frac{dh}{dT} = \frac{d\hat{u}}{dT} + R$$

Hence

$$\boxed{C_p - C_v = R} \tag{11.8}$$

This relationship holds for all ideal gases, even if the specific heats vary with temperature. The specific heat ratio $\gamma$ is defined by

$$\gamma = \frac{C_p}{C_v} \tag{11.9}$$

For a perfect gas, $\gamma$ is a constant. Air behaves as a perfect gas over a relatively wide range of temperatures and pressures, and over this range the specific heat ratio is nearly constant and equal to 1.4 (see Tables Appendix-C.1 and C.2).

Equations 11.8 and 11.9 lead to

$$C_v = \frac{R}{\gamma - 1} \tag{11.10}$$

and

$$C_p = \frac{\gamma R}{\gamma - 1} \tag{11.11}$$

### 11.4.3   Entropy variations

For compressible flows, changes in *entropy* are important. Entropy is the subject of the second law of thermodynamics. The second law can be stated in a number of different ways, none of which is easy to understand. We will use the second law only indirectly, and it is sufficient for us to regard entropy simply as another variable of state defined by

$$T \, ds = d\hat{u} + p \, dv \tag{11.12}$$

We should also understand that the change in entropy during a process is intimately connected with the concept of *reversibility*. When a process is reversible, it means that no matter what heat and work interactions occur during the process, the original state of the system can be recovered by reversing the directions of all the interactions. For an adiabatic, reversible process, the entropy remains constant, and the process is called *isentropic*. For an adiabatic, irreversible process, the second law indicates that the entropy must increase.

Using the definition of enthalpy, we can write equation 11.12 as

$$T \, ds = dh - v \, dp \tag{11.13}$$

For a *perfect* gas (that is, a gas that obeys the ideal gas law and which has constant specific heats), equation 11.12 becomes

$$ds = C_v \frac{dT}{T} + R \frac{dv}{v} \tag{11.14}$$

and equation 11.13 becomes

$$ds = C_p \frac{dT}{T} - R \frac{dp}{p} \tag{11.15}$$

These two results can be integrated to obtain

$$\boxed{s_2 - s_1 = C_v \ln \frac{T_2}{T_1} - R \ln \frac{\rho_2}{\rho_1}} \tag{11.16}$$

and

$$\boxed{s_2 - s_1 = C_p \ln \frac{T_2}{T_1} - R \ln \frac{p_2}{p_1}} \tag{11.17}$$

When a flow is isentropic ($s_2 = s_1$) and obeys the ideal gas law, it follows that

$$\boxed{\frac{\rho}{\rho_r} = \left( \frac{T}{T_r} \right)^{\frac{1}{\gamma - 1}} \quad \text{and} \quad \frac{p}{p_r} = \left( \frac{T}{T_r} \right)^{\frac{\gamma}{\gamma - 1}}} \tag{11.18}$$

The parameters $T_r$, $\rho_r$ and $p_r$ are the values of the temperature, density and pressure at some reference point. It is common practice to use the "stagnation conditions" as the reference conditions (see Section 11.4.5).

## 11.4.4   Speed of sound

Sound waves are pressure disturbances that are small compared to the ambient pressure. For example, sound at $100\,dB$, which is a very noisy sound level,[4] corresponds to a pressure disturbance level of only $1\,Pa$ ($10^{-5}$ atmosphere).

The transmission of sound waves is an *isentropic*, compressible phenomenon, and sound waves travel at a speed given by

$$a = \sqrt{\left.\frac{\partial p}{\partial \rho}\right|_s} \tag{11.19}$$

That is, the speed of sound is determined by the rate of change of pressure with respect to density, at a constant entropy, $s$. For an ideal gas, the pressure and density in isentropic flow are related by

$$\frac{p}{\rho^\gamma} = \text{constant}$$

(see equation 11.18). By differentiating this relationship, we find that

$$\frac{dp}{p} - \gamma\frac{d\rho}{\rho} = 0$$

Therefore,

$$\left.\frac{\partial p}{\partial \rho}\right|_s = a^2 = \gamma\frac{p}{\rho}$$

For an ideal gas, therefore, the speed of sound is given by

$$\boxed{a = \sqrt{\gamma RT}} \tag{11.20}$$

For air at $20°\,C$ the speed of sound is $343\,m/s = 1,126\,ft/s = 768\,mph$.[5]

Since we can also write the bulk modulus of a fluid $K$ in terms of the rate of change of pressure with respect to density, that is, from equation 1.2,

$$K = \frac{dp}{d\rho/\rho} = \rho\frac{dp}{d\rho} \tag{11.21}$$

and so

$$a = \sqrt{K/\rho}$$

For fluids, therefore, the speed of sound and the bulk modulus of the fluid are directly related. For isentropic flow of a gas, it can be shown that $K = \gamma p$ (see Section 11.5), and so

$$a = \sqrt{\gamma p/\rho} \tag{11.22}$$

For an ideal gas, we obtain $a = \sqrt{\gamma RT}$, as before.

---

[4]The Occupational Safety and Health Administration (OSHA) requires ear protection for people exposed to noise levels exceeding $90\,dB$.

[5]It takes sound about 4.7 seconds to travel a mile. Since the noise made by thunder travels at approximately the isentropic speed of sound, the time delay between the thunder and the lightning flash can be used as a rough guide to determine how far away a lightning strike has occurred: after the flash, count 5 seconds for every mile.

### 11.4.5   Stagnation quantities

For steady, adiabatic flow in a streamtube, with no work interactions, the one-dimensional energy equation (equation 8.29) becomes

$$h_1 + \tfrac{1}{2}V_1^2 = h_2 + \tfrac{1}{2}V_2^2$$

where we have used $h = \hat{u} + p/\rho$, and gravity has been ignored.  This relationship can be written as

$$h_0 = h + \tfrac{1}{2}V^2 \tag{11.23}$$

where the constant $h_0$ is the enthalpy of the fluid at a point where $V = 0$.  The quantity $h_0$ is called the *stagnation enthalpy* or *total enthalpy*.  For steady adiabatic flow, the stagnation enthalpy is constant along a streamtube.  For an ideal gas with constant specific heats (a perfect gas), $h = C_p T$, and

$$C_p T_0 = C_p T + \tfrac{1}{2}V^2 \tag{11.24}$$

where $T_0$ is the *stagnation temperature* or *total temperature*.  Using

$$C_p = \frac{\gamma R}{\gamma - 1}, \quad \text{and} \quad M^2 = \frac{V^2}{\gamma R T}$$

we obtain

$$\boxed{\frac{T_0}{T} = 1 + \frac{\gamma - 1}{2}M^2} \tag{11.25}$$

which is a particular form of the one-dimensional energy equation for steady, adiabatic flow of a perfect gas.  Also

> For steady, adiabatic flow of a perfect gas, $T_0$ is constant along a streamtube.

Even if the flow does not obey all of these restrictions, it is still possible to compute a stagnation temperature at any point according to equation 11.25, so that this equation may be used as a definition of the stagnation or *total temperature*.  For an adiabatic, steady flow of a perfect gas, we know that $T_0$ is constant along a streamline, but if these conditions are not satisfied no conclusions can be drawn regarding the behavior of $T_0$.

We can also define stagnation or reservoir conditions for the density and pressure.  It is necessary to specify how the flow is brought to rest, and so we define $\rho_0$ and $p_0$ as the density and pressure of the gas if it was brought to rest isentropically.  The stagnation density and pressure are constant along a streamline only if the flow itself is isentropic.

The isentropic relationships are commonly referred to as stagnation conditions, so that

$$\frac{\rho}{\rho_0} = \left(\frac{T}{T_0}\right)^{\frac{1}{\gamma - 1}} \quad \text{and} \quad \frac{p}{p_0} = \left(\frac{T}{T_0}\right)^{\frac{\gamma}{\gamma - 1}} \tag{11.26}$$

where $\rho_0$ and $p_0$ are the density and pressure of the gas if it was brought to rest isentropically.  They are called the stagnation or total density and pressure.  Using equation 11.25, we find that for isentropic flow

$$\boxed{\frac{\rho_0}{\rho} = \left(1 + \frac{\gamma - 1}{2}M^2\right)^{\frac{1}{\gamma - 1}}} \tag{11.27}$$

and

$$\frac{p_0}{p} = \left(1 + \frac{\gamma - 1}{2} M^2\right)^{\frac{\gamma}{\gamma - 1}} \tag{11.28}$$

These functions are tabulated in Table Appendix-C.12 for $\gamma = 1.4$. Solutions to the isentropic flow relations may also be found using the compressible flow calculator available on the web at *http://www.engapplets.vt.edu/*.

## 11.5   Compressible Flow Through a Nozzle

We have seen how water passing through a constriction in an open channel can become supercritical (Chapter 10). Similarly, when a gas passes through a converging and diverging duct, a supersonic flow can be produced. The converging and diverging duct is called a *nozzle*, but the principles of its operation are very similar to what we have already discussed with respect to open channel flow. In a supersonic wind tunnel, for example, a subsonic flow accelerates as it passes through the converging part of the nozzle, and if the downstream pressure is low enough, the flow becomes sonic at the throat and expands to supersonic Mach numbers in the diverging part of the nozzle (see Figure 11.6). The nozzle can then be attached to a test section, where experiments in supersonic flow can be performed. When the downstream pressure is not low enough, shock waves can appear in the expansion, in the same way hydraulic jumps can appear in the diverging part of a channel flow. If the downstream pressure is too high, the whole flow will become subsonic and the tunnel is said to *choke* (see Section 11.5.3).

We will now consider the variations in pressure, temperature, density and velocity experienced by a compressible gas flowing isentropically through a nozzle similar to that shown in Figure 11.6 (sometimes called a Laval nozzle, after the Swedish engineer Karl Gustav Patrik de Laval, who invented the convergent-divergent nozzle for steam turbine applications in 1888).

### 11.5.1   Isentropic flow analysis

For isentropic flow, there is no heat transfer and all processes are reversible. No shocks are allowed. The flow is steady, and quasi-one-dimensional. We assume a perfect gas, and neglect the effects of gravity. By differentiating equation 11.18, we obtain

$$\frac{d\rho}{\rho} = \frac{1}{\gamma - 1} \frac{dT}{T} \tag{11.29}$$

and

$$\frac{dp}{p} = \frac{\gamma}{\gamma - 1} \frac{dT}{T} \tag{11.30}$$
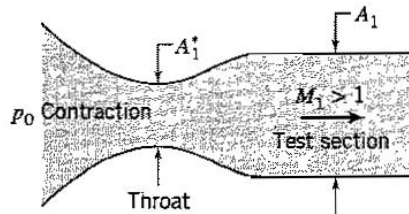


Figure 11.6: Isentropic, compressible flow through a converging and diverging duct.

Consider an elemental control volume that follows the inside contours of the nozzle, as shown in Figure 11.7. The one-dimensional continuity equation, $\rho A V = constant$, can be differentiated to give

$$\frac{d\rho}{\rho} + \frac{dA}{A} + \frac{dV}{V} = 0 \tag{11.31}$$

Similarly, we apply the momentum equation for steady flow (equation 3.20) to this control volume. For isentropic flow, there is no wall friction, and so

$$pA + \rho V^2 A + p\,dA = (p + dp)(A + dA) + (\rho + d\rho)(V + dV)^2 (A + dA)$$

Note that the term $p\,dA$ on the left hand side of the equation represents the force due to pressure acting on the side walls of the control volume. Neglecting all higher order terms, this becomes

$$A\,dp + AV^2\,d\rho + \rho V^2\,dA + 2\rho V A\,dV = 0$$

With $\rho A V = constant$, we obtain

$$dp + \rho V\,dV = 0 \tag{11.32}$$

This is the momentum equation for steady, quasi-one-dimensional flow, in the absence of viscous and gravitational forces. For isentropic (inviscid, no heat transfer) flow, this equation can be written as

$$V\,dV = -\frac{dp}{\rho} = -\frac{dp}{d\rho}\frac{d\rho}{\rho} = -a^2\frac{d\rho}{\rho} \tag{11.33}$$

since the speed of sound (squared) is equal to the rate of change of pressure with density at constant entropy (equation 11.19). Introducing the Mach number (equation 1.5) and using the continuity equation (equation 11.31), we obtain

$$\frac{dV}{dx} = -\frac{\frac{V}{A}}{1 - M^2}\frac{dA}{dx}$$

In addition, by using the isentropic relationships given in equations 11.29 and 11.30, we find that

$$\frac{d\rho}{dx} = \frac{\frac{\rho}{A}M^2}{1 - M^2}\frac{dA}{dx}$$

$$\frac{dp}{dx} = \frac{\frac{p}{A}\gamma M^2}{1 - M^2}\frac{dA}{dx}$$

$$\text{and} \quad \frac{dT}{dx} = \frac{\frac{p}{A}(\gamma - 1)M^2}{1 - M^2}\frac{dA}{dx}$$
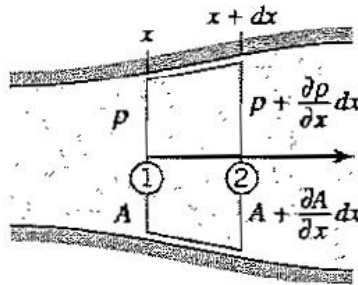


Figure 11.7: Elemental control volume for the derivation of the momentum equation for steady, quasi-one-dimensional flow.

If we avoid the case where $M = 1$, and consider the two cases where $M < 1$ everywhere, or $M > 1$ everywhere:

**1.** When $M < 1$ everywhere, then with

(a)   $\dfrac{dA}{dx} < 0, \quad \dfrac{dp}{dx} < 0, \quad \dfrac{d\rho}{dx} < 0, \quad \dfrac{dT}{dx} < 0, \quad \text{and} \quad \dfrac{dV}{dx} > 0$

(b)   $\dfrac{dA}{dx} > 0, \quad \dfrac{dp}{dx} > 0, \quad \dfrac{d\rho}{dx} > 0, \quad \dfrac{dT}{dx} > 0, \quad \text{and} \quad \dfrac{dV}{dx} < 0$

**2.** When $M > 1$ everywhere, then with

(a)   $\dfrac{dA}{dx} < 0, \quad \dfrac{dp}{dx} > 0, \quad \dfrac{d\rho}{dx} > 0, \quad \dfrac{dT}{dx} > 0, \quad \text{and} \quad \dfrac{dV}{dx} < 0$

(b)   $\dfrac{dA}{dx} > 0, \quad \dfrac{dp}{dx} < 0, \quad \dfrac{d\rho}{dx} < 0, \quad \dfrac{dT}{dx} < 0, \quad \text{and} \quad \dfrac{dV}{dx} > 0$

These results are summarized in Figure 11.8. The similarity with respect to the frictionless flow of a liquid in an open channel is clear by comparing Figures 10.14 and 11.8.

We see that when the Mach number is subsonic everywhere, the pressure, density and temperature drop as the flow speeds up in the converging part of the nozzle, and they rise as the flow slows down in the diverging part of the nozzle. When the Mach number is supersonic everywhere, the pressure, density and temperature rise as the flow slows down in the converging part of the nozzle, and they fall as the flow speeds up in the diverging part of the nozzle. In particular, for supersonic flow downstream of the throat (Case 2b above), the velocity increases and the temperature decreases as the area continues to expand. The Mach number is therefore set by the amount the area increases downstream of the throat. That is, the Mach number depends on the area ratio $A/A^*$, where $A^*$ is the cross-sectional area of the nozzle throat. To obtain a Mach number of 8, for example, an area ratio of about 200 is required (see also Section 11.5.2). Note that the flow in a subsonic diffuser (a diffuser is a duct of increasing area) has a falling velocity and a rising pressure, but the flow in a supersonic diffuser has a rising velocity and a falling pressure.

The downstream pressure level defines a series of flow regimes, much as the downstream water level did in the case of open channel flow through a smooth constriction:

**1.**   Only two solutions exist with $M = 1$ at the throat when there are no losses (Figure 11.9, cases $c$ and $i$);
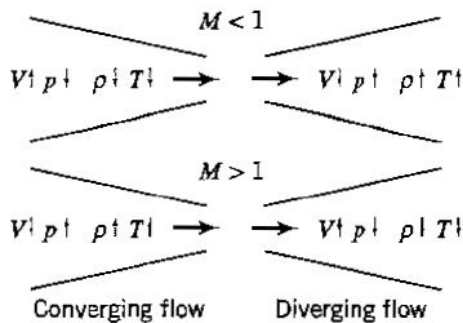


Figure 11.8: Summary of flow variation in subsonic and supersonic ducts.
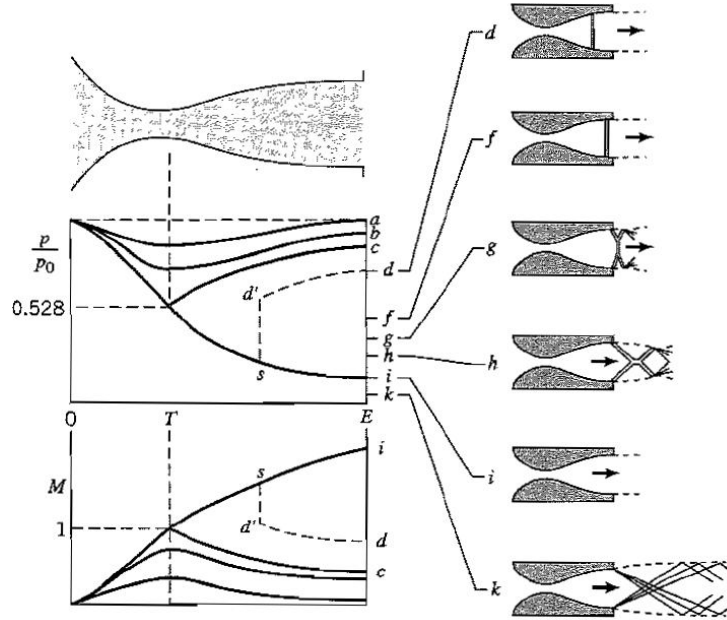
Figure 11.9: Pressure and Mach number distributions through a converging-diverging nozzle. From Liepmann & Roshko, *Elements of Gasdynamics*, John Wiley & Sons Inc., 1957.

**2.** Normal shocks are found in the nozzle for exit pressures in the range marked by points $c$ and $f$;

**3.** Oblique shocks form outside the nozzle for the range between points $f$ and $i$; and

**4.** Oblique expansion waves form outside the nozzle for exit pressures below point $i$.

Shocks and expansion waves are considered further in Sections 11.6 to 11.10.

## 11.5.2   Area ratio

We saw that the Mach number downstream of the throat depends on the ratio of the cross-sectional area of the nozzle to the cross-sectional area of the throat. To find this relationship, we write the continuity equation between the throat and a location in the nozzle

$$\rho V A = \rho^* V^* A^*$$

where the asterisk denotes the throat location. We will only consider flows where supersonic flow exists in the test section. At the throat, therefore, $M = 1$, and $U^* = a^*$. That is,

$$\frac{A}{A^*} = \frac{\rho^*}{\rho} \frac{a^*}{V} = \frac{\rho^*}{\rho_0} \frac{\rho_0}{\rho} \frac{a^*}{V}$$

By using the isentropic relations (equations 11.27 and 11.28), we can show that

$$\left(\frac{A}{A^*}\right)^2 = \frac{1}{M^2} \left[\frac{2}{\gamma+1}\left(1 + \frac{\gamma-1}{2}M^2\right)\right]^{(\gamma+1)/(\gamma-1)} \tag{11.34}$$

This is the area relation for isentropic, supersonic flow in a nozzle.
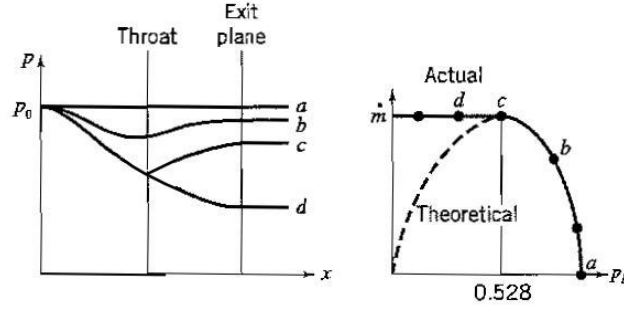
Figure 11.10: Variation of mass flow rate as a function of pressure for steady, isentropic flow in a converging-diverging duct. The "theoretical" curve corresponds to equation 11.35. The "actual" curve corresponds to choked flow.

### 11.5.3   Choked flow

What is the mass flow through the nozzle? For steady, one-dimensional nozzle flow, the mass flow rate $\dot{m}$ is given by

$$\dot{m} = \rho V A \; = \; \text{constant.}$$

The energy equation gives

$$C_p T_0 = C_p T + \tfrac{1}{2} V^2$$

That is,

$$\tfrac{1}{2} V^2 \;=\; C_p \left(T_0 - T\right)$$
$$\;=\; C_p T_0 \left(1 - \frac{T}{T_0}\right)$$

For isentropic flow this becomes

$$\tfrac{1}{2} V^2 \;=\; C_p T_0 \left[1 - \left(\frac{p}{p_0}\right)^{\frac{\gamma-1}{\gamma}}\right]$$

Hence,

$$\dot{m} \;=\; \rho V A \;=\; \rho_0 \left(\frac{p}{p_0}\right)^{\frac{1}{\gamma}} A \left[2 C_p T_0 \left(1 - \left(\frac{p}{p_0}\right)^{\frac{\gamma-1}{\gamma}}\right)\right]^{\frac{1}{2}}$$

so that

$$\dot{m} \;=\; A \left[\frac{2\gamma}{\gamma-1} p_0 \rho_0 \left(\left(\frac{p}{p_0}\right)^{\frac{2}{\gamma}} - \left(\frac{p}{p_0}\right)^{\frac{\gamma+1}{\gamma}}\right)\right]^{\frac{1}{2}} \tag{11.35}$$

This curve is plotted in Figure 11.10 for a flow that exits to a pressure $p_b$, called the *back pressure*. We see that the mass flow rate curve has a maximum. To find the pressure ratio at which the maximum mass flow rate occurs, we differentiate equation 11.35 with respect to the pressure ratio $p/p_0$

$$\left.\frac{\partial \dot{m}}{\partial \frac{p}{p_0}}\right|_A \;=\; \frac{A^2}{2\dot{m}} \frac{2\gamma}{\gamma-1} p_0 \rho_0 \left[\frac{2}{\gamma}\left(\frac{p}{p_0}\right)^{\frac{2-\gamma}{\gamma}} - \frac{\gamma+1}{\gamma}\left(\frac{p}{p_0}\right)^{\frac{1}{\gamma}}\right]$$

This derivative is zero when

$$\frac{2}{\gamma}\left(\frac{p}{p_0}\right)^{\frac{2-\gamma}{\gamma}} \;=\; \frac{\gamma+1}{\gamma}\left(\frac{p}{p_0}\right)^{\frac{1}{\gamma}}$$

That is, when

$$\frac{p}{p_0} \;=\; \left(\frac{\gamma+1}{2}\right)^{\frac{\gamma}{1-\gamma}} \;=\; 0.528 \quad \text{for air} \tag{11.36}$$

We can now find where this pressure ratio occurs in the nozzle. For isentropic flow, we have

$$\frac{p_0}{p} \;=\; \left(1+\frac{\gamma-1}{2}M^2\right)^{\frac{\gamma}{\gamma-1}}$$

Substituting the pressure ratio at which the maximum mass flow rate occurs from equation 11.36, we find that this critical pressure ratio occurs when $M=1$, that is, it occurs at the throat.

Since the maximum mass flow rate occurs when the Mach number at the throat is sonic, it cannot be affected by the pressure distribution downstream of the throat: the pressure changes cannot propagate upstream of the point where the flow is sonic. As a result, lowering the back pressure cannot increase the mass flow rate. Once the flow at the throat is sonic, the nozzle is said to be "choked." At this point, the mass flow rate has reached its maximum value and it remains fixed at that value even when the back pressure is lowered. Therefore, equation 11.35 does not apply at pressure ratios below the critical value given by equation 11.36. This fact is indicated in Figure 11.10 by the "actual" curve (choked flow) compared to the "theoretical" curve (equation 11.36).

## 11.6   Normal Shocks

So far, we have qualitatively discussed the formation of shock waves in compressible flow. To understand this phenomenon more quantitatively,, we will now analyze a one-dimensional flow containing a stationary normal shock. In this framework, the flow is steady. The gas is assumed to be "perfect" so that it obeys the ideal gas law and its specific heats are constant.

Consider the control volume shown in Figure 11.11. Stations 1 and 2 are placed well outside the shock so that all gradients are zero. That is, the velocity, pressure and temperature are all constant at these locations, and the one-dimensional equations of motion apply between stations 1 and 2. With no temperature gradients at the control volume boundaries, the flow is taken to be adiabatic, so that the total temperature is constant (see Section 11.4.5).

---

For steady, adiabatic flow of a perfect gas, $T_0$ is constant across a shock wave.

---

The flow is not reversible, however, because the entropy is expected to change. The equations describing this flow are

Continuity:     $\rho_1 V_1 = \rho_2 V_2$

Momentum:     $p_1 + \rho_1 V_1^2 = p_2 + \rho_2 V_2^2$
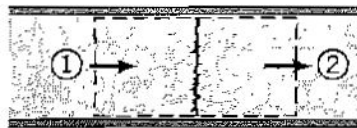


Figure 11.11: A normal shock in one-dimensional flow.

$$\text{Energy:} \quad C_p T_1 + \tfrac{1}{2} V_1^2 = C_p T_2 + \tfrac{1}{2} V_2^2 = C_p T_0 = \text{constant}$$

$$\text{Second law:} \quad s_2 - s_1 = C_p \ln (T_2/T_1) - R \ln (p_2/p_1)$$

$$\text{Equation of state:} \quad p = \rho R T$$

We have five equations and five unknowns ($\rho$, $u$, $p$, $s$, $T$), which implies that for any given upstream state a unique downstream state exists.

By using these equations in different ways, a number of results can be obtained, as shown below. It should be emphasized that all these results stem from the one-dimensional equations of motion, and no new phenomena are introduced. We simply manipulate the equations to obtain some useful results called the normal shock relations.

### 11.6.1 Temperature ratio

The temperature ratio across the shock can be expressed in terms of the upstream and downstream Mach number and the ratio of specific heats, as follows.

$$\frac{T_2}{T_1} = \frac{T_2}{T_{02}} \cdot \frac{T_{02}}{T_{01}} \cdot \frac{T_{01}}{T_1}$$

Since $T_{01} = T_{02}$ across a shock, we use the definition of the stagnation temperature to obtain

$$\frac{T_2}{T_1} = \frac{1 + \frac{\gamma-1}{2} M_1^2}{1 + \frac{\gamma-1}{2} M_2^2} \tag{11.37}$$

### 11.6.2 Velocity ratio

From the definition of the Mach number

$$\frac{V_2}{V_1} = \frac{M_2 a_2}{M_1 a_1} = \frac{M_2 \sqrt{\gamma R T_2}}{M_1 \sqrt{\gamma R T_1}}$$

Using equation 11.37,

$$\frac{V_2}{V_1} = \frac{M_2}{M_1} \left[ \frac{1 + \frac{\gamma-1}{2} M_1^2}{1 + \frac{\gamma-1}{2} M_2^2} \right]^{\frac{1}{2}} \tag{11.38}$$

### 11.6.3 Density ratio

From the continuity equation,

$$\frac{\rho_2}{\rho_1} = \frac{V_1}{V_2} = \frac{M_1}{M_2} \left[ \frac{1 + \frac{\gamma-1}{2} M_2^2}{1 + \frac{\gamma-1}{2} M_1^2} \right]^{\frac{1}{2}} \tag{11.39}$$

### 11.6.4 Pressure ratio

From the momentum equation and the ideal gas law,

$$p_1 \left( 1 + \frac{V_1^2}{RT_1} \right) = p_2 \left( 1 + \frac{V_2^2}{RT_2} \right)$$

and since

$$\frac{V^2}{RT} = \frac{M^2 a^2}{RT} = \frac{M^2 \gamma RT}{RT} = M^2 \gamma$$

then

$$\frac{p_2}{p_1} = \frac{1 + \gamma M_1^2}{1 + \gamma M_2^2} \tag{11.40}$$

## 11.6.5   Mach number ratio

From the equation of state,

$$\frac{p_2}{p_1} = \frac{\rho_2 T_2}{\rho_1 T_1}$$

Using equations 11.37, 11.39, and 11.40, this relationship can be expressed in terms of $M_1$ and $M_2$. Two solutions can be found:

$$M_2 = M_1 \tag{11.41}$$

$$\text{or} \quad M_2^2 = \frac{M_1^2 + \frac{2}{\gamma - 1}}{\frac{2\gamma}{\gamma - 1} M_1^2 - 1} \tag{11.42}$$

The first solution implies a shock of zero strength, since we see from equation 11.40 that the pressure does not change across the shock. The second solution indicates that, for $M_1 > 1$, it is possible to have a shock of finite strength in a one-dimensional steady flow. It can also be shown that the downstream Mach number $M_2$ will always be subsonic. Therefore

> A normal shock occurs only if $M_1 > 1$. As a result, $M_2 < 1$.

Substituting for $M_2$ in equations 11.39 and 11.40, we obtain

$$\boxed{\frac{\rho_2}{\rho_1} = \frac{V_1}{V_2} = \frac{(\gamma + 1)M_1^2}{(\gamma - 1)M_1^2 + 2}} \tag{11.43}$$

and

$$\boxed{\frac{p_2}{p_1} = 1 + \frac{2\gamma}{(\gamma + 1)}\left(M_1^2 - 1\right)} \tag{11.44}$$

## 11.6.6   Stagnation pressure ratio

The stagnation pressure ratio across the shock can be found as follows. Using the definitions of the total temperature and pressure (equations 11.25 and 11.28), we have

$$\frac{p_{02}}{p_{01}} = \frac{p_{02}}{p_2} \cdot \frac{p_1}{p_{01}} \cdot \frac{p_2}{p_1} = \frac{p_2}{p_1}\left(\frac{T_{02}}{T_2}\right)^{\frac{\gamma}{\gamma - 1}}\left(\frac{T_1}{T_{01}}\right)^{\frac{\gamma}{\gamma - 1}}$$

Since $T_{02} = T_{01}$ across the shock,

$$\frac{p_{02}}{p_{01}} = \frac{p_2}{p_1}\left(\frac{T_1}{T_2}\right)^{\frac{\gamma}{\gamma - 1}} \tag{11.45}$$

Alternatively,

$$\frac{p_{02}}{p_{01}} = \frac{p_{02}}{p_2} \cdot \frac{p_2}{p_1} \cdot \frac{p_1}{p_{01}}$$

so that

$$\frac{p_{02}}{p_{01}} = \left(1 + \frac{\gamma - 1}{2}M_2^2\right)^{\frac{\gamma}{\gamma - 1}}\left(\frac{1 + \gamma M_1^2}{1 + \gamma M_2^2}\right)\left(1 + \frac{\gamma - 1}{2}M_1^2\right)^{\frac{1 - \gamma}{\gamma}}$$

Using equation 11.42 to eliminate $M_2$

$$\frac{p_{02}}{p_{01}} = \left[\frac{\frac{\gamma+1}{2}M_1^2}{1+\frac{\gamma-1}{2}M_1^2}\right]^{\frac{\gamma}{\gamma-1}} \left[\frac{2\gamma}{\gamma-1}M_1^2 - \frac{\gamma-1}{\gamma+1}\right]^{\frac{-1}{\gamma-1}} \qquad (11.46)$$

Equation 11.46 is plotted in Figure 11.12. The figure is very similar to that given for the height ratio across a planar hydraulic jump in Figure 10.10. The interpretation of these results requires a consideration of the entropy changes that occur.

### 11.6.7 Entropy changes

Figure 11.12 indicates that for a shock with For $M_1 > 1$ (a "compression" shock), $p_{02} < p_{01}$, and for a shock with $M_1 < 1$ (an "expansion" shock), $p_{02} > p_{01}$. We will now use the second law of thermodynamics to show that only compression shocks can occur.[6]

The entropy change across the shock is given by equation 11.17:

$$s_2 - s_1 = C_p \ln\frac{T_2}{T_1} - R \ln\frac{p_2}{p_1}$$

Since $R = C_p(\gamma - 1)/\gamma$,

$$s_2 - s_1 = C_p \ln\left[\frac{T_2/T_1}{(p_2/p_1)^{\frac{\gamma-1}{\gamma}}}\right] = C_p \ln\left[\frac{\frac{T_2}{T_{02}} \cdot \frac{T_{02}}{T_{01}} \cdot \frac{T_{01}}{T_1}}{\left(\frac{p_2}{p_{02}} \cdot \frac{p_{02}}{p_{01}} \cdot \frac{p_{01}}{p_1}\right)^{\frac{\gamma-1}{\gamma}}}\right]$$

By using the definitions of the stagnation temperature (equation 11.25) and stagnation pressure (equation 11.28), this relationship can be simplified to give a very elegant result

$$s_2 - s_1 = C_p \ln\left[\left(\frac{p_{01}}{p_{02}}\right)^{\frac{\gamma-1}{\gamma}}\right] = R \ln\frac{p_{01}}{p_{02}} \qquad (11.47)$$

---

[6]This is true for all gases obeying the ideal gas law.
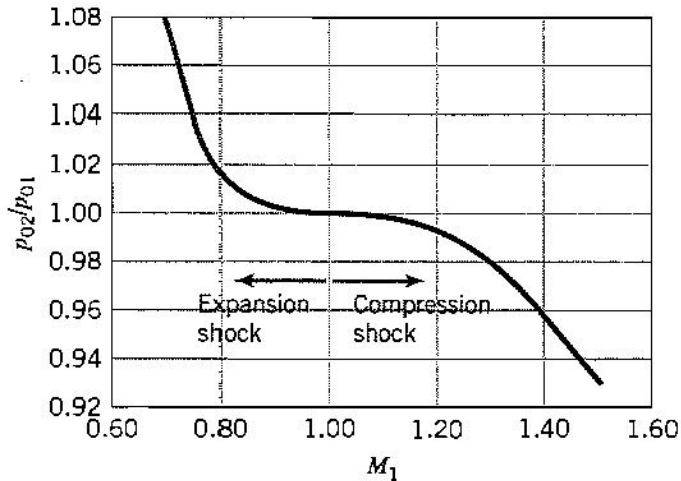


Figure 11.12: Stagnation pressure ratio across a normal shock as a function of Mach number, according to equation 11.46. Note the similarity to Figure 10.10.

Therefore the entropy change is related to the change in stagnation pressure. Since the entropy can only increase across a shock, we see that $p_{02} < p_{01}$, and Figure 11.12 indicates that $M_1$ must be supersonic. If $p_{02}$ were greater than $p_{01}$ the entropy would decrease across a shock, which is impossible.

### 11.6.8   Summary: normal shocks

The normal shock relations were derived directly from the equations of motion for one-dimensional flow. Nevertheless, some of the relations are quite complicated, and for convenience they are often presented in tabulated form (see Table Appendix-C.16). Since we are most commonly interested in air flows, the tables are given only for $\gamma = 1.4$. The compressible flow calculator available on the Web at *http://www.engapplets.vt.edu/*, can also be used.

In many problems the initial conditions are known, but we need to find the downstream conditions. In that case, equation 11.42 represents the starting point of the solution. Once $M_2$ is found using equation 11.42, all the other downstream variables can be determined using the normal shock relations. Alternatively, we can use equation 11.42 to express the normal shock relations in terms of $M_1$:

$$\frac{\rho_2}{\rho_1} = \frac{V_1}{V_2} = \frac{(\gamma + 1) M_1^2}{(\gamma - 1) M_1^2 + 2} \tag{11.48}$$

and

$$\frac{p_2}{p_1} = 1 + \frac{2\gamma}{\gamma + 1} \left(M_1^2 - 1\right) \tag{11.49}$$

The temperature rise is most conveniently found using

$$\frac{T_2}{T_1} = \frac{p_2}{p_1} \frac{\rho_1}{\rho_2} \tag{11.50}$$

and the stagnation pressure ratio can be expressed as

$$\frac{p_{02}}{p_{01}} = \frac{p_2}{p_1} \left(\frac{T_1}{T_2}\right)^{\frac{\gamma}{\gamma - 1}} \tag{11.51}$$

The entropy rise is given by

$$\frac{s_2 - s_1}{R} = \ln\left(\frac{p_{01}}{p_{02}}\right) \tag{11.52}$$

## 11.7   Weak Normal Shocks

The pressure ratio across a normal shock is given by equation 11.49. This can be written in terms of the pressure jump $\Delta p$, where $\Delta p = p_2 - p_1$, so that

$$\frac{\Delta p}{p_1} = \frac{2\gamma}{\gamma + 1} \left(M_1^2 - 1\right) \tag{11.53}$$

The ratio $\Delta p/p_1$ is often called the *shock strength*. When the shock is weak, an interesting relationship may be obtained between the shock strength and the change in entropy. Weak shocks are found when $M_1$ is close to one, and so the parameter $m$, defined by $m = M_1^2 - 1$,
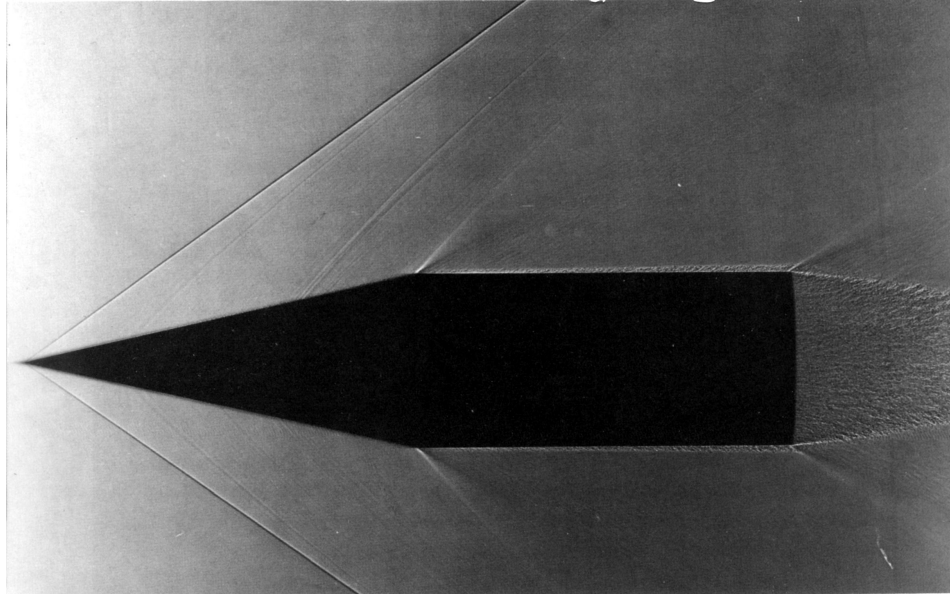
Figure 11.13: A cone-cylinder body is shot through air at Mach 1.84. Oblique shocks are formed as the flow deflects to pass over the body, and expansion fans are formed at the shoulder, and at the start of the wake. A turbulent boundary layer is visible over the main part of the body. Photograph courtesy of A.C. Charters.

is small compared to one. This allows a series expansion of the equation 11.52 in the small quantity $m$ (using equations 11.49, 11.50 and 11.51). The final result is[7]

$$\frac{s_2 - s_1}{R} \approx \frac{\gamma + 1}{12\gamma^2} \left( \frac{\Delta p}{p_1} \right)^3 \tag{11.54}$$

For the small pressure change that accompanies a weak normal shock, the entropy rise is therefore very small. A weak shock produces a nearly isentropic change of state. In the limit, a very weak shock becomes an isentropic acoustic wave, that is, a Mach wave (see Section 11.2).

## 11.8 Oblique Shocks

What happens in a supersonic flow that is not one-dimensional? For example, what happens when a supersonic flow is deflected through an angle $\alpha$? From experiment, we know that an oblique shock forms, as illustrated in Figure 11.13 for a cone-cylinder body.

The flow through a plane oblique shock may be examined using the velocity diagrams shown in Figure 11.14. We will assume that the flow upstream and downstream of the shock is uniform, and that all changes occur discontinuously across the shock.

The incoming velocity $V_1$ can be resolved into a component normal to the shock, $V_{1n}$, and a component parallel to the shock, $V_{1p}$. Similarly, we resolve the downstream velocity $V_2$ into its components $V_{2n}$ and $V_{2p}$. The angle between $V_1$ and the shock wave is $\beta$, and the deflection of the flow is $\alpha$.

Conservation of mass across the shock gives

$$\rho_1 V_{1n} = \rho_2 V_{2n} \tag{11.55}$$

---

[7]For details, see Liepmann & Roshko, *Elements of Gasdynamics*, John Wiley & Sons, 1957.

Conservation of momentum normal and parallel to the shock gives

$$p_1 + \rho_1 V_{1n}^2 = p_2 + \rho_2 V_{2n}^2 \tag{11.56}$$

and

$$\rho_1 V_{1n} V_{1p} = \rho_2 V_{2n} V_{2p} \tag{11.57}$$

From equations 11.55 and 11.57 we see that

$$V_{1p} = V_{2p} \tag{11.58}$$

This is a very useful result since it indicates that

> Any velocity change introduced by the oblique shock depends solely on the component normal to it, and the component parallel to the shock is unchanged.

## 11.8.1 Oblique shock relations

The conditions before and after the shock can now be found using the normal shock relations with the normal Mach number $M_1 \sin \beta$ replacing $M_1$. We obtain the following oblique shock relations:

$$\frac{\rho_2}{\rho_1} = \frac{V_{1n}}{V_{2n}} = \frac{(\gamma + 1) M_1^2 \sin^2 \beta}{(\gamma - 1) M_1^2 \sin^2 \beta + 2} \tag{11.59}$$

and

$$\frac{p_2}{p_1} = 1 + \frac{2\gamma}{\gamma + 1} \left( M_1^2 \sin^2 \beta - 1 \right) \tag{11.60}$$

The change in Mach number may be found by replacing $M_2$ in the normal shock relation 11.42 with the normal component $M_2 \sin (\beta - \alpha)$. That is:

$$M_2^2 \sin^2 (\beta - \alpha) = \frac{M_1^2 \sin^2 \beta + \frac{2}{\gamma - 1}}{\frac{2\gamma}{\gamma - 1} M_1^2 \sin^2 \beta - 1} \tag{11.61}$$

The relationships between the upstream and downstream variables depend only on the normal components of the Mach numbers. The incoming component must be supersonic, so that $M_1 \sin \beta \geq 1$. This condition sets the minimum wave angle for an oblique shock. The maximum angle corresponds to a normal shock, where $\beta = \pi/2$, so that

$$\sin^{-1} \frac{1}{M_1} \leq \beta \leq \frac{\pi}{2} \tag{11.62}$$

Also, the outgoing component $M_2 \sin (\beta - \alpha)$ will be subsonic since it is downstream of a normal shock, although $M_2$ can remain supersonic.
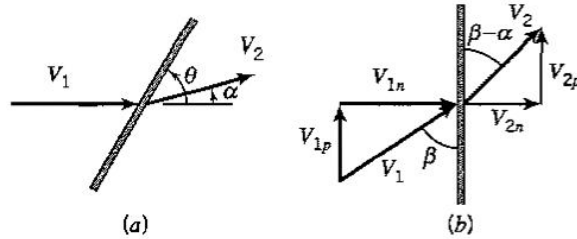


Figure 11.14: (a) Flow through an oblique shock. (b) Resolution of velocity components.
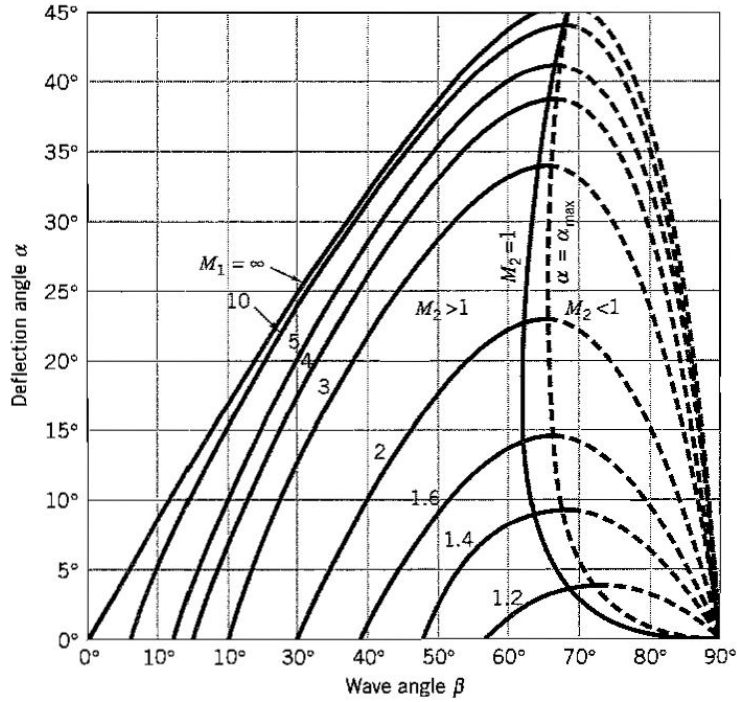
Figure 11.15: Variation of shock angle $\beta$ with turning angle $\alpha$, as a function of Mach number. Adapted from Liepmann & Roshko, *Elements of Gasdynamics*, John Wiley & Sons, 1957.

## 11.8.2 Flow deflection

From Figure 11.14 we see that

$$\tan \beta = \frac{V_{1n}}{V_{1p}}, \qquad \text{and} \qquad \tan (\beta - \alpha) = \frac{V_{2n}}{V_{2p}}$$

Since $V_{1p} = V_{2p}$ (equation 11.58), we can use equation 11.59 to show that

$$\frac{\tan \beta}{\tan (\beta - \alpha)} = \frac{\rho_2}{\rho_1} = \frac{V_{1n}}{V_{2n}} = \frac{(\gamma + 1) M_1^2 \sin^2 \beta}{(\gamma - 1) M_1^2 \sin^2 \beta + 2} \tag{11.63}$$

or, after a considerable amount of algebra,

$$\tan \alpha = 2 \cot \beta \frac{M_1^2 \sin^2 \beta - 1}{M_1^2 (\gamma + \cos 2\beta) + 2} \tag{11.64}$$

Equation 11.64 has the right limiting behavior, since $\alpha = 0$ for $\beta = \pi/2$ and $\beta = \sin^{-1}(1/M_1)$, as required by the limits given in equation 11.62. Between these two extremes where $\alpha = 0$, the deflection angle $\alpha$ must be positive, and therefore it has a maximum value somewhere, as shown in Figure 11.15. For each value of $M_1$, there is a corresponding $\alpha_{max}$, which is the maximum deflection angle for which an oblique shock solution can be found.

When $\alpha > \alpha_{max}$, however, no solution can be found. The analysis given here no longer applies. By experiment, we know that a new phenomenon occurs: the shock *detaches* from the body, so that it moves upstream away from the body, and it curves, so that portions of the shock become normal to the direction of the flow. An example is given by the bow shock shown in Figure 11.5. Downstream of a detached shock, regions of mixed supersonic

and subsonic flow occur, and the analysis becomes very complicated. Detached shocks will not be considered any further.

In addition, when $\alpha < \alpha_{max}$, there are two solutions for the shock angle $\beta$ for each value of $\alpha$ and $M_1$, one to the left of the dashed line in Figure 11.15, called the *weak solution*, and one to the right, called the *strong solution*. In solutions with the stronger shock (on the right), the flow becomes subsonic as it passes through the shock. In solutions with the weaker shock (on the left), the flow remains supersonic, except for a small range of values of $\alpha$. In practice, the solution adopted by a particular flow depends on the downstream flow condition. The weak solution is the one that is most commonly observed. Unless otherwise indicated, the weak solution is usually assumed to hold.

### 11.8.3   Summary: oblique shocks

Equation 11.64 is the key to solving many oblique shock problems: when the shock angle can be found for a given deflection angle, the other variables can be found using the normal shock relations (equations 11.48 to 11.52), or the normal shock tables (Table Appendix-C.16). It is also possible to write a short computer program to solve these relationships, even using a hand-held calculator. The compressible flow calculator provided on the web at *http://www.engapplets.vt.edu/* provides solutions to the relations for isentropic flow, normal shock and oblique shocks.

## 11.9   Weak Oblique Shocks and Compression Waves

What happens when the deflection angle for an oblique shock becomes very small? Obviously, the strength of the shock becomes weak, and the changes in temperature, density, and entropy become small. It is particularly interesting to compare the change in entropy to the change in the other variables. We will assume that the downstream Mach number remains supersonic.

If we rearrange equation 11.63, we obtain[8]

$$\frac{1}{M_1^2 \sin^2 \beta} = \frac{\gamma + 1}{2} \frac{\tan(\beta - \alpha)}{\tan \beta} - \frac{\gamma - 1}{2}$$

Further rearrangement gives

$$M_1^2 \sin^2 \beta - 1 = \frac{\gamma + 1}{2} M_1^2 \frac{\sin \beta \cos \beta}{\cos(\beta - \alpha)} \tag{11.65}$$

When the deflection angle is small, $\sin \alpha \approx \alpha$, and $\cos(\beta - \alpha) \approx \cos \beta$, so that

$$M_1^2 \sin^2 \beta - 1 \approx \left( \frac{\gamma + 1}{2} M_1^2 \tan \beta \right) \alpha \tag{11.66}$$

Also, from equation 11.64 and Figure 11.15, we see that for the cases where $M_2 > 1$

$$\tan \beta \approx \tan \alpha_M$$

That is, the angle of the shock approaches the angle of a Mach wave. Since

$$\tan \alpha_M = \frac{1}{\sqrt{M_1^2 - 1}}$$

---

[8]See Liepmann & Roshko, *Elements of Gasdynamics*, published by John Wiley & Sons, 1957.
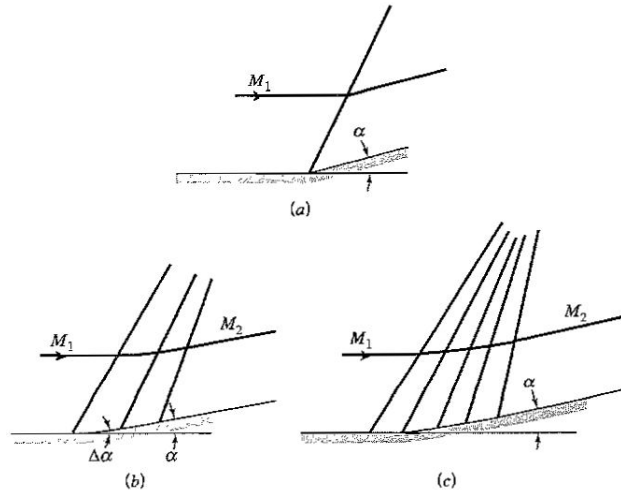
Figure 11.16: Compression of a supersonic flow by turning an angle $\alpha$. (a) Single oblique shock; (b) Series of weak compression waves; (c) Smooth, continuous turning. From Liepmann & Roshko, *Elements of Gasdynamics*, John Wiley & Sons, 1957.

(Section 11.2) then

$$M_1^2 \sin^2 \beta - 1 \approx \frac{\gamma + 1}{2} \frac{M_1^2}{\sqrt{M_1^2 - 1}} \, \alpha \qquad (11.67)$$

Equation 11.67 provides the basis for deriving all the other relationships that apply to weak oblique shocks. For example, by using equations 11.67 and 11.60, we obtain

$$\frac{p_2 - p_1}{p_1} = \frac{\Delta p}{p_1} = \frac{\gamma M_1^2}{\sqrt{M_1^2 - 1}} \, \alpha \qquad (11.68)$$

We see that the strength of the wave is proportional to the deflection angle. The changes in the other flow quantities, except entropy, are also proportional to $\alpha$. Entropy, however, is proportional to the third power of the shock strength (equation 11.54). A weak oblique shock, therefore, causes a finite change in pressure, temperature and flow angle, but these changes occur almost isentropically. In the limit of a very weak wave, all changes are isentropic, and so we can compress a flow isentropically using a succession of weak oblique Mach waves. For example, a supersonic flow can be deflected through a certain angle by a single shock [Figure 11.16(a)], and the stagnation pressure will decrease. However, if we replaced the single turn by a series of smaller turns [Figure 11.16(b)], each generating a weak oblique shock or *compression wave*, there will be almost no change in entropy or stagnation pressure. In the limit of a smooth turn, the flow is exactly isentropic [Figure 11.16(c)].

In example 12.4, a Mach 3 flow was deflected by a single shock through an angle of $10°$, and we found that the rise in entropy was equal to $0.0334 R \, m^2/s^2 K$. If instead we accomplished the same turning in 10 steps, each of $1°$, we would find that the rise in entropy was equal to $0.00033 R \, m^2/s^2 K$, that is, 100 times smaller.

We see that compression by Mach waves is an isentropic process. Therefore, if we know the Mach number at any point, all the other flow variables can be found using the isentropic flow relationships derived in Section 11.4.5. The most important relationship that we need to know, therefore, is the relationship between the Mach number and the deflection angle. That is, we need to know the function

$$\alpha = \nu \, (M) \qquad (11.69)$$
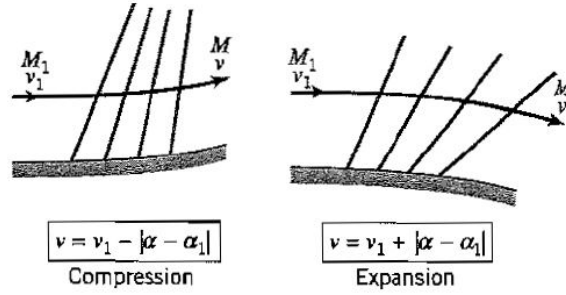
Figure 11.17: Simple isentropic deflections. (a) Compression; (b) Expansion. From Liepmann & Roshko, *Elements of Gasdynamics*, John Wiley & Sons, 1957.

This is called the Prandtl-Meyer function. It may be evaluated explicitly by finding how an infinitesimal flow deflection is related to the change in flow speed, and integrating the result for a finite deflection. The details are given in textbooks on gasdynamics and compressible flow.[9] Here we give only the final result

$$\nu\left(M\right) = \sqrt{\frac{\gamma+1}{\gamma-1}}\tan^{-1}\sqrt{\frac{\gamma-1}{\gamma+1}\left(M^2-1\right)} - \tan^{-1}\sqrt{M^2-1} \qquad (11.70)$$

For convenience, this function is tabulated in Table Appendix-C.19.

Any given supersonic flow with a Mach number $M$ has a particular value of $\nu$. To find the Mach number $M_2$ after an isentropic compression by a deflection of $\alpha$, we begin by finding the value of $\nu_1$ corresponding to the initial Mach number $M_1$. Then we find $\nu_2$ by *subtracting* the deflection angle from the upstream Prandtl-Meyer function [see Figure 11.17(a)]. That is,

$$\boxed{\nu_2 = \nu_1 - (\alpha - \alpha_1)} \qquad \text{isentropic compression} \qquad (11.71)$$

which gives $M_2$, either from equation 11.70 or Table Appendix-C.19. All other variables can then be found using the isentropic relationships (or the compressible flow calculator available at *http://www.engapplets.vt.edu/*). Note that $\nu_2 < \nu_1$, so that $M_2 < M_1$.

## 11.10   Expansion Waves

A most remarkable result can now be obtained. Since the compression by weak oblique shocks (Mach waves) is isentropic, it is *reversible*. In other words, the flow direction can be altered without violating any of the laws of thermodynamics.

It is therefore possible to describe isentropic expansions using the same Prandtl-Meyer function derived for isentropic compressions.

For an isentropic expansion, the only difference is the sign convention on $\alpha$. To determine the Mach number $M_2$ after an isentropic expansion caused by a flow deflection of $\alpha$ [Figure 11.17(b)], we find $\nu_2$ by *adding* the deflection angle to the upstream Prandtl-Meyer

[9]For example, see Liepmann & Roshko, *Elements of Gasdynamics*, John Wiley & Sons, 1957.

function [see Figure 11.17(b)]. That is,

$$\boxed{\nu_2 = \nu_1 + (\alpha - \alpha_1)} \qquad \text{isentropic expansion} \qquad (11.72)$$

Note that $\nu_2 > \nu_1$, so that $M_2 > M_1$.

## 11.11   Wave Drag on Supersonic Vehicles

The formation of shocks on vehicles traveling at supersonic speeds gives rise to a drag on the vehicle called *wave drag*. It is most easily demonstrated by considering the flow over a diamond-shaped airfoil, such as that shown in Figure 11.2. The oblique shock attached to the leading edge causes the pressure to rise above its ambient value. This pressure acts on the front part of the airfoil, and it has a resultant component in the downstream direction equal to the pressure downstream of the shock times the cross-sectional area of the airfoil, $A_c$. The flow then expands isentropically through a series of expansion waves centered on the apex of the diamond (this is called an *expansion fan*), so that the pressure drops below the ambient value, thereby augmenting the drag force on the airfoil. The wave drag is equal to the total force due to pressure differences acting on the airfoil in the streamwise direction.

The rise in pressure and its subsequent fall can be computed using the oblique shock relations and the Prandtl-Meyer function, so for the diamond-shaped airfoil the total wave drag can be computed quite easily. For three-dimensional shapes, estimating the wave drag can be very difficult, but it is very important to do it accurately since for supersonic vehicles it is the dominant source of drag.

In addition to causing drag, the wave pattern formed over the vehicle translates into a sonic boom problem on the ground. For the flow over the diamond-shaped airfoil, we see that the wave pattern impinging on the ground would consist of a shock, followed by an expansion, and then another shock attached to the trailing edge (which turns the flow back into its original direction). The pressure signal looks like the letter N (see Figure 11.18), and it is sometimes called the "N-wave." The environmental nuisance caused by sonic booms is one of the principal problems that needs to be solved before the extensive use of supersonic passenger transports becomes commonplace.
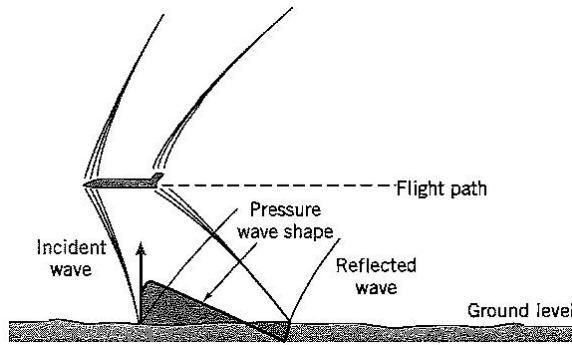


Figure 11.18: Sonic boom pattern generated by a supersonic transport. From *Compressible Flow*, M.A. Saad, Prentice-Hall, 1985.

# Chapter 12

# Turbomachines

## 12.1    Introduction

In this chapter we examine the performance and design of turbomachinery. Turbomachines are widely used in engineering applications, and many different types of machine exist. They can be classified according to whether they add energy to $(+\dot{W}_{shaft})$, or extract mechanical energy from, the fluid stream $(+\dot{W}_{shaft})$. See Figure 12.1. Pumps, fans, blowers, compressors and propellers are examples of turbomachines that add energy to a fluid, and windmills and water turbines are examples of turbomachines that extract energy from the fluid.

Turbomachines come in many different shapes, sizes and geometries, but their common feature is that they have a *rotor* or *impeller*, that is, a wheel equipped with blades. In the case of a water turbine, the fluid stream acts on the rotor blades to produce a force with a significant component in the circumferential direction, and in the case of a pump, the blades act on the fluid with a significant torque to increase the pressure of the stream.

Turbomachines are further subdivided according to the direction the exit flow takes compared to the entry flow. For example, a propeller turbine is an *axial-flow* machine since
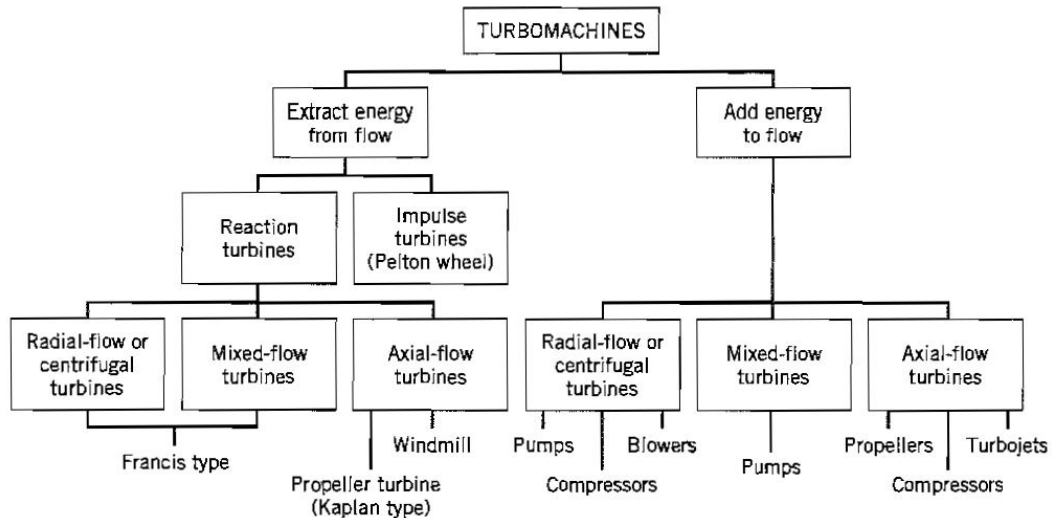


Figure 12.1: Classification of turbomachines, with examples.
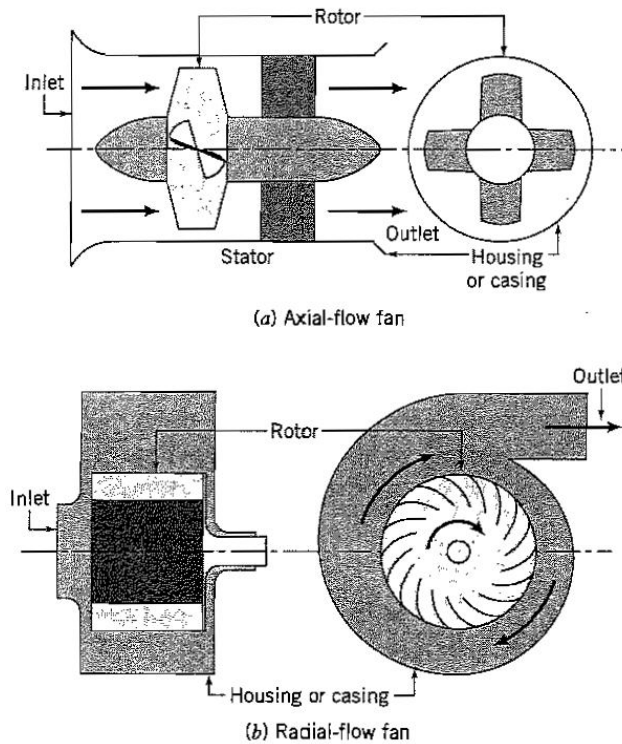
Figure 12.2: (a) Axial-flow (or propeller) turbine. (b) Radial-flow (or centrifugal) fan. Adapted from Munson, Young & Okishii *Fundamentals of Fluid Mechanics*, John Wiley & Sons, 1998.

the directions of the entry and exit flow are aligned along a common axis [Figure 12.2(a)]. The fan shown in Figure 12.2(b) is a *radial-flow* or *centrifugal* machine since the directions of the inlet end entry flow are orthogonal. There are also *mixed-flow* devices that fall somewhere in between the axial- and radial-flow machines (Figure 12.3). The design of each machine is adapted to a particular application. Sometimes a high flow rate is required, sometimes a high pressure, and at other times, a high flow rate and a high pressure are needed.

We will consider some common examples of turbomachines such as pumps, turbines, propellers and windmills. Before we analyze these particular devices, we will consider the
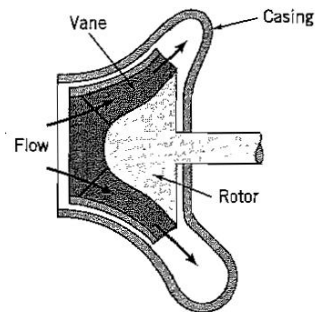


Figure 12.3: Mixed-flow pump. From John & Haberman *Introduction to Fluid Mechanics*, Prentice Hall, 1988.

underlying momentum and energy principles that apply to all turbomachinery.

## 12.2  Angular Momentum Equation for a Turbine

Since we are dealing with machines where the blades or rotors spin on an axis, angular momentum is an important variable. In Chapter 3, we applied Newton's second law to the flow of fluid through a fixed control volume to derive a linear momentum equation in integral form. Here, we will derive a similar equation for the angular momentum. The basic angular momentum principle for a system of fixed mass is

$$\mathbf{T} = \left. \frac{d\mathbf{H}}{dt} \right|_{sys} \tag{12.1}$$

where $\mathbf{T}$ is the total torque or moment applied to the system by its surroundings, and $\mathbf{H}$ is the angular momentum of the system given by the integral of the moment over all the mass in the system. That is,

$$\mathbf{H} = \int_{sys} \mathbf{r} \times \mathbf{V} \, dm = \int_{sys} \mathbf{r} \times \mathbf{V} \rho \, dv \tag{12.2}$$

($\mathbf{V}$ is the velocity of any point, and $\mathbf{r}$ is the distance of the point from the center of rotation).

We can now relate the system formulation to the fixed control volume formulation in the same way we did in deriving the continuity and linear momentum equations (see Chapter 3).[1] We consider the mass of fluid that is coincident with the control volume at time $t = 0$ (the system). At time $t + \Delta t$, the mass has moved a small distance downstream, and in terms of the control volume, there is a certain amount of angular momentum that has entered the control volume, and a certain amount that has left. In addition, if the flow is unsteady, the angular momentum of the system can change internal to the system. At the instant the system and the control volume occupy the same space, the rate of change of the angular momentum of the system is given by the sum of the unsteady rate of change of the angular momentum of the fluid contained in the control volume, and the net flux of angular momentum leaving the control volume. That is,

$$\left. \frac{d\mathbf{H}}{dt} \right|_{sys} = \frac{\partial}{\partial t} \int \mathbf{r} \times \mathbf{V} \rho \, dv + \int (\mathbf{n} \cdot \rho \mathbf{V}) \, \mathbf{r} \times \mathbf{V} \, dA \tag{12.3}$$

The sum is equal to the total torque applied to the mass of fluid that is contained in the control volume at time $t$, and so for a fixed control volume

$$\mathbf{T} = \frac{\partial}{\partial t} \int \mathbf{r} \times \mathbf{V} \rho \, dv + \int (\mathbf{n} \cdot \rho \mathbf{V}) \, \mathbf{r} \times \mathbf{V} \, dA \tag{12.4}$$

This is the integral form of the momentum equation for a fixed control volume, in a three-dimensional, time-dependent flow.

In all the applications considered here, the flow is steady and the only external torque is applied by a shaft. In that case

$$\mathbf{T}_{shaft} = \int (\mathbf{n} \cdot \rho \mathbf{V}) \, \mathbf{r} \times \mathbf{V} \, dA \tag{12.5}$$

A fixed coordinate system is chosen so that the axis of rotation of the machine coincides with the $z$-axis (Figure 12.4). The rotor spins inside an annular control volume at a fixed angular speed, $\omega$ ($rad/s$). One-dimensional flow is assumed, so that the fluid enters the

---

[1]We could also use the Reynolds transport theorem, as outlined in Section A.15.
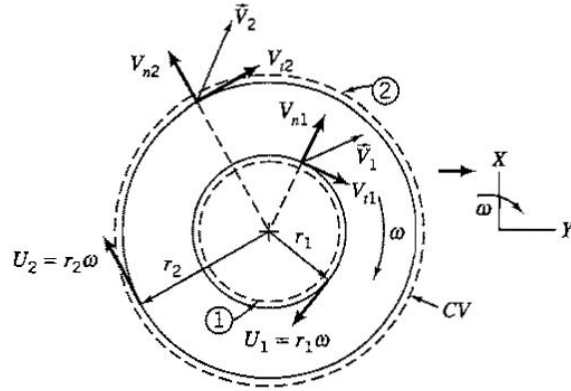
Figure 12.4: Fixed annular control volume and absolute velocity components for angular momentum analysis. From Fox & Macdonald, *Introduction to Fluid Mechanics*, John Wiley & Sons, 4th ed., 1992.

rotor at the radial location $r_1$ with a uniform absolute velocity $V_1$, and it leaves the rotor at the radial location $r_2$ with a uniform absolute velocity $V_2$. Equation 12.5 reduces to

$$
\begin{aligned}
T_{shaft}\mathbf{k} &= \int (\mathbf{n} \cdot \rho\mathbf{V})\,\mathbf{r} \times \mathbf{V}\,dA_1 + \int (\mathbf{n} \cdot \rho\mathbf{V})\,\mathbf{r} \times \mathbf{V}\,dA_2 \\
&= \rho\dot{q}\,(r_2 V_{t2} - r_1 V_{t1})\,\mathbf{k}
\end{aligned}
$$

where $\dot{q}$ is the volume flow rate and $V_{t1}$ and $V_{t2}$ are the tangential components of the absolute velocities of the fluid crossing the surface of the control volume. In scalar form

$$
\boxed{T_{shaft} = \rho\dot{q}\,(r_2 V_{t2} - r_1 V_{t1})}
\tag{12.6}
$$

The tangential velocities $V_{t1}$ and $V_{t2}$ are positive when they point in the same direction as the blade speed. This sign convention gives positive torques for machines that do work on the fluid (for example, pumps, fans, blowers and compressors), and negative torques for machines that extract work from the fluid (for example, hydraulic turbines and windmills).

Equation 12.6 is the basic relationship between torque and angular momentum for all turbomachines. It is sometimes called the *Euler momentum equation*.

The rate of work done on a turbomachine rotor, that is, the mechanical power $\dot{W}_{shaft}$, is given by $\omega T_{shaft}$, so that

$$
\dot{W}_{shaft} = \omega T_{shaft} = \rho\dot{q}\omega\,(r_2 V_{t2} - r_1 V_{t1})
\tag{12.7}
$$

We see that the mechanical power increases linearly with the mass flow rate $\dot{m} = \rho\dot{q}$, the rotational speed $\omega$ $(rad/s)$, and the change in angular momentum.

By dividing the mechanical power by $\dot{m}g$, we obtain a quantity with the dimensions of length, called the *head*:

$$
H = \frac{\dot{W}_{shaft}}{\dot{m}g} = \frac{1}{g}\,(r_2 V_{t2} - r_1 V_{t1})
\tag{12.8}
$$

## 12.3   Velocity Diagrams

We see that, to find the torque produced by or applied to a turbomachine, it is necessary to know the velocity components at the entry and exit sections. *Velocity diagrams* are used for
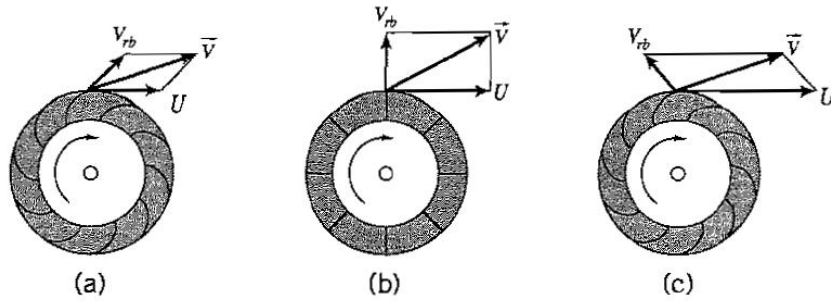
Figure 12.5: Velocity diagrams for three types of centrifugal fans. (a) Forward-curved blades; (b) flat blades; (c) backward-curved blades. **V** is the absolute velocity of air leaving the blade (shown equal for all three blade types); $V_{rb}$ is the velocity of air leaving the blade relative to the blade, $U$ is the velocity of the blade tip.

this purpose, and some examples are given in Figure 12.5 for different types of centrifugal fan. A velocity diagram is simply a vector diagram showing the relationship between the absolute and relative velocities. The symbol **V** is used for absolute velocities, $V_{rb}$ denotes a velocity relative to the blade, and $U$ is the velocity of the blade tip.

It is always assumed that the flow relative to the rotor enters and leaves tangent to the blade profile. The blade angles, $\beta$, are measured relative to the circumferential direction, as shown in Figure 12.6(a). The absolute speed of the fluid is the vector sum of the impeller velocity and the flow velocity relative to the blade, and this sum may be found graphically, as shown in Figures 12.6(b) and 12.6(c). Here, $U_1 = \omega R_1$, and $U_2 = \omega R_2$. The absolute fluid velocity makes an angle $\alpha_1$ relative to the normal direction at the inlet, and an angle $\alpha_2$ relative to the normal direction at the outlet. At each section, the normal component of the absolute velocity, $V_n$, is equal to the normal component of the velocity relative to the blade, $V_{rb_n}$.
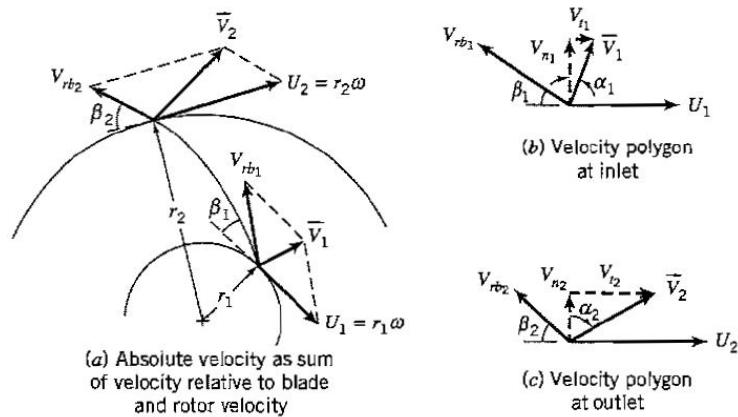


Figure 12.6: Velocity diagram for a typical radial-flow machine. From Fox & Macdonald, *Introduction to Fluid Mechanics*, John Wiley & Sons, 4th ed., 1992.

## 12.4 Hydraulic Turbines

A hydraulic turbine converts gravitational potential energy of water into shaft work. As water passes through the wheel of the turbine, which is fitted with vanes or buckets, its momentum changes. The forces resulting from this momentum change turn the wheel against some external load, causing it to do work. The difference between the initial and final water levels is called the head $H$ (see equation 12.8), and it measures the change in potential energy.[2] Different types of turbine are used, depending on the size of the available head. When the head is high (greater or equal to about $300\,m$, or $1000\,ft$), *impulse* turbines are used almost exclusively. In this design, one or more jets of water at atmospheric pressure are directed against buckets on the rim of the wheel (Figure 12.7). Most of the kinetic energy of the water is converted into work, and the discharge has just enough velocity left to clear the buckets and fall into the low-level reservoir or *tail water*. The water loses kinetic energy as it passes through an impulse wheel but it enters and leaves at the same pressure.

For lower heads, *reaction* turbines are used. Here, the flow through the wheel, or "runner," is completely enclosed by a housing, and the pressure and velocity at the exit are different from their values at the entry. There are two basic types of reaction turbines: *radial-flow* turbines and *axial-flow* turbines, which refer to the direction of water movement through the runner.

We will now examine the performance of impulse, radial-flow and axial-flow turbines in more detail.

### 12.4.1 Impulse turbine

The Pelton wheel shown in Figure 12.7 was developed in California about 1880. It is named after Lester A. Pelton (1829–1908), who developed the first efficient design. The concept

---

[2]The available head will always be greater than the head produced by the turbine because the turbine efficiency will always be less than one (see Section 12.6).
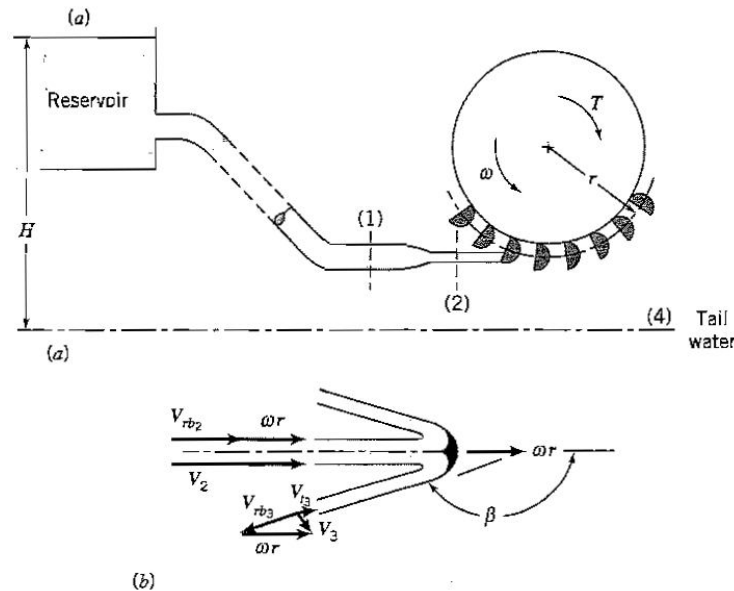


Figure 12.7: The Pelton wheel (an impulse turbine). (a) Side elevation. (b) Section through bucket. From Hunsaker & Rightmire, *Engineering Applications of Fluid Mechanics*, McGraw-Hill, 1947.

dates back to the simple water wheels used by the Sumerians. In the case of the Pelton wheel, high velocity water jets strike the buckets, which are shaped like a spoon with a central ridge. The ridge divides the impinging jet in half, and each half is deflected back through an angle of about 165°. The torque exerted on the runner is given by the change in momentum of the water.

The performance of the impulse turbine can be analyzed using the tools developed in Section 12.2. From equation 12.6, the torque is given by

$$T_{shaft} \; = \; \rho \dot{q} r \left( V_2 - V_{t3} \right) \tag{12.9}$$

where $V_2$ and $V_{t3}$ are the absolute tangential velocities, which are assumed to have the same moment arm, $r$. When there are no losses upstream of the nozzle, $V_2 = \sqrt{2gH}$, but in practice $V_2$ may be significantly less than this value.

We can also use Bernoulli's equation in this flow, but we need to follow a streamline, and we need to move with the buckets so that we are in a steady frame of reference. Since the pressure is atmospheric everywhere, and we neglect changes in height

$$\tfrac{1}{2}V_{rb_2}^2 = \tfrac{1}{2}V_{rb_3}^2$$

so that

$$V_{rb_2} = V_{rb_3}$$

where $V_{rb_2}$ and $V_{rb_3}$ are the magnitudes of the velocities relative to the bucket (see Figure 12.7). That is,

$$V_2 = V_{rb_2} + \omega r \quad \text{and} \quad V_{t3} = \omega r - V_{rb_3} \cos \left( \pi - \beta \right)$$

Therefore

$$\begin{aligned} T_{shaft} \; &= \; \rho \dot{q} r \left( V_{rb_2} - V_{rb_3} \cos \beta \right) \\ &= \; \rho \dot{q} r \left( V_2 - \omega r \right) \left( 1 - \cos \beta \right) \end{aligned} \tag{12.10}$$

Due to losses in the system, the actual torque available in practice has a maximum value of about $0.91 T_{shaft}$.

The mechanical power generated by the turbine is given by

$$\dot{W}_{shaft} \; = \; \rho \dot{q} r \omega \left( V_2 - \omega r \right) \left( 1 - \cos \beta \right) \tag{12.11}$$

In nondimensional terms,

$$C_P \; = \; \frac{\dot{W}_m}{\tfrac{1}{2}\rho \dot{q} V_2^2} \; = \; 2\xi \left( 1 - \xi \right) \left( 1 - \cos \beta \right) \tag{12.12}$$

where $C_P$ is a power coefficient and the parameter $\xi$ represents the ratio of the speed of the bucket to the absolute speed of the impinging water jet. That is,

$$\xi = \frac{\omega r}{V_2}$$

For a given value of $\beta$, the power coefficient is maximum when the speed of the bucket is half the absolute speed of the water jet, so that $\xi = 0.5$ (this can be shown by differentiating equation 12.12 with respect to $\xi$). In an actual turbine, the optimum value of $\xi$ is a little less, closer to 0.45, because of losses in the system. We also see that the maximum power coefficient is achieved when $\beta$ is as close as possible to 180°. In practice, the angle must be less than 180° since the flow must clear the following bucket. As we indicated earlier, a practical maximum is probably close to 165°.
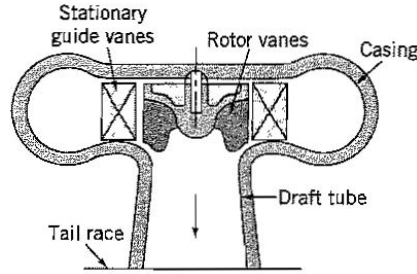
Figure 12.8: Radial-flow hydraulic turbine of the Francis type. From Fox & Macdonald, *Introduction to Fluid Mechanics*, John Wiley & Sons, 4th ed., 1992.

## 12.4.2   Radial-flow turbine

An example of a radial-flow hydraulic turbine is shown in Figure 12.8. The flow is completely enclosed in a casing, so that the pressure in the machine can be different from atmospheric. The water enters the stationary guide vanes directly from the inlet duct. The guides impart angular momentum to the water before it enters the rotating runner, where its angular momentum is reduced as work is done by the flow. This type of turbine is also known as the Francis turbine after James B. Francis, who developed it in 1849. The purely radial type shown in Figure 12.8 is suited to relatively small volume flow rates and high heads, whereas the mixed-flow type shown in Figure 12.9 works efficiently with larger volume flow rates and lower heads. Taken together, it is possible to run these machines at heads from as low as $5\,m$ to as high as $250\,m$. Efficiencies can be as high as 94%.

To analyze the performance of a radial-flow turbine, we need to find the change in angular momentum. Consider the velocity diagrams for the runner shown in Figure 12.10. For steady, one-dimensional flow, we obtain from equation 12.6

$$T_{shaft} \; = \; \rho \dot{q} \left( r_2 V_{t2} - r_{2'} V_{t2'} \right) \tag{12.13}$$

where $V_{t2}$ and $V_{t2'}$ are the absolute tangential velocities, which are assumed to have the moment arms $r_2$ and $r_{2'}$, respectively.
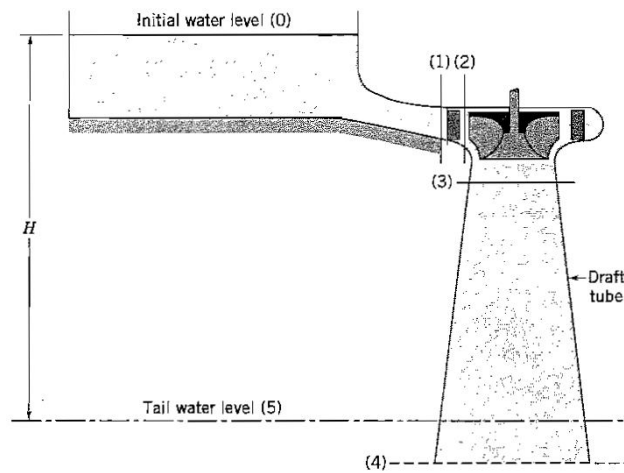


Figure 12.9: Schematic of a mixed-flow hydraulic turbine. From Hunsaker & Rightmire, *Engineering Applications of Fluid Mechanics*, McGraw-Hill, 1947.
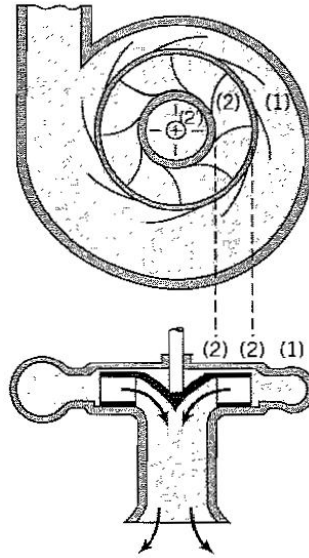
Figure 12.10: Notation for a radial-flow turbine. From Hunsaker & Rightmire, *Engineering Applications of Fluid Mechanics*, McGraw-Hill, 1947.

### 12.4.3   Axial-flow turbine

An example of an axial-flow turbine is shown in Figure 12.11. Axial-flow (or propeller) turbines are usually fitted with blades that can be adjusted to suit the operating conditions, a feature developed by a Czech engineer named Viktor Kaplan. It is more compact than the Francis type, runs faster, and it maintains a high efficiency over a broad range of conditions because of the flexibility afforded by the adjustable blades. It is more costly than the Francis type because of its greater complexity, but an efficiency of greater than 92% is possible with units up to $60,000\,hp$ capacity.

As shown in Figure 12.11, the guide vanes are arranged in the same way as in a Francis turbine, and they serve the same purpose, which is to turn the flow. Before entering the runner, however, the stream turns through a right angle and is assumed to have no radial velocity component as it passes through the runner. It is also assumed that the axial component is uniform across the outlet, and that the flow is steady. In this case, we obtain from equation 12.6 between stations 2' and 3

$$T_{shaft} \;=\; \rho\dot{q}\left(r_{2'}V_{t2'} - r_3 V_{t3}\right) \tag{12.14}$$

where $V_{t2'}$ and $V_{t3}$ are the absolute tangential velocities, which are assumed to have the mean moment arms $r_{2'}$ and $r_3$, respectively. A more detailed analysis would allow deviation from one-dimensional flow, and require the torque to be found by integration over the inlet and outlet areas.

## 12.5   Pumps

Rotary pumps, like turbines, come in three types: radial-flow or centrifugal pumps, mixed-flow or screw pumps, and axial-flow or propeller pumps (Figure 12.12). For centrifugal pumps, the inlet is typically on one side of the impeller, in line with the axis of rotation, but the flow may enter from both sides to balance the thrust. The inlet flow can be assumed to have no swirl, so that its tangential velocity is zero. Centrifugal pumps are used for high
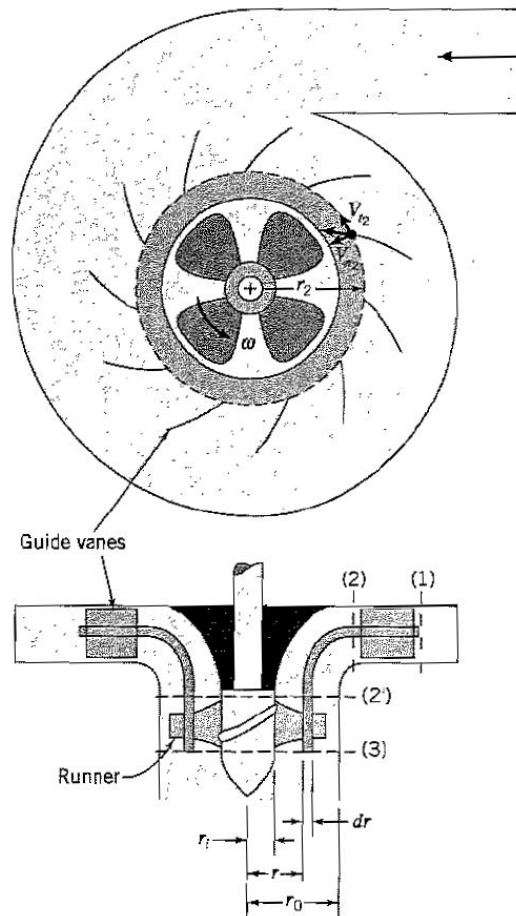
Figure 12.11: Notation for an axial-flow turbine of the Kaplan type. From Hunsaker & Rightmire, *Engineering Applications of Fluid Mechanics*, McGraw-Hill, 1947.

head ($\geq 6\,m$), low volume flow rate applications. Screw pumps have a number of screw-shaped blades, and are used for heads between 3 to $5\,m$. Propeller pumps are used for low head ($< 6\,m$), high volume flow rate applications. They also have the advantage of being able to handle solids in suspensions, and they are used to pump foodstuffs, slurries and sewage. All rotary pumps generally need *priming*, which means that if they are filled with air they cannot suck up a liquid from below their inlet.

All three types of pump are widely used in industry. However, the centrifugal pump is undoubtedly the most common of the three, and it is the only type considered here.[3]

## 12.5.1   Centrifugal pumps

As shown in Figure 12.12, a centrifugal pump has an impeller rotating within a casing. The fluid enters along the axis of rotation, moves through the impeller radially outward gaining velocity and pressure, and then discharges into the volute or diffuser, where the velocity decreases and the pressure increases. The flow leaves the impeller with a velocity which has an outward and backward component relative to the impeller. The absolute

---

[3]For a discussion on mixed-flow and axial-flow pump performance, see F.M. White, *Fluid Mechanics*, 2nd.ed., McGraw-Hill, 1986.
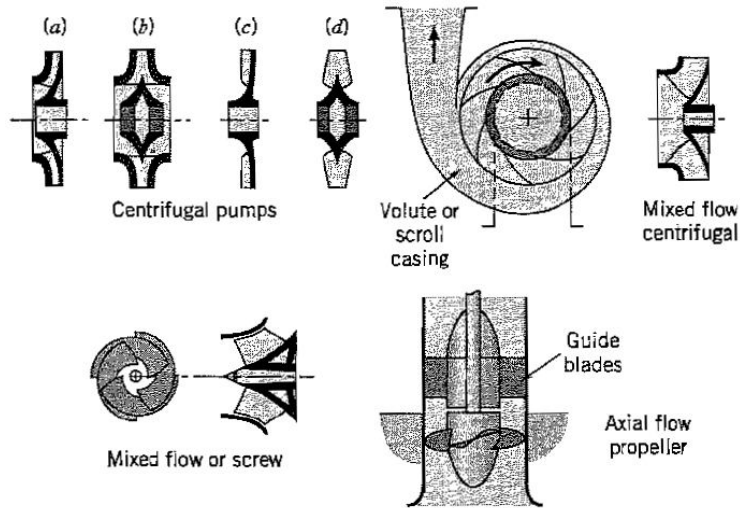
Figure 12.12: Typical pump impeller types. Adapted from Duncan, Thom & Young, *Mechanics of Fluids*, Edward Arnold, 2nd ed., 1970.

tangential component, $V_{t2}$, is then the tip speed of the impeller, $U_2 = \omega r_2$, less the tangential component of the relative velocity, $V_{rb_2} \cos \beta_2$. A typical velocity diagram is shown in Figure 12.13.

If the flow enters the impeller with purely axial absolute velocity, the entering fluid has no angular momentum and $V_{t1} = 0$. The torque is then given by equation 12.6, so that

$$T_{shaft} \;=\; \rho \dot{q} r_2 V_{t2} \tag{12.15}$$

The mechanical power input to the pump is given by:

$$\dot{W}_{shaft} \;=\; \omega T_{shaft} \;=\; \rho \dot{q} \omega r_2 V_{t2} \tag{12.16}$$

The performance of a particular centrifugal pump is shown in Figure 12.14 as a function of discharge. Performance charts are usually plotted for a constant shaft rotation speed,
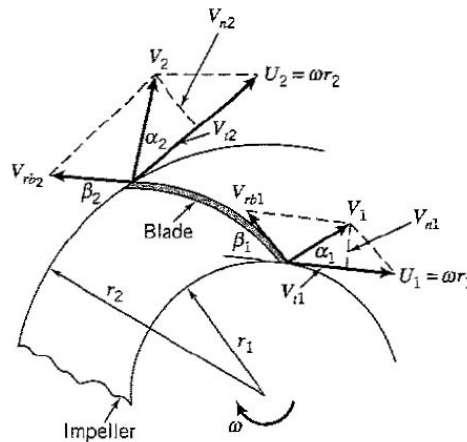


Figure 12.13: Velocity diagram at the exit from a centrifugal pump impeller.
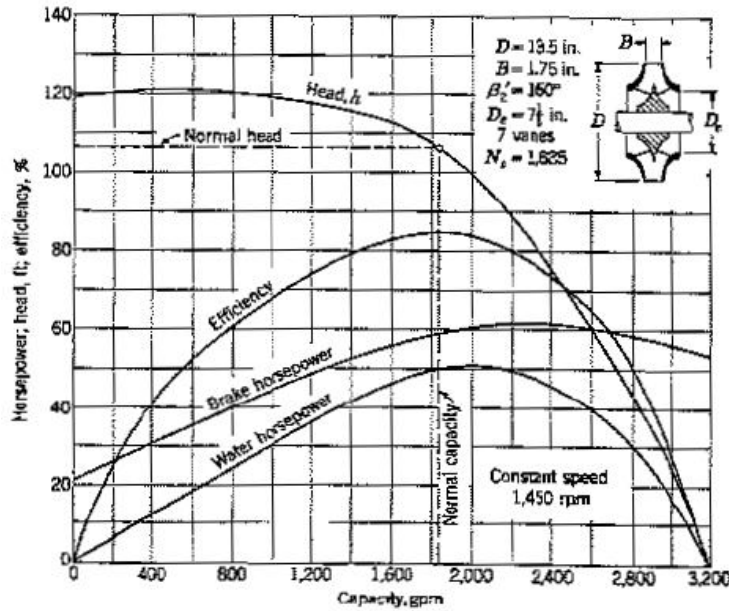
Figure 12.14: Typical characteristic performance curves for a centrifugal pump. From Daugherty, Franzini and Finnemore, *Fluid Mechanics with Engineering Applications*, 8th ed., published by McGraw-Hill, 1985.

as shown in Figure 12.15. The independent variable is the discharge or volume flow rate, $\dot{q}$, and the dependent variables are the output head, $H$, the input power, $\dot{W}_{shaft}$, and the efficiency, $\eta$ (see also Section 12.7). In practice, the variables are almost always expressed dimensionally.

## 12.5.2   Cavitation

Cavitation can occur in turbomachines when the local pressure falls below the vapor pressure of the liquid. Small bubbles of gas will form, which can have a devastating effect on the impeller. As they collapse on the impeller surface, intense pressures are developed which can cause pitting damage to the impeller, with the possibility of eventual failure of the surface material.

There are two sources of cavitation in pumps: the velocities at the tip of the impeller can produce very low pressure regions where bubbles can form, and the inlet pressures may be so low that bubbles are formed on the inlet side. The first source of cavitation can occur in hydraulic turbines, but the second source is restricted to pumps. The pump inlet is the low-pressure side where cavitation will first occur and the bubbles are then entrained into the impeller, where they can collapse and cause erosion.

Near the top of the graphs given in Figure 12.15 for centrifugal water pumps is plotted the *net positive-suction head* (NPSH), which is the head required at the pump inlet to keep the liquid at the inlet from cavitating. The NPSH is defined as

$$\text{NPSH} \;=\; \frac{p_i - p_v}{\rho g} + \frac{V_i^2}{2g} \tag{12.17}$$

where $p_i$ and $V_i$ are the pressure and velocity on the inlet side, and $p_v$ is the vapor pressure of the liquid. If the pump inlet is located a distance $h$ above the reservoir, and there are no
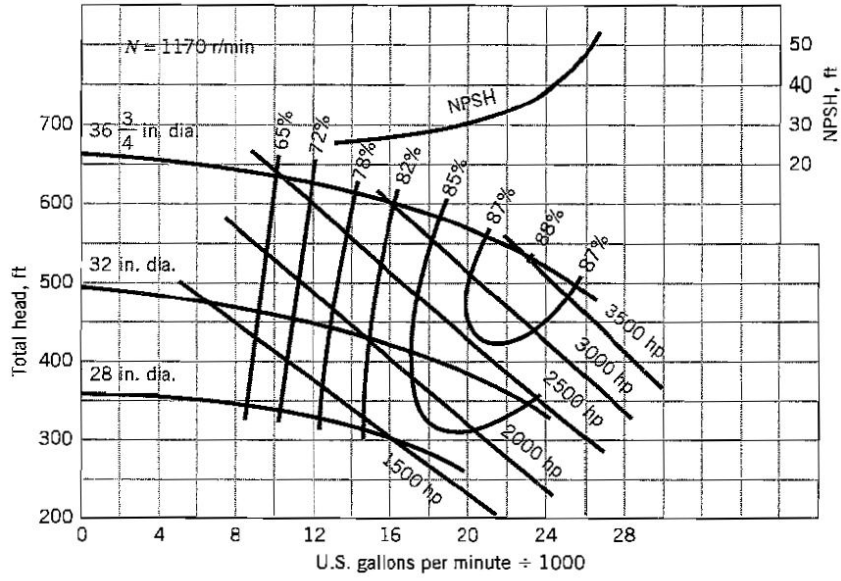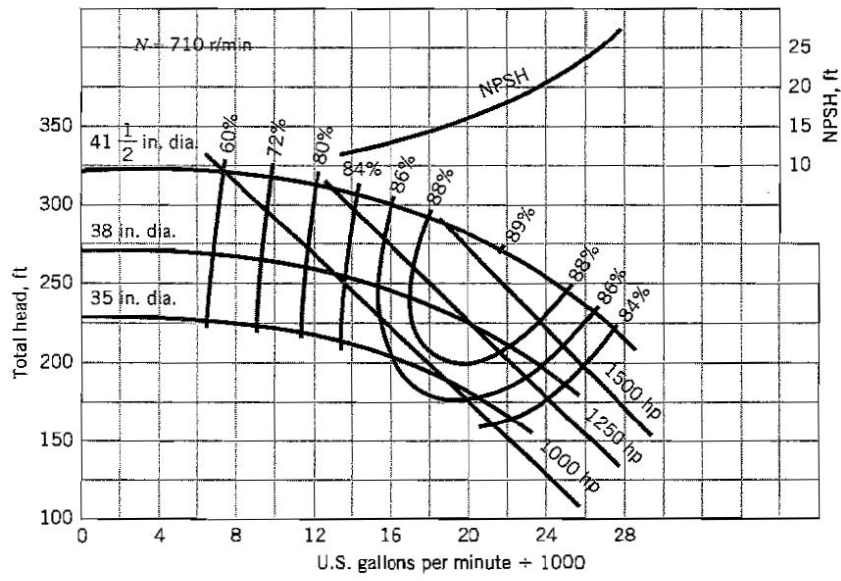
Figure 12.15: Measured performance curves for two models of a centrifugal water pump. (a) Basic casing with three impeller sizes; (b) Twenty percent larger casing with three larger impellers at slower speed. From the Ingersoll-Rand Corporation, Cameron Pump Division.

significant losses in the inlet piping, then, by Bernoulli's equation for steady flow,

$$\frac{p_i}{\rho g} + \frac{V_i^2}{2g} + h_i \;=\; \frac{p_r}{\rho g}$$

where $p_r$ is the pressure at the surface of the reservoir. That is,

$$\mathrm{NPSH} \;=\; \frac{p_r - p_v}{\rho g} - h_i$$
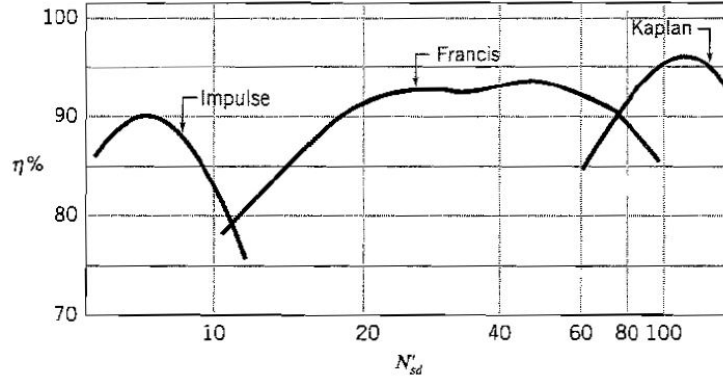
Figure 12.16: Optimum efficiency of hydraulic turbines as a function of specific speed. The specific speed $N'_{sd}$ (equation 12.21) is calculated in U.S. customary units of *rpm*, *hp*, and *ft*, so it is not dimensionless. From Munson, Young & Okishii *Fundamentals of Fluid Mechanics*, John Wiley & Sons, 1998.

As long as the machine is operated above the NPSH line, there should be no problems with cavitation at the pump inlet.

## 12.6    Relative Performance Measures

An important parameter is the efficiency of the turbine, which measures how much useful work is done compared to the theoretical maximum.

For a hydraulic turbine with a head difference $H$ (the difference between the highest and lowest water levels), there is a certain amount of ideal power available called the hydraulic power $\dot{W}_h$, given by

$$\dot{W}_h \;=\; \rho \dot{q} g H \tag{12.18}$$

and the efficiency is defined as $\eta_t = \dot{W}_{shaft}/\dot{W}_h$, so that

$$\eta_t = \frac{\dot{W}_{shaft}}{\dot{W}_h} = \frac{\omega T_{shaft}}{\rho \dot{q} g H} \tag{12.19}$$

For pumps, $\dot{W}_h$ measures the power produced by the pump and $\dot{W}_{shaft}$ the power applied to the pump, so that the efficiency is defined as $\eta_p = \dot{W}_h/\dot{W}_{shaft}$, and

$$\eta_p = \frac{\dot{W}_h}{\dot{W}_{shaft}} = \frac{\rho \dot{q} g H}{\omega T_{shaft}} \tag{12.20}$$

The optimum efficiency of turbines as a function of specific speed is shown in Figure 12.16. Here, the specific speed $N'_{sd}$ is defined by

$$N'_{sd} = \frac{N(rpm)\sqrt{\dot{W}_{shaft}(hp)}}{[H(ft)]^{5/4}} \tag{12.21}$$

and it is calculated in U.S. customary units of *rpm*, *hp*, and *ft*, so it is not dimensionless. The figure illustrates that the three different types of hydraulic turbine are suited to different operating ranges, based on the value of the specific speed.

> The specific speed is the principal factor determining the choice of turbine.

These curves may be compared to the optimum efficiencies of different pump types, which are shown as a function of specific speed in Figure 12.17. Here, the specific speed $N_s$ is defined by:

$$N_s = \frac{N(rpm)\sqrt{\dot{q}(gpm)}}{[H(ft)]^{3/4}} \tag{12.22}$$

and it is calculated in U.S. customary units of $rpm$, $gpm$, and $ft$, so it is not dimensionless. We see a very similar behavior based on the value of the specific speed: radial-flow machines are suited to low values, mixed-flow devices are suited to intermediate values, and axial-flow machines are suited to high values.

The efficiency behavior of two models of a particular commercial centrifugal water pump is shown for a range of sizes and discharge values in Figure 12.15. The behavior is quite complex, and the challenge to the designer is to design or specify the pump so that it operates as close as possible to its optimum value for its given duty cycle.

## 12.7 Dimensional Analysis

As we have seen, it is possible to derive relatively simple equations to describe the performance of turbomachines. However, the equations were obtained under the assumption of steady, one-dimensional flow, and in most cases the actual flow through a turbomachine is extremely complex. The actual performance will differ from the ideal performance through the effects of nonuniform velocity distributions, viscous losses, separation losses, and mechanical friction. To estimate the losses in a given machine, the full equations of motion need to be solved. However, an analytical approach is not generally possible. Even computer-generated solutions of the governing equations can provide only a limited set of guidelines for design purposes, and therefore new designs always need to be tested experimentally, usually by building a model. Then, in order to make predictions regarding the full-scale performance, we need to use dimensional analysis. Scale modeling, dimensional analysis,
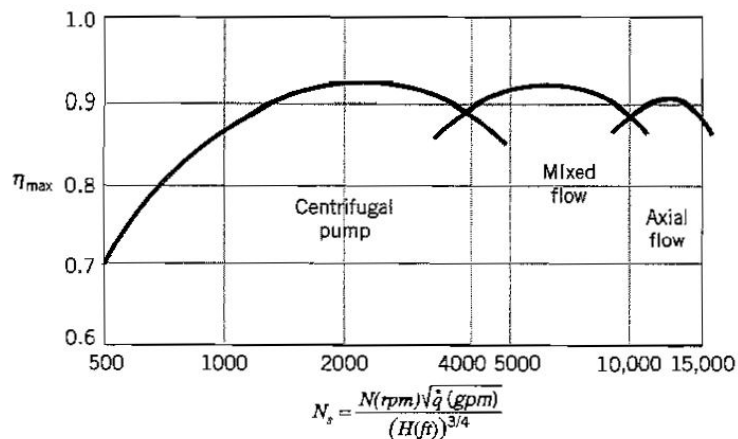


Figure 12.17: Optimum efficiency of pump types as a function of specific speed. The specific speed $N_s$ is calculated in U.S. customary units of $rpm$, $gpm$, and $ft$, so it is not dimensionless. From F.M. White, *Fluid Mechanics*, 2nd ed., McGraw-Hill, New York, 1986.

and experiment are often the only practical approaches, although a basic understanding of the underlying physical phenomena is essential.

The performance of a turbomachine is described in terms of the pressure difference across the machine $\Delta p$, the flow rate through the machine $\dot{q}$, the size of the machine (indicated by, for example, the diameter of the rotor $D$), the rotational speed $N$ (usually measured in $rev/s$ or $rps$), and the properties of the fluid, $\rho$ and $\mu$. That is,

$$\Delta p = f''(D, N, \dot{q}, \rho, \mu) \tag{12.23}$$

By dimensional analysis we obtain

$$\frac{\Delta p}{\rho N^2 D^2} = f'\left(\frac{\dot{q}}{ND^3}, \frac{ND^2}{\nu}\right) \tag{12.24}$$

The pressure difference is often expressed in terms of the total head difference $H$, where $\Delta p \sim gH$, so that

$$\frac{gH}{N^2 D^2} = f_1\left(\frac{\dot{q}}{ND^3}, \frac{ND^2}{\nu}\right) \tag{12.25}$$

Alternatively, we could write the left hand side of equation 12.24 in terms of the power of the machine $\dot{W}_{shaft}$, where $\dot{W}_{shaft} \propto \Delta p A V$, where $A$ and $V$ are a representative area and velocity, respectively. In terms of the primary variables $D$ and $N$, we could write $\dot{W}_{shaft} \propto \Delta p D^3 N$, so that

$$\frac{\dot{W}_{shaft}}{\rho N^3 D^5} = f_2\left(\frac{\dot{q}}{ND^3}, \frac{ND^2}{\nu}\right) \tag{12.26}$$

Similarly, we can write the left hand side of equation 12.24 in terms of the torque of the machine $T_{shaft}$, where $T_{shaft} \propto \Delta p A D$, so that in terms of the primary variables $T_{shaft} \propto \Delta p D^3$, and

$$\frac{T_{shaft}}{\rho N^2 D^5} = f_3\left(\frac{\dot{q}}{ND^3}, \frac{ND^2}{\nu}\right) \tag{12.27}$$

As we saw in Section 12.2, the definition of the efficiency $\eta$ depends on whether the shaft work is done on the fluid or whether the fluid does work on the shaft. For the case of a hydraulic turbine, the mechanical output power is less than the hydraulic power, so that

$$\eta_t = \frac{\rho \dot{q} \, gH}{T_{shaft} N} = f_t\left(\frac{\dot{q}}{ND^3} \frac{ND^2}{\nu}\right) \tag{12.28}$$

For a pump, the input power is greater than the hydraulic power produced, so that

$$\eta_p = \frac{T_{shaft} N}{\rho \dot{q} \, gH} = f_p\left(\frac{\dot{q}}{ND^3}, \frac{ND^2}{\nu}\right) \tag{12.29}$$

The dimensionless parameters developed here have the following names.

$$\frac{gH}{N^2 D^2} \qquad \text{head coefficient} \quad C_H$$

$$\frac{\dot{W}_{shaft}}{\rho N^3 D^5} \qquad \text{power coefficient} \quad C_P$$

$$\frac{T_{shaft}}{\rho N^2 D^5} \qquad \text{torque coefficient}$$

$$\frac{\dot{q}}{ND^3} \qquad \text{flow coefficient} \quad C_Q$$

$$\frac{g(\text{NPSH})}{N^2 D^2} \qquad \text{suction-head coefficient} \quad C_{HS}$$

$$\frac{ND^2}{\nu} \qquad \text{Reynolds number}$$

Here, $N$ is usually measured in $rev/s$, not $rad/s$. Note that the power coefficient defined here differs from that given in equation 12.12 by the exclusion of some dimensional constants such as $\frac{1}{2}$ and $\pi$.

An additional dimensionless parameter called the *specific speed* $N_s''$ can be formed by dividing the flow coefficient by the head coefficient and taking the square root

$$N_s'' = \frac{\sqrt{\frac{\dot{q}}{ND^3}}}{\sqrt{\frac{gH}{N^2 D^2}}} = \frac{N\sqrt{\dot{q}}}{(gH)^{\frac{3}{4}}} \qquad \text{specific speed} \qquad (12.30)$$

From equation 12.25 we then have

$$N_s'' = \frac{N\sqrt{\dot{q}}}{(gH)^{\frac{3}{4}}} = f_4\left(\frac{\dot{q}}{ND^3}, \frac{ND^2}{\nu}\right) \qquad (12.31)$$

The parameter $N_s''$ is nondimensional , but the quantities $N_{sd}'$ and $N_s$, defined by equations 12.21 and 12.22, are not.

The Reynolds number for most turbomachines is large, even for scale models, so that turbulent flow will usually occur in the model and the prototype. In that case, it has been found that the effects of viscosity can be neglected. It is generally assumed, therefore, that

$$\frac{gH}{N^2 D^2} = g_1\left(\frac{\dot{q}}{ND^3}\right) \qquad (12.32)$$

$$\frac{P}{\rho N^3 D^5} = g_2\left(\frac{\dot{q}}{ND^3}\right) \qquad (12.33)$$

$$\frac{T}{\rho N^2 D^5} = g_3\left(\frac{\dot{q}}{ND^3}\right) \qquad (12.34)$$

$$\eta_{t,p} = g_{t,p}\left(\frac{\dot{q}}{ND^3}\right) \qquad (12.35)$$

These functional relationships provide the basis for model testing, presenting experimental data, and for presenting performance data. It is not uncommon, however, to see mixed dimensionless and dimensional parameters being used to describe the performance of pumps and turbines, as shown in Figure 12.17 describing the average efficiency of commercial water pumps.

To demonstrate the scaling laws for pump performance, the dimensional data given in Figure 12.15 are replotted in nondimensional form in Figure 12.18. The collapse of the data is reasonably convincing, especially for the power and suction-head coefficients. The nondimensional curves can then be used to scale a wide variety of pumps of the same family, as long as the performance does not depart too far from the range covered by the original experimental data.

## 12.8 Propellers and Windmills

Another topic of interest is the performance of propellers and windmills. They are considered separately from pumps and turbines, in that they usually operate in a free flow, that is, they are usually unshrouded.

Propellers and windmills are devices that use airfoil sections to change the fluid pressure in order to produce a force, and the change in pressure occurs because the fluid momentum changes. The blade of an airplane propeller, for example, has an airfoil cross-section at each radial position. The speed of rotation is proportional to the radius, and therefore the
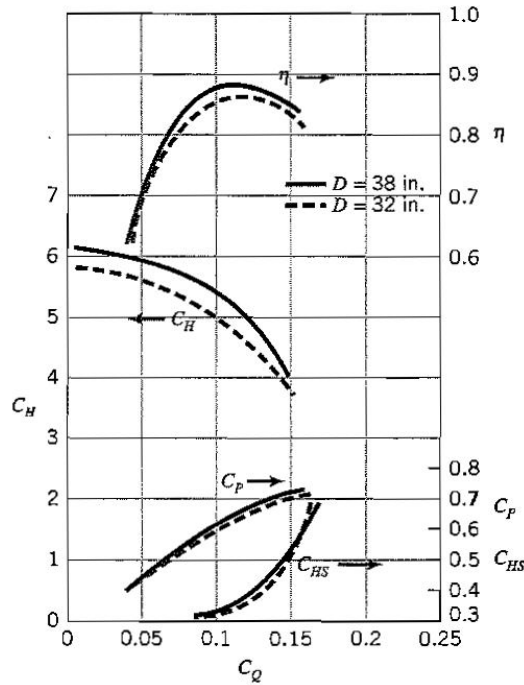
Figure 12.18: Nondimensional plot of the pump performance data given in Figure 12.15. These data are not representative of other pump designs. The coefficients are evaluated using $N$ in $revs/s$. From F.M. White, *Fluid Mechanics*, 2nd ed., McGraw-Hill, 1986.

direction of the resultant velocity also changes with radial distance. The propeller blade is twisted so that the angle of attack stays within the design limits of the airfoil, and that lift is produced efficiently at each section. The blades that drive a simple cooling fan are also a type of propeller, but they are usually made of a twisted sheet of metal or plastic to reduce costs. Ship propellers, on the other hand, need to be designed for maximum thrust while limiting the tip speed to avoid cavitation (Figure 7.1).

A propeller increases the fluid momentum, and a windmill decreases it, but the analysis of their performance is very similar and only the direction of the resultant force is different. We begin our analysis of a propeller by assuming that the force due to pressure differences accelerates the flow in the axial direction without swirl, and that flow friction can be neglected. Under these assumptions, we can find the thrust and relative speed $V$ across the propeller. Let $F$ be the force exerted by the propeller on the fluid (Figure 12.19). Relative to the propeller, the velocity of the flow far upstream is $V_1$. We choose a frame of reference moving with the propeller (we need to move at a velocity $V_1$), so that the flow is steady with respect to the observer. The fluid is assumed to be incompressible, and the propeller sweeps out an area $A$.

The propeller draws fluid in over an area larger than $A$, and expels it over an area smaller than $A$. If we draw the streamlines that bound the fluid flow through the propeller, we define a *slipstream* boundary. The volume defined by the slipstream boundary and the areas 1 and 4, where the flow velocity is parallel and in the streamwise direction, is often used as the control volume for the analysis of a propeller or windmill ($CV1$). A second control volume is used to enclose the propeller itself ($CV2$). This volume is approximated to be rectangular. Under the assumption of one-dimensional flow, the continuity and $x$-momentum equations
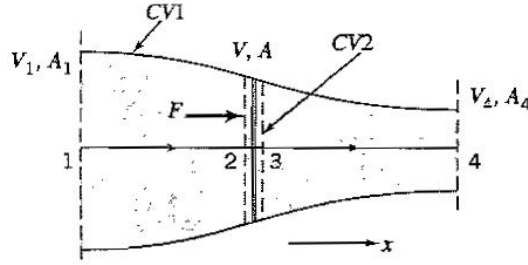
Figure 12.19: Control volume for a propeller.

for $CV2$, are

$$\rho V_2 A = \rho V_3 A$$

$$\text{and} \quad F + p_2 A - p_3 A = -\rho V_2^2 A + \rho V_3^2 A$$

respectively. The continuity equation gives $V_2 = V_3$: there is no jump in velocity across the propeller, only a jump in pressure. Hence,

$$F = (p_3 - p_2) A$$

Bernoulli's equation cannot be applied across $CV2$ because the propeller increases the energy of the flow (the pressure rise does work on the flow). However, for $CV1$, Bernoulli's equation applies between sections 1 and 2, and between sections 3 and 4. So

$$p_1 + \tfrac{1}{2}\rho V_1^2 + \rho g h_1 = p_2 + \tfrac{1}{2}\rho V_2^2 + \rho g h_2$$

$$p_3 + \tfrac{1}{2}\rho V_3^2 + \rho g h_3 = p_4 + \tfrac{1}{2}\rho V_4^2 + \rho g h_4$$

The pressure on the slipstream boundary will assumed to be equal to atmospheric pressure so that $p_1 = p_4 = p_a$. Also, from continuity, $V_2 = V_3(= V)$, and if we neglect hydrostatic head differences across the streamlines (this is reasonable if they are small compared to $p_3 - p_2$), then

$$\tfrac{1}{2}\rho V_1^2 = p_2 + \tfrac{1}{2}\rho V^2$$

and

$$p_3 + \tfrac{1}{2}\rho V^2 = \tfrac{1}{2}\rho V_4^2$$

Therefore

$$p_3 - p_2 = \tfrac{1}{2}\rho \left( V_4^2 - V_1^2 \right)$$

and

$$F = \tfrac{1}{2}\rho \left( V_4^2 - V_1^2 \right) A \tag{12.36}$$

If we now apply the continuity and $x$-momentum equations between sections 1 and 4 on $CV1$, we obtain, respectively,

$$\rho V_1 A_1 = \rho V_4 A_4 = \dot{m}$$

and

$$F = (-\dot{m}) V_1 + (+\dot{m}) V_4 = \dot{m} (V_4 - V_1) \tag{12.37}$$

Eliminating $F$ from equations 12.36 and 12.37, we find

$$V = \tfrac{1}{2} (V_1 + V_4) \tag{12.38}$$

so that the velocity through the propeller disk is just the average of the velocities at stations upstream and downstream of the propeller. In other words, there is the same increase of velocity ahead of the propeller as there is behind it.

Finally, consider the power required to drive the propeller. The work done by the propeller is equal to the thrust $F$, multiplied by a distance. In a time $\Delta t$, the propeller moves a distance $V_1 \Delta t$, and so the work done per unit time (= the power $\dot{W}_{shaft}$), is given by:

$$\dot{W}_{shaft} = FV_1 = \dot{m}\left(V_4 - V_1\right)V_1$$

The rate of change in the kinetic energy of the slipstream between sections 1 and 4, $P_{KE}$, is given by the mass flow rate times half the difference in the velocities squared, so that

$$P_{KE} = \tfrac{1}{2}\dot{m}\left(V_4^2 - V_1^2\right)$$

(see Section 3.3). The ideal efficiency of the propeller is then given by

$$\eta_{prop} = \frac{P}{P_{KE}} = \frac{V_1}{V}$$

and since $V > V_1$, the efficiency of an ideal propeller is always less than 100% (actual ship and airplane propellers approach 80%).

The magnitude of the thrust produced by a windmill is the same as that calculated for a propeller, but it acts in the opposite direction. The average velocity through the windmill is still given by equation 12.38, but since the windmill reduces the kinetic energy of the flow, the rate of change in the kinetic energy is now given by

$$P_{KE} = \tfrac{1}{2}\dot{m}\left(V_1^2 - V_4^2\right)$$

For a windmill, $V_1$ is the undisturbed wind speed.

The efficiency for a windmill is defined by comparing the rate of change of the kinetic energy produced by the windmill $P_{KE}$ to the kinetic energy flux through a streamtube of undisturbed flow, equal in area to the area of the windmill itself. This energy flux, $P_{KEF}$, is given by

$$P_{KEF} = \tfrac{1}{2}\rho V_1 A V_1^2$$

The ideal efficiency of a windmill is then given by

$$\eta_w = \frac{P_{KE}}{P_{KEF}} = \frac{\left(V_1 + V_4\right)\left(V_1^2 - V_4^2\right)}{2V_1^3}$$

The maximum efficiency is found by differentiating $\eta_w$ with respect to $V_4/V_1$ and setting the result equal to zero. This gives a maximum efficiency of 59.3%.[4] Because of friction and other losses, this efficiency is not found in practice: the highest possible efficiency for a real windmill appears to be about 50% (Figure 12.20), but example 13.3 shows that the traditional Dutch windmill operates at an efficiency of only about 15%.

In this analysis we have made a number of assumptions. In particular, we assumed that the pressure on the slipstream boundary was equal to atmospheric pressure. At the same time, we assumed that the pressures over sections 2 and 3 were different from atmospheric, which leads to a mismatch in pressures at the tips of the propeller. In reality, the pressure cannot be uniform over the propeller disk.

An alternative control volume is sometimes used to avoid these difficulties. Here, a cylindrical control volume is used with a very large diameter (Figure 12.21). The following boundary conditions are then applied: (1) the pressure is atmospheric on the control volume

---

[4]Glauert, H. Airplane Propellers. *Aerodynamic Theory*, Vol. IV, ed. W.F. Durand. Published by Dover Publications, New York, 1963.
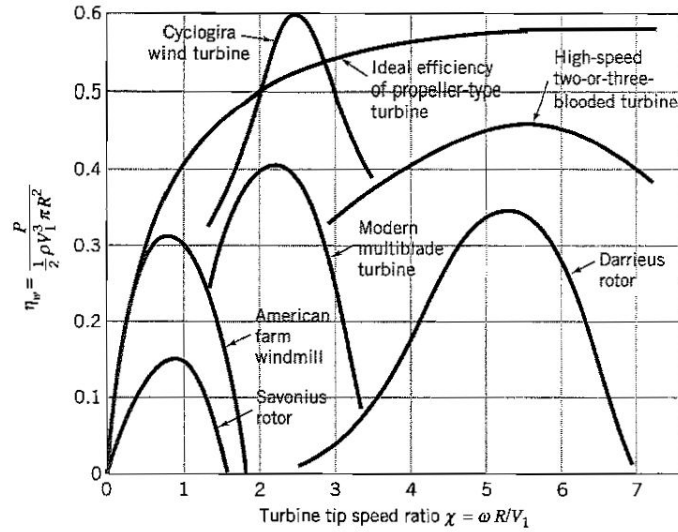
Figure 12.20: Efficiency trends for wind turbine types ($\eta_w$) versus tip speed ratio $\chi$ ($= \omega R/V_1$). From Baumeister, T., Avallone, E.A. and Baumeister, T. III, eds., *Mark's Standard Handbook for Mechanical Engineers*, 8th. ed. McGraw-Hill, New York, 1986.

surface; (2) there is negligible flow across the cylindrical part of the control volume surface, and (3) the change of fluid momentum outside the slipstream boundary is negligible. The first assumption seems reasonable, since the effects of pressure die off as velocity squared. However, even if the flow velocities $v_c$ across the area $A_c$ of the cylindrical part of the surface are very small, the product $v_c A_c$ may still be important. Also, the change in momentum of the fluid outside the slipstream boundary may not be negligible. It turns out that the error in the second assumption cancels out the error in the third assumption, and the same answer is obtained as in our original analysis. In fact, it can be shown that these two assumptions are equivalent to that made for the boundary conditions on the slipstream boundary control volume $CV_1$.

## 12.9 Wind Energy Generation

We saw that the theoretical upper limit on the efficiency of a propeller is 100%, so that in the absence of losses, in an ideal flow, all the energy supplied by the propeller is converted
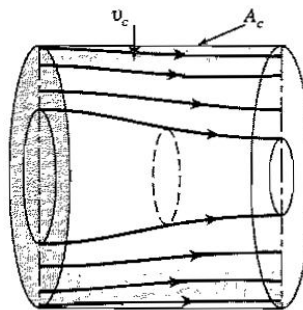


Figure 12.21: Alternative control volume for a propeller.

into flow energy. In contrast, the efficiency of a windmill is limited to about 59%, and in practice it is often much less. This limits the generation of power using wind turbines, and great efforts have been made to improve the efficiency and performance of wind turbines.

The conventional wind turbine is mounted horizontally, and a vane is used to align the propeller with the wind direction. Vertical axis machines, such as the Savonius rotor and the Darrieus turbine, have the advantage that their operation is independent of the wind direction. The Savonius rotor consists of two curved blades forming an S-shaped passage for the airflow, and the Darrieus turbine has two or three airfoils attached to a vertical shaft (Figures 12.22). They are typically shaped so that under load the stress distribution is constant along the length of the airfoil. The maximum efficiency of a Savonius rotor is only about 15%, whereas the Darrieus turbine has a superior maximum efficiency of about 32%, but the Darrieus turbine is not self starting.

The efficiency of a wind turbine $\eta_w$ is a strong function of the tip speed ratio $\chi$, which is the ratio of the maximum speed seen by the blade (which occurs at the tip of a propeller blade) and the speed of the incoming air stream. That is,

$$\chi = \frac{\omega R}{V_1} \tag{12.39}$$

where $\omega$ is the rotation rate in $rads/s$, $R$ is the radius of the turbine, and $V_1$ is the wind speed. Figure 12.20 illustrates that each type of wind-powered system has a corresponding tip speed ratio for maximum efficiency.

There are three main difficulties in designing a wind-powered generating system. First, the wind strength and direction continually change. The variation in the wind direction is not a severe problem, because the machine can be designed to be self-aligning, but the variation in the wind strength is. The variation in average wind strength in the United States is illustrated in Figure 12.23, and locations with little or no prevailing wind strength are obviously not suitable for producing wind energy. On the other hand, "runaway" can occur when storms produce unusually strong winds. The rotor can then begin to turn at such high speeds that the material strength limits are exceeded and the blade elements fail. A governor is required to limit the rotation rate, or the blades can be designed to twist, so that at high wing loading corresponding to high wind speeds the blades produce less lift and runaway is prevented.

Perhaps the most severe shortcoming due to variable wind strength is the long-term variations that result in power output. This is not a particular limitation for pumping water from a well, where a large reservoir is used to average out the fluctuations in the water flow. However, when the windmill is used to generate electricity, a battery storage
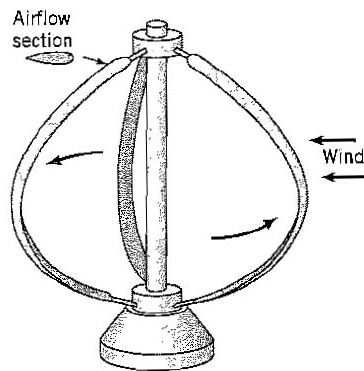


Figure 12.22: Darrieus rotor. From Baumeister, T., Avallone, E.A. and Baumeister, T. III, eds., *Mark's Standard Handbook for Mechanical Engineers*, 8th. ed. McGraw-Hill, New York, 1986.
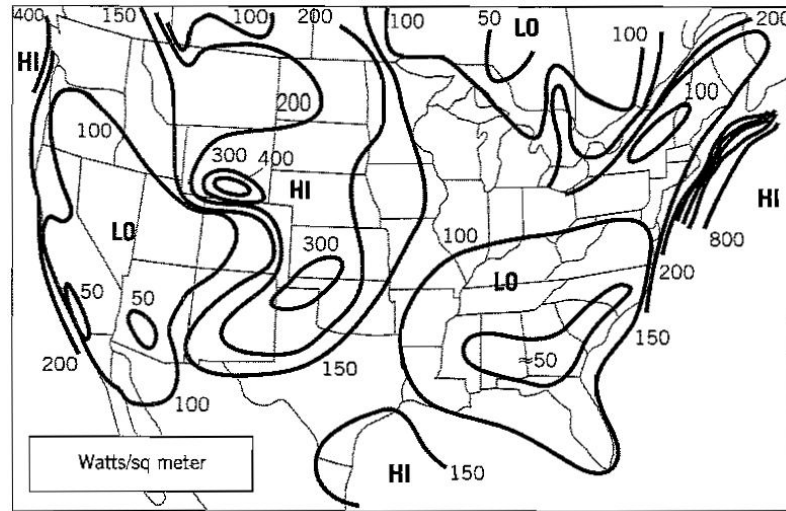
Figure 12.23: Annual average available wind power in the U.S.A, in $W/m^2$. From Baumeister, T., Avallone, E.A. and Baumeister, T. III, eds., *Mark's Standard Handbook for Mechanical Engineers*, 8th. ed. McGraw-Hill, New York, 1986.

system is required, or the windmill must be combined with another source of electricity (such as a fossil-fuel driven system) to produce a constant power output. In commercial systems, the wind-driven system is usually connected to a "grid," that is, a common distribution system which receives energy from a variety of sources and regulates and distributes the power supply to the customers. Alternatively, the irregular power output from the windmill can be used to pump water to a reservoir located on top of a nearby hill, and then a water-powered turbine can be used to generate electricity in response to the demand.

The second difficulty in designing a wind-powered generating system is that the flow energy contained in the wind is rather low. For example, if we took a wind speed of $15\,m/s$ (about $33\,mph$, a rather stiff breeze), and a rotor diameter of $3\,m$ (about $10\,ft$), we find that the maximum power available (with a theoretical maximum efficiency of 59.3%) is given by

$$\text{max theoretical power} \;=\; \tfrac{1}{2}\eta_w \rho V_1^3 \pi R^2 \;=\; 8.49\,kW$$

which is enough to run a typical house. However, the average power generated by this system will be much lower because of variability in the wind speed and the much lower efficiencies found in actual systems. There are great benefits to increasing the size of the rotor; doubling the rotor diameter will increase the power by a factor of four. However, the static stresses in the blades due to wind loads will double and the deflection will increase by a factor of eight. With rotation, the static load will be augmented by the inertia force due to the centripetal acceleration. At any location along the blade, this force is proportional to $(\omega R)^2/R = \omega^2 R$, so that it increases linearly with the size and quadratically with the rotational speed. We see that the size and rotation rate of a wind-powered turbine are limited by the possibility of material failure, and to generate significant amounts of electricity a large number of machines will be required. Such wind "farms" exist, and a large scale example is located east of San Francisco (see Figure 12.24).

The third difficulty is that the rotational speeds generated by common wind turbines are not well matched to generator speeds. Generators in the United States are typically designed to run at $3600\,rpm$, to produce alternating electric current at $60\,Hz$. If we choose a high-speed two-bladed design, operating at peak efficiency, we see from Figure 12.20 that the tip speed ratio $\chi$ should equal about 5.5. For the example given earlier, we will need a

Figure 12.24: Wind farm located in Altamont Pass, near Livermore, CA. Maximum power output is $5\,MW$ at a wind speed of $15\,mph$. Courtesy U.S. Department of Energy.

rotational speed $\omega = V_1 \chi / R = 55\,rads/s = 525\,rpm$. So, even if the wind speed was constant at $15\,m/s$, a speed-up gearbox will be required. The variability of the wind speed will mean that the gearbox will need to operate over a large speed range, and that the frequency of the alternating current will vary with wind speed. Consequently, a considerable amount of control and regulation circuitry is necessary for the output to be useful for running standard appliances, or to be acceptable to a grid.

# Chapter 13

# Environmental Fluid Mechanics

## 13.1    Atmospheric Flows

The understanding of wind flows and atmospheric transport processes is crucial to, for example, the ability to predict and quantify the dispersion of pollutants in the atmosphere, estimating the greenhouse effect, and predicting the weather.

The atmosphere is made up of two basic layers: the *troposphere* and the *stratosphere*. In the troposphere, the temperature decreases linearly with height (the slope of the curve is called the *lapse rate*), whereas in the stratosphere the temperature remains approximately constant with height. The lapse rate, and the height of the troposphere, vary with time and location but the U.S Weather Service has compiled a set of average conditions over the United States at $40°$ N latitude called the U.S. Standard Atmosphere.

According to this standard atmosphere, which does not necessarily give an accurate description of the atmosphere at any one time or place, the stratosphere extends from sea level to a height of $11\,km$ $(36,000\,ft)$, with a lapse rate of $6.50°\,K/km$ (called the *standard lapse rate*). The stratosphere begins at the top of the troposphere and extends to an altitude of $32.2\,km$ $(106,000\,ft)$, and its temperature is constant at $216.7°\,K$ $(-56.5°\,C)$ up to an altitude of $20.1\,km$ $(66,000\,ft)$.[1] The troposphere contains 80 to 85% of the total mass of the atmosphere and virtually all of its water, and therefore it plays the major role in determining our weather and climate. Above $20.1\,km$, the temperature gradually increases with height, due to the absorption of the sun's infrared radiation by ozone, which is formed by the intense ultraviolet radiation from the sun. It is also this absorption by ozone that protects living things on earth from the destructive effects of ultra-violet rays. The temperature profile of the U.S. Standard Atmosphere is shown in Figure 13.1.

To put these altitudes into perspective, Mount Everest has a height of about $29,000\,ft$ $(8840\,m)$, long range airplanes travel near the top of the troposphere at about $35,000\,ft$ $(10,670\,m)$, and Concorde traveled well into the stratosphere at about $56,000\,ft$ $(17,070\,m)$. Most clouds appear at heights less than about 10 to $12\,km$ so that they are mainly confined to the troposphere, although occasionally the top of particularly large clouds may extend to $18\,km$ or higher.

The atmosphere extends well beyond the stratosphere, but the air densities become very small. For example, at the top of the stratosphere the density is only 1% of the sea level value. Vehicles traveling in the upper reaches of the atmosphere (called the *ionosphere*) experience very low density conditions where the continuum approximation may no longer apply.

---

[1]Some authors consider the stratosphere to extend only up to $20.1\,km$, so that it is confined to the region of constant temperature.
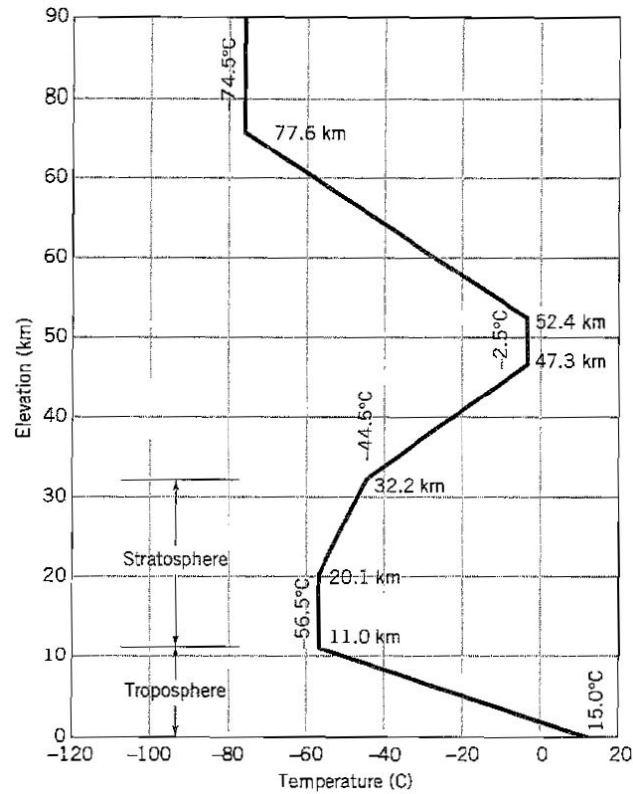
Figure 13.1: Temperature variation with altitude in the U.S. Standard Atmosphere. Data from *The U.S. Standard Atmosphere*, U.S. Government Printing Office, Washington, D.C., 1976.

## 13.2    Equilibrium of the Atmosphere

The lower part of the atmosphere, that is, the troposphere, is constantly being mixed by convection.[2] Water vapor is taken up and then precipitated, and there are great movements of polar air and of tropical air into the temperate regions. In the tropics, due to the intense heating of the ground, air is rising. This produces a general large scale circulation of air from the temperate regions toward the tropics (*trade winds*) and a drift near the top of the troposphere from the tropics toward the poles. Cold air from the higher levels will settle toward the ground to maintain continuity. This convective mixing of the atmosphere is due to unequal heating of the earth's surface, caused by the variation of solar intensity with latitude and by the unequal heat-absorption characteristics of land and water areas. As a result, the troposphere is kept in some relatively stable thermal and mechanical equilibrium which determines our climate. Departures from this equilibrium are what we know as weather. Weather varies from day to day or even from hour to hour in an irregular manner.

Climate is the average weather at a given place at a particular time of year, over many seasons, and climatology predicts from past records the safe date for planting crops, for example. Meteorology predicts tomorrow's weather from a knowledge of the present condition of the atmosphere near a given locality.

The fundamental nature of convection suggests that the lower atmosphere should have an approximately adiabatic temperature gradient. Air next to the ground that is heated

---

[2]The material in this section was adapted from *Engineering Applications of Fluid Mechanics*, by J.C. Hunsaker & B.G. Rightmire, McGraw-Hill, 1947.
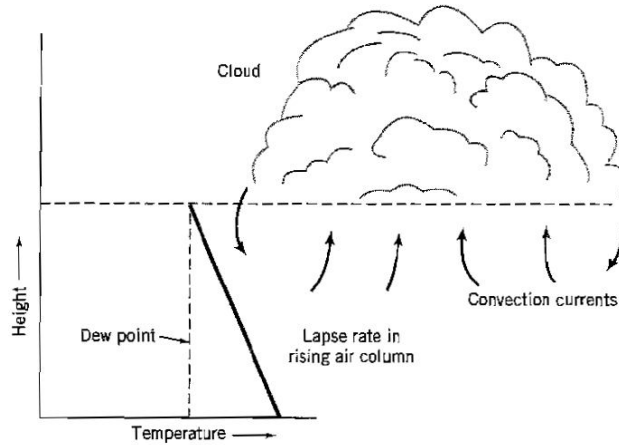
Figure 13.2: Cloud formation by condensation of water vapor carried upward in a rising column of air. Hunsaker & Rightmire 2.23, p.51

more in one place than in another will rise like warm air in a chimney. Colder and denser air will flow in to take its place. The rising air will cool almost adiabatically, for air is a poor conductor. To find this cooling rate, we start with the hydrostatic equation ($dp/dz = -\rho g$) and use the thermodynamic relationships given for adiabatic, inviscid flow (that is, isentropic flow) by equation 11.18. We obtain the *adiabatic lapse rate*:

$$\text{adiabatic lapse rate } = \left(-\frac{dT}{dz}\right)_{ad} = \frac{\gamma - 1}{\gamma R}\, g \tag{13.1}$$

which is equal to $0.00098°C/m$ for dry air.

It is interesting to observe that the natural temperature lapse rate makes for stability of the lower atmosphere; that is, an air mass, displaced vertically for some reason, tends to return to its original level. Consider a mass of air rising by convection because it became slightly unstable at ground level due to local heating. This air will cool at the adiabatic lapse rate of $0.98°C$ per $100\,m$. At any level, however, it will be subject to the same pressure as the surrounding atmosphere. Hence, since the usual atmospheric lapse rate is less than the adiabatic lapse rate (it is only $0.65°C$ per $100\,m$), the displaced air mass will be denser than its surroundings and will tend to fall back.

Usually, the air is stable, and large-scale convection does not occur. However, when the atmospheric lapse rate exceeds the adiabatic rate, the air is unstable. Thunderstorms arise in an unstable atmosphere in which the lapse rate is temporarily excessive from abnormal heating of the ground and the lower levels of the air. This condition frequently occurs in summer. In winter, when the ground is covered with snow, the lower levels are cold, the lapse rate is small, and the air is likely to be stable. On a clear summer night the ground cools quickly by radiation, and the lower level of air may become cooler than that lying above it. Here the lapse rate may be zero or even reversed. This is called a *temperature inversion* and makes for great stability.

The formation of cumulus clouds and thunderstorms is a result of instability. Warm, moist air next to the ground becomes unstable and rises, cooling adiabatically until the *dew point* is reached, when condensation of water vapor creates a cloud (see Figure 13.2). If the initial uprush is violent, the rising air may overshoot its equilibrium altitude. If there is an inversion or a stable layer of air at this elevation, further upward motion is stopped. However, if the upper air is neutral or slightly unstable, the latent heat released by condensation may be enough to carry the convection current to greater heights. As we

indicated earlier, storm clouds have been found to extend up to $50,000\,ft$, although the air is usually clear above $20,000\,ft$.

Air motion is invariably turbulent, and clouds are usually turbulent also. The Reynolds number is based on an approximate characteristic dimension of the cloud such as its height or width (both are generally of the same order). With a cloud dimension of about $500\,m$, and a characteristic internal motion of $5\,m/s$, then with $\nu = 10^{-5}\,m^2/s$ (it is approximately the same for water vapor as it is for air), the Reynolds number $= (500 \times 5)/10^{-5} = 2.5 \times 10^8$. It is no surprise that clouds always have a turbulent appearance.

## 13.3    Circulatory Patterns and Coriolis Effects

The sun, the earth, and the earth's atmosphere form one very large dynamic system. The differential heating of the air gives rise to horizontal pressure gradients, which in turn lead to horizontal motions in the atmosphere.[3] The temperature difference between the atmosphere at the poles and at the equator, and between the atmosphere over the continents and over the oceans, causes the large-scale motions of the atmosphere. Local winds, such as lake breezes, are also caused by temperature differences. The land surface generally heats and cools faster by radiation than a large body of water, and so during the day the air tends to rise over the land, causing the air to move from the water to the land. At night, the land surface cools at a faster rate so that the air over the land gradually becomes cooler and more dense than that over the water, and the movement of air is from the land to the water.

If the earth were not rotating, air would normally tend to flow down the pressure gradient, that is, from regions of higher pressure to lower pressure. The flow would be perpendicular to the isobars (contours of constant pressure). However, the rotation of the earth prevents this from happening, at least on the scale of large weather patterns. If we are an observer located in a rotating reference frame, such as we are on earth, there are apparent forces that can act, in addition to the effects of pressure gradient, gravity, and viscous forces. The most important is the *Coriolis* force.

The "truest" inertial frame is the distant stars. On the earth's surface, we are actually accelerating because of the motion about the sun, the spinning of the earth about its axis of rotation, and by other motions we are not aware of. The most important of these is the spin, being 365 times greater than the angular velocity about the sun. So the center of the earth is a good choice as an *inertial* reference frame ($[X, Y, Z]$ in Figure 13.3).

The positions, velocities and accelerations that we see (fixed to the earth's surface) are not those seen by an observer fixed to the earth's center. For many applications, the difference between the two reference frames is negligible. The differences are evident only on a large scale, such as in atmospheric and oceanic movements.

We can develop expressions for the equations of motion with reference to the earth's surface, and we will see that we can add a term to Euler's equation that represents an "apparent" acceleration and treat it mathematically and conceptually as a force.

The earth spins on its axis from west to east, so that the rotation looking down from the North Pole is counterclockwise (see Figure 13.3). If the angular velocity vector of the earth's rotation is $\vec{\Omega}$, that is equal to the angular rotation of a particle of fluid at a latitude of $\beta$, and we know that $\Omega = 2\pi\,rad/day$. The angular momentum of the particle per unit mass relative to the inertial frame of reference (the earth's center) will be $\mathbf{r} \times \mathbf{V}$, where $\mathbf{r}$ is the radius of rotation and $\mathbf{V}$ its velocity, where $\mathbf{V} = \vec{\Omega} \times \mathbf{r}$. Since $\mathbf{r}$ is measured from the axis of rotation, $r = R\cos\beta$, where $R$ is the radius of the earth ($= 6380\,km$).

---

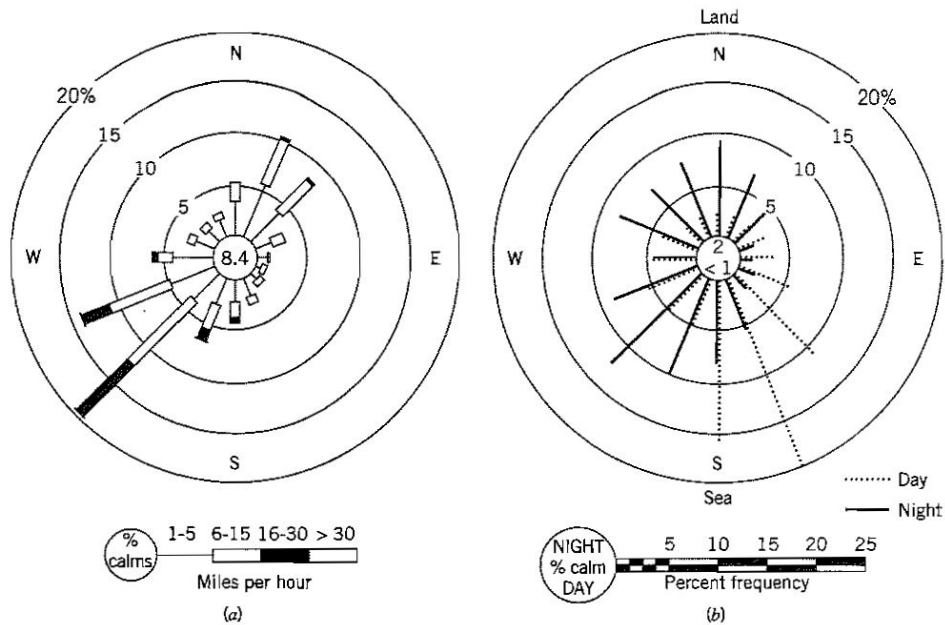[3] *Air Pollution: Its Origin and Control*, K. Wark, C.F. Warner & W.T. Davis, published by Addison-Wesley, 1998.
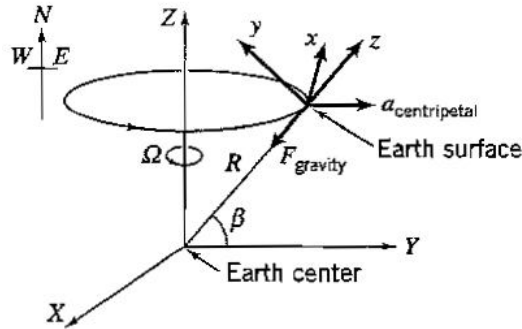
Figure 13.3: Coordinate system for the earth spinning around its axis. $XYZ$ is the inertial coordinate system with its origin at the center of the earth, and $xyz$ is the local coordinate system at the latitude $\beta$ (at the equator, the latitude is zero). $R$ is the radius of the earth.

A particle in the northern hemisphere, moving in the northerly direction, will be moving toward the axis of rotation. In the absence of friction, angular momentum will be conserved, and the fluid will acquire a greater angular velocity since its radius is decreasing ($\beta$ increases). This is the familiar effect seen when a spinning skater pulls in his arms to increase her rate of rotation. So a north-bound particle will deflect to the right (the east) in the northern hemisphere. A south-bound particle acquires a lower angular velocity to conserve angular momentum, and it will deflect to the west.

We can also consider motions in the east-west direction, at a constant latitude. A particle in the northern hemisphere, moving in the easterly direction, will increase its angular velocity. To conserve its angular momentum, it will experience a tendency to move to a larger radius of rotation; it is deflected to the right (to the south). Similarly, a west-bound particle will have a lower angular velocity and experience a tendency to deflect to the north to conserve angular momentum.

The overall result of these Coriolis effects is to create clockwise circulatory patterns for the northern hemisphere, and counter-clockwise circulatory patterns for the southern hemisphere. This is true for the atmosphere, and for the oceans. Coriolis effects are the dominant mechanisms controlling these circulatory patterns, and therefore they effectively control weather patterns.

To see how the Coriolis effects enter into the equations of motion, we note that the acceleration of a particle (fluid or otherwise) near the earth's surface in the earth's inertial reference frame can be written as the sum of a number of accelerations seen by an observer on the earth's surface in the $[x, y, z]$-coordinate system (where the positive $z$-direction is in the direction of increasing altitude). These include the rectilinear acceleration, the centripetal acceleration, and the Coriolis acceleration, $2\vec{\Omega} \times \mathbf{V}$. The centripetal acceleration is usually very small for motions in the atmosphere, and therefore the acceleration of a fluid particle in the inertial reference frame (based on the earth's center) is given by the sum of its acceleration in the local reference frame plus the Coriolis acceleration. That is,

$$\frac{D\mathbf{V}}{Dt} + 2\vec{\Omega} \times \mathbf{V}$$

If we ignore viscous effects, we obtain

$$\frac{D\mathbf{V}}{Dt} + 2\vec{\Omega} \times \mathbf{V} = -\frac{1}{\rho}\nabla p - \mathbf{g}$$

or

$$\frac{D\mathbf{V}}{Dt} = -2\vec{\Omega} \times \mathbf{V} - \frac{1}{\rho}\nabla p - \mathbf{g} \tag{13.2}$$

An apparent force, the Coriolis force, appears in the equations of motion due to the earth's rotation. Since the vertical velocities are typically much smaller than the velocities in the horizontal plane, we have

$$2\vec{\Omega} \times \mathbf{V} = -f_c v\mathbf{i} + f_c u\mathbf{j}$$

where $f_c$ is the Coriolis parameter defined by

$$f_c = 2\Omega \sin\beta \tag{13.3}$$

On earth, $0 \leq f_c \leq 1.44 \times 10^{-4}\, s^{-1}$.

If we non-dimensionalize equation 13.2 (as we did with the Navier-Stokes equation in Section 7.7), we find that the Coriolis term becomes

$$\left(\frac{2\sin\beta}{Ro}\right)\mathbf{V}'$$

where $\mathbf{V}'$ is the velocity non-dimensionalized by the characteristic velocity scale $V_0$, and

$$Ro = \frac{V_0}{\Omega L}$$

This is the Rossby number, which measures the importance of the inertia force relative to the Coriolis force. For a typical $40\,km/hr$ wind, for the Rossby number to be of order one, the Coriolis force must act over a characteristic distance $L$ of about $150\,km$. As it acts over a greater and greater distance, the Coriolis effect becomes more and more important.

For example, in the atmosphere the boundary layer thickness varies bewteen $200\,m$ and $1\,km$ (see Section 13.4). Outside this region, in the *free layer*, friction is negligible under "normal" conditions. In the free layer, without Coriolis effects, the acceleration term in the momentum equation is balanced by the force due to pressure differences, and the flow tends to be in the direction of the pressure gradient (from high to low pressure). However, in the simplest possible wind system, that of straight uniform flow, there is no acceleration and the force due to pressure differences is balanced by the Coriolis force. So the velocity vector is turned at right angles to the direction of the pressure gradient. Streamlines are therefore almost *parallel* to the isobars. This is called *geostrophic balance*. It follows that in the atmosphere the pressure in a uniform flow is always higher to the right (looking downstream).

Geostrophic balance approximates the conditions found at altitudes a few hundred meters or more above the surface of the earth. Except in the case of very light winds, the direction and magnitude of the actual winds at this height generally do not differ by more than $10°$ and $20\%$, respectively, from their geostrophic values. For this reason isobaric maps can be used to determine wind speed and direction. The isobars yield direction, and the magnitude of the gradient (the distance between the isobars, which are also streamlines) determines the speed.

When the wind follows a curved path, the centripetal acceleration needs to be taken into account. This effect is only important near the center of high- or low-pressure region where the isobars have significant curvature. The wind then deviates from its geostrophic value and is called the *gradient wind*.

Within the earth's boundary layer, that is, at heights less than a few hundred meters, viscous effects become important. In particular, the variation of horizontal velocity with height also produces Coriolis effects which vary with height, and the wind direction near the earth's surface will be skewed from its geostrophic or gradient direction.

## 13.4    Planetary Boundary Layer

The nature of the terrain, the location and density of the trees, the location and size of lakes, rivers, hills, and buildings strongly affects the velocity distribution in the atmospheric
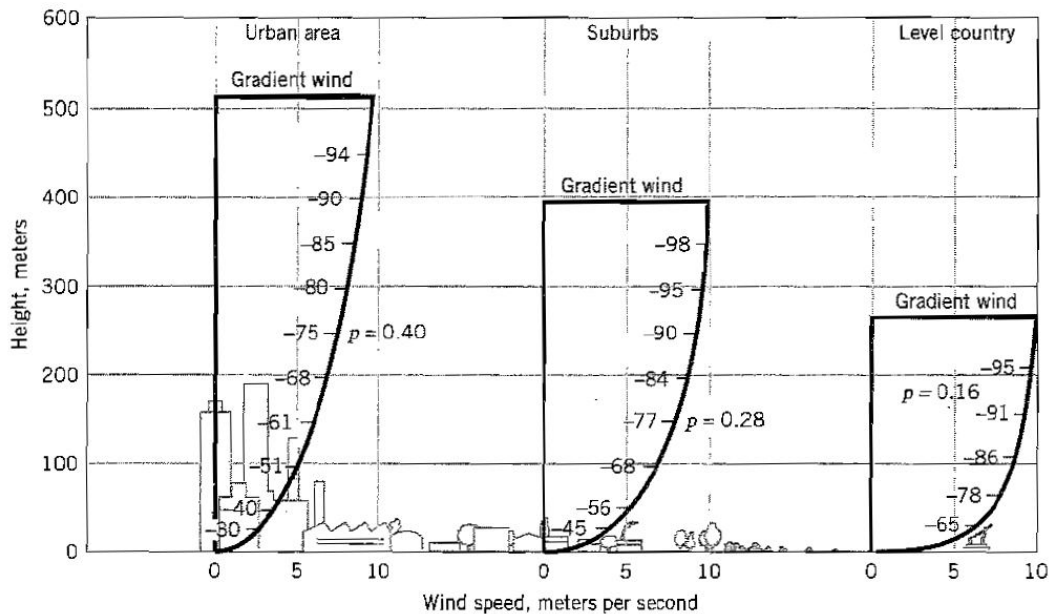
Figure 13.4: Effect of terrain roughness on the planetary boundary layer velocity profile. From *Air Pollution: Its Origin and Control*, K. Wark, C.F. Warner & W.T. Davis, Addison-Wesley, 1998.

or *planetary* boundary layer.[4] The depth of the boundary layer can vary from a few hundred meters to several kilometers, and it is greater for unstable conditions than for stable conditions.

The general effect of terrain roughness on the velocity profile is shown in Figure 13.4. In this particular example, the change in the overall boundary layer thickness is from approximately $500\,m$ to $280\,m$, for decreasing roughness. Because of the change in wind speed with height, any wind speed value must be quoted with respect to the elevation at which it is measured. The international standard height for surface wind measurements is $10\,m$. The profile is often modeled as a power law similar to that given in Section 9.4 for a flat plate turbulent boundary layer. When the lapse rate is approximately adiabatic and the terrain is generally level with little surface cover, the exponent $p$ is approximately 0.15, which is close to the 1/7th value used in Section 9.4, but it can vary widely depending on the roughness and the stability of the atmosphere.

The variation in wind profile is important for a number of reasons, but it is felt most directly in the approach of an airplane to a landing strip. The speed of the airplane relative to the wind speed determines its lift and drag performance, but the speed of the airplane relative to the ground dictates its landing pattern. The wind speed naturally decreases with altitude due to the presence of the planetary boundary layer, and this needs to be taken into account by the pilot. The rapid variation in the wind profile close to the ground adds to the difficulty in judging the approach.

# 13.5   Prevailing Wind Strength and Direction

The large-scale circulatory patterns in the atmosphere are modified by local conditions, which can vary with time. For example, in the mid-latitudes, in the free layer of the

---

[4] *Air Pollution: Its Origin and Control*, K. Wark, C.F. Warner & W.T. Davis, published by Addison-Wesley, 1998.

Figure 13.5: (a) A typical wind rose representation of wind-speed data. (b) A day-night wind rose for New York City showing diurnal effect of the sea breeze. From *Air Pollution: Its Origin and Control*, K. Wark, C.F. Warner & W.T. Davis, Addison-Wesley, 1998.

atmosphere, the air currents meander, forming the zonal currents which are a type of wave motion. Nevertheless, there are recurring patterns, which help to set the average conditions at any location. At any particular time, in any given season, we have expectations for the average condition including the temperature, precipation, and the prevailing wind strength and direction. Charts are available for most locations indicating the prevailing wind strength and direction, averaged over many years, as shown by the example given in Figure 13.5. In addition, data are available for maximum wind conditions, rainfall rate, and snow deposits, which are important for designing buildings and providing services such as storm drains. Such data are often incorporated in building codes or national standards for drainage systems or other services.

The prevailing wind conditions provide vital information for other purposes as well. Predicting the probable distribution by air currents of a toxic emission from an industrial site requires the use of charts such as that shown in Figure 13.5. Choosing the location of a wind turbine and predicting its likely power output, requires similar data, as do long-distance sailing and tracking weather balloons.

## 13.6    Atmospheric Pollution

Atmospheric pollution is a very broad term, which describes the dispersion of airborne particles and reactive agents, and their chemical interaction in the presence of sunlight. Here, we are concerned with the dispersion of airborne particles and other material, of which there is a great variety.

Airborne particles are produced by two very different mechanisms.[5] The larger particles are fragments of still larger ones which, through weathering, mechanical breakage, solution,

---

[5]V.J. Schaefer and J.A. Day, *A Field Guide to the Atmosphere*, The Peterson Field Guide Series, published by Houghton Mifflin, 1981.

or some other attrition process, finally become small enough to float in the atmosphere when lifted up by the wind. These particles may sometimes be reduced in size to $1\,\mu m$ or smaller, but when found in the air are generally $5\,\mu m$ or larger, the smaller ones may be joined to the larger ones by adhesion, electrical forces, or surface tension. Many of these larger particles are of natural origin, although some are of human origin, resulting from processes such as the production of cement, quarrying and strip mining.

The other major mechanism of small-particle formation begins in the vapor phase and proceeds by condensation, crystalization, or related mechanisms. The cooling of hot saturated or supersaturated vapor, the combination of chemicals, photolytic reactions, and other condensation processes typically produce such particles. Their sizes range from molecular clusters of $0.001$ to $0.003\,\mu m$ to about $1\,\mu m$. In the presence of high temperatures and a rich source of condensable material, as in a volcano or the exhaust gases from a coal-burning power plant, some particles can grow to sizes considerably larger than $1\,\mu m$.

The largest airborne particles may be in the air for minutes or hours. The intermediate sizes are likely to be suspended for hours or days, and the smallest particles may reside in the atmosphere for weeks, months, and even years. All particles in the atmosphere will tend to fall to the ground under its own weight. In the absence of air resistance, a particle experiences a constant acceleration of $g$, and its velocity increases linearly with time. As its velocity increases, however, the aerodynamic drag increases. If we ignore the buoyancy, then at some point the drag force will balance the weight of the particle, and the particle reaches a constant velocity called the *terminal velocity*. The terminal velocity $V_p$ of a spherical particle of radius $R$ may be found from an equilibrium force balance, where

$$\rho_p g \tfrac{4}{3}\pi R^3 = \tfrac{1}{2}\rho_a V_p^2 \pi R^2 C_D \tag{13.4}$$

where $\rho_p$ is the density of the particle material, $\rho_a$ is the air density, and $C_D$ is the particle drag coefficient. Small particles settle very slowly, and therefore their Reynolds numbers are typically much less than one. Stokes showed analytically that the drag coefficient for spheres for Reynolds numbers less than one is given by:[6]

$$\text{drag force} \;=\; 6\pi R \mu V_p$$

or

$$C_D \;=\; \frac{24}{Re} \tag{13.5}$$

where the Reynolds number is based on the diameter. Flows at these low Reynolds numbers are dominated by viscous effects, and they are often called *creeping* flows (see Figure 9.14). Equation 13.4 becomes

$$V_p = \frac{2\rho_p g R^2}{9\mu}$$

A particle of soot, for example, with $R = 1\,\mu m$ and a density similar to that of pure carbon ($\rho_p = 1,600\,kg/m^3$) has a terminal velocity in air at sea level of $0.02\,mm/s$, which is equal to $1.7\,m/day$. We see that small particles are extremely slow to settle to the ground once they have become airborne. Their terminal velocity increases with size. Larger particles may have Reynolds numbers considerably larger than one, and Stokes' drag law (equation 13.5) will not apply. In that case, the terminal velocity may be found using equation 13.4, in combination with the results given in Figure 9.14.

# 13.7    Dispersion of Pollutants

The dispersion of pollutants in the lower atmosphere is greatly aided by thermal convection and turbulent mixing. Buoyancy effects determine the depth of the convective mixing layer, called the *maximum mixing depth* (MMD). The MMD is the height where a thermally

---

[6]Stokes, G. *Transactions of the Cambridge Philosophical Society*, **8**, 1845; **9**, 1851.
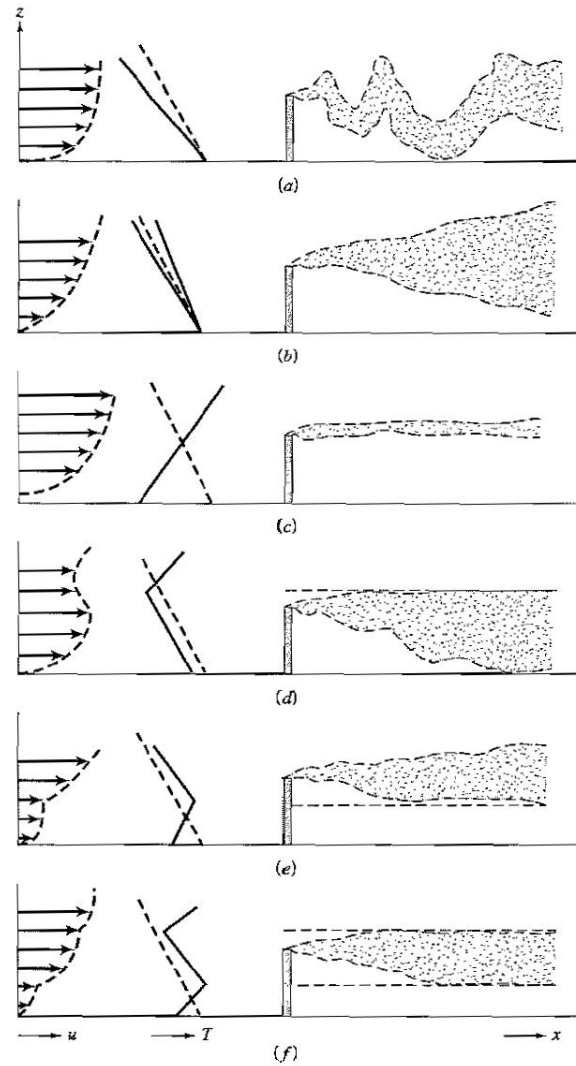
Figure 13.6: Typical velocity profile, temperature profile, and plume shape for various atmospheric conditions ( ——— ambient lapse rate; − − − − dry adiabatic lapse rate). (a) Strong instability; (b) Near neutral stability; (c) Surface inversion; (d) Inversion above stack; (e) Inversion below stack; (f) Inversion below and above stack. From *Air Pollution: Its Origin and Control*, K. Wark, C.F. Warner & W.T. Davis, Addison-Wesley, 1998.

heated fluid particle will stop rising, and it is given approximately by the intersection of the air temperature profile with the adiabatic lapse line. When the atmosphere is very stable, so that the air temperature increases with altitude, the MMD can be very small. These temperature inversions can produce very high pollution levels in urban areas.

Turbulence in the atmosphere is usually defined as the fluctuations in velocity with frequencies greater than 2 cycles per hour ($0.6 \times 10^{-3}\,Hz$), with the most energetic fluctuations in the 0.01 to $1\,Hz$ range. There are fluctuations due to the "mechanical" turbulence produced by velocity gradients, and there is also turbulence produced by thermal eddies associated with temperature gradients (these eddies are much smaller than the convective motions that transport pollutants up to the MMD). Thermal eddies are prevalent on sunny days when light winds occur and the temperature gradient is unstable. They typically have
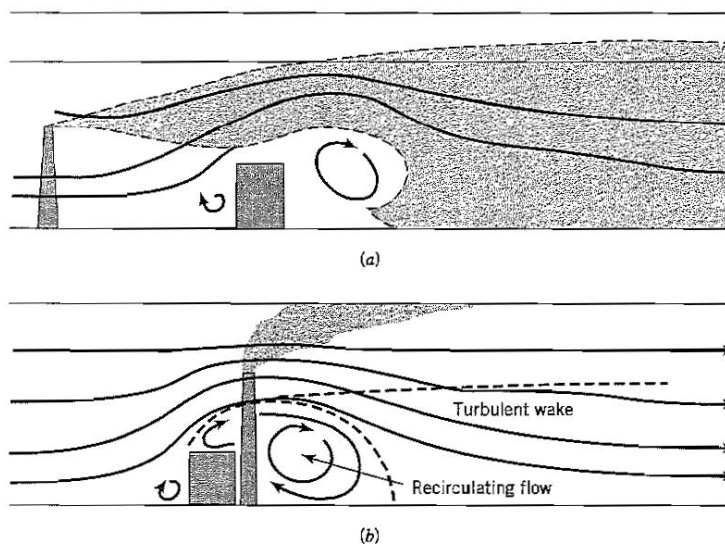
Figure 13.7: Effect of local flow patterns on the dispersion of gaseous effluent from a stack. From *Air Pollution: Its Origin and Control*, K. Wark, C.F. Warner & W.T. Davis, Addison-Wesley, 1998.

periods measured in minutes. Mechanical eddies predominate on windy nights with neutral stability, and they have periods on the order of seconds.

The wind, the stability of the atmosphere, and the resulting level of atmospheric turbulence will all affect the shape of the plume produced by a tall smoke stack, as illustrated in Figure 13.6. A wide range of possibilities is shown, and the strong influence of the temperature stability can be seen.

Another significant influence is the terrain surrounding the stack. The proximity of buildings can have a particularly strong effect, as seen in Figure 13.7. If the stack is placed improperly, or it is too low, the backflow in the wake of the building can cause heavy pollutant concentrations in the vicinity of the building.

## 13.8 Diffusion and Mixing

It is of great interest to know how the properties of a fluid at one point influence the properties at another point. For example, we know that when dye is introduced into a fluid, it slowly diffuses throughout the fluid. How does this process occur, and at what rate? Think of how a scent travels through a room. If a perfume bottle is opened in one corner of the room, there will be a high concentration of perfume molecules near the bottle and a low concentration elsewhere. The molecules will move and mix with the surrounding air by diffusion, even in the complete absence of drafts, so that after a sufficiently long time they will be distributed uniformly throughout the room. The rate at which this happens depends on the diffusion coefficient (a property of the perfume), and the strength of the concentration gradient. So the diffusion will happen quickly to begin with and then slow down as the concentration becomes more uniform and the strength of the gradients decrease (see Figure 13.8). This type of diffusion, where there is no mean flow, is described by Fick's first law of diffusion,

$$J = -D_m \frac{dC}{dx} \tag{13.6}$$

where $J$ is the mass of perfume crossing a unit area per unit time (the mass flux of perfume), $D_m$ is the mass diffusion coefficient for perfume in air, with dimensions $= L^2T^{-1}$, and $C$ is
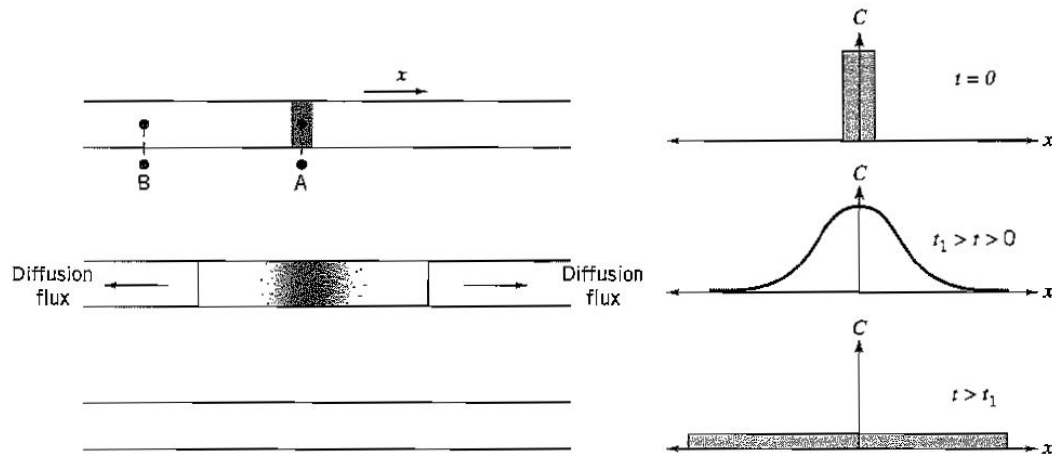
Figure 13.8: One-dimensional spreading of perfume in air as a function of time. From Potter & Wiggert, *Mechanics of Fluids*, 2nd ed., Prentice Hall, with permission.

the local concentration of perfume (mass per unit volume). The minus sign indicates that the diffusion of perfume is from regions of high to low concentration. Note how similar this equation is to equation 1.7, which described the diffusion of momentum by viscosity due to velocity differences, and also to the Fourier heat conduction equation

$$q \; = \; -k\frac{dT}{dx} \tag{13.7}$$

which describes the diffusion of heat due to temperature differences.

Since diffusion is a molecular transport process, the amount of diffusion across an interface is proportional to the surface area. Increasing the surface area will increase the rate of mixing proportionally. This is why we stir a fluid to mix it. When we add sugar to coffee, we could sit and wait for the sugar to diffuse into the coffee. For it to mix thoroughly by diffusion, we would have to wait a long time (molecular diffusion processes are typically very slow) and the coffee would undoubtedly be very cold. Instead, we stir the coffee. The resulting turbulence stretches and distorts the fluid particles that contain high concentrations of sugar molecules, which increases their surface area, and allows the molecular mixing process to occur in a very short time, before the coffee has cooled.

Mixing also enhances the diffusion of heat, and therefore turbulent flows are very efficient for cooling a surface. The turbulent eddies mix the flow very thoroughly, so that hot fluid can be quickly transported to regions where the surrounding fluid is cold, and vice versa. The turbulent eddies also stretch and distort the fluid particles, thereby increasing the surface area over which the heat conduction takes place.

In addition, mixing enhances the diffusion of momentum. For example, whenever velocity gradients are present, we also have gradients of momentum. As we saw in Section 1.6.3, viscosity diffuses momentum by molecular exchanges which cause slower fluid to speed up, and faster fluid to speed up. This is typically a slow process. However, in turbulent flows we have strong, large-scale mixing present, and the momentum is redistributed very much faster. Because of this stirring process, the momentum distribution becomes more uniform and the strength of the velocity gradients tends to be reduced. As we indicated in Section 8.7, this process is similar to viscous diffusion, except that it is more effective. Turbulent "diffusion" is often modeled using an equivalent "eddy" viscosity, which is typically orders of magnitude larger than the molecular viscosity. Since the turbulent diffusion of heat, mass , and momentum all depend on the fluctuating velocity field, the eddy viscosities

for each transport process are all about the same magnitude.

# Appendices

# Appendix A

# Analytical Tools

Here, we consider a number of basic analytical skills necessary for the study of fluid mechanics. This material is by way of summary only, and neither the selection nor its treatment is comprehensive. It is in the nature of a review, and it will be assumed that you have seen this material elsewhere in greater depth.

## A.1 Rank of a Matrix

The customary notation for a determinant $A$ of order $n$ consists of a square array of $n^2$ quantities enclosed between vertical bars

$$|A| = |a_{ij}| = \begin{vmatrix} a_{11} & a_{12} & . & a_{1n} \\ a_{21} & a_{22} & . & a_{2n} \\ . & . & . & . \\ a_{n1} & a_{n2} & . & a_{nn} \end{vmatrix}$$

This notation implies a particular summation process that applies to the elements of the determinant. For a determinant of order 2, the summation is

$$\begin{vmatrix} a_{11} & a_{12} \\ a_{21} & a_{22} \end{vmatrix} = a_{11}a_{22} - a_{12}a_{21}$$

For a determinant of order 3, the summation is

$$\begin{vmatrix} a_{11} & a_{12} & a_{13} \\ a_{21} & a_{22} & a_{23} \\ a_{31} & a_{32} & a_{33} \end{vmatrix} = \begin{aligned} & a_{11}\left(a_{22}a_{33} - a_{23}a_{32}\right) - a_{12}\left(a_{21}a_{33} - a_{23}a_{31}\right) \\ & \quad + a_{13}\left(a_{21}a_{32} - a_{22}a_{31}\right) \end{aligned}$$

The order of a determinant gives the rank of a matrix. The rank of a matrix $r$ is given by the largest non-zero determinant that fits in the matrix. For example, a 3 by 6 matrix (3 rows by 6 columns) has a maximum rank of 3, since a determinant is by definition square. However, four different determinants can be found, depending on which column of the matrix corresponds to the first column of the determinant. The first two possibilities for the matrix $\|A\|$ are

$$\begin{Vmatrix} \begin{vmatrix} a_{11} & a_{12} & a_{13} \\ a_{21} & a_{22} & a_{23} \\ a_{31} & a_{32} & a_{33} \end{vmatrix} & \begin{matrix} a_{14} & a_{15} & a_{16} \\ a_{24} & a_{25} & a_{26} \\ a_{34} & a_{35} & a_{36} \end{matrix} \end{Vmatrix}$$

and

$$\begin{Vmatrix} \begin{matrix} a_{11} \\ a_{21} \\ a_{31} \end{matrix} & \begin{vmatrix} a_{12} & a_{13} & a_{14} \\ a_{22} & a_{23} & a_{24} \\ a_{32} & a_{33} & a_{34} \end{vmatrix} & \begin{matrix} a_{15} & a_{16} \\ a_{25} & a_{26} \\ a_{35} & a_{36} \end{matrix} \end{Vmatrix}$$

If any of the four possible determinants of order 3 is non-zero, the rank of this matrix is 3.

## A.2     Scalar Product

Consider two vectors $\mathbf{A}$ and $\mathbf{B}$, in Cartesian coordinates, so that

$$\begin{aligned}
\mathbf{A}(x, y, z, t) &= A_x \mathbf{i} + A_y \mathbf{j} + A_z \mathbf{k} \\
\text{and} \quad \mathbf{B}(x, y, z, t) &= B_x \mathbf{i} + B_y \mathbf{j} + B_z \mathbf{k}
\end{aligned}$$

Then the scalar product is given by

$$\mathbf{A} \cdot \mathbf{B} \;=\; |\mathbf{A}|\,|\mathbf{B}| \cos\theta \;=\; \mathbf{B} \cdot \mathbf{A}$$

where $\theta$ is the angle between $\mathbf{A}$ and $\mathbf{B}$. The scalar product, or the *dot product*, of two vectors is a scalar, and it is *commutative*, which means that

$$\mathbf{A} \cdot \mathbf{B} = \mathbf{B} \cdot \mathbf{A}$$

In other words, the scalar product is independent of the sign of $\theta$, as indicated by the cosine: it may be measured from $\mathbf{A}$ to $\mathbf{B}$, or $\mathbf{B}$ to $\mathbf{A}$. We also have

$$\mathbf{A} \cdot \mathbf{B} = A_x B_x + A_y B_y + A_z B_z$$

A very useful scalar product is the one where one of the vectors is a unit vector, say, $\mathbf{n}$. Then

$$\mathbf{n} \cdot \mathbf{A} = |\mathbf{n}|\,|\mathbf{A}| \cos\theta = A \cos\theta$$

which gives the component of $\mathbf{A}$ in the direction of $\mathbf{n}$. This particular scalar product can be used whenever we need to find the component of the velocity or momentum in a given direction. For example, the $x$-component of the velocity $\mathbf{V}$ is given by $\mathbf{i} \cdot \mathbf{V} = u$, the $y$-component is given by $\mathbf{j} \cdot \mathbf{V} = v$, and the $z$-component is given by $\mathbf{k} \cdot \mathbf{V} = w$. In general, the component of $\mathbf{V}$ in the direction of $\mathbf{n}$ is given by $\mathbf{n} \cdot \mathbf{V}$.

## A.3     Vector Product

For the vectors $\mathbf{A}$ and $\mathbf{B}$ we have the vector product

$$\mathbf{A} \times \mathbf{B} = |\mathbf{A}|\,|\mathbf{B}| \sin\theta\,\mathbf{e} = -\mathbf{B} \times \mathbf{A}$$

where $\theta$ is the (smaller) angle between $\mathbf{A}$ and $\mathbf{B}$, and the direction of the unit vector $\mathbf{e}$ is given by the right-hand-screw rule. The vector product, or the *cross product*, of two vectors is not commutative, which means that

$$\mathbf{A} \times \mathbf{B} = -\mathbf{B} \times \mathbf{A}$$

and it depends on the sign of $\theta$, as indicated by the sine: for $\mathbf{A} \times \mathbf{B}$ it must be measured *from $\mathbf{A}$ to $\mathbf{B}$*, and for $\mathbf{B} \times \mathbf{A}$ it must be measured *from $\mathbf{B}$ to $\mathbf{A}$*. To find the components of the vector product in Cartesian coordinates we can use the determinant form

$$\mathbf{A} \times \mathbf{B} \;=\; \begin{vmatrix} \mathbf{i} & \mathbf{j} & \mathbf{k} \\ A_x & A_y & A_z \\ B_x & B_y & B_z \end{vmatrix}$$

$$= \; (A_y B_z - A_z B_y)\,\mathbf{i} - (A_x B_z - A_z B_x)\,\mathbf{j} + (A_x B_y - A_y B_x)\,\mathbf{k}$$

# A.4    Gradient Operator $\nabla$

The gradient of a scalar quantity $\phi$ is the rate of change of that quantity in space. The gradient operator, $\nabla$, or *grad*, operates on a scalar so that $\nabla\phi$ is a vector. For example, we can find the grad of the pressure field, the temperature field or the density field. The gradient vector $\nabla\phi$ has the property that its projection in any direction is equal to the derivative of $\phi$ in that direction. That is, for a unit vector $\mathbf{n}$, the scalar product $\mathbf{n}\cdot\nabla\phi$ gives the rate of change of $\phi$ in the direction of $\mathbf{n}$. Since the maximum projection of a vector is in the direction of the vector itself, it is clear that $\nabla\phi$ extends in the direction of the maximum rate of change of $\phi$.

Consider a closed volume $V$ with a surface area $A$. Then the gradient of any scalar such as $\phi$ is formally defined as

$$\nabla\phi \equiv \lim_{V\to 0} \frac{1}{V} \int \mathbf{n}\phi\, dA$$

where $\mathbf{n}$ is an outward facing unit normal vector. So the gradient of $\phi$ is the ratio of the integral of $\mathbf{n}\phi$ over an area $A$, to the volume $V$ enclosed by $A$, as the volume shrinks to zero about some point.

In Cartesian coordinates,

$$\nabla\phi \;=\; \frac{\partial\phi}{\partial x}\mathbf{i} + \frac{\partial\phi}{\partial y}\mathbf{j} + \frac{\partial\phi}{\partial z}\mathbf{k}$$

In cylindrical coordinates,

$$\nabla\phi \;=\; \frac{\partial\phi}{\partial r}\mathbf{e_r} + \frac{1}{r}\frac{\partial\phi}{\partial\theta}\mathbf{e_\theta} + \frac{\partial\phi}{\partial z}\mathbf{e_z}$$

Note that the operator $\nabla$ looks like a vector. In fact, it has many properties that are similar to the properties vectors have. However, it differs from a vector in some important ways, as we shall see, and it is best thought of as an *operator* with special properties. We can write $\nabla\phi$ in Cartesian coordinates as

$$\nabla\phi \;=\; \left( \frac{\partial}{\partial x}\mathbf{i} + \frac{\partial}{\partial y}\mathbf{j} + \frac{\partial}{\partial z}\mathbf{k} \right)\phi$$

which emphasizes that $\nabla\phi$ is shorthand for the result obtained when $\nabla$ operates on a scalar $\phi$.

# A.5    Divergence Operator $\nabla\cdot$

The divergence of a vector quantity is the outflow of that quantity per unit time per unit volume. The divergence operator $\nabla\cdot$ operates on a vector, and the result is a scalar. That is, the divergence of a vector is a scalar (note the contrast with the gradient operator $\nabla$). The divergence of any vector, such as the velocity $\mathbf{V}$, is formally defined as

$$\nabla\cdot\mathbf{V} \equiv \lim_{V\to 0} \frac{1}{V} \int \mathbf{n}\cdot\mathbf{V}\, dA$$

So the divergence of the velocity is the ratio of the integral of $\mathbf{n}\cdot\mathbf{V}$ over an area $A$, to the volume $V$ enclosed by $A$, as the volume shrinks to zero about some point, say $P$. More physically, $\mathbf{V}$ is the velocity through any small surface element $dA$, and $\mathbf{n}\cdot\mathbf{V} = |\mathbf{V}|\cos\theta$ is the volume flux per unit area. The area integral is the total volume flux through the surface area $A$, and the divergence of $\mathbf{V}$ is the volume flux per unit volume at the point $P$.

In Cartesian coordinates, the divergence of $\mathbf{V}(\mathbf{x}, t) = \mathbf{V}(x, y, z, t)$ is simply

$$\nabla \cdot \mathbf{V} \;=\; \left( \frac{\partial}{\partial x}\mathbf{i} + \frac{\partial}{\partial y}\mathbf{j} + \frac{\partial}{\partial z}\mathbf{k} \right) \cdot (u\mathbf{i} + v\mathbf{j} + w\mathbf{k})$$

That is,

$$\nabla \cdot \mathbf{V} \;=\; \frac{\partial u}{\partial x} + \frac{\partial v}{\partial y} + \frac{\partial w}{\partial z}$$

In cylindrical coordinates,

$$\nabla \cdot \mathbf{V} = \frac{1}{r} \frac{\partial r u_r}{\partial r} + \frac{1}{r} \frac{\partial u_\theta}{\partial \theta} + \frac{\partial u_z}{\partial z}$$

**Note:** We see that the divergence operator $\nabla\cdot$ behaves in some ways like a scalar product. However, as we have already noted, $\nabla$ differs from a vector in some important ways, and it is best thought of as an operator with special properties. In particular, $\nabla\cdot$ is not commutative, so that $\nabla \cdot \mathbf{V} \neq \mathbf{V} \cdot \nabla$ (see Section A.11).

Also, a vector field that has zero divergence (for example, $\nabla \cdot \mathbf{A} = 0$) is sometimes called a *solenoidal* vector field. A velocity field that has zero divergence ($\nabla \cdot \mathbf{V} = 0$) is called an *incompressible* velocity field.

## A.6    Laplacian Operator $\nabla^2$

The Laplacian operator is composed of second derivatives in space. When it operates on a scalar, the result is a scalar; when it operates on a vector, the result is a vector.

In Cartesian coordinates,

$$\nabla^2 \phi \;=\; \frac{\partial^2 \phi}{\partial x^2} + \frac{\partial^2 \phi}{\partial y^2} + \frac{\partial^2 \phi}{\partial z^2} \tag{A.1}$$

In cylindrical coordinates,

$$\nabla^2 \phi \;=\; \frac{\partial^2 \phi}{\partial r^2} + \frac{1}{r} \frac{\partial \phi}{\partial r} + \frac{1}{r^2} \frac{\partial^2 \phi}{\partial \theta^2} + \frac{\partial^2 \phi}{\partial z^2} \tag{A.2}$$

We see that the Laplacian operator behaves in some ways like the scalar product $\nabla \cdot \nabla$. However, as we have already noted, $\nabla$ differs from a vector in some important ways, and it is best thought of as an operator with special properties.

Also, when a parameter $\phi$ is operated on by the Laplacian $\nabla^2$, and the result is zero, it is said to satisfy Laplace's equation $\nabla^2 \phi \;=\; 0$.

## A.7    Curl Operator $\nabla\times$

The curl operator $\nabla\times$ operates on a vector and the result is another vector. That is, the curl of a vector is a vector. A physical interpretation relevant to fluid dynamics is that the curl of the velocity field $\nabla \times \mathbf{V}$ is equal to twice the angular velocity of the flow field at a given point (this is not obvious, of course, but it is useful to realize that $\nabla \times \mathbf{V}$ is related to the rotation of the flow — see Section 6.1). The curl of any vector, such as the velocity $\mathbf{V}$, is formally defined as

$$\nabla \times \mathbf{V} \equiv \lim_{V \to 0} \frac{1}{V} \int \mathbf{n} \times \mathbf{V} \, dA$$

So the curl of the velocity is the ratio of the integral of $\mathbf{n} \times \mathbf{V}$ over an area $A$, to the volume $V$ enclosed by $A$, as the volume shrinks to zero about some point.

In Cartesian coordinates, the curl of $\mathbf{V}(\mathbf{x}, t) = \mathbf{V}(x, y, z, t)$ is given in the shorthand, determinant form by

$$\nabla \times \mathbf{V} = \begin{vmatrix} \mathbf{i} & \mathbf{j} & \mathbf{k} \\ \frac{\partial}{\partial x} & \frac{\partial}{\partial y} & \frac{\partial}{\partial z} \\ u & v & w \end{vmatrix}$$

That is,

$$\nabla \times \mathbf{V} = \left( \frac{\partial w}{\partial y} - \frac{\partial v}{\partial z} \right) \mathbf{i} - \left( \frac{\partial w}{\partial x} - \frac{\partial u}{\partial z} \right) \mathbf{j} + \left( \frac{\partial v}{\partial x} - \frac{\partial u}{\partial y} \right) \mathbf{k}$$

In cylindrical coordinates,

$$\nabla \times \mathbf{V} = \left( \frac{1}{r} \frac{\partial u_z}{\partial \theta} - \frac{\partial u_\theta}{\partial z} \right) \mathbf{e_r} - \left( \frac{\partial u_z}{\partial r} - \frac{\partial u_r}{\partial z} \right) \mathbf{e_\theta} + \left( \frac{1}{r} \frac{\partial r u_\theta}{\partial r} - \frac{1}{r} \frac{\partial u_r}{\partial \theta} \right) \mathbf{e_z}$$

We see that the curl operator $\nabla \times$ behaves in some ways like a vector product. For example, it is true that $\nabla \times \mathbf{V} = -\mathbf{V} \times \nabla$. However, $\nabla$ differs from a vector in some important ways, and it is best thought of as an operator with special properties.

A vector field that has zero curl (for example, $\nabla \times \mathbf{V} = 0$) is commonly called an *irrotational* vector field.

## A.8   Div, Grad, and Curl

$$\nabla \phi = \lim_{V \to 0} \frac{1}{V} \int \mathbf{n} \phi \, dA$$

$$\nabla \cdot \mathbf{V} = \lim_{V \to 0} \frac{1}{V} \int \mathbf{n} \cdot \mathbf{V} \, dA$$

$$\nabla \times \mathbf{V} = \lim_{V \to 0} \frac{1}{V} \int \mathbf{n} \times \mathbf{V} \, dA$$

where $\phi$ is a scalar and $\mathbf{V}$ is a vector.

We also have the differential forms, and in Cartesian coordinates,

$$\nabla \phi = \frac{\partial \phi}{\partial x} \mathbf{i} + \frac{\partial \phi}{\partial y} \mathbf{j} + \frac{\partial \phi}{\partial z} \mathbf{k}$$

$$\nabla \cdot \mathbf{V} = \frac{\partial u}{\partial x} + \frac{\partial v}{\partial y} + \frac{\partial w}{\partial z}$$

$$\nabla \times \mathbf{V} = \begin{vmatrix} \mathbf{i} & \mathbf{j} & \mathbf{k} \\ \frac{\partial}{\partial x} & \frac{\partial}{\partial y} & \frac{\partial}{\partial z} \\ u & v & w \end{vmatrix}$$

$$= \left( \frac{\partial w}{\partial y} - \frac{\partial v}{\partial z} \right) \mathbf{i} - \left( \frac{\partial w}{\partial x} - \frac{\partial u}{\partial z} \right) \mathbf{j} + \left( \frac{\partial v}{\partial x} - \frac{\partial u}{\partial y} \right) \mathbf{k}$$

In cylindrical coordinates,

$$\nabla \phi = \frac{\partial \phi}{\partial r} \mathbf{e_r} + \frac{1}{r} \frac{\partial \phi}{\partial \theta} \mathbf{e_\theta} + \frac{\partial \phi}{\partial z} \mathbf{e_z}$$

$$\nabla \cdot \mathbf{V} = \frac{1}{r} \frac{\partial r u_r}{\partial r} + \frac{1}{r} \frac{\partial u_\theta}{\partial \theta} + \frac{\partial u_z}{\partial z}$$

$$\nabla \times \mathbf{V} = \left( \frac{1}{r} \frac{\partial u_z}{\partial \theta} - \frac{\partial u_\theta}{\partial z} \right) \mathbf{e_r} - \left( \frac{\partial u_z}{\partial r} - \frac{\partial u_r}{\partial z} \right) \mathbf{e_\theta} + \left( \frac{1}{r} \frac{\partial r u_\theta}{\partial r} - \frac{1}{r} \frac{\partial u_r}{\partial \theta} \right) \mathbf{e_z}$$

## A.9    Integral Theorems

Stokes' Theorem relates the line integral of the velocity to the area integral of the vorticity. That is,

$$\int \mathbf{n} \cdot \vec{\Omega}\, dS \;\; = \;\; \int \mathbf{n} \cdot \nabla \times \mathbf{V}\, dS \;\; = \;\; \oint_C \mathbf{V} \cdot d\vec{\ell}$$

where the line integral is taken around the closed curve $C$ defining the perimeter of the area $S$, where the direction of integration around $C$ is positive with respect to the side of $S$ om which the unit normals are drawn (by the right hand screw rule).

   Additional theorems relate area integrals to volume integrals. For a closed volume $V$ with surface area $A$,

$$\int \mathbf{n}\, p\, dA \;\; = \;\; \int \nabla p\, dV$$

$$\int \mathbf{n} \cdot \mathbf{V}\, dA \;\; = \;\; \int \nabla \cdot \mathbf{V}\, dV$$

$$\int \mathbf{n} \times \mathbf{V}\, dA \;\; = \;\; \int \nabla \times \mathbf{V}\, dV$$

The second of these is sometimes called the divergence theorem.

## A.10    Taylor-Series Expansion

The Taylor-series expansion allows us to estimate the variation of a quantity in the neighborhood of a known point in a formal and complete way. To find how the pressure $p$ varies with $z$, for example, the pressure is expanded in a power series in the neighborhood of $z = \alpha$, where $\alpha$ is a known point (see Figure A.1). The expansion is given by

$$p(z) = p(\alpha) + (z - \alpha)\left.\frac{\partial p}{\partial z}\right|_{z=\alpha} + \frac{(z-\alpha)^2}{2!}\left.\frac{\partial^2 p}{\partial z^2}\right|_{z=\alpha} + \ldots$$

We need to assume that the pressure and its derivatives exist at $z = \alpha$ (it is obvious that if the function $p(z)$ has a discontinuity close to the point $\alpha$ where the derivative takes an infinite value, the Taylor-series expansion will not give a good estimate). With $(z - \alpha) = \delta z$, we can write this relationship as

$$p(\alpha + \delta z) = p(\alpha) + \delta z\left.\frac{\partial p}{\partial z}\right|_{\alpha} + \frac{(\delta z)^2}{2!}\left.\frac{\partial^2 p}{\partial z^2}\right|_{\alpha} + \frac{(\delta z)^3}{3!}\left.\frac{\partial^3 p}{\partial z^3}\right|_{\alpha} + \ldots$$
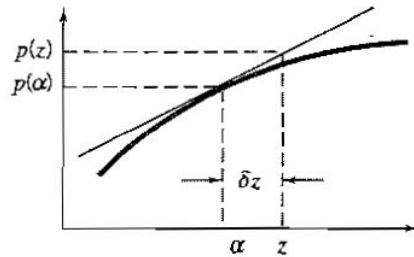


Figure A.1: Estimating the pressure at $z$ by using the pressure at $\alpha$, by applying the Taylor-series expansion.

The dots represent higher order terms, that is, terms which contain $\delta z$ in a higher order (for example, $(\delta z)^2$ is one order higher than $\delta z$, and $(\delta z)^3$ is one order higher than $(\delta z)^2$). If $\delta z$ is very small, $(\delta z)^2$ is much smaller still, and in the limit of $\delta z$ going to very small values, higher order terms can usually be neglected. This may be illustrated by using some numerical values. For a quantity $\Delta$ that is small compared to unity, $\Delta \ll 1$, then $\Delta^2 \ll \Delta$. For example,

$$
\begin{array}{rclcrcl}
\Delta & = & 0.1 & \Delta^2 & = & 0.01 \\
\Delta & = & 0.01 & \Delta^2 & = & 0.0001, \quad \text{etc.}
\end{array}
$$

Therefore, higher order terms rapidly become small, and in the limit of an infinitesimally small value of $\Delta$, terms that contain $\Delta^2$ can normally be neglected. This approach is called linearization (since quadratic terms are neglected), and it can be very useful, as we shall see.

# A.11 Total Derivative and the Operator $\mathbf{V} \cdot \nabla$

In Cartesian coordinates,

$$
\begin{aligned}
\frac{D\mathbf{V}}{Dt} &= \left( \frac{\partial u}{\partial t} + u\frac{\partial u}{\partial x} + v\frac{\partial u}{\partial y} + w\frac{\partial u}{\partial z} \right) \mathbf{i} \\
&+ \left( \frac{\partial v}{\partial t} + u\frac{\partial v}{\partial x} + v\frac{\partial v}{\partial y} + w\frac{\partial v}{\partial z} \right) \mathbf{j} \\
&+ \left( \frac{\partial w}{\partial t} + u\frac{\partial w}{\partial x} + v\frac{\partial w}{\partial y} + w\frac{\partial w}{\partial z} \right) \mathbf{k}
\end{aligned}
$$

In cylindrical coordinates,

$$
\begin{aligned}
\frac{D\mathbf{V}}{Dt} &= \left( \frac{\partial u_r}{\partial t} + u_r\frac{\partial u_r}{\partial r} + \frac{u_\theta}{r}\frac{\partial u_r}{\partial \theta} + u_z\frac{\partial u_r}{\partial z} - \frac{u_\theta^2}{r} \right) \mathbf{e_r} \\
&+ \left( \frac{\partial u_\theta}{\partial t} + u_r\frac{\partial u_\theta}{\partial r} + \frac{u_\theta}{r}\frac{\partial u_\theta}{\partial \theta} + u_z\frac{\partial u_\theta}{\partial z} + \frac{u_r u_\theta}{r} \right) \mathbf{e_\theta} \\
&+ \left( \frac{\partial u_z}{\partial t} + u_r\frac{\partial u_z}{\partial r} + \frac{u_\theta}{r}\frac{\partial u_z}{\partial \theta} + u_z\frac{\partial u_z}{\partial z} \right) \mathbf{e_z}
\end{aligned}
$$

By writing the total derivative as

$$
\frac{D\mathbf{V}}{Dt} = \frac{\partial \mathbf{V}}{\partial t} + (\mathbf{V} \cdot \nabla) \mathbf{V}
$$

we define a new operator $\mathbf{V} \cdot \nabla$. In this form, the total derivative is written in a way that is independent of the coordinate system. The expansion of $\mathbf{V} \cdot \nabla$ depends on the coordinate system. In Cartesian coordinates,

$$
\mathbf{V} \cdot \nabla = u\frac{\partial}{\partial x} + v\frac{\partial}{\partial y} + w\frac{\partial}{\partial z}
$$

Compare this with the divergence of $\mathbf{V}$, where

$$
\nabla \cdot \mathbf{V} = \frac{\partial u}{\partial x} + \frac{\partial v}{\partial y} + \frac{\partial w}{\partial z}
$$

In cylindrical coordinates,

$$
\mathbf{V} \cdot \nabla = u_r\frac{\partial}{\partial r} + \frac{u_\theta}{r}\frac{\partial}{\partial \theta} + u_z\frac{\partial}{\partial z}
$$

The operator $\mathbf{V}\cdot\nabla$ should not be thought of as a dot product of the velocity and a "vector" $\nabla$. As we indicated earlier, $\nabla$ is not a true vector, and it only behaves like a vector sometimes. It is best to think of $\mathbf{V}\cdot\nabla$ as an operator in its own right. To make this clear, it is preferable to write it in parentheses, as $(\mathbf{V}\cdot\nabla)$, although formally there is no ambiguity.[1]

Care must be taken in expanding $\mathbf{V}\cdot\nabla$ in other than Cartesian coordinates. In fact, $\mathbf{V}\cdot\nabla$ is an example of a *dyad*, and it is more easily handled in tensor notation. It can be expressed in true vector form using the (very useful) vector identity:

$$(\mathbf{V}\cdot\nabla)\,\mathbf{V} = \nabla\left(\tfrac{1}{2}V^2\right) - \mathbf{V}\times(\nabla\times\mathbf{V}) \tag{A.3}$$

## A.12  Integral and Differential Forms

Instead of deriving the differential forms of the continuity and momentum equations for inviscid flow (the Euler equation) using elemental control volumes, as we did in sections 5.2 and 5.3, we can obtain them directly from their integral forms.

The continuity equation for a fixed control volume (equation 3.9) states

$$\frac{\partial}{\partial t}\int\rho\,dV + \int\mathbf{n}\cdot\rho\mathbf{V}\,dA \;=\; 0$$

Since the control volume is fixed, the derivative can be moved inside the integral, so that

$$\int\frac{\partial\rho}{\partial t}\,dV + \int\mathbf{n}\cdot\rho\mathbf{V}\,dA \;=\; 0$$

The area integral can be converted to a volume integral using the divergence theorem (see Section A.9). Hence,

$$\int\left(\frac{\partial\rho}{\partial t} + \nabla\cdot\rho\mathbf{V}\right)dV \;=\; 0$$

Since the control volume is arbitrary, the integrand itself must be zero, so that

$$\frac{\partial\rho}{\partial t} + \nabla\cdot\rho\mathbf{V} \;=\; 0$$

as before (equation 5.8).

The momentum equation for a fixed control volume (equation 3.20) states

$$\mathbf{R_{ext}} + \mathbf{F_v} - \int\mathbf{n}\,p\,dA + \int\rho\mathbf{g}\,dV \;=\; \frac{\partial}{\partial t}\int\rho\mathbf{V}\,dV + \int(\mathbf{n}\cdot\rho\mathbf{V})\,\mathbf{V}\,dA$$

If we examine the the interior of the fluid, and ignore viscous forces, $\mathbf{R_{ext}}$ and $\mathbf{F_v}$ can be neglected. Since the control volume is fixed, the derivative can be moved inside the integral, so that

$$-\int\mathbf{n}\,p\,dA + \int\rho\mathbf{g}\,dV \;=\; \int\frac{\partial\rho\mathbf{V}}{\partial t}\,dV + \int(\mathbf{n}\cdot\rho\mathbf{V})\,\mathbf{V}\,dA$$

Changing the area integrals to volume integrals and collecting terms,

$$-\int(\nabla p + \rho\mathbf{g})\,dV \;=\; \int\left(\frac{\partial\rho\mathbf{V}}{\partial t} + (\nabla\cdot\rho\mathbf{V})\,\mathbf{V} + (\rho\mathbf{V}\cdot\nabla)\,\mathbf{V}\right)dV$$

$$=\; \int\left(\rho\frac{\partial\mathbf{V}}{\partial t} + \rho\,(\mathbf{V}\cdot\nabla)\,\mathbf{V} + \mathbf{V}\frac{\partial\rho}{\partial t} + \mathbf{V}\,(\nabla\cdot\rho\mathbf{V})\right)dV$$

---

[1]Gibbs, "Vector Analysis," Dover Publications, Chapter III.

Using the continuity equation yields

$$\int \left( \rho \frac{\partial \mathbf{V}}{\partial t} + \rho \left( \mathbf{V} \cdot \nabla \right) \mathbf{V} + \nabla p - \rho \mathbf{g} \right) dV \;=\; 0$$

Since the control volume is arbitrary, the integrand itself must be zero, so that

$$\rho \left( \frac{\partial \mathbf{V}}{\partial t} + \left( \mathbf{V} \cdot \nabla \right) \mathbf{V} \right) + \nabla p - \rho \mathbf{g} \;=\; 0$$

That is,

$$\rho \frac{D\mathbf{V}}{Dt} \;=\; -\nabla p + \rho \mathbf{g}$$

as before (equation 5.10).

# A.13   Gravitational Potential

To take the next step, we need to introduce the concept of a potential function. We will simply define a function $\phi_g$ such that

$$\mathbf{g} = -g\nabla \phi_g$$

The vector $\nabla \phi_g$ is a unit vector that points in the direction opposite to the vector $\mathbf{g}$. The parameter $\phi_g$ is called a *potential function*, and in this case is identified with the altitude or elevation. Here the term "potential" is clearly connected with the idea of potential energy, which is only a function of elevation. If a body moves from point $a$ to point $b$, its potential energy will be unchanged as long as the two points have the same elevation. Gravity is called a "conservative" force field since the potential energy of a body depends only on the elevation and not on the particular path used to get from $a$ to $b$. The quantity that measures the change in potential energy is the elevation, which is also the potential function associated with the conservative force field due to gravity, $\phi_g$.

The Euler equation may then be written as

$$\frac{D\mathbf{V}}{Dt} = -\frac{1}{\rho}\nabla p + \mathbf{g} = -\frac{1}{\rho}\nabla p - g\nabla \phi_g \tag{A.4}$$

Therefore, in Cartesian coordinates, we have

$$\frac{\partial u}{\partial t} + u\frac{\partial u}{\partial x} + v\frac{\partial u}{\partial y} + w\frac{\partial u}{\partial z} \;=\; -\frac{1}{\rho}\frac{\partial p}{\partial x} - g\frac{\partial \phi_g}{\partial x}$$

$$\frac{\partial v}{\partial t} + u\frac{\partial v}{\partial x} + v\frac{\partial v}{\partial y} + w\frac{\partial v}{\partial z} \;=\; -\frac{1}{\rho}\frac{\partial p}{\partial y} - g\frac{\partial \phi_g}{\partial y}$$

$$\frac{\partial w}{\partial t} + u\frac{\partial w}{\partial x} + v\frac{\partial w}{\partial y} + w\frac{\partial w}{\partial z} \;=\; -\frac{1}{\rho}\frac{\partial p}{\partial z} - g\frac{\partial \phi_g}{\partial z}$$

In cylindrical coordinates, we have

$$\frac{\partial u_r}{\partial t} + u_r\frac{\partial u_r}{\partial r} + \frac{u_\theta}{r}\frac{\partial u_r}{\partial \theta} + u_z\frac{\partial u_r}{\partial z} - \frac{u_\theta^2}{r} \;=\; -\frac{1}{\rho}\frac{\partial p}{\partial r} - g\frac{\partial \phi_g}{\partial r}$$

$$\frac{\partial u_\theta}{\partial t} + u_r\frac{\partial u_\theta}{\partial r} + \frac{u_\theta}{r}\frac{\partial u_\theta}{\partial \theta} + u_z\frac{\partial u_\theta}{\partial z} + \frac{u_r u_\theta}{r} \;=\; -\frac{1}{\rho}\frac{1}{r}\frac{\partial p}{\partial \theta} - g\frac{1}{r}\frac{\partial \phi_g}{\partial \theta}$$

$$\frac{\partial u_z}{\partial t} + u_r\frac{\partial u_z}{\partial r} + \frac{u_\theta}{r}\frac{\partial u_z}{\partial \theta} + u_z\frac{\partial u_z}{\partial z} \;=\; -\frac{1}{\rho}\frac{\partial p}{\partial z} - g\frac{\partial \phi_g}{\partial z}$$

## A.14    Bernoulli's Equation

Bernoulli's equation holds for steady, inviscid, constant density flow between two points along a streamline, or across streamlines if the flow is irrotational. In Section 4.2, it was derived by considering the forces acting on a particle of fluid moving along a streamline. It may also be derived directly from the Navier-Stokes equation, which reduces to the Euler equation (equation A.4) under the condition of inviscid flow. With the added condition of steady flow, and using the vector identity given in equation A.3, the Euler equation reduces to

$$\nabla \left(\tfrac{1}{2}V^2\right) - \mathbf{V} \times (\nabla \times \mathbf{V}) = -\frac{1}{\rho}\nabla p - g\nabla\phi_g$$

If the flow is of constant density, then

$$\nabla \left(\tfrac{1}{2}V^2\right) - \mathbf{V} \times (\nabla \times \mathbf{V}) = -\nabla\left(\frac{p}{\rho}\right) - g\nabla\phi_g = -\nabla\left(\frac{p}{\rho} + g\phi_g\right)$$

That is,

$$\nabla \left(\tfrac{1}{2}V^2 + \frac{p}{\rho} + gz\right) = \mathbf{V} \times (\nabla \times \mathbf{V}) \tag{A.5}$$

We have used $z = \phi_g$, where $z$ is the altitude or elevation above a horizontal reference plane.

For irrotational flows, $\nabla \times \mathbf{V} = 0$, so that

$$\nabla \left(\tfrac{1}{2}V^2 + \frac{p}{\rho} + gz\right) = 0$$

and we find that

$$p + \tfrac{1}{2}\rho V^2 + \rho gz = B_i$$

where $B_i$ is a constant throughout the (irrotational) flow field.

For rotational flows, we take the component of equation A.5 along a streamline. That is, we take a dot product with a unit vector $\mathbf{ds}$ that lies along the direction of the streamline, so that

$$\nabla \left(\tfrac{1}{2}V^2 + \frac{p}{\rho} + gz\right) \cdot \mathbf{ds} = \mathbf{V} \times (\nabla \times \mathbf{V}) \cdot \mathbf{ds}$$

Since $\mathbf{V}$ and $\mathbf{ds}$ lie in the same direction, $\mathbf{V} \times (\nabla \times \mathbf{V}) \cdot \mathbf{ds} = 0$, and by integrating along the streamline we obtain

$$p + \tfrac{1}{2}\rho V^2 + \rho gz = B$$

where $B$ is a constant along the streamline.

## A.15    Reynolds Transport Theorem

In Sections 3.4 and 3.6, the integral forms of the continuity and the momentum equations for a fixed control volume (equations 3.9 and 3.20) were derived from first principles. It is possible to express the conservation concepts embodied in these equations in a more general way. The left hand sides of the continuity and momentum equations describe the total rate of change in a property of the fluid (mass, momentum) contained in a given volume, accounting for the flow in and out of the control volume and the changes that may be occurring inside the control volume. In other words, they provide a link between the total rate of change of a property of a fixed *mass* of fluid and the rate of change of that property in a fixed *volume* of fluid. For instance, for a fixed mass of fluid, the rate of change of the property called mass is obviously zero. For a fixed volume of fluid, the same principle is expressed as a balance between the rate of change of mass in the control volume and the net mass transported out across the surface of the control volume.

In more general terms, we can define an *extensive* property of the fluid $B$, which could be mass, momentum, energy, and so on. An *intensive* property $b$ can also be defined, which is simply the property $B$ per unit mass, so that

$$B = mb,$$

where $m$ is the mass of fluid being considered. The value of $B$ is directly proportional to the amount of mass being considered, whereas the value of $b$ is independent of the amount of mass. It follows that

$$B_{CV} \; = \; \int_{CV} \rho b \, dv$$

where the integral is over the control volume $CV$.

The question is, therefore, what is the rate of change of $B_{sys}$, which is the rate of change of $B$ following a system (that is, a fixed mass of fluid) in terms of the rate of change of $B_{CV}$, which is the amount of $B$ contained in the control volume at any time. The Reynolds transport theorem for a fixed control volume states that the rate of change of $B$ (following a given mass of fluid) is equal to the rate of change of $B$ contained in the control volume plus the net outflux of $B$ through the surface of the control volume. That is,

$$\frac{DB_{sys}}{dt} \; = \; \frac{\partial B_{CV}}{\partial t} + \int (\mathbf{n} \cdot \rho \mathbf{V}) \, b \, dA$$

and therefore

$$\frac{DB_{sys}}{dt} \; = \; \frac{\partial}{\partial t} \int \rho b \, dv + \int (\mathbf{n} \cdot \rho \mathbf{V}) \, b \, dA \tag{A.6}$$

The Reynolds transport theorem provides a link between control volume and system concepts. It serves the same function for a large control volume as the total derivative serves for a small control volume (see Section 5.1). We have not given a formal derivation here, but the link with the continuity and momentum equations is clear.[2] For example, when the property $B$ is mass,

$$B = m \qquad \text{and} \qquad b = \frac{dB}{dm} = 1$$

and we obtain the left hand side of the continuity equation (equation 3.9). When the property $B$ is linear momentum,

$$\mathbf{B} = m\mathbf{V} \qquad \text{and} \qquad b = \frac{d\mathbf{B}}{dm} = \mathbf{V}$$

and we obtain the left hand side of the momentum equation (equation 3.20). When the property $B$ is the total energy $E$,

$$B = E = me \qquad \text{and} \qquad b = \frac{dB}{dm} = e$$

and we obtain the left hand side of the energy equation (equation 3.25).

The power of the Reynolds' transport theorem lies in the fact that the property $B$ can be anything that is *transported* by the fluid: mass, linear momentum, angular momentum, kinetic energy, and so forth.

---

[2]Formal derivations can be found in White *Fluid Mechanics*, McGraw-Hill 1986; Shapiro *Elements of Gasdynamics*, Wiley 1962; Munson, Young & Okiishi *Fundamentals of Fluid Mechanics*, Wiley 1998;and Potter & Wiggert *Mechanics of Fluids*, Prentice-Hall 1997.

# Appendix B

# Conversion Factors

| | | | | | | | | |
|---|---|---|---|---|---|---|---|---|
| Length | $1\ m$ | $=$ | $1,000\ mm$ | $=$ | $39.4\ in$ | $=$ | $3.281\ ft$ | |
| | $1\ km$ | $=$ | $0.622\ mile$ | | | | | |

| | | | | | | | | |
|---|---|---|---|---|---|---|---|---|
| Velocity | $1\ m/s$ | $=$ | $3.281\ ft/s$ | $=$ | $3.60\ km/hr$ | $=$ | $2.28\ mph$ | |
| | $1\ knot$ | $=$ | $0.5155\ m/s$ | | | | | |

Volume $\quad\quad 1\ m^3\ =\ 1000\ liters\ =\ 35.31\ ft^3$
$\quad\quad\quad\quad\quad\quad\ 1\ ft^3\ =\ 28.32\ liters\ =\ 7.48\ gal\ (U.S.)$
$\quad\quad\quad 1\ gal\ (U.S.)\ =\ 3.785\ liters$

Mass $\quad\quad\quad 1\ kg\ =\ 1,000\ g\ =\ 2.205\ lb_m\ =\ 0.0685\ slug$
$\quad\quad\quad\quad\ 1\ slug\ =\ 32.174\ lb_m$

Density $\quad 1\ kg/m^3\ =\ 0.00194\ slug/ft^3\ =\ 0.06243\ lb_m/ft^3$
$\quad\quad\quad\quad\quad\quad\quad\quad =\ 36.13\times 10^{-6}\ lb_m/in^3$

Force $\quad\quad\quad\quad 1\ N\ =\ 0.2248\ lb_f$

Pressure $\quad 1\ Pascal\ =\ 1\ N/m^2\ =\ 10^{-5}\ bar\ =\ 10\ dyne/cm^2$
$\quad\quad\quad\quad\quad\quad\quad\quad =\ 0.14504\times 10^{-3}\ psi\quad or\quad lb_f/in^2$
$\quad\quad\quad\quad\quad\quad\quad\quad =\ 0.02088\ psf\quad or\quad lb_f/ft^2$

$\quad\quad\quad\quad\quad 1\ atm\ =\ 101,325\ N/m^2\quad or\quad Pa$
$\quad\quad\quad\quad\quad\quad\quad\quad =\ 1.01325\ bar$
$\quad\quad\quad\quad\quad\quad\quad\quad =\ 760\ Torr$
$\quad\quad\quad\quad\quad\quad\quad\quad =\ 14.70\ psi\quad or\quad lb_f/in^2$
$\quad\quad\quad\quad\quad\quad\quad\quad =\ 2,116\ psf\quad or\quad lb_f/ft^2$
$\quad\quad\quad\quad\quad\quad\quad\quad =\ 29.92\ in\ Hg\ =\ 760.0\ mm\ Hg$
$\quad\quad\quad\quad\quad\quad\quad\quad =\ 10.33\ m\ H_2O\ =\ 33.90\ ft\ H_2O$

Viscosity $\quad 1\ Pa\cdot s\ =\ 1\ N\ s/m^2$
$\quad\quad\quad\quad\quad\quad\quad\quad =\ 10\ poise\ =\ 1,000\ cp\ (centipoise)$
$\quad\quad\quad\quad\quad\quad\quad\quad =\ 0.02088\ lb_f\ s/ft^2$
$\quad\quad\ 1\ lb_f\ s/ft^2\ =\ 32.174\ lb_m/s\ ft^2$

Kinematic
  viscosity     $1\ m^2/s$  $=$  $10^4\ Stokes$
                                  $=$  $10.76\ ft^2/s$

Energy          $1\ N \cdot m$  $=$  $1\ Joule$
                                  $=$  $0.7375\ ft \cdot lb_f$  $=$  $0.000948\ BTU$
                                  $=$  $0.2388\ cal$

Power            $1\ W$  $=$  $1\ J/s$
                                    $=$  $0.7375\ ft \cdot lb_f/s$
              $1\ kW$  $=$  $1.341\ hp$  $=$  $737.5\ ft \cdot lb_f/s$

Temperature    $1\ ^\circ C$  $=$  $1\ ^\circ K$  $=$  $\frac{9}{5}\ ^\circ R$
                  $0\ ^\circ C$  $=$  $273.15\ ^\circ K$
                                  $=$  $32\ ^\circ F$  $=$  $459.67\ ^\circ R$

# Appendix C

# Fluid and Flow Properties

**TABLE C.1   Physical Properties of Air at Standard Atmospheric Pressure (SI Units)[a]**

| Temperature (°C) | Density, $\rho$ (kg/m³) | Dynamic viscosity, $\mu$ (N·s/m²) | | Kinematic viscosity, $\nu$ (m²/s) | | Specific heat ratio, $\gamma$ |
|---|---|---|---|---|---|---|
| −40 | 1.514 | 1.57 | E − 5 | 1.04 | E − 5 | 1.401 |
| −20 | 1.395 | 1.63 | E − 5 | 1.17 | E − 5 | 1.401 |
| 0 | 1.292 | 1.71 | E − 5 | 1.32 | E − 5 | 1.401 |
| 5 | 1.269 | 1.73 | E − 5 | 1.36 | E − 5 | 1.401 |
| 10 | 1.247 | 1.76 | E − 5 | 1.41 | E − 5 | 1.401 |
| 15 | 1.225 | 1.80 | E − 5 | 1.47 | E − 5 | 1.401 |
| 20 | 1.204 | 1.82 | E − 5 | 1.51 | E − 5 | 1.401 |
| 25 | 1.184 | 1.85 | E − 5 | 1.56 | E − 5 | 1.401 |
| 30 | 1.165 | 1.86 | E − 5 | 1.60 | E − 5 | 1.400 |
| 40 | 1.127 | 1.87 | E − 5 | 1.66 | E − 5 | 1.400 |
| 50 | 1.109 | 1.95 | E − 5 | 1.76 | E − 5 | 1.400 |
| 60 | 1.060 | 1.97 | E − 5 | 1.86 | E − 5 | 1.399 |
| 70 | 1.029 | 2.03 | E − 5 | 1.97 | E − 5 | 1.399 |
| 80 | 0.9996 | 2.07 | E − 5 | 2.07 | E − 5 | 1.399 |
| 90 | 0.9721 | 2.14 | E − 5 | 2.20 | E − 5 | 1.398 |
| 100 | 0.9461 | 2.17 | E − 5 | 2.29 | E − 5 | 1.397 |
| 200 | 0.7461 | 2.53 | E − 5 | 3.39 | E − 5 | 1.390 |
| 300 | 0.6159 | 2.98 | E − 5 | 4.84 | E − 5 | 1.379 |
| 400 | 0.5243 | 3.32 | E − 5 | 6.34 | E − 5 | 1.368 |
| 500 | 0.4565 | 3.64 | E − 5 | 7.97 | E − 5 | 1.357 |
| 1000 | 0.2772 | 5.04 | E − 5 | 1.82 | E − 4 | 1.321 |

[a] Based on data from R. D. Blevins, *Applied Fluid Dynamics Handbook*, Van Nostrand Reinhold Co., Inc., New York, 1984.

**TABLE C.2  Physical Properties of Air at Standard Atmospheric Pressure (BG Units)[a]**

| Temperature (°F) | Density, $\rho$ (slug/ft³) | | Dynamic viscosity, $\mu$ (lb$_f \cdot$ s/ft²) | | Kinematic viscosity, $\nu$ (ft²/s) | | Specific heat ratio, $\gamma$ |
|---|---|---|---|---|---|---|---|
| −40  | 2.939 | E − 3 | 3.29 | E − 7 | 1.12 | E − 4 | 1.401 |
| −20  | 2.805 | E − 3 | 3.34 | E − 7 | 1.19 | E − 4 | 1.401 |
| 0    | 2.683 | E − 3 | 3.38 | E − 7 | 1.26 | E − 4 | 1.401 |
| 10   | 2.626 | E − 3 | 3.44 | E − 7 | 1.31 | E − 4 | 1.401 |
| 20   | 2.571 | E − 3 | 3.50 | E − 7 | 1.36 | E − 4 | 1.401 |
| 30   | 2.519 | E − 3 | 3.58 | E − 7 | 1.42 | E − 4 | 1.401 |
| 40   | 2.469 | E − 3 | 3.60 | E − 7 | 1.46 | E − 4 | 1.401 |
| 50   | 2.420 | E − 3 | 3.68 | E − 7 | 1.52 | E − 4 | 1.401 |
| 60   | 2.373 | E − 3 | 3.75 | E − 7 | 1.58 | E − 4 | 1.401 |
| 70   | 2.329 | E − 3 | 3.82 | E − 7 | 1.64 | E − 4 | 1.401 |
| 80   | 2.286 | E − 3 | 3.86 | E − 7 | 1.69 | E − 4 | 1.400 |
| 90   | 2.244 | E − 3 | 3.90 | E − 7 | 1.74 | E − 4 | 1.400 |
| 100  | 2.204 | E − 3 | 3.94 | E − 7 | 1.79 | E − 4 | 1.400 |
| 120  | 2.128 | E − 3 | 4.02 | E − 7 | 1.89 | E − 4 | 1.400 |
| 140  | 2.057 | E − 3 | 4.13 | E − 7 | 2.01 | E − 4 | 1.399 |
| 160  | 1.990 | E − 3 | 4.22 | E − 7 | 2.12 | E − 4 | 1.399 |
| 180  | 1.928 | E − 3 | 4.34 | E − 7 | 2.25 | E − 4 | 1.399 |
| 200  | 1.870 | E − 3 | 4.49 | E − 7 | 2.40 | E − 4 | 1.398 |
| 300  | 1.624 | E − 3 | 4.97 | E − 7 | 3.06 | E − 4 | 1.394 |
| 400  | 1.435 | E − 3 | 5.24 | E − 7 | 3.65 | E − 4 | 1.389 |
| 500  | 1.285 | E − 3 | 5.80 | E − 7 | 4.51 | E − 4 | 1.383 |
| 750  | 1.020 | E − 3 | 6.81 | E − 7 | 6.68 | E − 4 | 1.367 |
| 1000 | 8.445 | E − 4 | 7.85 | E − 7 | 9.30 | E − 4 | 1.351 |
| 1500 | 6.291 | E − 4 | 9.50 | E − 7 | 1.51 | E − 3 | 1.329 |

[a] Based on data from R. D. Blevins, *Applied Fluid Dynamics Handbook,* Van Nostrand Reinhold Co., Inc., New York, 1984.

**TABLE C.3  Physical Properties of Water (SI Units)[a]**

| Temperature (°C) | Density, $\rho$ (kg/m³) | Dynamic viscosity, $\mu$ (N·s/m²) | Kinematic viscosity, $\nu$ (m²/s) | Surface tension[b], $\sigma$ (N/m) | Vapor pressure, $p_v$ [N/m²(abs)] |
|---|---|---|---|---|---|
| 0 | 999.9 | 1.787 E − 3 | 1.787 E − 6 | 7.56 E − 2 | 6.105 E + 2 |
| 5 | 1000.0 | 1.519 E − 3 | 1.519 E − 6 | 7.49 E − 2 | 8.722 E + 2 |
| 10 | 999.7 | 1.307 E − 3 | 1.307 E − 6 | 7.42 E − 2 | 1.228 E + 3 |
| 20 | 998.2 | 1.002 E − 3 | 1.004 E − 6 | 7.28 E − 2 | 2.338 E + 3 |
| 30 | 995.7 | 7.975 E − 4 | 8.009 E − 7 | 7.12 E − 2 | 4.243 E + 3 |
| 40 | 992.2 | 6.529 E − 4 | 6.580 E − 7 | 6.96 E − 2 | 7.376 E + 3 |
| 50 | 988.1 | 5.468 E − 4 | 5.534 E − 7 | 6.79 E − 2 | 1.233 E + 4 |
| 60 | 983.2 | 4.665 E − 4 | 4.745 E − 7 | 6.62 E − 2 | 1.992 E + 4 |
| 70 | 977.8 | 4.042 E − 4 | 4.134 E − 7 | 6.44 E − 2 | 3.116 E + 4 |
| 80 | 971.8 | 3.547 E − 4 | 3.650 E − 7 | 6.26 E − 2 | 4.734 E + 4 |
| 90 | 965.3 | 3.147 E − 4 | 3.260 E − 7 | 6.08 E − 2 | 7.010 E + 4 |
| 100 | 958.4 | 2.818 E − 4 | 2.940 E − 7 | 5.89 E − 2 | 1.013 E + 5 |

[a] Based on data from *Handbook of Chemistry and Physics*, 69th Ed., CRC Press, 1988.
[b] In contact with air.

**TABLE C.4  Physical Properties of Water (BG Units)[a]**

| Temperature (°F) | Density, $\rho$ (slugs/ft³) | Dynamic viscosity, $\mu$ (lb$_f$·s/ft²) | Kinematic viscosity, $\nu$ (ft²/s) | Surface tension[b], $\sigma$ (lb$_f$/ft) | Vapor pressure, $p_v$ [lb$_f$/in.²(abs)] |
|---|---|---|---|---|---|
| 32 | 1.940 | 3.732 E − 5 | 1.924 E − 5 | 5.18 E − 3 | 8.854 E − 2 |
| 40 | 1.940 | 3.228 E − 5 | 1.664 E − 5 | 5.13 E − 3 | 1.217 E − 1 |
| 50 | 1.940 | 2.730 E − 5 | 1.407 E − 5 | 5.09 E − 3 | 1.781 E − 1 |
| 60 | 1.938 | 2.344 E − 5 | 1.210 E − 5 | 5.03 E − 3 | 2.563 E − 1 |
| 70 | 1.936 | 2.037 E − 5 | 1.052 E − 5 | 4.97 E − 3 | 3.631 E − 1 |
| 80 | 1.934 | 1.791 E − 5 | 9.262 E − 6 | 4.91 E − 3 | 5.069 E − 1 |
| 90 | 1.931 | 1.500 E − 5 | 8.233 E − 6 | 4.86 E − 3 | 6.979 E − 1 |
| 100 | 1.927 | 1.423 E − 5 | 7.383 E − 6 | 4.79 E − 3 | 9.493 E − 1 |
| 120 | 1.918 | 1.164 E − 5 | 6.067 E − 6 | 4.67 E − 3 | 1.692 E + 0 |
| 140 | 1.908 | 9.743 E − 6 | 5.106 E − 6 | 4.53 E − 3 | 2.888 E + 0 |
| 160 | 1.896 | 8.315 E − 6 | 4.385 E − 6 | 4.40 E − 3 | 4.736 E + 0 |
| 180 | 1.883 | 7.207 E − 6 | 3.827 E − 6 | 4.26 E − 3 | 7.507 E + 0 |
| 200 | 1.869 | 6.342 E − 6 | 3.393 E − 6 | 4.12 E − 3 | 1.152 E + 1 |
| 212 | 1.860 | 5.886 E − 6 | 3.165 E − 6 | 4.04 E − 3 | 1.469 E + 1 |

[a] Based on data from *Handbook of Chemistry and Physics,* 69th Ed., CRC Prass, 1988.
[b] In contact with air.

**TABLE C.5　Properties of the U.S. Standard Atmosphere (SI Units)[a]**

| Altitude (m) | Temperature (°C) | Acceleration of gravity, $g$ (m/s²) | Pressure, $p$ [N/m²(abs)] | | Density, $\rho$ (kg/m³) | | Dynamic viscosity, $\mu$ (N·s/m²) | |
|---|---|---|---|---|---|---|---|---|
| −1,000 | 21.50 | 9.810 | 1.139 | E + 5 | 1.347 | E + 0 | 1.821 | E − 5 |
| 0 | 15.00 | 9.807 | 1.103 | E + 5 | 1.225 | E + 0 | 1.789 | E − 5 |
| 1,000 | 8.50 | 9.804 | 8.988 | E + 4 | 1.112 | E + 0 | 1.758 | E − 5 |
| 2,000 | 2.00 | 9.801 | 7.950 | E + 4 | 1.007 | E + 0 | 1.726 | E − 5 |
| 3,000 | −4.49 | 9.797 | 7.012 | E + 4 | 9.093 | E − 1 | 1.694 | E − 5 |
| 4,000 | −10.98 | 9.794 | 6.166 | E + 4 | 8.194 | E − 1 | 1.661 | E − 5 |
| 5,000 | −17.47 | 9.791 | 5.405 | E + 4 | 7.364 | E − 1 | 1.628 | E − 5 |
| 6,000 | −23.96 | 9.788 | 4.722 | E + 4 | 6.601 | E − 1 | 1.595 | E − 5 |
| 7,000 | −30.45 | 9.785 | 4.111 | E + 4 | 5.900 | E − 1 | 1.561 | E − 5 |
| 8,000 | −36.94 | 9.782 | 3.565 | E + 4 | 5.258 | E − 1 | 1.527 | E − 5 |
| 9,000 | −43.42 | 9.779 | 3.080 | E + 4 | 4.671 | E − 1 | 1.493 | E − 5 |
| 10,000 | −49.90 | 9.776 | 2.650 | E + 4 | 4.135 | E − 1 | 1.458 | E − 5 |
| 15,000 | −56.50 | 9.761 | 1.211 | E + 4 | 1.948 | E − 1 | 1.422 | E − 5 |
| 20,000 | −56.50 | 9.745 | 5.529 | E + 3 | 8.891 | E − 2 | 1.422 | E − 5 |
| 25,000 | −51.60 | 9.730 | 2.549 | E + 3 | 4.008 | E − 2 | 1.448 | E − 5 |
| 30,000 | −46.64 | 9.715 | 1.197 | E + 3 | 1.841 | E − 2 | 1.475 | E − 5 |
| 40,000 | −22.80 | 9.684 | 2.871 | E + 2 | 3.996 | E − 3 | 1.601 | E − 5 |
| 50,000 | −2.50 | 9.654 | 7.978 | E + 1 | 1.027 | E − 3 | 1.704 | E − 5 |
| 60,000 | −26.13 | 9.624 | 2.196 | E + 1 | 3.097 | E − 4 | 1.584 | E − 5 |
| 70,000 | −53.57 | 9.594 | 5.221 | E + 0 | 8.283 | E − 5 | 1.438 | E − 5 |
| 80,000 | −74.51 | 9.564 | 1.052 | E + 0 | 1.846 | E − 5 | 1.321 | E − 5 |

[a] Data from *U.S. Standard Atmosphere,* 1976, U.S. Government Printing Office, Washington, D.C.

**TABLE C.6  Properties of the U.S. Standard Atmosphere (BG Units)[a]**

| Altitude (ft) | Temperature (°F) | Acceleration of gravity, $g$ (ft/s²) | Pressure, $p$ [lb$_f$/in.²(abs)] | Density, $\rho$ (slugs/ft³) | Dynamic viscosity, $\mu$ (lb$_f \cdot$ s/ft²) |
|---|---|---|---|---|---|
| −5,000 | 76.84 | 32.189 | 17.554 | 2.745 E − 3 | 3.836 E − 7 |
| 0 | 59.00 | 32.174 | 14.696 | 2.377 E − 3 | 3.737 E − 7 |
| 5,000 | 41.17 | 32.159 | 12.228 | 2.048 E − 3 | 3.637 E − 7 |
| 10,000 | 23.36 | 32.143 | 10.108 | 1.756 E − 3 | 3.534 E − 7 |
| 15,000 | 5.55 | 32.128 | 8.297 | 1.496 E − 3 | 3.430 E − 7 |
| 20,000 | −12.26 | 32.112 | 6.759 | 1.267 E − 3 | 3.324 E − 7 |
| 25,000 | −30.05 | 32.097 | 5.461 | 1.066 E − 3 | 3.217 E − 7 |
| 30,000 | −47.83 | 32.082 | 4.373 | 8.907 E − 4 | 3.107 E − 7 |
| 35,000 | −65.61 | 32.066 | 3.468 | 7.382 E − 4 | 2.995 E − 7 |
| 40,000 | −69.70 | 32.051 | 2.730 | 5.873 E − 4 | 2.969 E − 7 |
| 45,000 | −69.70 | 32.036 | 2.149 | 4.623 E − 4 | 2.969 E − 7 |
| 50,000 | −69.70 | 32.020 | 1.692 | 3.639 E − 4 | 2.969 E − 7 |
| 60,000 | −69.70 | 31.990 | 1.049 | 2.256 E − 4 | 2.969 E − 7 |
| 70,000 | −67.42 | 31.959 | 0.651 | 1.392 E − 4 | 2.984 E − 7 |
| 80,000 | −61.98 | 31.929 | 0.406 | 8.571 E − 5 | 3.018 E − 7 |
| 90,000 | −56.54 | 31.897 | 0.255 | 5.610 E − 5 | 3.052 E − 7 |
| 100,000 | −51.10 | 31.868 | 0.162 | 3.318 E − 5 | 3.087 E − 7 |
| 150,000 | 19.40 | 31.717 | 0.020 | 3.658 E − 6 | 3.511 E − 7 |
| 200,000 | −19.78 | 31.566 | 0.003 | 5.328 E − 7 | 3.279 E − 7 |
| 250,000 | −88.77 | 31.415 | 0.000 | 6.458 E − 8 | 2.846 E − 7 |

[a] Data from *U.S. Standard Atmosphere,* 1976, U.S. Government Printing Office, Washington, D.C.

**TABLE C.7  Densities of Some Common Solids and Fluids (kg/m³) at Atmospheric Pressure and 20°C**

| | | | |
|---|---|---|---|
| Gold | 19,300 | Lead | 11,370 |
| Silver | 10,510 | Copper | 8906 |
| Steel | 7850 | Aluminum | 2770 |
| Plexiglass | 1180 | Water (20°C) | 998 |
| Oak (red) | 660 | Ice | 920 |
| Pine (Eastern, white) | 370 | Sea water | 1025 |
| Mercury | 13,550 | SAE 30 oil | 917 |
| Kerosene | 809 | Gasoline | 680 |
| Ethyl alcohol | 789 | Air (sea level) | 1.204 |
| Carbon dioxide | 1.85 | Argon | 1.679 |
| Methane (natural gas) | 0.677 | Propane | 1.854 |
| Hydrogen | 0.0851 | Helium | 0.169 |
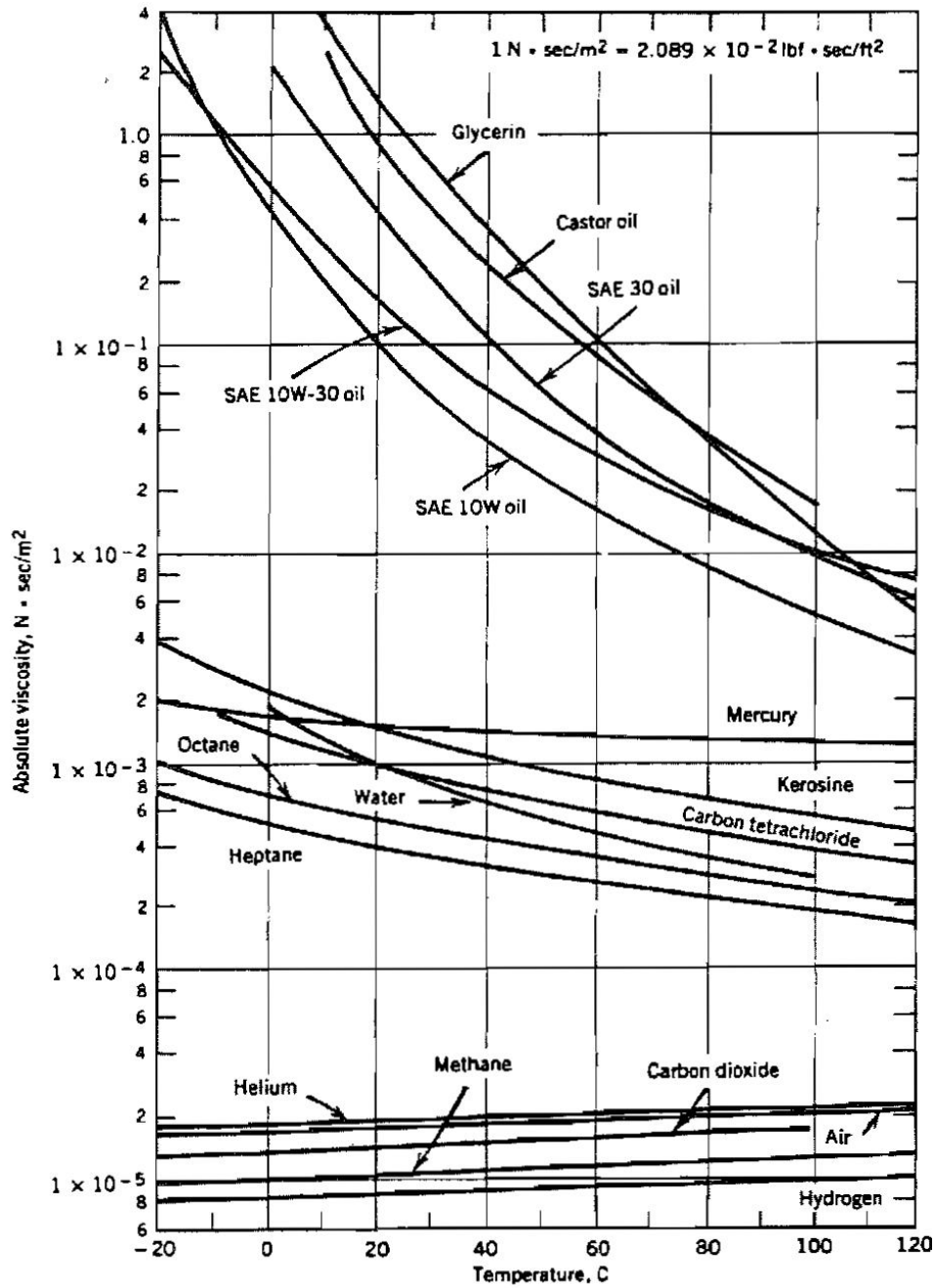
Figure C.1: Dynamic viscosity of common fluids as a function of temperature (at one atmosphere). Adapted from Fox & Macdonald, *Introduction to Fluid Mechanics.*
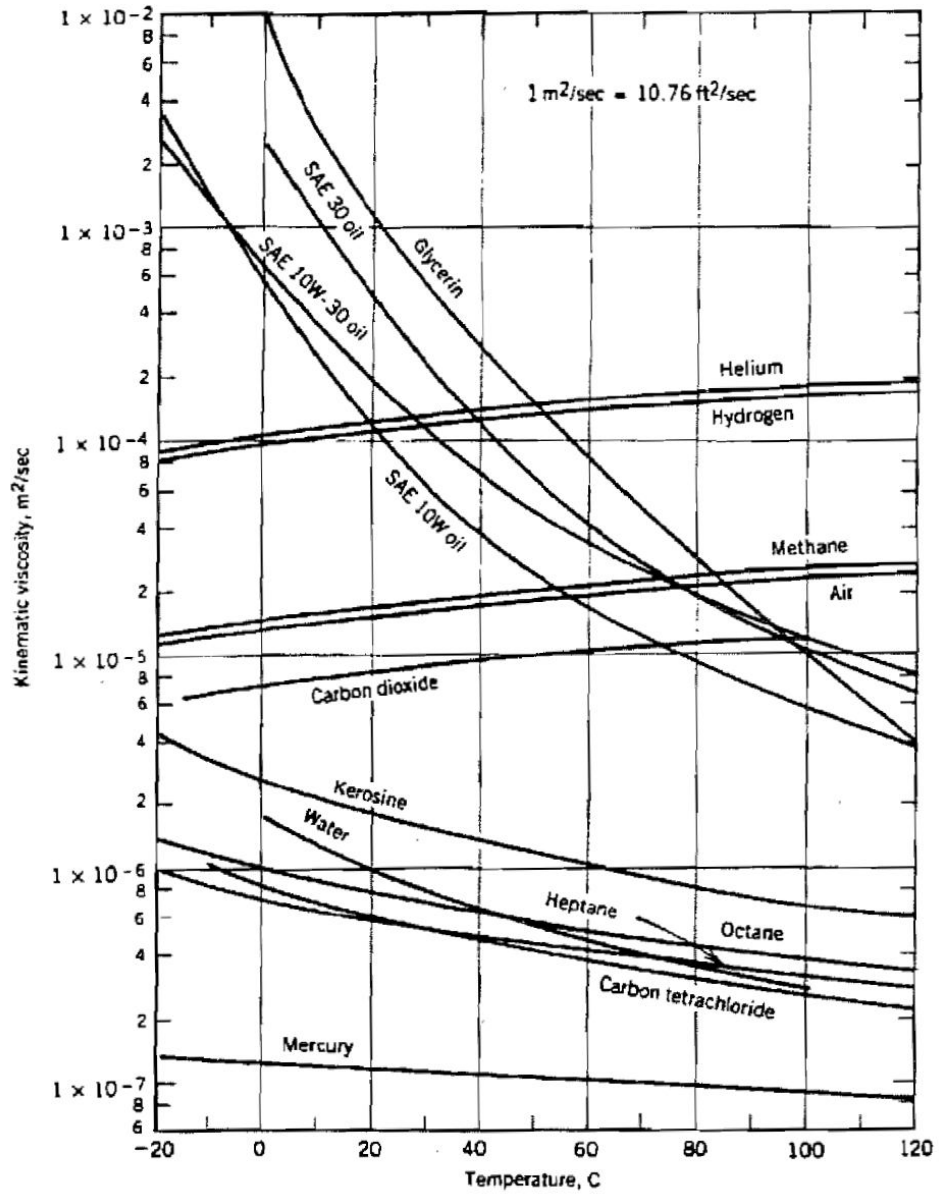
Figure C.2: Kinematic viscosity of common fluids as a function of temperature (at one atmosphere). Adapted from Fox & Macdonald, *Introduction to Fluid Mechanics*.

**TABLE C.8   Properties of Common Gases at Atmospheric Pressure and 20°C**

| Gas | Molecular weight | $R$ [m²/(s²·K)] | $\rho$ (kg/m³) | $\mu$ [(N·s)/m²] | Specific heat ratio $\gamma$ |
|------|------|------|------|------|------|
| $H_2$ | 2.016 | 4124 | 0.0838 | 9.05 E − 6 | 1.41 |
| He | 4.003 | 2077 | 0.166 | 1.97 E − 5 | 1.66 |
| $H_2O$ | 18.02 | 461 | 0.749 | 1.02 E − 5 | 1.33 |
| Ar | 39.944 | 208 | 1.66 | 2.24 E − 5 | 1.67 |
| Dry air | 28.96 | 287 | 1.20 | 1.80 E − 5 | 1.40 |
| $CO_2$ | 44.01 | 189 | 1.83 | 1.48 E − 5 | 1.30 |
| CO | 28.01 | 297 | 1.16 | 1.82 E − 5 | 1.40 |
| $N_2$ | 28.02 | 297 | 1.16 | 1.76 E − 5 | 1.40 |
| $O_2$ | 32.00 | 260 | 1.34 | 2.00 E − 5 | 1.40 |
| NO | 30.01 | 277 | 1.23 | 1.90 E − 5 | 1.40 |
| $N_2O$ | 44.02 | 189 | 1.83 | 1.45 E − 5 | 1.31 |
| $Cl_2$ | 70.91 | 117 | 2.95 | 1.03 E − 5 | 1.34 |
| $CH_4$ | 16.04 | 518 | 0.667 | 1.34 E − 5 | 1.32 |

Adapted from White, *Fluid Mechanics,* McGraw-Hill, 1986.

**TABLE C.9   Properties of Common Liquids at Atmospheric Pressure and 20°C**

| Liquid | $\rho$ (kg/m³) | $\mu$ [(N·s)/m²] | $\sigma$ (N/m) | $p_v$ (N/m²) | Bulk modulus, (N/m²) |
|------|------|------|------|------|------|
| Ammonia | 608 | 2.20 E − 4 | 2.13 E − 2 | 9.10 E + 5 | |
| Benzene | 881 | 6.51 E − 4 | 2.88 E − 2 | 1.01 E + 4 | 1.05 E + 9 |
| Carbon tetrachloride | 1,590 | 9.67 E − 4 | 2.70 E − 2 | 1.20 E + 4 | 9.65 E + 8 |
| Ethanol | 789 | 1.20 E − 3 | 2.28 E − 2 | 5.7 E + 3 | 8.96 E + 8 |
| Gasoline | 680 | 2.92 E − 4 | 2.16 E − 2 | 5.51 E + 4 | 9.58 E + 8 |
| Glycerin | 1,260 | 1.49 | 6.33 E − 2 | 1.4 E − 2 | 4.34 E + 9 |
| Kerosene | 804 | 1.92 E − 3 | 2.8 E − 2 | 3.11 E + 3 | 1.43 E + 9 |
| Mercury | 13,550 | 1.56 E − 3 | 4.84 E − 1 | 1.1 E − 3 | 2.55 E + 10 |
| Methanol | 791 | 5.98 E − 4 | 2.25 E − 2 | 1.34 E + 4 | 8.27 E + 8 |
| SAE 10 oil | 917 | 1.04 E − 1 | 3.6 E − 2 | | 1.31 E + 9 |
| SAE 30 oil | 917 | 2.90 E − 1 | 3.5 E − 2 | | 1.38 E + 9 |
| Water | 998 | 1.00 E − 3 | 7.28 E − 2 | 2.34 E + 3 | 2.19 E + 9 |
| Seawater | 1,025 | 1.07 E − 3 | 7.28 E − 2 | 2.34 E + 3 | 2.28 E + 9 |

Adapted from White, *Fluid Mechanics,* McGraw-Hill, 1986.

**TABLE C.10   Isentropic Flow Functions
(One-Dimensional, Ideal Gas, $\gamma = 1.4$)**

| M | $T/T_0$ | $p/p_0$ | $\rho/\rho_0$ | $A/A^*$ |
|------|--------|--------|--------|--------|
| 0.00 | 1.0000 | 1.0000 | 1.0000 | $\infty$ |
| 0.02 | 0.9999 | 0.9997 | 0.9998 | 28.94 |
| 0.04 | 0.9997 | 0.9989 | 0.9992 | 14.48 |
| 0.06 | 0.9993 | 0.9975 | 0.9982 | 9.666 |
| 0.08 | 0.9987 | 0.9955 | 0.9968 | 7.262 |
| 0.10 | 0.9980 | 0.9930 | 0.9950 | 5.822 |
| 0.12 | 0.9971 | 0.9900 | 0.9928 | 4.864 |
| 0.14 | 0.9961 | 0.9864 | 0.9903 | 4.182 |
| 0.16 | 0.9949 | 0.9823 | 0.9873 | 3.673 |
| 0.18 | 0.9936 | 0.9777 | 0.9840 | 3.278 |
| 0.20 | 0.9921 | 0.9725 | 0.9803 | 2.964 |
| 0.22 | 0.9904 | 0.9669 | 0.9762 | 2.708 |
| 0.24 | 0.9886 | 0.9607 | 0.9718 | 2.496 |
| 0.26 | 0.9867 | 0.9541 | 0.9670 | 2.317 |
| 0.28 | 0.9846 | 0.9470 | 0.9619 | 2.166 |
| 0.30 | 0.9823 | 0.9395 | 0.9564 | 2.035 |
| 0.32 | 0.9799 | 0.9315 | 0.9506 | 1.922 |
| 0.34 | 0.9774 | 0.9231 | 0.9445 | 1.823 |
| 0.36 | 0.9747 | 0.9143 | 0.9380 | 1.736 |
| 0.38 | 0.9719 | 0.9052 | 0.9313 | 1.659 |
| 0.40 | 0.9690 | 0.8956 | 0.9243 | 1.590 |
| 0.42 | 0.9659 | 0.8857 | 0.9170 | 1.529 |
| 0.44 | 0.9627 | 0.8755 | 0.9094 | 1.474 |
| 0.46 | 0.9594 | 0.8650 | 0.9016 | 1.425 |
| 0.48 | 0.9560 | 0.8541 | 0.8935 | 1.380 |
| 0.50 | 0.9524 | 0.8430 | 0.8852 | 1.340 |
| 0.52 | 0.9487 | 0.8317 | 0.8766 | 1.303 |
| 0.54 | 0.9449 | 0.8201 | 0.8679 | 1.270 |
| 0.56 | 0.9410 | 0.8082 | 0.8589 | 1.240 |
| 0.58 | 0.9370 | 0.7962 | 0.8498 | 1.213 |
| 0.60 | 0.9328 | 0.7840 | 0.8405 | 1.188 |
| 0.62 | 0.9286 | 0.7716 | 0.8310 | 1.166 |
| 0.64 | 0.9243 | 0.7591 | 0.8213 | 1.145 |
| 0.66 | 0.9199 | 0.7465 | 0.8115 | 1.127 |
| 0.68 | 0.9154 | 0.7338 | 0.8016 | 1.110 |
| 0.70 | 0.9108 | 0.7209 | 0.7916 | 1.094 |
| 0.72 | 0.9061 | 0.7080 | 0.7814 | 1.081 |
| 0.74 | 0.9013 | 0.6951 | 0.7712 | 1.068 |
| 0.76 | 0.8964 | 0.6821 | 0.7609 | 1.057 |
| 0.78 | 0.8915 | 0.6691 | 0.7505 | 1.047 |
| 0.80 | 0.8865 | 0.6560 | 0.7400 | 1.038 |
| 0.82 | 0.8815 | 0.6430 | 0.7295 | 1.030 |
| 0.84 | 0.8763 | 0.6300 | 0.7189 | 1.024 |
| 0.86 | 0.8711 | 0.6170 | 0.7083 | 1.018 |
| 0.88 | 0.8659 | 0.6041 | 0.6977 | 1.013 |
| 0.90 | 0.8606 | 0.5913 | 0.6870 | 1.009 |

**TABLE C.10   Isentropic Flow Functions**
(Continued)

| M | $T/T_0$ | $p/p_0$ | $\rho/\rho_0$ | $A/A^*$ |
|------|--------|--------|--------|--------|
| 0.92 | 0.8552 | 0.5785 | 0.6764 | 1.006 |
| 0.94 | 0.8498 | 0.5658 | 0.6658 | 1.003 |
| 0.96 | 0.8444 | 0.5532 | 0.6551 | 1.001 |
| 0.98 | 0.8389 | 0.5407 | 0.6445 | 1.000 |
| 1.00 | 0.8333 | 0.5283 | 0.6339 | 1.000 |
| 1.02 | 0.8278 | 0.5160 | 0.6234 | 1.000 |
| 1.04 | 0.8222 | 0.5039 | 0.6129 | 1.001 |
| 1.06 | 0.8165 | 0.4919 | 0.6024 | 1.003 |
| 1.08 | 0.8108 | 0.4801 | 0.5920 | 1.005 |
| 1.10 | 0.8052 | 0.4684 | 0.5817 | 1.008 |
| 1.12 | 0.7994 | 0.4568 | 0.5714 | 1.011 |
| 1.14 | 0.7937 | 0.4455 | 0.5612 | 1.015 |
| 1.16 | 0.7880 | 0.4343 | 0.5511 | 1.020 |
| 1.18 | 0.7822 | 0.4232 | 0.5411 | 1.025 |
| 1.20 | 0.7764 | 0.4124 | 0.5311 | 1.030 |
| 1.22 | 0.7706 | 0.4017 | 0.5213 | 1.037 |
| 1.24 | 0.7648 | 0.3912 | 0.5115 | 1.043 |
| 1.26 | 0.7590 | 0.3809 | 0.5019 | 1.050 |
| 1.28 | 0.7532 | 0.3708 | 0.4923 | 1.058 |
| 1.30 | 0.7474 | 0.3609 | 0.4829 | 1.066 |
| 1.32 | 0.7416 | 0.3512 | 0.4736 | 1.075 |
| 1.34 | 0.7358 | 0.3417 | 0.4644 | 1.084 |
| 1.36 | 0.7300 | 0.3323 | 0.4553 | 1.094 |
| 1.38 | 0.7242 | 0.3232 | 0.4463 | 1.104 |
| 1.40 | 0.7184 | 0.3142 | 0.4374 | 1.115 |
| 1.42 | 0.7126 | 0.3055 | 0.4287 | 1.126 |
| 1.44 | 0.7069 | 0.2969 | 0.4201 | 1.138 |
| 1.46 | 0.7011 | 0.2886 | 0.4116 | 1.150 |
| 1.48 | 0.6954 | 0.2804 | 0.4032 | 1.163 |
| 1.50 | 0.6897 | 0.2724 | 0.3950 | 1.176 |
| 1.52 | 0.6840 | 0.2646 | 0.3869 | 1.190 |
| 1.54 | 0.6783 | 0.2570 | 0.3789 | 1.204 |
| 1.56 | 0.6726 | 0.2496 | 0.3711 | 1.219 |
| 1.58 | 0.6670 | 0.2423 | 0.3633 | 1.234 |
| 1.60 | 0.6614 | 0.2353 | 0.3557 | 1.250 |
| 1.62 | 0.6558 | 0.2284 | 0.3483 | 1.267 |
| 1.64 | 0.6502 | 0.2217 | 0.3409 | 1.284 |
| 1.66 | 0.6447 | 0.2152 | 0.3337 | 1.301 |
| 1.68 | 0.6392 | 0.2088 | 0.3266 | 1.319 |
| 1.70 | 0.6337 | 0.2026 | 0.3197 | 1.338 |
| 1.72 | 0.6283 | 0.1966 | 0.3129 | 1.357 |
| 1.74 | 0.6229 | 0.1907 | 0.3062 | 1.376 |
| 1.76 | 0.6175 | 0.1850 | 0.2996 | 1.397 |
| 1.78 | 0.6121 | 0.1794 | 0.2931 | 1.418 |
| 1.80 | 0.6068 | 0.1740 | 0.2868 | 1.439 |

**TABLE C.10  Isentropic Flow Functions**
(*Continued*)

| M | $T/T_0$ | $p/p_0$ | $\rho/\rho_0$ | $A/A^*$ |
|---|---------|---------|---------------|---------|
| 1.82 | 0.6015 | 0.1688 | 0.2806 | 1.461 |
| 1.84 | 0.5963 | 0.1637 | 0.2745 | 1.484 |
| 1.86 | 0.5911 | 0.1587 | 0.2686 | 1.507 |
| 1.88 | 0.5859 | 0.1539 | 0.2627 | 1.531 |
| 1.90 | 0.5807 | 0.1492 | 0.2570 | 1.555 |
| 1.92 | 0.5756 | 0.1447 | 0.2514 | 1.580 |
| 1.94 | 0.5705 | 0.1403 | 0.2459 | 1.606 |
| 1.96 | 0.5655 | 0.1360 | 0.2405 | 1.633 |
| 1.98 | 0.5605 | 0.1318 | 0.2352 | 1.660 |
| 2.00 | 0.5556 | 0.1278 | 0.2301 | 1.688 |
| 2.02 | 0.5506 | 0.1239 | 0.2250 | 1.716 |
| 2.04 | 0.5458 | 0.1201 | 0.2200 | 1.745 |
| 2.06 | 0.5409 | 0.1164 | 0.2152 | 1.775 |
| 2.08 | 0.5361 | 0.1128 | 0.2105 | 1.806 |
| 2.10 | 0.5314 | 0.1094 | 0.2058 | 1.837 |
| 2.12 | 0.5266 | 0.1060 | 0.2013 | 1.869 |
| 2.14 | 0.5219 | 0.1027 | 0.1968 | 1.902 |
| 2.16 | 0.5173 | 0.09956 | 0.1925 | 1.935 |
| 2.18 | 0.5127 | 0.09650 | 0.1882 | 1.970 |
| 2.20 | 0.5081 | 0.09352 | 0.1841 | 2.005 |
| 2.22 | 0.5036 | 0.09064 | 0.1800 | 2.041 |
| 2.24 | 0.4991 | 0.08784 | 0.1760 | 2.078 |
| 2.26 | 0.4947 | 0.08514 | 0.1721 | 2.115 |
| 2.28 | 0.4903 | 0.08252 | 0.1683 | 2.154 |
| 2.30 | 0.4859 | 0.07997 | 0.1646 | 2.193 |
| 2.32 | 0.4816 | 0.07751 | 0.1610 | 2.233 |
| 2.34 | 0.4773 | 0.07513 | 0.1574 | 2.274 |
| 2.36 | 0.4731 | 0.07281 | 0.1539 | 2.316 |
| 2.38 | 0.4689 | 0.07057 | 0.1505 | 2.359 |
| 2.40 | 0.4647 | 0.06840 | 0.1472 | 2.403 |
| 2.42 | 0.4606 | 0.06630 | 0.1440 | 2.448 |
| 2.44 | 0.4565 | 0.06426 | 0.1408 | 2.494 |
| 2.46 | 0.4524 | 0.06229 | 0.1377 | 2.540 |
| 2.48 | 0.4484 | 0.06038 | 0.1347 | 2.588 |
| 2.50 | 0.4444 | 0.05853 | 0.1317 | 2.637 |
| 2.52 | 0.4405 | 0.05674 | 0.1288 | 2.687 |
| 2.54 | 0.4366 | 0.05500 | 0.1260 | 2.737 |
| 2.56 | 0.4328 | 0.05332 | 0.1232 | 2.789 |
| 2.58 | 0.4289 | 0.05169 | 0.1205 | 2.842 |
| 2.60 | 0.4252 | 0.05012 | 0.1179 | 2.896 |
| 2.62 | 0.4214 | 0.04859 | 0.1153 | 2.951 |
| 2.64 | 0.4177 | 0.04711 | 0.1128 | 3.007 |
| 2.66 | 0.4141 | 0.04568 | 0.1103 | 3.065 |
| 2.68 | 0.4104 | 0.04429 | 0.1079 | 3.123 |
| 2.70 | 0.4068 | 0.04295 | 0.1056 | 3.183 |

**TABLE C.10   Isentropic Flow Functions**
(Continued)

| M | $T/T_0$ | $p/p_0$ | $\rho/\rho_0$ | $A/A^*$ |
|------|--------|----------|----------|--------|
| 2.72 | 0.4033 | 0.04166 | 0.1033 | 3.244 |
| 2.74 | 0.3998 | 0.04039 | 0.1010 | 3.306 |
| 2.76 | 0.3963 | 0.03917 | 0.09885 | 3.370 |
| 2.78 | 0.3928 | 0.03800 | 0.09671 | 3.434 |
| 2.80 | 0.3894 | 0.03685 | 0.09462 | 3.500 |
| 2.82 | 0.3860 | 0.03574 | 0.09259 | 3.567 |
| 2.84 | 0.3827 | 0.03467 | 0.09059 | 3.636 |
| 2.86 | 0.3794 | 0.03363 | 0.08865 | 3.706 |
| 2.88 | 0.3761 | 0.03262 | 0.08674 | 3.777 |
| 2.90 | 0.3729 | 0.03165 | 0.08489 | 3.850 |
| 2.92 | 0.3697 | 0.03071 | 0.08308 | 3.924 |
| 2.94 | 0.3665 | 0.02980 | 0.08130 | 3.999 |
| 2.96 | 0.3633 | 0.02891 | 0.07957 | 4.076 |
| 2.98 | 0.3602 | 0.02805 | 0.07788 | 4.155 |
| 3.00 | 0.3571 | 0.02722 | 0.07623 | 4.235 |
| 3.10 | 0.3422 | 0.02345 | 0.06852 | 4.657 |
| 3.20 | 0.3281 | 0.02023 | 0.06165 | 5.121 |
| 3.30 | 0.3147 | 0.01748 | 0.05554 | 5.629 |
| 3.40 | 0.3019 | 0.01512 | 0.05009 | 6.184 |
| 3.50 | 0.2899 | 0.01311 | 0.04523 | 6.790 |
| 3.60 | 0.2784 | 0.01138 | 0.04089 | 7.450 |
| 3.70 | 0.2675 | 0.009903 | 0.03702 | 8.169 |
| 3.80 | 0.2572 | 0.008629 | 0.03355 | 8.951 |
| 3.90 | 0.2474 | 0.007532 | 0.03044 | 9.799 |
| 4.00 | 0.2381 | 0.006586 | 0.02766 | 10.72 |
| 4.10 | 0.2293 | 0.005769 | 0.02516 | 11.71 |
| 4.20 | 0.2208 | 0.005062 | 0.02292 | 12.79 |
| 4.30 | 0.2129 | 0.004449 | 0.02090 | 13.95 |
| 4.40 | 0.2053 | 0.003918 | 0.01909 | 15.21 |
| 4.50 | 0.1980 | 0.003455 | 0.01745 | 16.56 |
| 4.60 | 0.1911 | 0.003053 | 0.01597 | 18.02 |
| 4.70 | 0.1846 | 0.002701 | 0.01463 | 19.58 |
| 4.80 | 0.1783 | 0.002394 | 0.01343 | 21.26 |
| 4.90 | 0.1724 | 0.002126 | 0.01233 | 23.07 |
| 5.00 | 0.1667 | 0.001890 | 0.01134 | 25.00 |

Adapted from Fox and Macdonald, *Introduction to Fluid Mechanics*, published by John Wiley & Sons, 4th ed., 1992.

**TABLE C.11   Normal Shock Flow Functions
(One-Dimensional, Ideal Gas, $\gamma = 1.4$)**

| $M_1$ | $M_2$ | $p_{0_2}/p_{0_1}$ | $T_2/T_1$ | $p_2/p_1$ | $\rho_2/\rho_1$ |
|------|-------|-------------|----------|----------|------------|
| 1.00 | 1.000 | 1.000 | 1.000 | 1.000 | 1.000 |
| 1.02 | 0.9805 | 1.000 | 1.013 | 1.047 | 1.033 |
| 1.04 | 0.9620 | 0.9999 | 1.026 | 1.095 | 1.067 |
| 1.06 | 0.9444 | 0.9998 | 1.039 | 1.144 | 1.101 |
| 1.08 | 0.9277 | 0.9994 | 1.052 | 1.194 | 1.135 |
| 1.10 | 0.9118 | 0.9989 | 1.065 | 1.245 | 1.169 |
| 1.12 | 0.8966 | 0.9982 | 1.078 | 1.297 | 1.203 |
| 1.14 | 0.8820 | 0.9973 | 1.090 | 1.350 | 1.238 |
| 1.16 | 0.8682 | 0.9961 | 1.103 | 1.403 | 1.272 |
| 1.18 | 0.8549 | 0.9946 | 1.115 | 1.458 | 1.307 |
| 1.20 | 0.8422 | 0.9928 | 1.128 | 1.513 | 1.342 |
| 1.22 | 0.8300 | 0.9907 | 1.141 | 1.570 | 1.376 |
| 1.24 | 0.8183 | 0.9884 | 1.153 | 1.627 | 1.411 |
| 1.26 | 0.8071 | 0.9857 | 1.166 | 1.686 | 1.446 |
| 1.28 | 0.7963 | 0.9827 | 1.178 | 1.745 | 1.481 |
| 1.30 | 0.7860 | 0.9794 | 1.191 | 1.805 | 1.516 |
| 1.32 | 0.7760 | 0.9757 | 1.204 | 1.866 | 1.551 |
| 1.34 | 0.7664 | 0.9718 | 1.216 | 1.928 | 1.585 |
| 1.36 | 0.7572 | 0.9676 | 1.229 | 1.991 | 1.620 |
| 1.38 | 0.7483 | 0.9630 | 1.242 | 2.055 | 1.655 |
| 1.40 | 0.7397 | 0.9582 | 1.255 | 2.120 | 1.690 |
| 1.42 | 0.7314 | 0.9531 | 1.268 | 2.186 | 1.724 |
| 1.44 | 0.7235 | 0.9477 | 1.281 | 2.253 | 1.759 |
| 1.46 | 0.7157 | 0.9420 | 1.294 | 2.320 | 1.793 |
| 1.48 | 0.7083 | 0.9360 | 1.307 | 2.389 | 1.828 |
| 1.50 | 0.7011 | 0.9298 | 1.320 | 2.458 | 1.862 |
| 1.52 | 0.6941 | 0.9233 | 1.334 | 2.529 | 1.896 |
| 1.54 | 0.6874 | 0.9166 | 1.347 | 2.600 | 1.930 |
| 1.56 | 0.6809 | 0.9097 | 1.361 | 2.673 | 1.964 |
| 1.58 | 0.6746 | 0.9026 | 1.374 | 2.746 | 1.998 |
| 1.60 | 0.6684 | 0.8952 | 1.388 | 2.820 | 2.032 |
| 1.62 | 0.6625 | 0.8876 | 1.402 | 2.895 | 2.065 |
| 1.64 | 0.6568 | 0.8799 | 1.416 | 2.971 | 2.099 |
| 1.66 | 0.6512 | 0.8720 | 1.430 | 3.048 | 2.132 |
| 1.68 | 0.6458 | 0.8640 | 1.444 | 3.126 | 2.165 |
| 1.70 | 0.6406 | 0.8557 | 1.458 | 3.205 | 2.198 |
| 1.72 | 0.6355 | 0.8474 | 1.473 | 3.285 | 2.230 |
| 1.74 | 0.6305 | 0.8389 | 1.487 | 3.366 | 2.263 |
| 1.76 | 0.6257 | 0.8302 | 1.502 | 3.447 | 2.295 |
| 1.78 | 0.6210 | 0.8215 | 1.517 | 3.530 | 2.327 |
| 1.80 | 0.6165 | 0.8127 | 1.532 | 3.613 | 2.359 |
| 1.82 | 0.6121 | 0.8038 | 1.547 | 3.698 | 2.391 |
| 1.84 | 0.6078 | 0.7947 | 1.562 | 3.783 | 2.422 |
| 1.86 | 0.6036 | 0.7857 | 1.577 | 3.870 | 2.454 |
| 1.88 | 0.5996 | 0.7766 | 1.592 | 3.957 | 2.485 |
| 1.90 | 0.5956 | 0.7674 | 1.608 | 4.045 | 2.516 |

**TABLE C.11   Normal Shock Flow Functions**
(*Continued*)

| $M_1$ | $M_2$ | $p_{0_2}/p_{0_1}$ | $T_2/T_1$ | $p_2/p_1$ | $\rho_2/\rho_1$ |
|------|--------|--------|--------|--------|--------|
| 1.92 | 0.5918 | 0.7581 | 1.624 | 4.134 | 2.546 |
| 1.94 | 0.5880 | 0.7488 | 1.639 | 4.224 | 2.577 |
| 1.96 | 0.5844 | 0.7395 | 1.655 | 4.315 | 2.607 |
| 1.98 | 0.5808 | 0.7302 | 1.671 | 4.407 | 2.637 |
| 2.00 | 0.5774 | 0.7209 | 1.687 | 4.500 | 2.667 |
| 2.02 | 0.5740 | 0.7115 | 1.704 | 4.594 | 2.696 |
| 2.04 | 0.5707 | 0.7022 | 1.720 | 4.689 | 2.725 |
| 2.06 | 0.5675 | 0.6928 | 1.737 | 4.784 | 2.755 |
| 2.08 | 0.5643 | 0.6835 | 1.754 | 4.881 | 2.783 |
| 2.10 | 0.5613 | 0.6742 | 1.770 | 4.978 | 2.812 |
| 2.12 | 0.5583 | 0.6649 | 1.787 | 5.077 | 2.840 |
| 2.14 | 0.5554 | 0.6557 | 1.805 | 5.176 | 2.868 |
| 2.16 | 0.5525 | 0.6464 | 1.822 | 5.277 | 2.896 |
| 2.18 | 0.5498 | 0.6373 | 1.839 | 5.378 | 2.924 |
| 2.20 | 0.5471 | 0.6281 | 1.857 | 5.480 | 2.951 |
| 2.22 | 0.5444 | 0.6191 | 1.875 | 5.583 | 2.978 |
| 2.24 | 0.5418 | 0.6100 | 1.892 | 5.687 | 3.005 |
| 2.26 | 0.5393 | 0.6011 | 1.910 | 5.792 | 3.032 |
| 2.28 | 0.5368 | 0.5921 | 1.929 | 5.898 | 3.058 |
| 2.30 | 0.5344 | 0.5833 | 1.947 | 6.005 | 3.085 |
| 2.32 | 0.5321 | 0.5745 | 1.965 | 6.113 | 3.110 |
| 2.34 | 0.5297 | 0.5658 | 1.984 | 6.222 | 3.136 |
| 2.36 | 0.5275 | 0.5572 | 2.002 | 6.331 | 3.162 |
| 2.38 | 0.5253 | 0.5486 | 2.021 | 6.442 | 3.187 |
| 2.40 | 0.5231 | 0.5402 | 2.040 | 6.553 | 3.212 |
| 2.42 | 0.5210 | 0.5318 | 2.059 | 6.666 | 3.237 |
| 2.44 | 0.5189 | 0.5234 | 2.079 | 6.779 | 3.261 |
| 2.46 | 0.5169 | 0.5152 | 2.098 | 6.894 | 3.285 |
| 2.48 | 0.5149 | 0.5071 | 2.118 | 7.009 | 3.310 |
| 2.50 | 0.5130 | 0.4990 | 2.137 | 7.125 | 3.333 |
| 2.52 | 0.5111 | 0.4910 | 2.157 | 7.242 | 3.357 |
| 2.54 | 0.5092 | 0.4832 | 2.177 | 7.360 | 3.380 |
| 2.56 | 0.5074 | 0.4754 | 2.198 | 7.479 | 3.403 |
| 2.58 | 0.5056 | 0.4677 | 2.218 | 7.599 | 3.426 |
| 2.60 | 0.5039 | 0.4601 | 2.238 | 7.720 | 3.449 |
| 2.62 | 0.5022 | 0.4526 | 2.259 | 7.842 | 3.471 |
| 2.64 | 0.5005 | 0.4452 | 2.280 | 7.965 | 3.494 |
| 2.66 | 0.4988 | 0.4379 | 2.301 | 8.088 | 3.516 |
| 2.68 | 0.4972 | 0.4307 | 2.322 | 8.213 | 3.537 |
| 2.70 | 0.4956 | 0.4236 | 2.343 | 8.338 | 3.559 |
| 2.72 | 0.4941 | 0.4166 | 2.364 | 8.465 | 3.580 |
| 2.74 | 0.4926 | 0.4097 | 2.386 | 8.592 | 3.601 |
| 2.76 | 0.4911 | 0.4028 | 2.407 | 8.721 | 3.622 |
| 2.78 | 0.4897 | 0.3961 | 2.429 | 8.850 | 3.643 |
| 2.80 | 0.4882 | 0.3895 | 2.451 | 8.980 | 3.664 |

**TABLE C.11   Normal Shock Flow Functions**
(*Continued*)

| $M_1$ | $M_2$ | $p_{0_2}/p_{0_1}$ | $T_2/T_1$ | $p_2/p_1$ | $\rho_2/\rho_1$ |
|------|--------|-------------------|-----------|-----------|-----------------|
| 2.82 | 0.4868 | 0.3829 | 2.473 | 9.111 | 3.684 |
| 2.84 | 0.4854 | 0.3765 | 2.496 | 9.243 | 3.704 |
| 2.86 | 0.4840 | 0.3701 | 2.518 | 9.376 | 3.724 |
| 2.88 | 0.4827 | 0.3639 | 2.540 | 9.510 | 3.743 |
| 2.90 | 0.4814 | 0.3577 | 2.563 | 9.645 | 3.763 |
| 2.92 | 0.4801 | 0.3517 | 2.586 | 9.781 | 3.782 |
| 2.94 | 0.4788 | 0.3457 | 2.609 | 9.918 | 3.801 |
| 2.96 | 0.4776 | 0.3398 | 2.632 | 10.06 | 3.820 |
| 2.98 | 0.4764 | 0.3340 | 2.656 | 10.19 | 3.839 |
| 3.00 | 0.4752 | 0.3283 | 2.679 | 10.33 | 3.857 |
| 3.10 | 0.4695 | 0.3012 | 2.799 | 11.05 | 3.947 |
| 3.20 | 0.4644 | 0.2762 | 2.922 | 11.78 | 4.031 |
| 3.30 | 0.4596 | 0.2533 | 3.049 | 12.54 | 4.112 |
| 3.40 | 0.4552 | 0.2322 | 3.180 | 13.32 | 4.188 |
| 3.50 | 0.4512 | 0.2130 | 3.315 | 14.13 | 4.261 |
| 3.60 | 0.4474 | 0.1953 | 3.454 | 14.95 | 4.330 |
| 3.70 | 0.4440 | 0.1792 | 3.596 | 15.81 | 4.395 |
| 3.80 | 0.4407 | 0.1645 | 3.743 | 16.68 | 4.457 |
| 3.90 | 0.4377 | 0.1510 | 3.893 | 17.58 | 4.516 |
| 4.00 | 0.4350 | 0.1388 | 4.047 | 18.50 | 4.571 |
| 4.10 | 0.4324 | 0.1276 | 4.205 | 19.45 | 4.624 |
| 4.20 | 0.4299 | 0.1173 | 4.367 | 20.41 | 4.675 |
| 4.30 | 0.4277 | 0.1080 | 4.532 | 21.41 | 4.723 |
| 4.40 | 0.4255 | 0.09948 | 4.702 | 22.42 | 4.768 |
| 4.50 | 0.4236 | 0.09170 | 4.875 | 23.46 | 4.812 |
| 4.60 | 0.4217 | 0.08459 | 5.052 | 24.52 | 4.853 |
| 4.70 | 0.4199 | 0.07809 | 5.233 | 25.61 | 4.893 |
| 4.80 | 0.4183 | 0.07214 | 5.418 | 26.71 | 4.930 |
| 4.90 | 0.4167 | 0.06670 | 5.607 | 27.85 | 4.966 |
| 5.00 | 0.4152 | 0.06172 | 5.800 | 29.00 | 5.000 |

Adapted from Fox and Macdonald, *Introduction to Fluid Mechanics,*
published by John Wiley & Sons, 4th ed., 1992.

**TABLE C.12   Prandtl–Meyer Function (one-dimensional, ideal gas, $\gamma = 1.4$)**

| $\nu$ (degrees) | $M$ | $\alpha_M$ (degrees) | $\nu$ (degrees) | $M$ | $\alpha_M$ (degrees) |
|---|---|---|---|---|---|
| 0.0 | 1.000 | 90.000 | 17.5 | 1.689 | 36.293 |
| 0.5 | 1.051 | 72.099 | 18.0 | 1.706 | 35.874 |
| 1.0 | 1.082 | 67.574 | 18.5 | 1.724 | 35.465 |
| 1.5 | 1.108 | 64.451 | 19.0 | 1.741 | 35.065 |
| 2.0 | 1.133 | 61.997 | 19.5 | 1.758 | 34.673 |
| 2.5 | 1.155 | 59.950 | 20.0 | 1.775 | 34.290 |
| 3.0 | 1.177 | 58.180 | 20.5 | 1.792 | 33.915 |
| 3.5 | 1.198 | 56.614 | 21.0 | 1.810 | 33.548 |
| 4.0 | 1.218 | 55.205 | 21.5 | 1.827 | 33.188 |
| 4.5 | 1.237 | 53.920 | 22.0 | 1.844 | 32.834 |
| 5.0 | 1.256 | 52.738 | 22.5 | 1.862 | 32.488 |
| 5.5 | 1.275 | 51.642 | 23.0 | 1.879 | 32.148 |
| 6.0 | 1.294 | 50.619 | 23.5 | 1.897 | 31.814 |
| 6.5 | 1.312 | 49.658 | 24.0 | 1.915 | 31.486 |
| 7.0 | 1.330 | 48.753 | 24.5 | 1.932 | 31.164 |
| 7.5 | 1.348 | 47.896 | 25.0 | 1.950 | 30.847 |
| 8.0 | 1.366 | 47.082 | 25.5 | 1.968 | 30.536 |
| 8.5 | 1.383 | 46.306 | 26.0 | 1.986 | 30.229 |
| 9.0 | 1.400 | 45.566 | 26.5 | 2.004 | 29.928 |
| 9.5 | 1.418 | 44.857 | 27.0 | 2.023 | 29.632 |
| 10.0 | 1.435 | 44.177 | 27.5 | 2.041 | 29.340 |
| 10.5 | 1.452 | 43.523 | 28.0 | 2.059 | 29.052 |
| 11.0 | 1.469 | 42.894 | 28.5 | 2.078 | 28.769 |
| 11.5 | 1.486 | 42.287 | 29.0 | 2.096 | 28.491 |
| 12.0 | 1.503 | 41.701 | 29.5 | 2.115 | 28.216 |
| 12.5 | 1.520 | 41.134 | 30.0 | 2.134 | 27.945 |
| 13.0 | 1.537 | 40.585 | 30.5 | 2.153 | 27.678 |
| 13.5 | 1.554 | 40.053 | 31.0 | 2.172 | 27.415 |
| 14.0 | 1.571 | 39.537 | 31.5 | 2.191 | 27.155 |
| 14.5 | 1.588 | 39.035 | 32.0 | 2.210 | 26.899 |
| 15.0 | 1.605 | 38.547 | 32.5 | 2.230 | 26.646 |
| 15.5 | 1.622 | 38.073 | 33.0 | 2.249 | 26.397 |
| 16.0 | 1.639 | 37.611 | 33.5 | 2.269 | 26.151 |
| 16.5 | 1.655 | 37.160 | 34.0 | 2.289 | 25.908 |
| 17.0 | 1.672 | 36.721 | 34.5 | 2.309 | 25.668 |

**TABLE C.12  Prandtl–Meyer Function** (*Continued*)

| $\nu$ (degrees) | $M$ | $\alpha_M$ (degrees) | $\nu$ (degrees) | $M$ | $\alpha_M$ (degrees) |
|---|---|---|---|---|---|
| 35.0 | 2.329 | 25.430 | 52.5 | 3.146 | 18.532 |
| 35.5 | 2.349 | 25.196 | 53.0 | 3.176 | 18.366 |
| 36.0 | 2.369 | 24.965 | 53.5 | 3.202 | 18.200 |
| 36.5 | 2.390 | 24.736 | 54.0 | 3.230 | 18.036 |
| 37.0 | 2.410 | 24.510 | 54.5 | 3.258 | 17.873 |
| 37.5 | 2.431 | 24.287 | 55.0 | 3.287 | 17.711 |
| 38.0 | 2.452 | 24.066 | 55.5 | 3.316 | 17.551 |
| 38.5 | 2.473 | 23.847 | 56.0 | 3.346 | 17.391 |
| 39.0 | 2.495 | 23.631 | 56.5 | 3.375 | 17.233 |
| 39.5 | 2.516 | 23.418 | 57.0 | 3.406 | 17.076 |
| 40.0 | 2.538 | 23.206 | 57.5 | 3.436 | 16.920 |
| 40.5 | 2.560 | 22.997 | 58.0 | 3.467 | 16.765 |
| 41.0 | 2.582 | 22.790 | 58.5 | 3.498 | 16.611 |
| 41.5 | 2.604 | 22.585 | 59.0 | 3.530 | 16.458 |
| 42.0 | 2.626 | 22.382 | 59.5 | 3.562 | 16.306 |
| 42.5 | 2.649 | 22.182 | 60.0 | 3.594 | 16.155 |
| 43.0 | 2.671 | 21.983 | 60.5 | 3.627 | 16.005 |
| 43.5 | 2.694 | 21.786 | 61.0 | 3.660 | 15.856 |
| 44.0 | 2.718 | 21.591 | 61.5 | 3.694 | 15.708 |
| 44.5 | 2.741 | 21.398 | 62.0 | 3.728 | 15.561 |
| 45.0 | 2.764 | 21.207 | 62.5 | 3.762 | 15.415 |
| 45.5 | 2.788 | 21.017 | 63.0 | 3.797 | 15.270 |
| 46.0 | 2.812 | 20.830 | 63.5 | 3.832 | 15.126 |
| 46.5 | 2.836 | 20.644 | 64.0 | 3.868 | 14.983 |
| 47.0 | 2.861 | 20.459 | 64.5 | 3.904 | 14.840 |
| 47.5 | 2.886 | 20.277 | 65.0 | 3.941 | 14.698 |
| 48.0 | 2.910 | 20.096 | 65.5 | 3.979 | 14.557 |
| 48.5 | 2.936 | 19.916 | 66.0 | 4.016 | 14.417 |
| 49.0 | 2.961 | 19.738 | 66.5 | 4.055 | 14.278 |
| 49.5 | 2.987 | 19.561 | 67.0 | 4.094 | 14.140 |
| 50.0 | 3.013 | 19.386 | 67.5 | 4.133 | 14.002 |
| 50.5 | 3.039 | 19.213 | 68.0 | 4.173 | 13.865 |
| 51.0 | 3.065 | 19.041 | 68.5 | 4.214 | 13.729 |
| 51.5 | 3.092 | 18.870 | 69.0 | 4.255 | 13.593 |
| 52.0 | 3.119 | 18.701 | 69.5 | 4.297 | 13.459 |

**TABLE C.12   Prandtl–Meyer Function** (*Continued*)

| $\nu$ (degrees) | $M$ | $\alpha_M$ (degrees) | $\nu$ (degrees) | $M$ | $\alpha_M$ (degrees) |
|---|---|---|---|---|---|
| 70.0 | 4.339 | 13.325 | 87.5 | 6.390 | 9.003 |
| 70.5 | 4.382 | 13.191 | 88.0 | 6.472 | 8.888 |
| 71.0 | 4.426 | 13.059 | 88.5 | 6.556 | 8.774 |
| 71.5 | 4.470 | 12.927 | 89.0 | 6.642 | 8.660 |
| 72.0 | 4.515 | 12.795 | 89.5 | 6.729 | 8.546 |
| 72.5 | 4.561 | 12.665 | 90.0 | 6.819 | 8.433 |
| 73.0 | 4.608 | 12.535 | 90.5 | 6.911 | 8.320 |
| 73.5 | 4.655 | 12.406 | 91.0 | 7.005 | 8.207 |
| 74.0 | 4.703 | 12.277 | 91.5 | 7.102 | 8.095 |
| 74.5 | 4.752 | 12.149 | 92.0 | 7.201 | 7.983 |
| 75.0 | 4.801 | 12.021 | 92.5 | 7.302 | 7.871 |
| 75.5 | 4.852 | 11.894 | 93.0 | 7.406 | 7.760 |
| 76.0 | 4.903 | 11.768 | 93.5 | 7.513 | 7.649 |
| 76.5 | 4.955 | 11.642 | 94.0 | 7.623 | 7.538 |
| 77.0 | 5.009 | 11.517 | 94.5 | 7.735 | 7.428 |
| 77.5 | 5.063 | 11.392 | 95.0 | 7.851 | 7.318 |
| 78.0 | 5.118 | 11.268 | 95.5 | 7.970 | 7.208 |
| 78.5 | 5.174 | 11.145 | 96.0 | 8.092 | 7.099 |
| 79.0 | 5.231 | 11.022 | 96.5 | 8.218 | 6.989 |
| 79.5 | 5.289 | 10.899 | 97.0 | 8.347 | 6.881 |
| 80.0 | 5.348 | 10.777 | 97.5 | 8.480 | 6.772 |
| 80.5 | 5.408 | 10.656 | 98.0 | 8.618 | 6.664 |
| 81.0 | 5.470 | 10.535 | 98.5 | 8.759 | 6.556 |
| 81.5 | 5.532 | 10.414 | 99.0 | 8.905 | 6.448 |
| 82.0 | 5.596 | 10.294 | 99.5 | 9.055 | 6.340 |
| 82.5 | 5.661 | 10.175 | 100.0 | 9.210 | 6.233 |
| 83.0 | 5.727 | 10.056 | 100.5 | 9.371 | 6.126 |
| 83.5 | 5.795 | 9.937 | 101.0 | 9.536 | 6.019 |
| 84.0 | 5.864 | 9.819 | 101.5 | 9.708 | 5.913 |
| 84.5 | 5.935 | 9.701 | 102.0 | 9.885 | 5.806 |
| 85.0 | 6.006 | 9.584 | | | |
| 85.5 | 6.080 | 9.467 | | | |
| 86.0 | 6.155 | 9.350 | | | |
| 86.5 | 6.232 | 9.234 | | | |
| 87.0 | 6.310 | 9.119 | | | |

Adapted from Liepmann and Roshko, *Elements of Gasdynamics,* John Wiley & Sons, 1957.

# Index